UNCLASSIFIED

AD NUMBER

AD276249

NEW LIMITATION CHANGE

TO

Approved for public release, distribution unlimited

FROM

Distribution authorized to U.S. Gov't. agencies and their contractors; Mar 1962. Other requests shall be referred to Air Force Systems Command, ASD, Wright-Patterson AFB, OH 43433.

AUTHORITY

AFWAL ltr, 21 Nov 1984

THIS PAGE IS UNCLASSIFIED

AD 276249

AUTHORITY: AFWAL ltr 21 Nov 84

UNCLASSIFIED

AD 276249

DEFENSE DOCUMENTATION CENTER

FOR

SCIENTIFIC AND TECHNICAL INFORMATION

CAMERON STATION ALEXANDRIA, VIRGINIA



UNCLASSIFIED

# DISCLAIMER NOTICE

THIS DOCUMENT IS BEST QUALITY PRACTICABLE. THE COPY FURNISHED TO DTIC CONTAINED A SIGNIFICANT NUMBER OF PAGES WHICH DO NOT REPRODUCE LEGIBLY.

NOTICE: When government or other drawings, specifications or other data are used for any purpose other than in connection with a definitely related government procurement operation, the U. S. Government thereby incurs no responsibility, nor any obligation whatsoever; and the fact that the Government may have formulated, furnished, or in any way supplied the said drawings, specifications, or other data is not to be regarded by implication or otherwise as in any manner licensing the holder or any other person or corporation or conveying any rights or permission to manufacture, use or sell any patented invention that may in any way be related thereto.

276 249

22 62
CATALOGUED BY ASTIA
AS AD NO.

# AN ENGINEERING EVALUATION OF METHODS FOR THE PREDICTION OF FATIGUE LIFE IN AIRFRAME STRUCTURES

TECHNICAL REPORT No. ASD-TR-61-434

MARCH 1962

FLIGHT DYNAMICS LABORATORY
AERONAUTICAL SYSTEMS DIVISION
AIR FORCE SYSTEMS COMMAND
WRIGHT-PATTERSON AIR FORCE BASE, OHIO

Project No. 1367, Task No. 136710

(Prepared under Contract No. AF 33(616)-6574 by Lockheed-California, Lockheed Aircraft Corporation, J. A. Young and M. A. Melcon.)

## NOTICES

When Government drawings, specifications, or other data are used for any purpose other than in connection with a definitely related G[illegible]ment procurement operation, the United States Government thereby incurs no responsibility nor any obligation whatsoever; and the fact that the Government may have formulated, furnished, or in any way supplied the said drawings, specifications, or other data, is not to be regarded by implication or [illegible] licensing the holder or any other person or corporation, or [illegible] or permission to manufacture, use, or sell any patented invention that may in any way be related thereto.

Qualified requesters may obtain copies of this report from the Armed Services Technical Information Agency, (ASTIA), Arlington Hall Station, Arlington 12, Virginia.

ASTIA release to OTS NOT authorized

Copies of ASD Technical Reports and Technical Notes should not be returned to the Aeronautical Systems Division unless return is required by security considerations, contractual obligations, or notice on a specific document.

300 - May 1962 - 33-1463 & 1464

# FOREWORD

This report was prepared by the Lockheed-California Company, a Division of Lockheed Aircraft Corporation, Burbank, California, under USAF Contract No. AF 33(616)-6574. This contract was performed under Project No. 1367, "Structural Design Criteria," Task No. 136710, "Structural Analysis Methods." This Project and Task are part of Air Force Systems Command's Applied Research Program 750A, "The Mechanics of Flight." The contract was administered initially under the technical direction of the Aircraft Laboratory by the Project Engineer, Mr. Bernard Nasal. It was completed in the Flight Dynamics Laboratory under the direction of Mr. Vincent Kearney.

The program was conducted at the Lockheed-California Company under the technical administration of Mr. M. A. Melcon, Department Manager, Structural Methods. Technical supervision was under the direction of Mr. W. J. Critchlow, Group Engineer, Structural Statics, and Mr. A. J. McCulloch. The details of the methods review and computations were performed by Mr. Louis Young with the assistance of other technical personnel in the Structural Methods Development and from the Mathematical Analysis Department in programming for digital computer. Statistical analysis of the S-N data was performed by Dr. F. M. Mueller.

The laboratory experimental program was under the technical administration of Mr. H. W. Foster, Division Manager, Lockheed Structures Research Laboratory. The design and assembly of the experimental equipment and the development of operational techniques were under the technical supervision of Mr. J. Redman, Group Engineer, Structural Development Research. He was also assisted in the assembly of electronic equipment for magnetic tape signal analysis, the recording of special loading spectra, and for fatigue test and test control equipment by Mr. W. B. Brewer, Group Engineer, Electrical Instrumentation, aided by Mr. R. A. Meyer, electrical design; Mr. J. B. Parlan, tape equipment; Mr. P. A. [illegible], electrical calibration, monitoring, and maintenance.

The testing performed under this contract was under the direct supervision of Mr. H. W. Grebe, Mr. R. H. Wells, and Mr. J. D. Ryan, assisted by Mr. [illegible] J. Cox, Mr. R. L. Lowe, and Mr. L. Silvas.

Typing of the report was done by Mrs. Emily A. Baldwin, assisted by Mrs. Joyce Ponder and Miss Pat Daly.

---

The assembly of the electronic equipment for magnetic tape reading, counting, tape recording of special loading spectra, and for the magnetic tape controlled fatigue test equipment, along with the development of the calibration and monitoring techniques, and the testing of the spectrum loaded coupons reported herein, was shared between this contract and the companion contract, No. AF 33(616)-6575, "Research Study to Establish Fatigue Test Loading Spectra from Flight Records."

## ABSTRACT

The results of a research study are presented for the comparison and verification of methods of fatigue life prediction suitable for handling the complex problems encountered in the design and operation of modern aircraft. A general introduction to the problems of airframe fatigue analysis is given from the overall viewpoint of a system of design, development testing, and interpretation of fleet service history to maintain a necessary comparative basis for relating a practical fatigue life prediction method to operational results. From a study of twenty proposed fatigue life prediction methods ten of the procedures were chosen for evaluation numerically with a group of seventy-eight complex spectral test results representing approximately 200 individual specimens.

An experimental program generated constant amplitude axial load S-N type data on simple notched coupons of 7075-T6 aluminum alloy sheet for use in the analysis procedures. Covered spectral fatigue test data from these same type coupons were utilized from another concurrent AFD fatigue research program. New magnetic tape controlled fatigue test machines were utilized to apply simple spectra of gust, maneuver, ground, composite spectra of flight gust, ground taxi, and ground-air-ground transitions and composite spectra of flight maneuver, ground taxi, and ground-air-ground transitions. A series of specimens of a complex joint were also [illegible] the same simple covered gust and maneuver spectra, and to the composite spectra of flight gust, ground taxi, and ground-air-ground transition cycles, and to composite flight maneuver, ground taxi, and ground-air-ground transition cycles. These data were analyzed by the selected procedures to confirm or provide a possible means of improving the selected fatigue life prediction methods.


PUBLICATION REVIEW

This report has been reviewed and is approved.

FOR THE COMMANDER

William C. Nielsen

WILLIAM C. NIELSEN
Colonel, USAF
Chief, Flight Dynamics Laboratory

TABLE OF CONTENTS


| SECTION | | Page |
|---|---|---|
| I | Introduction and Background | 1 |
| II | Methods of Analysis | 5 |
| III | Evaluation and Selection of Fatigue Life Prediction Methods | 25 |
| IV | Investigation of the Influence of Spectrum Shape on Fatigue Life Predictions | 53 |
| V | Analysis of Complex Joint Specimens | 99 |
| VI | Summary and Conclusions | 113 |
| | References | 119 |
| | Appendix A: Description of Fatigue Life Prediction Methods | 122 |
| | Appendix B: Application of Selected Fatigue Life Prediction Methods to Published Test Data | 161 |
| | Appendix C: Spectral Fatigue Test Data for the Evaluation of Fatigue Life Prediction Methods | 196 |
| | Appendix D: Original Test Results | 264 |

## LIST OF ILLUSTRATIONS


| FIGURE | | PAGE |
|---|---|---|
| 1 | Fatigue Notch Factors for Simulation Elements | 8 |
| 2 | Development of Gust Loading Spectra | 13 |
| 3 | Development of Maneuver Loading Spectra | 15 |
| 4 | Schematic of Composite Loading Spectrum | 17 |
| 5 | Comparison of Predicted and Experimental Fatigue Life - Gust Loading Spectra | 32-38 |
| 6 | Comparison of Predicted and Experimental Fatigue Life - Maneuver Loading Spectra | 39 |
| 7 | Cumulative Distributions for the Ratio of Test Life to Predicted Life | 41 |
| 8 | Cumulative Distributions for the Ratio of Test Stress to Adjusted Stress | 42 |
| 9 | Log Cumulative Distributions for the Ratio of Test Life to Predicted Life | 44 |
| 10 | Variation of the Test Derived Fatigue Quality Index K verses Slope of the Loading Spectra | 48 |
| 11 | General View of Tape Handling Equipment | 60 |
| 12 | General View of Specimen Loading Apparatus | 60 |
| 13 | Close-Up of Test Specimen Installation | 61 |
| 14 | Comparison of Servo Valve Input Signal with Specimen Loading History | 62 |
| 15 | Notched Sheet Test Coupons - 7075-T6 Aluminum Alloy | 63 |
| 16 | Sample Flight Loading Trace | 64 |
| 17 | Comparison of Trace Reductions - Wing Root Random Loading Trace | 65 |
| 18 | Schematic of High Peak, Concave Upward, and Concave Downward Gust Loading Spectra | 66 |

LIST OF ILLUSTRATIONS (Continued)


| FIGURE | | PAGE |
|---|---|---|
| 19 | Comp[illegible] of Military Maneuver Loading Spectrum w[illegible]ation Specified in MIL-A-8866 for Class "A" Aircraft | 67 |
| 20 | Sample of Random Military Maneuver Loading Trace | 68 |
| 21 | Development of Ordered Loading Spectrum | 69 |
| 22 | Schematic Representation of Sequence, Stress Interval, and Unit Spectrum Size | 70 |
| 23 | Partial Trace of an Ordered Gust Loading History | 71 |
| 24 | Sample of Ordered Military Maneuver Loading Trace | 72 |
| 25 | Schematic Diagrams of Maneuver Loading Sequences for Coupons | 73 |
| 26 | Schematic Representation of Ordered Loading Trace - Gust and Ground Loadings Plus Ground-to-Air Cycles | 74 |
| 27 | Sample Random Loading Trace - Composite of Military Maneuver and Ground Loadings | 75 |
| 28 | Variation in Quality Index (K) with Slope of Gust Loading Spectra in the High Stress Range | 78 |
| 29 | Variation in Quality Index (K) with Slope of Gust Loading Spectra in the Midstress Range of Maximum Calculated Fatigue Damage | 79 |
| 30 | Varying Stress versus Slope of Gust Loading Spectra | 80 |
| 31 | Varying Stress versus Slope of Maneuver Loading Spectra | 81 |
| 32 | Varying Stress versus Slope of Composite Gust Loading Spectra | 82 |
| 33 | Varying Stress versus Slope of Composite Maneuver Spectrum | 83 |
| 34 | Standardized S-N Curves for Calculating Fatigue Damage and Fatigue Life | 86 |
| 35 | Illustrations of Gust Loading Spectra and the Corresponding Curves for Fatigue Damage at Quality Indexes of 2, 4 and 6 | 87 |

LIST OF ILLUSTRATIONS (Continued)


| FIGURE | | PAGE |
|---|---|---|
| 36 | Illustration of Procedure Used to Correlate Quality Index and Slope of Loading Spectra in Stress Range of Maximum Fatigue Damage | 88 |
| 37 | Comparison between Predicted and Experimental Fatigue Lives for Gust Spectra on Coupons | 95 |
| 38 | Comparison between Predicted and Experimental Fatigue Lives for Gust Spectra on Coupons | 96 |
| 39 | Comparison between Predicted and Experimental Fatigue Lives for Maneuver, Ground, and Composite Spectra on Coupons | 97 |
| 40 | Cumulative Distributions for the Ratio of Test Life to Predicted Life | 98 |
| 41 | Detail Sketch of Panel Assembly | 100 |
| 42 | Basic Ordered Unit Gust and Unit Composite Gust Loading Spectra | 101 |
| 43 | Two Joint Test Panel Assemblies Installed in Fatigue Test Machine | 102 |
| 44 | Schematic Diagram of 500,000 - pound Fatigue Machine | 102 |
| 45 | Basic Ordered Unit Maneuver and Unit Composite Maneuver Loading Spectra | 105 |
| 46 | Comparison Between Predicted and Experimental Fatigue Lives | 111 |
| 47 | S-N Data for Notched Sheet Specimens | 127 |
| 48 | Analytical Representation of S-N Data | 132 |
| 49 | Analytical Interpretation of Unit Loading Spectrum | 134 |
| 50 | Equivalent Cycle Ratio $(n/N)_1$ for Lo-Hi and Hi-Lo Sequence of Loading | 137 |
| 51 | The Influence of Prior Fatigue Loading on the Selection of an Equivalent S-N Curve | 139 |
| 52 | Typical Variation in Fatigue Life with the Exponents b and c for a Specific Unit Loading Spectrum | 149 |

## LIST OF ILLUSTRATIONS (Continued)


| FIGURE | | PAGE |
|---|---|---|
| 53 | Tangent Intercept Method of Spectrum Fatigue Test Interpretation | 156 |
| 54 | Schematic of Tangent Intercept Method | 157 |
| 55 | Method Used to Reduce Cumulative Stress-Frequency Spectrum into Simple Cyclic Loading Steps | 163 |
| 56 | Comparison of Analytical and Experimental Unit Gust Loading Spectrum for Notched Sheet Specimens | 165 |
| 57 | $(S_y - S_F)$ versus N for S-N Data on Notched Sheet Specimens | 166 |
| 58 | Standardized S-N Curves $f_{mean}$ = -10,000 psi | 170 |
| 59 | Standardized S-N Curves $f_{mean}$ = 0 | 171 |
| 60 | Standardized S-N Curves $f_{mean}$ = 10,000 psi | 172 |
| 61 | Standardized S-N Curves $f_{mean}$ = 20,000 psi | 173 |
| 62 | Standardized S-N Curves $f_{mean}$ = 30,000 psi | 174 |
| 63 | Schematic Diagrams of Gust Loading Sequences | 200-201 |
| 64 | Notched Sheet Specimen for which Fatigue Test Data are Presented in Reference 16 | 202 |
| 65 | Specimens for which Fatigue Test Data are Presented in Reference 17 | 203 |
| 66 | Riveted Lap Joint Specimens for which Fatigue Test Data are Presented in Reference 18 | 204 |
| 67 | Notched Plate Specimen for which Fatigue Test Data are Presented in Reference 19 | 205 |
| 68 | C-46 Wing Specimen for which Fatigue Test Data are Presented in References 20 and 23 | 206 |
| 69 | F5I Wing Specimen for which Fatigue Test Data are Presented in Reference 21 | 207 |
| 70 | Unit Gust Loading Spectra for Notched Sheet Specimens - 2024-T3 Aluminum Alloy | 221 |
| 71 | Unit Gust Loading Spectra for Notched Sheet Specimens - 7075-T6 Aluminum Alloy | 222 |

LIST OF ILLUSTRATIONS (Continued)


| FIGURE | | PAGE |
|---|---|---|
| 72 | Unit Gust Loading Spectra for Double Shear Riveted Joint Specimens - 2024-T3 Alclad Aluminum Alloy | 223 |
| 73 | Unit Gust Loading Spectra for Unnotched Sheet Specimens - 7075-T6 Alclad Aluminum Alloy | 224 |
| 74 | Unit Gust Loading Spectra for Butt Joint Specimens - 7075-T6 Alclad Aluminum Alloy | 225 |
| 75 | Unit Gust Loading Spectra for Strip Specimens with Centrally Located Hole - Cr-Mo Steel | 226 |
| 76 | Unit Gust Loading Spectra for Lap Joint Specimens with a Single Row of Flush Rivets - 2024-T3 Alclad Aluminum Alloy | 227 |
| 77 | Unit Gust Loading Spectrum for Lap Joint Specimens with a Double Row of Flush Rivets - 2024-T3 Alclad Aluminum Alloys | 228 |
| 78 | Unit Gust Loading Spectra for Lap Joint Specimens with a Single Row of Flush Rivets - 7075-T6 Alclad Aluminum Alloy | 229 |
| 79 | Unit Gust Loading Spectra for Notched Plate Specimens - D.T.D. 363A Aluminum Alloy | 230 |
| 80 | Unit Gust Loading Spectrum for C-46 Wing - 2024-T3 Aluminum Alloy | 231 |
| 81 | Unit Gust Loading Spectra for F51 Wing - 2024-T3 Aluminum Alloy | 232 |
| 82 | S-N Curves for Notched Sheet Specimens - 2024-T3 Aluminum Alloy | 233 |
| 83 | S-N Curves for Notched Sheet Specimens - 7075-T6 Aluminum Alloy | 234 |
| 84 | S-N Curves for Double Shear Riveted Joint Specimens - 2024-T3 Alclad Aluminum Alloy | 235 |
| 85 | S-N Curves for Unnotched Sheet Specimens - 7075-T6 Alclad Aluminum Alloy | 236 |
| 86 | S-N Curves for Butt Joint Specimens - 7075-T6 Alclad Aluminum Alloy | 237 |

LIST OF ILLUSTRATIONS (Continued)


| FIGURE | | PAGE |
|---|---|---|
| 87 | S-N Curves for Strip Specimens with Centrally Located Hole - Cr-Mo Steel | 238 |
| 88 | S-N Curves for Lap Joint Specimens with a Single Row of Flush Rivets - 2024-T3 Alclad Aluminum Alloy | 239 |
| 89 | S-N Curve for Lap Joint Specimen with a Double Row of Flush Rivets - 2024-T3 Alclad Aluminum Alloy | 240 |
| 90 | S-N Curve for Lap Joint Specimens with a Single Row of Flush Rivets - 7075-T6 Alclad Aluminum Alloy | 241 |
| 91 | S-N Curve for Notched Plate Specimens - D.T.D. 363A Aluminum Alloy | 242 |
| 92 | S-N Curves for Wing Stations 180, 214, 228, and 239 of C-46 Wing - 2024-T Aluminum Alloy | 243 |
| 93 | Average S-N Curves for Complete C-46 Wing - 2024-T Aluminum Alloy | 244 |
| 94 | S-N Curves for Initial Failure of P51 Wing - 2024-T Aluminum Alloy | 245 |
| 95 | S-N Curves for Final Failure of P51 Wing - 2024-T Aluminum Alloy | 246 |
| 96 | Schematic Diagrams of Lo-Hi-Lo Maneuver Loading Sequence | 247 |
| 97 | Unit Maneuver Loading Spectra for Double Shear Riveted Joint Specimens - 2024-T3 Alclad Aluminum Alloy | 252 |
| 98 | Unit Maneuver Loading Spectra for Unnotched Sheet Specimens - 7075-T6 Alclad Aluminum Alloy | 253 |
| 99 | Unit Maneuver Loading Spectra for Butt Joint Specimens- 7075-T6 Alclad Aluminum Alloy | 254 |
| 100 | Unit Maneuver Loading Spectra for Strip Specimens with a Centrally Located Hole - Cr-Mo Steel | 255 |
| 101 | S-N Curves for Double Shear Riveted Joint Specimens- Constant Minimum Stress (for Maneuver-Type Loading)- 2024-T3 Alclad Aluminum | 256 |

LIST OF ILLUSTRATIONS (Continued)


| FIGURE | | PAGE |
|---|---|---|
| 102 | S-N Curves for Unnotched Sheet Specimens - Constant Minimum Stress (for Maneuver-Type Loading) - 7075-T6 Alclad Aluminum Alloy | 257 |
| 103 | S-N Curves for Butt Joint Specimens - Constant Minimum Stress (for Maneuver Type Loading) - 7075-T6 Alclad Aluminum | 258 |
| 104 | S-N Curves for Strip Specimens with Centrally Located Hole - Constant Minimum Stress (for Maneuver-Type Loading) - Cr-Mo Steel | 259 |
| 105 | Deviation in $\Delta$ Log $S_v$ from the Least Square Best Fit Straight Line on a Plot of Log $S_v$ versus Log N | 266 |
| 106 | Experimental S-N Curve for Notched Sheet Coupons - $K_T = 3$, $f_{mean} = -10$ KSI | 274 |
| 107 | Experimental S-N Curve for Notched Sheet Coupons - $K_T = 3$, $f_{mean} = -5$ KSI | 275 |
| 108 | Experimental S-N Curve for Notched Sheet Coupons - $K_T = 3$, $f_{mean} = 10$ KSI | 276 |
| 109 | Experimental S-N Curve for Notched Sheet Coupons - $K_T = 3$, $f_{mean} = 15$ KSI | 277 |
| 110 | Experimental S-N Curve for Notched Sheet Coupons - $K_T = 4$, $f_{mean} = -10$ KSI | 278 |
| 111 | Experimental S-N Curve for Notched Sheet Coupons - $K_T = 4$, $f_{mean} = -5$ KSI | 279 |
| 112 | Experimental S-N Curve for Notched Sheet Coupons - $K_T = 4$, $f_{mean} = 0$ KSI | 280 |
| 113 | Experimental S-N Curve for Notched Sheet Coupons - $K_T = 4$, $f_{mean} = 10$ KSI | 281 |
| 114 | Experimental S-N Curve for Notched Sheet Coupons - $K_T = 4$, $f_{mean} = 15$ KSI | 282 |
| 115 | Experimental S-N Curve for Notched Sheet Coupons - $K_T = 7$, $f_{mean} = -10$ KSI | 283 |
| 116 | Experimental S-N Curve for Notched Sheet Coupons - $K_T = 7$, $f_{mean} = -5$ KSI | 284 |

## LIST OF ILLUSTRATIONS (Continued)


| FIGURE | | PAGE |
|---|---|---|
| 117 | Experimental S-N Curves for Notched Sheet Coupons - $K_T = 7$, $f_{mean} = 0$ KSI | 285 |
| 118 | Experimental S-N Curve for Notched Sheet Coupons - $K_T = 7$, $f_{mean} = 10$ KSI | 286 |
| 119 | Experimental S-N Curve for Notched Sheet Coupons - $K_T = 7$, $f_{mean} = 15$ KSI | 287 |
| 120 | Experimental S-N Curve for Notched Sheet Coupons - $K_T = 10$, $f_{mean} = -10$ KSI | 288 |
| 121 | Experimental S-N Curve for Notched Sheet Coupons - $K_T = 10$, $f_{mean} = -5$ KSI | 289 |
| 122 | Experimental S-N Curve for Notched Sheet Coupons - $K_T = 10$, $f_{mean} = 10$ KSI | 290 |
| 123 | Experimental S-N Curve for Notched Sheet Coupons - $K_T = 10$, $f_{mean} = 15$ KSI | 291 |
| 124 | Christensen Diagram - Axial Loading, Coupon Test S-N Data - $K_T = 7$ | 293 |
| 125 | Christensen Diagram - Axial Loading, Coupon Test S-N Data - $K_T = 4$ | 294 |
| 126 | Interpolated S-N Curves for Notched Sheet Coupons - $K_T = 7$ | 295 |
| 127 | Interpolated S-N Curves for Notched Sheet Coupons - $K_T = 4$ | 296 |
| 128 | Interpolated S-N Curves for Notched Sheet Coupons - Constant Minimum Stress of 5.4 KSI - $K_T = 4$ & $K_T = 7$ | 297 |
| 129 | Close-up of Specimen Installation | 299 |
| 130 | General View of Tape Construction and Data Reduction Equipment | 299 |
| 131 | Schematic of Transcription of Flight Record | 300 |
| 132 | Mean Crossing Peak Count - Wing Root and Modified Wing Root Traces | 301 |
| 133 | Schematic of System for Altering Spectrum Shapes | 303 |
| 134 | Schematic of Step Ordered Tape Generation | 306 |
| 135 | Schematic of Test Loading System | 312 |

## LIST OF ILLUSTRATIONS (Continued)


| FIGURE | | PAGE |
|---|---|---|
| 136 | General View of Specimen Loading Apparatus | 314 |
| 137 | Magnetic Tape Loading Control Units | 314 |
| 138 | Definition of the Zero Crossing Peak Count Method | 320 |
| 139 | Applications of Basic Computer Elements | 322 |
| 140 | Applications of Basic Computer Elements | 323 |
| 141 | Schematic of Computing Circuit for the Zero Crossing Peak Count | 324 |
| 142 | Schematic for Complete Testing, Monitoring, and Counting Process | 327 |
| 143 | Maximum Error Limits | 328 |
| 144 | 95% Probability Error Limits | 329 |
| 145 | Random Low Peak Gust Loading Test Data | 383 |
| 146 | Ordered Low Peak Gust Loading Test Data | 384 |
| 147 | Ordered Low Peak Gust Loading Test Data | 385 |
| 148 | Ordered Low Peak Gust Loading Test Data | 386 |
| 149 | Random Low Peak Gust Loading Test Data | 387 |
| 150 | Ordered Low Peak Gust Loading Test Data | 388 |
| 151 | Random High Peak Gust Loading Test Data | 389 |
| 152 | Ordered High Peak Gust Loading Test Data | 390 |
| 153 | Ordered High Peak Gust Loading Test Data | 391 |
| 154 | Ordered High Peak Gust Loading Test Data | 392 |
| 155 | Random High Peak Gust Loading Test Data | 393 |
| 156 | Ordered High Peak Gust Loading Test Data | 394 |
| 157 | Wing Root Random Loading Test Data | 395 |
| 158 | Wing Root Ordered Loading Test Data | 396 |
| 159 | Modified Wing Root Random Loading Test Data | 397 |

## LIST OF ILLUSTRATIONS (Continued)


| FIGURE | | PAGE |
|---|---|---|
| 160 | Modified Wing Root Ordered Loading Test Data | 398 |
| 161 | Random Ground Loading Test Data | 399 |
| 162 | Ordered Ground Loading Test Data | 400 |
| 163 | Random Military Maneuver Flight Loading Test Data | 401 |
| 164 | Ordered Military Maneuver Flight Loading Test Data | 402 |
| 165 | Ordered Military Maneuver Flight Loading Test Data | 403 |
| 166 | Ordered Composite Loading Test Data (Low Peak Gust Loadings in Flight) | 404 |
| 167 | Ordered Composite Loading Test Data (Low Peak Gust Loadings in Flight) | 405 |
| 168 | Ordered Composite Loading Test Data (High Peak Gust Loadings in Flight) | 406 |
| 169 | Ordered Composite Loading Test Data (High Peak Gust Loadings in Flight) | 407 |
| 170 | Random Composite Loadings (Military Maneuver Flight Loadings) | 408 |
| 171 | Panel Assembly No. 1 - Static Failure | 416 |
| 172 | Panel Assembly No. 9 - Fatigue Failure | 416 |
| 173 | Panel Assembly No. 2 - Fatigue Failure | 417 |
| 174 | Cross Section of the Tee - Fatigue Failure | 417 |
| 175 | Panel Assembly No. 4 - Fatigue Failure | 418 |
| 176 | Two Cross Section Views of the Fatigue Crack | 418 |
| 177 | Panel Assembly No. 8 - Fatigue Failures | 419 |
| 178 | Cross Section of the Failed Tee | 419 |
| 179 | Ordered Test Load Histories - Panel 1 | 426 |
| 180 | Ordered Test Loading History - Panels 2 and 3 | 427 |

LIST OF ILLUSTRATIONS (Continued)


| FIGURE | | PAGE |
|---|---|---|
| 181 | Ordered Test Loading History - Panels 4 to 6 | 428 |
| 182 | Ordered Test Loading History - Panels 7 to 9 | 429 |
| 183 | Ordered Composite Gust Loading Test Histories - Panels 10 and 13 | 430 |
| 184 | Ordered Composite Maneuver Loading Test Histories - Panels 14 and 15 | 431 |

## LIST OF TABLES


| TABLE | | PAGE |
|---|---|---|
| 1 | List of Coding Used in Figures | 31 |
| 2 | Statistical Parameters Estimated from the Cumulative Distribution Curves | 45 |
| 3 | Variation of the Fatigue Quality Index with Different Loading Spectra Slope | 47 |
| 4 | Lives Predicted by Miner's Method for Gust Spectra on Coupons | 76 |
| 5 | Fatigue Lives Predicted by Miner's Method for Maneuver, Ground, Composite Gust and Composite Maneuver Spectra on Coupons | 77 |
| 6 | Fatigue Lives Predicted for Coupons with Adjustments for Slope of Loading Spectra | 84 |
| 7 | Evaluation of Fatigue Damage for Quality Indexes of 2, 4 and 6 | 85 |
| 8 | Fatigue Quality Index for Gust Spectra on Coupons | 89 |
| 9 | Fatigue Quality Index for Maneuver, Ground and Composite Spectra on Coupons | 90 |
| 10 | Fatigue Lives Predicted for Composite Gust and Composite Maneuver Spectra on Coupons from Quality Index for First Specimen in a Similar Type of Simple Flight Spectra | 91 |
| 11 | Fatigue Lives Predicted for Maneuver and Composite Maneuver Spectra on Coupons from Quality Index for First Specimen in a Gust Spectrum | 92 |
| 12 | Comparison of Test Fatigue Life of Simple Loading Spectra with the Flight Portion of Composite Tests | 93 |
| 13 | Coding in Figures for Coupons and Panels | 94 |
| 14 | Influence of Ground-Air Transition | 103 |
| 15 | Quality Index for Minimum Gross Area Stresses in Gust, Maneuver, and Composite Spectra | 107 |
| 16 | Quality Index for Gross Area Stresses in Vicinity of Fracture in Gust, Maneuver, and Composite Spectra | 108 |
| 17 | Fatigue Lives Predicted for Maneuver, Composite Gust, and Composite Maneuver Spectra on Panels from Quality Index for First Specimen in a Simple Gust Spectrum | 109 |

LIST OF TABLES (Continued)


| TABLE | | PAGE |
|---|---|---|
| 18 | Fatigue Lives Predicted for Composite Maneuver Spectra on Panels from Quality Index for First Specimen in a Simple Maneuver Spectrum | 110 |
| 19 | Parameters for S-N Data and Unit Gust Loading Spectra | 176-177 |
| 20 | Parameters for S-N Data and Unit Maneuver Loading Spectra | 178 |
| 21 | Predicted Fatigue Lives for Gust Loading Spectra | 179-181 |
| 22 | Predicted Lives by the FFA and Modified Henry's Methods with Required Analytical Parameters Based on the Complete S-N Curve and Entire Gust Loading Spectra | 182-184 |
| 23 | Predicted Fatigue Lives for Maneuver Loading Spectra | 185 |
| 24 | Stress Adjustment Factors for Exactly Predicting the Geometric Mean of Test Life for Gust Loading Spectra | 186-188 |
| 25 | Stress Adjustment Factors for Exactly Predicting the Geometric Mean of Test Life under Maneuver Loading Spectra | 189 |
| 26 | Fatigue Quality Indexes for Gust Loading Spectra | 190-191 |
| 27 | Fatigue Quality Indexes for Maneuver Spectra | 192 |
| 28 | Exponents for the Modified Corten-Dolan and the Non-Linear Cumulative Damage Methods from Gust Loading Spectra | 193-194 |
| 29 | Exponents for the Modified Corten-Dolan and Non-Linear Cumulative Damage Methods from Maneuver Loading Spectra | 195 |
| 30 | Test Variables to be Considered with Mean and Varying Stress in Analyzing Fatigue Life Prediction Methods | 199 |
| 31 | Unit Gust Loading Spectra and S-N Data for Notched Sheet Specimens - 2024-T3 Aluminum Alloy | 208 |

## LIST OF TABLES (Continued)


| TABLE | | PAGE |
|---|---|---|
| 32 | Unit Gust Loading Spectra and S-N Data for Notched Sheet Specimens - 7075-T6 Aluminum Alloy | 209 |
| 33 | Unit Gust Loading Spectra and S-N Data for Double Shear Riveted Joints - 2024-T3 Alclad | 210 |
| 34 | Unit Gust Loading Spectra and S-N Data for Unnotched Sheet - 7075-T6 Alclad | 211 |
| 35 | Unit Gust Loading Spectra and S-N Data for Butt Joints - 7075-T6 Alclad | 212 |
| 36 | Unit Gust Loading Spectra and S-N Data for Strips with Centrally Located Hole - Cr-Mo Steel | 213 |
| 37 | Unit Gust Loading Spectra and S-N Data for Single-Row Flush-Riveted Lap Joints - 2024-T3 Alclad | 214 |
| 38 | Unit Gust Loading Spectrum and S-N Data for Double-Row Flush-Riveted Lap Joints - 2024-T3 Alclad | 215 |
| 39 | Unit Gust Loading Spectra and S-N Data for Single-Row Flush-Riveted Lap Joints - 7075-T6 Alclad | 216 |
| 40 | Unit Gust Loading Spectra and S-N Data for Notched Plate Specimens - D.T.D. 363A Aluminum Alloy | 217 |
| 41 | Unit Gust Loading Spectrum and S-N Data for Wing Stations 180, 214, 228, and 239 of C-46 Wing - 2024-T Aluminum Alloy | 218 |
| 42 | Unit Gust Loading Spectrum and S-N Data for Complete C-46 Wing - 2024-T Aluminum Alloy | 219 |
| 43 | Unit Gust Loading Spectra and S-N Data for F51 Wing - 2024-T Aluminum Alloy | 220 |
| 44 | Unit Maneuver Loading Spectra and S-N Data for Double Shear Riveted Joints - 2024-T3 Alclad | 248 |
| 45 | Unit Maneuver Loading Spectra and S-N Data for Unnotched Sheet - 7075-T6 Alclad | 249 |
| 46 | Unit Maneuver Loading Spectra and S-N Data for Butt Joints-7075-T6 Alclad | 250 |
| 47 | Unit Maneuver Loading Spectra and S-N Data for Strips with Centrally Located Hole - Cr-Mo Steel | 251 |

LIST OF TABLES (Continued)


| TABLE | | PAGE |
|---|---|---|
| 48 | Experimental Fatigue Lives for Gust Loading Spectra | 260-262 |
| 49 | Experimental Fatigue Lives for Maneuver Loading Spectra | 263 |
| 50 | Test Configurations for S-N Data | 265 |
| 51 | Student's t - Values for $\nu$ = 23 Degrees of Freedom | 268 |
| 52 | S-N Data for Notched Sheet Coupons | 270-272 |
| 53 | S-N Data for Notched Sheet Coupons | 273 |
| 54 | Static Tensile Properties of 7075-T6 Bare Aluminum Sheet, .040 Gage | 332 |
| 55 | Unit Low Peak Gust Loading Spectra and S-N Data for Notched Sheet Coupons - $K_T$ = 4 - 18 and 4 Loading Steps | 333 |
| 56 | Unit Low Peak Gust Loading Spectra and S-N Data for Notched Sheet Coupons - $K_T$ = 4 - 14 Loading Steps | 334 |
| 57 | Unit Low Peak Gust Loading Spectra and S-N Data for Notched Sheet Coupons - $K_T$ = 7 - 17 and 13 Loading Steps | 335 |
| 58 | Unit High Peak Gust Loading Spectra and S-N Data for Notched Sheet Coupons - $K_T$ = 4 - 23 and 5 Loading Steps | 336 |
| 59 | Unit High Peak Gust Loading Spectra and S-N Data for Notched Sheet Coupons $K_T$ = 4 - 19 Loading Steps | 337 |
| 60 | Unit High Peak Gust Loading Spectra and S-N Data for Notched Sheet Coupons - $K_T$ = 7 - 14 and 17 Loading Steps | 338 |
| 61 | Unit Concave Upward and Concave Downward Gust Loading Spectra and S-N Data for Notched Sheet Coupons - $K_T$ = 4 - 7 Loading Steps | 339 |
| 62 | Unit Fighter Maneuver Loading Spectra and S-N Data for Notched Sheet Coupons - $K_T$ = 4 - 11 Loading Steps | 340 |
| 63 | Unit Fighter Maneuver Loading Spectra and S-N Data for Notched Sheet Coupons - $K_T$ = 4 - 40 Loading Steps | 341 |

LIST OF TABLES (Continued)


| TABLE | | PAGE |
|---|---|---|
| 64 | Unit Ground Loading Spectra and S-N Data for Notched Sheet Coupons - $K_T$ = 7 - 18 and 11 Loading Steps | 342 |
| 65 | Unit Composite Low Peak Gust, Ground and Ground-Air-Ground Loading Spectrum, and S-N Data for Notched Sheet Coupons - $K_T$ = 4 - 26 Loading Steps | 343 |
| 66 | Unit Composite Low Peak Gust, Ground and Ground-Air-Ground Loading Spectrum, and S-N Data for Notched Sheet Coupons - $K_T$ = 7 - 21 Loading Steps | 344 |
| 67 | Unit Composite High Peak Gust, Ground and Ground-Air-Ground Loading Spectra, and S-N Data for Notched Sheet Coupons - $K_T$ = 4 - 28 Loading Steps | 345 |
| 68 | Unit Composite Fighter Maneuver, Ground and Ground-Air-Ground Loading Spectrum, and S-N Data for Notched Sheet Coupons - $K_T$ = 4 - 29 Loading Steps | 346 |
| 69 | Experimental Fatigue Lives for Gust Loading Spectra | 347-350 |
| 70 | Experimental Fatigue Lives for Ground Loading Spectra | 351 |
| 71 | Experimental Fatigue Lives for Fighter Maneuver Loading Spectra | 352 |
| 72 | Experimental Fatigue Lives for Composite Maneuver Loading Spectrum | 352 |
| 73 | Experimental Fatigue Lives for Composite Gust Loading Spectra | 353 |
| 74 | Low Peak Random Gust Loading Histories | 354 |
| 75 | Low Peak Ordered Gust Loading Histories | 355 |
| 76 | Low Peak Ordered Gust Loading Histories | 356 |
| 77 | Low Peak Ordered Gust Loading Histories | 357 |
| 78 | Low Peak Random Gust Loading Histories | 358 |
| 79 | Low Peak Ordered Gust Loading Histories | 359 |
| 80 | High Peak Random Gust Loading Histories | 360-361 |
| 81 | High Peak Ordered Gust Loading Histories | 362 |
| 82 | High Peak Ordered Gust Loading Histories | 363 |

LIST OF TABLES (Continued)


| TABLE | | PAGE |
|---|---|---|
| 83 | High Peak Ordered Gust Loading Histories | 364 |
| 84 | High Peak Random Gust Loading Histories | 365 |
| 85 | High Peak Ordered Gust Loading Histories | 366 |
| 86 | Test Loading Spectra | 367-371 |
| 87 | Random Military Maneuver Loading Histories | 372 |
| 88 | Ordered Military Maneuver Loading Histories | 373 |
| 89 | Ordered Military Maneuver Loading Histories | 374 |
| 90 | Random Ground Loading Histories | 375 |
| 91 | Ordered Ground Loading Histories | 376 |
| 92 | Ordered Composite Loading Histories - Low Peak Gust Loadings in Flight | 377 |
| 93 | Ordered Composite Loading Histories - Low Peak Gust Loadings in Flight | 378 |
| 94 | Ordered Composite Loading Histories - High Peak Gust Loadings in Flight | 379 |
| 95 | Ordered Composite Loading Histories - High Peak Gust Loadings in Flight | 380-381 |
| 96 | Random Composite Loading Histories - Military Maneuver Loadings in Flight | 382 |
| 97 | Mechanical Properties of Joint Material | 412 |
| 98 | Summary of Panel Test Results | 413-415 |
| 99 | Gust Loading History - Lo-Hi Loading Sequence -Panel 1 | 420 |
| 100 | Gust Loading History - Lo-Hi Loading Sequence - Panels 2 and 3 - Test Group No. G82 | 421 |
| 101 | Gust Loading History - Lo-Hi Loading Sequence - Panels 4 to 6 - Test Group No. G83 | 422 |
| 102 | Fighter Maneuver Loading Histories - Lo-Hi Loading Sequence - Panels 7 to 9.- Test Group No. M17 | 423 |

LIST OF TABLES (Continued)

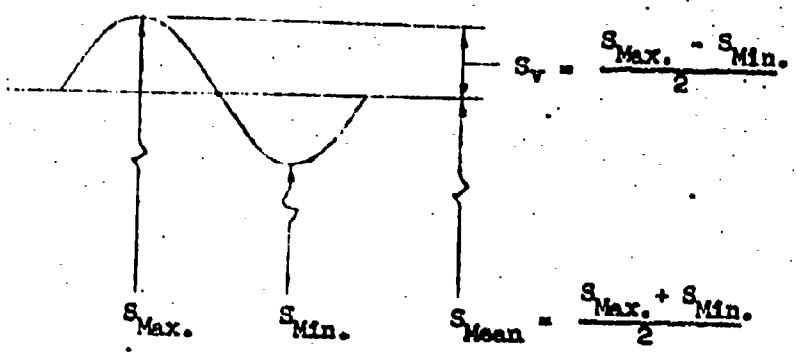

| TABLE | | PAGE |
|---|---|---|
| 103 | Composite Loading Histories - Gust Loadings in Flight - Lo-Hi Loading Sequence Panels 10 and 13 - Test Group No. CG5 | 424 |
| 104 | Composite Loading Histories - Fighter Maneuver Loadings in Flight - Lo-Hi Loading Sequence - Panels 14 and 15 - Test Group No. CM1 | 425 |
| 105 | Factors Used to Convert Panel Stresses for Minimum Gross Area into Stresses for Gross Area at Point of Fracture | 432 |
| 106 | Gross Area Stress Spectra in Vicinity of Fracture in Panel 2 at Tee and in Panel 3 at Stringer Run-Out | 433 |
| 107 | Gross Area Stress Spectra in Vicinity of Fracture in Panel 4 at Stringer Run-Out, in Panel 5 at Tee and in Panel 6 at Joint | 434 |
| 108 | Gross Area Stress Spectra in Vicinity of Fracture in Panels 7 and 9 at Joint and in Panel 8 at Tee | 435 |
| 109 | Gross Area Stress Spectra in Vicinity of Fracture in Panel 10 at Joint and Panel 13 at Stringer Run-Out | 436 |
| 110 | Gross Area Stress Spectra in Vicinity of Fracture in Panel 14 at Tee and in Panel 15 at Joint | 437 |

## LIST OF SYMBOLS

| | |
|---|---|
| a, b, c, d | exponents |
| e | exponential = 2.718282 |
| $f_v$ | varying stress in KSI |
| $f_E$ | varying stress at the endurance limit in KSI |
| $f_{max}$ | maximum stress in KSI |
| $f_{min}$ | minimum stress in KSI |
| $f_{mean}$, $f_m$ | mean stress in KSI |
| $f_{v_{peak}}$ | peak or largest varying stress |
| $f_{red}$ | reduced or equivalent constant stress which gives the same damage ratio as a spectrum of varying stresses above the endurance limit |
| g | load factor |
| h | parameter |
| k | proportionality factor |
| m | number of cracks |
| n | number of load cycles applied at a varying load of specific amplitude |
| p | $\alpha C^u$ |
| r | coefficient of crack propagation |
| u | $\frac{1}{a}$ |
| $u_i$ | number of load cycles applied before crack initiation |
| w | internal work absorbed by a material at a varying load of specific amplitude |
| x | log N |
| $x_i$ | number of load cycles applied between initiation of fatigue crack and the final failure of a specimen at a varying load of specific amplitude |
| y | log $(S_v - S_E)$ |
| $y_o$ | log p |

| | |
|---|---|
| $v$ | per cent of the number of cycles to failure that is used up in initiating cracks at a varying load of specific amplitude |
| $A$ | area |
| $D$ | damage ratio |
| $F_{varying}$ | allowable varying stress in KSI |
| $F_{mean}$ | allowable mean stress in KSI |
| $F_{tu}$ | tensile ultimate strength in KSI |
| G-A-G | ground-air-ground |
| $H$, $H_T$, $\Sigma n$ | total number of load cycles applied at or above a varying stress of specific amplitude |
| $H_o$ | value of H at $S_v$ equal zero |
| $H_s$ | total number of load cycles in one application of a unit loading spectrum |
| $K$ | damage boundary or $K_T$ of standardized S-N curves |
| $K_T$ | theoretical elastic stress concentration factor |
| $\frac{M}{h}$ | force due to bending moment in lbs. |
| $\frac{Mc}{I}$ | stress due to bending moment in KSI |
| $N$ | number of cycles to failure when a varying load of constant amplitude is applied to a specimen |
| $N_L$ | fatigue life in terms of the total number of load cycles that are applied at varying loads of two or more amplitudes prior to failure |
| $N'$ | number of cycles to failure when only the highest load in a unit loading spectrum is applied to a specimen |
| $N^m$ | number of cycles to failure at a varying load of constant amplitude for a "fictitious" S-N curve |
| $P$ | force or load in lbs. |
| $R$ | ratio of the coefficient of the rate of crack propagation at a lower varying load to that at the highest varying load in a unit loading spectrum |

| | |
|---|---|
| $S_v$ | relative or nondimensional varying stress = $\frac{f_{max} - f_{mean}}{F_{tu}} = \frac{fv}{F_{tu}}$ |
| $S_E$ | relative or nomdimensional varying stress at the endurance limit = $\frac{f_E}{F_{tu}}$ |
| $S_E'$ | relative varying stress at the endurance limit after fatigue damage is produced by the application of varying loads above the endurance limit |
| $S_R$ | relative or nondimensional reduced varying stress = $\frac{f_{red}}{F_{tu}}$ |
| $S_{max}$ | relative or nondimensional maximum stress = $\frac{f_{max}}{F_{tu}}$ |
| $S_{mean}$ | relative or nondimensional mean stress = $\frac{f_{mean}}{F_{tu}}$ |
| W | maximum amount of internal work that is absorbed by a material before failure |
| W.S. | wing station |
| $\alpha$, and $\sigma$ | S-N parameters |
| $\beta$, $\delta$, and $\psi$ | exponents |
| $\Gamma$ | gamma function |
| $\sigma$ | standard deviation and multiplicative standard deviation |
| $\omega$ | stress interaction factor having a value that always exceeds unity |
| $\sqrt[i]{N_{L_1} \cdot N_{L_2} \cdots N_{L_i}}$ | geometric mean of $N_L$ |




Definition of Maximum, Minimum, Mean and Varying Relative Stresses.

## SECTION I

## INTRODUCTION AND BACKGROUND

The problem of the fatigue of airframe structures is of vital importance not only to the operators of both military and commercial aircraft but also to the designers. The importance of fatigue of the airframe has been well recognized by the military and industry for many years. However, the complexities involved have successfully defied satisfactory solution in spite of the massive effort, time, and expense which have been invested in fatigue research in past years. In addition to the operational problems on current aircraft, future trends to high performance VTOL/STOL and spacecraft, with their acutely more critical weight problems, foretells even greater urgency of reaching a practical solution of the "fatigue problem."

A satisfactory analytical solution for the problem of fatigue life prediction has eluded the intense efforts of some of the best scientists, engineers and research specialists for the past 130 years. This is so because of the immense number of variables involved, the statistical qualities of nature, and the inherent limitations of the analytical achievements in detail stress analysis, impressive as these are. Progress is being made in the area of the statistical definition of the external loading environment, and in the area of the definition of the material resistance to fatigue cracking under complex loading environments.

There is, however, a most important middle area between these two which is the crux of the whole problem of fatigue life prediction. This area is that concerned with the definition of a "fatigue quality" as a property of complex, composite structure. The analytical assessment of this key property of a complex structure is fraught with the most formidable of difficulties. The purely analytical approach offers no immediate fruitfulness. This is not to imply neglect of this area, rather, that the solution must be pursued with vigor; but the primary approach must be experimental. Some of the reasons for this statement are as follows:

a. Joint friction and its attendant nonlinear slippage characteristics is highly unpredictable and nonrepeatable.

b. Local plastic yielding at points of high stress concentrations with resulting residual stresses, and, for some materials, the changing work hardening properties, is too complex a process to expect analytical solutions to follow clearly the path through intricate service histories.

c. Fretting and fretting corrosion can create unpredictable stress concentrations which often compound with normal design concentrations.

d. Repairs, reconstruction, and accidental damage place unforeseen and unpredictable fatigue-critical areas in the structure.

e. The micro-detailed geometrical stress analysis required at the multitudinous points in a complex structure is as yet beyond the capabilities of the modern analyst.

Manuscript released by the authors 21 August, 1961 for publication as an ASD Technical Report

Time and complexity preclude reliance on purely analytical solutions which would realistically encompass these variables.

An important distinction must be made between various stages of the external loads and stress analysis of a complex structure and a theory of fatigue damage. It is a process of definitive stress analysis that is required to define the complex stress history at a critical point in the structure. It is a process of fatigue damage that defines the formation of a crack in a critical point in the structure as a function of the definitive stress history.

Even if a perfect fatigue damage theory were available the fatigue life prediction problem would not be solved until the stress analysis problem is also solved.

However, the problem of fatigue life prediction is amenable to solution in spite of all the difficulties cited. This solution makes use of analytical formulations where feasible, and supported by the proper kind of laboratory fatigue testing and field service comparisons, a reasonably good job may be accomplished, consistent with the uncertainties which will always be inherent in the definition of the external basic loads.

It must be recognized from the outset that the development of fatigue cracks in metal is a statistically random process. The loads and stresses in the airframes of individual aircraft are subject to extremely wide variations. Many of the operating variables are beyond direct control. The integrated influence of all these variables yields a large scatter of results. Thus it cannot be expected to precisely predict the fatigue life of a single article. Life insurance companies with the best facilities and statisticians do not yet attempt to predict the life span of a single individual however well their prediction holds for a large-enough population.

A considerable background of successful service history on other aircraft models can provide a basis for significant comparisons. When coupled with this foundation of service history, and with judicious testing of critical areas of the structure, it is possible to develop a system which has good potential of achieving fatigue quality control as well as reasonable predictability of fatigue life.

## OBJECTIVES

The objectives of this research study are as follows:

1. To review, compare and evaluate proposed methods of fatigue life prediction suitable for application to the special problems of airframe structure.

2. To provide experimental fatigue life data of constant load amplitude S-N type for use in evaluating selected prediction methods.

3. To provide experimental fatigue life data under complex loading spectra representative of realistic airframe loading history on both coupon-type specimens and on specimens of a complex joint representative of contemporary airframe construction.

4. From an analysis of the new experimental data to verify the adequacy or provide a possible improvement in the selected fatigue life prediction method.

## PLAN OF THE STUDY

This research program was organized into three basic phases to meet the stated objectives:

**Phase I.**

A study of proposed methods for the prediction of fatigue life was made and those suitable for application to the problems of airframe fatigue were selected for evaluation using available published data. This portion is discussed in Sections I through III and Appendices A, B, and C.

**Phase II.**

Experimental fatigue data were generated to provide additional verification or a basis for the improvement of selected methods of fatigue life prediction under loadings more realistic of airframe environment than was previously available. These data are described in Appendix D.

**Phase III.**

Analyses were made of the experimental results of Phase II using the selected methods from Sections II and III. A summary of the results and conclusions drawn is presented in Section VI.

## SECTION II

## METHODS OF ANALYSIS

Fatigue analysis follows the same general pattern as developed in static strength analysis. These subjects may be classified into three broad fields.

1. External loads
2. Internal loads
3. Allowable loads

The differences in fatigue analysis compared with conventional static strength analysis are associated primarily with the specification of the multitudes of external loadings, with the detail requirements, or precision demanded of internal load (or stress) distributions, and with the form or specification of the allowable loads. Another major difference is the convention of expressing the results of static strength analysis as a comparison of internal loads (stresses) with allowable loads (stresses) to show a "Margin of Safety." Inherent in this "Margin of Safety" is the concept of a "Factor of Safety." Fatigue analyses for this discussion will not contain this concept of "Margins of Safety" nor "Factors of Safety," but will be limited to the direct prediction of a "fatigue life." That the predicted lifetime in whatever units measured (hours, cycles, missions, or any other) is "safe" or not is, of course, dependent not only upon the precision of all input data, precision of operations performed, but also on many other factors, some not even a part of the fatigue process.

1. Such factors as "fail safe" may change completely the complexion of a "Margin of Safety" in fatigue.

2. Periodic and special inspections, maintenance, and repair can have the quality of extending the "life" of an airframe to an indefinite period, probably determined by economic or performance obsolescence rather than fatigue.

The subject of factors or margins of safety will be discussed in a later section of the report (see Section III ).

A method of analysis is a formal procedure to attain the solution of a problem. The method chosen will depend heavily on two facets:

1. The problem to be solved, and

2. The data available on which to base the solution.

To illustrate, one of the oldest and simplest fatigue problems to be solved is that of the plain rotating shaft in bending. Assuming the external loading to be known, measured, or limited, the internal stresses may be simply computed by the engineering beam theory. The remaining question is the determination of

the allowable stresses for the lifetime desired or to predict the life of a given design. An impressive amount of experimental S-N data is available for most materials under this type of loading. This is highly important in the solution of this problem, which may be considered solved, provided:

A. External loads are

   1. Constant, known, or
   2. Measured, or
   3. Limited.

B. Internal loads (stresses) are

   1. Predictable or
   2. Measurable.

C. Allowable loads (stresses) are

   1. Known or
   2. Determinable for

      a. Material chosen,
      b. Processing variables,
      c. Environment,
      d. Rate of loading,
      e. Laboratory simulation compatible with service conditions, etc.

The effects of more than one load level on fatigue life were minimized in most industrial problems of this type by restricting the loads produced in service to levels below an endurance limit, or the maximum repeated load for an indefinite life on the S-N curve. This is still the practice for certain propeller and other rotating machinery for aircraft use.

The internal loads or stresses in the simple example were assumed predictable or measurable. The simple shaft, without notches, is both an easily predictable and an easily tested article. Years of laboratory experience have evolved specimen designs which achieve consistent fatigue failure in almost straight shafts unaffected by grips and loading fixtures. The experimentally determined allowable stresses are thus compatible with the actual part under its expected loading. This point is of primary importance to the precision and success of the solution to the assigned problem.

Suppose the shaft had a notch. The solution of the problem may now take one of two divergent paths.

Path 1. The influence of the notch may be computed in the second stage of the solution dealing with the prediction of internal loads or stresses. Geometrical analyses of stress concentration factors, supported by experimental measurements, photoelastic optical methods, and others, constitute a large body of data to accomplish this step. (References 1, 2 & 3)

Successfully accomplished, the predicted maximum repeated stress to be applied may be compared with the allowable S-N data of virgin unnotched material to predict a fatigue life or to design to a specific life.

However, attempts to follow Path 1 have run into difficulties. The theoretical elastic or photoelastically determined stress concentration factor is, in the actual part, profoundly affected by yielding, residual stresses, work hardening, and other effects so that the net fatigue effect is not directly predictable. This is well illustrated in Figure 1 taken from reference 4, which indicates the fatigue effective concentration factor compared with the geometrical stress concentration factor at several different fatigue lives. Some recent work at the NACA has provided empirical plasticity corrections which work well in certain steels (non-work hardenable), but these corrections are as yet unsuccessful in aluminum alloy (work hardenable). (Reference 3)

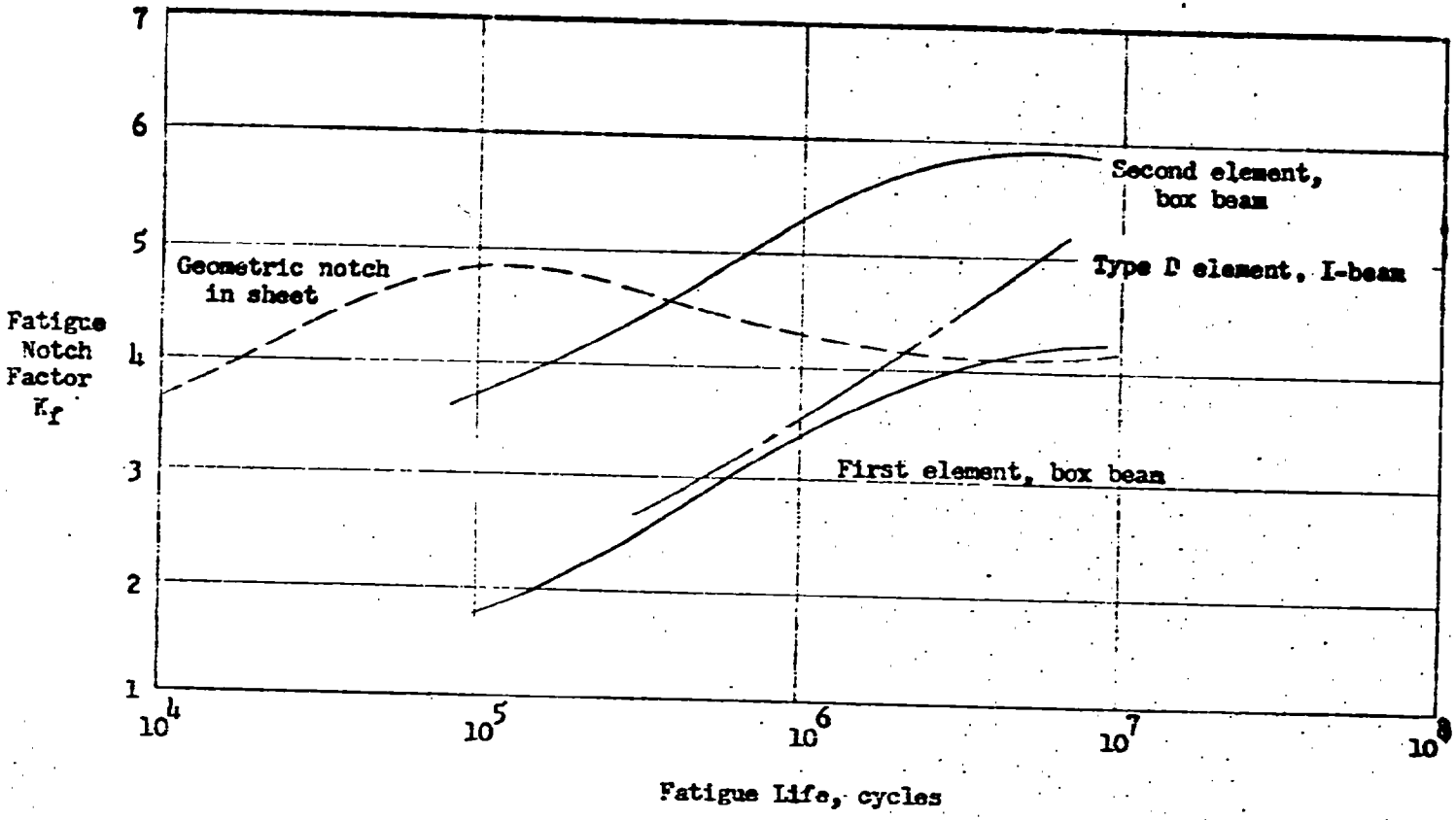



Figure 1 Fatigue notch factors for simulation elements. (Ref. No. 4 )

Path 2. The internal loads or stresses may be computed as if the notch were not there (gross area basis) or at the root of the notch (net area basis) without any influence of stress concentration.

The stress concentration influence of the notch is assigned to the third stage of the solution dealing with the allowable stress determination. The actual notch or a graded series of notches is fatigue tested and S-N or allowable data are plotted for the specific part. (Stresses must, of course, be consistent with the internal stresses of step 2.) The fatigue effectiveness of the notch is in this manner determined experimentally.

Following Path 2 is seen to be fundamentally an improvement over the method or procedure of Path 1 in that some of the previous difficulties unaccountable by analysis are now experimentally determined and the precision of prediction of the fatigue life of the notched part is improved. However, experimental data for the actual configuration must be made available for the achievement of this improvement. Lack of these data may force an estimate by the best means available (Path 1), but imprecision is then inevitable.

The type of experimental data required to assess the fatigue problem varies at different stages of a design. Broadly categorized, these may be scaled in complexity by the following list:

1. Material and Processing Data are needed in the earlier preliminary design stages. These are usually S-N type or simple spectrum-type fatigue tests to provide comparative data for decisions among possible design choices.

2. Development Tests are designed to assure achievement of a satisfactory fatigue quality at critical joints or discontinuities.

3. Full-Scale Component or Airframe Fatigue Test may be planned if the fleet size warrants the time and cost.

4. Fleet Service History is a factor of importance. The structure designed by the best means available must be observed in service. The integrated influence of many factors may reduce fatigue life below the best engineering and laboratory estimates. Some of these factors are:

    a. Service loading variations, changing operational demands,
    b. Installation stresses, misalignments,
    c. Workmanship, nicks, scratches not duplicated in laboratory test specimens,
    d. Material alloy, heat treat, batch variations,
    e. Environmental conditions, corrosive atmosphere,
    f. And many others.

The factors that bring about fatigue life reductions must be ferreted out and field service experience obtained to provide a feed-back loop to improve the life predictions. Engineering estimates of fatigue life conditioned by fleet-wide field service experience are another stage of improvement beyond that provided by calculations and laboratory experiments. Laboratory testing and analysis of parts which have a known service failure history provide a required overall check of the laboratory-analysis life-prediction system.

Within this context of an overall system approach for the deliberate scheduling of improvements in airframe fatigue life predictions, depending on the data available at various stages of a design, specific facets of the airframe life prediction problem will be examined in more detail.

EXTERNAL LOADING DATA

The aircraft exists and operates in a complex physical environment. The list of service loading is extensive. It includes:

1. Gust loadings

    1.1 In clear air
    1.2 In storms

2. Maneuver loadings

    2.1 Transport

        2.1.1 Routine route maneuvers
        2.1.2 Training maneuvers

    2.2 Military aircraft

        2.2.1 Operational maneuvers
        2.2.2 Training maneuvers

3. Landing impacts

4. Taxiing and ground handling

5. Ground-air cycle

6. Buffeting

    6.1 Stall
    6.2 Supersonic shock wave instability

7. Acoustical noise

    7.1 Propeller tip or jet noise
    7.2 Aerodynamic noise (boundary layer)

The contribution of some of these types of loading to fatigue damage has been debated for many years. Other concurrent research programs are investigating experimentally some important facets of these loadings. (See reference 5) Preliminary results indicate that the fatigue influence of some of these items may be unimportant while others are of considerable importance. It is too early to determine a clear cut simplification.

A detailed investigation of the generation of external applied loading data and its influence on the fatigue life prediction process is considered beyond the scope of this study. It will be assumed that complete external applied loading spectra for all the critical loading conditions can be developed for a mission phase synthesis utilizing basic environmental statistics currently available for each type of loading. However, a brief review of the general characteristics of several pertinent types of loading is given to describe the complex form of these external applied loads and to demonstrate the versatility required of a practical fatigue life prediction method necessary to handle this complexity.

1. Gust Loading

a. The gust loading record is characterized by a varying load factor or stress component oscillating about a substantially constant mean load level. At different positions in the structure and in different types of aircraft the mean load level can cover a wide range of values. This is significant for fatigue life predictions.

b. The natural sequence of varying gust loading magnitudes is substantially random. However, examination of sufficient length of record shows an eventual symmetry of positive loads and negative loads. Past practice has been to regroup positive half cycles with equal negative half cycles and re-order the sequence of occurrence into a graduated spectra of frequency of occurrence or probability of exceedance. This process is illustrated in Figure 2. It can be seen that a number of basic assumptions are involved in tampering with the original load record to convert it into the ordered spectrum. The fatigue significance of the order of load application has been well demonstrated. (Reference 16) Physical considerations of the process of crack propagation confirm the importance of order of loading. This information is not reported in the current service load data reduction methods. Some experimental evidence of the fatigue life significance of this property of ordered vs. random loading is being generated in a concurrent research project reported in reference 5.

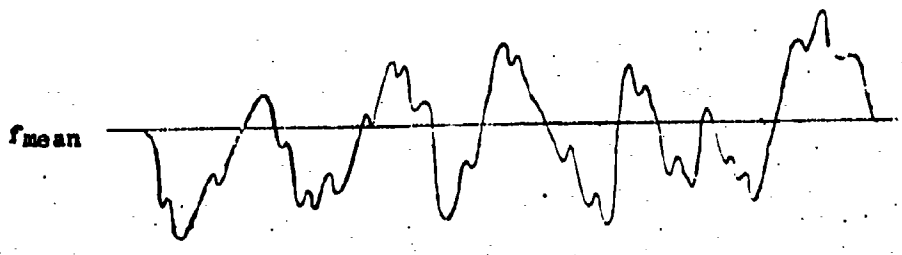
2. Maneuver Loading

a. Bomber, Transport, and Cargo-Type Aircraft

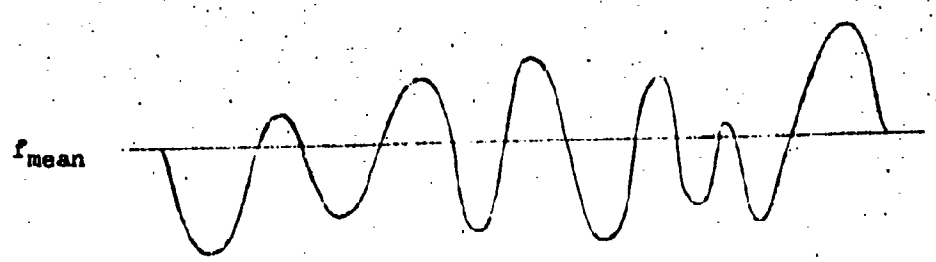
Maneuver loadings of large bomber, transport, and cargo-type aircraft are characterized by near symmetry of incremental or varying load component about the constant flight mean load level. For records of sufficient duration the loads are substantially random in sequence, and, in general, the above comments regarding gust loadings are applicable to maneuver loadings for this class of aircraft.

b. Military Fighter-Trainer Aircraft

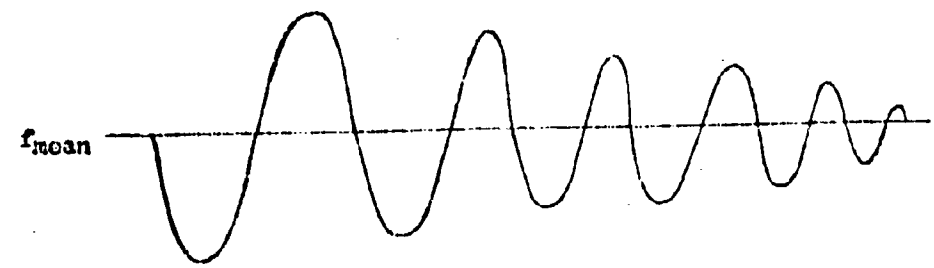
The maneuver load record for high load factor military fighter-trainer type aircraft has a considerable bias in the positive direction, reflecting the pilot's inherent avoidance of uncomfortable negative accelerations of any appreciable magnitude. The resulting load record has a substantially constant minimum load at the steady static 1g level. The positive acceleration increments rise from this level to a maximum load increment and return to the steady static 1g level with only minor excursions in the negative range. This is characterized by a varying mean load for each load cycle as contrasted with gust loads which occur with a substantially constant mean load level. The character




Random Sequence of Flight Loads




Random Grouping of Faired Flight Loads




Ordered Grouping of Faired Flight Loads

Figure 2 Development of Gust Loading Spectra

of this type of loading is illustrated in Figure 3 . Incremental load levels may approach random sequence over a long-enough time period. As discussed above, the sequence information is lost in current data reduction techniques. This fact produces a significant difference in handling the fatigue life predictions, which will be discussed in more detail in later sections.

3. Landing Impacts

Landing loads are applied to the airframe while it is in the flight steady mean load condition. The varying loads are a complex function of the dynamic response of the structure and are affected by the usually nonlinear characteristics of the tire-shock strut combination. The sequence of load application is not accounted for in the usual analysis.

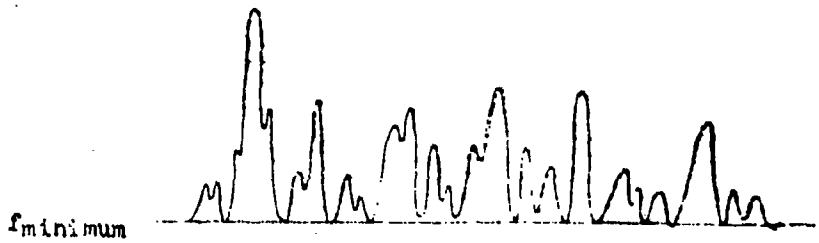
4. Taxi and Ground Handling

These conditions create varying loads of a generally random sequence oscillating about a ground-supported mean load level. Depending on the aircraft configuration, the mean load level for these conditions can become compressive for fatigue critical structures which are normally loaded in tension in the flight conditions. This condition can be aggravated by configurations which carry large external stores and/or tip tanks. Thus the range of the mean load can be quite large for each flight.

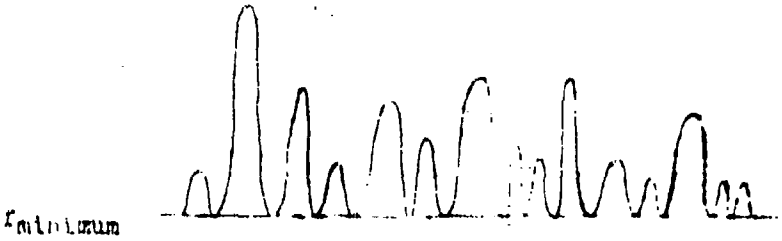
5. Ground-Air-Ground Cycle

The change in load distribution from ground borne to air borne during the take-off run and the transition from air borne to ground borne during the landing run is a loading cycle that takes place once each flight. There is general agreement that this cycle is an important contributor to fatigue damage. However, there is no general agreement on the specific definition of the effective amplitude of this loading. One definition could be the cycle of loading from the maximum negative (ground load) to the maximum positive (flight load) occurring in each flight. This overall load cycle per flight is not yet precisely defined; it may become a spectrum of load amplitudes over the life duration of a fleet. Another definition, popular in many quarters though not universally accepted, is the transition cycle from the ground-borne static mean load level to the air-borne static mean load, and return on each flight. Various other definitions have been proposed such as the RMS value of negative ground level loads to the RMS value of positive flight level loads and return for each flight.

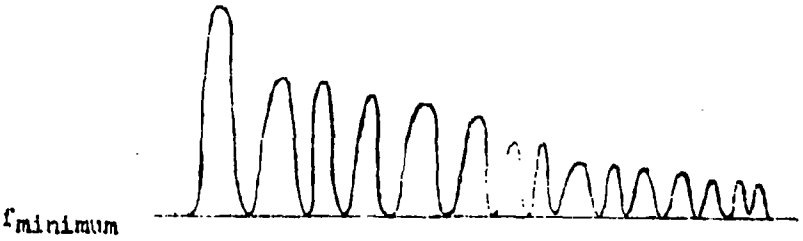
Whatever the load level definition, the ground-air-ground cycle is generally broken down into its own substantially constant varying load component acting once per flight about its own mean load level.




Random Sequence of Flight Loads




Random Grouping of Paired Flight Loads




Ordered Grouping of Paired Flight Loads

Figure 3 Development of Maneuver Loading Spectra

6. Buffeting

Buffeting from stall or supersonic shock wave instability is a phenomenon to be avoided wherever possible. When fatigue accounting is necessary, these loads are generally considered random in sequence and act symmetrically about a specific mean or steady load condition. The comments on gust loads are therefore also applicable for buffet loadings.

7. Acoustic Noise

Although an important source of fatigue damage for some areas of structure in certain configurations, this specialized problem is not within the scope of this study.

8. Composite of Mission Loads

The total load history at a point on the airframe structure during one flight mission may be made up of each of the major types discussed above. These may be schematically illustrated as in Figure 4.

| | | |
|---|---|---|
| Pre-take-off ground handling and take-off run. | - | Taxi load spectrum at a negative mean load (compression). |
| Ground-air | - | Transition from ground- to airborne state. |
| Turbulence | - | Random loads varying about a positive mean load (tension). |
| Fighter Maneuver | - | Varying increments to a maximum above the static level flight mean load. |
| Landing impact | - | Nonrandom varying loads about a level flight mean load. |
| Air-ground | - | Transition from flight- to ground-borne state. |
| Landing run, taxi, and ground handling | - | Same as take-off and pre-take-off ground handling. |

Each of the several types of loadings may appear in each flight.

9. Summary

This discussion of the loads to which airframe structures are subjected during their lifetime is primarily to demonstrate the type of input data which the method of analysis for fatigue life prediction must be capable of handling in order to solve the problem posed. Some methods proposed for fatigue life prediction, while elegant and useful in certain

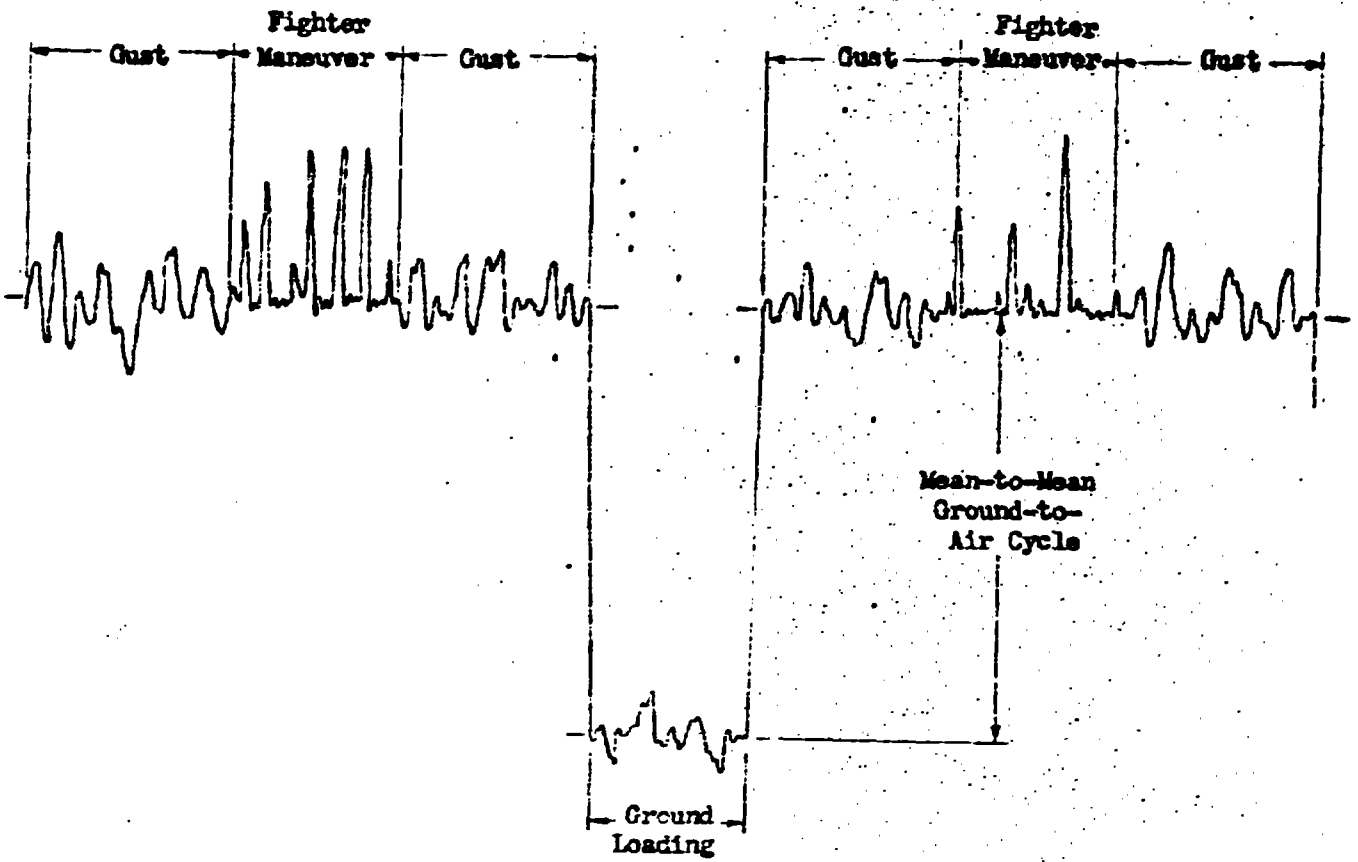



Figure 4 Schematic of Composite Loading Spectrum

fields, are limited in capability to handling only simple definitions of loads. These limited methods cannot be successful in the solution of the problem at hand.

## INTERNAL LOAD DISTRIBUTION

Structural designs which achieve the highest efficiency place the greatest amount of material into pure tension or compression, reducing bending stresses from local discontinuities to the least possible. Great pains are taken to achieve this desirable goal. The process of design and analysis goes through several circuits of ever increasing precision, each stage successively miniaturizing the structural element under consideration.

| Design Stage | Method of Analysis | Structural Size |
|---|---|---|
| 1. Preliminary design | $P = \frac{M}{h}$ , $f = \frac{P}{A}$ | Yards |
| 2. Project design | $f = \pm \frac{Mc}{I} + \frac{P}{A}$ | Feet |
| 3. Final design | Redundant analysis | Inches |
| 4. Proof of design | Experimental | Millimeters to microns |
| 5. Research | Experimental | Millimeters to microns. |

The precision of internal loads and stress distributions computed at various stages of the design is essentially consistent with the precision of the data available at that stage of design. However, it is well known that both the number of cycles to crack initiation and the additional cycles for growth to a critical crack size are extremely sensitive to small variations in the stress level existing at the critical points.

The desired precision of life prediction resolves into a required precision of stress prediction that is simply not attainable with the currently available analytical tools. This critical statement is not an indictment of the present state of the art of stress analysis for this is indeed impressive. Rather, it must be considered a recognition of critical factors which the current analysis techniques cannot handle and were never intended to handle. As discussed in the introduction, some of these factors are:

1. Joint friction with unpredictable, nonrepeatable, nonlinear slippage characteristics.

2. Local plastic yielding at points of high stress concentration with the resulting ever-changing residual stresses, and work hardening properties.

3. Fretting and fretting corrosion resulting from joint slippage under repeated loads.

4. The complexity of practical structures most generally results in shapes not readily amenable to the analytical approach.

Consideration of the formidable difficulties involved in this brief list indicates that the purely analytical approach cannot in the immediate future offer any hope of adequate solution. Therefore the only practical approach is to refer this problem to the experimental laboratory for solution. This is Path 2 of the analysis methods discussed in the introduction. However, for timely success in this approach a number of conditions must be considered.

1. There must be a specimen design to test. The designer is called upon to make decisions without benefit of final test knowledge. The best tools available and the data on hand at decision time are used to make the best possible estimates. These estimates can only be considered crude at best. The stress concentration factor procedure finds its greatest usefulness at this stage. As explained in the sample problem in the introduction, by judicious use of a large body of stress concentration literature (for example, reference 1) and with the full realization of the limitations on fatigue effectiveness of these predictions, design comparisons and choices can be made, subject to later confirmation and refinement.

2. The fatigue test specimen must be complete. The test specimen must be a large-enough sample of the structure to encompass local redistributions of load due to yielding, joint slippage; it must contain an exact representation of all critical local eccentricities and a reasonable representation of local supporting structure. It must have all secondary attachments which would in any way affect the fatigue life of the primary element; for example, attachment holes for hose clamps, tubing, electrical wiring bundles, drain holes, and holes for secondary support brackets may be fatigue critical but are too easily overlooked. All processing operations, cleaning, coating, etching, sealing, etc., which the airframe parts undergo during manufacture should also be included in the build-up of the fatigue test specimen.

3. Nominal structure adjacent to joint. The loads introduced into a complex joint or material discontinuity are generally controlled by the stress state of the average material in the structure surrounding the joint. It is also often considered good practice that joints and fatigue-critical discontinuities, and especially blind areas, should be as good as or better than adjacent structure with a nominal hole. To most directly demonstrate achievement of this quality level and to aid in the definition and monitoring of the test load spectra, the test specimen should include such sections.

4. The full range of loads are necessary. There is considerable evidence accumulated from full-scale airframe fatigue tests (references 20 and 21 and others) and from laboratory attempts to duplicate service failures, that the location of fatigue failures in complex structure is dependent on the applied load levels. Constant load amplitude S-N type tests on multiple specimens must therefore cover the full range of the anticipated operational service loads. Spectrum-type tests offer the advantage of requiring fewer specimens to cover the full range of operational loads. However, the test variables of unit spectrum block size, stress interval, order of load application, etc., exert some influence on the test results. The influence of these test variables must be minimized by judicious choices. (Reference 5)

The internal loads from the normal static stress analysis are generally considered adequate to define the test spectra for development tests of the joint or discontinuity. Strain gage surveys taken during component or full-scale static tests are an aid in either setting the fatigue test load level, or, if scheduled later, provide data for corroboration or corrective analyses to improve the precision of prediction when necessary.

The successful fatigue test of a fully detailed specimen of a critical area of the airframe structure under the full range of expected loads provides experimentally the micro-detailed analysis which includes most of the factors which current purely analytical approaches find insurmountable.

It is necessary, however, that allowable fatigue data for complex structure be provided by laboratory development tests of fully detailed specimen(s) of the critical areas of the structure, tested under the full range of loads representative of those expected in service. To define an S-N curve for a specific element of structure requires a minimum of six to nine specimens with sixteen or twenty desirable depending upon the statistical confidence level required. In the interests of economy, schedule, and the availability of large scale fatigue equipment, in addition to the technical reasons discussed above, it is advantageous to perform the development tests on fewer specimens with each to experience the full spectrum of loadings anticipated for operational service. This aspect is especially important in the consideration of a full scale airframe fatigue test in which the economic justification of a single test specimen is of paramount importance.

The interpretation of the results of these more complex specimen tests is not quite so simple as the interpretation of the allowable fatigue life (vs. Stress) of constant amplitude type loadings. However, a number of methods have been used such as the comparison of the test results with the results of tests of a (good quality) standard joint, or the Tangent Intercept Method, or the Fatigue Quality Index procedure. The latter two are described in detail in Appendix A.

One of the objectives of this study is to explore the possibilities and limitations in the use of spectrum type fatigue test results as a means for fatigue life prediction.

SUMMARY

A discussion of the complexities involved in the prediction of the fatigue life of airframe structure and the requirements of a practical method has emphasized these points.

1. External loadings are complex in range and sequence. A fatigue life prediction method must be versatile in scope to handle the many types of loadings likely to be critical.

2. The prediction of the fatigue life of complex structure requires a precision and reliability of local stress history under complex external loading which is not currently available by purely analytical means, nor likely to be available in the near future.

3. A satisfactory fatigue damage theory is not available for the analytical prediction of the allowable stress history of complicated structure under complex loadings.

4. The crux of the problem of fatigue life prediction is, therefore, a fatigue quality of complex structure which embodies the effects of the complex internal stress history and the allowable stress history for the formation of a critical crack, both of which are dependent on the range and sequence of applied loading.

5. Laboratory development tests of fully detailed specimens of fatigue critical structure are required to assess this fatigue quality of complex structure. Either spectrum type tests which cover the full range of loads anticipated for operational service, or constant amplitude S-N type tests may be used for this purpose.

6. For spectrum type tests, test variables such as loading block size, stress interval size, and loading sequence affect the laboratory results. These effects must be eliminated, reduced to insignificance, or accounted for by some empirical means.

7. Interpretation of operational service history by consistent laboratory testing and analysis means is required to provide a comparative base for any method of fatigue life prediction.

## SECTION III

## EVALUATION AND SELECTION OF FATIGUE LIFE PREDICTION METHODS

From a search of the literature a number of methods for the prediction of fatigue life proposed by various authors was selected for comparative study and evaluation. During this study, simplifications, modifications, and generalizations were developed to better adapt some of these methods to the problem of fatigue life prediction of aluminum airframe structure. For brevity and continuity of this section, these methods and their extensions are described in detail in Appendix A.

While all these methods (except one, the Tangent Intercept Method) were fundamentally the concept of the gradual accumulation of fatigue damage during the progress of loading, each author emphasized some particular aspect or formula for the representation of either or both the applied loading spectra or the allowable S-N data. These variations could be considered in three general categories. The methods studied in this phase of the project are classified in the three categories as listed below, with the Tangent Intercept method unclassified. In addition, those methods chosen for comparison by numerical evaluation with the selected test data are indicated by the asterisk.

Class I. Linear Cumulative Damage (based on specific S-N data for each specimen type).

* 1. Miner's Method (reference 6)

This is the well-known linear summation of the fractions of fatigue damage expressed as the cycle ratio $(\frac{n_i}{N_i})$ where failure is hypothesized when the sum of all cycle ratios is one.

* 2. Lundberg's FFA Method (reference 7)

Lundberg and his associates at the Aeronautical Research Institute of Sweden (FFA) utilized mathematical formulas for representing the applied loading spectrum and the allowable S-N data and, based on Miner's linear cumulative damage hypothesis, obtained a closed form solution for the total damage, and, thus, for the corresponding predicted fatigue life. This method was evaluated in two parts, one utilizing equations for the applied load spectra and for the S-N curves with parameters determined by an average best fit for the full stress range, while the second application, in an attempt to improve the precision of prediction, restricted the best fit to the mid-range of stress levels in the region of highest cycle ratios.

* 3. Shanley's "1X" Method (references 8, 9 and 10)

Based on a concept of rate of formation of slip bands, Shanley's "1X" method derives an equation for the fatigue damage which results in the linear cumulative damage expression of Miner, utilizing a mathematical formula for the S-N curve.

4. Langer's Method (reference 11)

Langer separated the fatigue process into two parts - first, the initiation of cracks, and second the growth of the cracks, and, based on linear accumulation of cycle ratios, derived a prediction of fatigue life.

5. Grover's Method (reference 12)

Grover's method is essentially the same as Langer's method. Both of these methods require experimental S-N data which separate the crack initiation stage from the crack growth stage. These data were not available for this evaluation.

6. Smith's Residual Stress Method (reference 13)

Using Miner's linear cumulative damage, Smith proposes inclusion of the residual stresses from plastic yielding at higher load levels with the stresses from external loads. This very elegant method of stress analysis is not practical for the complexity of loading history met in service, and could not be evaluated in this study.

Class II. Nonlinear Cumulative Damage (based on specific S-N data for each specimen type.)

7. Henry's Method (reference 14)

Henry developed a procedure for reducing the allowable S-N curve in a step-by-step procedure to account for damage of prior loadings. By ingenious means of cycle ratio corrections, the reductions are achieved by reference to only the original S-N curve. The result is a nonlinear accumulation of damage. Knowledge of the order of load application is necessary for the use of this method. In its original form the mathematical representation of the S-N data could be applied only to a limited class of materials.

* 8. Generalization of Henry's Method

Henry's original development is extended in this report to accept a more general representation of the S-N data. This development is discussed in detail in Appendix "A".

9. Corten and Dolan's Method (reference 15)

Corten and Dolan based their method on a concept of relating fatigue damage to the number of cracks formed as a function of the largest varying load in the sequence, with the growth of such cracks to occur at all load levels of the sequence. The result is a form of nonlinear cumulative damage in terms of stress ratios of the various loads in the spectrum, and, as such, contributes damage from the low stresses below the endurance limit. This point is discussed in detail in Appendix A.

* 10. Modified Corten and Dolan Method

The Corten and Dolan method is modified to convert the basic formula to a cycle ratio basis, which assumes no contribution from loadings below the endurance limit. The nonlinearity coefficient, evaluated by the available test data in Appendix B, indicates the results to be so closely equivalent to the Linear Cumulative Damage Method that further evaluation was discontinued.

* 11. A Simplified Nonlinear Cumulative Damage Method

A simplified form of a nonlinear cumulative damage method is developed from the results of this survey by introducing an empirical exponent into the equation representing the damage ratio summation. This nonlinearity coefficient, evaluated from the available test data in Appendix B, indicates the results to be so closely equivalent to the Linear Cumulative Damage Method that further evaluation was discontinued.

* 12. Shanley's "2X" Method (reference 8)

Based on essentially the same reasoning as was used to develop his linear "1X" method, Shanley assumed one of the coefficients in the rate equation to be stress dependent. This increased strongly the rate of crack growth and resulted in a nonlinear form of the cumulative damage summation.

Class III. Cumulative Damage (Linear or Nonlinear) from Damage Boundaries or Modified S-N Curves

13. Kommers' Nonlinear Damage Hypothesis (reference 22)

Kommers pointed out the essential nonlinearity of the damage boundaries determined experimentally from two-step load tests of steel coupons. The damage boundaries were found to be functions of both the load levels and the cycle ratios in each load level.

14. Richart and Newmark's Method (reference 24)

Richart and Newmark devised a formal procedure with additional experimental verification for utilizing Kommers' nonlinear

damage hypothesis to create damage boundaries which vary with both stress level and the cycle ratio.

15. Marco and Starkey's Method (reference 25)

A method of defining damage boundaries by use of a power relation of the cycle ratio was developed by Marco and Starkey. The exponent was made stress or load dependent, which resulted in essentially a mathematical formulation of the damage boundaries for use in the procedure described previously by Richart and Newmark, and suggested by Kommers' earlier work.

16. Freudenthal and Heller's Method (reference 26)

Freudenthal and Heller have developed a procedure to construct a "fictitious" S-N curve by the use of a stress interaction factor, which is derived from a statistical analysis of a large number of samples tested under a number of spectra of loading. Lack of both the type and quantity of the necessary data precludes its practical application.

17. Levy's Method (reference 27)

Levy suggested a fatigue life prediction procedure based on deriving, from test data, empirical constants as exponents for each cycle ratio of a step spectrum, with one additional constant coefficient required for the life prediction equation. This method requires (q + 1) sets of test data and the solution of as many simultaneous equations where q is the number of steps of the loading spectrum. Data were not available in a form required to evaluate this method.

* 18. Stress Concentration Method

The stress concentration method in practice is a procedure of refined stress analysis to define the ratio of peak stress in a discontinuity of structure to the nominal stress in a region remote from the disturbance. It must be coupled with a damage theory to complete a life prediction method. The linear cumulative damage hypothesis is taken for that purpose in this study. The stress concentration factor derived analytically may be used in either of two ways:

A. When used to specifically define the peak stress, the allowable stress (or cycles) may be determined from an appropriate S-N curve for the virgin unnotched material.

B. The stress concentration factor may be used to select an appropriate S-N curve from a graded set of notched specimens of the material. This S-N curve may be arbitrarily considered as the damage boundary for the design for which no specific test data exist.

Once the peak stress history is defined (as in A.) or the equivalent notch concentration factor specified (as in B.) any of the fatigue life prediction methods could, in principle, be used.

* 19. Fatigue Quality Index Method

A fatigue test of a completely detailed specimen is conducted under the full spectrum of loads expected on the structure in service. The results of the spectrum test are analyzed with a set of standardized S-N data fixed for the purpose of providing a scale of measurement of fatigue quality. That stress concentration factor is determined which, by interpolation, makes the linear cumulative damage equation exactly unity under the application of the full test history. This concentration factor, defined as the Fatigue Quality Index for the tested specimen, is compared with an acceptance standard.

As a fatigue life prediction method, the establishment of the Fatigue Quality Index provides an arbitrary damage boundary based on a fatigue test of the specimen under its own anticipated load spectrum. By the linear cumulative damage procedure, fatigue life predictions are made from this damage boundary for the structure under other similar loading spectra.

Unclassified

* 20. Tangent Intercept Method (reference 28)

Originally developed as a method of interpretation of simple spectrum test results to derive a fatigue quality acceptance standard, the Tangent Intercept procedure has been proposed as a fatigue life prediction method. (reference 31)

Essentially a graphical procedure, the spectrum test result in cumulative cycles is plotted in an appropriate field of S-N curves. The interpolated $K_T$ value of the S-N curve which is tangent to the total test spectrum becomes the Tangent Intercept Quality Index of the specimen.

As a fatigue life prediction method, an S-N curve of the specimen is provided by constant amplitude tests. The fatigue life under a spectrum of loads is defined by the multiple of the unit spectrum which becomes just tangent to the S-N curve.

## EVALUATION OF METHODS OF PREDICTION

For use in evaluating numerically the various methods of fatigue life prediction which were chosen, an extensive search of the available published data turned up seventy-six groups of tests conducted on approximately 266 specimens suitable for application to most of the proposed methods. These are all spectrum-type experiments in which spectrum shapes, unit spectrum block size, stress intervals, sequence of loadings, etc., cover a wide range of variations. Included also are pertinent spectrum test results from the Australian P-51 and the NACA C-46 wing full scale fatigue tests. Detailed descriptions of these test data are given in Appendix "C".

The evaluation was conducted in two forms, depending on the scale on which the comparisons are measured.

1. Comparisons of Life Cycles

Each of the methods chosen for evaluation was required to predict the fatigue life of the test specimen from the unit applied loading spectrum, using whichever form of the allowable data that was specifically applicable to the method.

The details of this numerical work pertinent to each method are given in Appendix "B".

The results of the life predictions of each group of specimens are plotted in Figure 5 for sixty-five groups of gust-type spectrum results, and in Figure 6 for thirteen groups of maneuver-type spectrum results. The code identification of the various methods is given in Table 1. The experimental results are also plotted for direct comparison, indicating the geometrical mean of the group, and a vertical bar showing the band spread between the minimum and maximum experimental values of the group.

Another comparison of the prediction with the actual test result is made by the ratio:

$$\text{Degree of conservatism} = \frac{N_{L_{(Test)}}}{N_{L_{(Predicted)}}}$$

If $\frac{N_{L_{(Test)}}}{N_{L_{(Predicted)}}} < 1.00$, the prediction is unconservative.

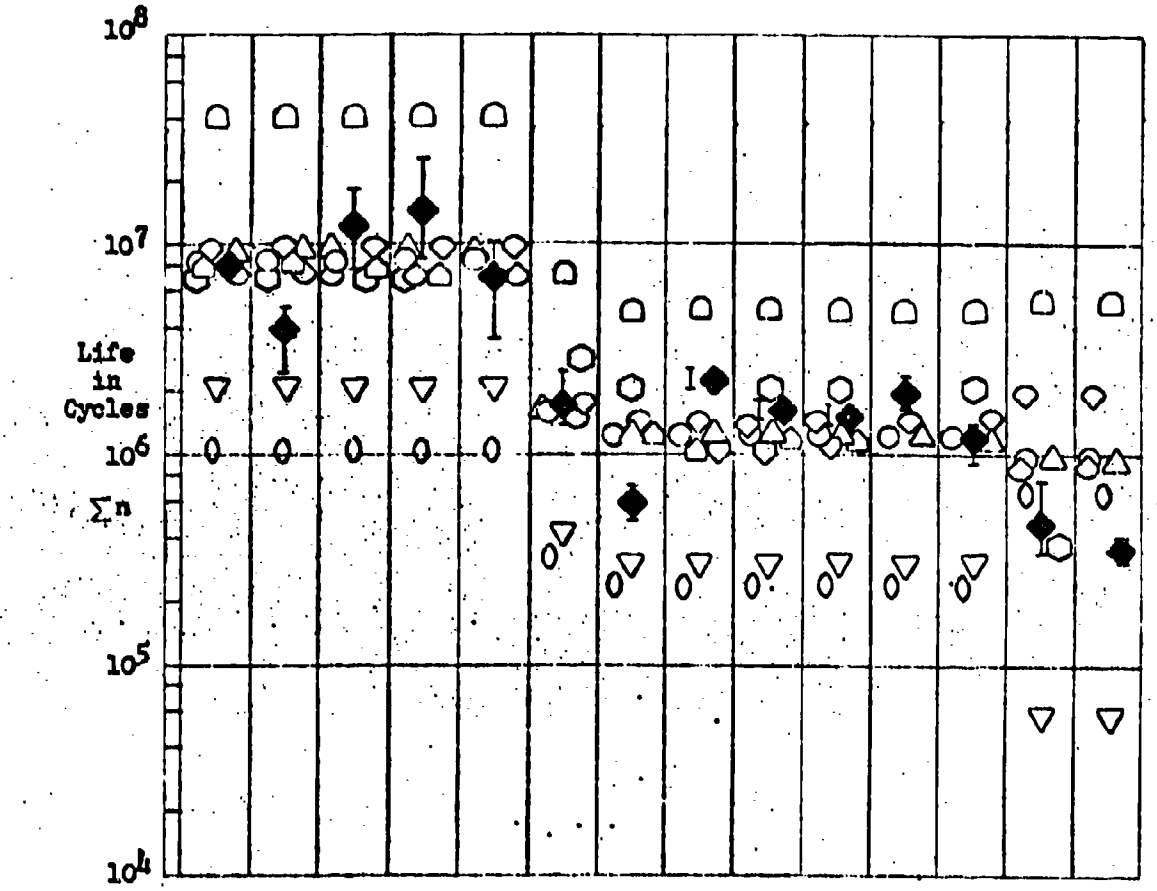
If $\frac{N_{L_{(Test)}}}{N_{L_{(Predicted)}}} \geq 1.00$, the prediction is conservative.

TABLE 1

LIST OF CODING USED IN FIGURES

| Symbol | Meaning | |
|---|---|---|
| ◆ | Geometric Mean of Test Data | |
| \| | Scatter Band for Test Data | |
| ○ | Miner's | |
| ◇ | FFA | Loading Spectrum and S-N Equations Best Fit in the Midstress Range. |
| ◇ | FFA | Loading Spectrum and S-N Equations Best Fit in the Full Stress Range. |
| △ | Shanley "1X" | |
| ▽ | Shanley "2X" | |
| ⌂ | Modified Henry | S-N Equation Best Fit in the Midstress Range. |
| ▽ | Modified Henry | S-N Equation Best Fit in the Full Stress Range. |
| ⌂ | Tangent Intercept | |
| ⬡ | Quality Index-Based on Standardized S-N Data of Figs. 58 to 62. | |
| 0 | Stress Concentration Factor-Based on Standardized S-N Data of Figs. 58 to 62. | |

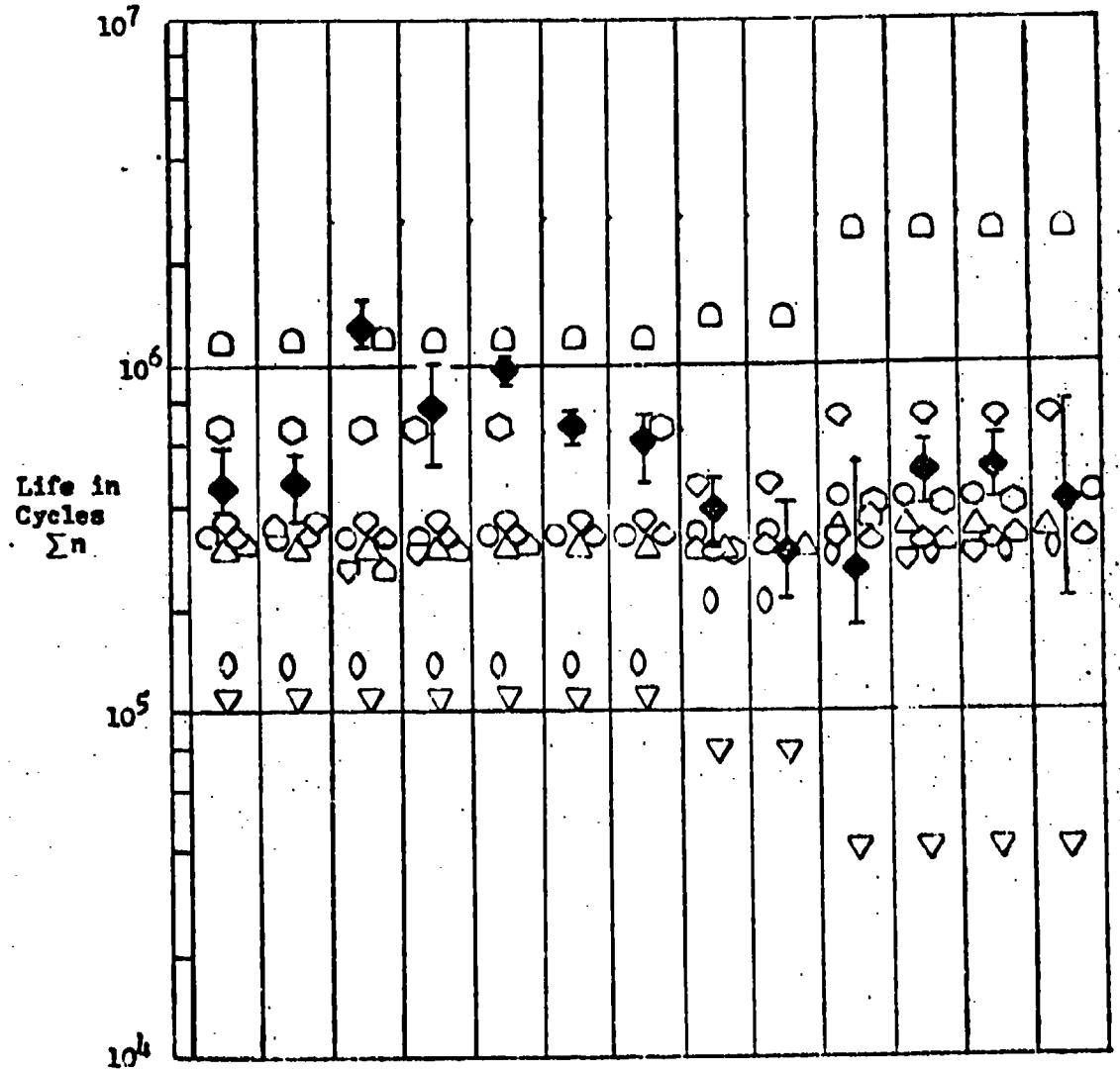
| Loading Sequence in the Unit Spectrum Block | |
|---|---|
| L-H | Low to High Loading Sequence |
| H-L | High to Low Loading Sequence |
| L-H-L | Low to High to Low Loading Sequence |
| H-L-H | High to Low to High Loading Sequence |
| QR | Quasi-Random Loading Sequence |
| TR | True Random Loading Sequence |




| Test Group No. | G1 | G2 | G3 | G4 | G5 | G6 | G7 | G8 | G9 | G10 | G11 | G12 | G13 | G14 |
|---|---|---|---|---|---|---|---|---|---|---|---|---|---|---|
| Sequence | L-H | | H-L | | QR | | L-H | H-L | L-H-L | H-L-H | QR | | | |
| Block Size (cycles) | 100000 | 500000 | 100000 | 500000 | 100000 | | 100200 | | | | 50100 | 100200 | 50000 | 100000 |
| Loading Steps | 18 | | | | | | 8 | | | | | | | |
| Mean Stress | 17.4 KSI | | | | | | | | | | | | 0 KSI | |
| Spectrum | Gust B | | | | | Gust A | | | | | | | | |
| Specimen | Notched Sheet | | | | | | | | | | | | | |
| Material | 2024-T3 | | | | | | | | | | | | | |
| Reference for Test Data | 16 | | | | | | | | | | | | | |

Coding for Points is Given in Table 1

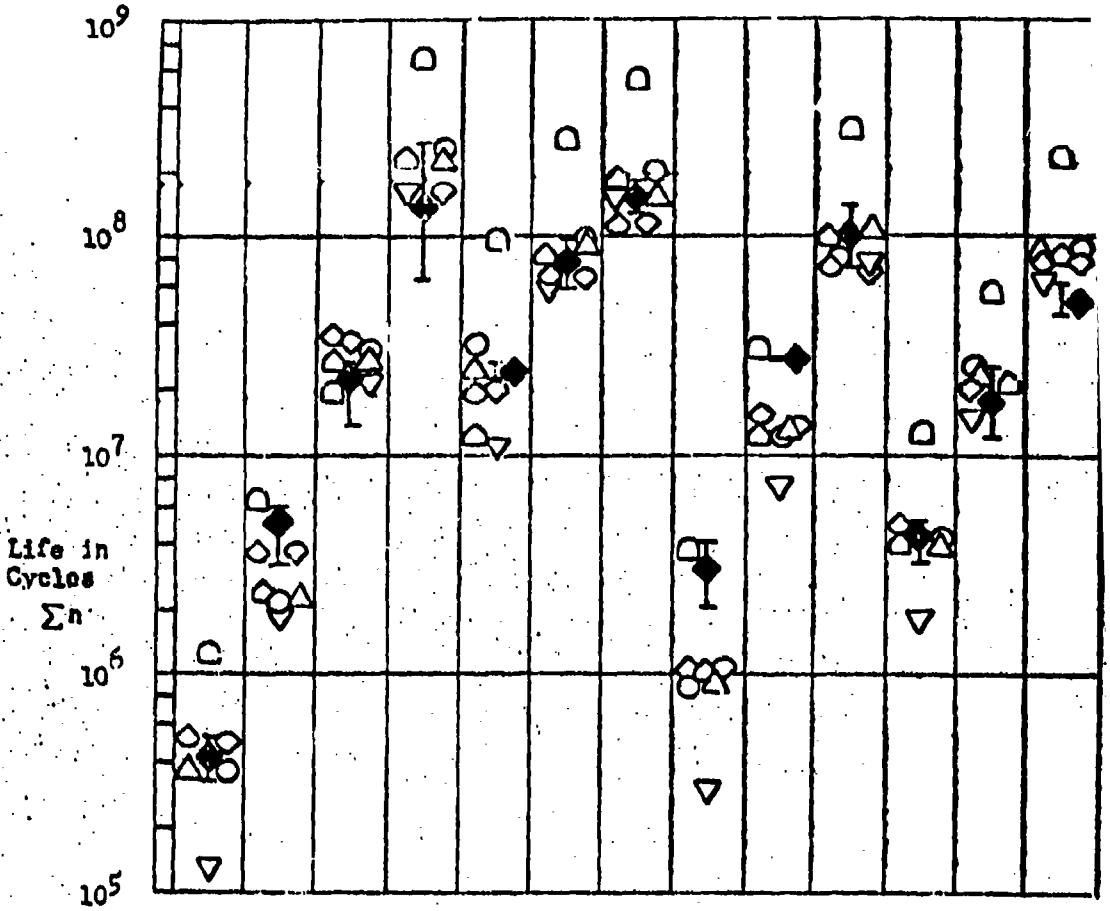
Figure 5. Comparison of Predicted and Experimental Fatigue Life




| Test Group No. | G15 | G16 | G17 | G18 | G19 | G20 | G21 | G22 | G23 | G24 | G25 | G26 | G27 |
|---|---|---|---|---|---|---|---|---|---|---|---|---|---|
| Sequence | L-H | | H-L | L-H-L | H-L-H | QR | | L-H-L | GR | L-H | E-L | L-E-L | QR |
| Block Size (cycles) | 10200 | 50900 | | 10200 | 50900 | 10200 | 50900 | 30200 | | 30000 | | | |
| Loading Steps | 8 | | | | | | | | | | | | |
| Mean Stress | 20 KSI | | | | | | | 10 KSI | | 0 KSI | | | |
| Spectrum | Gust A | | | | | | | | | | | | |
| Specimen | Notched Sheet | | | | | | | | | | | | |
| Material | 7075-T6 | | | | | | | | | | | | |
| Reference for Test Data | 16 | | | | | | | | | | | | |

Coding for Points is Given in Table 1.

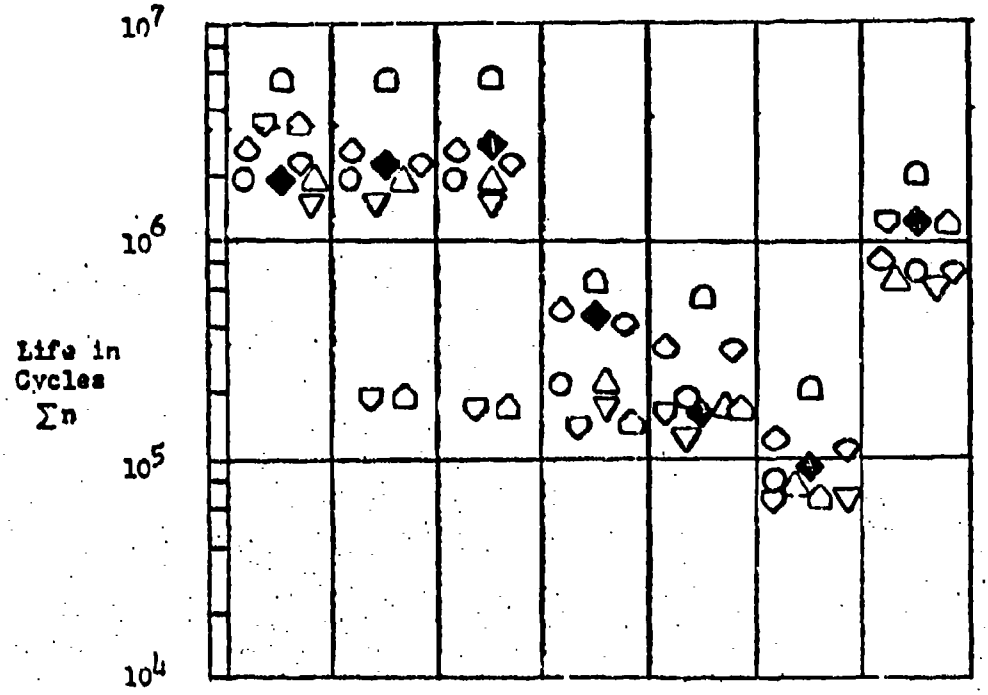
Figure 5 (continued) Comparison of Predicted and Experimental Fatigue Li




| Test Group No. | G28 | G29 | G30 | G31 | G32 | G33 | G34 | G35 | G36 | G37 | G38 | G39 | G40 |
|---|---|---|---|---|---|---|---|---|---|---|---|---|---|
| Sequence | L-H-L | | | | | | | | | | | | |
| Block Size (cycles) | 360280 | | | | | | | | | | | | |
| Loading Steps | 9 | | | | | | | | | | | | |
| Mean Stress KSI | 15.5 | 9.3 | 6.2 | 4.9 | 15.4 | 12.4 | 11.1 | 13.2 | 8.9 | 6.6 | 43.1 | 33.5 | 27.5 |
| Spectrum | Gust | | | | | | | | | | | | |
| Specimen | Double Shear Riveted Joint | | | | Unnotched Sheet | | | Butt Joint | | | Strips with Hole | | |
| Material | 2024-T3 Alclad | | | | 7075-T6-Alclad | | | | | | Cr-Mo Steel | | |
| Reference for Test Data | 17 | | | | | | | | | | | | |

Coding for Points is Given in Table 1.

Figure 5. (continued) Comparison of Predicted and Experimental Fatigue Life

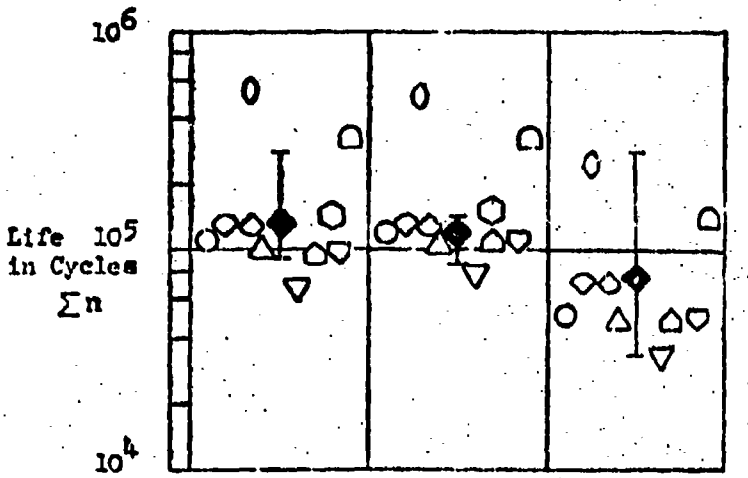



| Test Group No. | G41 | G42 | G43 | G44 | G45 | G46 | G47 |
|---|---|---|---|---|---|---|---|
| Sequence[a] | L-H | H-L | | | | | L-H |
| Block Size (cycles) | Same as Experimental Life | | | | | | |
| Loading Steps | 6 | | | 5 | | | 6 |
| Mean Load LBS | 975 | | | | 1140 | 1055 | |
| Spectrum | Gust | | | | | | |
| Specimen | Lap Joint with One Row of Flush Rivets | | | | b | c | |
| Material | 2024-T3 Alclad | | | | | 7075-T6 Alclad | |
| Reference for Test Data | 18 | | | | | | |

a sequence applied only once
b Lap Joint with two rows of flush rivets
c Lap Joint with one row of flush rivets

Coding for Points is Given in Table 1.

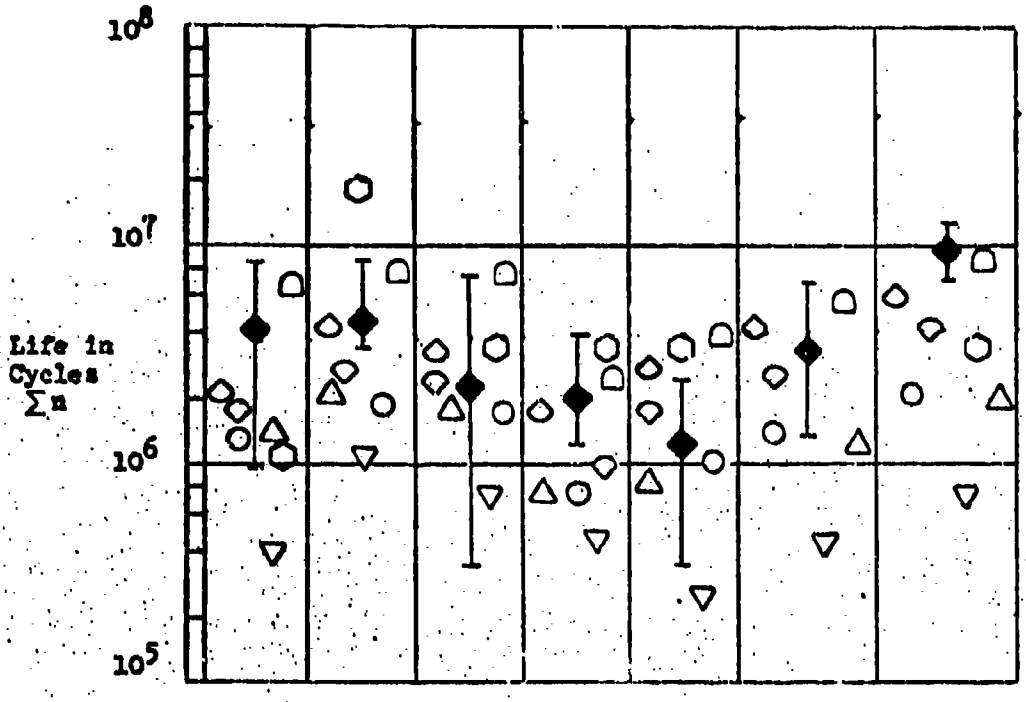
Figure 5. (Continued) Comparison of Predicted and Experimental Fatigue Life




| Test Group No. | G48 | G49 | G50 |
|---|---|---|---|
| Sequence | L-H-L | | |
| Block Size (cycles) | 13290 | 6290 | 5410 |
| Loading Steps | 9 | | 10 |
| Mean Stress | 14 KSI | | |
| Spectrum | Gust | | |
| Specimen | Notched Plate | | |
| Material | D.T.D. 363A Aluminum Alloy | | |
| Reference for Test Data | 19 | | |

Coding for Points is Given in Table 1

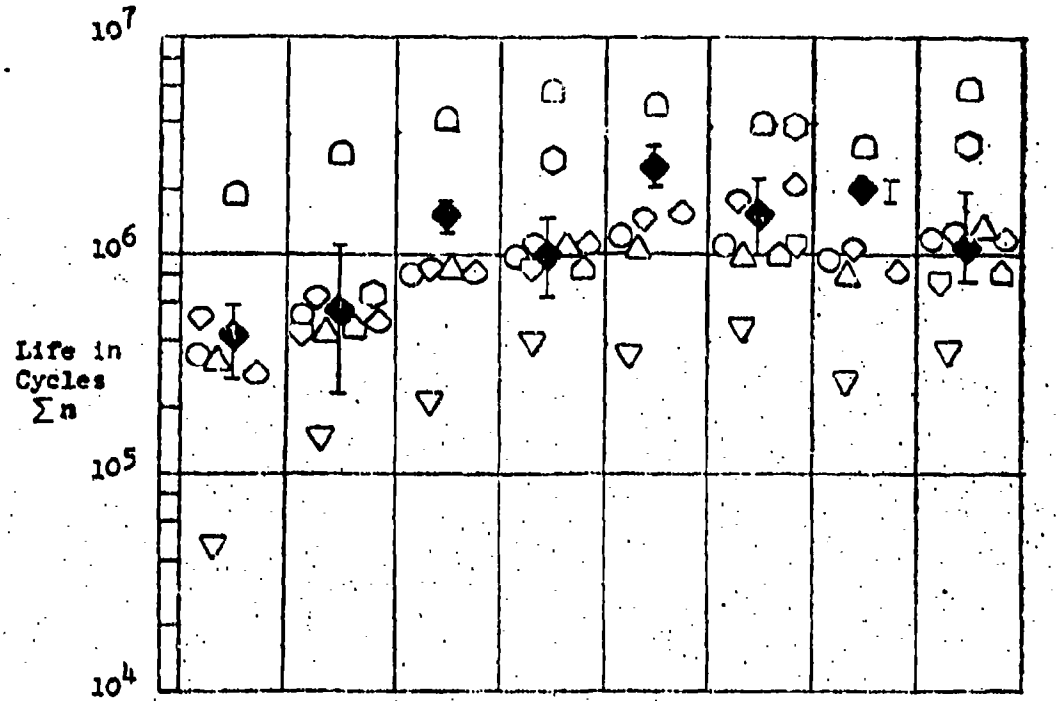
Figure 5. (continued) Comparison of Predicted and Experimental Fatigue Life




| Test Group No. | G51 | G52 | G53 | G54 | G55 | G56 | G57 |
|---|---|---|---|---|---|---|---|
| Type of Failure | Crack Initiation | | | | First Crack | Critical Crack | Final Failure |
| Sequence | Quasi-Random | | | | | | |
| Block Size (cycles) | 59670 | | | | | | |
| Loading Steps | 16 | | | | | | |
| Mean Load Factor | Unit Gravitational Acceleration | | | | | | |
| Spectrum | Gust | | | | | | |
| Location on C-46 Wing | Wing Station | | | | Complete Wing | | |
| | 180 | 214 | 228 | 239 | | | |
| Material | 2024-T | | | | | | |
| Reference for Test Data | 20 | | | | | | |

Coding for Points is Given in Table 1.

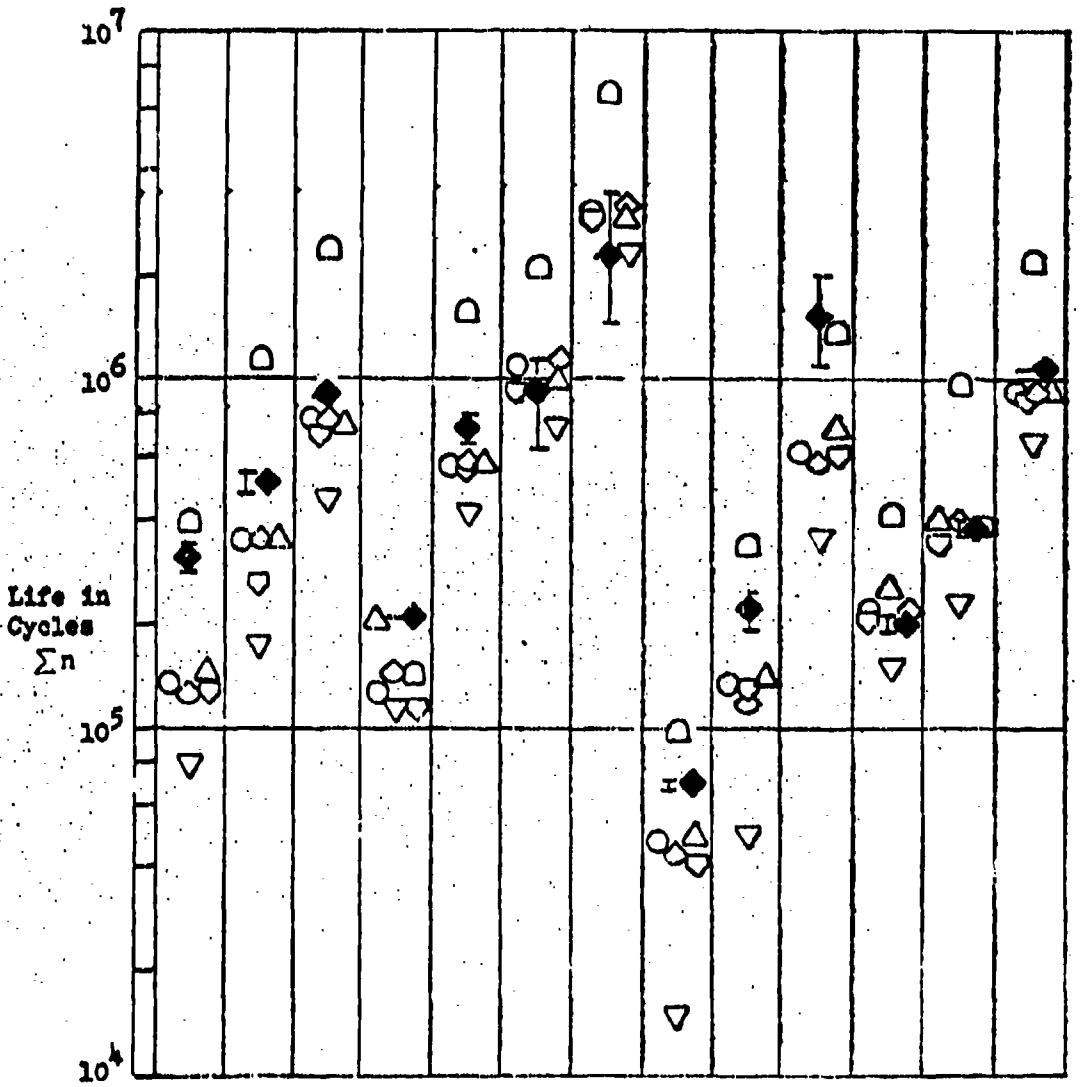
Figure 5. (continued) Comparison of Predicted and Experimental Fatigue Life




| Test Group No. | G58 | G59 | G60 | G61 | G62 | G63 | G64 | G65 |
|---|---|---|---|---|---|---|---|---|
| Type of Failure | Initial | | | | Final | | | |
| Sequence | T R | L-H-L | T R | L-H-L | T R | L-H-L | T R | L-H-L |
| Block Size (cycles) | 500000 | 32860 | 500000 | 32860 | 500000 | 32860 | 500000 | 32860 |
| Loading Steps | 11 | 3 | 11 | 3 | 11 | 3 | 11 | 3 |
| Mean Load LBS | 17900 | | | | | | | |
| Spectrum | Gust | | | | | | | |
| Location on P-51 Wing | Gun bay | | Tank bay | | Gun bay | | Tank bay | |
| Material | 2024-T | | | | | | | |
| Reference for Test Data | 21 | | | | | | | |

Coding for Points is Given in Table 1

Figure 5. (continued) Comparison of Predicted and Experimental Fatigue Life




| Test Group No. | M1 | M2 | M3 | M4 | M5 | M6 | M7 | M8 | M9 | M10 | M11 | M12 | M13 |
|---|---|---|---|---|---|---|---|---|---|---|---|---|---|
| Sequence | L-H-L | | | | | | | | | | | | |
| Block Size | 7477 | | | | | | | | | | | | |
| Loading Steps | 9 | | | | | | | | | | | | |
| Minimum Stress KSI | 5.1 | 3.8 | 3.1 | 9.6 | 7.7 | 6.4 | 4.8 | 5.3 | 4.4 | 3.3 | 16.8 | 15.1 | 12.6 |
| Spectrum | Maneuver | | | | | | | | | | | | |
| Specimen | Double Shear Riveted Joint | | | Unnotched Sheet | | | | Butt Joint | | | Strips with Hole | | |
| Material | 2024-T3 Alclad | | | 7075-T6 Alclad | | | | | | | Cr-Mo Steel | | |
| Reference for Test Data | 17 | | | | | | | | | | | | |

Coding for Points is given in Table I.

Figure 6. Comparison of Predicted and Experimental Fatigue Life.

This scale of comparison is most informative in assessing the life prediction effectiveness of the various methods and in providing information on the scatter factors which need consideration for assessing reliability on the life cycle scale.

2. Comparisons of the Change in Stress Level Required to Predict Exactly the Test Life

The stress scale may be used to evaluate the various prediction methods by the determination of a proportionality factor, k, by which all stress levels of the test spectrum are raised or lowered to arrive at the exact prediction of the specific test life.

The comparison of the prediction with the actual test result is made by the ratio:

$$\text{Degree of conservatism} = \frac{S_{v_{(Test)}}}{S_{v_{(Adjusted)}}} = \frac{S_{v_{(Test)}}}{k\, S_{v_{(Test)}}} = \frac{1}{k}$$

If $\frac{S_{v_{(Test)}}}{S_{v_{(Adjusted)}}} = \frac{1}{k} < 1.00$, the prediction is unconservative.

If $\frac{S_{v_{(Test)}}}{S_{v_{(Adjusted)}}} = \frac{1}{k} \geq 1.00$, the prediction is conservative.

This scale of comparison is informative to the designer with respect to the amount of material (and its corresponding weight) which is necessary to achieve a given fatigue life, and in the assessment of any factor of safety on loads which may need consideration in achieving any required degree of reliability of fatigue life.

The ratios of $\frac{N_{L_{(Test)}}}{N_{L_{(Predicted)}}}$, and $\frac{S_{v_{(Test)}}}{S_{v_{(Adjusted)}}}$ were ranked in ascending order and the percentage of the total number of samples equal to or less than a given degree of conservatism was determined and plotted as a function of that degree of conservatism. These correlation graphs are shown in Figures 7 and 9 for the life cycle prediction and in Figure 8 for the stress adjustment ratio.

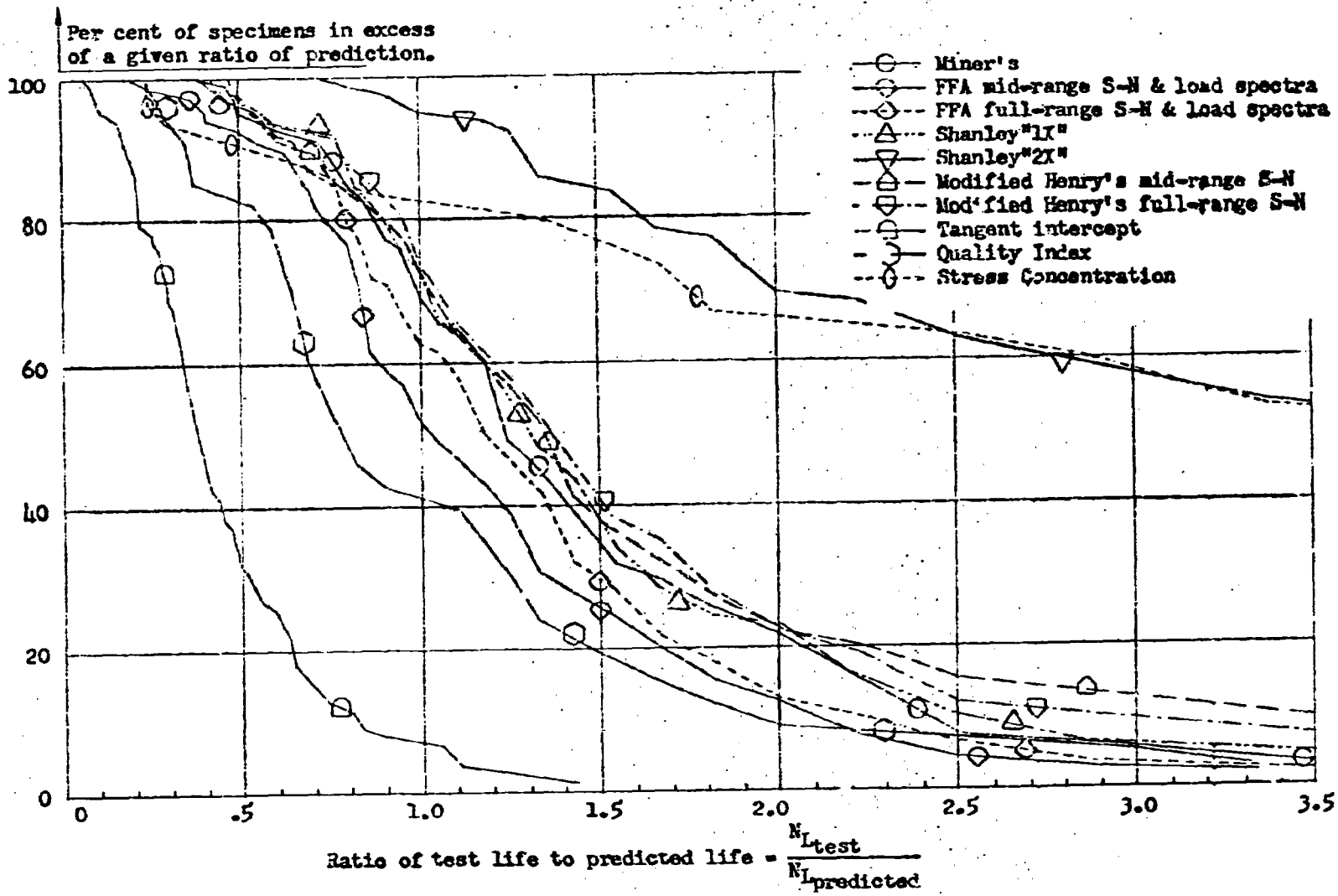



Figure 7. Cumulative Distributions for the Ratio of Test Life to Predicted Life

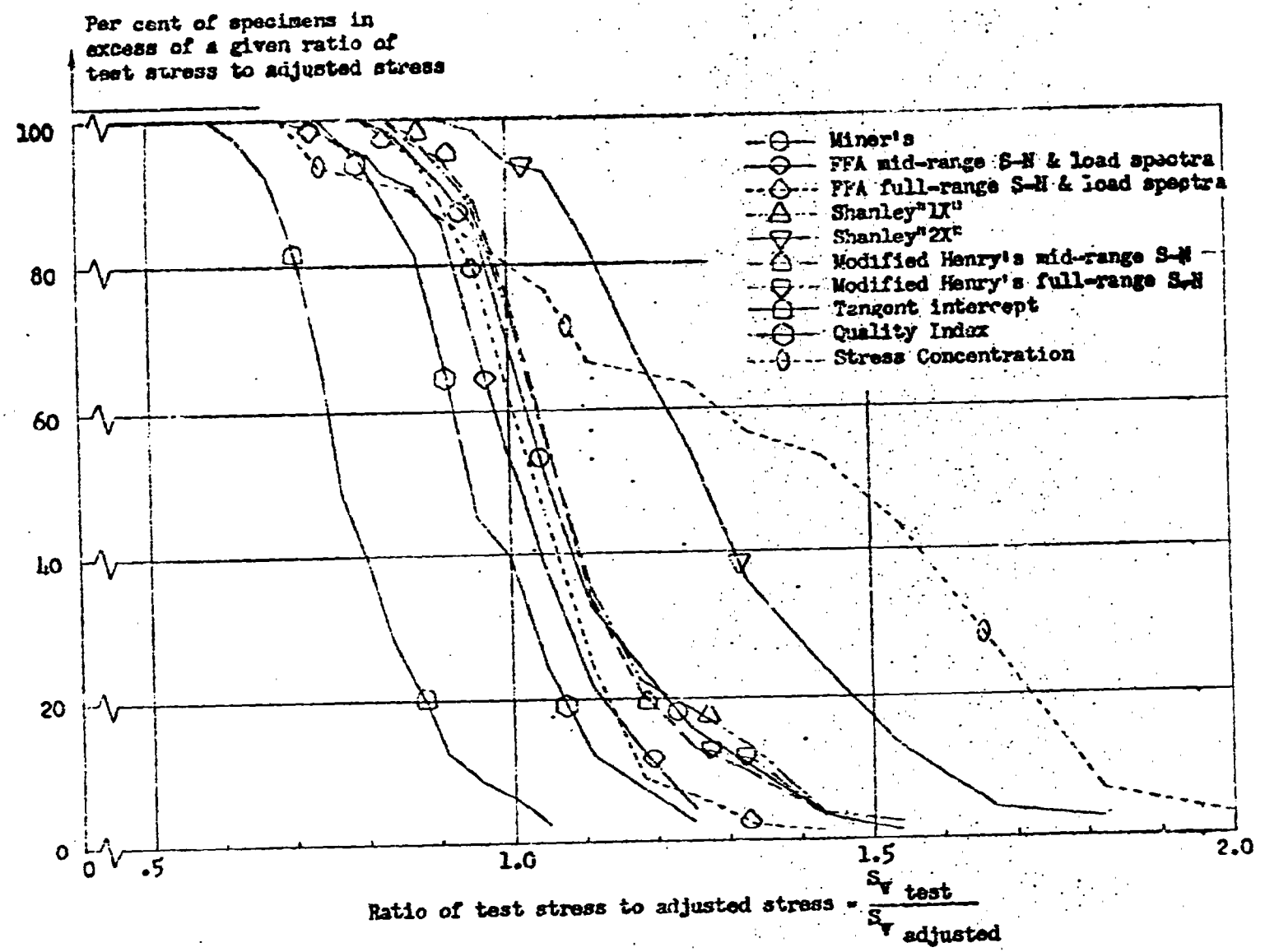



Figure 8. Cumulative Distributions for the Ratio of Test Stress to Adjusted Stress

The inherent spread of fatigue life predictions is evident in the rectilinear scale of Figure 7. To encompass a wider range of data, Figure 9 is presented with the degree of conservatism on a log scale. This latter figure also has the advantage that equal distances on each side of the ordinate of perfect correlation (degree of conservatism = 1.00) represent equal degrees of conservatism, whereas in the rectilinear plots of Figures 7 and 8, these distances are distorted between the unconservative and the conservative sides of the diagrams.

The appearance of these diagrams is roughly similar to the Gaussian normal distribution curve. Table 2 was therefore prepared from these data to indicate a quasi-statistical analysis of the error spread in terms of standard deviations (one sigma). From the properties of the logarithmic increments, the resulting multiplicative standard deviation is a factor to be multiplied or divided, not added or subtracted as is the case for the standard deviation.

Examination of these curves shows the Tangent Intercept method to be very unconservative for predicting the fatigue life of this group of tests. Also evident is the large degree of conservatism in the fatigue life predictions of Shanley's "2X" method and the lack of agreement, both conservative and unconservative, for the stress concentration procedure when using the concept of linear cumulative damage with standardized S-N curves. All other methods evaluated by these data group closely to the same band generally consistent with the linear cumulative damage prediction. This agreement is to be expected since all of these methods except the Tangent Intercept are variations of the basic cumulative damage procedure, some of which vary only in details of mathematical curve fitting.

Some of the methods which introduce nonlinearities do not demonstrate for these tests any strong divergence from the linear accumulation process, with the single exception of Shanley's "2X" method.

The evaluation of the two variants of the least squares best fit of the S-N data in the two methods showed no detectable difference in the generalized Henry method. A relatively minor overall improvement can be observed in Lundberg's FFA method when the best fit of S-N and loading spectra data is restricted to the midstress region of most damaging stresses.

In Figure 8 the correlation of the various methods as measured on the stress scale reveals the same general pattern among the various methods as was discussed above for the life cycle scale of comparison. The significant difference, from the viewpoint of design and control for the prevention of fatigue failures, is the relatively small change in the stress adjustment factor required to achieve a given degree of improvement on the life cycle scale.

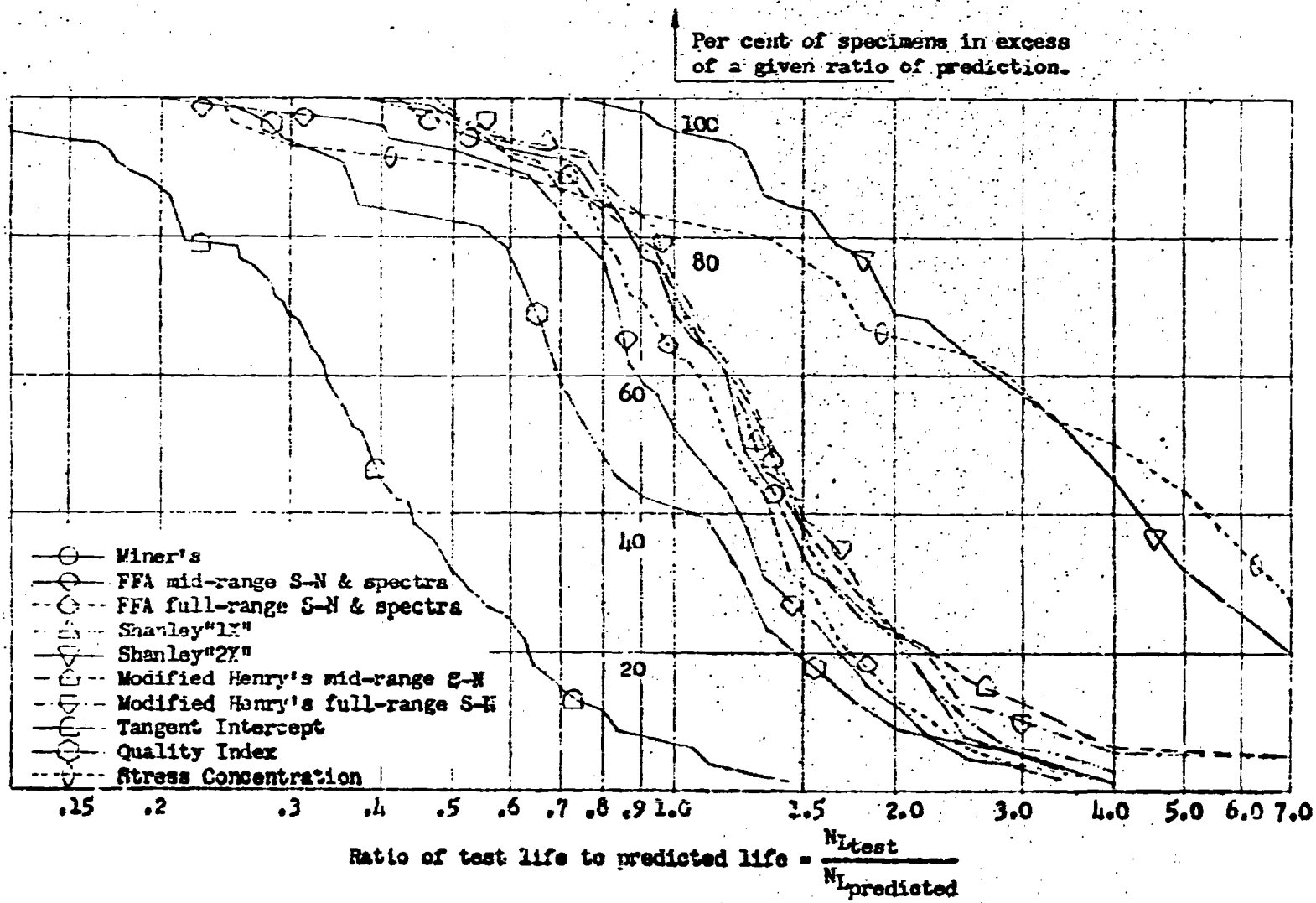



Figure 9. Log Cumulative Distributions for the Ratio of Test Life to Predicted Life

TABLE 2

STATISTICAL PARAMETERS ESTIMATED FROM THE CUMULATIVE DISTRIBUTION CURVES

| Method Codes in Table 1 | Ratio, $\frac{NI_{test}}{NI_{predicted}}$ Multiplicative Mean | Ratio, $\frac{NI_{test}}{NI_{predicted}}$ Multiplicative Standard Deviation One $\sigma$ | Ratio, $\frac{S_{Vtest}}{S_{Vadjusted}}$ Mean | Ratio, $\frac{S_{Vtest}}{S_{Vadjusted}}$ Standard Deviation One $\sigma$ |
|---|---|---|---|---|
| Tangent Intercept | .38 | 1.84 | .79 | ±.10 |
| FFA Code ○ | 1.07 | 1.74 | 1.02 | ±.12 |
| FFA Code ◇ | 1.20 | 1.62 | 1.05 | ±.12 |
| Miner's | 1.29 | 1.64 | 1.09 | ±.16 |
| Henry's Code △ | 1.42 | 1.85 | 1.09 | ±.14 |
| Henry's Code ▽ | 1.43 | 1.78 | 1.09 | ±.14 |
| Shanley's 1X | 1.34 | 1.65 | 1.10 | ±.15 |
| Shanley's 2X | 3.74 | 2.13 | 1.30 | ±.20 |
| Quality Index | .87 | 1.93 | .97 | ±.12 |
| Stress Concentration | 2.40 | 2.81 | 1.36 | ±.36 |

Derived from Figures 8 and 9.

## THE FATIGUE QUALITY INDEX METHOD

The potential advantages of basing a fatigue life prediction method on one or a few spectrum test results of specimens of critical structure is worthy of special study. The simplest test of the effectiveness of the procedure is to compare the values of the test-derived quality index determined from all available tests in which two or more different loading spectra were applied to one specimen. If these quality indices are invariant (within a reasonable scatter factor) for all load spectra test results on the same type of specimen, the predictability of fatigue life is assured.

The fatigue quality index was derived for all the pertinent data available from the test groups chosen for this evaluation. These values are listed in Table 3 . The test data of these groups are of a similarly shaped spectrum of varying loads in which the general slope was changed as well as the mean stresses. Comparisons of the fatigue quality index values in Table 3 for a given specimen, however, indicate a considerable variance. The variance due to scatter of the test results is also indicated.

Groups 28 through 31 inclusive show the influence of progressively reduced slope of a gust-type spectrum on the derived fatigue quality index for a double shear riveted joint of 2024-T3 Aluminum Alloy. The maximum K-value (minimum life of each test group) is progressively higher for each reduction in slope of the loading spectrum. The geometric mean and the minimum K-value (maximum life of each test group) show a slight reversal in the general trend for the lowest sloped loading spectrum. However, the change in slope between these last two groups (G30 and G31 in Figure 10) is relatively much smaller than the changes among the others of the set. The trend of increasing K-value with decreasing slope of the loading spectrum is, in general, stronger than the scatter (except for the last two groups).

Groups G35, G36, and G37 provide a similar comparison for a butt-joint specimen of 7075-T6 Aluminum Alloy. The trend is clearer for this group, there being no overlapping of the minimum and maximum K-values of any of the groups.

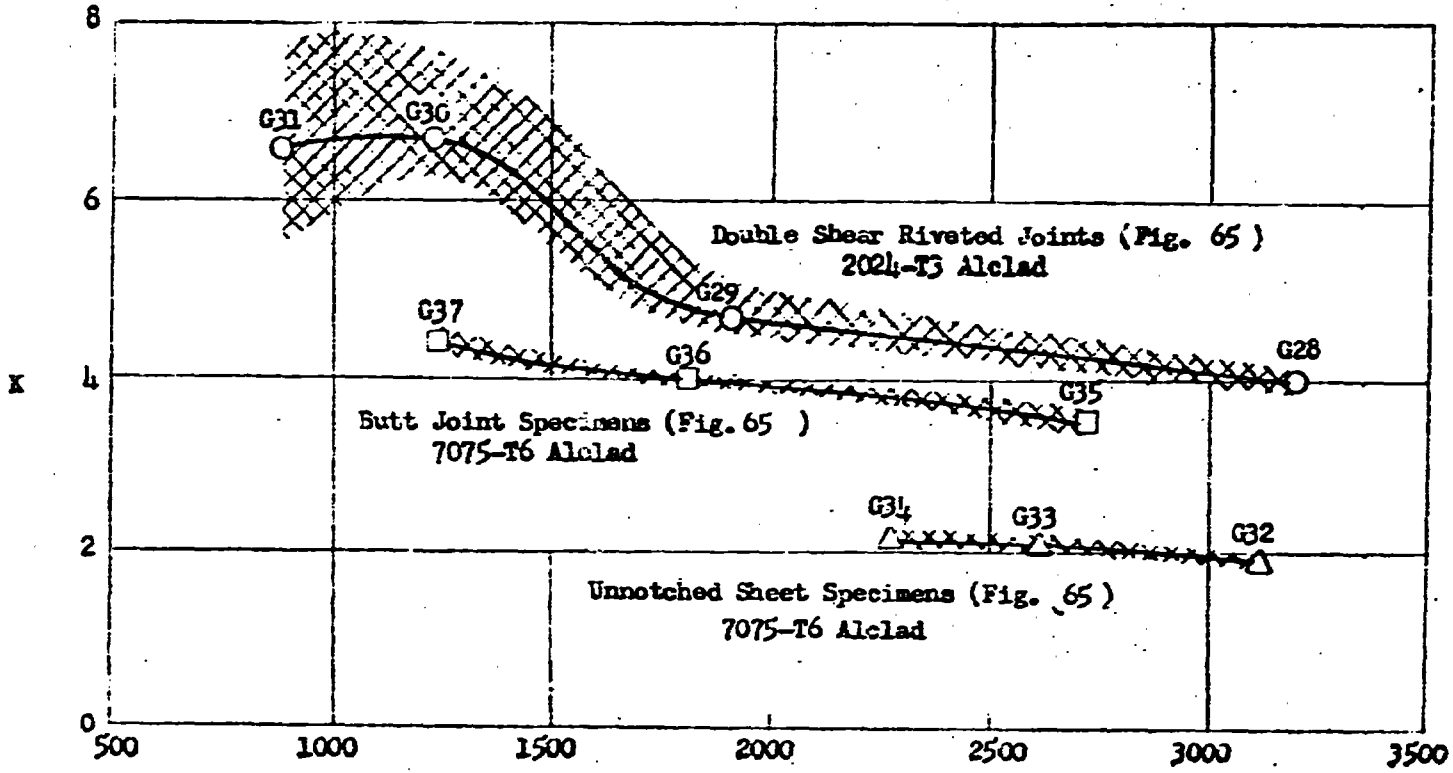
Groups G32, G33, and G34 indicate, for 7075-T6 aluminum alloy unnotched sheet specimens, the same general trend of increasing K-value with reduction of loading spectrum slope. However, the variance is much weaker, and there is more overlap of minimum and maximum values of the groups from scatter. Contributing to this conclusion, however, is the relatively small difference in slope as indicated by Figure 10.

It is therefore concluded from this brief study that the relative maximum load content of a service record as exemplified by the mean load changes and the slope of the statistical load frequency spectrum has an important influence on the fatigue life of airframe structure.

TABLE 3

VARIATION OF THE FATIGUE QUALITY INDEX
WITH DIFFERENT LOADING SPECTRA SLOPE

| Test Group | Slope Sequence | No. of Spec. | | Max. K Min. Life | Geometric Mean | Min. K Max. Life |
|---|---|---|---|---|---|---|
| | 2024-T3 Double Shear Rivited Joint - 2(3/16)Round Head Rivets | | | | | |
| G28 | High Lo-Hi-Lo | 2 | K | 4.13 | 3.97 | 3.82 |
| | | | Life | $.324 \times 10^6$ | $.411 \times 10^6$ | $.522 \times 10^6$ |
| G29 | High Intermediate Lo-Hi-Lo | 3 | K | 5.06 | 4.70 | 4.52 |
| | | | Life | $3.20 \times 10^6$ | $5.98 \times 10^6$ | $4.788 \times 10^6$ |
| G30 | Low Intermediate | 3 | K | 7.73 | 6.71 | 6.29 |
| | | | Life | $13.69 \times 10^6$ | $21,73 \times 10^6$ | $27.4 \times 10^6$ |
| G31 | Low Lo-Hi-Lo | 2 | K | 7.83 | 6.59 | 5.52 |
| | | | Life | $62.4 \times 10^6$ | $129.7 \times 10^6$ | $270.0 \times 10^6$ |
| | 7075-T6 Butt Joint Specimens 5/32 CSK Rivets | | | | | |
| G35 | High Lo-Hi-Lo | 4 | K | 3.69 | 3.52 | 3.30 |
| | | | Life | $2.05 \times 10^6$ | $2.99 \times 10^6$ | $4.03 \times 10^6$ |
| G36 | Intermediate Lo-Hi-Lo | 2 | K | 3.98 | 3.97 | 3.96 |
| | | | Life | $27.00 \times 10^6$ | $27.56 \times 10^6$ | $28.10 \times 10^6$ |
| G37 | Low Lo-Hi-Lo | 2 | K | 4.59 | 4.41 | 4.25 |
| | | | Life | $72.75 \times 10^6$ | $101.00 \times 10^6$ | $140.00 \times 10^6$ |
| | 7075-T6 Unnotched Sheet | | | | | |
| G32 | High | 2 | K | 1.91 | 1.90 | 1.89 |
| | | | Life | $24.1 \times 10^6$ | $25.71 \times 10^6$ | $27.4 \times 10^6$ |
| G33 | Intermediate | 2 | K | 2.22 | 2.10 | 1.98 |
| | | | Life | $58.7 \times 10^6$ | $75.875 \times 10^6$ | $98.0 \times 10^6$ |
| G34 | Low | 2 | K | 2.26 | 2.17 | 2.07 |
| | | | Life | $127.00 \times 10^6$ | $152.00 \times 10^6$ | $181.00 \times 10^6$ |




h - Slope of Loading Spectra in High Stress Range

Figure 10 Variation of the Test Derived Fatigue Quality Index K versus Slope of the Loading Spectra

## FACTORS OR MARGINS OF SAFETY FOR FATIGUE

Diagrams of the type of Figure 7 are often used for discussion on the necessity of factors of safety or margins of safety on fatigue life. Diagrams of the type of Figure 8 are correspondingly used for discussions of factors or margins on loads or stresses to achieve the same end; namely, a "safe-life" philosophy of design. However, there are many other facets of the problem which must be considered in the establishment of safety factors. A brief discussion of some of these facets is given, although it is not the purpose nor within the scope of this study to establish factors or margins of safety for fatigue.

### Mission Objectives

The trend of design toward achievement of higher performance goals has led to an ever higher degree of specialization. For each major project, therefore, the subject of reassessment of factors of safety in relation to the specific mission objectives is a necessity.

### Fail-Safe Philosophy

One of the most important aspects to be considered is the "fail-safe" philosophy of design. The "safe-life" and the "fail-safe" philosophy have been the subject of considerable controversy in the past by proponents of one or the other approaches to built-in safety in the flight structure. From practical considerations, both have a place, they are not mutually exclusive philosophies, and even though reliance may be placed on a "fail-safe" approach, the fatigue qualities of the structure cannot have any less degree of attention. However, in the case of successful "fail-safe" design, the need for reliance on fatigue life for flight safety is considerably reduced. The consideration of factors of safety on fatigue life thus may have an entirely different complexion in the presence of a "fail-safe" structure than it assuredly must have in a "safe-life" structure which is not "fail-safe."

### Loads

The evaluation diagrams referred to above cover only a portion of the life prediction process; uncertainties in the external load predictions are not contained. The external loads as well as the interrelation of the static strength level loads and their factors of safety should be considered simultaneously in assessing factors of safety for designing against fatigue.

### Inspection, Maintenance, and Repair

Inspection, maintenance, and repair as a means of prolonging indefinitely the "fatigue useful life" of a structure is another important subject, often overlooked in the assessment of factors of safety for fatigue. Catastrophic fatigue cracking of major structure early in the operational life of a fleet is not to be condoned. On the other hand, an airframe used long enough can be expected to develop fatigue cracks. The fatigue characteristics of some materials show no specific endurance limit, and the severe performance

requirements of flight force the use of the highest possible design allowable tensile stresses. However, means are available for designing to any specific fatigue life required, performance permitting. Scheduled inspection, maintenance, and repair or replacement of components may become a deliberate policy in the attainment of higher performance with safety from fatigue problems. Helicopter parts are an example.

Test Procedures

Factors in the laboratory testing procedures also affect the scatter of results, which should be considered in assessing factors for design. Constant amplitude loading appears to give wider scatter in results when compared with spectral load testing techniques. Notched coupon-type specimens appear also to give wider scatter in results than complex specimens in which load redistributions may take place. These factors should be taken into account, particularly in assessing a broad range of specimen types and loadings as represented in the Figures 5 and 6 of the methods evaluation phase of this study.

It may be concluded, therefore, that the results of this study demonstrates a need for factors or margins of safety in certain classes of structures (non-fail-safe). However, additional considerations are necessary, some of which are specific for each type of project. An evaluation of the need and the particular values for factors of safety should, therefore, be a process in the establishment of design criteria for each project.

## CONCLUSIONS OF THE EVALUATION STUDY

From considerations of the problems involved in the prediction of fatigue life of airframe structure when this process is used as a tool for the prevention of fatigue failures in an operational fleet, and based on the test data utilized in this evaluation, the following conclusions may be drawn.

1. The Linear Cumulative Damage Method is currently the most practical, simple, and yet versatile method available and has sufficient accuracy commensurate with the other uncertainties, such as service load history, not included in this evaluation.

2. The Stress Concentration Factor Method of refined stress analysis, coupled with a fatigue damage theory such as the linear cumulative damage hypothesis used in this evaluation, is shown to be less than adequate as a fatigue life prediction method. However, since these procedures usually are the only means available for preliminary design assessments, their use must be followed up by development tests of fatigue critical areas.

   Development tests of fatigue critical joints and structural discontinuities are required to assess a fatigue quality of the structure which is as yet not attainable by theoretical means. To achieve satisfactory reliability from the laboratory results, the critical areas of the specimen must be as exact a simulation of the critical area as possible, including local eccentricities, supports, manufacturing processes and finishes, local attachments for secondary elements, etc., and should also include a nominal area of surrounding structure for load and stress monitoring and for comparing the joint results with the fatigue life of the nominal structure, if this is required. These development tests must encompass the full range of load magnitudes expected in service to properly assess location of cracks, crack growth, and final fracture. While the objectives of these tests might be achieved by constant load amplitude S-N type tests or the full spectral-type tests, there is considerable evidence (reference 20) for recommending the latter.

3. The Fatigue Quality Index Procedure, which was originally a means of interpreting spectrum-type fatigue tests, is investigated as a test-based method of fatigue life prediction. A spectrum test result is analyzed by the linear cumulative damage equation coupled with a fixed standard set of S-N data to define which K-value of the set will make the cumulative damage summation exactly unity. For success as a fatigue life prediction method, the test-defined K-value should be invariant for similar types of test spectra applied to identical specimens. Study of the applicable test data shows this not to be the case. Further exploration is therefore necessary to determine whether a consistent trend exists which might be used as an adjustment factor to improve the life prediction process.

4. The Tangent Intercept Method demonstrated the largest degree of unconservatism when applied to these test data. Graphical limitations make this method impractical to handle the more complex composite loading histories, often at several different mean load levels in each flight.

5. Shanley's "2X" Method of nonlinear cumulative damage, based on a more accelerated rate of crack growth than his "1X" method, demonstrated a larger degree of conservatism than all other methods investigated.

6. The remaining prediction methods which were evaluated (Lundberg's FFA method, Shanley's "1X", and the generalized Henry method) all show relatively small differences in reliability of life prediction, considering the large uncertainties remaining, for instance, in the service loads and operational history. The limitations of mathematical curve fitting in some of these methods and the complexity and lack of statistical information for other methods preclude their widespread application for aircraft fatigue life prediction.

7. The assessment of reliability on the scale of the stress adjustments necessary to achieve exact prediction of the fatigue test results show generally the same relationship among the various methods as for the scale of life cycles. However, as would be expected, far less absolute deviation occurred on the stress adjustment scale than on the life cycle scale.

8. The results of this study demonstrate a need for factors or margins of safety in certain classes of structures (non-fail safe). However, additional considerations are necessary, some of which are specific for each type of project. An evaluation of the need and the particular values for factors of safety should, therefore, be a process in the establishment of design criteria for each project.

## SECTION IV

## INVESTIGATION OF THE INFLUENCE OF SPECTRUM SHAPE ON FATIGUE LIFE PREDICTIONS

Based on the test data available, the evaluation study of fatigue life prediction methods discussed in Section III arrived at two basic conclusions. First, when adequate S-N data is available on the specific structure, fatigue life prediction under complex loading spectra by the simple linear cumulative damage procedure is of sufficient accuracy commensurate with other intangibles remaining in the problem. Secondly, the direct use of the fatigue quality index procedure was shown to be less capable of analysing different spectra of loads applied to identical specimens. While some of the discrepancy is attributable to artificial test variables, sufficient variation remains to indicate a considerable influence from the statistical load frequency content as exemplified by the spectrum shape (slope).

It is the purpose of this section of the study to explore the circumstances of this difference in fatigue life predictions for similar structure tested under different shaped loading spectra. The objective is to determine whether any regularity in the trend of fatigue life with shape of loading spectra exists which might be used an an empirical adjustment factor to improve the predictability under different types of loading spectra. An experimental program was conducted to generate data for this purpose.

### EXPERIMENTAL PROGRAM

The experimental program was conducted in two parts to provide evidence for this study. The first part, using simple notched sheet coupons of 7075-T6 aluminum alloy, explored a variety of test spectra shapes including the use of the original random load record from which the ordered loading spectra was derived. The results of these tests, reported in detail in Appendix D, are analyzed in this section of the report. The second part of the experimental program was conducted on specimens of a complex joint design to determine whether the results of the coupon test program could be reproduced in complex structure more representative of contemporary aircraft. These results, reported in detail also in Appendix D, are analyzed in the following section of this report.

### FATIGUE TEST EQUIPMENT

A magnetic tape controlled fatigue loading machine was assembled from available equipment. The system consisted essentially of a magnetic tape playback unit, associated electronic amplifiers, calibration equipment, load monitoring tape recording system, and an oscillograph. The amplified magnetic tape load demand signal was fed through a summing junction to a highly sensitive electrohydraulic servo-valve which controls the pressure on each side of a 17,000 lb. capacity, double-acting hydraulic loading jack. The fatigue test specimen was coupled to the hydraulic jack, in series through a calibrated electrical strain-gage load-measuring cell. The instantaneous load signal from the monitoring cell was amplified and fed through a specially tailored lead network to the tape demand signal summing junction. The error between the measured load signal and the

demand signal, suitable amplified, was applied to the servo valve in a direction to reduce the error to zero. This negative feed-back loop stabilizes the system up to relatively high frequence of load application, in this case approximately 60 cps for simple loading forms, determined primarily by the dynamics of the mechanical system and the hydraulic flow characteristics of the valve and associated power supply.

While most of the equipment is of commercially available units and the test arrangement is simple and straightforward, the precision and repeatability, demanded for quality results, require considerable efforts to develop control, maintenance, calibration, and monitoring techniques to a satisfactory degree of reliability. These techniques consist essentially of careful calibration of each set-up, and recording sampling load monitoring tapes which are counted on the electronic analogue computer set up for this purpose. The test data records reported herein are based on the load cell monitor count. The details of the equipment and a description of the complete test technique are more fully outlined in Appendix D, Part 2. Figures 11, 12, and 13 illustrate the test equipment, electronic control system, and a test specimen in place. Figure 14 illustrates the precision finally achieved by comparing the calibrated load cell output with the demand signal applied to the servo valve input terminals.

## COUPON TEST SPECIMENS

The test specimens for the first phase of this program were made of a three-inch-wide strip of 0.040-inch thick 7075-T6 aluminum alloy sheet, Material Spec. QQ-A-277. Static tensile properties, taken in the longitudinal grain direction, are reported in Appendix D, Part 2, for samples from each sheet purchased for this program. The tensile test specimen conformed to ASTM standard E8-57T. These results indicate adequate uniformity and conformity of this material to the specification standards.

The specimens were notched by a series of central holes designed for two values of $K_T$ = 4 and 7. The dimensions were as indicated in Figure 15. Floating edge-grooved stiffener blocks were installed to prevent buckling under the maximum compressive loads.

## TEST SPECTRA ON MAGNETIC TAPE

A sample reproduced from a short length of an actual load trace from a B-47 aircraft flying in turbulence is shown in Figure 16. The general characteristics of varying magnitude cyclic loads are apparent, along with other irregularities of a nonrepetitive nature. There have been a number of methods proposed to reduce this type of load record to ordered cyclic load frequency spectra, three of which were explored in some detail in the research program reported in reference 5. A line through the average of the amplitudes of a short length of trace defines the local mean static load measured from a calibrated reference line. Perhaps the simplest of the counting methods is the mean crossing peak count which records each excursion from the local mean line to a maximum peak and return to the next crossing of the mean line as one half cycle of load, ignoring any secondary excursions within the time interval of mean line crossings. For records of sufficient duration, varying

magnitudes of positive peaks and negative peaks are substantially equal in number. Positive and negative half cycles are regrouped to form full cycles. These cycles are rearranged in order of magnitude and plotted in cumulative load frequency form as illustrated in Figure 17. The majority of service loading data is customarily reported in this form.

The other counting methods that were investigated, the range count and the interval crossing count, are defined in detail in reference 5. For the available loading traces, these were shown to be equivalent to the mean crossing peak count method described above. For this reason all the spectral fatigue results of this report are recorded in the form of mean crossing peak counts.

Analogue computing components were assembled to perform the counting procedure as described in Appendix D, Part 2. The computing techniques were calibrated against an average of several manual counts of approximately five minutes' length of the B-47 wing root bending moment record, which had been recorded on oscillograph paper for this purpose.

The relatively short length of B-47 data record (ninety-six minutes) produced a continuous frequency distribution spectra, with no gaps and discontinuities in the load intervals. However, the record was modified to provide a variety of spectra more suitable for testing. The modifications are discussed below.

1. The varying component of load was recorded separately from the local mean load so that independent amplification ratios could be applied to each load channel. An inequality of the maximum negative and the maximum positive load was equalized by nonlinear re-recording.

2. The varying spectra of loads were extended in length by linear amplifications and splicing, and was modified by special nonlinear amplifications to introduce the seldom encountered higher loads found on longer records. The technique used in producing this master gust spectrum tape is described in detail in Appendix D, Part 2.

3. During testing, suitable linear amplification ratios were used to produce high-slope high peak spectra, as illustrated in Figure 18.

4. Nonlinear amplification of the varying load record changed the spectrum shape to be predominately concave downward as illustrated in Figure 18.

5. The use of a diode rectifier suppressed all negative load peaks and resulted in a master record substantially representative of the random positive maneuver excursions from a constant minimum load level. The spectrum shape was modified by non-linear amplification to produce the characteristics of the maneuver spectrum of Specification MIL-A-8866. See Figure 19. A sample of the resulting random military maneuver loading trace is given in Figure 20. This type of trace represents the true random maneuver loading sequence denoted in Figure 25.

6. Unit step spectra were constructed and recorded on tape, from the average fatigue life on the various random mean crossing peak count curves of each type of spectrum, by the breakdown illustrated in Figure 21. The unit spectrum sizes were 1/10 and 1/20 of the total random test life.

and the stress interval was 1000 psi in each block size. One additional combination was produced with 4000 psi stress interval and 1/20 block size, as illustrated in Figure 22. A typical trace of an ordered step or Lo-Hi loading spectrum of a gust history is shown in Figure 23. The unit maneuver spectrum size was 1/20 of the total random test life with stress intervals of either 1000 or 4000 psi. A sample of an ordered military maneuver loading trace is shown in Figure 24, and the ordered or Lo-Hi maneuver loading sequence is illustrated in Figure 25.

7. Ordered composite gust and ground loading was simulated as sketched schematically in Figure 26, based on the 1/20 unit spectrum block size and 1000 psi stress interval. The load activity was the same as for the random composite tests in Reference 5 with approximately 11 to 12 gust loads per flight and approximately 6 to 7 taxi loads per flight. Test group CG4 had approximately 100 gust loads and 10 ground taxi loads per flight.

8. Random composite maneuver loading and ground taxi loading were simulated by running the master random maneuver tape during the flight portion and switching to the master gust random tape at the mean load level and amplification commensurate with ground taxi loads. The load activity was approximately 30 maneuver loads and approximately 35 taxi loadings per flight. A trace of this record is shown in Figure 27. Only those tests are used that were deemed of sufficient duration to provide adequate statistical sampling of both the maneuver and ground (gust) records.

The results of the fatigue tests conducted are tabulated and plotted in Appendix D, Part 2.

## ANALYSIS OF THE COUPON TEST DATA

Miner's method was applied to the unit spectra using the specific S-N data for these coupons from Appendix D. The resulting predictions are compared with test results in Tables 4 and 5 and in Figures 37, 38, and 39. The fatigue life predictions by Miner's method for these coupons are in general less conservative than the results of the application of this method to the test data from the literature. This is illustrated in Figure 40 by the comparison of curve number 2 with curve number 1 taken from Figure 7 of Section III. The largest degree of unconservatism is shown for coupons of $K_T = 7.00$ loaded with the ground taxi spectra at compressive mean stress levels of $f_m = -3000$ psi. (Test group numbers T1 and T2.)

The effects of the shape of the loading spectra on fatigue life predictions by the Fatigue Quality Index method was investigated in two ways:

1. Adjustment of the Fatigue Quality Index by a function of the slope of the air loading spectrum in the high stress range.

2. Adjustment of the Fatigue Quality Index by a function of the slope of the air loading spectrum in the stress range of maximum fatigue damage as denoted by the largest cycle ratio $\left(\frac{n}{N}\right)_{max}$ in the unit loading spectrum.

The slope of the airloading portion of each test spectra is plotted as a function of the varying stress level for gust and maneuver type loading spectra in Figures 30 and 31, respectively, and for composite gust and composite maneuver load spectra in Figures 32 and 33, respectively.

The test results of Groups G74, G79, and G81 were selected to provide the empirical adjustment function for the variation of the Fatigue Quality Index with the slope of the test spectra. The test results of each of the three shapes of loading spectra in Figure 18 were used to derive the Fatigue Quality Index for the coupon specimen of $K_T = 4$. The geometric mean of the Quality Index for the test groups G74, G79, and G81 are plotted in Figure 28 as a function of the slope of the varying load spectra at 90% of the maximum peak load applied. Figure 29 is a graph of the same test derived Fatigue Quality Index values plotted as a function of the slope of the loading diagrams in the region of the stress level for maximum calculated fatigue damage, $(\frac{n}{N})_{max}$.

To predict the fatigue life of similar specimens tested under other types of loading spectra, the slope of the new unit loading spectrum is determined at the appropriate stress level, for example, at the level of 90% of the maximum applied load in the sequence. At this value of slope, the corresponding Fatigue Quality Index read from Figure 28 establishes the standard S-N curve set that is to be used in the prediction of fatigue life by the linear cumulative damage procedure. This is accomplished for twelve sets of data in Table 6, including low slope gust spectra, composite gust and ground load spectra, and composite maneuver and ground load spectra. These predictions are graphically compared with the corresponding test results in Figures 37 to 39. The degree of conservatism is indicated in Table 6 by the ratio of test fatigue life to predicted fatigue life. These degrees of conservatism are ranked in ascending order, and the percentage of the total number of samples equal to or less than a given degree of conservatism is determined and plotted as a function of that degree of conservatism as curve No. 4 in Figure 40.

The second procedure of adjustment is not quite so direct. As indicated in Table 7 and Figure 35, the stress level of the maximum cycle ratio $(\frac{n}{N})_{max}$ is a function of the Quality Index which, from Figure 29, is a function of the slope of the loading spectra at the stress level for maximum cycle ratio. The graphical procedure illustrated in Figure 36 was used to determine the compatible stress level, slope of the loading spectra, and Fatigue Quality Index. As an example, Figure 36 illustrates the procedure for Test Group No. G66. Arbitrarily chosen Fatigue Quality Index values were utilized to obtain the stress level at which the maximum cycle ratio exists for the unit loading spectra. These values of stress level are plotted as a function of the chosen Quality Index, K, in the center graph of Figure 36. The slope of the loading spectra is given as a function of the varying stress level in the graph to the left of Figure 36 (see Figures 30, 31, 32, and 33 for slope data from other loading spectra). Values of slope "h" and Quality Index "K" are determined at several trial varying stress levels a, b, and c, from the left and center graph as indicated, and these values are cross plotted on the right hand graph at points a, b, and c. The intersection of the interpolating curve abc with the curve of Figure 29 provides the value of the Fatigue Quality Index compatible with the other parameters as desired.

The adjusted value of the Fatigue Quality Index is used to predict fatigue lives of these specimens with the standard set of S-N data as in the normal procedure. Results of life predictions for thirteen of the sixteen groups of coupons of this series are given in Table 6. Two cases (G75 and G80) provided no compatible values. A third case (CM1) was of a slope beyond the range of the control test data of Figure 29 and was therefore omitted.

The comparison of these predicted results with their test results is given in Figures 37, 38, and 39. The ratio of the test life to the predicted life is determined, ranked, and the percentage of the total number of samples exceeding a given degree of conservatism is plotted as a function of that degree of conservatism as described previously. This is Curve No. 5 in Figure 40.

The basic version of the Fatigue Quality Index procedure was also applied to these coupon data. The Fatigue Quality Index values, derived from the 26 groups of coupon test results by the use of the standardized S-N curves, are listed in Tables 8 for simple gust type spectra of various shapes and in Table 9 for the simple fighter maneuver and the ground-taxi type of loading spectra, and for the composite gust and the composite maneuver flight type of loading spectra. The minimum, the maximum, and the geometrical mean of the test derived Fatigue Quality Index are given. In addition, the FQI value from the first specimen of each group is given. Its purpose is to assess the effectiveness of a reduced number of test results in the evaluation of other loading spectra on similar specimens. This is of importance in consideration of large size specimens, components, and full-scale airframe tests in which only one specimen may be economically feasible.

Comparison may be made of the results of Test Groups G66 through 69 which are low peak load, low slope gust spectra (at a low mean stress level) with those of Test Groups G72 through G75 which are high peak load, high slope gust spectra (with a high mean stress level) on the same type specimen ($K_T$ = 4.). This comparison indicates a considerable variation in the derived Fatigue Quality Index. A life prediction derived from a test of the low slope variety of gust spectrum would under-predict the result of the high slope gust spectrum whereas the reverse situation would provide an unconservative prediction. It was not possible to evaluate the results of the specimen of $K_T$ = 7.0 because the derived Fatigue Quality Index, in most cases, exceeded the maximum scale value of K = 8.0.

The comparison of the test derived FQI values for the first specimen of each of these two simple gust groups shows a similar trend. For the low slope spectra the geometric mean of the first specimen FQI values is 5.46 which compares well with the geometric mean of the means of all specimens of this group which is K = 5.45, even though by chance the first specimen of the first group was the maximum value of all in this group. The similar comparison for the high slope group has a geometric mean of the first specimen of K = 4.43 to compare with the geometric mean of the means for all the specimens of this group of K = 4.53. The first specimen basis for life predictions in this case would be only slightly unconservative.

The two groups G78 and G79 (concave upward loading spectra) and G80 and G81 (concave downward loading spectra) show a somewhat reversed trend from that discussed above in that the concave upward group has a relatively higher Fatigue Quality Index value although this spectra has higher peak stresses and slope than the concave downward loading spectra.

The simple fighter maneuver spectra test results from groups M14, M15, and M16 show derived Fatigue Quality Index values more closely approximating the concave upward gust spectra (group G78 and G79) than any of the others. However, the results of these simple maneuver spectra encompass the widest scatter of all the groups. The values of the Fatigue Quality Index range from the minimum of K = 3.60 to the maximum of K = 7.10.

The derived FQI values for the composite test results bear no close correspondence to their counterparts in the simple spectrum groups. From Tables 8 and 9, compare, for instance, groups G66 through G69 with composite gust Group C01 (low slope spectra) and groups G72 through G75 with composite gust groups C03 and C04 (high peak, high slope spectra), and the fighter maneuver groups M14, M15 and M16 with the composite maneuver group CM1. Fatigue life predictions are made in Table 10 for the composite loading spectra by the use of the derived Fatigue Quality Index value from the first coupon specimen result of the corresponding simple spectra of flight loads. As indicated these results were unconservative in the composite tests by approximately 12% of the predicted value for the low slope gust spectra, 43 to 60% of the prediction for the high slope gust spectra and 33% of the prediction for the maneuver spectra. Comparisons in Tables 4 and 5, of the fatigue life predictions for these same groups by Miner's method utilizing the specific S-N curves for these coupons show only moderately improved predictions. This is a fundamental result inherent in the test data which none of the life prediction methods studied in this report can cope with in their current form.

To determine the effectiveness of a Fatigue Quality Index derived from a gust test spectra as a means of predicting the fatigue life of coupons under maneuver type spectra, Table 11 was prepared. This comparison indicates results ranging from relatively conservative predictions to values of test results of half the predictions. While this range of the ratios of test life to predicted life is within the normal scatter band of other prediction methods, this data group is much too small for reliance.

An unexpected result of this series of tests is indicated in the comparisons shown in Table 12. The flight portion of the composite spectrum tests is compared with the simple spectrum test results for corresponding types of loading. The ratio of the number of cycles of flight loadings in the composite spectrum test to the number of cycles of loading in the simple spectrum test may be considered to be the damage fraction for this portion of the loading. Assigning the remaining fraction $(1-\Delta D_{(flight)})$ to the rest of the loadings and noting that the damage due to ground taxi loadings is relatively small, the ground-air-transition cycle is seen to be a predominant producer of fatigue damage. This portion of the loading is seen to provide approximately 50% to 73% of the total damage ratio for this series of tests. The importance of this transition cycle is thus established on an experimental basis. Reviewing the results in Table 5 of the simple linear cumulative damage procedure (Miner's method) utilizing the specific S-N data for these specimens indicates that the effect of the ground-air transition cycle is not predictable by this method either. The test results vary unconservatively from approximately 24% to 86% of the predicted value.

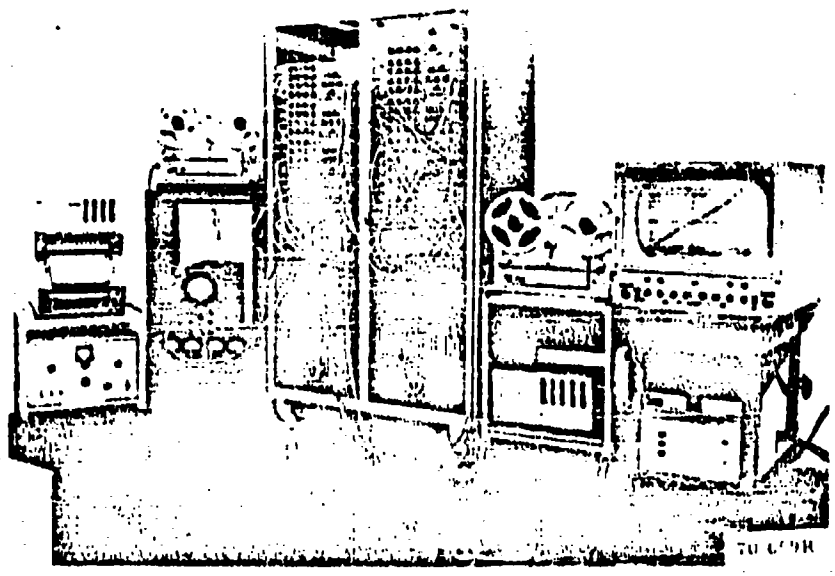


Figure 11 General View of Tape Handling Equipment

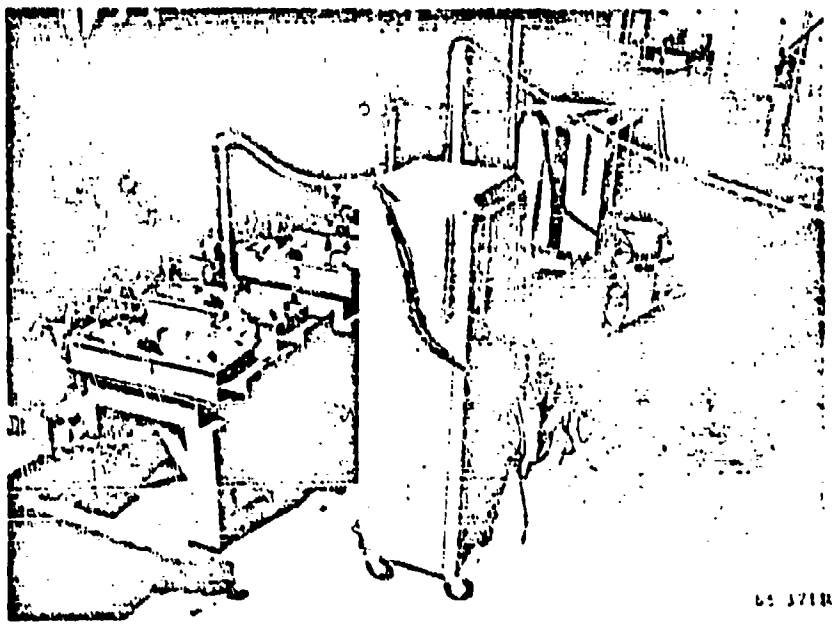


Figure 12 General View of Specimen Loading Apparatus

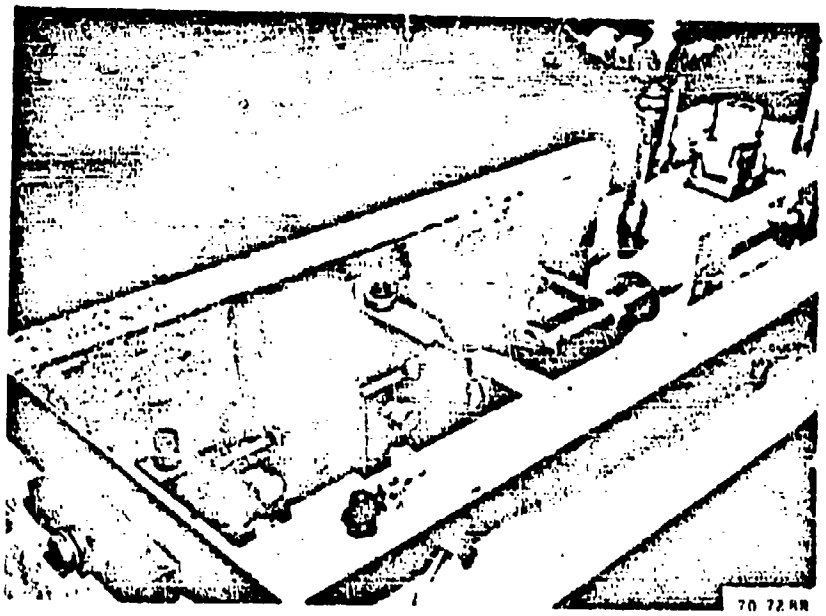


Figure 13 Close-up of Test Specimen Installation

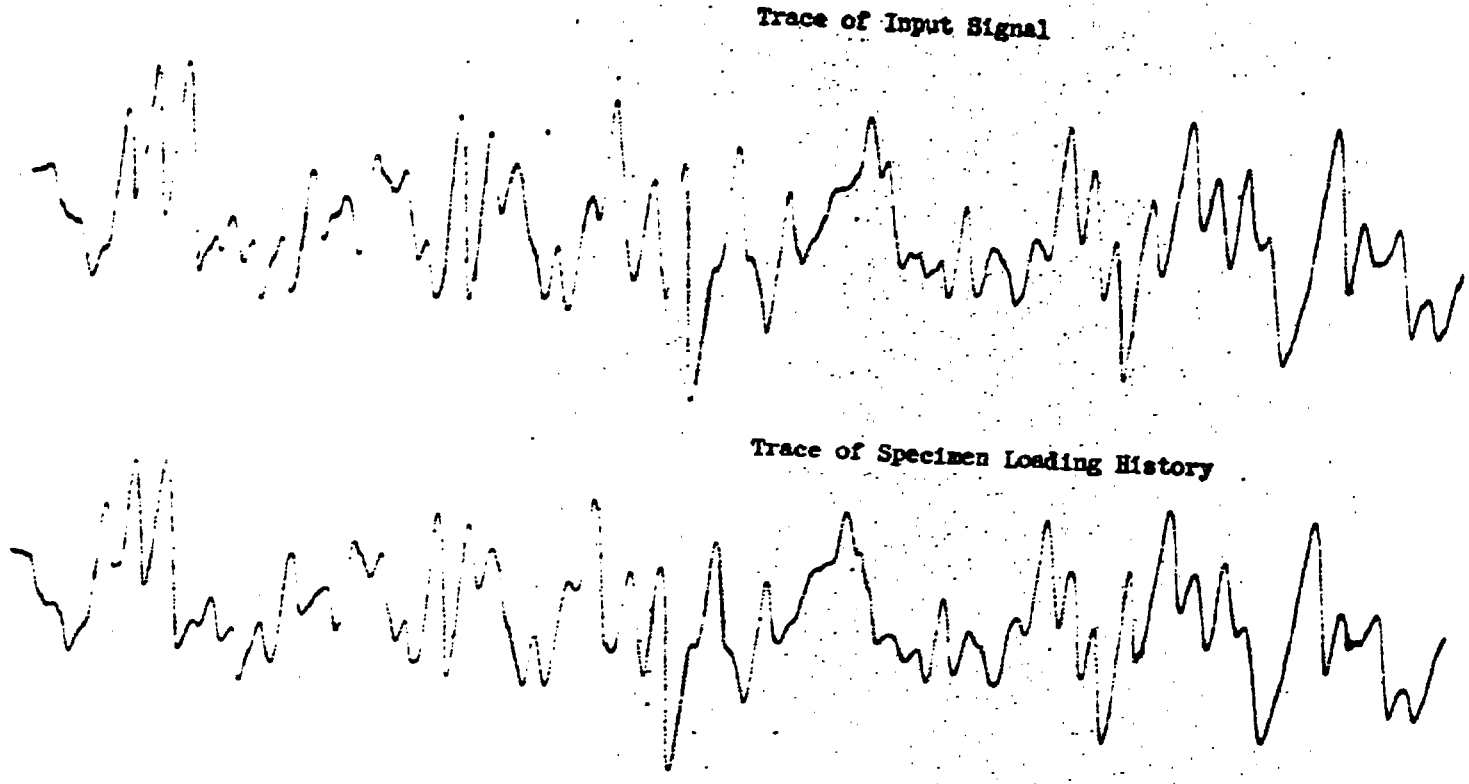
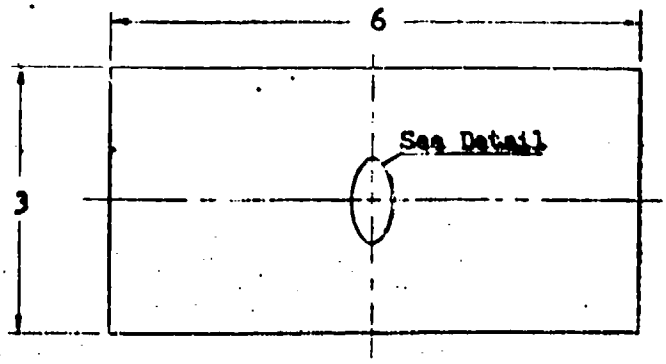
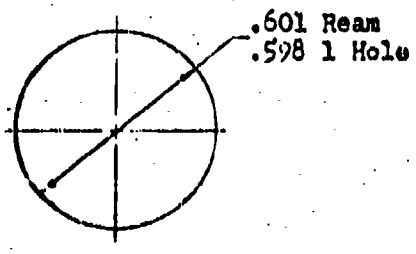
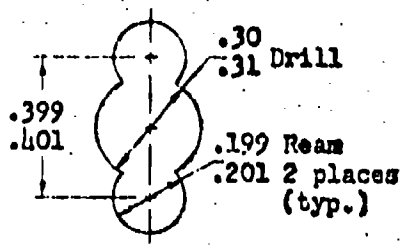



Figure 14 Comparison of Servo Valve Input Signal with Specimen Loading History

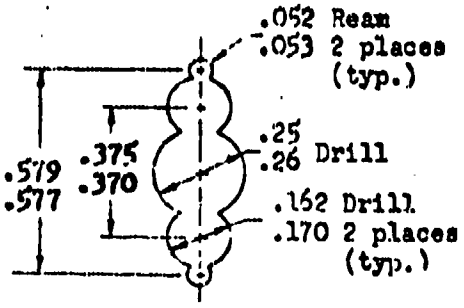


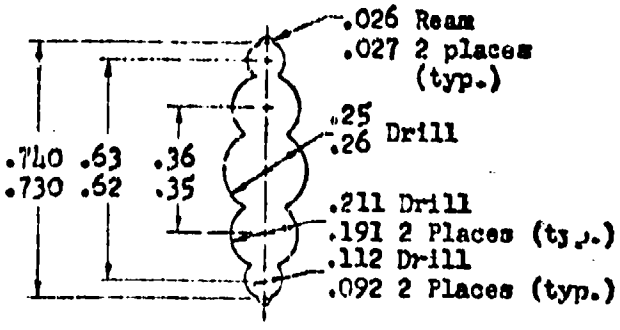

$K_T$ = 3.0




$K_T$ = 4.0




$K_T$ = 7.0




$K_T$ = 10.0

Note: All Dimensions Given In Inches

**MATERIAL:** 7075-T6 Bare Aluminum Alloy Sheet (.04 inches thick)
**FABRICATION:** Specimen Blanks Sheared to Size
Holes Drilled and Reamed
Burrs Removed by Light Stoning

Figure 15. Notched Sheet Test Coupons

Figure 16 Sample Flight Loading Trace

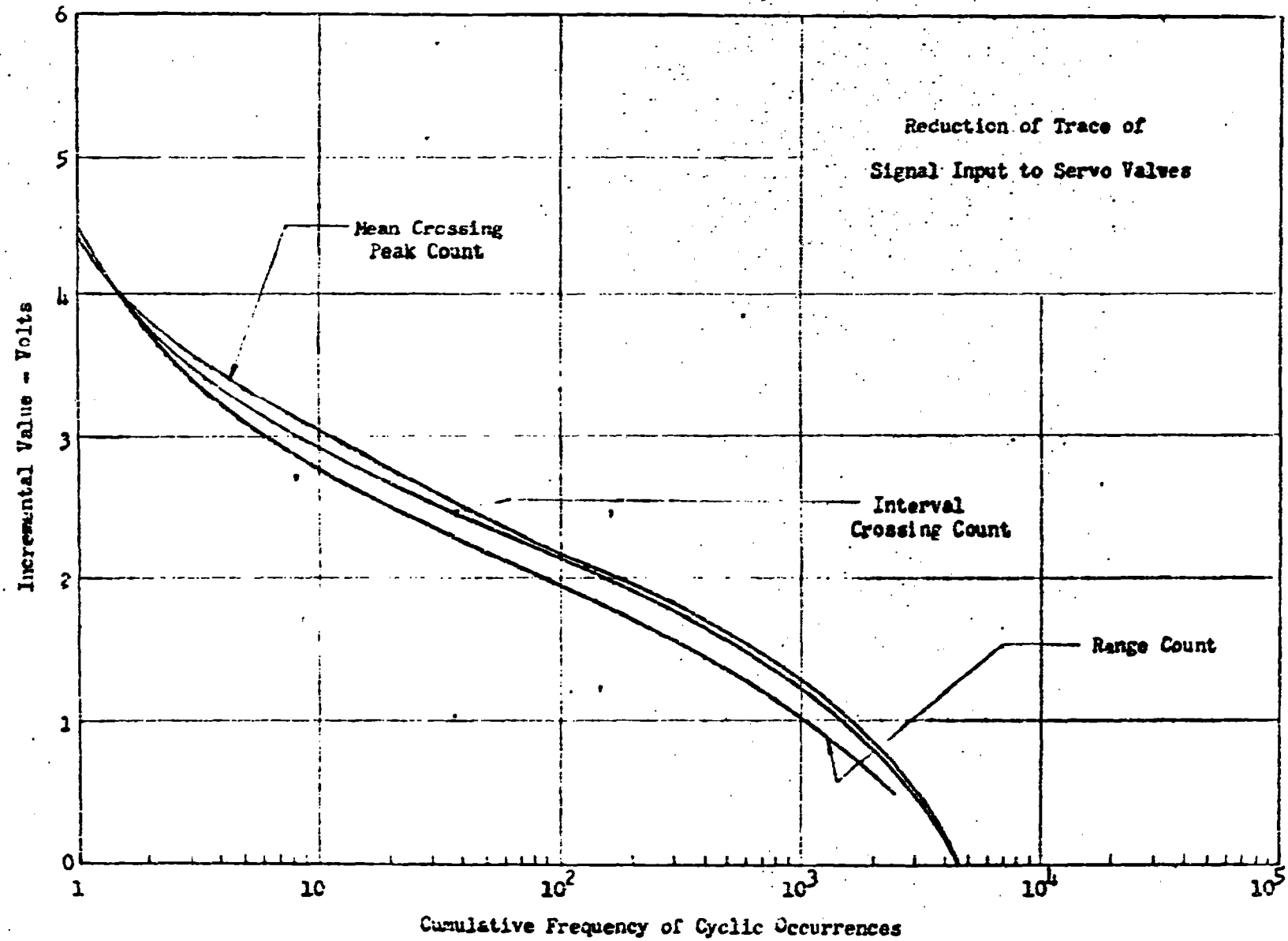



Figure 17 Comparison of Trace Reductions - Wing Root Random Loading Trace

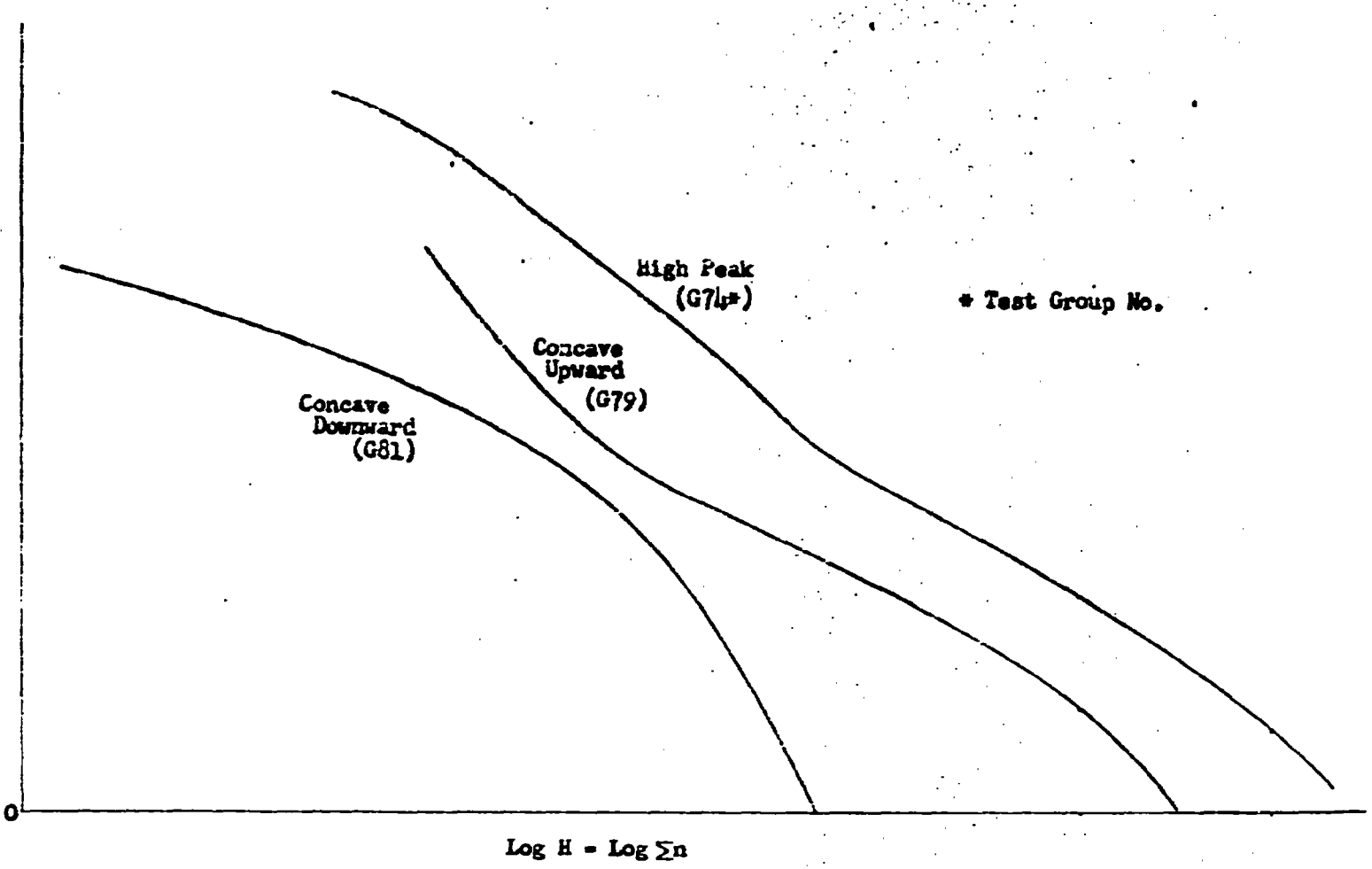



Figure 18. Schematic of High Peak, Concave Upward and Concave Downward Gust Loading Spectra.

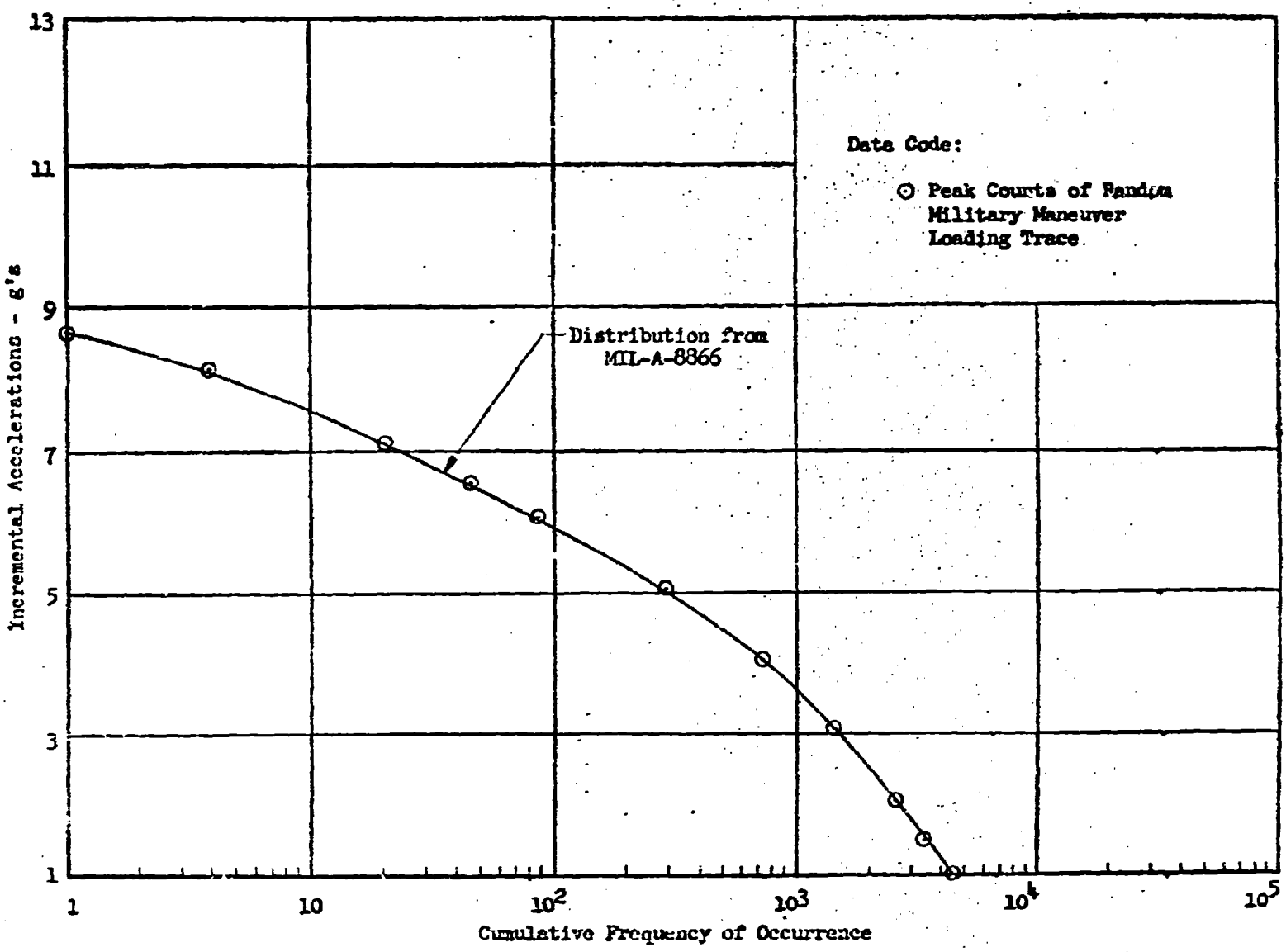



Figure 19 Comparison of Military Maneuver Loading Spectrum with Distribution Specified in MIL-A-8866 for Class "A" Aircraft

Figure 20 Sample of Random Military Maneuver Loading Trace

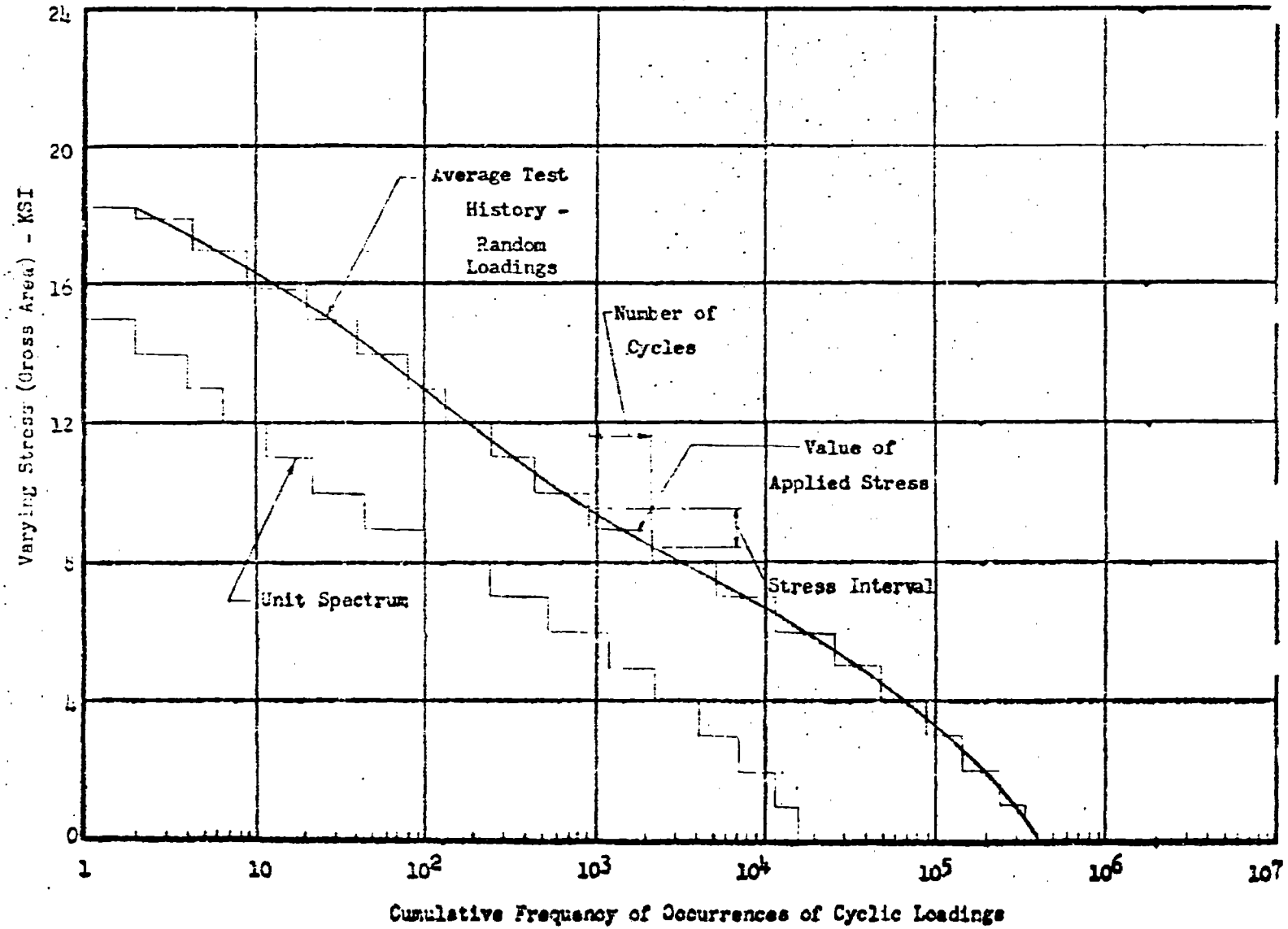
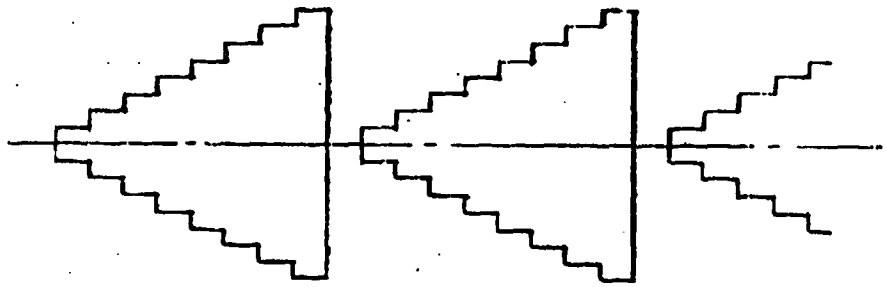
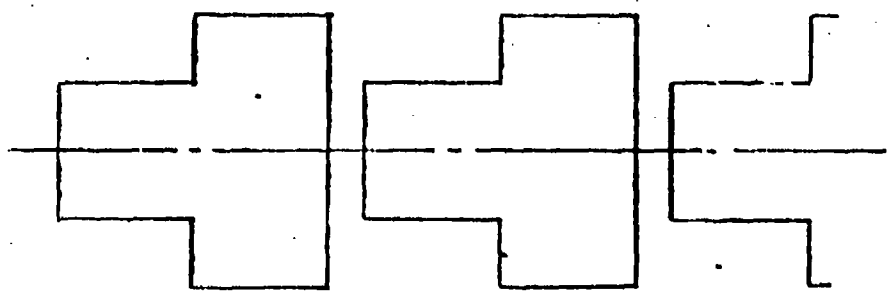


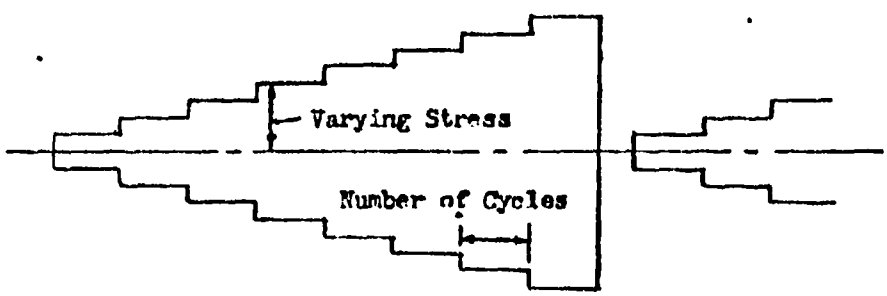

Figure 21 Development of Ordered Loading Spectrum



Low-High Sequence, Small Stress Interval, Small Unit Spectrum



Low-High Sequence, Large Stress Interval, Small Unit Spectrum




Low-High Sequence, Small Stress Interval, Large Unit Spectrum

Figure 22. Schematic Representation of Sequence Stress Interval, and Unit Spectrum Size

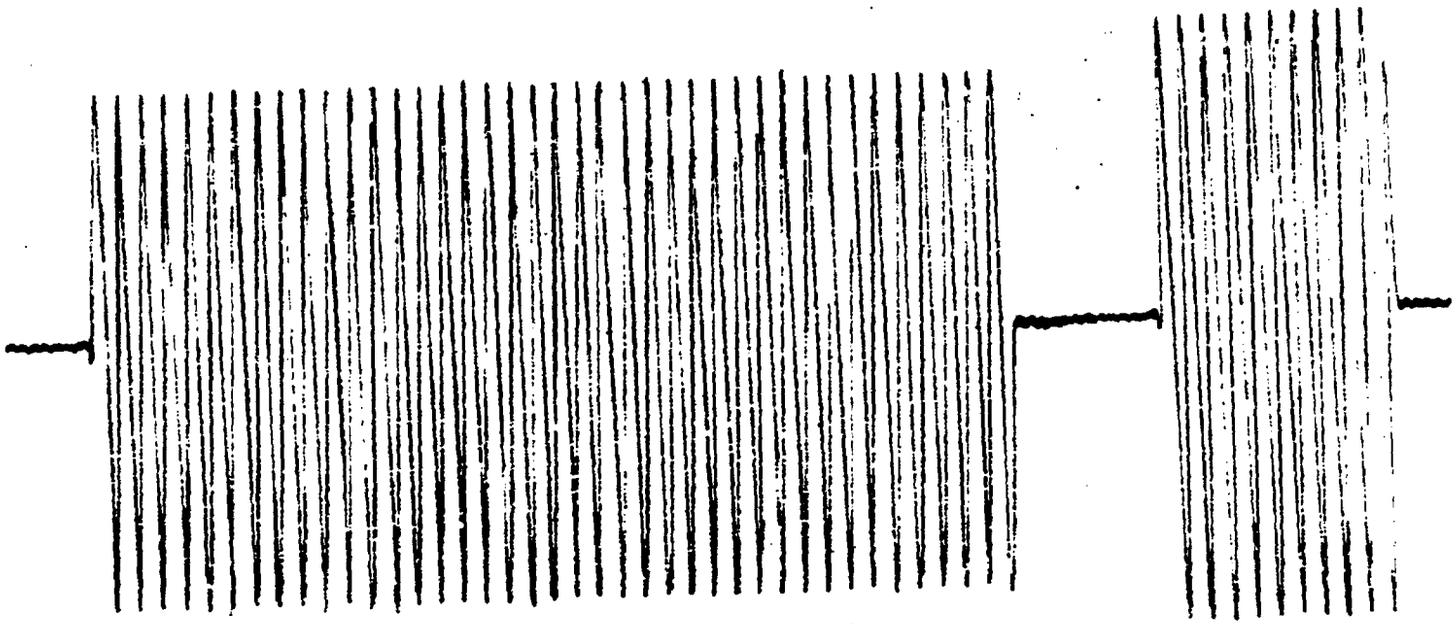


Figure 23 Partial Trace of an Ordered Gust Loading History

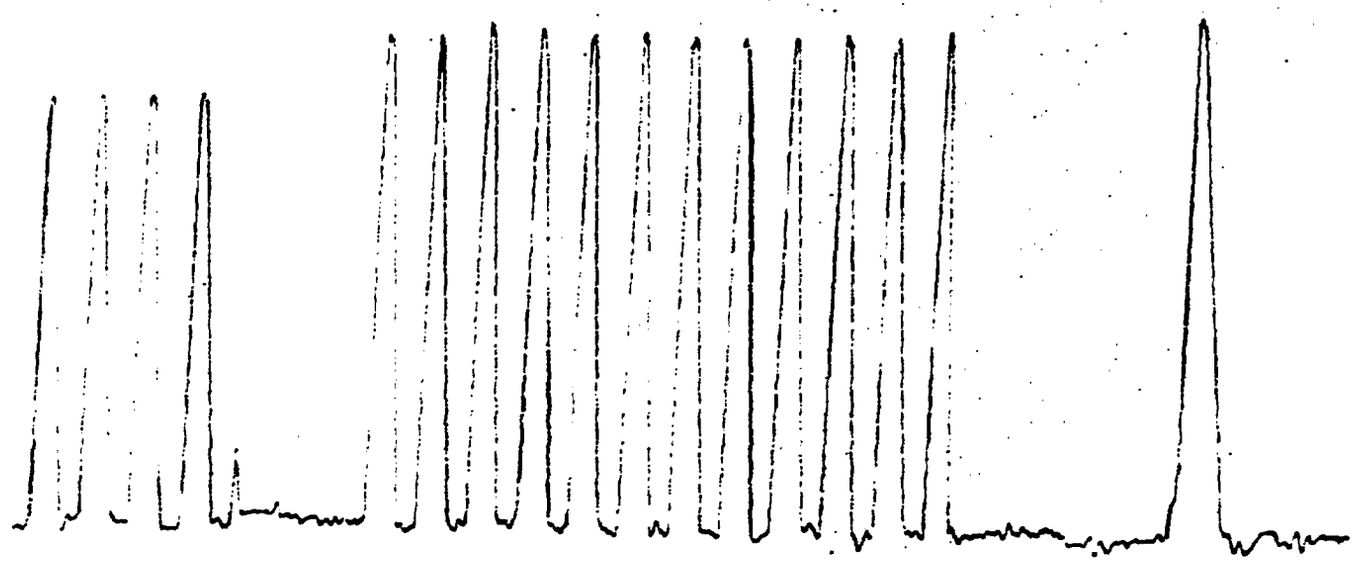


Figure 24 Sample of Ordered Military Maneuver Loading Trace

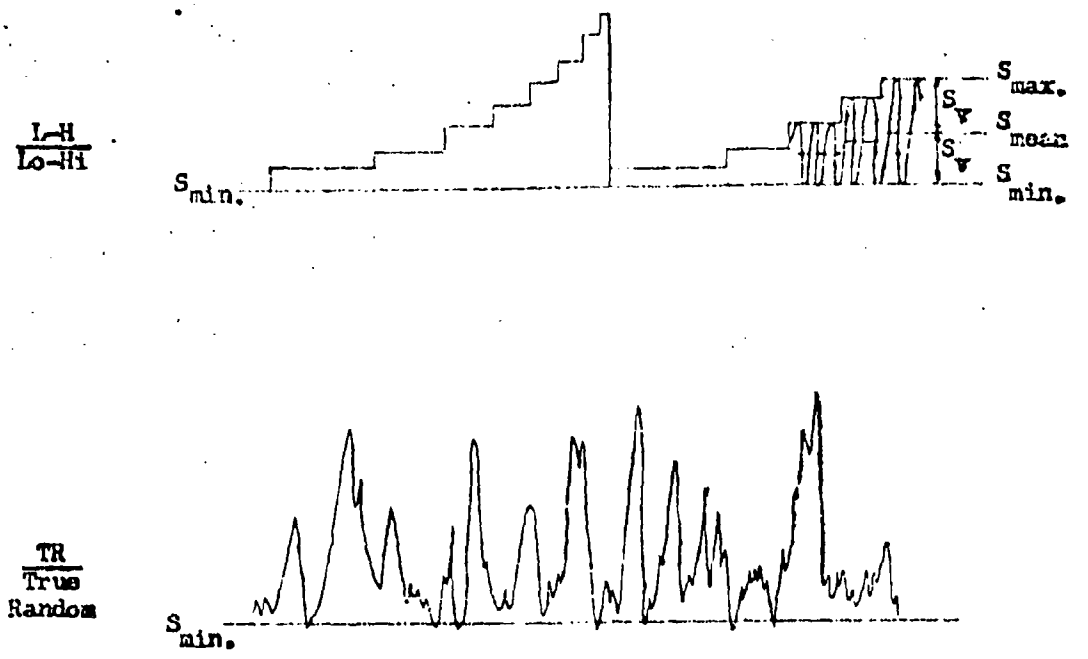



Figure 25. Schematic Diagrams of Maneuver Loading Sequences for Coupons

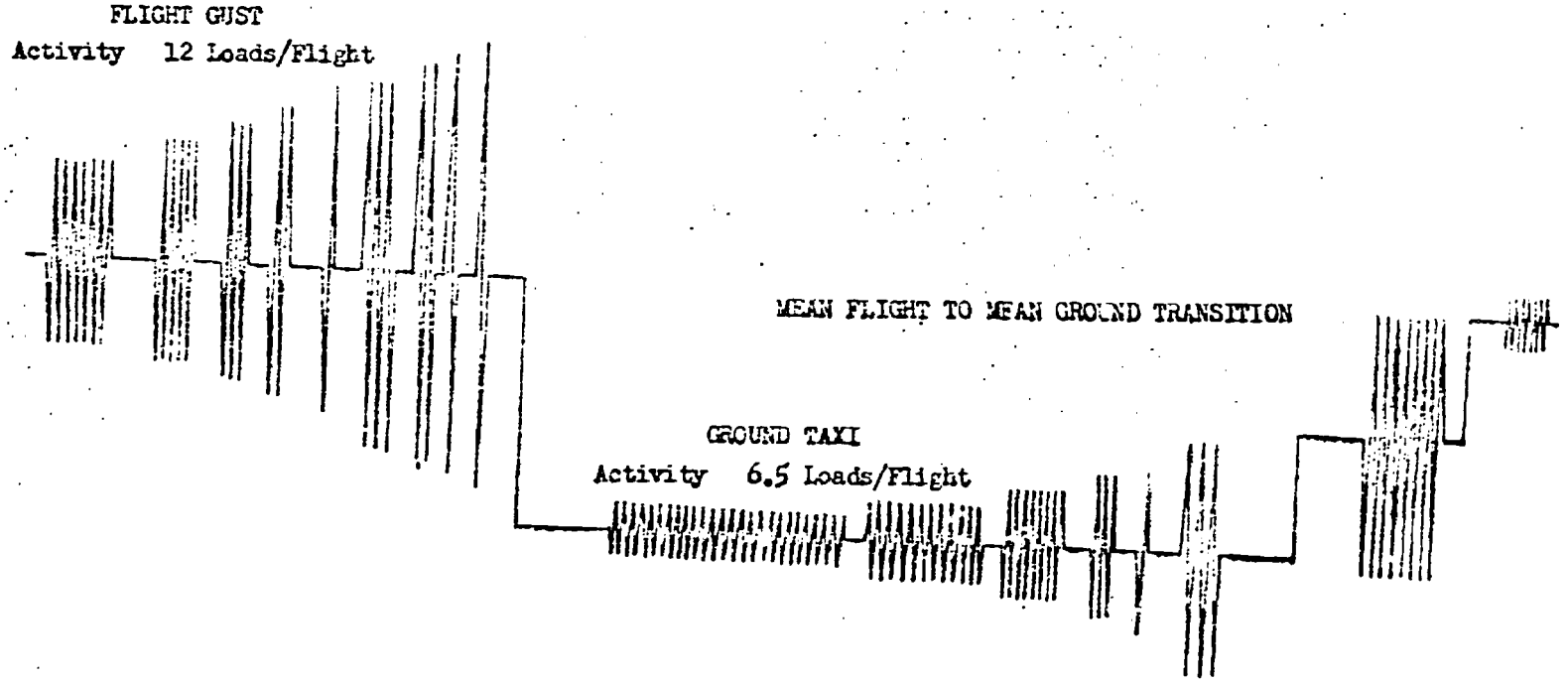



Figure 26 Schematic Representation of Ordered Loading Trace -- Gust and Ground Loadings plus Ground-to-Air Cycles.

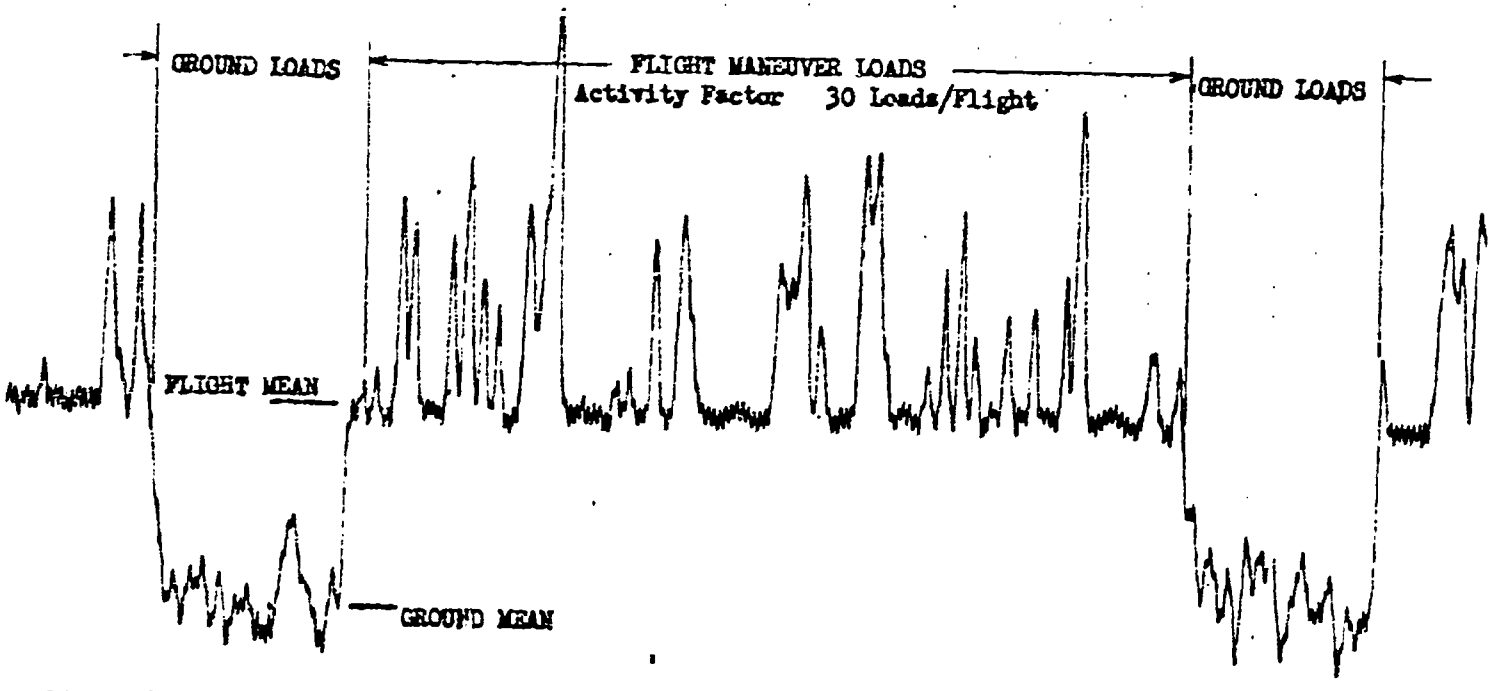



Figure 27 Sample Random Loading Trace - Composite of Military Maneuver and Ground Loadings

TABLE 4

FATIGUE LIVES PREDICTED BY MINER'S METHOD FOR GUST SPECTRA ON COUPONS

| Test Group No. | Sequence | Geometric Mean of Test Life ($10^6$ cycles) | Predicted Life ($10^6$ cycles) Miner's Method | $\frac{N_L \text{ Test}}{N_L \text{ Pred.}}$ |
|---|---|---|---|---|
| G66 | True Random | 1.650 | 4.296 | .384 |
| G67 | Lo-Hi | 1.230 | .668 | 1.841 |
| G68 | Lo-Hi | 4.165 | 3.074 | 1.355 |
| G69 | Lo-Hi | 6.005 | 3.178 | 1.890 |
| G70 | True Random | .229 | .484 | .473 |
| G71 | Lo-Hi | .255 | .518 | .492 |
| G72 | True Random | .359 | .290 | 1.238 |
| G73 | Lo-Hi | .248 | .099 | 2.505 |
| G74 | Lo-Hi | .579 | .353 | 1.640 |
| G75 | Lo-Hi | .274 | .196 | 1.398 |
| G76 | True Random | .057 | .057 | 1.000 |
| G77 | Lo-Hi | .058 | .055 | 1.055 |
| G78 | True Random | .270 | .317 | .852 |
| G79 | Lo-Hi | .804 | .453 | 1.775 |
| G80 | True Random | .193 | .082 | 2.354 |
| G81 | Lo-Hi | .144 | .052 | 2.769 |

)UND,

| $\frac{N_L \text{ Test}}{N_L \text{ Pred.}}$ |
|---|
| 1.780 |
| 1.133 |
| .769 |
| .078 |
| .112 |
| .271 |
| .238 |
| .597 |
| .862 |
| .611 |

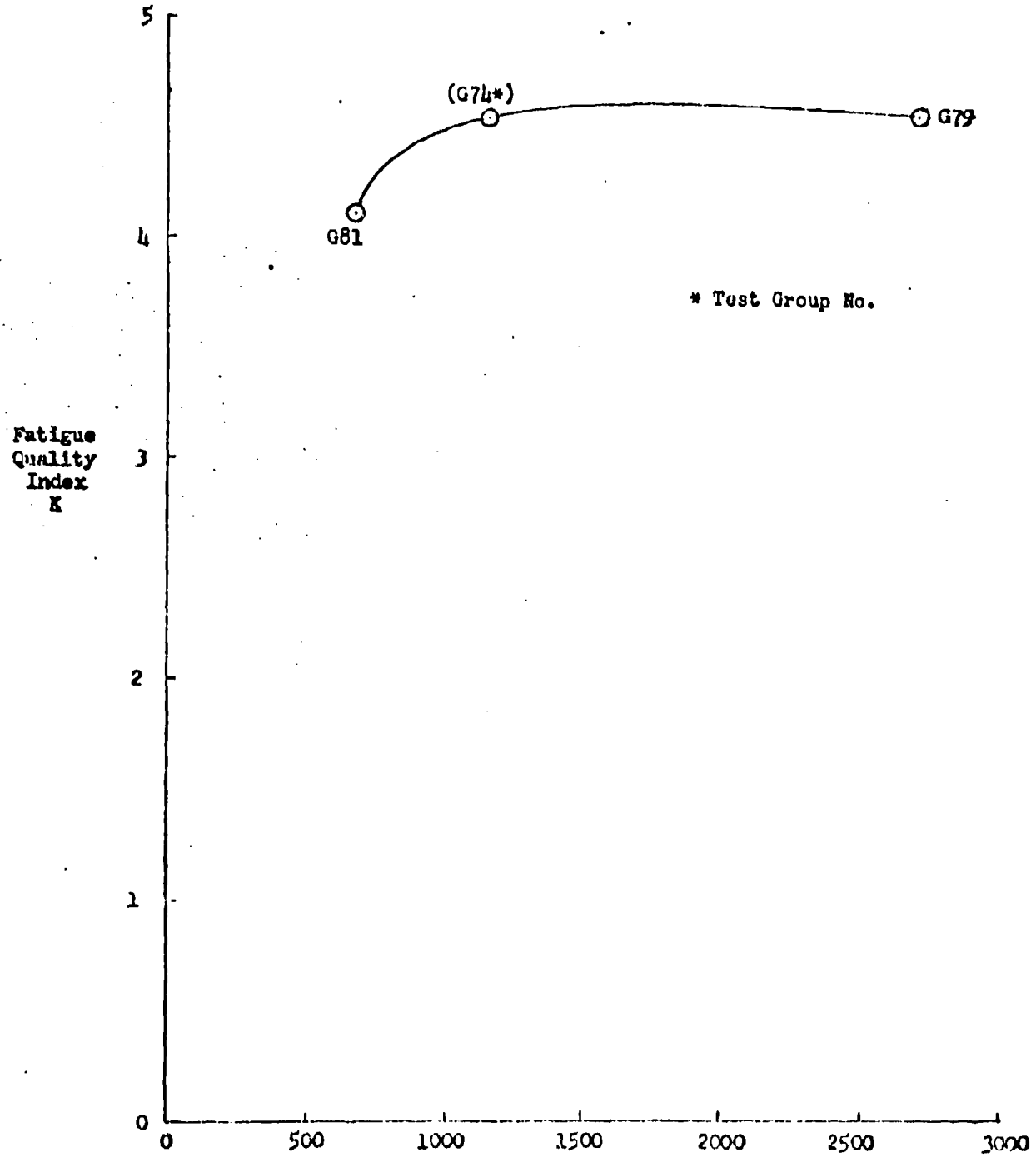



Figure 28. Variation in Quality Index (K) with slope of gust loading spectra in the high stress range.

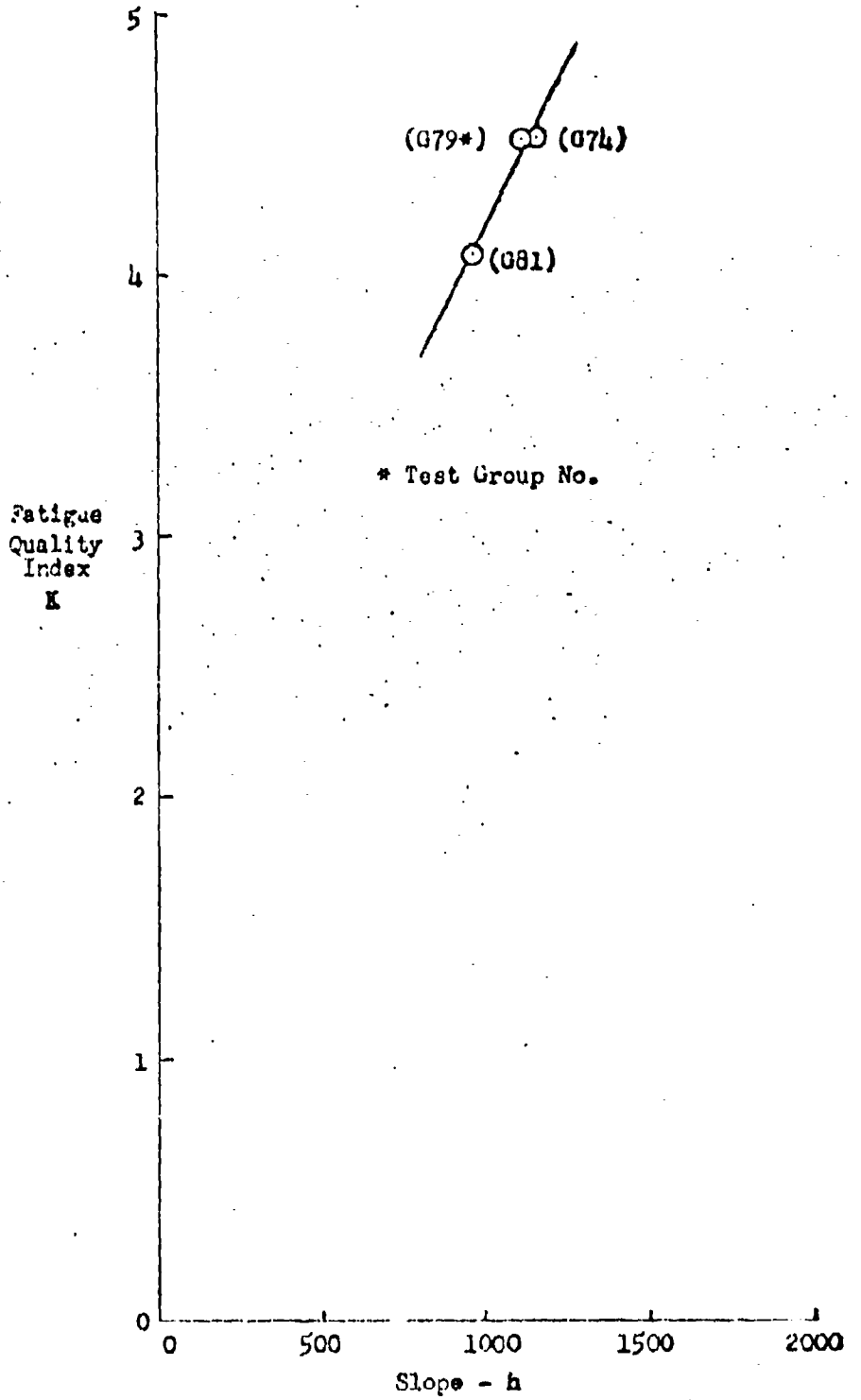



Figure 29 Variation in Quality Index (K) with Slope of Gust Loading Spectra in Midstress Range of Maximum Calculated Fatigue Damage.

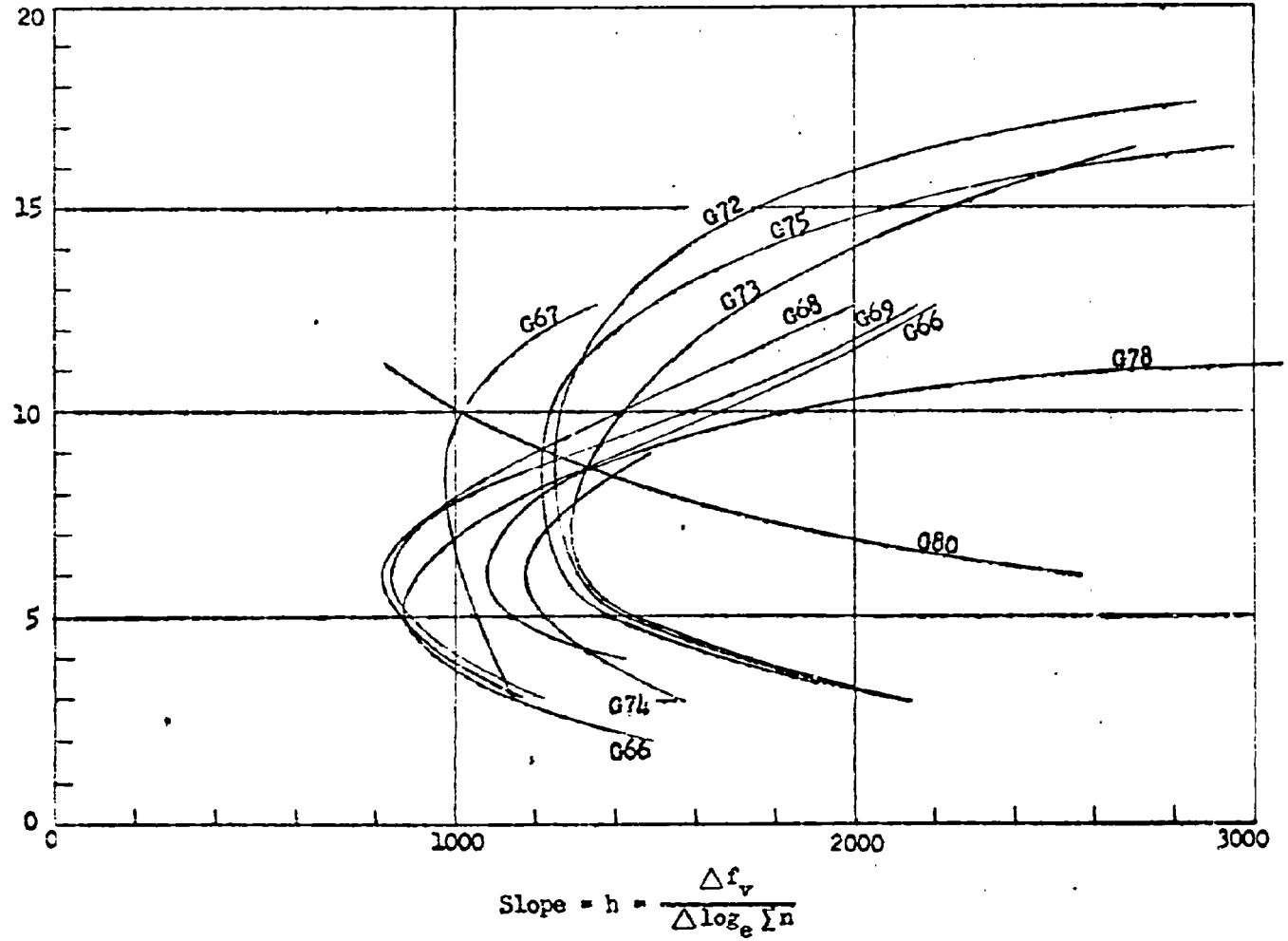



Figure 30. Varying Stress versus Slope of Gust Loading Spectra

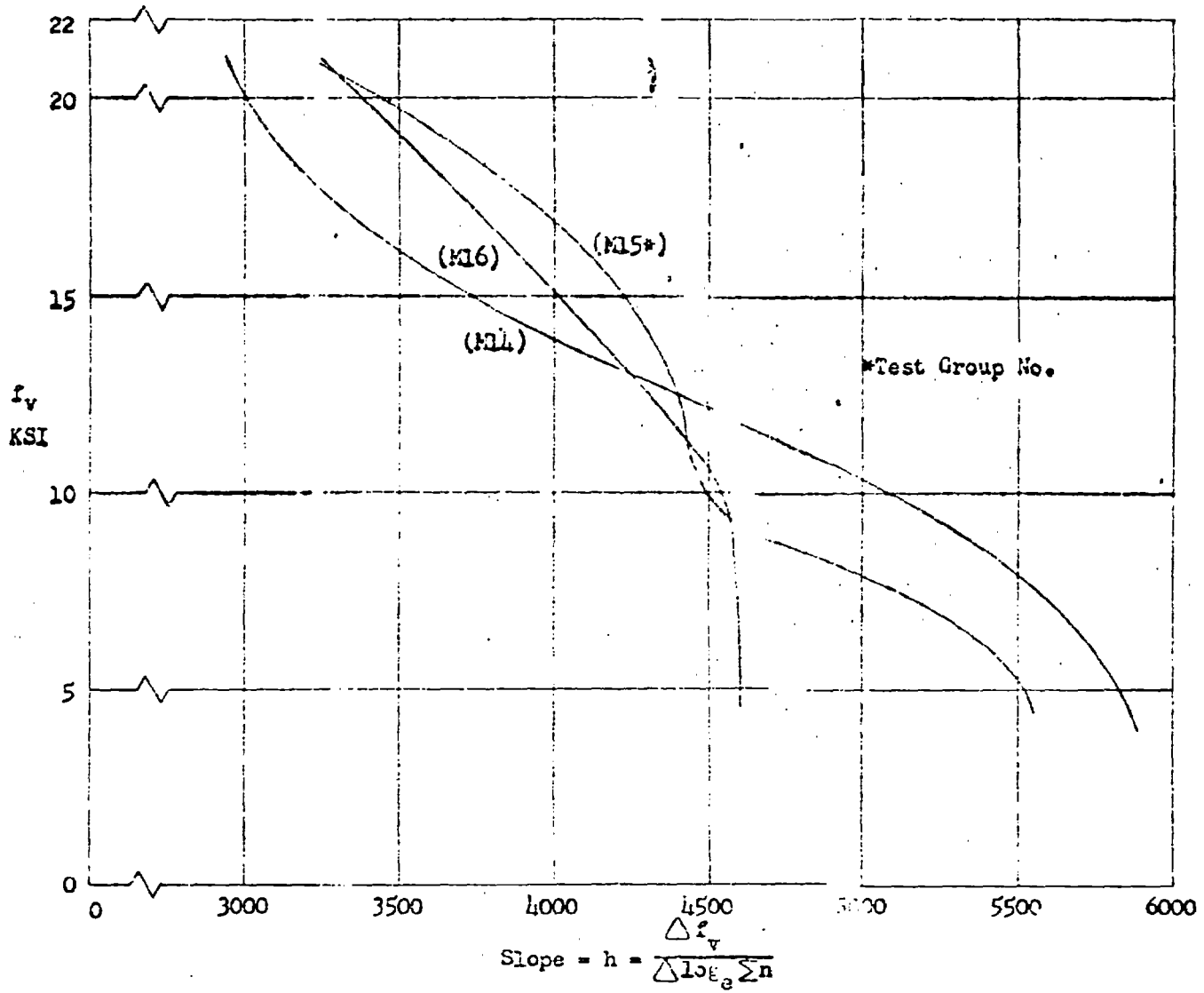



Figure 31 Varying Stress versus Slope of Maneuver Load Spectra

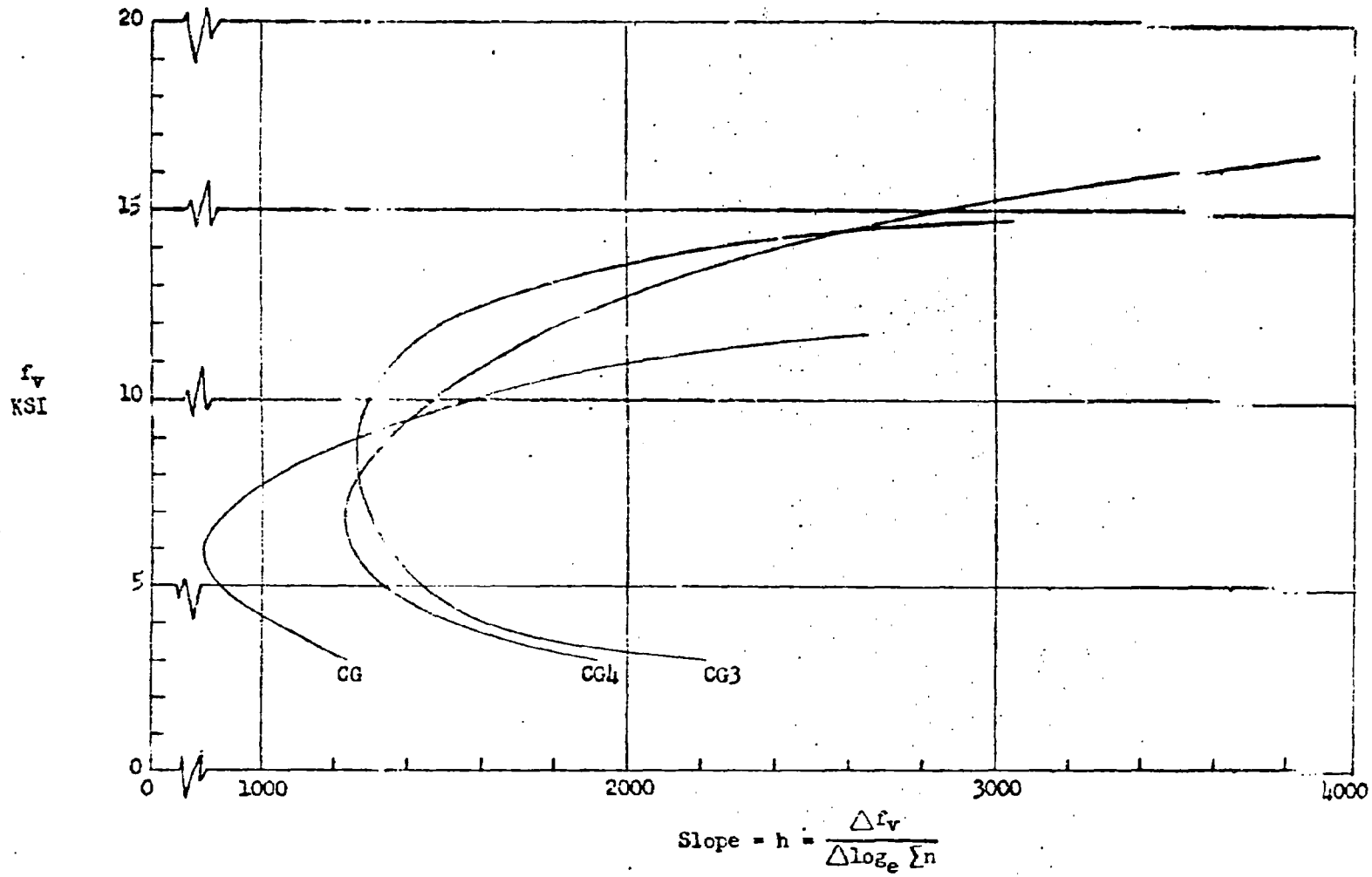



Figure 32 Varying Stress versus Slope of Composite Gust Loading Spectra

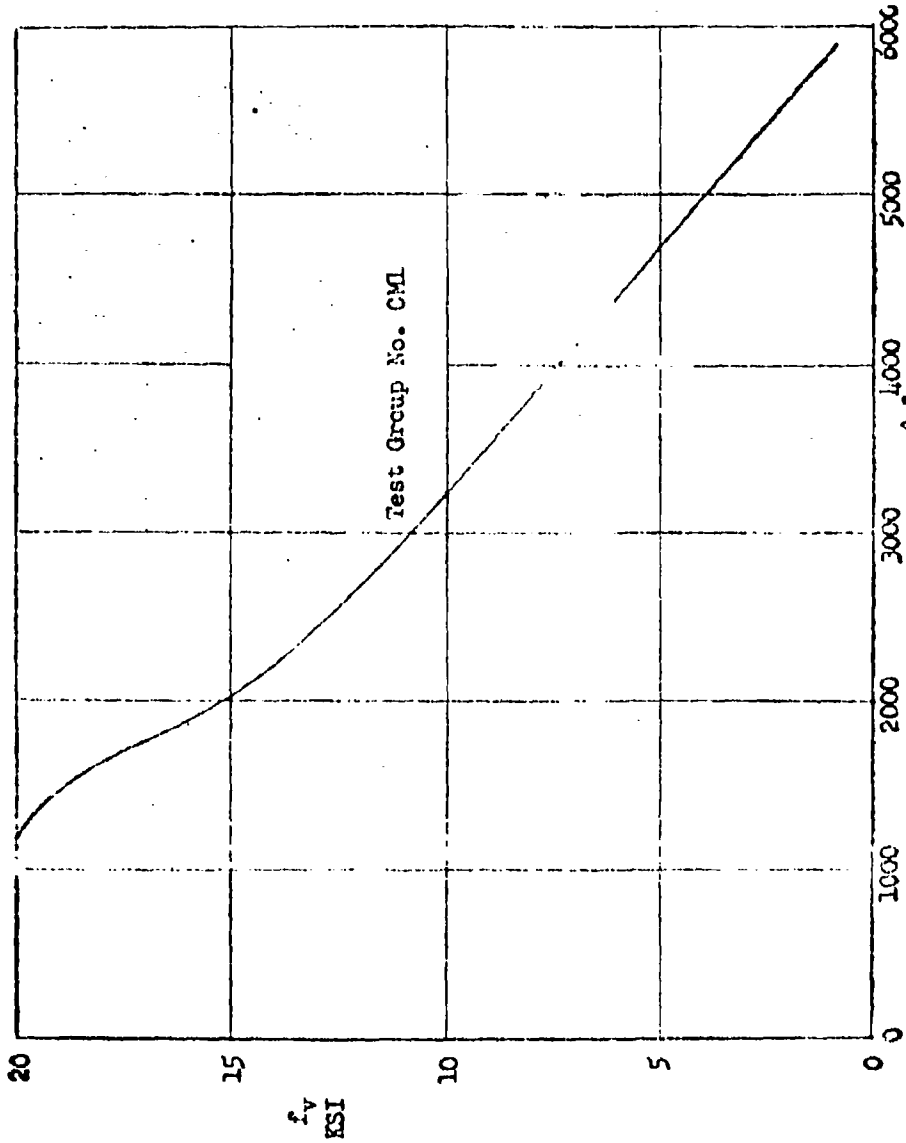



Figure 33 Varying Stress versus Slope of Composite Maneuver Spectrum

TABLE 6

FATIGUE LIVES PREDICTED FOR COUPONS WITH ADJUSTMENTS IN K FOR SLOPE OF LOADING SPECTRA

| Test Group No. | $f_{mean}$ KSI (Air Load Only) | Geom. Mean of Test Life ($10^6$ Cycles) | Midstress Slope Adjustment (a) | | | | | High Stress Slope Adjustment (b) | | | | | |
|---|---|---|---|---|---|---|---|---|---|---|---|---|---|
| | | | $f_v$ KSI Max. Cal. Dam. | $h_{@f_v}$ $\frac{\Delta psi}{\Delta Log_2 n}$ | K Fig. 29 | $N_{L_{pred}}$ ($10^6$ Cycles) | $\frac{N_{L_{Test}}}{N_{L_{Pred}}}$ | $f_{v_{peak}}$ KSI (Air Load Only) (c) | $0.9f_{v_{peak}}$ KSI | $h_{@.9f_{v_{peak}}}$ $\frac{\Delta psi}{\Delta Log_2 n}$ | K Fig. 28 | $N_{L_{pred}}$ ($10^6$ Cycles) | $\frac{N_{L_{Test}}}{N_{L_{Pred}}}$ |
| G66 | 6 | 1.650 | 6.50 | 940 | 4.02 | 50.000 | .033 | 14.00 | 12.60 | 2200 | 4.56 | 19.000 | .087 |
| G67 | | 1.230 | 8.15 | 980 | 4.18 | 4.300 | .286 | 14.00 | 12.60 | 1350 | 4.55 | 2.100 | .585 |
| G68 | | 4.165 | 6.20 | 840 | 3.76 | 100.000 | .0416 | 14.00 | 12.60 | 2000 | 4.57 | 8.400 | .496 |
| G69 | | 6.005 | 6.30 | 820 | 3.70 | 90.000 | .0667 | 14.00 | 12.60 | 2150 | 4.56 | 8.400 | .715 |
| G72 | 6 | .359 | 5.35 | 1370 | 5.00 | .280 | 1.282 | 19.52 | 17.57 | 2850 | 4.50 | .480 | .748 |
| G73 | 12 | .248 | 6.60 | 1290 | 4.91 | .110 | 2.253 | 18.30 | 16.47 | 2700 | 4.52 | .170 | 1.460 |
| G75 | | .274 | | | (f) | | | 18.30 | 16.47 | 2950 | 4.49 | .350 | .783 |
| G78 | | .312 | 5.65 | 1080 | 4.41 | .620 | .504 | 13.50 | 11.15 | 3080 | 4.47 | .600 | .520 |
| G80 | 12 | .226 | | | (f) | | | 13.50 | 11.15 | 830 | 4.38 | .110 | 2.053 |
| M14 | (d) | .027 | 12.42 | 890 | 3.89 | .032 | .844 | 20.81 | 17.73 | 3680 | (e) | | |
| M15 | (d) | .014 | 13.50 | 870 | 3.83 | .026 | .539 | 21.00 | 18.90 | 4750 | (e) | | |
| M16 | (d) | .012 | 14.70 | 810 | 3.62 | .044 | .273 | 21.00 | 18.90 | 3620 | (e) | | |
| CG1 | 6 | .998 | 7.77 | 1000 | 4.18 | 33.900 | .0294 | 13.00 | 11.70 | 2650 | 4.52 | 1.800 | .554 |
| CG3 | 12 | .142 | 6.10 | 1340 | 5.00 | .266 | .534 | 16.30 | 14.67 | 3050 | 4.48 | .462 | .307 |
| CG4 | 12 | .250 | 5.70 | 1270 | 4.90 | .374 | .669 | 18.30 | 16.47 | 3900 | (e) | | |
| CM1 | (d) | .011 | 12.50 | 2570 | (g) | | | 21.20 | 19.00 | 2480 | 4.56 | .025 | .44 |

(a) Prediction Based on Quality Index Adjustment for Slope of Loading Spectra in Midstress Range of Maximum Calculated Fatigue Damage.
(b) Prediction Based on Quality Index Adjustment for Slope of Loading Spectra at 90% of the Peak Varying Stress.
(c) Peak or Largest Varying Stress in Spectra.
(d) $f_{min}$ of 5.4 KSI
(e) Slope of Loading Spectra is Outside Range of Figure 28.
(f) Compatible Combinations of K and h do not Satisfy Curve in Figure 29.
(g) Slope of Loading Spectra is Outside Range of Figure 29.

TABLE 7

EVALUATION OF FATIGUE DAMAGE FOR QUALITY INDICES OF 2, 4, AND 6

Unit Spectra for Test Group No. 366

| Varying Stress $f_v$ KSI | Applied Cycles n | Cycles to Failure N $f_m$ = 6 KSI | Cycle Ratio $10^{-5}(\frac{n}{N})$ | Fatigue Damage % $\frac{n}{N}$ | Cycles to Failure N $f_m$ = 6 KSI | Cycle Ratio $10^{-3}(\frac{n}{N})$ | Fatigue Damage % $\frac{n}{N}$ | Cycles to Failure N $f_m$ = 6 KSI | Cycle Ratio $10^{-1}(\frac{n}{N})$ | Fatigue Damage % $\frac{n}{N}$ |
|---|---|---|---|---|---|---|---|---|---|---|
| | | K = 2 | | | K = 4 | | | K = 6 | | |
| .55 | 612800 | - | 0 | | - | 0 | 0 | - | 0 | 0 |
| 1.55 | 460000 | - | 0 | | - | 0 | 0 | - | 0 | 0 |
| 2.55 | 310000 | - | 0 | | - | 0 | 0 | - | 0 | 0 |
| 3.55 | 180000 | - | 0 | | - | 0 | 0 | 4200000 | .43 | 6.3 |
| 4.55 | 64000 | - | 0 | | - | 0 | 0 | 430000 | 1.49 | 21.9 |
| 5.55 | 25500 | - | 0 | | 5200000 | 4.90 | 13.2 | 120000 | 2.13 | 31.4 |
| 6.55 | 7000 | - | 0 | | 880000 | 7.95 | 21.4 | 88000 | 1.21 | 17.8 |
| 7.55 | 2300 | - | 0 | | 300000 | 7.67 | 20.6 | 34000 | .68 | 10.0 |
| 8.55 | 650 | - | 0 | | 135000 | 4.81 | 12.9 | 21000 | .31 | 4.6 |
| 9.55 | 280 | - | 0 | | 73000 | 3.84 | 10.3 | 14000 | .20 | 2.9 |
| 10.55 | 150 | 7000000 | 2.14 | 12.8 | 46000 | 3.26 | 8.8 | 10000 | .15 | 2.3 |
| 11.55 | 70 | 1500000 | 4.67 | 27.9 | 30000 | 2.33 | 6.3 | 7100 | .10 | 1.5 |
| 12.55 | 32 | 590000 | 5.42 | 32.4 | 20500 | 1.56 | 4.2 | 5400 | .06 | .9 |
| 13.55 | 13 | 290000 | 4.48 | 26.9 | 15000 | .87 | 2.3 | 3900 | .03 | .4 |
| | | | $\Sigma$ 16.71 | $\Sigma$ 100.0 | | $\Sigma$ 37.19 | $\Sigma$ 100.0 | | $\Sigma$ 6.79 | $\Sigma$ 100.0 |

$K_T = 2$
$K_T = 4$
$K_T = 6$
Hard Aluminum Alloys
$f_{mean}$ = 6 KSI
$f_v$ KSI
14
13
12
11
10
9
8
7
6
5
4
3
2
$10^3$
$10^4$
$10^5$
$10^6$
$10^7$

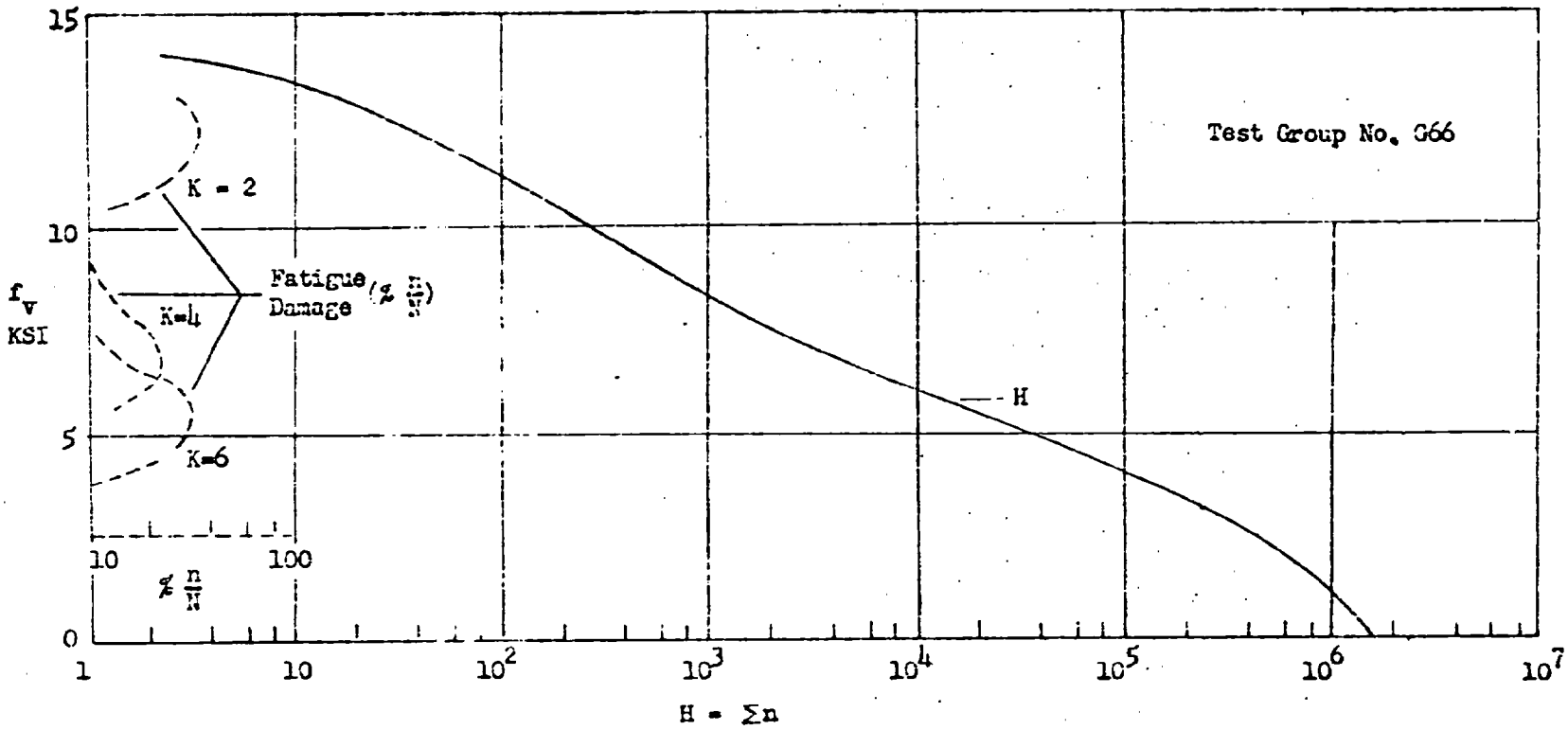



Figure 35. Illustration of a Gust Loading Spectra and the Corresponding Curves for Fatigue Damage at Quality Indices of 2, 4, and 6.

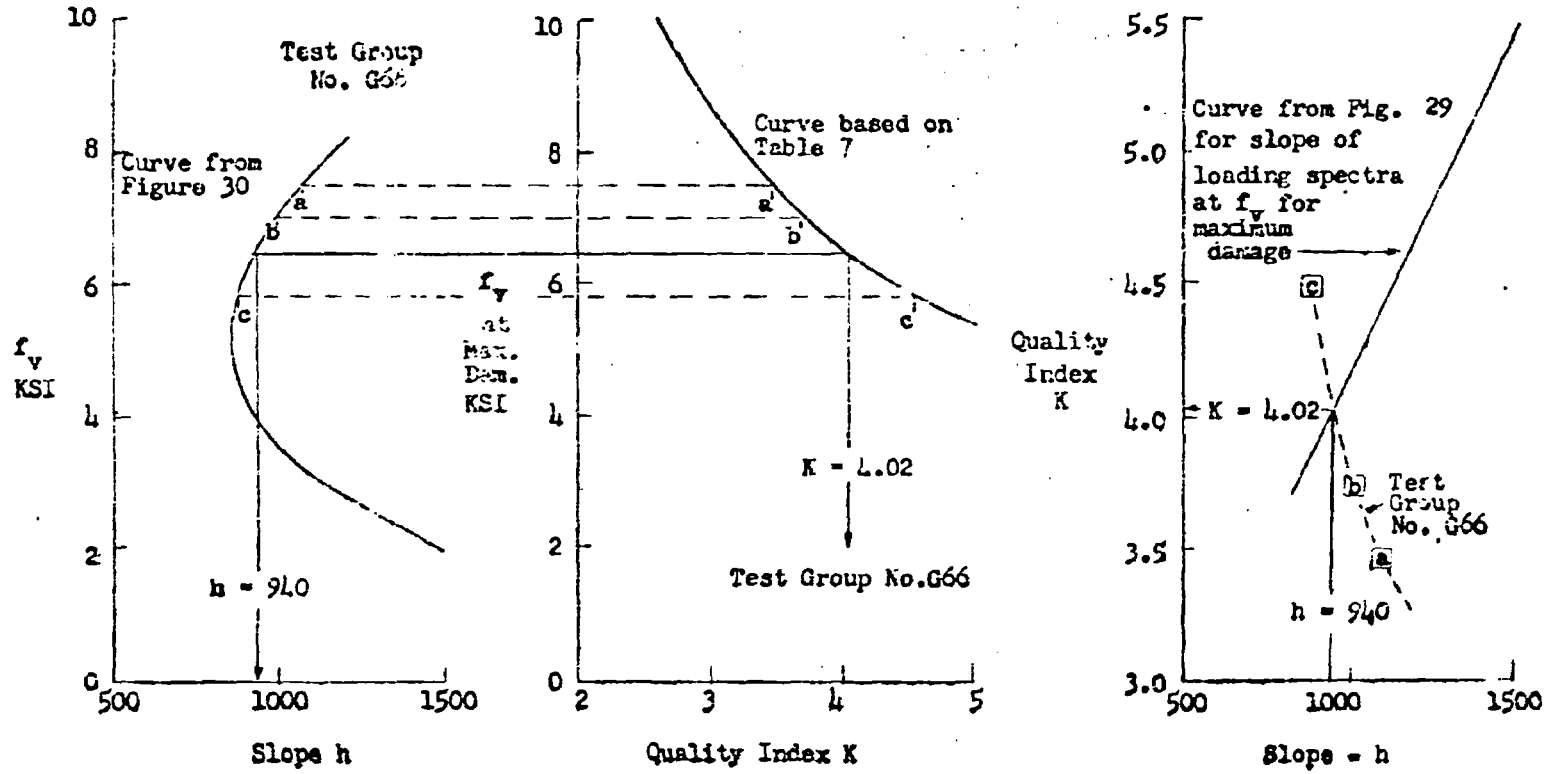



Figure 36. Illustration of procedure used to correlate quality index and slope of loading spectra in stress range of maximum fatigue damage.

TABLE 8

FATIGUE QUALITY INDEX FOR GUST SPECTRA ON COUPONS

Specimen, Figure 15

| Test Group No. | Type of Spectrum | Sequence | Number of Specimens | Geometric $K_T$ | K First Specimen in Test Group | K Quality Index Method | | |
|---|---|---|---|---|---|---|---|---|
| | | | | | | Minimum | Maximum | Geometric Mean |
| G66 | | True Random | 4 | 4 | 7.18 | 6.62 | 7.18 | 6.92 |
| G67 | | Lo-Hi | 5 | 4 | 4.63 | 4.57 | 6.23 | 5.05 |
| G68 | Low | Lo-Hi | 5 | 4 | 5.01 | 4.97 | 5.50 | 5.19 |
| G69 | Peak | Lo-Hi | 5 | 4 | 5.11 | 4.53 | 5.11 | 4.85 |
| G70 | | True Random | 6 | 7 | >8 | 7.38 | >8 | >8 |
| G71 | | Lo-Hi | 5 | 7 | >8 | >8 | >8 | >8 |
| G72 | | True Random | 7 | 4 | 4.32 | 4.32 | 5.27 | 4.78 |
| G73 | | Lo-Hi | 8 | 4 | 4.12 | 3.81 | 4.63 | 4.24 |
| G74 | High | Lo-Hi | 5 | 4 | 4.78 | 4.22 | 4.78 | 4.52 |
| G75 | Peak | Lo-Hi | 5 | 4 | 4.52 | 4.52 | 4.76 | 4.61 |
| G76 | | True Random | 6 | 7 | >8 | 7.58 | >8 | >8 |
| G77 | | Lo-Hi | 6 | 7 | >8 | >8 | >8 | >8 |
| G78 | Concave | True Random | 10 | 4 | 5.25 | 4.87 | 5.60 | 5.33 |
| G79 | upward | Lo-Hi | 5 | 4 | 4.20 | 4.36 | 4.74 | 4.52 |
| G80 | Concave | True Random | 4 | 4 | 4.30 | 3.98 | 4.30 | 4.17 |
| G81 | downward | Lo-Hi | 5 | 4 | 4.40 | 3.81 | 4.22 | 4.08 |

TABLE 9

FATIGUE QUALITY INDEX FOR MANEUVER GROUND AND COMPOSITE SPECTRA ON COUPONS

Specimen, Figure 15

| Test Group No. | Type of Spectrum | Sequence | Number of Specimens | Geometric $K_T$ | K First Specimen in Test Group | K Quality Index Method | | |
|---|---|---|---|---|---|---|---|---|
| | | | | | | Minimum | Maximum | Geometric Mean |
| ML4 | Fighter Maneuver | True Random | 7 | 4 | 4.15 | 3.60 | 4.75 | 4.18 |
| ML5 | | Lo-Hi | 5 | 4 | 4.85 | 4.20 | 5.40 | 4.76 |
| ML6 | | Lo-Hi | 5 | 4 | 7.10 | 4.80 | 7.10 | 5.61 |
| T1 | Ground | True Random | 6 | 7 | >8 | >8 | >8 | >8 |
| T2 | | Lo-Hi | 6 | 7 | >8 | >8 | >8 | >8 |
| CG1 | Low Peak | Lo-Hi | 5 | 4 | 8.00 | 6.80 | >8 | >8 |
| CG2 | Composite | Lo-Hi | 5 | 7 | >8 | >8 | >8 | >8 |
| CG3 | High Peak | Lo-Hi | 5 | 4 | 5.70 | 5.40 | 6.20 | 5.85 |
| CG4 | Composite | Lo-Hi | 8 | 4 | 5.60 | 5.00 | 5.80 | 5.35 |
| CM1 | Composite Maneuver | True Random | 5 | 4 | 7.45 | 5.87 | 7.45 | 6.69 |

TABLE 10

FATIGUE LIVES PREDICTED FOR COMPOSITE GUST AND COMPOSITE MANEUVER SPECTRA ON COUPONS FROM QUALITY INDEX FOR FIRST SPECIMEN IN A SIMILAR TYPE OF SIMPLE FLIGHT SPECTRA

| Test Group No. | Geometric Mean of Test Life ($10^6$ Cycles) | Low Peak Gust | | High Peak Gust | | Fighter Maneuver | |
|---|---|---|---|---|---|---|---|
| | | $N_{L_{Pred}}$ ($10^6$ Cycles) | $\frac{N_{L_{Test}}}{N_{L_{Pred}}}$ | $N_{L_{Pred}}$ ($10^6$ Cycles) | $\frac{N_{L_{Test}}}{N_{L_{Pred}}}$ | $N_{L_{Pred}}$ ($10^6$ Cycles) | $\frac{N_{L_{Test}}}{N_{L_{Pred}}}$ |
| | | K = 5.01* | | K = 4.78** | | K = 4.15*** | |
| CG1 | .998 | 8.475 | .118 | | | | |
| CG3 | .142 | | | .332 | .428 | | |
| CG4 | .250 | | | .414 | .604 | | |
| CM1 | .011 | | | | | .033 | .333 |

* K for first specimen in Test Group No. G68 (Specimen No. 372)
** K for first specimen in Test Group No. G74 (Specimen No. 313)
*** K for first specimen in Test Group No. M14 (Specimen No. 342)

TABLE 11

FATIGUE LIVES PREDICTED FOR MANEUVER AND COMPOSITE MANEUVER SPECTRA ON COUPONS FROM QUALITY INDEX FOR FIRST SPECIMEN IN A GUST SPECTRUM

| Test Group No. | Geometric Mean of Test Life ($10^6$ Cycles) | Based on Low Peak Gust Spectrum | | Based on High Peak Gust Spectrum | |
|---|---|---|---|---|---|
| | | $N_{L_{Pred}}$ ($10^6$ Cycles) | $\frac{N_{L_{Test}}}{N_{L_{Pred}}}$ | $N_{L_{Pred}}$ ($10^6$ Cycles) | $\frac{N_{L_{Test}}}{N_{L_{Pred}}}$ |
| | | K = 5.01* | | K = 4.78** | |
| M14 | .027 | .015 | 1.800 | .017 | 1.588 |
| M15 | .014 | .012 | 1.167 | .013 | 1.077 |
| M16 | .012 | .016 | .750 | .018 | .667 |
| CM1 | .011 | .019 | .579 | .022 | .500 |

* K for first specimen in Test Group No. G68 (Specimen No. 372)
** K for first specimen in Test Group No. G74 (Specimen No. 313)

TABLE 12

COMPARISON OF TEST FATIGUE LIFE OF SIMPLE LOADING SPECTRA WITH THE FLIGHT PORTION OF COMPOSITE TESTS

| Composite Spectra | | Simple Spectra | | | |
|---|---|---|---|---|---|
| Test Group No. | $N_{L_{Test}}$ ($10^6$ Cycles) | Test Group No. | $N_{L_{Test}}$ ($10^6$ Cycles) | $\frac{N_{L_{Test\ Composite}}}{N_{L_{Test\ Simple}}}$ | Damage Attributed to All Other Loadings* |
| CG1 | .615 | G67 | 1.23 | .500 | .500 |
| CG2 | .068 | G71 | .255 | .267 | .733 |
| CG3 | .090 | G73 | .248 | .363 | .637 |
| CG4 | .223 | G74 | .579 | .385 | .615 |
| CM1 | .0086 | M14 | .0267 | .322 | .678 |

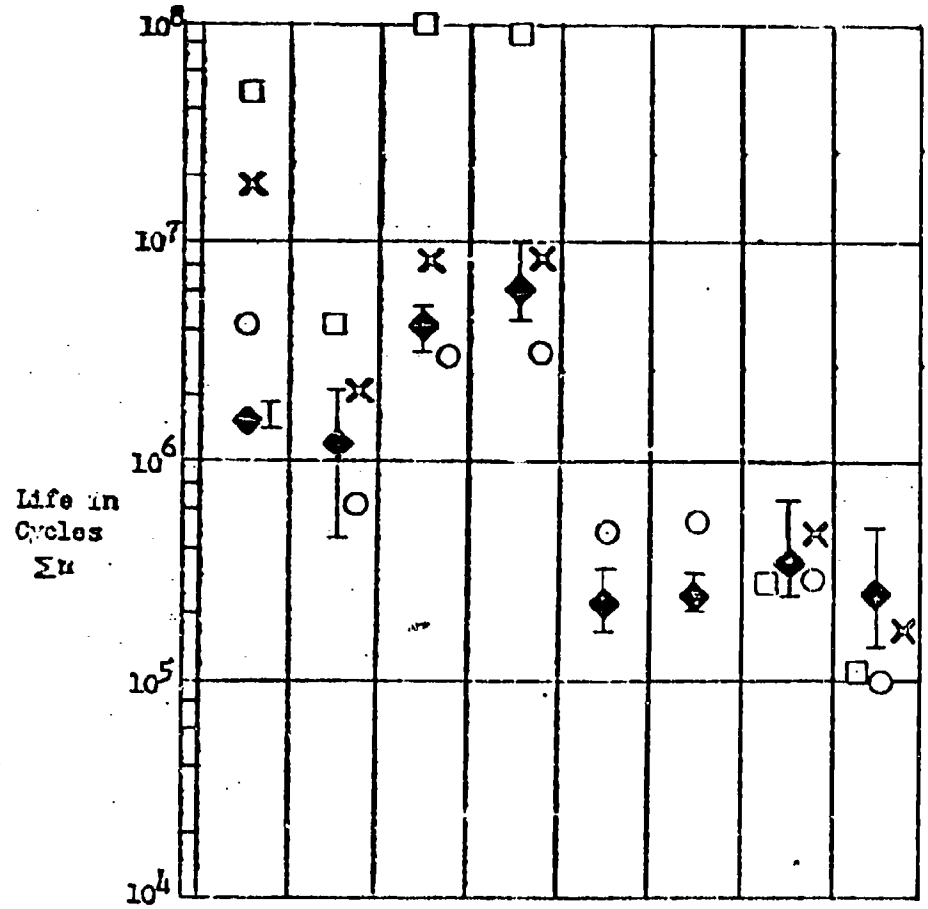
* Damage Attributable to All Other Loadings is $\Delta D = 1 - \frac{N_{L_{composite}}}{N_{L_{simple}}}$

TABLE 13

CODING IN FIGURES FOR COUPONS AND PANELS

(All Predictions are Based on Linear Cumulative Damage.)

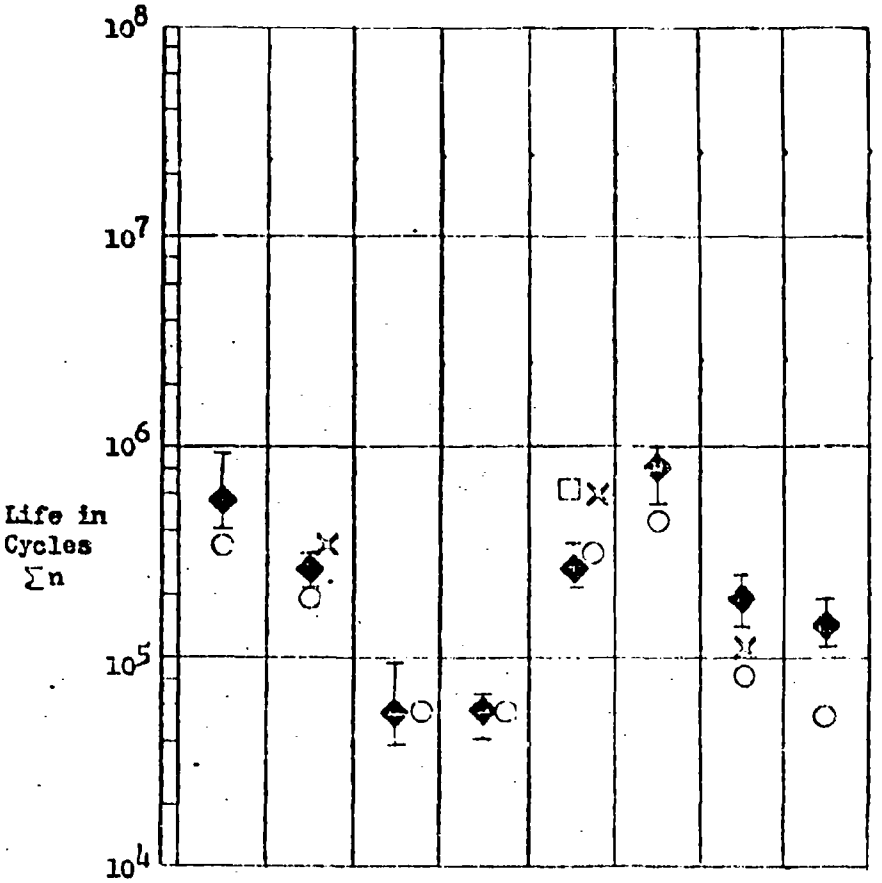
| Symbol | Meaning |
|---|---|
| ◆ | Geometric mean of test data. |
| I | Scatter band for test data. |
| ○ | Prediction based on actual S-N curve for specimen configuration (Coupons). (Miner's Method) |
| □ | Prediction based on standardized S-N curves with adjustment in K for slope of loading spectra in the mid-stress range. (Coupons) |
| ✕ | Prediction based on standardized S-N curves with adjustment in K for slope of loading spectra in the high stress range. (Coupons) |
| | Prediction based on standardized S-N curve corresponding to the Quality Index for the first specimen in a simple gust spectrum. |
| | a) S-N data based on stresses for minimum gross area. |
| ○ | 1) Quality Index for first panel in gust spectrum. |
| ⬭ | 2) Quality Index for first coupon in a low peak gust spectrum. |
| ⬭ | 3) Quality Index for first coupon in a high peak gust spectrum. |
| ○ | b) S-N data based on stresses for local gross area in fractured structural element. (Panels) |
| | Prediction based on standardized S-N curve corresponding to the Quality Index for the first specimen in a simple maneuver spectrum. |
| ◇ | a) S-N data based on stresses for minimum gross area. (Coupons and panels) |
| ◇ | b) S-N data based on stresses for local gross area in fractured structural element. (Panels) |




| Test Group No. | G66 | G67 | G68 | G69 | G70 | G71 | G72 | G73 |
|---|---|---|---|---|---|---|---|---|
| Sequence | TR | L-H | | | TR | L-H | TR | L-H |
| Block Size ($10^3$ Cycles) | 1663 | 26 | 60 | 120 | 233 | 9 | 379 | 9.25 |
| Number of Loading Steps | 18 | 4 | 14 | | 17 | 13 | 23 | 5 |
| Mean Stress KSI | 6 | | | | | 12 | | |
| Type of Spectrum | Gust | | | | | | | |
| Specimen | Notched Sheet Coupons | | | | | | | |
| $K_T$ | 4 | | | | 7 | 4 | | |
| Material | 7075-T6 | | | | | | | |

For Coding See Table 13

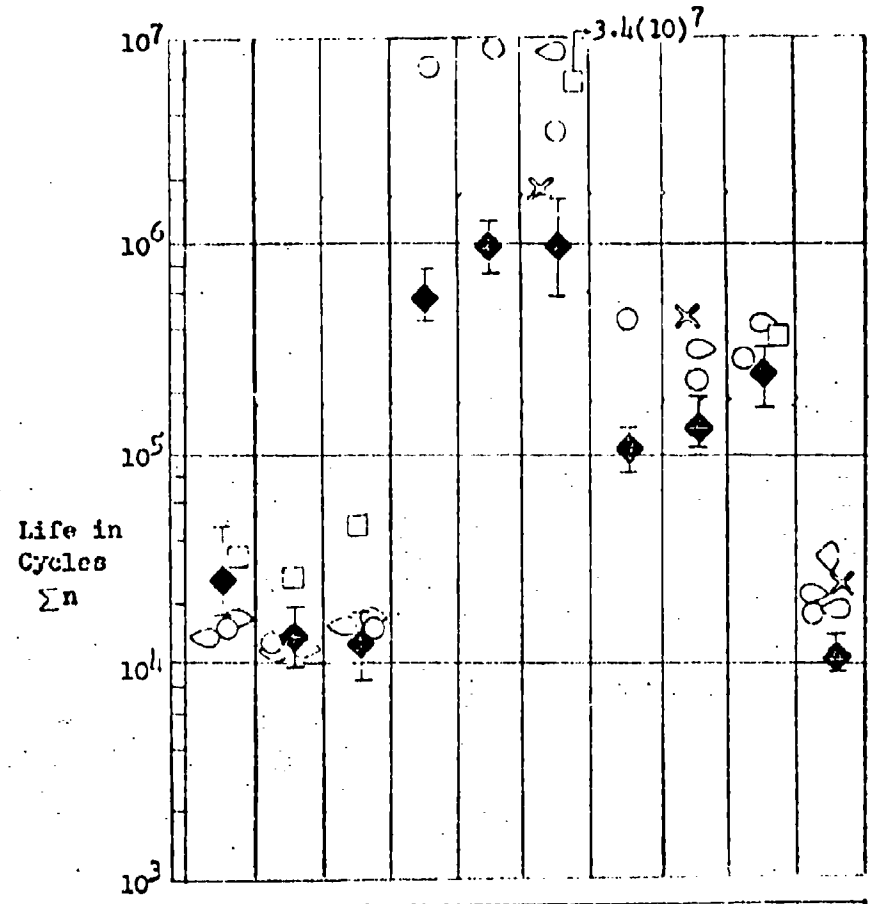
Figure 37. Comparison between Predicted and Experimental Fatigue Lives for Gust Spectra on Coupons




| Test Group No. | G74 | G75 | G76 | G77 | G78 | G79 | G80 | G81 |
|---|---|---|---|---|---|---|---|---|
| Sequence | L-H | | TR | L-H | TR | L-H | TR | L-H |
| Block Size ($10^3$ Cycles) | 16 | 32 | 58.7 | 2.5 | 273 | 826 | 197 | 115 |
| Number of Loading Steps | 19 | | 14 | 17 | 7 | | | |
| Mean Stress KSI | 12 | | | | | | | |
| Type of Spectrum | Gust | | | | | | | |
| Specimen | Notched Sheet Coupons | | | | | | | |
| $K_T$ | 4 | | 7 | | 4 | | | |
| Material | 7075-T6 | | | | | | | |

For Coding See Table 13

**Figure 38.** Comparison between Predicted and Experimental Fatigue Lives for Gust Spectra on Coupons




| Test Group No. | | | M14 | M15 | M16 | T1 | T2 | CG1 | CG2 | CG3 | CG4 | CM1 |
|---|---|---|---|---|---|---|---|---|---|---|---|---|
| Sequence | | | TR | L-H | | TR | L-H | | | | | TR |
| Block Size ($10^3$ Cycles) | | | 27.7 | 1.1 | 1 | 560 | 21.5 | 21.2 | 1.9 | 3.3 | 10.1 | 11 |
| Number of Loading Steps | | | 11 | | 40 | 18 | 11 | 26 | 21 | 29 | | |
| Minimum Stress | | Air | 5.4 | | | | | | | | | 5.45 |
| Mean Stress | K S I | Air | | | | | | 6 | | 12 | | |
| | | Ground | | | | -3 | | | | | | |
| | | G-A-G | | | | | | 1.5 | | 4.5 | | 1.22 |
| Type of Spectrum | | | Maneuver | | | Ground | | Composite Gust | | | | * |
| Specimen | | | Notched Sheet Coupons | | | | | | | | | |
| $K_T$ | | | 4 | | | 7 | | 4 | 7 | 4 | | |
| Material | | | 7075-T6 | | | | | | | | | |

* Composite Maneuver
For Coding See Table 13

Figure 39 Comparison between Predicted and Experimental Fatigue Lives for Maneuver, Ground, and Composite Spectra on Coupons

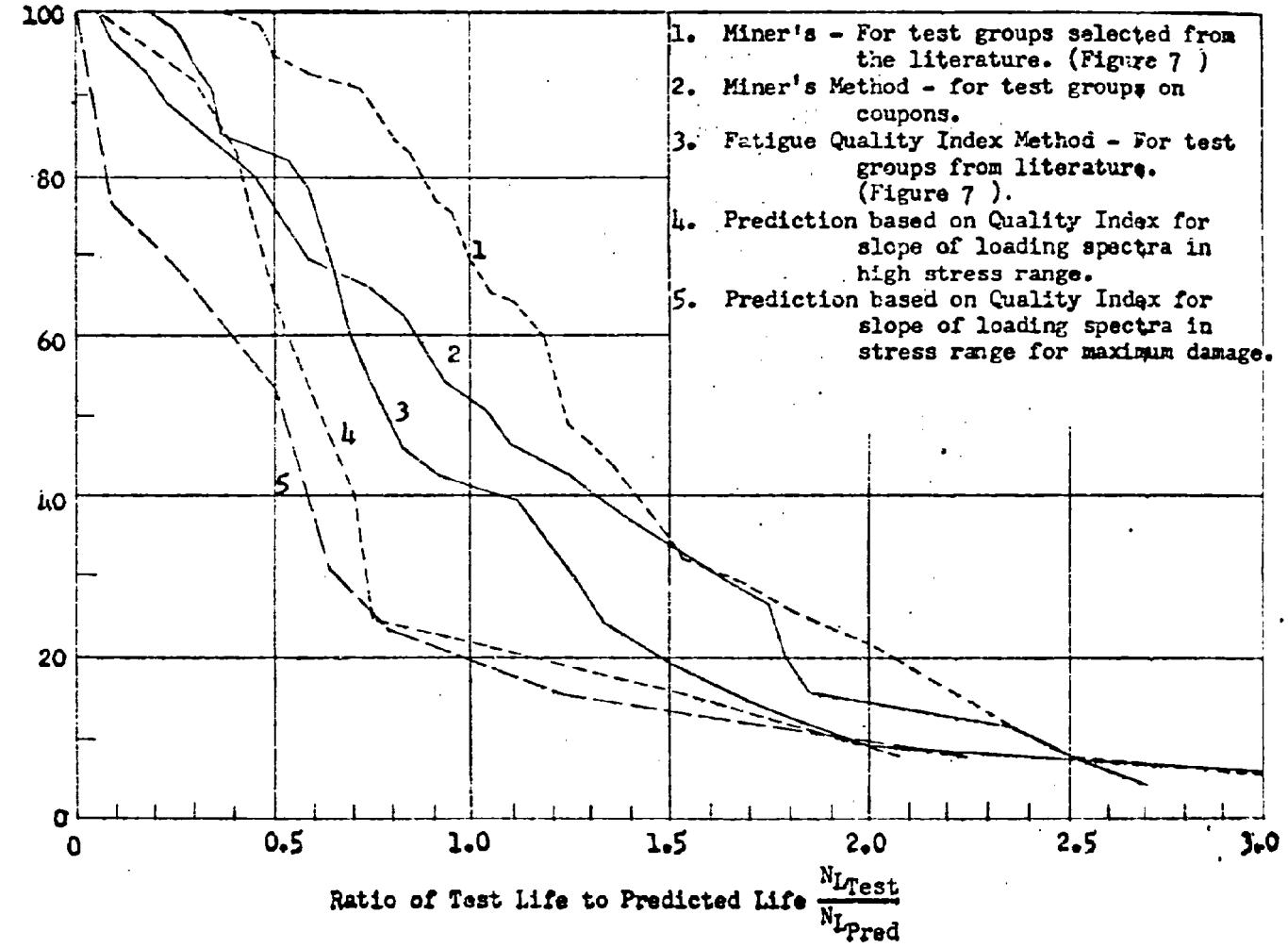



Figure 40. Cumulative Distributions for the Ratio of Test Life to Predicted Life

## SECTION V

## ANALYSIS OF COMPLEX JOINT SPECIMENS

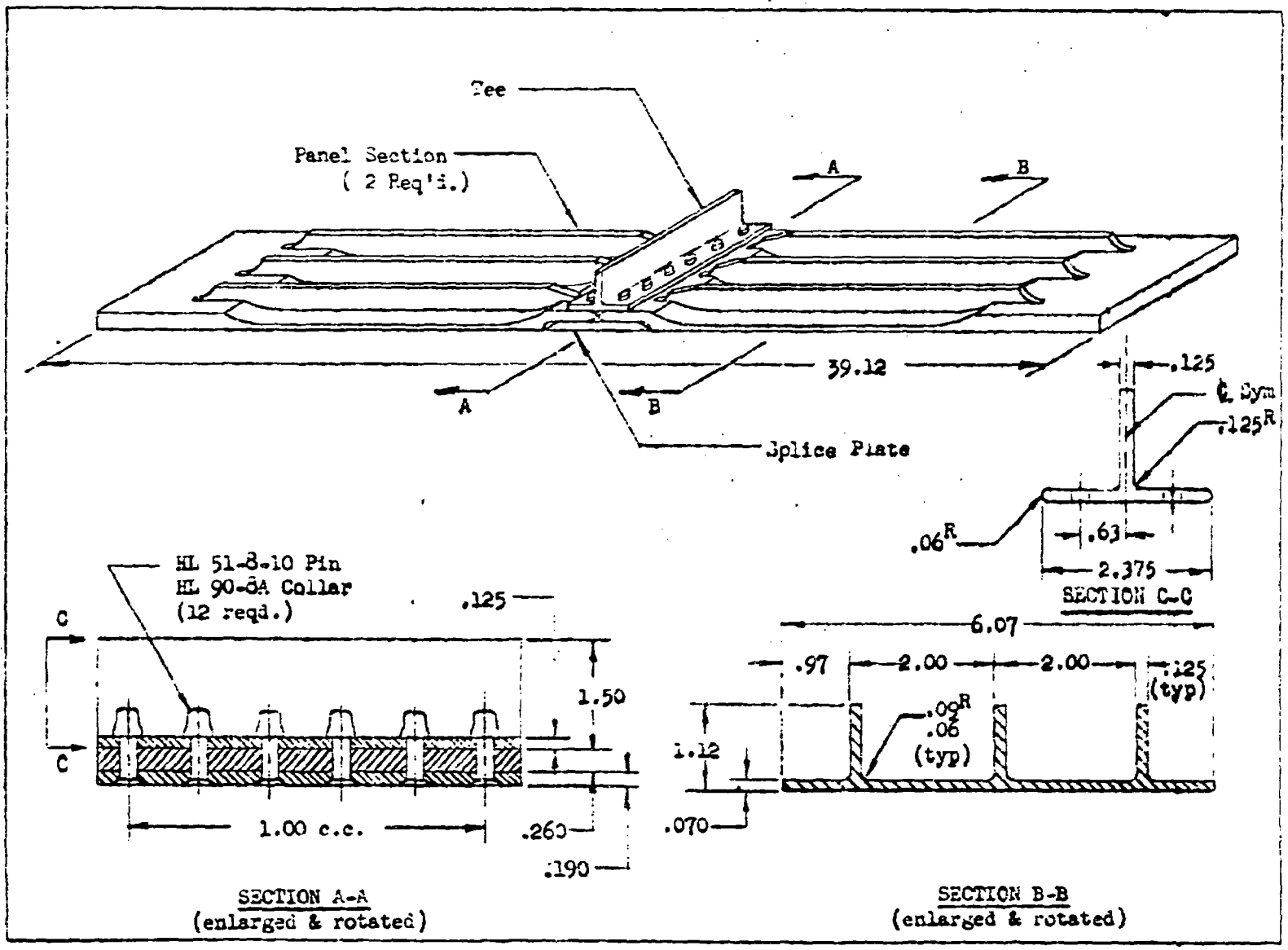
Many of the problems of full scale complex structure are not present in the simple notched strip coupon-type specimen used in the majority of research projects for reasons of economy. To determine the effectiveness of the selected life prediction method on specimens more representative of aircraft structure, a series of spectrum-type fatigue tests was conducted on a splice design adapted from an integrally stiffened tension surface of a current wing structure. A splice joint is made of two panels consisting of machined plates of 7075-T6 extrusion material approximately six inches wide, each containing three vertical stiffeners which run out or taper off into a tongue flange across the width of the plates. A double butt splice is formed by a flush recessed outer surface splice plate and an inner tee splice plate with an integral flange for a rib connection. Attachments are by twelve one-quarter inch diameter Hi-Lok fasteners, six on each side of the splice. The neutral axis location throughout the length was carefully tailored in the aircraft design to reduce as much as possible eccentrically induced bending stresses. The recessed outer splice plate, in addition to providing flush aerodynamic surfaces, also aids materially in achieving a uniform load axis. The details of the panel are sketched in Figure 41.

The panels were to be tested in an adaptation of the magnetic tape controlled fatigue test machine described in the preceding section. Two electro-servo controlled loading jacks were coupled in tandem to operate on one magnetic tape demand signal, providing 34,000 lb. load capacity. This proved insufficient, however, when the first panel had not failed after approximately 350 applications (over $5.25 \times 10^6$ cycles) of the unit low peak-low slope gust spectra illustrated in Figure 42. After careful inspection of this panel had revealed no visible damage, it was reassembled in the large 500,000 lb. fatigue machine illustrated in Figure 43. The principle of operation of this machine is illustrated schematically in Figure 44. Static loading was applied to determine the ultimate strength of the panel as a guide to stress levels to apply in the remaining fatigue tests.

Pertinent data are as follows:

| | |
|---|---|
| Static failure load | = 66,000 lbs. |
| Minimum gross area | = 0.815 in.$^2$ (Section BB in Figure 41) |
| Minimum gross area ultimate tensile strength | = 81,000 psi |

The remaining panels were fatigue tested in the large 500,000 lb. fatigue machine (Figure 43) as described in detail in Appendix D Part 3. Two additional panels, No. 11 and 12, were accidentally destroyed by compression collapse through malfunction of a loading valve in the hydraulic loading system.


Tee
Panel Section
( 2 Req'd.)
A
B
39.12
Splice Plate
.125
℄ Sym
.125R
.06R
.63
2.375
SECTION C-C
HL 51-8-10 Pin
HL 90-8A Collar
(12 reqd.)
.125
C
C
1.50
1.00 c.c.
.260
.190
SECTION A-A
(enlarged & rotated)
6.07
.97
2.00
2.00
.125
(typ)
.09R
.06
(typ)
1.12
.070
SECTION B-B
(enlarged & rotated)

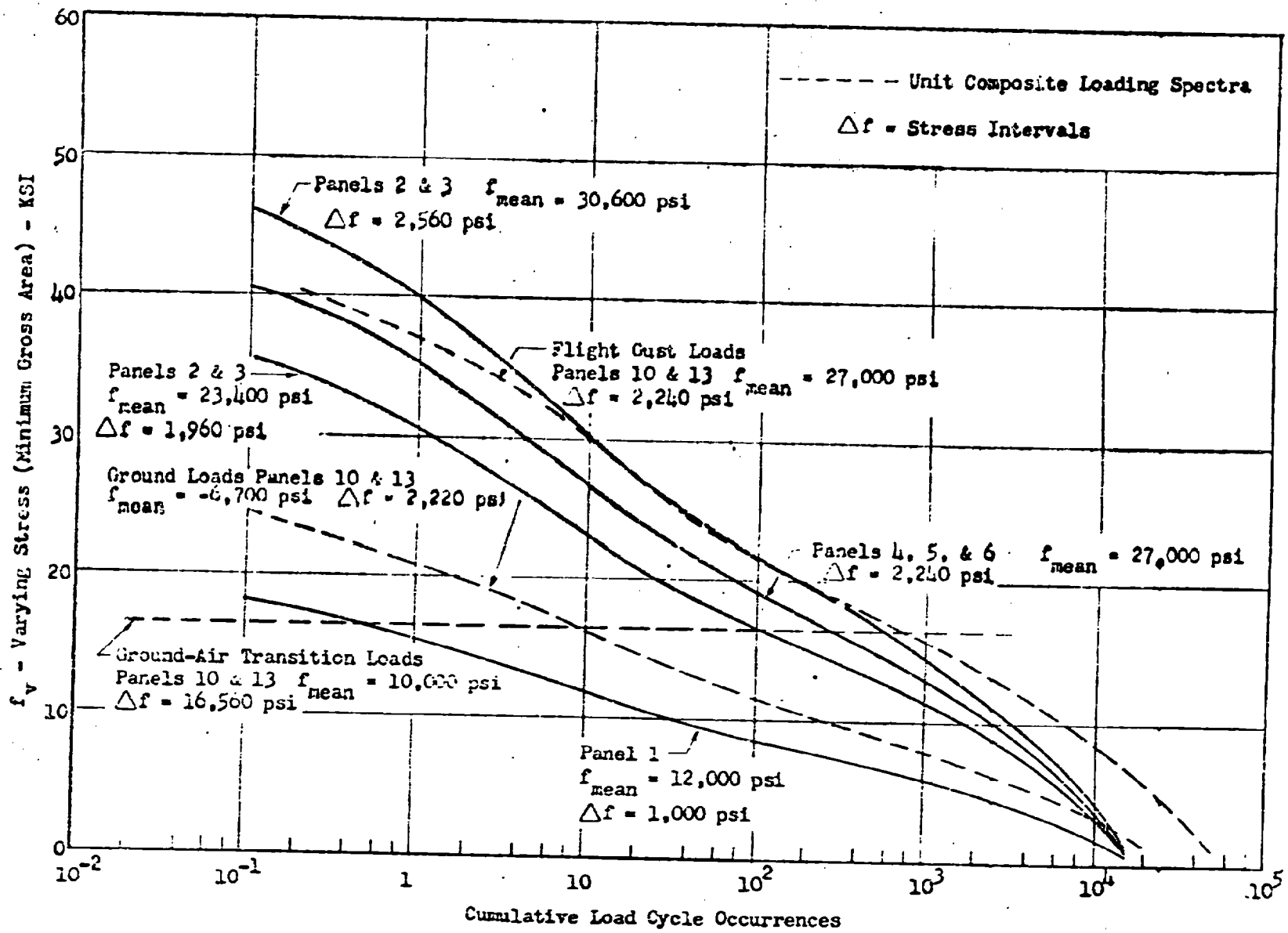



Figure 42. Basic Ordered Unit Gust and Unit Composite Gust Loading Spectra

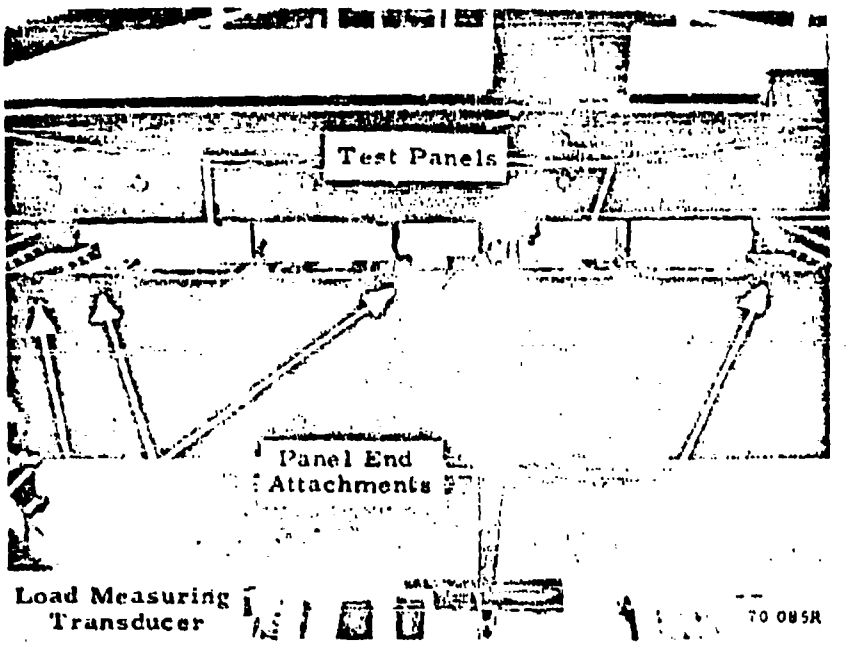



Figure 43 Two-Joint Test Panel Assemblies Installed in Tandem in a Lockheed 500,000-pound Fatigue Test Machine

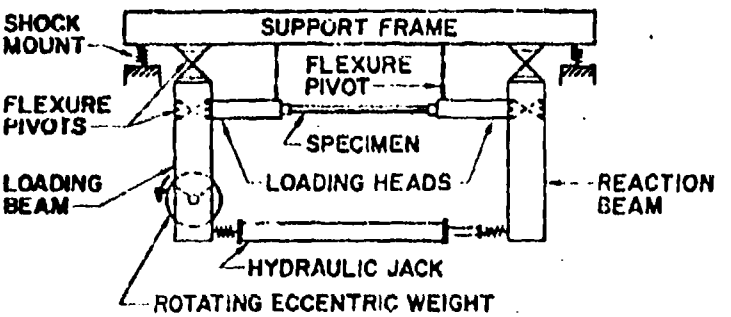



Figure 44 Schematic Diagram of the 500,000-pound Fatigue Machine Shown in the Above Photograph

Eight of the twelve panels successfully fatigue tested were apportioned five to the unit gust spectra that is illustrated in Figure 42, and three to the unit maneuver spectra in Figure 45. The remaining four were tested two to the composite gust, ground taxi, and mean load level ground-air transition cycle shown in Figure 42 and two to the composite maneuver, ground taxi, and mean load level ground-air transition cycle shown in Figure 45. The spectral test results are presented in terms of minimum gross area stress in Tables 99 to 104 and Figures 179 to 184 of Appendix D, Part 3. These same test results are also presented in terms of gross area stress at the point of fracture in Tables 106 to 110 of Appendix D. Photographs of the various types of failures that occurred are also presented there.

In the composite tests, the gust loading activity was approximately 12 loads per flight along with approximately 6.5 ground taxi loads per flight. The maneuver load activity was 30 loads per flight along with 35 ground loads per flight. In both cases, the ground-air cycle applied was the mean ground load transition to the mean flight load. These loads were grouped into ordered step spectra broken down to approximately 2000 to 2500 psi stress intervals in the gust and ground taxi loadings, and approximately 5500 psi intervals for the maneuver loadings. Block sizes varied from 1/48th to 1/600th of the final test life for the simple ordered spectral loading tests. However, due to the unexpectedly shorter test life under the composite loadings, these block sizes were from 1/5th to 1/10th of the final test life. The low-to-high load sequence was applied within the block interval. Further test details are given in Appendix D Part 3.

GROUND-AIR TRANSITION CYCLE

The importance of the ground-to-air-to-ground transition cycle discussed in connection with the analysis of the coupon data in Section IV was confirmed by these tests of the complex joint. The following comparison is developed relating the geometric mean of the number of flight cycles in the composite tests to the geometric mean of the number of flight cycles of a simple spectrum test:

TABLE 14 INFLUENCE OF GROUND-AIR TRANSITION

| Simple Spectra | | Composite Spectra | | | |
|---|---|---|---|---|---|
| Panel or (Group) Numbers | $N_L$ (test) ($10^6$ Cycles) | Panel or (Group) Numbers | $N_L$ (test) ($10^6$ Cycles) | $\frac{N_L \text{ (composite)}}{N_L \text{ (simple)}}$ | $1 - \frac{N_L \text{ (composite)}}{N_L \text{ (simple)}}$ |
| 4 | .912 | | | | |
| 5 | .783 | 10 | .397 | | |
| 6 | .928 | 13 | .516 | | |
| (C83) | .872* | (C05) | .452* | .518 | .482 |
| 7 | .298 | | | | |
| 8 | .421 | 14 | .099 | | |
| 9 | .474 | 15 | .179 | | |
| (M17) | .391* | (CM2) | .133* | .340 | .660 |

* Geometric mean of the group.

Assuming the ratio of the number of flight loading cycles in the composite test to the number of cycles in the simple spectrum test to be representative of fatigue damage done by the flight loads, the residual damage due to other than flight loadings of the composite spectra is seen to be 0.48 for the gust loading case and 0.66 for the fighter maneuver case. Since it is known that the damage contributed by the ground taxi portion of the spectra is relatively small, it can be concluded that the ground-air-ground transition cycle per flight is the predominant contributor of this residual damage. It should be noted also that the mean ground load to mean flight load level as used in these tests is a minimum (conservative) definition of this transition cycle per flight. The predominance of the ground-air transition would be expected to vary with the flight duration, reducing in importance with increased duration to the flight phase per landing. The gust loading spectra of these tests represents relatively short range flights; the fighter maneuver activity, however, is moderately high for long time average usage.

MINER'S METHOD

There were no specific S-N data available for this joint design, consequently Miner's method of simple linear cumulative damage could not be directly applied.

FATIGUE QUALITY INDEX PROCEDURE

Since a consistent influence of the shape or slope of the cumulative load frequency spectrum on the Fatigue Quality Index was not apparent in the analysis of the coupon data discussed in the previous section, this type of analysis was not applied to the data from the complex joint tests. However, several combinations of the Fatigue Quality Index procedure were applied.

The Fatigue Quality Index was derived for each of the test groups utilizing the standardized S-N data in the usual manner. Each of two base stress levels was used:

Stress Basis I. Minimum gross area stress in the uniform panel adjacent to the joint,

Stress Basis II. Actual gross area stress through the section of fracture.

The derived FQI values for Stress Basis I are given in Table 15, while those for Stress Basis II are given in Table 16. Examination of these values shows the general separation of the groups by the type of load spectra. In both bases of stress definition, the simple and composite gust loading values of K are similar within moderate scatter, and the simple and composite maneuver loading values are similar to each other but considerable different than the values from the gust-type spectra tests.

The Fatigue Quality Index is seen to be not invariant as would be required for satisfactory predictability of fatigue life. However, for similar spectra the predictability of variations on the basic load frequency spectrum is of interest. The large leverage factor between the Fatigue Quality Index value "K" and the corresponding fatigue life in number of cycles makes difficult the assessment of predictability. Therefore, several combinations of Fatigue Quality Index calculations were made to compare with the test results.

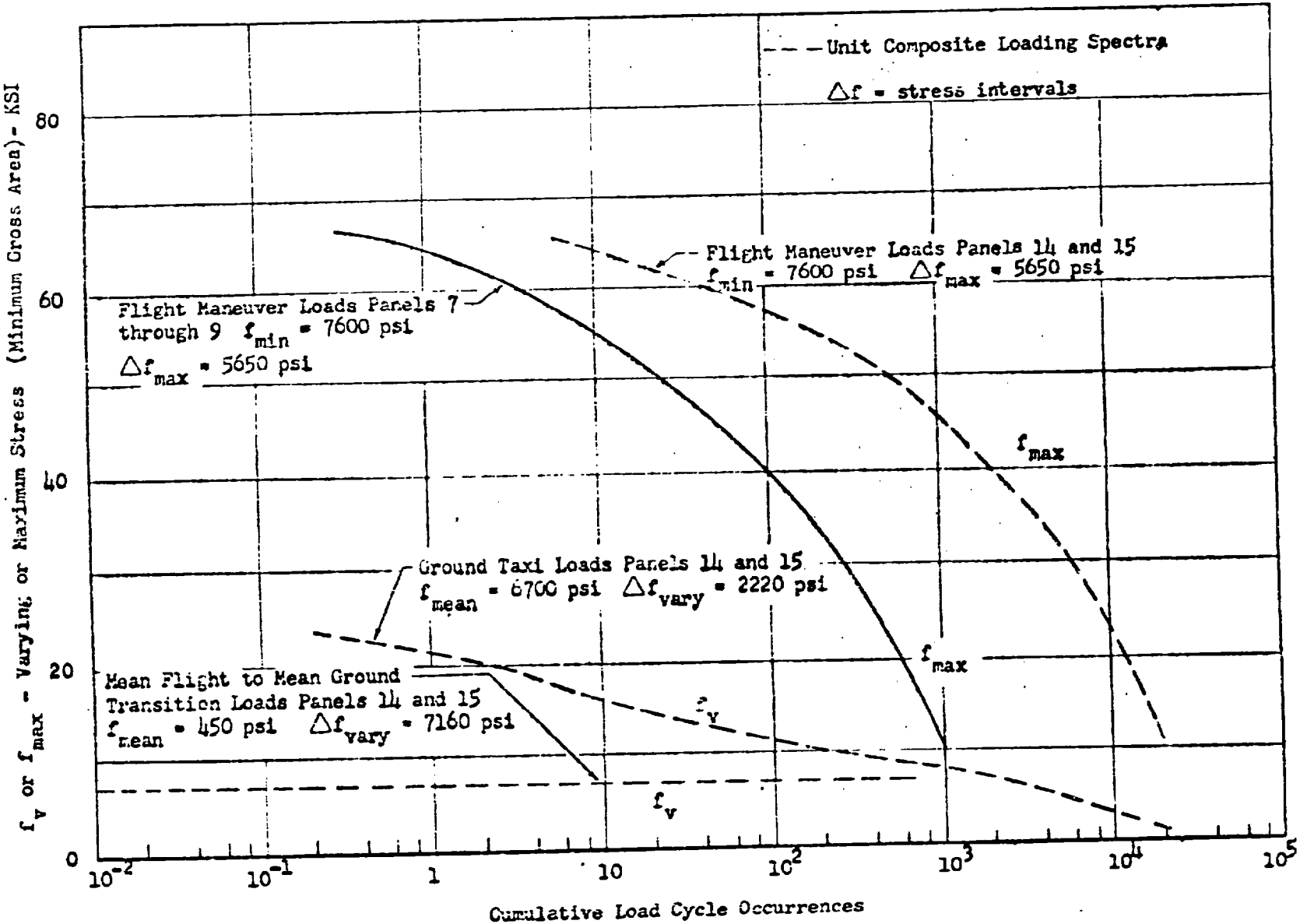



Figure 45. Basic Ordered Unit Maneuver and Unit Composite Maneuver Loading Spectra

## FATIGUE QUALITY INDEX FROM FIRST PANEL TEST RESULT

### A. SIMPLE GUST SPECTRUM

Fatigue life predictions based on a single specimen test result are an important consideration for large component and airframe fatigue tests in which more than one specimen is economically unfeasible. This investigation therefore utilizes the results of the gust spectrum test on Panel No. 4 to derive the Fatigue Quality Index with the standardized S-N curves. This value of Quality Index is used to predict the fatigue life of each specimen under the composite gust, simple maneuver, and composite maneuver load frequency spectra. Comparison of these predictions with the test results is given in Table 17 for both bases of stress definition.

The composite gust fatigue life by test is approximately 63.9 per cent and 75.8 per cent of the prediction when based on the Fatigue Quality Index for the simple gust load spectra and the minimum gross area stress outside the joint (Stress Basis I). When the stress is defined by the gross area at the point of fracture, the test result is 17.6 per cent to 30.4 per cent of the prediction.

The simple maneuver loading results are conservatively predicted by the Fatigue Quality Index from the simple gust spectrum test result, by factors of 10.5 to 74.5 times the predicted lifetime by the minimum gross area Stress Basis I. The corresponding composite maneuver test result is 6.36 to 8.07 times the predicted value on the same stress basis. However, on the basis of the stress through the point of fracture (Stress Basis II), the simple maneuver load spectrum test results were from 23.4 per cent of prediction (unconservative) to 206 per cent of prediction (conservative), whereas the composite maneuver load spectra test result was only 5.2 per cent and 58.8 per cent of the predicted lifetime (unconservative) on this stress basis. These variations in predictability are much greater than the test scatter within each group.

### B. SIMPLE MANEUVER SPECTRUM

The first test result from a simple maneuver loading spectrum (Panel No. 7) was also used to derive a Fatigue Quality Index with the standard S-N curves for use in predictions of the panel fatigue life under the composite maneuver loading spectra. These results are shown in Table 18. Predictions for both bases of stress definition were unconservative, comparing test lives with approximately 5.2 per cent and 6.6 per cent of the predicted values for a panel interpreted for each stress basis and 48.4 per cent and 61.6 per cent for the alternate panel in each case. This wide divergence is greater than the test scatter.

The results of these predictions are graphically compared with the test results from each of the panels in Figure 46. Too few test results were available to justify the statistical rank ordering of the ratio of test life to predicted life as was done for the more numerous coupon test data.

TABLE 15

CLASS I FATIGUE

QUALITY INDEX FOR MINIMUM GROSS AREA STRESSES IN GUST, MANEUVER, AND COMPOSITE SPECTRA

Specimen, Figure 41

| Test Group No. | Type of Spectrum | Sequence | Number of Specimens | K First Specimen in Test Group | K Quality Index Method | | |
|---|---|---|---|---|---|---|---|
| | | | | | Minimum | Maximum | Geometric Mean |
| G82 | Gust | Lo-Hi | 2 | 1.52 | 1.20 | 1.52 | 1.35 |
| G83 | Gust | | 3 | 1.24 | 1.24 | 1.33 | 1.29 |
| M17 | Maneuver | | 3 | .60 | .60 | .98 | .83 |
| CG5 | Composite Gust | | 2 | 1.40 | 1.38 | 1.40 | 1.39 |
| CM2 | Composite Maneuver | Lo-Hi | 2 | .70 | .70 | .99 | .83 |

TABLE 16

CLASS II FRACTURE

QUALITY INDEX FOR GROSS AREA STRESSES IN VICINITY OF FRACTURE IN GUST, MANEUVER, AND COMPOSITE SPECTRA

| Test Group No. | Type of Spectrum | Sequence | Number of Specimens | K First Specimen in Test Group | K Quality Index Method | | |
|---|---|---|---|---|---|---|---|
| | | | | | Minimum | Maximum | Geometric Mean |
| G82 | Gust | Lo-Hi | 2 | 5.01 | 4.01 | 5.01 | 4.48 |
| G83 | Gust | | 3 | 3.26 | 3.26 | 4.57 | 3.74 |
| M17 | Maneuver | | 3 | 3.28 | 2.81 | 4.04 | 3.34 |
| CG5 | Composite Gust | | 2 | 3.88 | 3.88 | 4.12 | 4.00 |
| CM2 | Composite Maneuver | Lo-Hi | 2 | 5.41 | 3.61 | 5.41 | 4.41 |

TABLE 17

FATIGUE LIVES PREDICTED FOR MANEUVER, COMPOSITE GUST, AND COMPOSITE MANEUVER SPECTRA ON PANELS FROM QUALITY INDEX FOR FIRST SPECIMEN IN A SIMPLE GUST SPECTRUM

| Test Group No. | Panel No. | $N_L$ Test ($10^6$ Cycles) | $N_L$ Pred. ($10^6$ Cycles) | $\frac{N_L \text{ Test}}{N_L \text{ Pred.}}$ | $N_L$ Pred. ($10^6$ Cycles) | $\frac{N_L \text{ Test}}{N_L \text{ Pred.}}$ |
|---|---|---|---|---|---|---|
| | | | K based on stresses for minimum gross area | | K based on stresses for local gross area at fracture | |
| | | | K = 1.24 * | | K = 3.26 * | |
| M17 | 7 | .298 | .004 | 74.500 | .310 | .961 |
| | 8 | .421 | .040 | 10.525 | 1.800 | .234 |
| | 9 | .474 | .040 | 11.850 | .230 | 2.061 |
| CG5 | 10 | .639 | 1.000 | .639 | 2.100 | .304 |
| | 13 | .758 | 1.000 | .758 | 4.300 | .176 |
| C42 | 14 | .218 | .027 | 8.074 | 4.200 | .052 |
| | 15 | .394 | .062 | 6.355 | .670 | .588 |

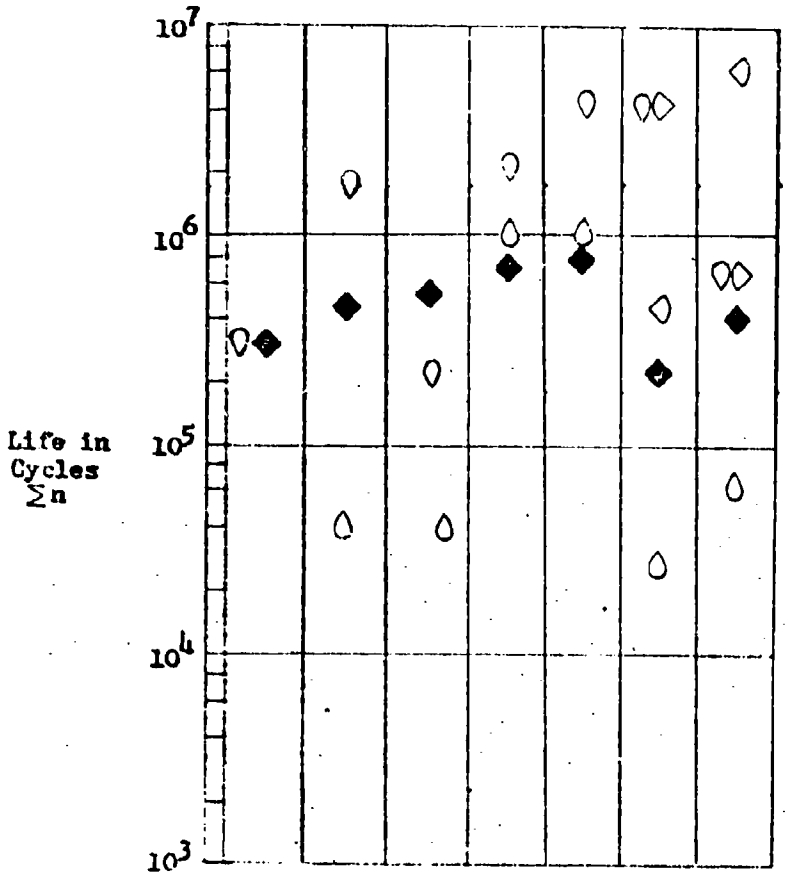
* K for Panel No. 4 in Test Group No. G83

TABLE 18

FATIGUE LIVES PREDICTED FOR COMPOSITE MANEUVER SPECTRA ON PANELS FROM QUALITY INDEX FOR FIRST SPECIMEN IN A SIMPLE MANEUVER SPECTRUM

| Test Group No. | Panel No. | $N_L$ Test ($10^6$ Cycles) | $N_L$ Pred. ($10^6$ Cycles) | $\frac{N_L \text{ Test}}{N_L \text{ Pred.}}$ | $N_L$ Pred. ($10^6$ Cycles) | $\frac{N_L \text{ Test}}{N_L \text{ Pred.}}$ |
|---|---|---|---|---|---|---|
| | | | K based on stresses for minimum gross area | | K based on stresses for local gross area at fracture | |
| | | | K = .6 * | | K = 3.28 * | |
| CM2 | 14 | .218 | .450 | .484 | 4.200 | .052 |
| | 15 | .394 | 6.000 | .066 | .640 | .616 |

* K for Panel No. 7 in Test Group No. M17




| Panel No. | | 7 | 8 | 9 | 10 | 13 | 14 | 15 |
|---|---|---|---|---|---|---|---|---|
| Test Group No. | | M17 | | | C05 | | CM2 | |
| Sequence | | Lo - Hi | | | | | | |
| Block Size ($10^3$ Cycles) | | 1 | | | 76 | | 44 | |
| Number of Loading Steps | | 11 | | | 32 | | 24 | |
| Mean Stress KSI | Air | 7.7* | | | 26.6 | | 7.7* | |
| | Ground | | | | -6.6 | | -6.7 | |
| | G-A-G | | | | 9.9 | | .45 | |
| Type of Spectrum | | Maneuver | | | Composite Gust | | Composite Maneuver | |
| Specimen | | Panel | | | | | | |
| Material | | 7075-T6 | | | | | | |

* $f_{min}$ for maneuver loading

For coding see Table 13

Figure 46. Comparison between Predicted and Experimental Fatigue Lives

## CONCLUSIONS FROM THE PANEL TESTS

The analysis of the spectral fatigue tests conducted on the complex panels result in the following conclusions.

1. The influence of the ground-air-ground transition cycle which occurs once per flight was found to be important in reducing the fatigue life of these joints when compared with the results of similar panels tested by the flight load spectra alone. This confirms the conclusions reached in the analysis of the coupon test results.

2. A Fatigue Quality Index derived from the first test result of a simple gust spectrum by use of standard S-N curves was used as a test-based fatigue life prediction procedure for other types of loading spectra. The predictions were somewhat unconservative for composite gust loading spectra which included the ground-air-ground cycle based on the mean ground to mean flight load transition. When based on the minimum gross area stress adjacent to the joint, this Fatigue Quality Index produced unduly conservative predictions for both the simple and the composite fighter maneuver test results. When based on the gross area through the point of fracture, they were both conservative and unconservative for the simple maneuver results and unconservative for the composite maneuver results.

3. The use of a Fatigue Quality Index derived from a simple fighter maneuver test spectrum was unconservative in predicting the composite fighter maneuver which contained the ground-air cycle based on the transition of mean ground to mean flight load.

## SECTION VI

## SUMMARY AND CONCLUSIONS

The main difficulty in the task of the prediction of fatigue life lies in the definition of a fatigue quality of complex structure. This quality embodies an intergration of the dual effects of a complicated localized internal stress history and the physics of the creation and propagation of a fatigue crack. The problem is complicated by a very complex loading history, plastic yielding at peak stress points, progressive work hardening of some materials, changing residual stress patterns, nonlinear, nonrepeatable slippage of friction joints, redistribution of local internal loads, and many other factors not amenable to analytical treatment. Means of analytical prediction of this fatigue quality of a complex structure will not likely be available in the near future. The statistical nature of many facets of the fatigue problem precludes hope of any specific fatigue life prediction of a simple article. The best that can be achieved is broad comparisons of the expectations of new structure compared with current and past fleet performance. However, the problem of fatigue control is amenable to solution.

An engineering evaluation of the available practical methods of fatigue life prediction was conducted by the application of selected procedures to a large body of experimental fatigue test results. From this study, the use of the Linear Cumulative Damage Hypothesis is recommended as best qualified from the standpoint of simplicity, versatility, and of sufficient accuracy (in view of other intangibles in the problem) for use in three areas of design:

1. Preliminary Design

   The Stress Concentration Method (essentially a refined method of stress analysis) must be coupled with a damage theory to constitute a life prediction method. The direct use of theoretical (or photoelastic or experimental) elastic stress concentration factors coupled with the linear cumulative damage procedure is inadequate and may provide misleading comparisons. Therefore, development tests of fatigue-critical areas are required.

2. Development Tests

   The development tests are an important link in any system for the control of fatigue cracks in fleet operations. The specimens must be complete in all fatigue-critical details. Where feasible, constant amplitude S-N type tests may be conducted to provide specific S-N data for fatigue life predictions by the simple cumulative damage procedure. This requires a considerable number of identical specimens for any reasonable degree of confidence. Where constant amplitude S-N type testing is not economically feasible (for large size specimen, component, or airframe testing) it is recommended that spectral type tests impose the full range of loading anticipated for operational

service. Spectral tests results are known to depend on many variables and assumptions made in the reduction of service loading records to practical test loading history. Some of these include unit spectrum size and stress interval size, both of which should be made relatively small (block size 1/20 or less of anticipated life; stress interval 1000-2000 psi). Flight by flight load sequence is one means of avoiding arbitrary definitions of the ground-air-ground transition cycle.

The sequence of the higher loads in the schedule has a large influence on the results; if applied early in the loading history, the test life may be unconservatively prolonged. Only the Henry Method, extended for more general application, had the potential of accounting for block size and loading sequence. However, for the test data used in this evaluation, the Generalized Henry Method offered no overall improvement over the more simple Linear Cumulative Damage Hypothesis. This problem cannot be satisfactorily resolved until sufficient statistical information on the sequence of occurrence of the highest loadings is made available from service records.

An interpretation of the full spectrum type fatigue test is outlined by a special application of the Linear Cumulative Damage Procedure in connection with a standardized set of S-N curves. The procedure is to find, by interpolation, which set of $K_T$ curves from the standardized group is required to make the cumulative damage equation exactly unity for the total applied test history. This K-value defines the Fatigue Quality Index demonstrated by the specimen under these test conditions.

3. Analysis of Service History

Many intangibles remain in the laboratory test based analysis system, including the wide range of operational loads in service, among others. It is necessary, therefore, to maintain a comparative base in service history by the consistent application of any analysis system to laboratory tests of structure which has a known operational history - both successful and unsuccessful. This is most important in the establishment of the fatigue quality acceptance standards for new structure.

The application of the Linear Cumulative Damage procedure in the prediction of the fatigue life of airframe structure as described has many unexplored areas. One of the most pertinent questions raised is the validity of the extrapolation of one or a few test results to other loading conditions. The experimental program conducted for this study explored briefly the influence of the statistical load content, as exemplified by the shape of the cumulative load frequency spectra, on the Fatigue Quality Index derived from the tests and their use in a test-based fatigue life prediction method for loading spectra of other shapes. A number of different loading spectra were applied to notched 7075-T6 aluminum alloy coupon specimens, including both the random loading sequences based on actual flight load measurements, and various ordered cyclic loading spectra derived from this flight record, and from various modifications of it.

A new magnetic tape controlled fatigue test machine and auxiliary equipment was assembled and testing, calibration, monitoring and maintenance techniques perfected to precisely reproduce almost any desired loading record which could be imposed on magnetic tape.

The experimental data derived from these tests were analyzed to determine what correlation, if any, existed between the derived quality index values and the slopes of the various loading spectra, and whether there was any trend that could be used as a corrective step for the improvement of the fatigue life prediction method. The slopes of the loading spectra were measured both at the high stress region and in the mid-stress level in the region of the maximum computed damage ratios. Fatigue life predictions using the experimentally derived relationship between spectrum slopes and the quality index were compared with the normal predictions based on the fatigue quality index derived from the first test result of a group.

The second group of experiments was conducted on a complex joint specimen representative of contemporary aircraft construction. Except for one specimen, these tests were conducted in a 500,000 lb. resonant pendulum type fatigue test machine. The same step-ordered cyclic load spectra were used as for some of the coupon experiments. These included gust type spectra of various slopes and maneuver type loadings, and two composite spectra of ground taxi loads, ground-to-air cycles based on the transition from ground mean load to flight mean load, and containing, in one case spectra of high peak-high slope flight gust loads, and in the other case spectra of military maneuver flight loads.

From an analysis of the experimental results of coupon tests, no consistent trend in the derived fatigue quality index could be developed as a function of the slope of the various loading spectra curves in either the high stress region or the mid-stress range of maximum computed fatigue damage. Fatigue life predictions of coupon type specimens loaded by composite spectra, including a ground-to-air transition based on the mean load level, from a test derived fatigue quality index based on a simple spectrum test of similar specimens loaded only by the flight portion of the spectrum of loads were less conservative than predictions by the simple linear cumulative damage hypothesis. This conclusion is equally applicable for gust-type loads or for military maneuver-type flight loads.

The use of a fatigue quality index based on a gust-type test to predict the fatigue life of specimens loaded by military maneuver-type spectra was not satisfactory.

These conclusions, with respect to the Fatigue Quality Index procedure initially based on coupon tests, were confirmed by a brief series of tests on a complex joint specimen.

A general observation is made that the scatter of coupon data obtained by spectrum-type tests is somewhat smaller than the scatter obtained in the constant amplitude-type tests, and that the scatter in results of the limited number of complex joints under spectral loading is even less than that on coupons tested by either constant amplitude or spectral-type loading. This may be significant in any study which might be conducted to establish factors of safety or margins of safety on fatigue loads or life. It is suggested that

these factors or margins of safety for fatigue cannot be established from a study of fatigue results alone, but must be considered in perspective with many other considerations such as static design criteria, fail-safe philosophy, and inspection, maintenance, and repair policy, as well as performance penalties which might accrue. These considerations are beyond the scope of this study.

## CONCLUSIONS

Based on the test data applied in the engineering evaluations conducted in this study and the analysis of the experimental results generated for the investigation of extrapolations of a test-based fatigue life prediction method for airframe structure, the following conclusions may be drawn.

1. When satisfactory constant amplitude S-N type data can be provided for the specific structure, the Linear Cumulative Damage procedure is recommended for its simplicity, versatility, and sufficient accuracy commensurate with the data currently available for this type of analysis.

2. Development tests are required for all fatigue-suspect areas of the structure. Either constant amplitude S-N type tests or full load range spectrum-type tests can be used for this purpose.

3. An important link in a fatigue quality control system is the establishment of realistic fatigue quality acceptance standards. These should be based on the consistent analysis of laboratory test results of structure with known service history, both successful and unsuccessful.

4. For spectral type tests, the technique for load simulation such as unit spectrum block size, stress intervals, and the order in which the higher peak loads appear in the sequence of loading has an important bearing on the fatigue life predictions based on test results. The unit block size and the stress interval should be relatively small. The question of where in the sequence of loading to place the highest loads cannot be satisfactorily resolved until this type of statistical information is made available from service records. A compromise is to place the highest loads approximately into the mid-range of the anticipated life sequence.

5. A special use of the Linear Cumulative Damage procedure in the interpretation of test results under complex composite spectral-type loading histories is a useful tool to accomplish two functions:

   a. To provide a simple index number on a scale of fatigue quality by which various structures may be compared and evaluated against fatigue quality acceptance standards established by similar consistent analysis of service history.

   b. To provide a test basis for the extrapolation of fatigue life predictions of complex structure under other similar loading spectra than the specific test condition, when specific constant amplitude S-N type data cannot be made available.

6. Test results indicate that the ground-air-ground transition cycle which occurs once per flight has a strong influence in reducing the fatigue life of coupons and complex panel specimens when compared with spectral tests with flight loads alone.

7. The use of simple gust-type spectral test results to derive a Fatigue Quality Index is less adequate for the life prediction of gust-type composite spectrum tests which include ground taxi, and ground-air transition cycles as well as flight gust loads. The same conclusion is made for the military maneuver-type loading conditions. The use of a Quality Index derived from a simple gust loading condition was completely inadequate to predict the fatigue life of specimens under military manouver-type of loads, and vice versa. More experimental data are needed to explore the problems of composite loading. In the meantime, it is concluded that development tests should contain the best possible representation of all loads expected in service. Flight by flight spectral loading technique is recommended to avoid arbitrary definition of the ground-air-ground transition cycle.

8. A versatile magnetic tape controlled fatigue test machine is now available with adequate calibration and monitoring techniques for precisely reproducing onto test specimens actual flight records and almost any simulation of ordered loading spectra which may be required.

## REFERENCES


1. Peterson, R.E., Stress Concentration Design Factor, John Wiley and Sons., 1953

2. Neuber, H., Theory of Notch Stresses: Principles of Exact Stress Calculations, J.W. Edwards, Ann Arbor, Michigan, 1946

3. Hardrath, H.F. and Ohman, L., A Study of Elastic and Plastic Stress Concentration Factors Due to Notches and Fillets in Flat Plates NACA Tech. Report No. 1117, 1953

4. Hyler, W.S., Popp, H.G., et al., Fatigue Behavior of Aircraft Structural Beams, NACA Tech. Note No. 4137, January 1958

5. McCulloch, A.J., Melcon, M.A., Crichlow, W.J., Foster, H.W., and Rebman, J., Investigation of the Representation of Aircraft Service Loading in Fatigue Tests, WADD Contract No. AF 33(616)-6575, Project No. 1367, Task 14025, ASD TR 61 - 435, September. 1961

6. Miner, M.A., Cumulative Damage in Fatigue. J. Appl. Mech., Vol. 12, No. 3, pp. A-159 - A-164, Sept. 1945

7. Lundberg, B., Fatigue Life of Airplane Structures, J. Aero. Sci. Vol. 22, No. 6, pp. 349 - 402, June 1955

8. Shanley, F.R., A Theory of Fatigue Based on Unbonding during Reversed Slip. RAND Corp. Report P-350-1, 11 Nov. 1952

9. Shanley, F.R., A Theory of Fatigue Based on Unbonding during Reversed Slip: Supplement. RAND Corp. Report P-350-Supplement, 1 May 1953

10. Shanley, F.R., Fatigue Analysis of Aircraft Structures, RAND Corp. Paper No. RM1127, 31 July 1953; AD 210794

11. Langer, B.F., Fatigue Failure from Stress Cycles of Varying Amplitude, J. Appl. Mech., Vol. 4, pp. A-160 - A-162, December, 1937

12. Grover, H.J., Cumulative Damage Theories. (In Proceedings of the Symposium on Fatigue of Aircraft Structures) WADC Tech. Rept. 59-507, pp. 207-225, August 1959

13. Smith, C.R., Prediction of Fatigue Failures in Aluminum Alloy Structures, SESA Proceedings, Vol. 12, No. 2, pp. 21-28, 1955

14. Henry, D.L., A Theory of Fatigue-Damage Accumulation in Steel. ASME Trans., Vol. 77, No. 6, pp. 913-918, August 1955

15. Corten, H.T. and Dolan, T.J., Cumulative Fatigue Damage. Session 3-Paper 2 (Advance copy of paper presented at the International Conference on Fatigue of Metals at the IME, London, 10-14 Sept. 1956, and at the ASME, N.Y., 28-30 November 1956)

16. Naumann, E.C., Hardrath, H.F., and Guthrie, D.E., Axial-Load Fatigue Tests of 2024-T3 and 7075-T6 Aluminum-Alloy Sheet Specimens under Constant-and Variable-Amplitude Loads, NASA Tech. Note No. D-212, December 1959

17. Wallgren, G., Fatigue Tests with Stress Cycles of Varying Amplitude, FFA Report No. 28, 1949

18. Russell, H.W., Jackson, L.R., et al., Fatigue Strength and Related Characteristics of Aircraft Joints - Part II - Fatigue Characteristics of Sheet and Riveted Joints of 0.040-inch 24S-T, and R 303-T275 Aluminum Alloys, NACA Tech. Note No. 1485, February 1948

19. Fisher, W.A.P., Programme Fatigue Tests on Notched Bars to a Gust Load Spectrum, R. A. E. Tech. Note No. Structures 236, March 1958

20. Whaley, R.E., Fatigue Investigation of Full-Scale Transport-Airplane Wings: Variable-Amplitude Tests with a Gust-Loads Spectrum, NACA Tech. Note No. 4132, November 1957

21. Payne, A.O., Random and Programmed Load Sequence Fatigue Tests on 24ST Aluminum Alloy Wings, Dept. of Supply, Melbourne, A.R.L. Report No. SM 244, Sept. 1956

22. Kommers, J.B., The Effect of Overstress in Fatigue on the Endurance Life of Steel, ASTM Proceedings, Vol. 45, pp. 532-541, 1945

23. McGuigan, Jr., M.J., Bryan, D.F., and Whaley, R.E., Fatigue Investigation of Full-Scale Transport-Airplane Wings: Summary of Constant-Amplitude Tests through 1953, NACA Tech. Note No. 3190, March 1954

24. Richart, Jr., F.E., and Newmark, N.M., A Hypothesis for the Determination of Cumulative Damage in Fatigue, ASTM Proceedings, Vol. 48, pp. 767-798, 1948

25. Marco, S.M. and Starkey, W.L., A Concept of Fatigue Damage. ASME Trans., Vol. 76, No. 4, pp. 627-632, May 1954

26. Freudonthal, A.M. and Heller, R.A., On Stress Interaction in Fatigue and a Cumulative Damage Rule - Part I - 2024 Aluminum and SAE 4340 Steel Alloys, WADC Tech. Rept. 58-69-Pt. 1, June 1958, AD 155687

27. Levy, J.C., Cumulative Damage in Fatigue - A Design Method Based on the S-N Curves, J. Royal Aero. Soc. Vol. 61, No. 559, pp. 485-491, July 1957

28. Foster, H.W., and Wells, R.H. "Fatigue Test of Lower Wing Surface Splice at Station 317" Lockheed Aircraft Corp., Lockheed Report No. 4612, 11 Feb 1944

29. Roylance, T.F., "A Review of Cumulative Damage in Fatigue", British Ministry of Supply S and T Memo No. 8/57 Dated May 1957

30. Kuhn, P. and Hardrath, H.F. "An Engineering Method for Estimating Notch Size Effect in Fatigue Tests on Steel NACA TN 2805 - Oct 1952

31. Aircraft Fatigue Handbook - Vol. II - Design and Analysis - Aircraft Industries Association - ARTC/W-76 Aircraft Structural Fatigue Panel, January 1957

32. Rhode, R.V., and Donely, P., Frequency of Occurrence of Atmospheric Gusts and of Related Loads on Airplane Structures, NACA War Report No. L-121, 1944

33. Weibull, W., Statistical Handling of Fatigue Data and Planning of Small Test Series. The Aeronautical Research Institute of Sweden (FFA), Report No. 69, October 1956

34. Cramer, H., Mathematical Methods of Statistics. Princeton Univ. Press, Princeton, N.J. (1954)

35. Pearson, K., Tables of the Incomplete $\Gamma$ - Function, Cambridge, 1951

## APPENDIX A

## DESCRIPTION OF FATIGUE LIFE PREDICTION METHODS

A survey of the literature revealed some seventeen procedures by different authors dealing with some aspect of fatigue life predictions. This section of the report presents a detailed description of most of these methods. In a number of cases, study of the methods revealed essentially a common basis with variations in handling certain aspects of the problem. For instance, the form of the mathematical equations for representing the loading spectra, or the S-N data were subject to differences by different authors who, nevertheless, were each performing, in a slightly different way, the basic linearly cumulative damage analysis.

In addition, study of some of these methods showed that modifications, extensions, and generalizations could be derived which would improve the application of certain specific methods. These extensions are derived and explained in detail. They provide three additional procedures for consideration, making twenty in all.

Study of these methods revealed some which could not be evaluated because of the lack of proper data. The methods which were studied include the following: (Those underlined were chosen for comparative evaluation.)

1. Linear Cumulative Damage - Miner's Method
2. Shanley's "1X" Method
3. Shanley's "2X" Method
4. Lundberg's FFA Method
5. Henry's Method
6. Generalization of Henry's Method
7. Corten and Dolan's Method
8. Modified Corten and Dolan Method
9. A Simplified Nonlinear Cumulative Damage
10. Kommers' Method
11. Richart and Newmark's Method
12. Marco and Starkey's Method
13. Freudenthal-Heller's Method

14. Langer's Method

15. Grover's Method

16. Levy's Method

17. Smith's Residual Stress Method

18. Tangent Intercept Method

19. Stress Concentration Method

20. A Fatigue Quality Index Method

LINEAR CUMULATIVE DAMAGE - MINER'S METHOD

In 1945 Miner derived, in reference 6, the first logical basis for the method of linear cumulative damage, which had been previously proposed by Palmgren in 1924. In deriving this method, the following assumptions were applied to a simple distribution of discrete loads:

1. The amount of internal work absorbed by the material during each load cycle was constant at a given load level.

2. The maximum amount of internal work that could be absorbed from cyclic loads prior to failure was always the same.

3. The amount of internal work absorbed at each discrete load level in a simple loading spectrum was linearly cumulative and independent of the sequence of loading.

The first two assumptions lead to the following relationship between the amount of internal work absorbed and the number of load cycles applied at a specific load level.

$$\frac{w_i}{W} = \frac{n_i}{N_i} \qquad \text{(A1)}$$

where

$w_i$ = work absorbed at the $i^{th}$ varying load,

$W$ = maximum amount of internal work that is absorbed by a material before failure (note that $W = W_i$ = constant),

$n_i$ = number of cycles applied at the $i^{th}$ varying load, and

$N_i$ = number of cycles required for failure at the $i^{th}$ varying load.

Assumptions two and three were used to derive the equation which is given below for relating the increments of internal work absorbed at two or more load levels to the maximum amount of internal work absorbed before failure.

$$\sum w_i = W$$

or (A2)

$$\sum \frac{w_i}{W} = 1$$

Elimination of $\frac{W_i}{W}$ in Equations (A1) and (A2) results in the following expression.

$$\sum \frac{n_i}{N_i} = 1 \qquad (A3)$$

Failure is specified by the above equation in terms of a damage level of unity when the left hand side of the equation is considered to represent fatigue damage in the form

$$D = \sum \frac{n_i}{N_i} \qquad (A4)$$

where

D = damage ratio or the fraction of fatigue life used up by the total number of load cycles that are applied at all load levels.

In using this expression, a unit distribution of discrete loads is usually selected that represents some specific service time or flight distance. When the damage ratio D has been calculated for this unit distribution, the predicted life is obtained as follows:

$$\text{Predicted Life (in hours or miles)} = \frac{1}{D} \times \text{(Life in hours or miles associated with a unit spectrum of discrete loads)}$$

or, in terms of the predicted fatigue life in cycles

$$N_L = \frac{\sum n_i}{D} = \frac{(\sum n_i)_{flight} + (\sum n_i)_{G\text{-}A\text{-}G} + (\sum n_i)_{ground}}{\left(\sum \frac{n_i}{N_i}\right)_{flight} + \left(\sum \frac{n_i}{N_i}\right)_{G\text{-}A\text{-}G} + \left(\sum \frac{n_i}{N_i}\right)_{ground}} \qquad (A5)$$

where

$N_L$ = predicted total number of cycles applied at loads of all magnitudes,

$\sum n_i$ = total number of load cycles in the unit distribution, and

D = damage ratio for the unit distribution.

SHANLEY'S "IX" METHOD

Shanley's "IX" method (references 8, 9, and 10) is similar to Miner's method in using the concept of linear cumulative damage that is expressed in Equation (A4). In this method S-N data are represented by an equation of the form:

$$N = \frac{\gamma}{S_v^{\delta}} \tag{A6}$$

where

$\gamma$ = a parameter which is equal to the vertical intercept at N = 1 of the straight line fit to a plot of log $S_v$ versus log N, and

$\delta$ = exponent defining the slope of the straight line fit.

This equation provides a linear approximation for the log-log form of S-N data that is illustrated in Figure 47.

A relative reduced stress or equivalent stress is also used in this method. This equivalent reduced stress is associated with a load of constant magnitude that may be applied the same number of times as all the loads above the endurance limit in a unit loading spectrum and may be defined in terms of Equation (A6) as

$$S_R = \left(\frac{\gamma}{N_R}\right)^{\frac{1}{\delta}} \tag{A7}$$

where

$S_R$ = relative equivalent or reduced stress of constant amplitude, and

$N_R$ = the total number of cycles that may be applied at all load levels above the endurance limit prior to failure.

Equation (A5) may be modified so that it becomes applicable to only the loads applied above the endurance limit in a unit loading spectrum. This is accomplished by multiplying this equation by the ratio of load cycles above the endurance limit $(\sum n_i)_{S_{v_i} > S_E}$ to the block size of the spectrum or $(\sum n_i)_{\text{all } S_{v_i}}$. Use of this ratio in Equation (A5) will lead to

$$N_R = \frac{(\sum n_i)_{S_{v_i} > S_E}}{\sum \frac{n_i}{N_i}} \tag{A8}$$

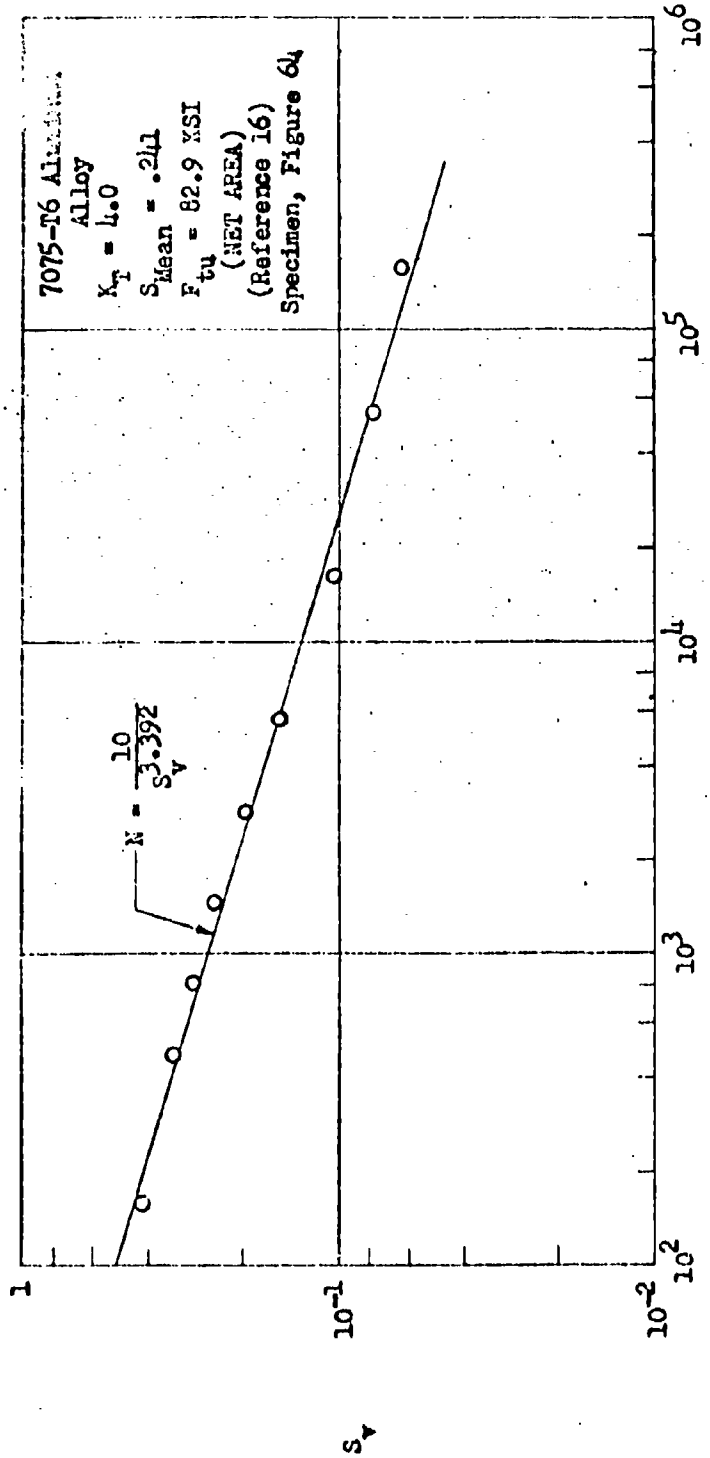



Figure 47. S-N Data for Notched Sheet Specimens

The following equation will result when Equations (A6) and (A7) are used to eliminate $N_i$ and $N_R$ in Equation (A8).

$$S_R = \left[ \frac{\sum n_i S_{v_i}^{\delta}}{\sum n_i} \right]^{\frac{1}{\delta}} \qquad S_{v_i} > S_R \tag{A9}$$

This equation was derived in reference 8 from a concept of crack growth that leads to the following relationship for depth of crack:

$$h = Ae^{an} \tag{A10}$$

where

h = depth of crack,

A = constant,

e = exponential,

a = factor that depends on the magnitude of the varying load, and

n = number of loading cycles.

To complete the derivation of the "1X" method in terms of the quantities specified in Equation (A10) the reduced stress in Equation (A9) was assumed to cause the same crack growth as the unit loading spectrum for which the reduced stress was calculated.

SHANLEY'S "2X" METHOD

By using an assumption that the constant, A, in Equation (A10) was dependent on stress level, Shanley derived his "2X" method in the preceding reference. This assumption leads to a rate of crack growth which is higher than that used in the "1X" method, with the reduced stress expressed in the form:

$$S_R = \left[ \frac{\sum n_i \, S_{v_i}^{2\delta}}{\sum n_i} \right]^{\frac{1}{2\delta}}_{S_{v_i} > S_E} \tag{A11}$$

By using Equations (A6) and (A7) to eliminate the relative stress terms in Equation (A11), the "2X" method may be expressed in terms of cycles as:

$$N_R = \sqrt{\frac{(\sum n_i)_{S_{v_i} > S_E}}{\sum \frac{n_i}{N_i^2}}} \tag{A12}$$

The relative reduced stress in Equations (A9) or (A11) may be used to predict fatigue life with the "1X" or "2X" method. To evaluate the reduced stress, S-N data must be analytically defined by Equation (A6) to evaluate the exponent $\delta$ that is used in Equations (A9) and (A11). The value of the relative reduced stress from either of these equations is used to read from an S-N curve the appropriate number of cycles $N_R$ that may be applied at load levels above the endurance limit. Fatigue life is predicted by "1X" and "2X" methods when $N_R$ is multiplied by the ratio of the total number of cycles of the associated unit loading spectrum to the total number of cycles above the endurance limit.

$$N_L = N_R \frac{\left[ \sum n_i \right]_{\text{unit block size}}}{\left[ \sum n_i \right]_{S_{v_i} > S_E}} \tag{A13}$$

The value of $N_R$ could be evaluated by substituting the relative reduced stress in Equation (A7) or (A14). When these equations provide a good fit to the S-N curve in the vicinity of $S_R$, their analytical definition will be the same as

the value of $N_R$ obtained by reading an S-N curve. Equations (A8) and (A12) may also be used to determine the value of $N_R$ without requiring an analytical definition of S-N data or of reduced stress. However, these equations were not used in making predictions from the "1X" and "2X" methods.

## THE FFA METHOD

Bo Lundberg and his colleagues at the Aeronautical Research Institute of Sweden (FFA) developed mathematical equations in reference 7 for simplified forms of the gust loading spectra and S-N data. By use of these equations in the linear cumulative damage concept, a closed form solution was obtained for fatigue life predictions.

In this method, S-N curves are represented by equations of the form:

$$N = \frac{\alpha}{(S_V - S_E)^\beta} \qquad (A14)$$

where

$N$ = number of cycles to failure at a varying load of constant magnitude corresponding to the relative varying stress, $S_V$,

$S_V$ = relative varying stress,

$S_E$ = relative varying stress at the endurance limit (may be arbitrarily defined by the relative varying stress at $N = 10^7$),

$\alpha$ = S-N curve parameter, given by the vertical intercept at $N = 1$ of the straight line fit to S-N data, when $\log (S_V - S_E)$ is plotted vs. $\log N$, and

$\beta$ = exponent defined by the slope of the straight line fit.

A graphical picture of S-N data is given in Figure 48 to illustrate the basis for this equation. This figure also indicates that Equation (A14) may not closely represent the behavior of S-N data in both the high and low stress ranges.

The cumulative loading spectrum is [illegible] in the FFA method [illegible] functions of the form:

$$H = H_0 e^{-h S_V} \qquad (A15)$$

where

$H$ = total number of load cycles applied at or above the relative varying stress corresponding to $S_V$,

$H_0$ = intercept of the straight line fit to the cumulative unit loading spectrum at $S_V = 0$ when $S_V$ is plotted versus $\log H$,

$h$ = slope of the straight line fit to the cumulative unit loading spectrum, and

$e$ = exponential.

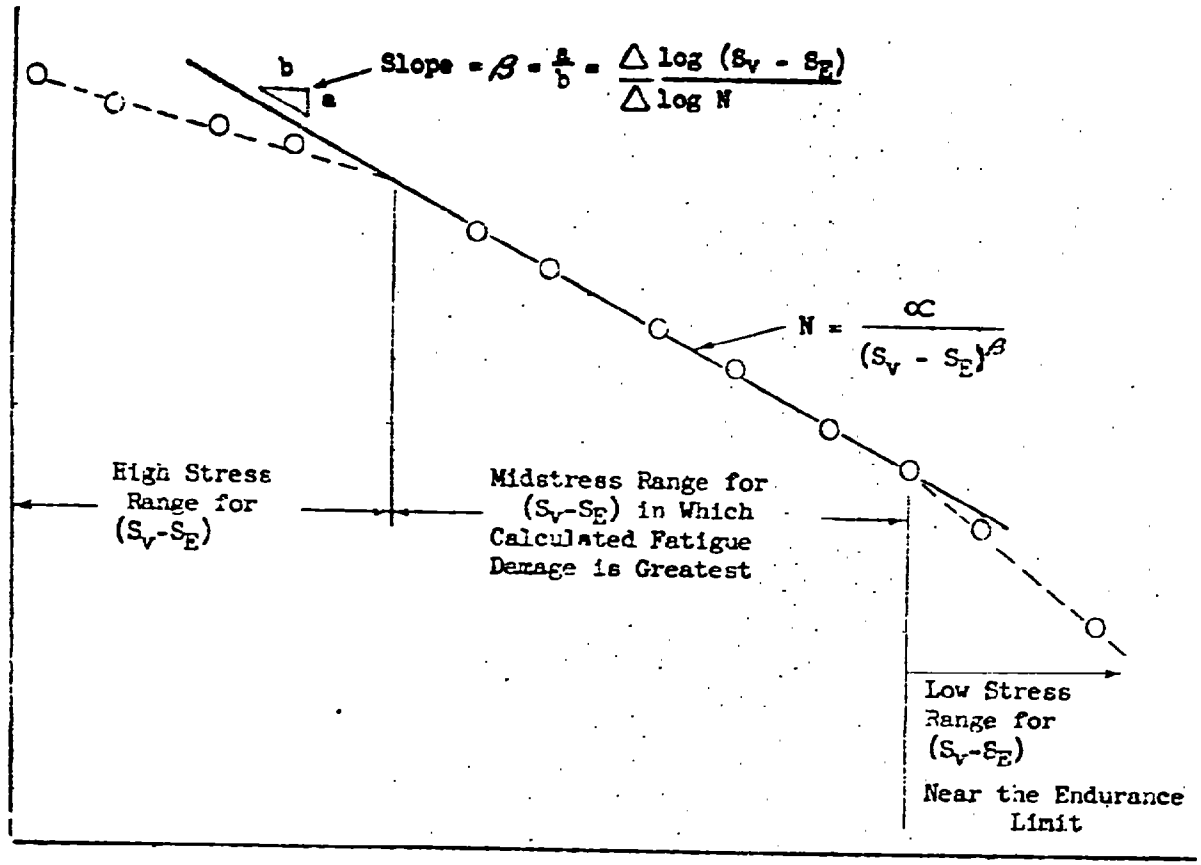



Figure 48. Analytical Representation of S-N Data

The type of curve fitting that is required for an adequate representation of cumulative loading spectra by this equation is illustrated in Figure 49. When more complex analytical functions are used, the solution of the resulting damage equation in the method can become very difficult. Complications are also involved when the shape of the unit loading spectrum cannot be adequately defined by a straight line fit in the stress range for maximum calculated fatigue damage.

To show how Equations (A14) and (A15) are used, Equation (A4) must be written in the form:

$$D = \sum \frac{-\Delta H}{N} \tag{A16}$$

where

$\Delta H$ = the number of cycles applied within the varying load interval represented by $\Delta S_v$.

The minus sign is required in the above definition for consistency with the negative exponent in Equation (A15).

For an infinitesimal increment in relative varying stress, $\Delta S_v$, Equation (A16) may be transformed into the following equation for defining fatigue damage over a wide range of varying stress.

$$D = -\int_{S_E}^{\infty} \frac{dH}{dS_v} \frac{1}{N} \, dS_v \tag{A17}$$

S. Eggwertz used Equations (A14) and (A15) in Appendix A of Reference 7 to eliminate $\frac{dH}{dS_v}$ and N in Equation (A17). He then integrated Equation (A17) between limits of $S_E$ to $\infty$ arrive at the following approximate solution.

$$D = \frac{H_o}{\alpha} h^{-\beta} e^{-h S_E} \Gamma(\beta + 1) \tag{A18}$$

where

$\Gamma(\beta + 1)$ = Gamma function of $(\beta + 1)$ which

may be obtained from mathematical tables such as Reference 35.

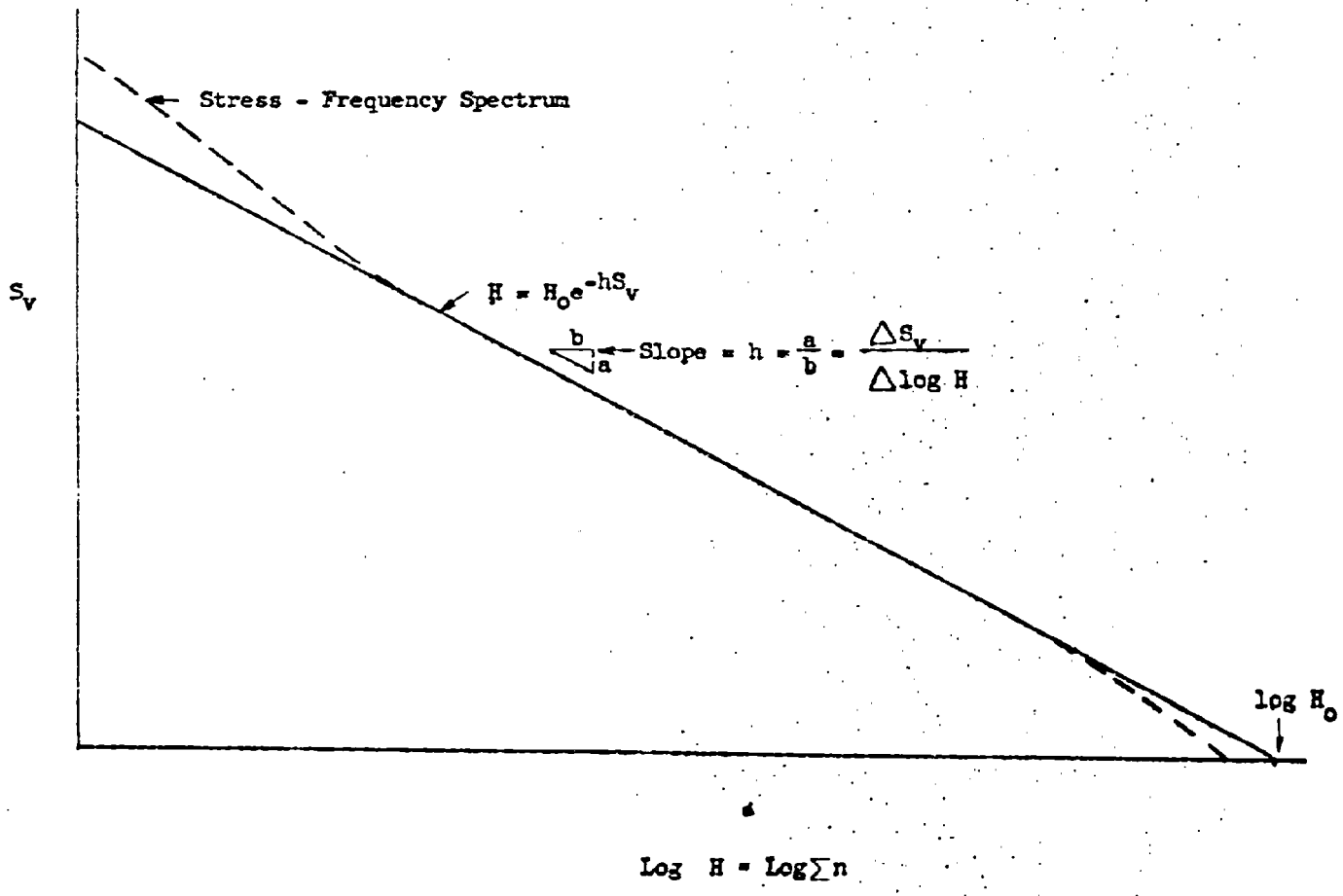



Figure 49. Analytical Interpretation of Unit Loading Spectrum

Within the usual accuracy of S-N and loading spectrum data, the approximate solution in Equation (A18) was considered to be more than adequate in Reference 7 for all practical applications of the FFA method.

When unit cumulative loading spectra are considered, fatigue damage may be calculated by using Equation (A18); and the predicted total number of cycles to failure may be obtained by using Equation (A5). In this last step, the actual total number of loading cycles in the unit spectrum must be used rather than the value of $H_o$ that was determined in the analytical definition of the spectrum.

HENRY'S METHOD

Henry (reference 14 ) derived a method of nonlinear cumulative damage by defining fatigue damage in terms of a reduction in the S-N curve. This decrease in fatigue strength reflected the effects of increased local stress concentration when loading cycles were applied at any load level above the endurance limit. As originally proposed, Henry's method could be used only with materials which had S-N curves which fit the following equation:

$$N = \frac{\alpha}{S_V - S_E} \tag{A19}$$

Fatigue damage at any varying stress greater than $S_E$ but less than 1.5 $S_E$ was evaluated in this method from the following equation:

$$D = \frac{S_E - S_E'}{S_E} = \frac{n/N}{1 + \frac{S_E}{S_V - S_E}\,(1 - n/N)} \tag{A20}$$

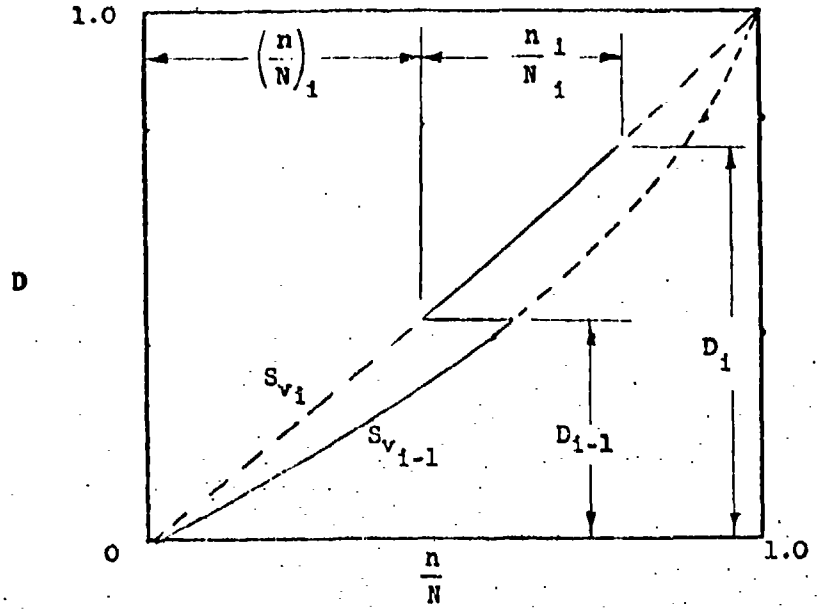
where

$S_E$ = relative varying stress at the endurance limit from S-N data prior to the initiation of any fatigue damage, and

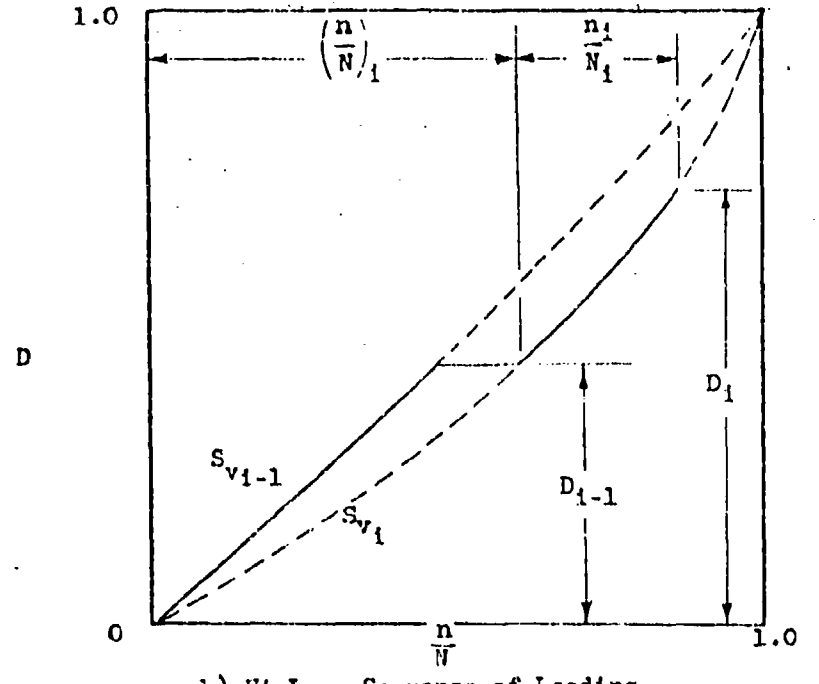
$S_E'$ = relative varying stress at the endurance limit after fatigue damage is produced by applying varying loads associated with relative stresses larger than $S_E$.

The above equation becomes indeterminate when $S_V = S_E$ and cannot be used when $S_V \leq S_E$. Equation (A20) is also used to compute fatigue damage when two or more varying loads are applied above the endurance limit. The damage after applying one or more varying loads is first defined in terms of an equivalent cycle ratio $\left(\frac{n}{N}\right)_1$ at the next varying load above the endurance limit.

This equivalent cycle ratio is then used as the starting point from which additional damage will be computed by Equation (A20) at the new varying load. This is shown in Figure 50. The equation for the equivalent cycle ratio is




a) Lo-Hi - Sequence of Loading




b) Hi-Lo - Sequence of Loading

Figure 50 Equivalent Cycle Ratio $\left(\frac{n}{N}\right)_i$ For Lo-Hi and Hi-Lo Sequence of Loading

$$\left(\frac{n}{N}\right)_i = \frac{D_{i-1}\left(1 + \frac{S_{v_i} - S_E}{S_E}\right)}{D_{i-1} + \frac{S_{v_i} - S_E}{S_E}} \qquad (A21)$$

where

$\left(\frac{n}{N}\right)_i$ = equivalent cycle ratio at a new relative varying stress greater than $S_E$ that computes the level of damage reached by applying loading cycles at other relative varying stresses.

$D_{i-1}$ = damage ratio after applying loading cycles at the last previous relative varying stress greater than $S_E$, and

$S_{v_i}$ = the new relative varying stress greater than $S_E$ at which damage is to be calculated.

The use of an equivalent cycle ratio may be further clarified in terms of stress levels and equivalent S-N curves by referring to the Hi-Lo loading sequence in Figure 51. In this figure, $n_1$ load cycles are applied at the larger relative varying stress of $S_{v_i}$. The constant amplitude fatigue life of $N_1$ on the original S-N curve is reduced by $n_1$ cycles to $(N_1 - n_1)$. An equivalent S-N curve that accounts for this reduction is defined in terms of a new relative endurance limit $S'_E$. The cycles to failure on the equivalent S-N curve at $S_{v_i}$ can be read from the original S-N curve at the increased stress level of $C_1 \cdot S_{v1}$ where $C_1$ is a functio of the new relative endurance limit. The cycles to failure on the equivalent S-N curve at a new relative varying stress of $S_{v_2}$ are also read from the original S-N curve, but not at $S_{v_2}$. They are read at the adjusted stress level defined by multiplying the new varying stress by $C_1$ which was previously evaluated at $S_{v1}$. This results in the definition of a fatigue life under constant amplitude loading of $S_{v_2}$ that is shorter than the original S-N curve by $\Delta N_2$ cycles or the equivalen cycle ratio $\left(\frac{n}{N}\right)_2$ in Equation (A21). Applying $n_2$ load cycles at the relative varyi stress of $S_{v2}$ will result in another new equivalent S-N curve with a still lower endurance limit of $S'_{E_1}$. Points on this second equivalent S-N curve in Figure 51 other relative varying stresses $S_{v_i}$ are defined by reading the original S-N curve

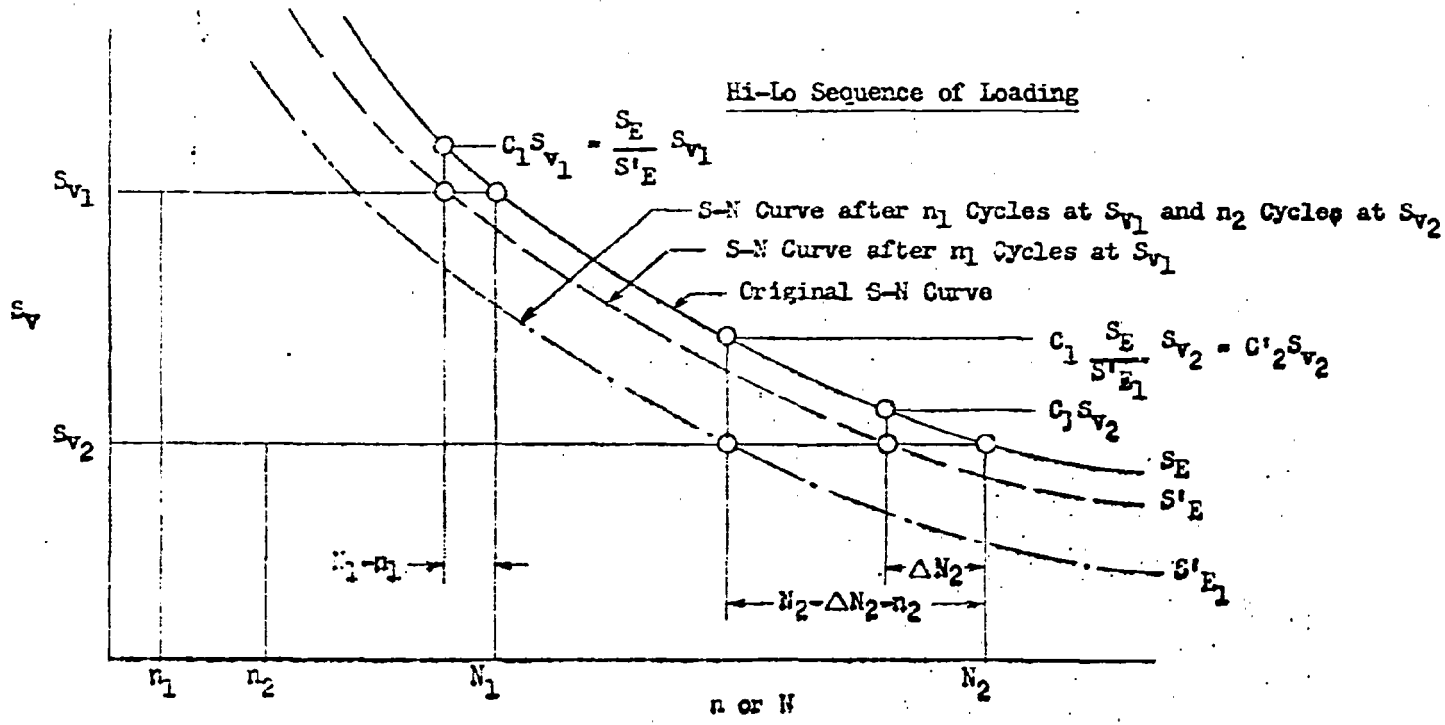



Figure 51. The Influence of Prior Fatigue Loading on the Selection of an Equivalent S-N Curve

stress levels of $C_2' S_{v_i}$. In this manner, the equivalent S-N data after any number of loading steps may be defined in terms of the original S-N curve. Since the exponent on $(S_v - S_E)$ in Equation (A19) has a fixed value of unity, the equivalent S-N curves have the same slope and are parallel to the original S-N curve when log $(S_v - S_E)$ is plotted versus log N.

If subscripts are added to Equation (A20), the equivalent cycle ratio in Equation (A21) could be used in the following manner to evaluate damage at the end of applying cycles of the next relative varying stress:

$$D_i = \frac{\left(\frac{n}{N}\right)_i + \frac{n_i}{N_i}}{1 + \frac{S_E}{S_{v_i} - S_E}\left[1 - \left\{\left(\frac{n}{N}\right)_i + \frac{n_i}{N_i}\right\}\right]} \qquad \text{(A22)}$$

where

$D_i$ = damage ratio after applying cycles at the next relative varying stress greater than $S_E$,

$n_i$ = number of cycles applied at the next relative varying stress, and

$N_i$ = the number of cycles to failure from S-N data for the next relative varying stress.

Fatigue damage can be determined through repeated use of Equation (A22) as a function of the magnitude and sequence of application of varying loads above the endurance limit. The block size of a simple spectrum of discrete load levels affects the cycle ratio $n_i/N_i$ used in this equation. Hence, the effects of block size are also a parameter in Henry's method.

After two loading steps, Equation (A22) would take the form given below, with $n_1$ load cycles applied in the first loading step and $n_2$ cycles in the second loading step.

$$D_2 = \frac{\frac{n_1}{N_1} + \frac{n_2}{N_2} - \frac{n_1}{N_1}\frac{S_E}{S_{v_1}}\left(1 + \frac{n_2}{N_2}\right) - \frac{n_2}{N_2}\cdot\frac{S_E}{S_{v_2}}\left(1 - \frac{n_1}{N_1}\right)}{1 - \frac{n_1}{N_1}\frac{S_E}{S_{v_1}} - \frac{n_2}{N_2}\frac{S_E}{S_{v_2}} - \frac{n_1}{N_1}\frac{n_2}{N_2}\frac{S_E^2}{S_{v_1}\cdot S_{v_2}}\left(\frac{S_{v_1} - S_{v_2}}{S_{v_2} - S_E}\right)} \qquad \text{(A23)}$$

All terms except the first and second in the numerator and the first in the denominator are zero when $S_E$ is zero, or tend to become zero when $S_{v_1}$ and $S_{v_2}$ are much greater than the relative endurance limit $S_E$. In such a case, Equation (A23) reduces to Equation (A4) in Miner's method. The added complexity in considering more than two load levels in Equation (A22) obscures this simple picture. When $S_{v_1}$ and $S_{v_2}$ are of the same order of magnitude as $S_E$, the difference in the fatigue damage predicted by Equations (A4) and (A23) will depend largely on the values of the cycle ratios $\frac{n_1}{N_1}$ and $\frac{n_2}{N_2}$. While this difference in fatigue damage would be slight for small cycle ratios, the difference will increase essentially as a linear function of these cycle ratios for fixed values of $S_{v_1}$ and $S_{v_2}$.

Another important feature indicated by Equation (A23) is the effects of the order in which the larger varying load is applied to the specimen. When the larger relative varying load is applied first as $S_{v_1}$, the last term in the denominator is negative. This makes the resulting damage larger and the fatigue life shorter than it would be when the larger varying load is applied in the second loading step as $S_{v_2}$. Test results, however, tend to indicate that the fatigue damage is smaller and the resulting fatigue life longer when the largest of two or more varying loads is applied first. This may be seen by comparing the test lives for Hi-Lo and Lo-Hi loading sequences such as Test Groups No. G1 and G3 in Table 48. In certain loading ranges this effect may be due to beneficial residual stresses resulting from plastic yielding. (Reference 30)

GENERALIZATION OF HENRY'S METHOD

A more general version of Henry's method is derived to cover the cases where S-N data can be expressed in terms of Equation (A14). Unlike the S-N function expressed in Equation (A9) and used in the original derivation of Henry's method, Equation (A14) permits the slope of S-N data to have values other than unity. Removal of this slope restriction on S-N data permits Henry's method to have much wider application and to be used with many more materials than previously possible.

The general equation for damage is given by

$$D = \frac{1 - \left(1 - \frac{n}{N}\right)^{1/\beta}}{1 + \frac{S_E}{S_v - S_E}\left(1 - \frac{n}{N}\right)^{1/\beta}} \qquad (A24)$$

where

$\beta$ = exponent from Equation (A14).

The equation replacing Equation (A2) for the equivalent cycle ratio at a subsequent relative varying stress is given below.

$$\left(\frac{n}{N}\right)_i = 1 - \left[\frac{\frac{S_{v_i} - S_E}{S_E}\left(1 - D_{i-1}\right)}{D_{i-1} + \frac{S_{v_i} - S_E}{S_E}}\right]^{\beta} \qquad (A25)$$

Equations (A24) and (A25) reduce to Equations (A20) and (A21) when the exponent $\beta$ is unity.

This modified set of equations for Henry's method was used to calculate fatigue damage for most of the test spectra used in this report, with the exception of spectra employing random sequences. The random sequences were generally inadequately defined for the required step-by-step application of the equations.

CORTEN AND DOLAN'S METHOD

Corten and Dolan (reference 15) base the evaluation of fatigue damage on the number of fatigue cracks that are formed and the rate of crack propagation. While cracks are propagated at all load levels, the number of cracks is considered to be a function only of the largest varying load used in a fatigue test. With these basic concepts, fatigue damage is assumed on the first cycle of loading and is related to the number of cycles applied at each varying load through the following equation:

$$D = m r n^{a} \tag{A26}$$

where

m = number of cracks,

r = coefficient of the rate of crack propagation, and

a = exponent that could change with the amplitude of the varying load.

The total calculated damage for a periodically repeated sequence of two different varying loads was generalized from this equation in terms of applied load cycles. This generalization considered the actual number of cycles applied at the larger varying load , and the equivalent number of cycles required at the larger varying load to obtain damage increments equal to those accrued at the smaller varying load. In subsequent development of the equations, however, the authors used the actual number of cycles applied in each step at the smaller load rather than the equivalent number of cycles at the larger load, as mentioned in reference 29. Because of this, their resulting equation for fatigue life falls within the original concept of their theory only when the exponent "a" does not depend on the magnitude of the varying load, and fails to do so when the exponent is affected by changes in the magnitude of the varying load. Hence, the method must be used with a load invariant exponent, where the total number of cycles applied in a periodically repeated sequence of two different varying loads is given by

$$N_L = \frac{N_2}{\frac{n_2}{n_1 + n_2} + R^{1/a}\left(1 - \frac{n_2}{n_1 + n_2}\right)} \tag{A27}$$

where

$N_2$ = number of cycles to failure at the larger varying load when it is the only varying load applied to the specimen,

$n_2$ = the number of cycles applied at the larger varying load,

$n_1$ = the number of cycles applied at the smaller varying load, and

R = ratio of the coefficient of the rate of crack propagation at the smaller varying load to that at the larger varying load = $\frac{r_1}{r_2}$

The ratio R in the above equation was empirically related in reference 15 to the ratio of the smaller to the larger varying stress as shown below.

$$R^{1/a} = \left[ \frac{S_{v_1}}{S_{v_2}} \right]^d \qquad (A28)$$

where

$S_{v_1}$ = relative varying stress, at the smaller load;

$S_{v_2}$ = relative varying stress, at the higher load; and

d = stress invariant exponent.

Equation (A28) was eventually used to extend equation (A27) into a more general equation for fatigue spectra involving any number of varying loads. The resulting equation is:

$$N_L = \frac{N'}{\frac{1}{\sum n_i} \sum n_i \left[ \frac{S_{v_i}}{S'_v} \right]^d} \qquad (A29)$$

where

N' = number of cycles to failure from S-N data for the largest varying load, and

$S'_v$ = relative varying stress for the largest load.

Use of the above equation will be discussed in the following section of this report.

MODIFIED CORTEN AND DOLAN METHOD

The method of Corten and Dolan is modified by replacing the stress ratios in Equation (A29) by a ratio involving the number of cycles to failure. This is readily accomplished when S-N data for a material can be analytically represented by Equation (A6).

In such cases, the following relationship between cycles to failure and relative varying stresses can be derived for the two-step spectrum under the restrictive condition where the relative varying stresses $S_{v_1}$ and $S_{v_2}$ are both greater than the relative endurance limit, $S_E$.

$$\frac{N_2}{N_1} = \left(\frac{S_{v_1}}{S_{v_2}}\right)^{\delta} \tag{A30}$$

or

$$\left(\frac{S_{v_1}}{S_{v_2}}\right)^{d} = \left(\frac{N_2}{N_1}\right)^{d/\delta} = \left(\frac{N_2}{N_1}\right)^{b}$$

with

$$b = \frac{m}{\delta}$$

By generalizing Equation (A30) to cover any number of varying loads, this last equation can be used to eliminate the relative varying stress in Equation (A29). This results in

$$N_L = \frac{N'}{\frac{1}{\sum n_i} \sum n_i \left(\frac{N'}{N_i}\right)^{b}} \tag{A31}$$

Since Equation (A29) was derived in terms of stresses, it implies that all varying loads, including those below the endurance limit, are effective in propagating fatigue damage. On the other hand, Equation (A31) does not consider fatigue damage to be propagated below the endurance limit. This is because the number of cycles to failure, $N_i$, is infinite in this region of the S-N data.

Values of the exponents d in Equation (A29) or b in Equation (A31) can be determined by using test data to define all other terms in the applicable equations.

S-N curves define $N'$ and $N_i$, the unit loading spectra define $S_{v_i}$ or $n_i$, while $N_v$ may best be defined by the geometric means of the test lives of a set of nominally identical specimens. Evaluation of the exponent b from the test data is discussed in Section III.

## A SIMPLIFIED NONLINEAR CUMULATIVE DAMAGE METHOD

While several of the methods which have been described use nonlinear accumulations of damage, an investigation of the simplest type of nonlinear representation was considered to be desirable. For this purpose the available test data will be used to evaluate the exponent in the equation

$$N_L = \frac{\sum n_i}{\sum \left[ \frac{n_i}{N_i} \right]^c} \tag{A32}$$

where

c = empirical exponent that is independent of the magnitude of the varying load.

When the exponent c is assumed independent of load amplitude, it is found to vary with material, specimen configuration, number of loading cycles in the unit spectrum, the number of loading steps, and the sequence in which the varying loads are applied to the specimen.

The exponent c is related to the exponent b in the modified version of Corten-Dolan's method. For a spectrum involving just two loading steps, the relationship between these exponents may be found by equating $N_L$ in Equations (A31) and (A32). This will result in:

$$b = \frac{\log_e\left(\frac{N_2}{n_1}\right) + \log_e \left[ \left(\frac{n_1}{N_1}\right)^c + \left(\frac{n_2}{N_2}\right)^c - \frac{n_2}{N_2} \right]}{\log_e \left(\frac{N_2}{N_1}\right)} \tag{A33}$$

where

$n_1$ = number of cycles applied in the spectrum at the smaller varying load,

$n_2$ = number of cycles applied at the larger varying load,

b = exponent in Equation (A31), and

c = exponent in Equation (A32).

The above relationship becomes rather complex and neither exponent can be expressed as a simple function of the other when a loading spectrum contains more than two different varying loads.

One pertinent difference between the exponent b in Equation (A31) and the exponent c in Equation (A32) lies in the fact that the value of c is more dependent upon block size than the exponent b. If the exponent c were evaluated for a unit loading spectrum which had the same fatigue life when applied at two different block sizes, the value of this exponent would be larger for the smaller block size as illustrated in Figure 52. The value of c is affected by block size through the number of applied load cycles that appear under different exponents in the numerator and denominator of Equation (A32). Figure 52 also indicates that the value of the exponent b is independent of block size at a specific fatigue life. The only effect that block size can have on the exponent b in Equation (A31) is from experimental variations in the fatigue lives used to evaluate this exponent.

Equations (A31) and (A32) both reduce to the simple linearly cumulative damage hypothesis, Equation (A5), when the exponents b and c are made equal to unity.

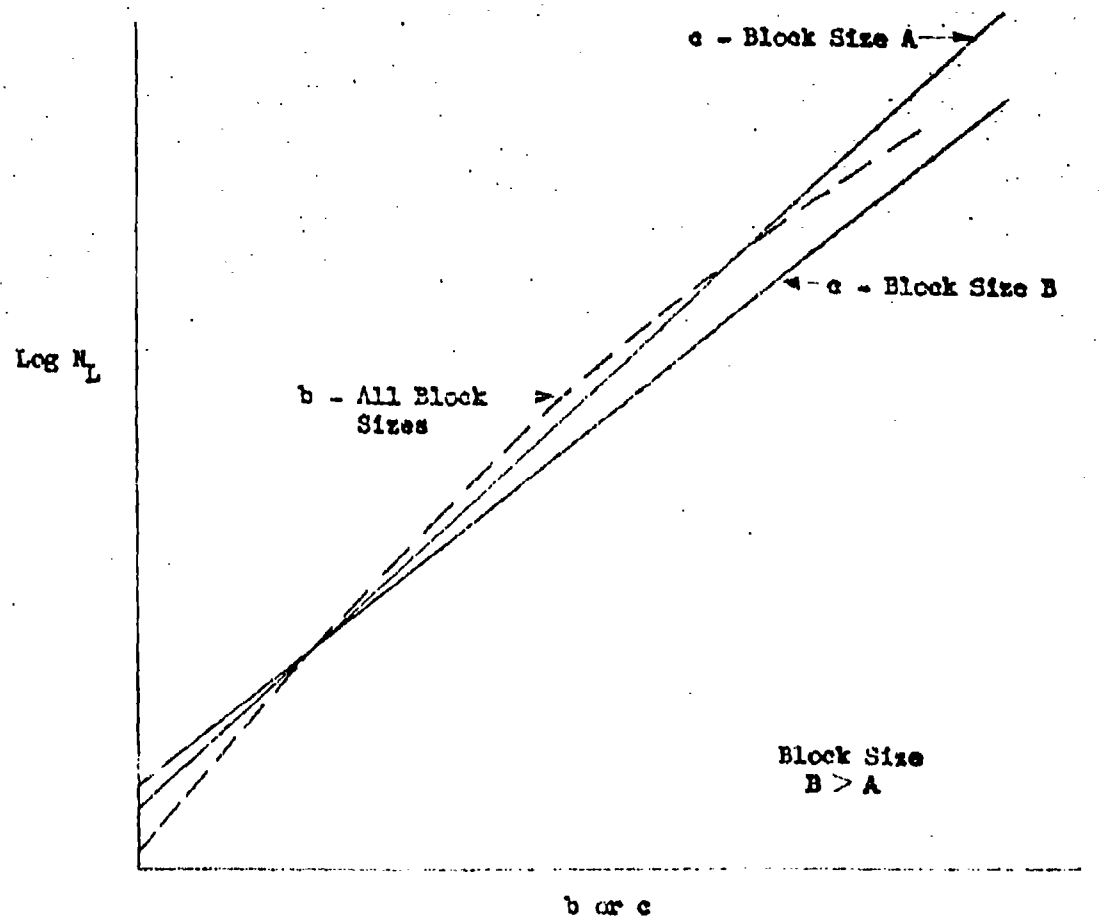



Figure 52 Typical Variation in Fatigue Life with the Exponents b and c for a Specific Unit Loading Spectrum.

## KOMMERS' HYPOTHESIS AND RICHART-NEWMARK'S AND MARCO-STARKEY'S METHODS

The concept that damage curves are a function of both the varying load and the cycle ratio, n/N, was first presented as a hypothesis by Kommers in 1945 (Reference 22). In 1948 Richart and Newmark (Reference 24) and later (1954) Marco and Starkey (Reference 25) proposed graphical and analytical methods for the application of these damage curves to fatigue life predictions. This hypothesis placed only one restriction on the curves. They could have any shape, but each curve was required to indicate a damage level of one when the cycle ratio was unity. Damage curves of this general type are shown in Figure 50. The evaluation of the actual damage curves is difficult because of the problems involved in assessing any degree of damage less than failure. The most important factor, however, is the relationship between damage curves rather than their absolute values. From this concept, Richart and Newmark developed a method for experimentally securing damage curves at a specific varying load relative to an arbitrary damage curve at any reference varying load.

Marco and Starkey (Reference 25) developed an analytical form for damage curves that is similar to that of Richart and Newmark. These authors make the shape of the damage curve at each load amplitude a function of the cycle ratio raised to a load or stress-dependent exponent.

$$D = \left(\frac{n}{N}\right)^{\psi} \qquad (A34)$$

where

D = damage at a specific varying load level,

n = number of cycles applied at the referenced varying load level,

N = number of cycles to failure, and

$\psi$ = load-dependent exponent

In applying the above methods to test results, specially obtained two-step loading test data would be required in large quantities to experimentally determine the relationship between damage boundaries. Since this type of data was not available in sufficient quantity for any of the test conditions being considered, Kommers', Richart-Newmark's, or Marco-Starkey's methods could not be applied.

FREUDENTHAL-HELLER'S METHOD

Freudenthal and Heller (reference 26) proposed the use of a stress-interaction factor to construct a fictitious S-N curve. The fatigue life, associated with a randomly applied unit spectrum of loading, is predicted from the fictitious S-N curve by the concept of linear cumulative fatigue damage, with Equation (A4) being replaced by

$$\sum \frac{n_i \omega_i}{N_i} = 1$$

or

$$\sum \frac{n_i}{N_i''} = 1 \qquad \text{(A35)}$$

where

$\omega_i$ = stress interaction factor that reduces the cycles to failure at the $i^{th}$ varying load after the specimen has had prior exposure to larger varying loads, and

$N_i'' = \frac{N_i}{\omega_i}$ = cycles to failure at the $i^{th}$ varying load from the fictitious S-N curve.

Determination of the stress interaction factor in the above equations depends on the statistical analysis of a large number of test results from a number of loading spectra applied to each type of specimen of interest. Experimental data may eventually be obtained that shows the nature of these interaction factors and some rules for their evaluation. Lack of both the type and quantity of data prevented application of this particular method to the test results used in this report.

## LANGER'S METHOD AND GROVER'S METHOD

Langer (reference 11) and Grover (reference 12) have each divided the process of fatigue damage development into two stages. The first stage involves crack initiation, and the other crack propagation. In Grover's development of this type of analysis, it is assumed that

$$\sum \frac{u_i}{v_i N_i} = 1 \qquad (A36)$$

and

$$\sum \frac{x_i}{N_i (1 - v_i)} = 1 \qquad (A37)$$

where

$$(u_i + x_i) = n_i$$

$u_i$ = number of load cycles applied before crack initiation,

$x_i$ = number of load cycles applied between crack initiation and final failure, and

$v_i$ = per cent of the number of cycles to failure that is used up in initiating cracks at the $i^{th}$ varying load level.

Use of Equations (A36) and (A37) requires information on the number of cycles at each load level for crack initiation and the additional number of cycles to critical fracture. However, if the S-N curves for crack initiation and for failure are parallel, this method reduces to the simple linear cumulative damage equation.

No evaluation of this method was possible because the information required was not reported in the available data selected for this study.

## LEVY'S METHOD

Another approach to analyzing fatigue has been developed by Levy (reference 27). In this approach the following equation was derived for two-step loading by assuming that less than one application of the higher load level in 10,000 total load cycles would have no effect on the S-N curve at the lower varying load.

$$N_L = \sqrt[4]{\left(N_2 \log_{10} \frac{10000\, n_2}{n_1 + n_2}\right)\left(N_1 \log_{10} \frac{n_1 + n_2}{n_2}\right)} \qquad \text{(A38)}$$

where

$N_L$ = predicted fatigue life,

$N_1$ = number of cycles to failure at the lower varying load,

$N_2$ = number of cycles to failure at the higher varying load,

$n_1$ = number of cycles applied at the lower varying load, and

$n_2$ = number of cycles applied at the higher varying loads.

This method was extended to three loading steps, with the following equation being suggested for fatigue life predictions with more than three loading steps:

$$\log N_L = a \log \frac{n_1}{\sum n_i} + b \log \frac{n_2}{\sum n_i} + \ldots + M \qquad \text{(A39)}$$

where a, b, . . . . and M are functions of $N_1$, $N_2$, etc.

This equation is tedious to apply, as it becomes necessary to evaluate (q + 1) constants in Equation (A39), where q is the total number of loading steps in a unit spectrum. An eight-loading-step spectrum, for example, would require nine different sets of relative load frequencies as well as nine corresponding test results in order to solve the resulting system of simultaneous equations for the applicable constants. Once the constants have been determined from this system of equations, only one equation involving these constants would be necessary to predict fatigue life for any one of the specified unit spectra. The type of test data used in this report could not generally be adapted to applications of Levy's method.

## SMITH'S METHOD

Smith, by considering two stress levels, has developed a method in Reference 13 that places primary emphasis on the effects of residual stresses in regions of stress concentration. These residual stresses are induced by plastic deformations during the first high load cycle. Their presence modifies the internal stresses associated with each additional loading, and, as such, is a stress analysis procedure rather than a damage theory or a life prediction method.

The modified stress, including the residual stress component, is used with the unnotched S-N curves and the linear cumulative damage equation to predict the fatigue life.

Since this method considers the influence of local stress variations on the fatigue strength of the material, an accurate stress history at the critical point is required. While this procedure has been demonstrated for simple two-step loading on a simple coupon, its application to multi-spectra in complex structure is not practical as yet. It was not possible to evaluate this method with the data chosen for this study.

TANGENT-INTERCEPT METHOD

The Tangent-Intercept approach (reference 28) was originally conceived to aid in interpretation of spectrum-type fatigue tests. It is in essence a graphical procedure of plotting the total cumulative load frequency spectrum of varying stresses achieved in the fatigue test at failure upon a graded set of S-N curves of the same mean stress level. The $K_T$ value of the S-N curve which is tangent to the test total cumulative load frequency curve becomes the effective fatigue quality associated with the joint tested. Since both the test spectrum and the S-N curves were standardized for all fatigue tests of this era, simply comparing the effective $K_T$ values gives a relative scale of joint quality. The method is schematically demonstrated in Figure 53. Joint A demonstrated a $K_T = 4.00$; Joint B did not last as long under the standardized test spectrum of loading and indicates a tangency to the S-N curve for $K_T = 8.00$. Fatigue tests of many joints which had proven satisfactory in service life showed better than, for example, $K_T = 4.5$. Some joints which developed cracks in service tested worse than $K_T$ of 4.5. By this means $K_T \leqslant 4.5$ became established as the fatigue quality acceptance standard. New joints were required to be redesigned and retested until they demonstrated acceptably low $K_T$ ( $\leqslant 4.5$).

The standard test spectrum was derived from a peak count reduction of flight test records from an instrumented (VGH) Lockheed Model 18 Transport flown approximately 1000 miles through Rocky Mountain weather. Later more extensive records reduced by NACA show that for small service times this spectrum is good. However, with longer service times, relatively greater number of high load levels are developed producing a concave upward shape to the load frequency curve. Other loadings such as landing, taxiing, ground-air cycle, etc., became known as prominent producers of fatigue damage, each at considerably different mean stress levels. When these loadings were included in the test program, the Tangent Intercept approach proved inadequate to handle the added complexities. Its use for the purpose of interpretation of spectrum fatigue tests has since been entirely superseded by the application of the linearly cumulative damage concept.

Proposals have been made to convert this graphical process into a procedure to predict fatigue life (reference 31). As a life prediction procedure, the tangent-intercept method is illustrated on Figure 54. In this method, the prediction of fatigue life is based on the number of times the complete unit loading spectrum can be applied to a specimen before the spectrum becomes tangent to (or intercepts) the S-N curve defined for the test specimen.

As indicated on Figure 54.

$$N_L = \frac{N_T}{H_T} H_S \qquad (440)$$

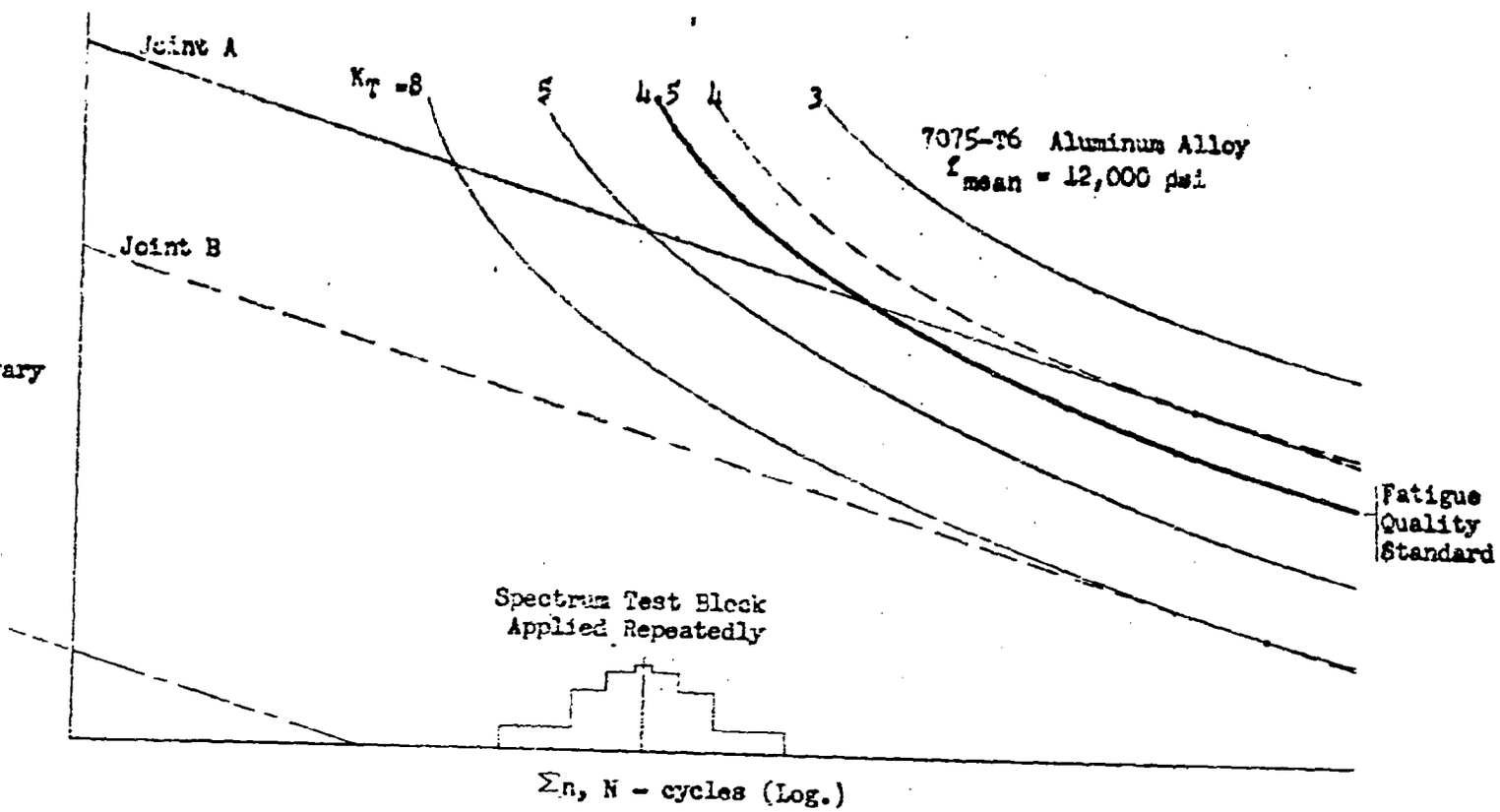



Figure 53 Tangent Intercept Method of Spectrum Fatigue Test Interpretation

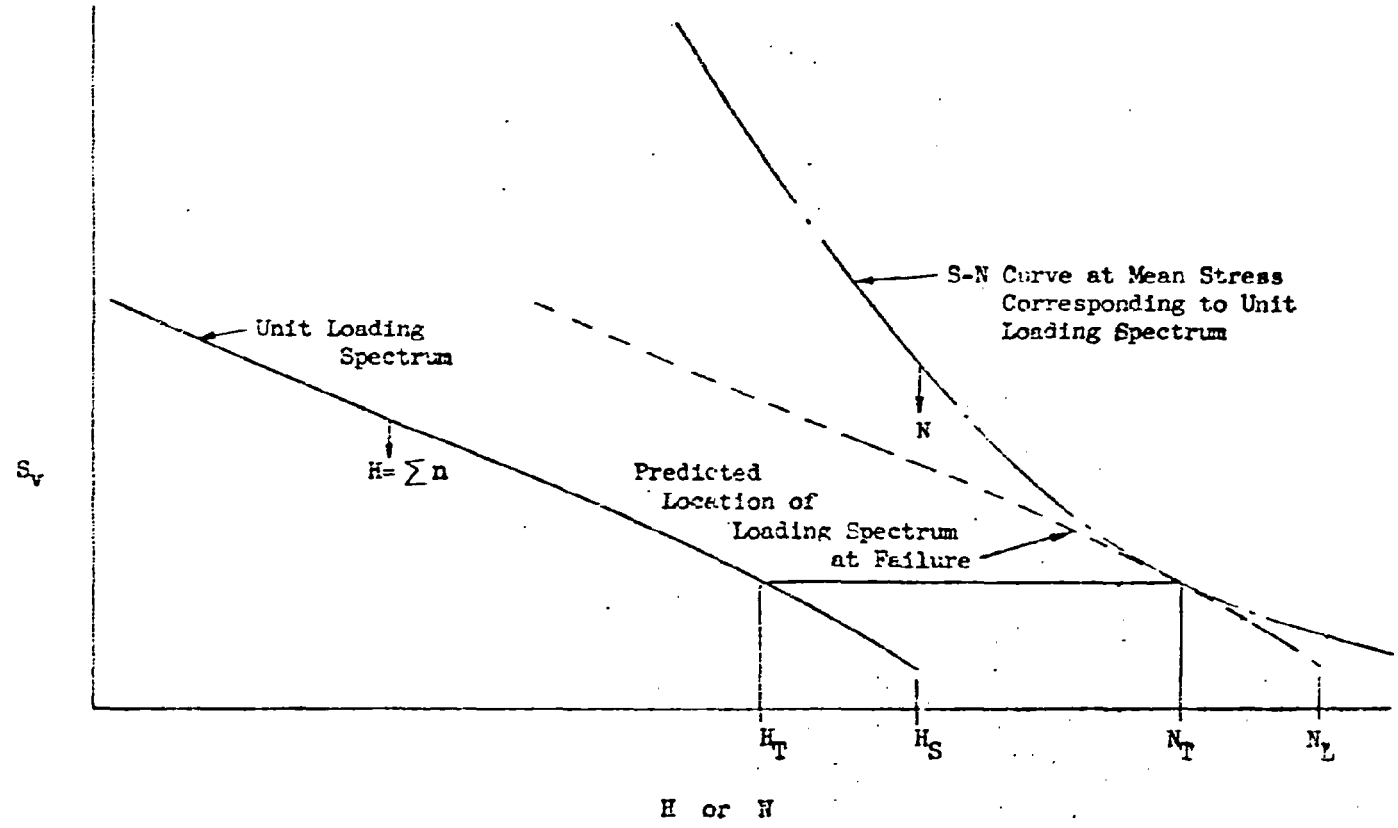



Figure 54 Schematic of Tangent Intercept Method

where

$N_T$ = number of cycles to failure at the point of tangency of the cumulative loading spectrum and S-N curves,

$H_T$ = the total number of cycles in the unit loading spectrum that are applied at or above the varying load at which the cumulative loading curve is tangent to the S-N curve, and

$H_S$ = total number of cycles applied at all varying loads in one complete application of the unit loading spectrum.

Once the unit loading spectrum and the S-N data are specified, the tangent intercept method will give the same predicted life irrespective of the loading sequence or the block size of the unit spectrum.

In terms of the linear cumulative damage process, the basic procedure outlined for the tangent-intercept method implies that the one constant amplitude load in the test spectrum at the point of tangency with the S-N curve is the only load which creates damage, and all other loads, both above and below this level, contribute no fatigue damage. This is, of course, known to be unconservative.

In the graphical application of the procedure, one test spectrum of a gust or a maneuver type may be conveniently compared with an appropriate set of S-N curves at a time. If the required total loading spectrum contains other significant types of loadings, such as combined gust, maneuver, ground taxi, and ground-air-ground transitions, the graphical procedure becomes hopelessly inadequate and impractical.

For these reasons no attempt was made to develop an empirically corrective procedure to reduce the unconservatism of the tangent-intercept fatigue life predictions.

## STRESS CONCENTRATION METHOD

The stress concentration procedure is a method of stress analysis to define as accurately as possible the stress distribution in local regions of discontinuities. (Typical references 1, 2 & 3 ) Before specific fatigue test data are available on a part, coupon, or joint specimen, the analytical assessment of the fatigue quality of a design is possible only through means of highly refined theoretical and/or photo-elastic or experimental stress analysis procedures. This type of analysis has in the past received a large amount of attention. This attention is currently no less, and work will continue to expand in the future. A large body of literature exists which provides solutions for many types of discontinuities and applied loading systems. However, for the reasons discussed in the introduction, applications of this analytical approach (including, as well, both experimental photoelasticity and static experimental stress analysis by means of strain gages and others) can only be considered a rough approximation until specific fatigue tests can be run.

To complete a life prediction method, the stress concentration procedure must be coupled with a fatigue damage theory. For evaluation in this study, the Miner's simple linear cumulative damage hypothesis was chosen. This method, used with a standardized set of S-N data for various geometrical $K_t$ values, constitutes the basic information usually available in early stages of design. The choice of the standard S-N curves is, in essence, arbitrarily specifying a damage boundary shape before this boundary has been determined or confirmed by tests. For important complex joints or critical areas of the structure, the timely confirmation or correction of the fatigue quality and the life prediction by fatigue tests through the full range of the loading spectrum is of utmost importance.

FATIGUE QUALITY INDEX METHOD

The Fatigue Quality Index method was developed to overcome the difficulties inherent in the use of the Tangent Intercept method for the interpretation of a composite spectrum test on a complex joint. The composite test spectrum is generally made up of a taxi-load spectrum at the ground static mean load level, a gust and/or maneuver and landing spectrum at the flight static mean load level, and ground-air-ground transition cycles for each flight. The spectrum fatigue results are interpreted by the use of the simple linearly cumulative damage equation to specifically define (by interpolation) which of the standardized S-N curves (identified by $K_T$ value), when used in conjunction with the actually applied test spectrum, will exactly satisfy the equation:

$$\sum \frac{n_i}{N_i} \equiv \quad \text{(A41)}$$

The stress concentration factor whi identifies these curves becomes the Fatigue Quality Index demonstrated l The test specimen under its expected loading spectrum. The Quality Inde ust be equal to or smaller than the established quality standard or else redesign and retest is necessary until satisfactory quality is achieved. established quality standard is based on the results obtained in an ident l, consistent analysis of many joints which have a known service history.

For comparative purposes the quali scale must remain fixed and the analysis system consistent between the anal of service history and the analysis of tests of new structure. Generally complete S-N curve is not available for each complete joint or critica rea of the structure. For these reasons one set of S-N data for the hard minum alloys has been fixed and all test interpretations and life predictic are based on the consistent use of this standardized set. This standardiz set of S-N curves may be considered an arbitrarily defined damage bounda nd, in the usage outlined, have no longer any significant relationship to th data from which they were derived.

For its use as a life prediction hod a Fatigue Quality Index is determined from a fatigue test in which a con ite spectrum of all anticipated service loads is applied to suspect areas the structure. The Fatigue Qualit derived from this test result may considered as a test-derived d boundary on which life predictions this structure may be made for similarly shaped loading spectra.

The Quality Index procedure as a prediction method is evaluated alon with the other selected methods by ication to suitable data from the literature and to the special fatig ta generated for this program. These evaluations are discussed in the appropriate places elsewhere in this report. See Sections III through VI.

## APPENDIX B

## APPLICATION OF SELECTED FATIGUE LIFE PREDICTION METHODS TO PUBLISHED TEST DATA

The study of the twenty proposed fatigue life prediction methods, conducted i Appendix "A", reduced the list to ten which were to be evaluated numerically by application and comparison with the selected spectral fatigue test data described in Appendix "C". It was also decided to vary the procedure of mathematical curve fitting in two of these methods to determine the significance of alternate equation parameters for S-N curves, one set derived for a least square "best fit" for all data points, and the other set derived for a least square "best fit" in the local region of the midstress levels, where usually the maximum calculated damage is found. These twelve applications ar those listed:

1. Miner's Linear Cumulative Damage Method.
2. Lundberg's FFA Method - Variant "A", with best fit to the midstress range of S-N and loading spectra data.
3. Lundberg's FFA Method - Variant "B", with best fit to the full-stress range of S-N and loading spectra data.
4. Shanley's "1X" Method.
5. Shanley's "2X" Method.
6. Henry's Method - Generalized Form - Variant "A", with best fit to the midstress range of S-N data.
7. Henry's Method - Generalized Form - Variant "B", with best fit to the full-stress range of S-N data.
8. Tangent Intercept Method.
9. Stress Concentration Procedure with Linear Cumulative Damage.
10. Fatigue Quality Index Method.
11. Modified Corten-Dolan.
12. Nonlinear Cumulative Damage.

The following sections explain the applications of each of these methods to the prediction of the fatigue lives of test specimens for which spectral and S-N data are listed in Appendix C.

The comparisons of the predicted fatigue life and experimental fatigue life are given in Section III of the main body of the report.

In addition to the direct comparison of fatigue lives on the cycle scale, a constant proportional adjustment in the varying stress levels was determined to make the predicted life exactly the experimental life for each test group by each method. The application of the proportionality factor to the mean

stress would, of course, make a more meaningful assessment of the effect of cross-section material changes in design. However, since the influence of the mean stress is not expected to change the order of ranking of the methods, the more simple comparison was chosen. The results of the analysis and comparisons of the various methods by the stress adjustment factor are given in Section III of the main body of the report.

1. Miner's Linear Cumulative Damage Method

The direct application of Miner's linear cumulative damage method is simple and straightforward. The unit cumulative frequency spectrum for the applied loads of each group is reduced to the simple number of cycles, $n_i$, in each stress interval in Tables 31 through 47 of Appendix C. The stress intervals are those used in each particular test, and the reduction from the accumulated spectrum to the simple spectrum is in accordance with the definitions given in Figure 55. Assuming all the cycles within one stress interval to act at the equivalent stress level approximately the mid point of the interval, the allowable number of cycles, $N_i$, at that stress level was interpolated from the appropriate form of the S-N curve; i.e., symmetrical varying stresses about a constant mean stress for gust-type spectra while varying stresses that maintain a constant minimum stress were used for the maneuver-type spectra. The interpolating function is a straight line segment in $S_y$ - Log N from tabulated input data taken at relatively close intervals. These values of $N_i$ are also listed in the Tables 31 through 47 . The individual damage ratios are formed and summed for all the stress intervals to form the damage for the unit spectrum. The life prediction for the group is then computed by Equation (B1):

$$N_L = \frac{\left(\sum n_i\right)_{\text{unit block}}}{\left(\sum \frac{n_i}{N_i}\right)_{\text{unit block}}} \qquad \text{(B1)}$$

These computations were performed on the IBM 7090 computer.

The stress adjustment ratio was determined by the change in slope of the accumulative spectra (i.e., constant proportional change to the stresses of all intervals) to require the process to exactly predict the test life. This was accomplished by an iteration procedur programmed for digital computation on the IBM 7090 computer.

Special handling was found necessary for some cases in which small changes of the stress adjustment factor would increase or decrease the mid-interval stress of the lower block in the vicinity of the endurance limit stress. Bringing in or dropping out of the large number of cycles in this last block could indicate a disproportionate

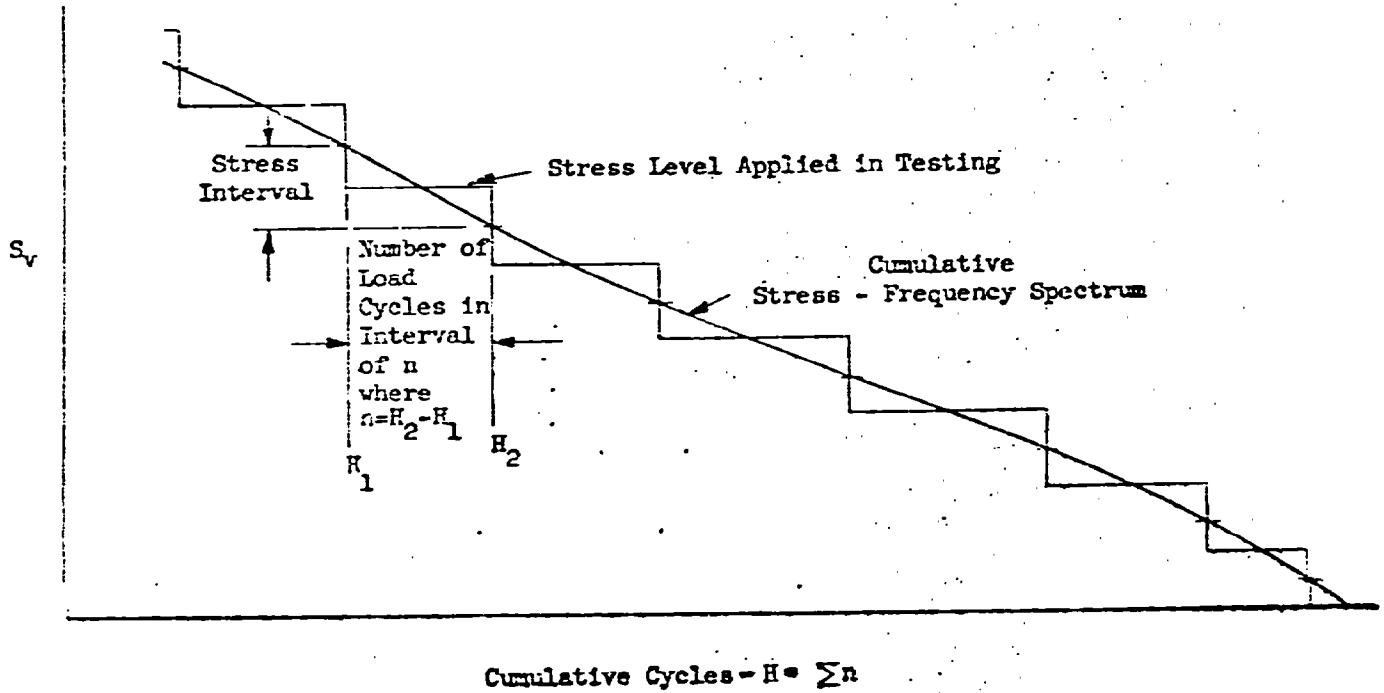



Figure 55 Method used to Reduce Cumulative Stress - Frequency Spectrum into Simple Cyclic Loading Steps.

shift in the predicted fatigue life for those cases where the S-N data indicate an actual endurance limit, or those cases in which an arbitrary endurance limit had been defined at $10^7$ cycles.

2. Lundberg's FFA Method

Since Lundberg's FFA method is basically an analytical form of the linear cumulative damage procedure, application consists of the determination of the mathematical curve parameters for the best fit to the unit applied loading spectrum, and those for best fit to the appropriate S-N curve. The suggested equation for gust-type spectra Equation (A15) has two adjustable parameters, $H_o$, the intercept, and h, the slope of the straight line, which is a best fit of the unit cumulative relative varying stress history when plotted in semi-log form of $S_V$ vs. log $\sum n$, as in Figure 56. The parameters for the S-N curve, $\alpha$ and $\beta$ from Equation (A14), represent, respectively, the intercept and the slope of the straight line which best fits the S-N data in a $\log(S_V - S_E)$ vs. log N plot as in Figure 57. These four parameters were determined for each test case using the applied unit loading spectra and the appropriate type of S-N data for gust spectra, or for maneuver-type spectra. The S-N curves for each type of specimen were determined for the applicable mean stress or minimum stress through interpolation on the Christensen diagram as discussed in Section D. Where necessary, parameters for the unit loading spectra were biased to best fit the midstress range in the region of maximum calculated damage. The parameters for the S-N curves were determined for two cases:

Case (A) for a best fit to the midstress range of S-N data in the region of maximum calculated fatigue damage ratios, and

Case (B) for a best fit to the full stress range.

The parameters for the equations of Case (A) are given in Table 19; those for Case (B) are given in Table 22 for the gust spectra tests. The unit damage computed from the unit spectra is given in terms of these four parameters by Equation (A18) of Appendix A, and the predicted fatigue life is computed by Equation (A5) of Appendix A. These fatigue life predictions are listed in Table 21 for the gust spectra by Case (A) and in Table 22 for Case (B). The fatigue life predictions for the maneuvering spectra tests are given in Table 23. The geometric mean of the experimental fatigue life of each group of tests is given in each table for direct comparison. These data are plotted in Figures 5 and 6 in Section III, where comparisons of those results with those of other methods are discussed.

The stress adjustments required to predict exactly the experimental fatigue life were determined for each test group by trial manipulations of the unit test spectra slope parameter h, maintaining $H_o$ the intercept constant. The resulting stress adjustment factors are listed in Table 24 for the gust loading spectra, and in Table 25 for the maneuvering-type spectra.

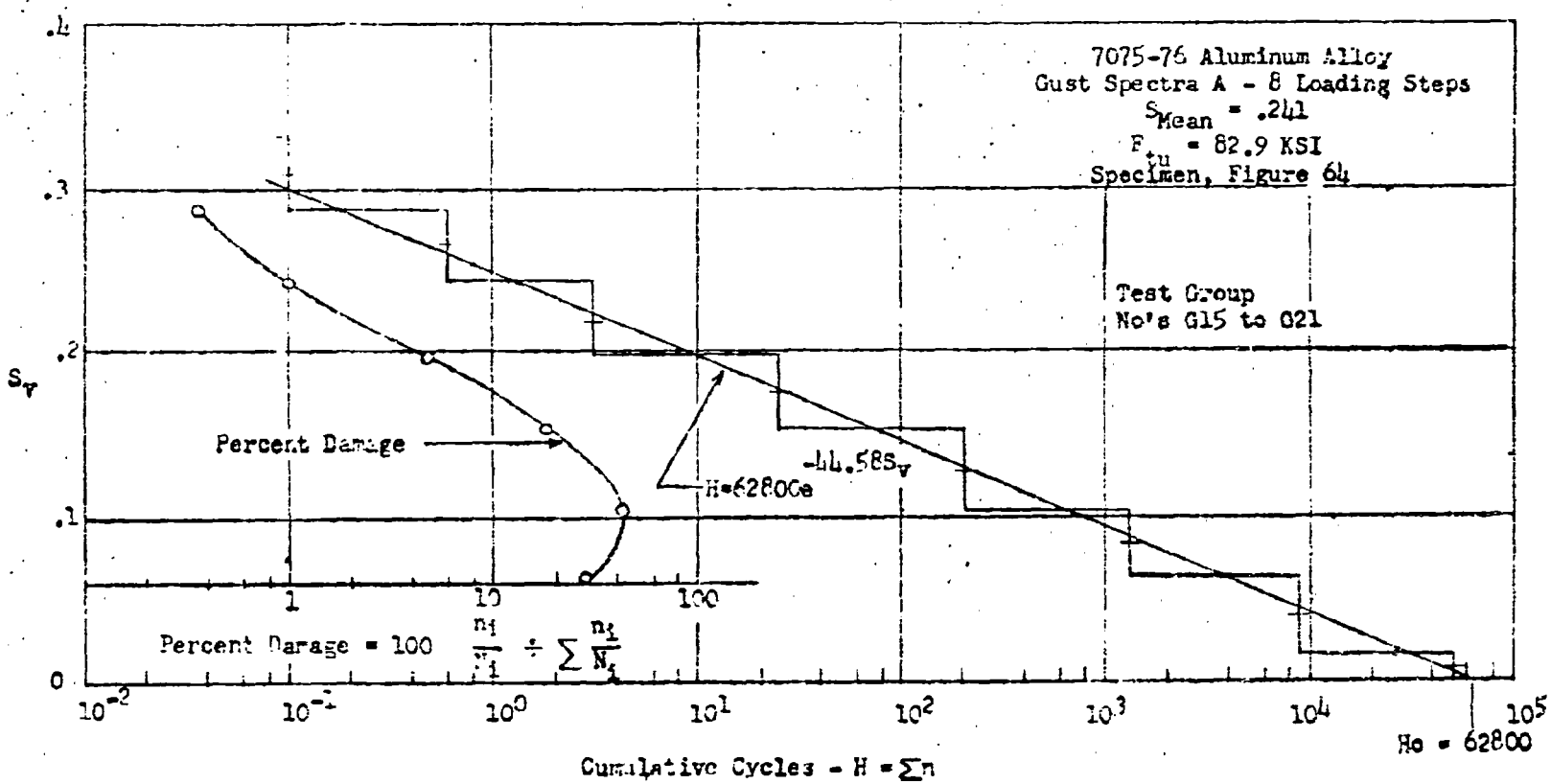



Figure 56 Comparison of Analytical and Experimental Unit Gust Loading Spectrum for Notched Sheet Specimens

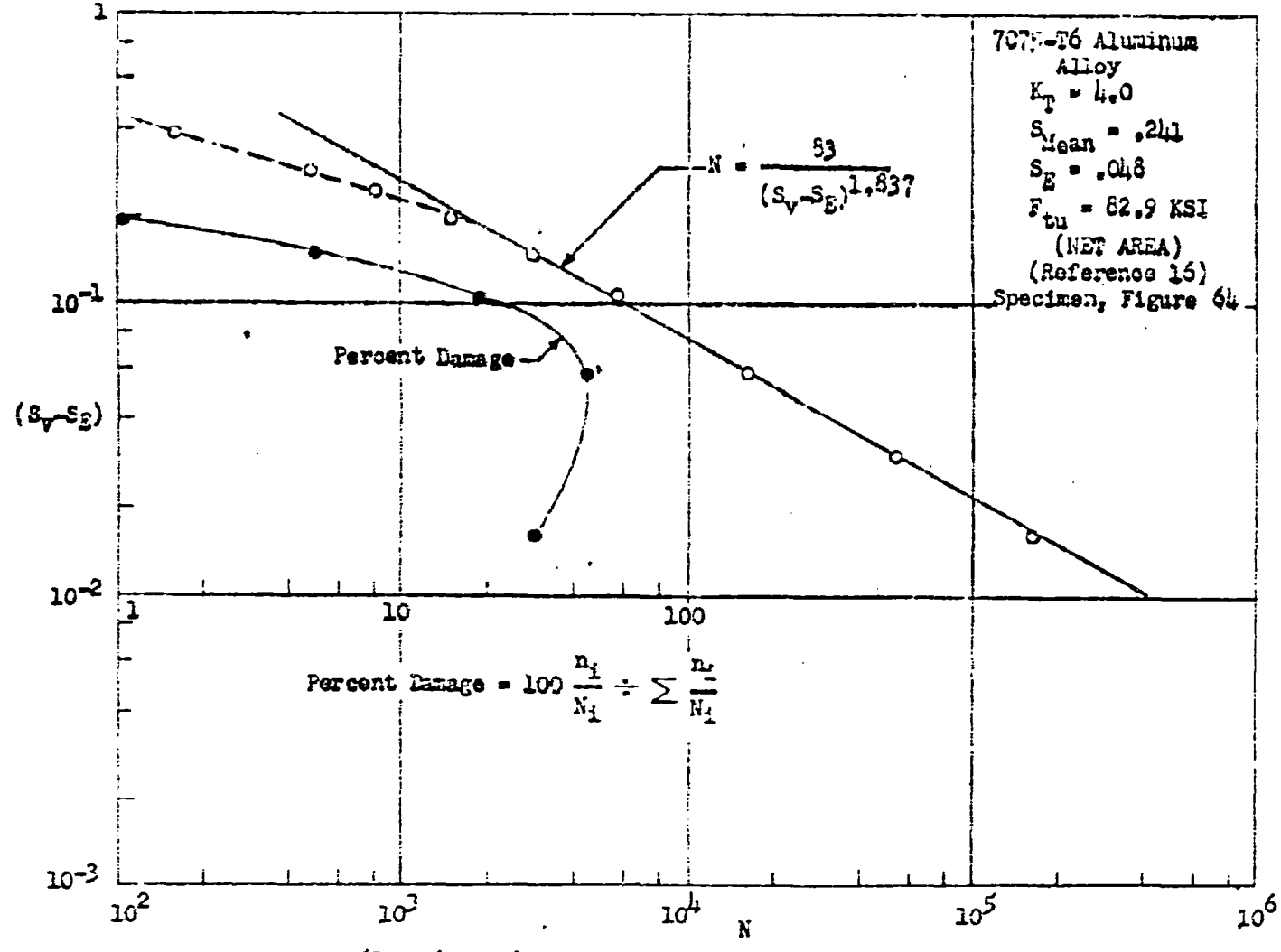



Figure 57 $(S_V-S_E)$ Versus N for S-N Data on Notched Sheet Specimens

3. Shanley's "1X" Method

In predicting fatigue life with Shanley's "1X" method, reduced varying stresses were computed for each of the loading spectra that were compared with test data. The number of applied cycles $n_i$ and the corresponding relative varying stresses $S_{V_i}$ above the endurance limit were provided from the test spectra in Tables 31 and 47 of Appendix C. The exponent $\delta$ in Equation (A6) was evaluated from the pertinent S-N data by a least square straight line fit to a plot of log $S_V$ versus log N. In securing this fit, S-N data points for the low stresses near the endurance limit were omitted because these stresses did not generally lie on or near the straight line which fit best the rest of the S-N data. After the exponent $\delta$ has been obtained from S-N data, the solution of Equation (A9) for a relative reduced stress $S_R$ corresponding to the stresses above the endurance limit in a loading spectrum is straightforward. The predicted number of cycles, $N_R$, to failure for load levels above the endurance limit are then read from the appropriate S-N curve at the computed value of $S_R$. Predictions of fatigue life in terms of cycles of applied loads at all levels, including those below the endurance limit, in a unit loading spectrum are then obtained from Equation (A13) by multiplying $N_R$ by the ratio of total number of cycles in the unit block to the number of load cycles applied above the endurance limit. The resulting life predictions, $N_L$, are listed in Table 21 for gust loading spectra and Table 23 for maneuver loading spectra.

Stress adjustments were also computed by interpolations to make the "1X" method exactly predict the test results. These adjustments are given in Tables 24 and 25.

4. Shanley's "2X" Method

The fatigue lives for Shanley's "2X" Method in Tables 21 and 23 were determined from Equations (A11) and (A13) in a similar manner as for Shanley's "1X" Method. The proportional stress adjustment factors determined by this method to exactly predict fatigue test lives are given in Tables 24 and 25.

5. Generalized Henry's Method

Fatigue life predictions by the generalized Henry's Method were computed for each of the test groups by the alternate application of Equations (A24) and (A25) of Appendix A, and accounting for the sequence of loading in the test block of each unit spectrum until the damage reached a value of unity. The number of blocks repeatedly applied to reach the damage value of unity is then the measure of the predicted fatigue life.

The parameters $\beta$ & $S_E$ in Equations (A24) and (A25) were determined for each of two cases of curve fitting.

Case (A) is the best fit line in the limited mid-stress range in the region of maximum calculated damage, from the graphs of log $(S_V - S_E)$ vs. log N.

Case (B) is the best fit line for the full stress range on the graphs of log $(S_V - S_E)$ vs. log N.

These parameters are given for each test group in Table 19 for the gust loading spectra utilizing the Case (A) curve parameters for the S-N data, and in Table 22 for the Case (B) curve parameters. The S-N curve parameters for the maneuvering spectra tests are given in Table 20. The cycles to failure N at each of the stress levels used in testing were read from an S-N curve.

The fatigue life calculated for each group of tests is given in Tables 21 and 22 for the gust spectra loadings with the Case (A) and Case (B) forms of S-N data, respectively, and in Table 23 for the maneuver spectra test groups in which only Case (B), the best fit for the full range of S-N data, was used. The experimental test results are also given in these tables for direct comparison. These predictions are plotted along with the prediction results of the other methods and with the experimental results for comparative evaluation of each of the methods in Section III in the main body of the report.

In addition to the fatigue life evaluation, the Generalized Henry procedure is used to determine the proportional stress adjustment factor required to predict exactly the test life. These factors are listed in Table 24 for the gust spectra test groups and in Table 25 for the maneuver spectra groups. These results are also compared with the results of other methods in Section III of the report.

In several of the test groups (G42 and G43) it was noted that a damage ratio in excess of unity was achieved within one of the stress intervals. The computing procedure, of course, recognizes this as failure and predicts life as less than the unit block size although, experimentally, these groups lasted from approximately twelve to sixteen times longer than predicted. These were extreme cases of the High-to-Low sequence of loading within the test block in which very few blocks were applied. Residual stresses from early plastic yielding no doubt greatly benefited the net effective fatigue stress at the peak stress point. These examples point up the important influence test variables often have on fatigue life in the laboratory. The probability of these type events occurring in service cannot be deduced from current data reduction procedures.

6. The Tangent Intercept Method

The fatigue lives predicted by the Tangent Intercept method were secured by locating the point at which the cumulative loading spectrum was tangent to the appropriate S-N curve and applying Equation (A40) to arrive at the total cumulative number of cycles in the tangent spectrum.

The stress adjustment factor was also derived by trial changes in the slope of the loading spectrum until the total cycles predicted agreed with the experimental test results.

The fatigue life predictions are listed in Table 21 for each group of gust loading spectra tests, and in Table 23 for each group of maneuver loading spectra tests. The experimental values are also given for direct comparison. The stress adjustment factors are listed in Tables 24 and 25 for the gust and maneuver loadings, respectively.

7. Stress Concentration Factor Method

The stress concentration factor method as described in Appendix A is an analytical stress analysis procedure for defining the local critical stress state which, when coupled with a fatigue damage theory, may be used to predict fatigue life. Its area of usage is limited to preliminary design assessments in which only minimum information is available. The application of this procedure makes use of the simple linear cumulative damage hypothesis. The appropriate S-N curve is selected from the group of standardized S-N data in Figures 58 to 62 by means of the theoretical stress concentration factor reported for each particular test specimen. Thirty groups of data from those listed in Appendix C were analyzed by this procedure. The resulting fatigue life predictions are listed in Table 21 for the gust spectra tests. The experimental fatigue life for each test group is also listed for comparison.

The stress adjustment factors were determined, using the same sets of data, to make the predicted fatigue life equal to the experimental fatigue life. These factors are listed in Table 24 for the gust spectra tests. Comparisons of the results of these predictions with those of the other methods chosen for evaluation are given in Section III in the main body of the report.

8. Fatigue Quality Index Method

The Fatigue Quality Index method was used to predict fatigue life for thirty-three test groups. The application of this method requires the use of one spectral fatigue test result to determine by interpolation which K curve, of the standard set of S-N data (Figures 58 to 62), is

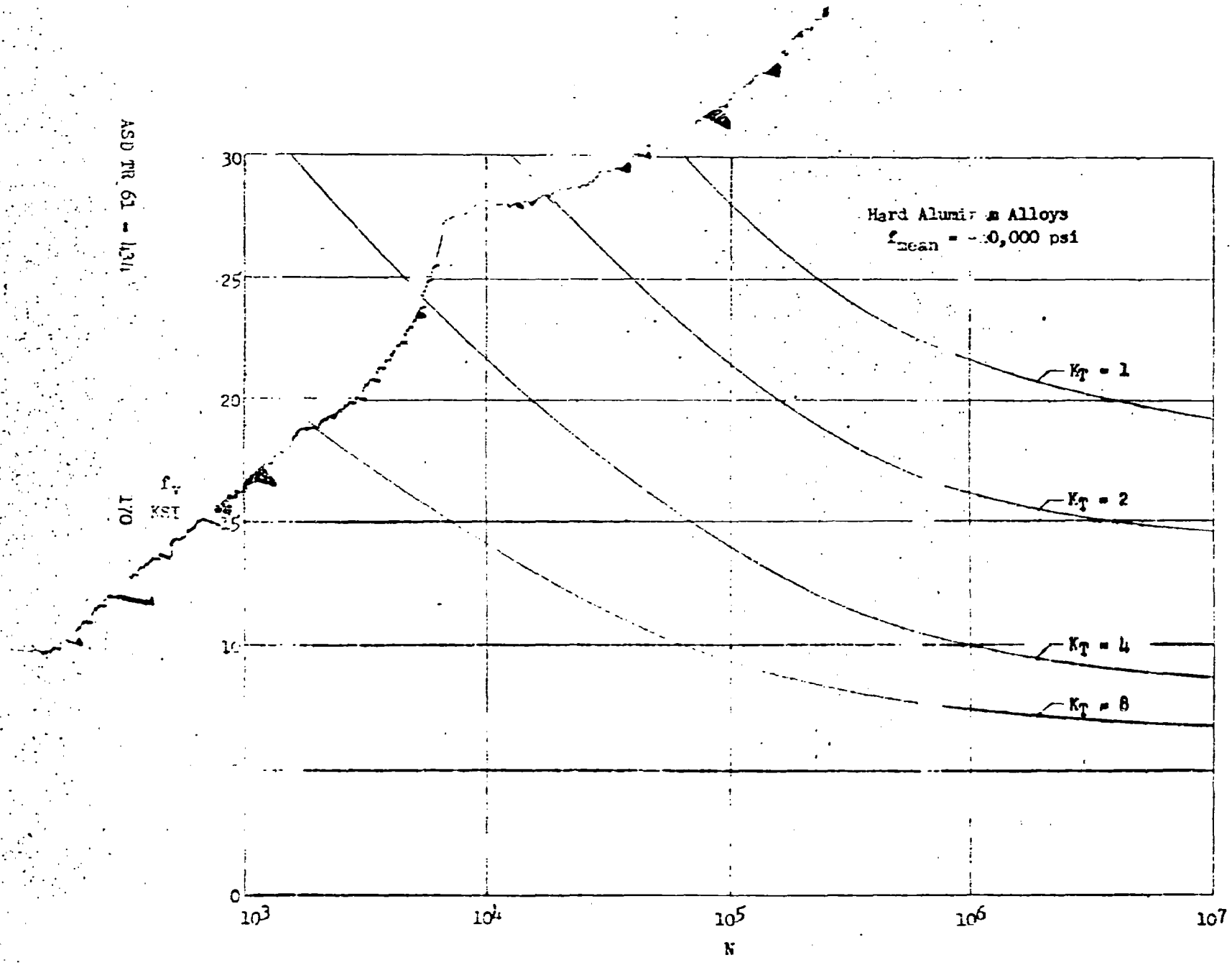



Figure 58 Standardized S-N Curves

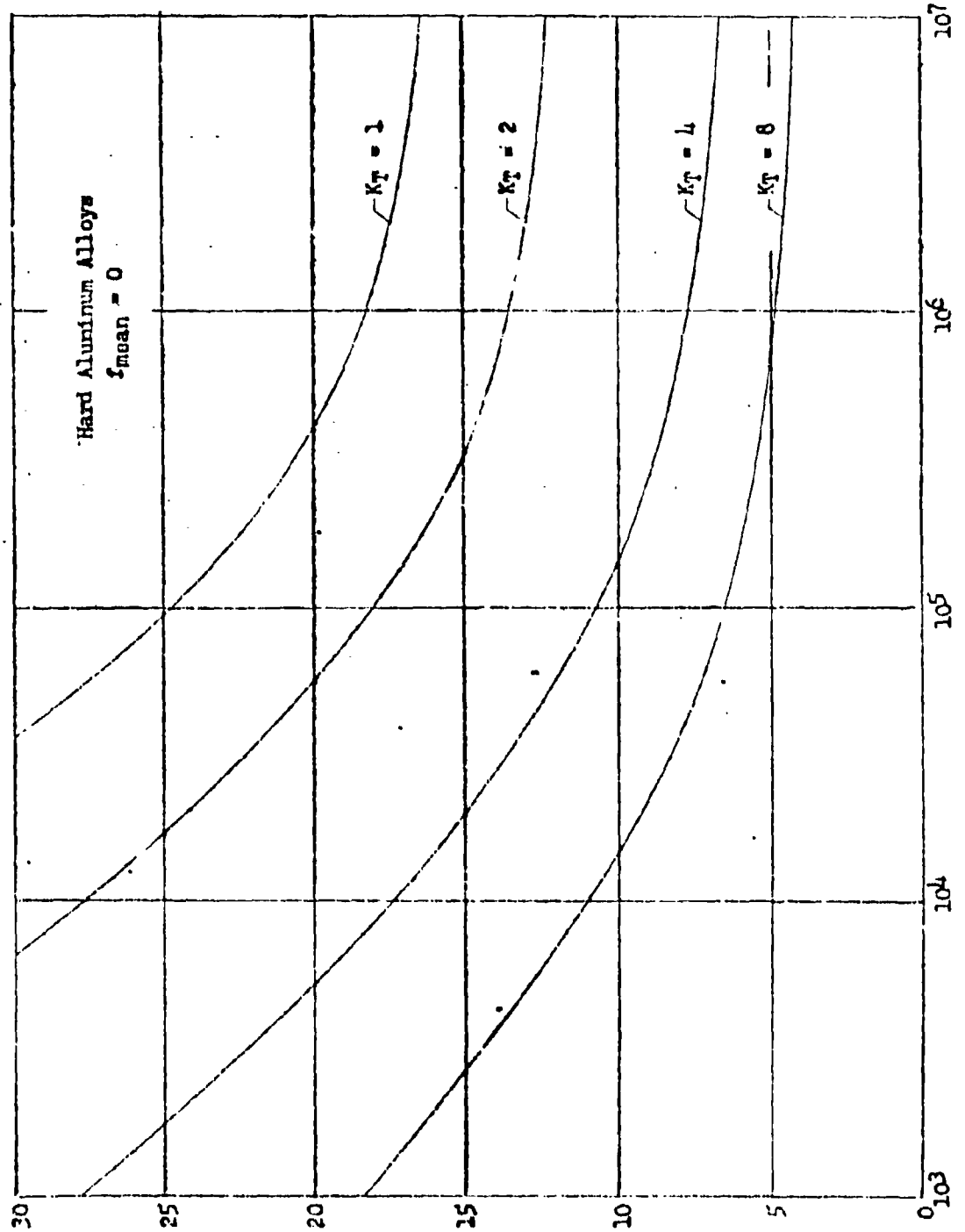



Figure 59 Standardized S-N Curves

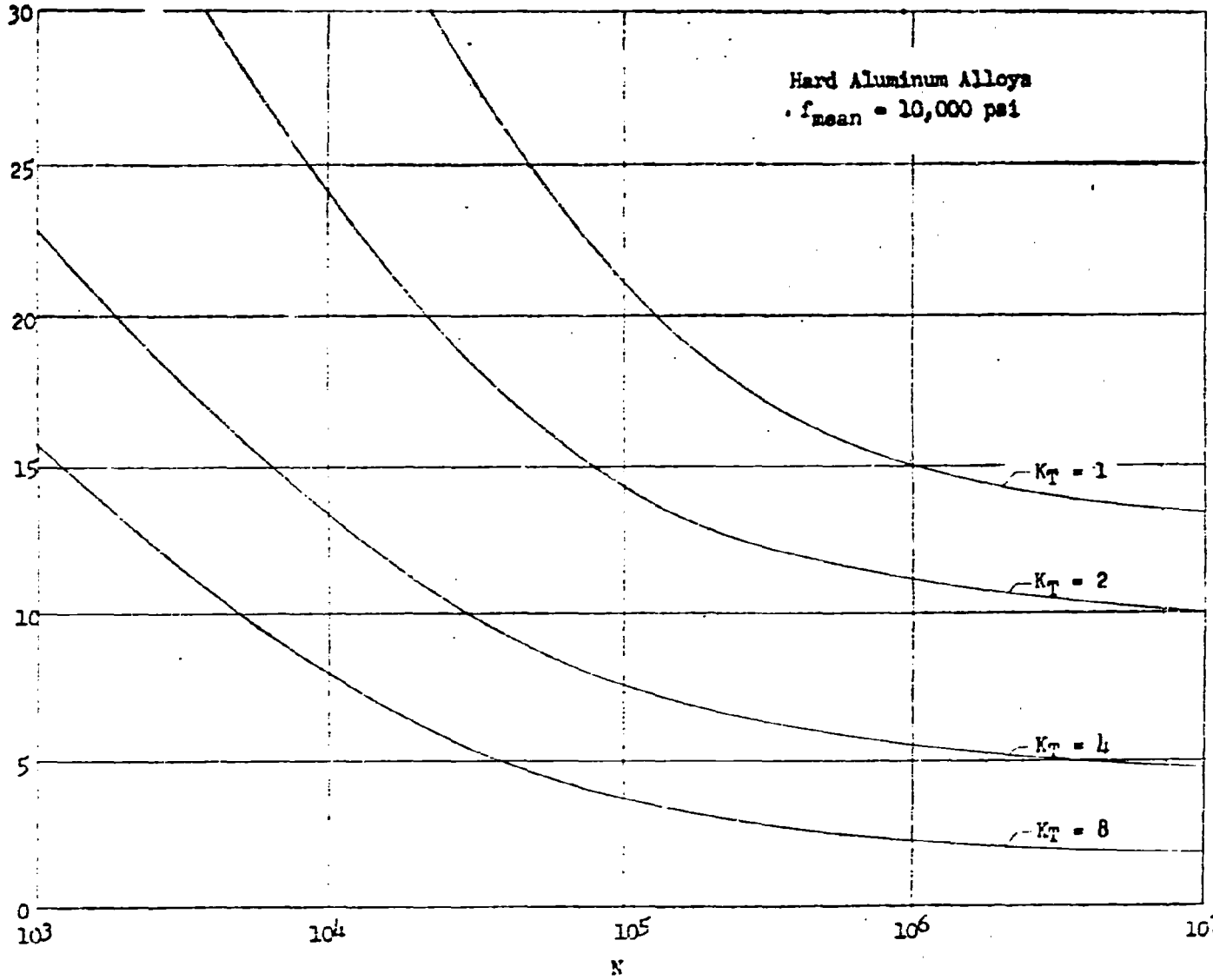



Figure 60 Standardized S-N Curves

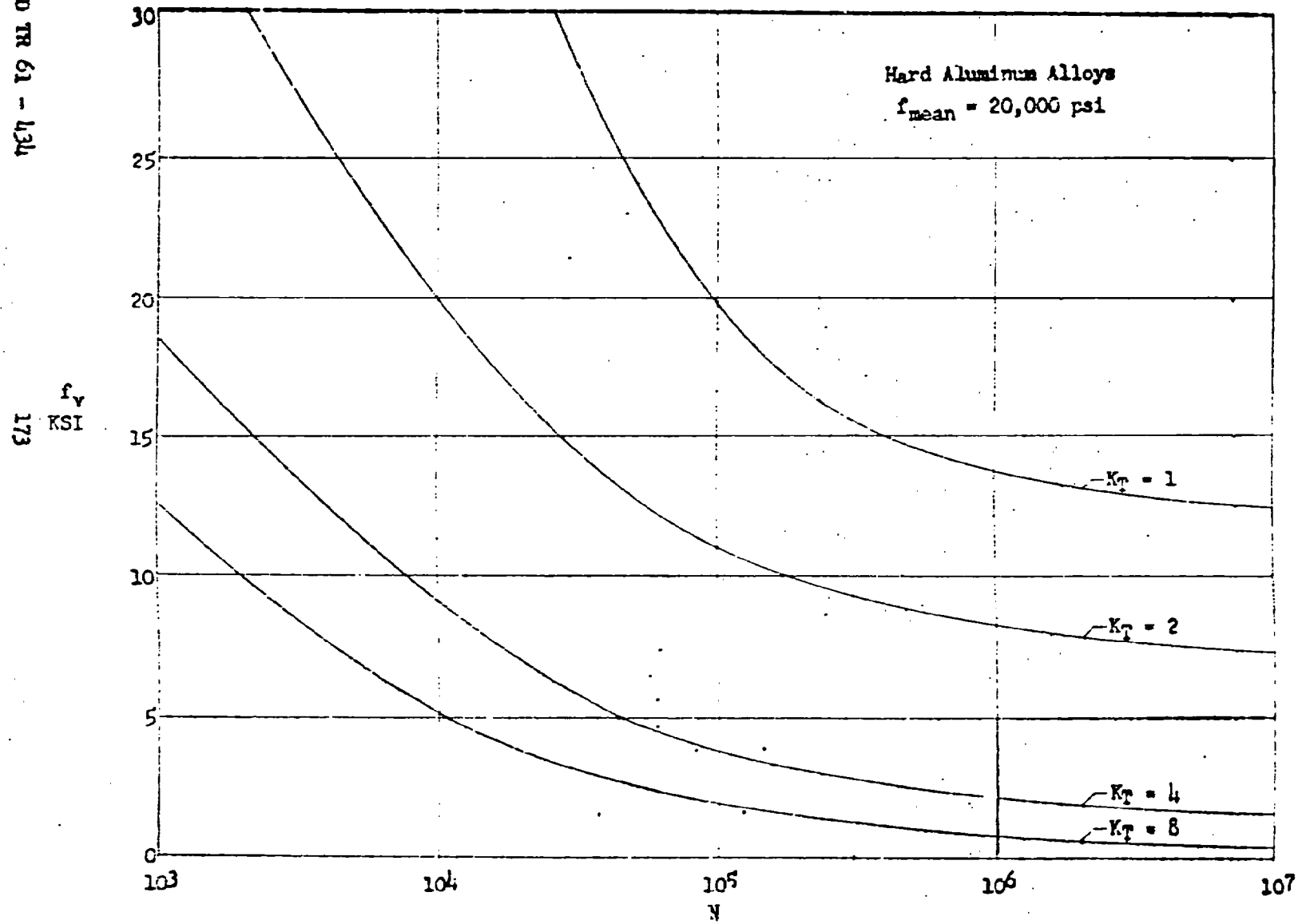
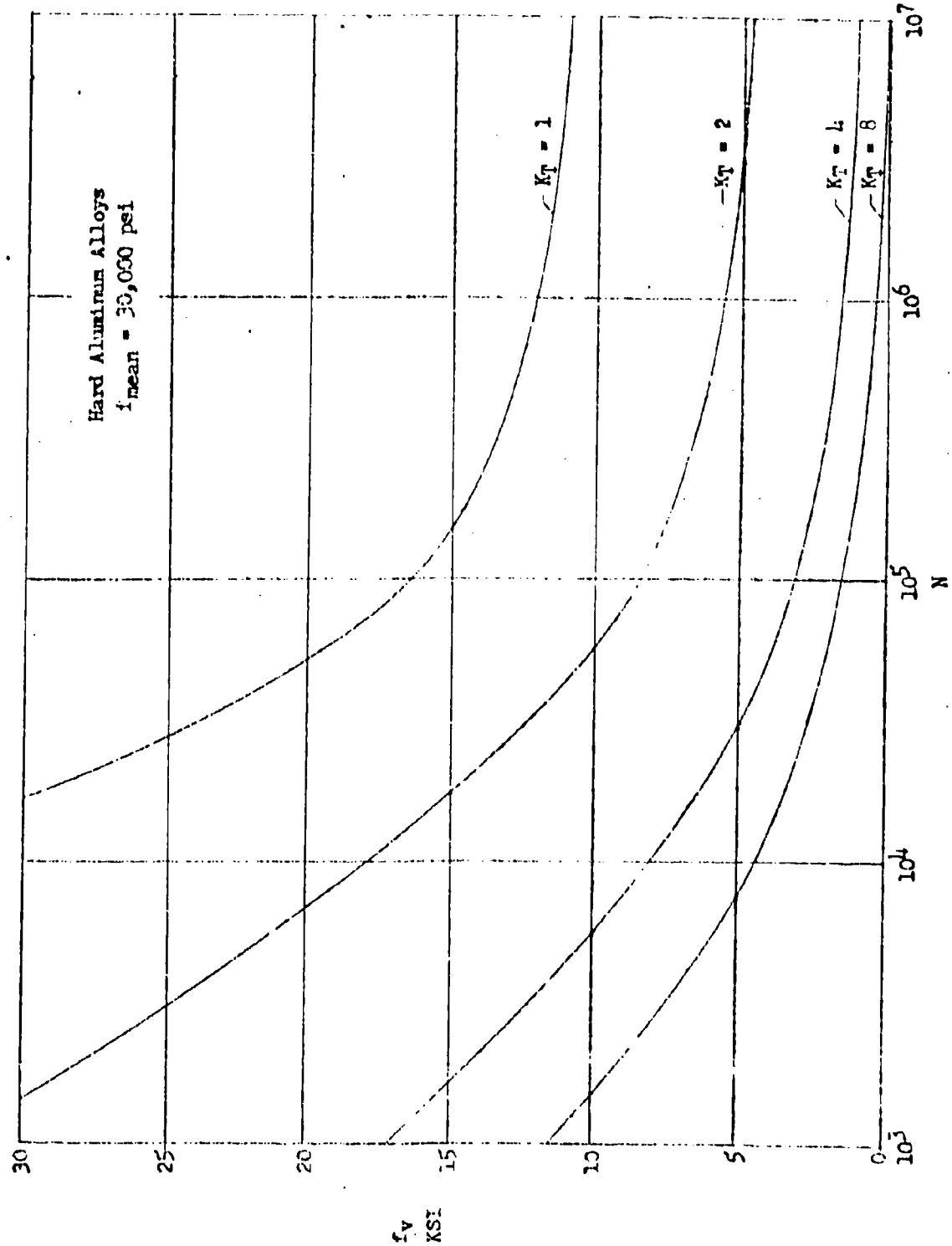



Figure 61 Standardized S-N Curves


Hard Aluminum Alloys
$f_{mean}$ = 30,000 psi
$K_T$ = 1
$K_T$ = 2
$K_T$ = 4
$K_T$ = 8
30
25
20
15
10
5
0
$f_v$ KSI
$10^3$
$10^4$
$10^5$
$10^6$
$10^7$
N

required to make the linear cumulative damage equation equal unity for this test result. Interpolation of these standardized S-N curves to the mean stress of each test group is made from Christensen diagrams similar to those described in Appendix D. The test-derived Fatigue Quality Index or K is listed in Table 26 for all of the gust spectra that were applied to aluminum specimens and in Table 27 for maneuver spectra applied to aluminum specimens. One of these test-derived K is used as a base test to predict the fatigue life of identical specimens loaded under other similar types of spectra.

To reduce the bias in choice of the base test, only those test groups were selected which had a quasi-random or Lo-Hi-Lo loading sequence in conjunction with the same and other types of loading sequences in similar test groups. These selected spectrum test groups were first used to derive the K for which Equation (A41) was exactly satisfied. The resulting value of K was then used to obtain fatigue life predictions for the test groups that are noted in Table 21.

The stress adjustment factors in Table 24 were also determined for this same set of test groups to make the predicted fatigue life exactly match the test life when using the previously derived Quality Index in the linear cumulative damage procedure.

The Quality Index Procedure is effective only when fatigue life predictions are made for loading spectra that have approximately the same shape of slope, the same number of loading steps, relatively similar stress increments, fairly close mean loads, equivalent block sizes, identical loading sequences and essentially the same point of fatigue failure. All of these conditions were not satisfied between any two of the Test Groups that were analyzed. Just to consider, for example, the point of failure on the C-46 wing, in Test Group No. G56 where the occurrence of a critical crack on the complete wing was used to select a test-derived K for analyzing Test Groups G51 to G55 and G57. A total of six critical cracks occurred in Test Group G56, four at Wing Station 195, one at Wing Station 204, and one at the corner of the inspection cutout B at WS214 in Figure 68. Out of these Wing Stations at which critical cracks occurred, only Wing Station 214 was analyzed by the Quality Index Method. This analysis of Wing Station 214, however, was for crack initiation at the corner of the inspection cutout plate at H in Figure 68 rather than the corner of the inspection cutout at B.

9. Modified Corten and Dolan and Nonlinear Cumulative Damage

The exponent b in Equation (A31) of the Modified Corten-Dolan method and the exponent c in Equation (A32) of the nonlinear cumulative damage method were evaluated from the test data in the manner described in Appendix A. The resulting values are tabulated in Table 28 for gust loading spectra and in Table 29 for maneuver loading spectra.

Fatigue life predictions, however, were not made with either the Modified Corten-Dolan's or nonlinear cumulative damage methods, since the resulting average values of 1.097 for b and 1.077 for c were extremely close to the value of unity. When either of these exponents reach this value, the corresponding method reduces to the concept of linear cumulative fatigue damage.

TABLE 19

PARAMETERS FOR S-N DATA AND UNIT GUST LOADING SPECTRA[a]

(Table is completed on next page)

| Material | Type of Specimen | $S_{Mean}$ | Type of Spectrum | No. of Loading Steps | Block Size | $\alpha$ (b) | $\beta$ (b) | $S_E$ (b) | $\delta$ (c) | $\Gamma(\beta+1)$ (d) | $H_o$ (d) | h (d) | Test Group No. |
|---|---|---|---|---|---|---|---|---|---|---|---|---|---|
| 2024-T3 | Notched Sheet | .241 | Gust B | 18 | 100000 | 67 | 2.473 | .053 | 4.318 | 3.225 | 124900 | 59.59 | G1-G5 |
| | | | Gust A | 18 | 100000 | 67 | 2.473 | .053 | 4.318 | 3.225 | 165200 | 45.22 | G6 |
| | | .241 | | 8 | 100200 | 67 | 2.473 | .053 | 4.318 | 3.225 | 176100 | 44.26 | G7-G12 |
| | | 0 | | | 50000 | 115 | 2.647 | .100 | 6.604 | 3.922 | 63900 | 26.55 | G13-G14 |
| 7075-T6 | | .241 | | | 50900 | 83 | 1.837 | .048 | 3.391 | 1.731 | 62800 | 44.58 | G15-G21 |
| | | .121 | | | 30200 | 159 | 1.828 | .074 | 4.419 | 1.716 | 51100 | 34.32 | G22-G23 |
| | Notched Sheet | 0 | Gust A | 8 | 30000 | 220 | 1.890 | .105 | 5.788 | 1.811 | 50200 | 27.60 | G24-G27 |
| 2024-T3 Alclad | Double Shear Riveted Joints | .253 | | 9 | 360280 | 1368 | 1.620 | .017 | 2.035 | 1.451 | 231800 | 26.99 | G28 |
| | | .152 | | | | 2650 | 1.684 | .018 | 1.904 | 1.525 | 230400 | 44.89 | G29 |
| | | .101 | | | | 12340 | 1.145 | .040 | 1.883 | 1.070 | 233700 | 67.66 | G30 |
| | | .0806 | | | | 26770 | .900 | .050 | 2.084 | .961 | 231500 | 84.37 | G31 |
| 7075-T6 Alclad | Unnotched Sheet | .201 | | | | 9364 | 1.130 | .097 | 2.875 | 1.062 | 231900 | 33.85 | G32 |
| | | .161 | | | | 10364 | 1.087 | .100 | 2.641 | 1.040 | 232200 | 42.37 | G33 |
| | | .145 | | | | 14434 | .976 | .100 | 2.623 | .990 | 230500 | 47.04 | G34 |
| | Butt Joints | .250 | | | | 243 | 2.370 | .042 | 3.376 | 2.388 | 232400 | 27.29 | G35 |
| | | .167 | | | | 988 | 2.080 | .052 | 3.460 | 2.156 | 230800 | 40.94 | G36 |
| | | .125 | | | | 4414 | 1.551 | .061 | 2.831 | 1.379 | 231300 | 54.55 | G37 |
| Cr-Mo Steel | Strips W/ Hole | .286 | | | | 1400 | 1.741 | .106 | 3.959 | 1.596 | 231800 | 23.85 | G38 |
| | | .222 | | | | 1237 | 1.721 | .124 | 3.628 | 1.571 | 234300 | 30.79 | G39 |
| | | .182 | | 9 | 360280 | 1327 | 1.669 | .130 | 3.700 | 1.508 | 227200 | 37.50 | G40 |

(a) $\alpha$, $\beta$, $S_E$, $\Gamma(\beta+1)$, $H_o$ & h for FFA method
$\beta$ and $S_E$ for modified Henry's method
$\delta$ for Shanley's "1X" and "2X" methods.

(b) Parameter in Equation (A14) (Best fit in the midstress range)

(c) Parameter in Equation (A6) (Best fit to the complete stress range.)

(d) Parameter in Equation (A18) (Best fit in the midstress range.)

TABLE 19

(Concluding Page of Table)

| Material | Type of Specimen | | $S_{Mean}$ | No. of Loading Steps | Block Size | $\alpha$ (b) | $\beta$ (b) | $S_E$ (b) | $\delta$ (c) | $\Gamma(\beta+1)$ (d) | $E_o$ (d) | h (d) | Test Group No. |
|---|---|---|---|---|---|---|---|---|---|---|---|---|---|
| 2024-T3 Alclad | (e) | | .212 | 6 | 189880c | 3045 | 1.598 | .049 | 2.601 | 1.428 | 2887000 | 34.96 | G41-G43 |
| | | | | 5 | 457700 | 3045 | 1.598 | .049 | 2.601 | 1.428 | 3040700 | 32.54 | G44 |
| | (f) | | | 5 | 164400 | 853 | 2.001 | .053 | 2.823 | 2.002 | 1146200 | 31.58 | G45 |
| 7075-T6 Alclad | (e) | | | 5 | 92900 | 3514 | 1.125 | .052 | 1.953 | 1.060 | 685600 | 31.25 | G46 |
| | | | .212 | 6 | 1228000 | 3514 | 1.125 | .052 | 1.953 | 1.060 | 1874800 | 35.01 | G47 |
| D.T.D. 363A Aluminum Alloy | Notched Plate | | .165 | 9 | 13290 | 222 | 1.422 | .033 | 2.532 | 1.260 | 52900 | 62.94 | G48 |
| | | | .165 | 9 | 6290 | 222 | 1.422 | .033 | 2.532 | 1.260 | 17100 | 56.18 | G49 |
| | | | .165 | 10 | 5410 | 222 | 1.422 | .033 | 2.532 | 1.260 | 30300 | 58.43 | G50 |
| 2024-T | C-46 Wing | WS 180 | .2 | 16 | 59670 | 472 | 2.372 | .039 | 3.624 | 2.893 | 202700 | 42.05 | G51 |
| | | WS 214 | | | | 2182 | 2.091 | .032 | 2.687 | 2.178 | | | G52 |
| | | WS 228 | | | | 1318 | 2.155 | .036 | 3.193 | 2.319 | | | G53 |
| | | WS 239 | | | | 1944 | 1.937 | .020 | 2.472 | 1.889 | | | G54 |
| | | (g) | | | | 309 | 2.676 | .030 | 4.020 | 4.054 | | | G55 |
| | | (h) | | | | 491 | 2.626 | .032 | 3.709 | 3.828 | | | G56 |
| | | (i) | | 16 | 59670 | 778 | 2.488 | .040 | 3.548 | 3.279 | 202700 | 42.05 | G57 |
| | P51 Wing | (j) | | 11 | 500000 | 129 | 2.394 | .039 | 4.881 | 2.964 | 998600 | 37.16 | G58 |
| | | Gun Bay | | 3 | 32860 | 129 | 2.394 | .039 | 4.881 | 2.964 | 115200 | 45.04 | G59 |
| | | (j) | | 11 | 500000 | 130 | 2.545 | .041 | 3.682 | 3.495 | 998600 | 37.16 | G60 |
| | | Tank Bay | | 3 | 32860 | 130 | 2.545 | .041 | 3.682 | 3.495 | 115200 | 45.04 | G61 |
| | | (k) | | 11 | 500000 | 504 | 2.270 | .039 | 3.782 | 2.602 | 998600 | 37.16 | G62 |
| | | Gun Bay | | 3 | 32860 | 504 | 2.270 | .039 | 3.782 | 2.602 | 115200 | 45.04 | G63 |
| | | (k) | | 11 | 500000 | 1624 | 1.549 | .052 | 3.574 | 1.377 | 998600 | 37.16 | G64 |
| 2024-T | | Tank Bay | .2 | 3 | 32860 | 1624 | 1.549 | .052 | 3.574 | 1.377 | 115200 | 45.04 | G65 |

(b), (c), and (d) See corresponding notes on previous pags.
(e) Lap joint with one row of flush rivets
(f) Lap joint with two rows of flush rivets
(g) First crack initiated in complete wing
(h) Critical crack initiated in complete wing
(i) Final failure of complete wing
(j) Initial failure
(k) Final failure

TABLE 20

PARAMETERS FOR S-N DATA AND UNIT MANEUVER LOADING SPECTRA(*)

| Material | Type of Specimen | $S_{Min.}$ | No. of Loading Steps | Block Size | $\alpha$ (**) | $\beta$ (**) | $S_E$ (**) | $\delta$ (***) | $\Gamma(\beta+1)$ (****) | $H_o$ (****) | h (****) | Test Group No. |
|---|---|---|---|---|---|---|---|---|---|---|---|---|
| 2024-T3 Alclad | Double Shear Rivited Joints | .0833 | 9 | 7497 | 914 | 1.647 | .033 | 2.544 | 1.481 | 9300 | 19.38 | M1 |
| | | .0625 | | | 1001 | 1.708 | .037 | 2.678 | 1.555 | 9400 | 25.83 | M2 |
| | | .050 | | | 5109 | 1.095 | .045 | 2.850 | 1.044 | 9300 | 32.30 | M3 |
| 7075-T6 Alclad | Unnotched Sheet | .125 | | | 558 | 2.077 | .095 | 4.028 | 2.150 | 9300 | 12.92 | M4 |
| | | .100 | | | 3172 | 1.459 | .099 | 2.955 | 1.292 | 9300 | 16.15 | M5 |
| | | .0833 | | | 4840 | 1.302 | .101 | 2.708 | 1.168 | 9300 | 19.38 | M6 |
| | | .0625 | | | 5477 | 1.346 | .092 | 3.015 | 1.200 | 9400 | 25.83 | M7 |
| | Butt Joints | .100 | | | 26 | 3.108 | .055 | 4.669 | 6.382 | 9300 | 16.15 | M8 |
| | | .0833 | | | 34 | 3.063 | .059 | 4.674 | 6.497 | 9300 | 19.38 | M9 |
| | | .0625 | | | 232 | 2.269 | .063 | 4.654 | 2.599 | 9300 | 25.83 | M10 |
| Cr-Mo Steel | Strips W/hole | .111 | | | 554 | 1.857 | .122 | 4.300 | 1.760 | 9300 | 14.53 | M11 |
| | | .100 | | | 556 | 1.962 | .122 | 4.122 | 1.931 | 9300 | 16.15 | M12 |
| | | .0833 | 9 | 7497 | 2105 | 1.397 | .122 | 3.689 | 1.240 | 9300 | 19.38 | M13 |

(*) $\alpha$, $\beta$, $S_E$, $\Gamma(\beta+1)$, $H_o$ & h are used in the FFA method
$\delta$ is used in the Shanley's "1X" and Shanley's "2X" methods
$\beta$ & $S_E$ are used in Henry's method.

(**) Parameter in Equation (A14) (Best fit to the full stress range.)
(***) Parameter in Equation (A6) (Best fit to the full stress range.)
(****) Parameter in Equation (A18) (Best fit to the full stress range.)

TABLE 21

PREDICTED FATIGUE LIVES FOR GUST LOADING SPECTRA
(Table is continued on next two pages)

| Test Group No. | Sequence | Geometric Mean of Test Life ($10^6$ Cycles) | Predicted Life ($10^6$ Cycles) | | | | | | | |
|---|---|---|---|---|---|---|---|---|---|---|
| | | | Miner | FFA Case A(a) | Shanley "1X" | Shanley "2X" | Modified Henry Case A (b) | Tangent Intercept | Quality Index | Stress Conc. Factor |
| G1 | Lo-Hi | 8.049 | 8.240 | 9.630 | 9.042 | 2.087 | 7.597 | 40.131 | 6.988 | 1.018 |
| G2 | Lo-Hi | 3.872 | | | | | 7.986 | | | |
| G3 | Hi-Lo | 11.888 | | | | | 7.403 | | | |
| G4 | Hi-Lo | 11.555 | | | | | 7.013 | | 6.988 | |
| G5 | QR | 6.988 | 8.240 | 9.630 | 9.042 | 2.087 | - | 40.131 | (c) | 1.018 |
| G6 | QR | 1.824 | 1.591 | 1.717 | 1.616 | .426 | - | 7.065 | 2.846 | .316 |
| G7 | Lo-Hi | .595 | 1.201 | 1.455 | 1.186 | .305 | 1.194 | 4.754 | 2.020 | .237 |
| G8 | Hi-Lo | 2.294 | | | | | 1.014 | | | |
| G9 | Lo-Hi-Lo | 1.612 | | | | | 1.145 | | | |
| G10 | Hi-Lo-Hi | 1.519 | | | | | 1.103 | | 2.020 | |
| G11 | QR | 2.020 | | | | | - | | (d) | |
| G12 | | 1.215 | 1.201 | 1.455 | 1.186 | .305 | - | 4.754 | 2.020 | .237 |
| G13 | | .479 | .944 | 1.913 | .942 | .058 | - | 5.361 | .364 | .656 |
| G14 | QR | .354 | .944 | 1.913 | .942 | .058 | - | 5.361 | (e) | .656 |
| G15 | Lo-Hi | .443 | .320 | .354 | .288 | .109 | .304 | 1.171 | .661 | .138 |
| G16 | Lo-Hi | .452 | | | | | .348 | | | |
| G17 | Hi-Lo | 1.268 | | | | | .257 | | | |
| G18 | Lo-Hi-Lo | .762 | | | | | .291 | | | |
| G19 | Hi-Lo-Hi | .976 | | | | | .304 | | .661 | |
| G20 | QR | .661 | | | | | - | | (f) | |
| G21 | QR | .600 | .320 | .354 | | .109 | - | 1.171 | .661 | .138 |
| G22 | Lo-Hi-Lo | .385 | .326 | .445 | | .076 | .287 | 1.360 | .282 | .209 |
| G23 | QR | .282 | .326 | .445 | .288 | .076 | - | 1.360 | (g) | .209 |
| G24 | Lo-Hi | .255 | .409 | .697 | .331 | .040 | .355 | 2.399 | .394 | .288 |
| G25 | Hi-Lo | .496 | | | | | .301 | | | |
| G26 | Lo-Hi-Lo | .498 | | | | | .316 | | .394 | |
| G27 | QR | .394 | .409 | .697 | .331 | .040 | - | 2.399 | (h) | .288 |

(a) Analytical representation of unit loading spectrum and S-N data is based on best fit in the midstress range.

(b) Analytical intrepretation of S-N data is based on best fit in the midstress range.

(c), (d), (e), (f), (g), and (h) See corresponding notes on last pages of table.

TABLE 21

PREDICTED FATIGUE LIVES FOR GUST LOADING SPECTRA
(Table is completed on next page)

| Test Group No. | Sequence | Geometric Mean of Test Life ($10^6$ Cycles) | Predicted Life ($10^6$ Cycles) Miner | FFA Case A (a) | Shanley "1X" | Shanley "2X" | Modified Henry Case A (b) | Tangent Intercept | Quality Index | Stress Conc. Factor |
|---|---|---|---|---|---|---|---|---|---|---|
| G28 | Lo-Hi-Lo | .411 | .368 | .482 | .370 | .132 | .364 | 1.171 | | |
| G29 | | 4.788 | 2.222 | 3.692 | 2.284 | 1.790 | 2.452 | 6.341 | | |
| G30 | | 21.732 | 29.959 | 33.146 | 27.496 | 22.860 | 28.473 | 18.566 | | |
| G31 | | 129.700 | 260.200 | 159.280 | 233.510 | 177.440 | 225.890 | 633.470 | | |
| G32 | | 25.710 | 31.627 | 19.522 | 24.928 | 10.758 | 13.344 | 92.350 | | |
| G33 | | 75.875 | 95.532 | 62.881 | 88.848 | 56.984 | 81.783 | 278.160 | | |
| G34 | | 151.966 | 195.450 | 108.070 | 148.540 | 147.150 | 186.980 | 501.790 | | |
| G35 | | 2.994 | .876 | 1.037 | .871 | .299 | 1.034 | 3.681 | | |
| G36 | | 27.558 | 12.133 | 13.560 | 12.167 | 7.030 | 11.879 | 30.003 | | |
| G37 | | 100.986 | 80.410 | 68.619 | 106.730 | 76.536 | 103.400(i) | 300.010 | | |
| G38 | | 4.060 | 4.130 | 4.266 | 3.734 | 1.739 | 3.956 | 12.215 | | |
| G39 | | 17.902 | 24.139 | 20.083 | 23.912 | 15.096 | 21.976 | 55.208 | | |
| G40 | Lo-Hi-Lo | 50.367 | 89.807 | 77.480 | 89.042 | 61.611 | 82.504 | 235.890 | | |
| G41 | Lo-Hi | 1.899 | 1.888 | 2.280 | 1.854 | 1.445 | 3.584 | 5.551 | | |
| G42 | Hi-Lo | 2.279 | 1.868 | 2.280 | 1.854 | 1.445 | .192 | 5.551 | | |
| G43 | | 2.818 | 1.888 | 2.280 | 1.854 | 1.445 | .173 | 5.551 | | |
| G44 | | .458 | .228 | .414 | .223 | .174 | .114 | .654 | | |
| G45 | | .164 | .138 | .326 | .174 | .125 | .166 | .568 | | |
| G46 | Hi-Lo | .093 | .079 | .110 | .075 | .065 | .066 | .207 | | |
| G47 | Lo-Hi | 1.226 | .705 | .732 | .680 | .601 | 1.178 | 2.050 | | |
| G48 | Lo-Hi-Lo | .133 | .107 | .127 | .100 | .068 | .096 | .330 | .143 | .529 |
| G49 | | .122 | .116 | .127 | .106 | .077 | .108 | .336 | .150 | .504 |
| G50 | Lo-Hi-Lo | .074 | .049 | .070 | .047 | .033 | .048 | .138 | (j) | .244 |

(a) See note on previous page.
(b) See note on previous page.
(i) Prediction ignored singularity at a varying stress equal to the endurance limit in the loading spectrum.
(j) Used as master spectrum to determine damage boundary with K of 5.27 for test groups No. G48 & G49. Reference Table 26.

TABLE 21

PREDICTED FATIGUE LIVES FOR GUST LOADING SPECTRA
(Concluding page of Tables)

| Test Group No. | Sequence | Geometric Mean of Test Life ($10^6$ Cycles) | Predicted Life ($10^6$ Cycles) Miner | FFA Case A (a) | Shanley "1X" | Shanley "2X" | Modified Henry Case A (b) | Tangent Intercept | Quality Index |
|---|---|---|---|---|---|---|---|---|---|
| G51 | QR | 4.179 | 1.305 | 1.759 | 1.408 | .393 | - | 6.667 | 1.099 |
| G52 | | 4.453 | 1.893 | 2.811 | 2.128 | 1.104 | - | 7.645 | 18.585 |
| G53 | | 2.307 | 1.695 | 2.402 | 1.751 | .719 | - | 7.435 | 3.305 |
| G54 | | 2.070 | .745 | .961 | .760 | .447 | - | 2.548 | 3.344 |
| G55 | | 1.252 | 1.010 | 1.750 | .810 | .261 | - | 3.947 | 3.344 |
| G56 | | 3.344 | 1.424 | 3.658 | 1.196 | .444 | - | 5.634 | (k) |
| G57 | QR | 9.666 | 2.126 | 4.116 | 1.957 | .715 | - | 8.452 | 3.344 |
| G58 | TR | .417 | .354 | .532 | .321 | .048 | - | 1.909 | (l) |
| G59 | Lo-Hi-Lo | .557 | .510 | .654 | .423 | .147 | .474 | 2.923 | .649 |
| G60 | TR | 1.521 | .798 | .851 | .870 | .214 | - | 4.128 | (m) |
| G61 | Lo-Hi-Lo | .953 | .956 | 1.092 | 1.086 | .400 | .865 | 5.557 | 2.715 |
| G62 | TR | 2.520 | 1.175 | 1.516 | 1.039 | .350 | - | 4.769 | (n) |
| G63 | Lo-Hi-Lo | 1.495 | 1.090 | 1.818 | .993 | .471 | 1.014 | 3.922 | 3.240 |
| G64 | TR | 2.017 | .939 | 1.103 | .806 | .275 | - | 3.142 | (o) |
| G65 | Lo-Hi-Lo | 1.039 | 1.181 | 1.275 | 1.312 | .372 | .818 | 5.708 | 3.311 |

(a), (b) See Corresponding note on first page of table
(c) Used as Master Spectrum to determine damage boundary with K of 3.22 for Test Group No. G 1 to G 4
(d) K of 2.95 G 6 to G12
(e) K of 4.71 G13
(f) K of 3.10 G15 to G19
(g) K of 3.78 G21
(h) K of 3.76 G23 to G26
(k) K of 8.26 G51 to G57
(l) K of 4.10 G57
(m) K of 3.33 G61
(n) K of 3.08 G63
(o) Used as Master Spectrum to determine damage boundary with K of 3.19 for Test Group No. G65

Ref. Table 26

TABLE 22

PREDICTED LIVES BY THE FFA AND MODIFIED HENRY'S METHODS WITH REQUIRED ANALYTICAL PARAMETERS BASED ON THE COMPLETE S-N CURVE AND ENTIRE GUST LOADING SPECTRUM

(Table is continued on the next two pages)

| TEST GROUP NO. | SEQUENCE | GEOMETRIC MEAN OF TEST LIFE ($10^6$ CYCLES) | PARAMETERS $\alpha$ (a) | $\beta$ (a) | $\Gamma(\beta+1)$ (b) | $H_o$ (b) | h (b) | PREDICTED LIFE ($10^6$ CYCLES) FFA Case B | PREDICTED LIFE ($10^6$ CYCLES) MODIFIED HENRY Case B |
|---|---|---|---|---|---|---|---|---|---|
| G1 | Lo-Hi | 8.049 | 24 | 2.652 | 4.995 | 52300 | 47.74 | 7.109 | 7.500 |
| G2 | Lo-Hi | 3.872 | | | | 261500 | | | 7.983 |
| G3 | Hi-Lo | 11.888 | | | | 52300 | | | 7.400 |
| G4 | Hi-Lo | 14.555 | | | | 261500 | | | 7.010 |
| G5 | QR | 6.968 | | | | 261500 | 47.74 | 7.109 | - |
| G6 | QR | 1.824 | | | | 121000 | 42.30 | 1.631 | - |
| G7 | Lo-Hi | .595 | | | | 147800 | 42.26 | 1.332 | 1.192 |
| G8 | Hi-Lo | 2.294 | | | | | | | 1.012 |
| G9 | Lo-Hi-Lo | 1.612 | | | | | | | 1.061 |
| G10 | Hi-Lo-Hi | 1.519 | | | | 147800 | | | 1.102 |
| G11 | QR | 2.020 | | | | 73900 | | | - |
| G12 | | 1.215 | 24 | 2.652 | 4.995 | 147800 | 42.26 | 1.332 | - |
| G13 | | .479 | 11 | 3.494 | 11.529 | 54800 | 25.44 | .873 | - |
| G14 | QR | .364 | 11 | 3.494 | 11.529 | 109600 | 25.44 | .873 | - |
| G15 | Lo-Hi | .443 | 41 | 2.053 | 2.102 | 11500 | 43.55 | .322 | .304 |
| G16 | Lo-Hi | .452 | | | | 57700 | | | .348 |
| G17 | Hi-Lo | 1.268 | | | | 57700 | | | .257 |
| G18 | Lo-Hi-Lo | .762 | | | | 11500 | | | .290 |
| G19 | Hi-Lo-Hi | .976 | | | | 57700 | | | .304 |
| G20 | QR | .661 | | | | 11500 | | | - |
| G21 | QR | .600 | 41 | 2.053 | 2.102 | 57700 | 43.55 | .322 | - |
| G22 | Lo-Hi-Lo | .385 | 24 | 2.420 | 3.048 | 42200 | 32.67 | .295 | .287 |
| G23 | QR | .282 | 24 | 2.420 | 3.048 | 42200 | 32.67 | .295 | - |

(a) Parameter in Equation (A14)
(b) Parameter in Equation (A18)

TABLE 22

(Table is completed on the next page)

| TEST GROUP NO. | SEQUENCE | GEOMETRIC MEAN OF TEST LIFE ($10^6$ CYCLES) | PARAMETERS $\alpha$ (a) | $\beta$ (a) | $\Gamma(\beta+1)$ (b) | $K_o$ (b) | h (b) | PREDICTED LIFE ($10^6$ CYCLES) FFA Case B | MODIFIED HENRY Case B |
|---|---|---|---|---|---|---|---|---|---|
| G24 | Lo-Hi | .255 | 23 | 2.552 | 3.522 | 40200 | 26.05 | .310 | .325 |
| G25 | Hi-Lo | .496 | \| | \| | \| | \| | \| | \| | .271 |
| G26 | Lo-Hi-Lo | .493 | \| | \| | \| | \| | \| | \| | .286 |
| G27 | CR | .394 | 23 | 2.552 | 3.522 | 40200 | 26.05 | .310 | - |
| G28 | Lo-Hi-Lo | .411 | 850 | 1.836 | 1.728 | 231800 | 26.99 | .514 | .364 |
| G29 | \| | 4.788 | 2650 | 1.684 | 1.525 | 230400 | 44.89 | 3.692 | 2.452 |
| G30 | \| | 21.732 | 9390 | 1.243 | 1.129 | 233700 | 67.66 | 36.226 | 27.034 |
| G31 | \| | 129.700 | 22000 | .953 | .952 | 231500 | 84.37 | 164.140 | 224.450 |
| G32 | \| | 25.710 | 6320 | 1.252 | 1.135 | 231900 | 33.85 | 19.008 | 12.617 |
| G33 | \| | 75.875 | 7370 | 1.206 | 1.105 | 232200 | 42.37 | 65.630 | 80.344 |
| G34 | \| | 151.966 | 12200 | 1.032 | 1.014 | 230500 | 47.04 | 110.080 | 186.980 |
| G35 | \| | 2.994 | 120 | 2.696 | 4.150 | 232400 | 27.29 | 1.060 | 1.032 |
| G36 | \| | 27.558 | 470 | 2.383 | 2.926 | 230800 | 40.94 | 14.700 | 11.578 |
| G37 | \| | 100.986 | 3210 | 1.667 | 1.505 | 231300 | 54.55 | 72.703 | 103.400 |
| G38 | \| | 4.060 | 320 | 2.458 | 3.176 | 231600 | 23.85 | 4.743 | 3.953 |
| G39 | \| | 17.902 | 910 | 1.856 | 1.758 | 234300 | 30.79 | 20.890 | 21.975 |
| G40 | Lo-Hi-Lo | 50.367 | 1330 | 1.659 | 1.508 | 227200 | 37.50 | 77.480 | 82.504 |
| G41 | Lo-Hi | 1.899 | 1400 | 1.941 | 1.896 | 2887000 | 34.96 | 2.674 | 3.584 |
| G42 | Hi-Lo | 2.279 | \| | \| | \| | 3464000 | 34.96 | 2.674 | .191 |
| G43 | \| | 2.848 | \| | \| | \| | 4330000 | 34.96 | 2.674 | .172 |
| G44 | \| | .458 | 1400 | 1.941 | 1.896 | 3041000 | 32.55 | .473 | .143 |
| G45 | \| | .164 | 850 | 2.001 | 2.002 | 1146000 | 31.58 | .326 | .166 |
| G46 | Hi-Lo | .093 | 1890 | 1.366 | 1.215 | 685500 | 31.25 | .118 | .065 |
| G47 | Lo-Hi | 1.228 | 1890 | 1.366 | 1.215 | 1875000 | 35.01 | .808 | 1.178 |
| G48 | Lo-Hi-Lo | .133 | 170 | 1.501 | 1.330 | 52900 | 62.94 | .128 | .096 |
| G49 | Lo-Hi-Lo | .122 | 170 | 1.501 | 1.330 | 17100 | 56.18 | .126 | .108 |
| G50 | Lo-Hi-Lo | .074 | 170 | 1.501 | 1.330 | 30300 | 58.43 | .070 | .048 |

(a), (b) See corresponding note on previous page

TABLE 22

(Concluding page of Table)

| TEST GROUP NO. | SEQUENCE | GEOMETRIC MEAN OF TEST LIFE ($10^6$ CYCLES) | PARAMETERS $\alpha$ (a) | $\beta$ (a) | $\Gamma(\beta+1)$ (b) | $H_o$ (b) | $h$ (b) | PREDICTED LIFE ($10^6$ CYCLES) FFA Case B | MODIFIED HENRY Case B |
|---|---|---|---|---|---|---|---|---|---|
| G51 | QR | 4.179 | 160 | 2.785 | 4.609 | 71800 | 34.60 | 2.196 | - |
| G52 | | 4.453 | 1710 | 2.192 | 2.404 | | | 4.229 | - |
| G53 | | 2.307 | 530 | 2.516 | 3.381 | | | 3.391 | - |
| G54 | | 2.070 | 1090 | 2.192 | 2.405 | | | 1.783 | - |
| G55 | | 1.252 | 65 | 3.444 | 10.773 | | | 2.836 | - |
| G56 | | 3.344 | 180 | 3.142 | 7.191 | | | 4.210 | - |
| G57 | QR | 9.656 | 350 | 2.867 | 5.086 | 71800 | 34.60 | 5.961 | - |
| G58 | TR | .417 | 5 | 3.584 | 13.077 | 805000 | 35.10 | .296 | - |
| G59 | Lo-Hi-Lo | .557 | 5 | 3.584 | 13.077 | 115200 | 45.04 | .490 | .463 |
| G60 | TR | 1.522 | 90 | 2.670 | 4.025 | 805000 | 35.10 | .814 | - |
| G61 | Lo-Hi-Lo | .953 | 90 | 2.670 | 4.025 | 115200 | 45.04 | 1.094 | .862 |
| G62 | TR | 2.520 | 100 | 2.932 | 5.509 | 805000 | 35.10 | 1.563 | - |
| G63 | Lo-Hi-Lo | 1.495 | 100 | 2.932 | 5.509 | 115200 | 45.04 | 2.199 | 1.004 |
| G64 | TR | 2.017 | 200 | 2.245 | 2.536 | 805000 | 35.10 | .887 | - |
| G65 | Lo-Hi-Lo | 1.039 | 200 | 2.245 | 2.536 | 115200 | 45.04 | 1.196 | .739 |

(a), (b) See corresponding note on first page of table.

TABLE 23

PREDICTED FATIGUE LIVES FOR MANEUVER LOADING SPECTRA

| Test Group No. | Sequence | Geometric Mean of Test Life ($10^6$ Cycles) | Predicted Life ($10^6$ Cycles) | | | | | |
|---|---|---|---|---|---|---|---|---|
| | | | Miner | FFA Case B | Shanley "1X" | Shanley "2X" | Modified Henry Case B | Tangent Intercept |
| M1 | Lo-Hi-Lo | .308 | .132 | .125 | .145 | .078 | .128 | .484 |
| M2 | | .499 | .342 | .346 | .341 | .171 | .259 | 1.127 |
| M3 | | .903 | .760 | .758 | .727 | .452 | .661 | 2.329 |
| M4 | | .206 | .126 | .145 | .203 | .113 | .115 | .139 |
| M5 | | .716 | .555 | .575 | .563 | .405 | .546 | 1.539 |
| M6 | | .903 | 1.008 | 1.122 | .963 | .714 | .921 | 2.076 |
| M7 | | 2.219 | 2.944 | 3.128 | 2.512 | 2.255 | 2.781 | 6.583 |
| M8 | | .069 | .047 | .043 | .048 | .015 | .040 | .096 |
| M9 | | .214 | .132 | .118 | .138 | .049 | .127 | .331 |
| M10 | | 1.477 | .611 | .582 | .712 | .348 | .592 | 1.332 |
| M11 | | .156 | .216 | .215 | .248 | .146 | .202 | .406 |
| M12 | | .370 | .382 | .390 | .381 | .227 | .338 | .962 |
| M13 | Lo-Hi-Lo | 1.042 | .903 | .915 | .890 | .637 | .848 | 2.141 |

TABLE 24

STRESS ADJUSTMENT FACTORS FOR EXACTLY PREDICTING THE GEOMETRIC MEAN OF TEST LIFE FOR GUST LOADING SPECTRA

(Table is continued on the next two pages)

| Test Group No. | Sequence | Stress Adjustment Factors | | | | | | | | | |
|---|---|---|---|---|---|---|---|---|---|---|---|
| | | Miner | FSA (a) Case A | FSA (d) Case B | Shanley "1X" | Shanley "2X" | Modified Henry (b) Case A | Modified Henry (d) Case B | Tangent Intercept | Quality Index | Stress Conc. Factor |
| G1 | Lo-Hi | 1.005 | 1.033 | .977 | 1.017 | .779 | .989 | .988 | 1.342 | .983 | .639 |
| G2 | Lo-Hi | 1.152 | 1.185 | 1.123 | 1.167 | .885 | 1.082 | 1.082 | 1.566 | 1.133 | .739 |
| G3 | Hi-Lo | .939 | .964 | .911 | .960 | .779 | .908 | .905 | 1.244 | .920 | .597 |
| G4 | Hi-Lo | .904 | .931 | .879 | .930 | .765 | .779 | .779 | 1.198 | .888 | .575 |
| G5 | CR | 1.037 | 1.060 | 1.003 | 1.038 | .793 | - | - | 1.381 | - | .650 |
| G6 | CR | .975 | .988 | .978 | .975 | .779 | - | - | 1.350 | 1.094 | .635 |
| G7 | Lo-Hi | 1.159 | 1.214 | 1.178 | 1.146 | .868 | 1.183 | 1.181 | 1.626 | 1.300 | .771 |
| G8 | Hi-Lo | .976 | .912 | .901 | .895 | (c) | .828 | .820 | 1.171 | .983 | .562 |
| G9 | Lo-Hi-Lo | .939 | .970 | .963 | .941 | \| | .918 | .916 | 1.263 | .936 | .609 |
| G10 | Hi-Lo-Hi | .951 | .991 | .975 | .949 | \| | .925 | .923 | 1.280 | .923 | .620 |
| G11 | CR | .899 | .935 | .923 | .912 | (c) | - | - | 1.203 | - | .579 |
| G12 | | .998 | 1.039 | 1.018 | .995 | .754 | - | - | 1.350 | 1.125 | .657 |
| G13 | | 1.109 | 1.322 | 1.107 | 1.086 | .848 | - | - | 1.476 | .943 | 1.058 |
| G14 | CR | 1.155 | 1.403 | 1.161 | 1.136 | .885 | - | - | 1.538 | - | 1.120 |
| G15 | Lo-Hi | .933 | .952 | .933 | .931 | (c) | .911 | .909 | 1.315 | 1.134 | .672 |
| G16 | Lo-Hi | .929 | .947 | .929 | .928 | (c) | .929 | .928 | 1.307 | 1.129 | .669 |
| G17 | Hi-Lo | .745 | (c) | .742 | .727 | .650 | .739 | .739 | .979 | .883 | .494 |
| G18 | Lo-Hi-Lo | .818 | .838 | .827 | .814 | .743 | (c) | (c) | 1.122 | .998 | .563 |
| G19 | Hi-Lo-Hi | .793 | .793 | .784 | .799 | .685 | (c) | (c) | 1.049 | .938 | .530 |
| G20 | CR | .844 | .866 | .853 | .875 | (c) | - | - | 1.168 | - | .590 |
| G21 | CR | .863 | .885 | .871 | .868 | (c) | - | - | 1.201 | 1.057 | .796 |
| G22 | Lo-Hi-Lo | .969 | 1.034 | .947 | .944 | .837 | .933 | .903 | 1.343 | .948 | .876 |
| G23 | CR | 1.033 | 1.114 | 1.009 | 1.004 | .860 | - | - | 1.446 | - | 1.004 |
| G24 | Lo-Hi | 1.087 | 1.251 | 1.038 | 1.042 | .858 | 1.082 | 1.076 | 1.495 | 1.072 | 1.021 |
| G25 | Hi-Lo | .970 | 1.075 | .917 | .955 | .760 | .955 | .955 | 1.326 | .959 | .908 |
| G26 | Lo-Hi-Lo | .969 | 1.074 | .916 | .955 | .759 | .955 | .955 | 1.325 | .958 | .907 |
| G27 | CR | 1.007 | 1.131 | .956 | .972 | .792 | - | - | 1.381 | - | .946 |

(a), (b), (c), and (d) See corresponding note on last page of table.

TABLE 24

STRESS ADJUSTMENT FACTORS FOR EXACTLY PREDICTING THE GEOMETRIC MEAN OF TEST LIFE FOR GUST LOADING SPECTRA

(Table is completed on the next page)

| Test Group No. | Sequence | Stress Adjustment Factors | | | | | | | | | |
|---|---|---|---|---|---|---|---|---|---|---|---|
| | | Miner | FFA (a) Case A | FFA (c) Case B | Shanley "1X" | Shanley "2X" | Modified Henry (b) Case A | Modified Henry (c) Case B | Tangent Intercept | Quality Index | Stress Conc. Factor |
| G28 | Lo-Hi-Lo | .958 | 1.080 | 1.104 | .954 | .680 | .831 | .831 | 1.654 | | |
| G29 | \| | .748 | .903 | .903 | .715 | .621 | .725 | .725 | 1.132 | | |
| G30 | \| | 1.120 | 1.121 | 1.145 | 1.107 | 1.026 | 1.109 | 1.103 | .956 | | |
| G31 | \| | 1.204 | 1.042 | 1.048 | 1.166 | 1.055 | 1.135 | 1.134 | 1.440 | | |
| G32 | \| | 1.027 | .941 | .937 | .996 | .990 | .990 | .990 | 1.306 | | |
| G33 | \| | 1.057 | .966 | .974 | 1.032 | .946 | 1.027 | 1.024 | 1.361 | | |
| G34 | \| | 1.033 | .943 | .946 | .964 | .914 | 1.010 | 1.010 | 1.305 | | |
| G35 | \| | .700 | .751 | .772 | .655 | .575 | .661 | .655 | 1.073 | | |
| G36 | \| | .782 | .851 | .874 | .734 | .642 | .751 | .748 | 1.021 | | |
| G37 | \| | (c) | .926 | .938 | (c) | .819 | (c) | (c) | 1.262 | | |
| G38 | \| | 1.005 | 1.012 | 1.032 | .973 | .757 | .968 | .963 | 1.396 | | |
| G39 | \| | 1.056 | 1.021 | 1.025 | 1.036 | .949 | 1.065 | 1.064 | 1.315 | | |
| G40 | Lo-Hi-Lo | 1.119 | 1.070 | 1.070 | 1.079 | 1.046 | 1.048 | 1.048 | 1.392 | | |
| G41 | Lo-Hi | .997 | 1.058 | 1.100 | .990 | .854 | 1.032 | 1.035 | 1.488 | | |
| G42 | Hi-Lo | .929 | 1.000 | 1.045 | .911 | .815 | .895 | .894 | 1.390 | | |
| G43 | \| | .853 | .936 | .983 | .834 | .745 | .813 | .813 | 1.266 | | |
| G44 | \| | .772 | .969 | 1.009 | .750 | .670 | .737 | .737 | 1.129 | | |
| G45 | \| | 1.048 | 1.215 | 1.215 | 1.023 | .890 | 1.010 | 1.010 | 1.561 | | |
| G46 | Hi-Lo | .950 | 1.063 | 1.084 | .898 | .828 | .915 | .914 | 1.321 | | |
| G47 | Lo-Hi | .843 | .847 | .861 | .824 | .773 | .869 | .871 | 1.181 | | |
| G48 | Lo-Hi-Lo | .939 | .987 | .990 | .921 | .816 | .916 | .917 | 1.344 | 1.019 | 1.380 |
| G49 | Lo-Hi-Lo | .984 | 1.011 | 1.011 | .959 | .854 | .961 | .960 | 1.397 | 1.056 | 1.419 |
| G50 | Lo-Hi-Lo | .886 | .984 | .985 | .873 | .779 | .868 | .867 | 1.211 | - | 1.318 |

(a), (b), (c), and (d) See corresponding note on next page of table.

TABLE 24

STRESS ADJUSTMENT FACTORS FOR EXACTLY PREDICTING THE GEOMETRIC MEAN OF TEST LIFE FOR GUST LOADING SPECTRA
(Concluding page of Table)

| Test Group No. | Sequence | Stress Adjustment Factors | | | | | | | | |
|---|---|---|---|---|---|---|---|---|---|---|
| | | Miner | FFA (a) Case A | FFA (d) Case B | Shanley "1X" | Shanley "2X" | Modified Henry (b) Case A | Modified Henry (d) Case B | Tangent Intercept | Quality Index |
| G51 | QR | .762 | .814 | .859 | .768 | .616 | - | - | 1.134 | .771 |
| G52 | ⋮ | .719 | .878 | .985 | .722 | .711 | - | - | 1.227 | 1.246 |
| G53 | ⋮ | .911 | 1.011 | 1.111 | .922 | .800 | - | - | 1.438 | 1.078 |
| G54 | ⋮ | .651 | .773 | .950 | .649 | .523 | - | - | 1.088 | 1.146 |
| G55 | ⋮ | .936 | 1.090 | 1.205 | .854 | .667 | - | - | 1.505 | 1.248 |
| G56 | ⋮ | .739 | .944 | 1.056 | .711 | .624 | - | - | 1.204 | - |
| G57 | QR | .649 | .822 | .894 | .646 | .533 | - | - | .940 | .876 |
| G58 | TR | .969 | 1.066 | .934 | .942 | .674 | - | - | 1.373 | - |
| G59 | Lo-Hi-Lo | .981 | 1.040 | .976 | .944 | .734 | .965 | .961 | 1.450 | 1.028 |
| G60 | TR | .858 | .870 | .862 | .874 | .679 | - | - | 1.257 | - |
| G61 | Lo-Hi-Lo | 1.001 | 1.032 | 1.031 | 1.027 | .823 | .974 | .974 | 1.464 | 1.245 |
| G62 | TR | .807 | .875 | .897 | .767 | .615 | - | - | 1.219 | - |
| G63 | Lo-Hi-Lo | .924 | 1.050 | 1.087 | .887 | .709 | .894 | .891 | 1.265 | 1.235 |
| G64 | TR | .843 | .847 | .825 | .794 | .688 | - | - | 1.137 | - |
| G65 | Lo-Hi-Lo | 1.031 | 1.055 | 1.032 | 1.031 | .945 | .945 | .945 | 1.361 | 1.277 |

(a) Analytical representation of S-N data and unit loading spectra is based on best fit in the midstress range of maximum calculated fatigue damage.

(b) Analytical definition of S-N data is based on best fit in the midstress range of maximum calculated fatigue damage.

(c) No incremental deviation because of mathematical discontinuity (See text)

(d) Analytical definitions are based on best fit over the full stress range.

TABLE 25

STRESS ADJUSTMENT FACTORS FOR EXACTLY PREDICTING THE GEOMETRIC MEAN OF TEST LIFE UNDER MANEUVER LOADING SPECTRA

| Test Group No. | Sequence | Stress Adjustment Factors | | | | | |
|---|---|---|---|---|---|---|---|
| | | Miner | FFA Case B | Shanley "1X" | Shanley "2X" | Modified Henry Case B | Tangent Intercept |
| M1 | Lo-Hi-Lo | .741 | .689 | .722 | .642 | .667 | 1.150 |
| M2 | | .877 | .875 | .887 | .746 | .867 | 1.337 |
| M3 | | .958 | .935 | .926 | .865 | .900 | 1.418 |
| M4 | | .959 | .901 | .994 | .815 | .948 | .923 |
| M5 | | .934 | .933 | .914 | .814 | .918 | 1.300 |
| M6 | | 1.041 | 1.070 | 1.024 | .819 | 1.009 | 1.493 |
| M7 | | 1.082 | 1.100 | 1.051 | 1.005 | 1.048 | 1.445 |
| M8 | | .931 | .888 | .932 | .752 | .915 | 1.076 |
| M9 | | .902 | .870 | .916 | .749 | .894 | 1.102 |
| M10 | | .837 | .797 | .834 | .723 | .811 | .978 |
| M11 | | 1.014 | 1.023 | 1.061 | .922 | 1.008 | 1.179 |
| M12 | | 1.008 | 1.014 | 1.007 | .877 | .979 | 1.253 |
| M13 | Lo-Hi-Lo | .972 | .966 | .958 | .881 | .958 | 1.222 |

TABLE 26

FATIGUE QUALITY INDEX FOR GUST LOADING SPECTRA

(Table is completed on next page)

| Test Group No. | Sequence | Number of Specimens | Geometric $K_T$ | K Quality Index Method | | |
|---|---|---|---|---|---|---|
| | | | | Minimum | Maximum | Geometric Mean |
| G1 | Lo-Hi | 3 | 4 | 3.17 | 3.17 | 3.17 |
| G2 | Lo-Hi | 9 | | 3.33 | 3.62 | 3.44 |
| G3 | Hi-Lo | 3 | | 2.92 | 3.19 | 3.04 |
| G4 | Hi-Lo | 6 | | 2.80 | 3.15 | 2.98 |
| G5 | QR | 8 | | 3.10 | 3.46 | 3.22 |
| G6 | QR | 4 | | 2.99 | 3.23 | 3.12 |
| G7 | Lo-Hi | 3 | | 3.43 | 3.61 | 3.52 |
| G8 | Hi-Lo | 3 | | 2.84 | 2.95 | 2.91 |
| G9 | Lo-Hi-Lo | 3 | | 2.98 | 3.09 | 3.05 |
| G10 | Hi-Lo-Hi | 3 | | 3.00 | 3.11 | 3.06 |
| G11 | QR | 3 | | 2.88 | 3.02 | 2.95 |
| G12 | " | 4 | | 3.10 | 3.30 | 3.16 |
| G13 | " | 6 | | 3.92 | 4.75 | 4.38 |
| G14 | QR | 3 | | 4.58 | 4.98 | 4.71 |
| G15 | Lo-Hi | 3 | | 3.19 | 3.41 | 3.32 |
| G16 | Lo-Hi | 4 | | 3.21 | 3.44 | 3.32 |
| G17 | Hi-Lo | 4 | | 2.77 | 2.91 | 2.85 |
| G18 | Lo-Hi-Lo | 4 | | 2.96 | 3.25 | 3.08 |
| G19 | Hi-Lo-Hi | 4 | | 2.93 | 3.03 | 2.97 |
| G20 | QR | 3 | | 3.04 | 3.15 | 3.10 |
| G21 | QR | 4 | | 3.11 | 3.30 | 3.18 |
| G22 | Lo-Hi-Lo | 3 | | 3.43 | 3.75 | 3.56 |
| G23 | QR | 6 | | 3.54 | 4.01 | 3.78 |
| G24 | Lo-Hi | 6 | | 3.53 | 4.58 | 4.19 |
| G25 | Hi-Lo | 5 | | 3.39 | 3.77 | 3.56 |
| G26 | Lo-Hi-Lo | 3 | | 3.37 | 3.73 | 3.55 |
| G27 | QR | 6 | 4 | 3.19 | 4.40 | 3.76 |

## TABLE 26

FATIGUE QUALITY INDEX FOR GUST LOADING SPECTRA

(concluding page of Table)

| Test Group No. | Sequence | Number of Specimens | Geometric $K_T$ | K Quality Index Method | | |
|---|---|---|---|---|---|---|
| | | | | Minimum | Maximum | Geometric Mean |
| G28 | Lo-Hi-Lo | 2 | | 3.82 | 4.13 | 3.97 |
| G29 | \| | 3 | | 4.53 | 5.06 | 4.70 |
| G30 | \| | 3 | | 6.29 | 7.73 | 6.71 |
| G31 | \| | 2 | | 5.52 | 7.83 | 6.59 |
| G32 | \| | 2 | 1 | 1.89 | 1.91 | 1.90 |
| G33 | \| | 2 | 1 | 1.98 | 2.22 | 2.10 |
| G34 | \| | 2 | 1 | 2.07 | 2.26 | 2.17 |
| G35 | \| | 4 | | 3.30 | 3.69 | 3.52 |
| G36 | \| | 2 | | 3.96 | 3.98 | 3.97 |
| G37 | \| | 2 | | 4.25 | 4.59 | 4.41 |
| G38 | \| | 2 | | - | - | - |
| G39 | \| | 2 | | - | - | - |
| G40 | Lo-Hi-Lo | 3 | | - | - | - |
| G41 | Lo-Hi | 1 | | - | - | >8 |
| G42 | Hi-Lo | 1 | | - | - | >8 |
| G43 | \| | 1 | | - | - | >8 |
| G44 | \| | 1 | | - | - | >8 |
| G45 | \| | 1 | | - | - | 4.47 |
| G46 | Hi-Lo | 1 | | - | - | >8 |
| G47 | Lo-Hi | 1 | | - | - | >8 |
| G48 | Lo-Hi-Lo | 6 | 3.95 | 4.41 | 5.75 | 5.23 |
| G49 | | 6 | 3.95 | 5.22 | 5.94 | 5.43 |
| G50 | Lo-Hi-Lo | 5 | 3.95 | 3.93 | 6.91 | 5.27 |
| G51 | QR | 4 | | 5.20 | >8 | 6.25 |
| G52 | \| | 6 | | >8 | >8 | >8 |
| G53 | \| | 5 | | 6.64 | >8 | >8 |
| G54 | \| | 5 | | >8 | >8 | >8 |
| G55 | \| | 6 | | >8 | >8 | >8 |
| G56 | \| | 6 | | 6.96 | >8 | 8.26 |
| G57 | QR | 6 | | 6.06 | 6.91 | 6.48 |
| G58 | TR | 3 | | 3.87 | 4.41 | 4.10 |
| G59 | Lo-Hi-Lo | 4 | | 3.77 | 4.62 | 4.11 |
| G60 | TR | 2 | | 3.23 | 3.44 | 3.33 |
| G61 | Lo-Hi-Lo | 7 | | 3.65 | 4.02 | 3.85 |
| G62 | TR | 4 | | 2.96 | 3.18 | 3.08 |
| G63 | Lo-Hi-Lo | 3 | | 3.46 | 3.83 | 3.64 |
| G64 | TR | 2 | | 3.12 | 3.25 | 3.19 |
| G65 | Lo-Hi-Lo | 5 | | 3.52 | 3.94 | 3.80 |

TABLE 27

FATIGUE QUALITY INDEX FOR MANEUVER SPECTRA

| Test Group No. | Sequence | Number of Specimens | Geometric $K_T$ | K Quality Index Method | | |
|---|---|---|---|---|---|---|
| | | | | Minimum | Maximum | Geometric Mean |
| M1 | Lo-Hi-Lo | 2 | | 2.50 | 2.60 | 2.55 |
| M2 | | 2 | | 3.50 | 4.20 | 3.83 |
| M3 | | 2 | | 4.00 | 4.20 | 4.10 |
| M4 | | 2 | 1 | .60 | .60 | .60 |
| M5 | | 2 | 1 | 1.15 | 1.22 | 1.19 |
| M6 | | 3 | 1 | 1.15 | 1.58 | 1.33 |
| M7 | | 2 | 1 | 1.51 | 1.92 | 1.70 |
| M8 | | 2 | | 3.50 | 3.60 | 3.55 |
| M9 | | 2 | | 3.20 | 3.50 | 3.35 |
| M10 | Lo-Hi-Lo | 2 | | 3.20 | 3.60 | 3.39 |

TABLE 28

EXPONENTS FOR THE MODIFIED CORTEN-DOLAN AND THE NON-LINEAR CUMULATIVE DAMAGE METHODS FROM GUST LOADING SPECTRA

(Table is completed on the next page)

| Test Group No. | Sequence | Geometric Mean of Test Life (cycles) | Exponents b Modified Corten & Dolan | Exponents c Non-linear Cumulative Damage |
|---|---|---|---|---|
| G1 | Lo-Hi | 804900 | .996 | .996 |
| G2 | Lo-Hi | 3872000 | .860 | .844 |
| G3 | Hi-Lo | 11888000 | 1.072 | 1.058 |
| G4 | Hi-Lo | 14555000 | 1.113 | 1.120 |
| G5 | QR | 6988000 | .969 | .966 |
| G6 | QR | 1824000 | 1.032 | 1.027 |
| G7 | Lo-Hi | 595000 | .846 | .822 |
| G8 | Hi-Lo | 2294000 | 1.156 | 1.168 |
| G9 | Lo-Hi-Lo | 1612000 | 1.069 | 1.065 |
| G10 | Hi-Lo-Hi | 1519000 | 1.055 | 1.051 |
| G11 | QR | 2020000 | 1.124 | 1.114 |
| G12 | \| | 1219000 | 1.003 | 1.003 |
| G13 | \| | 478600 | .865 | .855 |
| G14 | QR | 363600 | .816 | .762 |
| G15 | Lo-Hi | 442800 | 1.086 | 1.069 |
| G16 | Lo-Hi | 452400 | 1.091 | 1.113 |
| G17 | Hi-Lo | 1268000 | 1.389 | 1.457 |
| G18 | Lo-Hi-Lo | 762000 | 1.237 | 1.162 |
| G19 | Hi-Lo-Hi | 975700 | 1.209 | 1.299 |
| G20 | QR | 661400 | 1.196 | 1.155 |
| G21 | QR | 600300 | 1.169 | 1.206 |
| G22 | Lo-Hi-Lo | 385000 | 1.038 | 1.045 |
| G23 | QR | 282400 | .968 | .961 |
| G24 | Lo-Hi | 251600 | .898 | .886 |
| G25 | Hi-Lo | 496300 | 1.044 | 1.047 |
| G26 | Lo-Hi-Lo | 497700 | 1.045 | 1.041 |
| G27 | QR | 393900 | .991 | .991 |

TABLE 28

EXPONENTS FOR THE MODIFIED CORTEN-DOLAN AND THE NON-LINEAR CUMULATIVE DAMAGE METHODS FROM GUST LOADING SPECTRA

(Concluding page of table)

| Test Group No. | Sequence | Geometric Mean of Test Life (Cycles) | Exponents b Modified Corten & Dolan | Exponents c Non-linear Cumulative Damage |
|---|---|---|---|---|
| G28 | Lo-Hi-Lo | 410700 | 1.032 | 1.087 |
| G29 | \| | 4788000 | 1.293 | 1.282 |
| G30 | \| | 21732000 | .849 | .943 |
| G31 | \| | 129700000 | .589 | .914 |
| G32 | \| | 25710000 | .919 | .966 |
| G33 | \| | 75875000 | .871 | .968 |
| G34 | \| | 151966000 | .802 | .967 |
| G35 | \| | 2994000 | 1.323 | 1.549 |
| G36 | \| | 27558000 | 1.276 | 1.274 |
| G37 | \| | 100936000 | 1.088 | 1.032 |
| G38 | \| | 4060000 | .995 | .996 |
| G39 | \| | 17902000 | .865 | .948 |
| G40 | Lo-Hi-Lo | 50367000 | .647 | .918 |
| G41 | Lo-Hi | 1899000 | 1.004 | 1.016 |
| G42 | Hi-Lo | 2279000 | 1.065 | 1.442 |
| G43 | \| | 2848000 | 1.142 | - |
| G44 | \| | 457700 | 1.241 | - |
| G45 | \| | 164400 | .965 | .894 |
| G46 | Hi-Lo | 92900 | 1.073 | 1.296 |
| G47 | Lo-Hi | 1228000 | 1.232 | - |
| G48 | Lo-Hi-Lo | 132900 | 1.128 | 1.056 |
| G49 | \| | 121500 | 1.032 | 1.010 |
| G50 | Lo-Hi-Lo | 74100 | 1.214 | 1.101 |
| G51 | QR | 4179000 | 1.210 | 1.241 |
| G52 | \| | 4453000 | 1.186 | 1.171 |
| G53 | \| | 2307000 | 1.059 | 1.063 |
| G54 | \| | 2070000 | 1.232 | 1.257 |
| G55 | \| | 1252000 | 1.024 | 1.035 |
| G56 | \| | 3344000 | 1.138 | 1.180 |
| G57 | QR | 9666000 | 1.267 | 1.293 |
| G58 | TR | 416800 | 1.030 | 1.093 |
| G59 | Lo-Hi-Lo | 556600 | 1.063 | 1.025 |
| G60 | TR | 1521000 | 1.151 | 1.272 |
| G61 | Lo-Hi-Lo | 953300 | 1.145 | 1.046 |
| G62 | TR | 2520000 | 1.148 | 1.277 |
| G63 | Lo-Hi-Lo | 1495000 | 1.222 | 1.076 |
| G64 | TR | 2017000 | 1.164 | 1.312 |
| G65 | Lo-Hi-Lo | 1038700 | .948 | .983 |
| Average of Gust & Maneuver Spectra | | | 1.097 | 1.077 |

TABLE 29

EXPONENTS FOR THE MODIFIED CORTEN-DOLAN AND NON-LINEAR CUMULATIVE DAMAGE METHODS FROM MANEUVER LOADING SPECTRA

| Test Group No. | Sequence | Geometric Mean of Test Life (Cycles) | Exponents b Modified Corten & Dolan | Exponents c Non-linear Cumulative Damage |
|---|---|---|---|---|
| M1 | Lo-Hi-Lo | .308 | 1.685 | 1.173 |
| M2 | | .499 | 1.283 | 1.065 |
| M3 | | .903 | 1.131 | 1.026 |
| M4 | | .206 | 1.496 | 1.114 |
| M5 | | .716 | 1.203 | 1.042 |
| M6 | | .903 | .905 | .983 |
| M7 | | 2.219 | .715 | .963 |
| M8 | | .069 | 1.311 | 1.107 |
| M9 | | .214 | 1.462 | 1.105 |
| M10 | | 1.477 | 2.238 | 1.145 |
| M11 | | .198 | .945 | .983 |
| M12 | | .370 | .976 | .994 |
| M13 | Lo-Hi-Lo | 1.042 | 1.144 | 1.022 |
| Average of Gust + Maneuver Spectra | | | 1.097 | 1.077 |

## APPENDIX C

## SPECTRAL FATIGUE TEST DATA FOR THE EVALUATION OF FATIGUE LIFE PREDICTION METHODS

To evaluate and compare the fatigue life prediction methods studied in this program, a search was made for suitable experimental data. The suitability was judged on the basis of the following criteria:

1. Complexity - To cover the range and types of loading encountered in aircraft service, spectral fatigue test results were required.

2. Loading type was restricted to axial loading as more representative of the efficient stressing of the shell structure; bending data were considered unsatisfactory, except for the full scale airframe component test data.

3. Constant amplitude S-N data on each of the specific specimens were required in addition to the spectral results.

Within these criteria 78 sets of data suitable for most of the methods were collected covering approximately 266 individual specimens.

### GUST SPECTRA TEST RESULTS

While gust spectra were used in most of the tests, maneuvering type data were located for some specimens. These maneuver tests will be described in the next section. The gust spectra were applied to the various specimens in loading sequences that are shown in Figure 63. In the quasi-random loading tests, the order of application of the different varying loads was irregular, with the total number of cycles applied at each varying load being equal to those specified in the unit loading spectrum. The number of loading steps and the number of load cycles employed in the unit spectra covered wide ranges. Loading steps ranged from 3 to 18, the load cycles in the unit spectra ranged from approximately 5,000 to 3,000,000 cycles. Other pertinent test variables are noted in Table 30 and in the summary that follows. These include types of loading sequences, specimens, materials, and mean load levels used in the various tests. S-N data were also obtained on all fatigue specimens in part of each test program for which data are reported under loading of variable magnitude.

In general, the gust tests were conducted under the following conditions:

a. Lo-Hi, Hi-Lo, Lo-Hi-Lo, Hi-Lo-Hi, and quasi-random loading sequences were applied to the notched sheet specimens of Figure 64 which were made of 2024-T3 aluminum alloy and tested at net area mean stresses of 0 and 17.4 ksi; and of 7075-T6 aluminum alloy tested at net area mean stresses of 0, 10, and 20 ksi (reference 16). The gust spectra A and B specified in reference 32 were used in this testing. The

applicable unit loading spectra and S-N data are presented in Tables 31 and 32 and Figures 70, 71, 82, and 83. The brackets behind or under $F_{tu}$ in these tables and some of these figures (S-N curves only) denote that this value of $F_{tu}$ was divided into the net area stresses to obtain the relative varying and mean stresses, $S_v$ and $S_{mean}$. The magnitude of the relative varying stress in Figures 70 and 71 was increased as mean stress was reduced in this series of tests, maintaining essentially the same maximum stress spectrum.

b. Lo-Hi-Lo sequence was applied on the double shear riveted joints of Figure 65 which were made of 2024-T3 as presented from Reference 17. These were tested at net area mean stresses of 15.5, 9.3, 6.2, and 4.9 ksi. The same loading sequence was applied in tests to unnotched sheet of 7075-T6 (Figure 65) at net area mean stresses of 15.4, 12.4, and 11.1 ksi; to butt joints of 7075-T6 (Figure 65) at gross area mean stresses of 13.2, 8.9, and 6.6 ksi; and on strips of Cr-Mo steel (Figure 65) with a centrally located hole, at net area mean stresses of 43.1, 33.5, and 27.5 ksi. Unit loading spectra and S-N data for this series of tests are presented in Tables 33 to 36 and in Figures 72 to 75, and 84 to 87. In this series, the varying loads were decreased when reductions were made in mean stress levels. This may be seen in Figures 72 to 75.

c. Hi-Lo or Lo-Hi sequence was applied only once to lap joints of 2024-T3 with a single row of flush rivets (Figure 66) and tested at a gross area mean load of 975 lbs.; to lap joints of 7075-T6 with a single row of flush rivets (Figure 66) and tested at a gross area mean load of 1,055 lbs. (Reference 18) The unit loading spectra used in these tests and the related S-N data are given in Tables 37 to 39 and shown in Figures 76 to 78 and 88 to 90. In these tables and figures, the relative stresses, $S_v$ and $S_{mean}$ are based on the ratio of applied-to-ultimate static load while in Tables 40 and 41 to follow, they correspond to a similar ratio of load factors. The applicability of net or gross area in securing relative stress levels is denoted in the brackets near the ultimate load or load factor on each table or S-N curve.

d. Lo-Hi-Lo sequence is applied to notched plates of D.T.D 363A (a British zinc-aluminum alloy that is similar to 7075-T6) at a net area mean stress of 14 ksi (Reference 19). The unit loading spectra in Table 40 and in Figure 79 were used in testing. Applicable S-N data are presented in the same table and in Figure 91.

e. A quasi-random sequence of loads was applied to a complete C-46 wing for the purpose of determining the experimental load history at the initiation of the first crack; at the initiation of the critical crack that propagated to failure under continued loading, and at the

estimated time for final failure of the wing (reference 20). Test results were also screened for crack initiation at W.S. 180, W.S. 214, W.S. 228, and W.S. 239 which had measured local mean stresses of 7.1, 5.2, 6.3, and 6.0 ksi, respectively. All tests were conducted under the gross area loading spectrum described in Tables 41 and 42 or in Figure 80. S-N data are also presented in these tables or in Figures 92 and 93.

f. Lo-Hi-Lo and true random sequences of loading were applied to a complete P-51 wing at a mean load of 17,900 lbs. for determining initiation of failure. (Reference 21) Final failure resulted in the gun bay (approximately W.S. 28) and in the tank bay (W.S. 80). The two gross area loading spectra in Table 43 or Figure 81 were used in this series of tests with the related S-N data presented in the same Table and in Figures 94 and 95.

Experimental results for each of the preceding series of tests are tabulated in Table 48. This table sorts the data from 239 individual gust spectrum tests into 65 groups of test results according to material, specimen configurations, loading spectrum, and other pertinent experimental variables.

MANEUVER SPECTRA TEST RESULTS

Unit maneuver spectra were used in some of the tests that were selected from the literature to be correlated with fatigue life prediction methods. These unit maneuver spectra were applied in a series of tests that are reported in Reference 17. These tests were conducted under the Lo-Hi-Lo sequence of Figure 96 on double shear riveted joints of 2024-T3 (Figure 65) at net area minimum stresses of 5.1, 3.8, and 3.1 ksi, and on unnotched sheet of 7075-T6 at net area minimum stresses of 9.6, 7.7, 6.4, and 4.8 ksi. Butt joints of 7075-T6 (Figure 65) were tested at gross area minimum stresses of 5.3, 4.4, and 3.3 ksi; and strips of Cr-Mo steel with a centrally located hole (Figure 65) were tested at net area minimum stresses of 16.7, 15.1, and 12.6 ksi. The unit loading spectra and S-N data for this series of tests are presented in Tables 44 to 47 and in Figures 97 to 104. Similar to the series of tests conducted under unit gust loading spectra in Reference 17, the magnitude of the varying loads was decreased with reductions in mean load levels as shown in Figures 97, 98, 99, and 100. Twenty-seven experimental fatigue lives under these unit maneuver spectra were sorted into the 13 test groups listed in Table 49.

The application of these data to the numerical evaluation of ten of the fatigue life prediction methods selected for this phase of the study is described in detail in Appendix B. The results and conclusions drawn from the evaluation are given in Section III in the main body of the report.

TABLE 30

TEST VARIABLES TO BE CONSIDERED WITH MEAN AND VARYING STRESS IN ANALYZING FATIGUE LIFE PREDICTION METHODS

| SEQUENCE | NO. OF TEST GROUPS |
|---|---|
| Lo-Hi | 8 |
| Hi-Lo | 10 |
| Quasi-Random | 17 |
| Lo-Hi-Lo | 37 |
| Hi-Lo-Hi | 2 |
| True Random | 4 |

| NO. OF LOADING STEPS | NO. OF TEST GROUPS |
|---|---|
| 3 | 4 |
| 5 | 3 |
| 6 | 4 |
| 8 | 21 |
| 9 | 28 |
| 10 | 1 |
| 11 | 4 |
| 16 | 7 |
| 18 | 6 |

| BLOCK SIZE | NO. OF TEST GROUPS |
|---|---|
| 5410 | 1 |
| 6290 | 1 |
| 7500 | 13 |
| 10200 | 3 |
| 13290 | 1 |
| 30000 | 4 |
| 30200 | 2 |
| 32860 | 4 |
| 50000 | 1 |
| 50100 | 1 |
| 50900 | 4 |
| 59670 | 7 |
| 92900 | 1 |
| 100000 | 4 |
| 100200 | 5 |
| 164400 | 1 |
| 360280 | 13 |
| 457700 | 1 |
| 500000 | 7 |
| 1228000 | 1 |
| 1899000 | 1 |
| 2279000 | 1 |
| 2848000 | 1 |

| TYPE OF SPECTRUM | NO. OF TEST GROUPS |
|---|---|
| Gust | 65 |
| Maneuver | 13 |

| MATERIAL | NO. OF TEST GROUPS |
|---|---|
| 2024-T | 41 |
| 7075-T6 | 28 |
| Cr-Mo Steel | 6 |
| D.T.D. 363A | 6 |

| TYPE OF SPECIMEN | NO. OF TEST GROUPS |
|---|---|
| Notched Sheet | 27 |
| Double Shear Riveted Joints | 7 |
| Unnotched Sheet | 7 |
| Butt Joints | 6 |
| Strips with Hole | 6 |
| One Row Lap Joints | 6 |
| Two Row Lap Joints | 1 |
| Notched Plate | 3 |
| C-46 Wing | 7 |
| P-51 Wing | 8 |

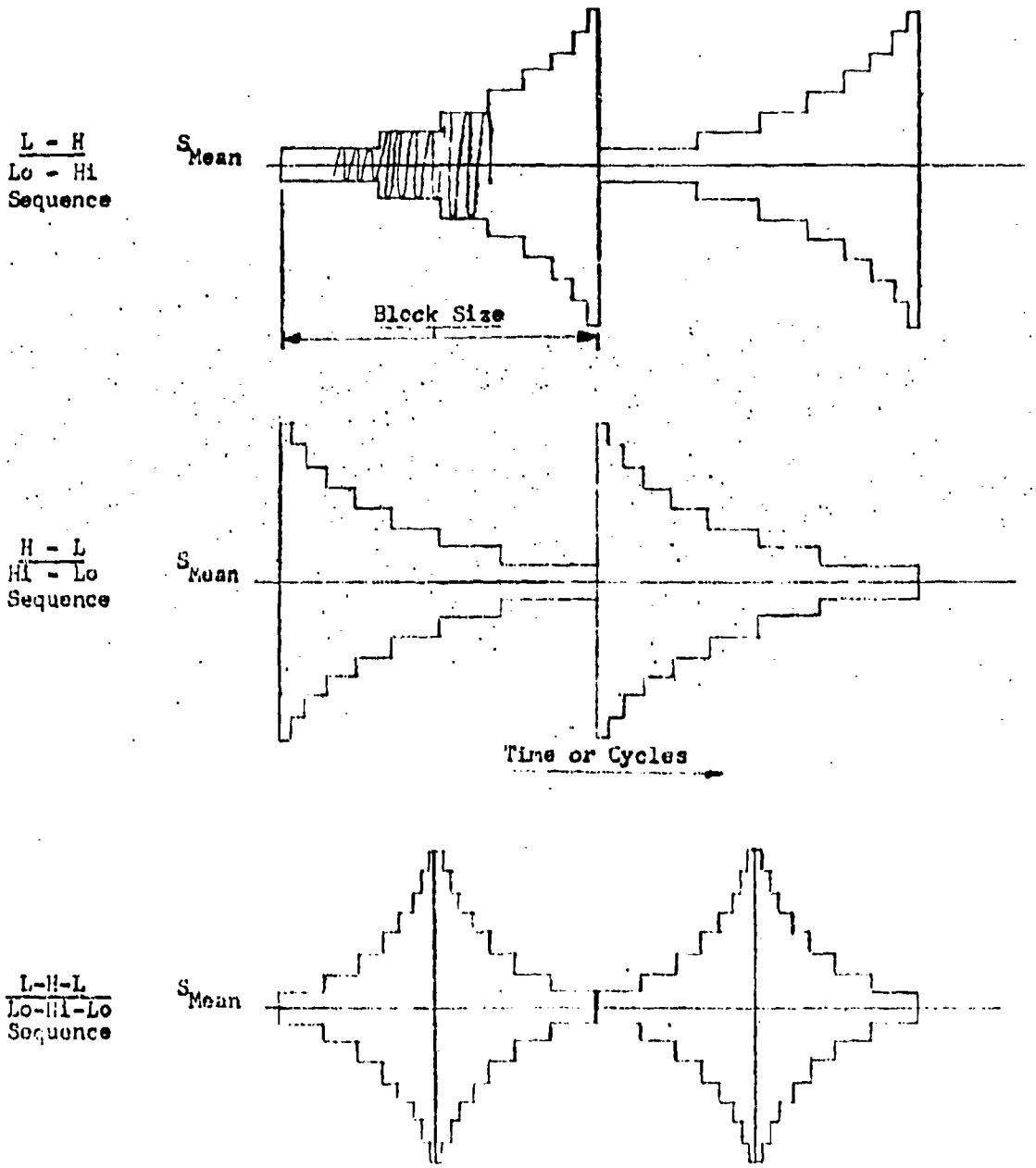



Figure 63. Schematic Diagrams of Gust Loading Sequences

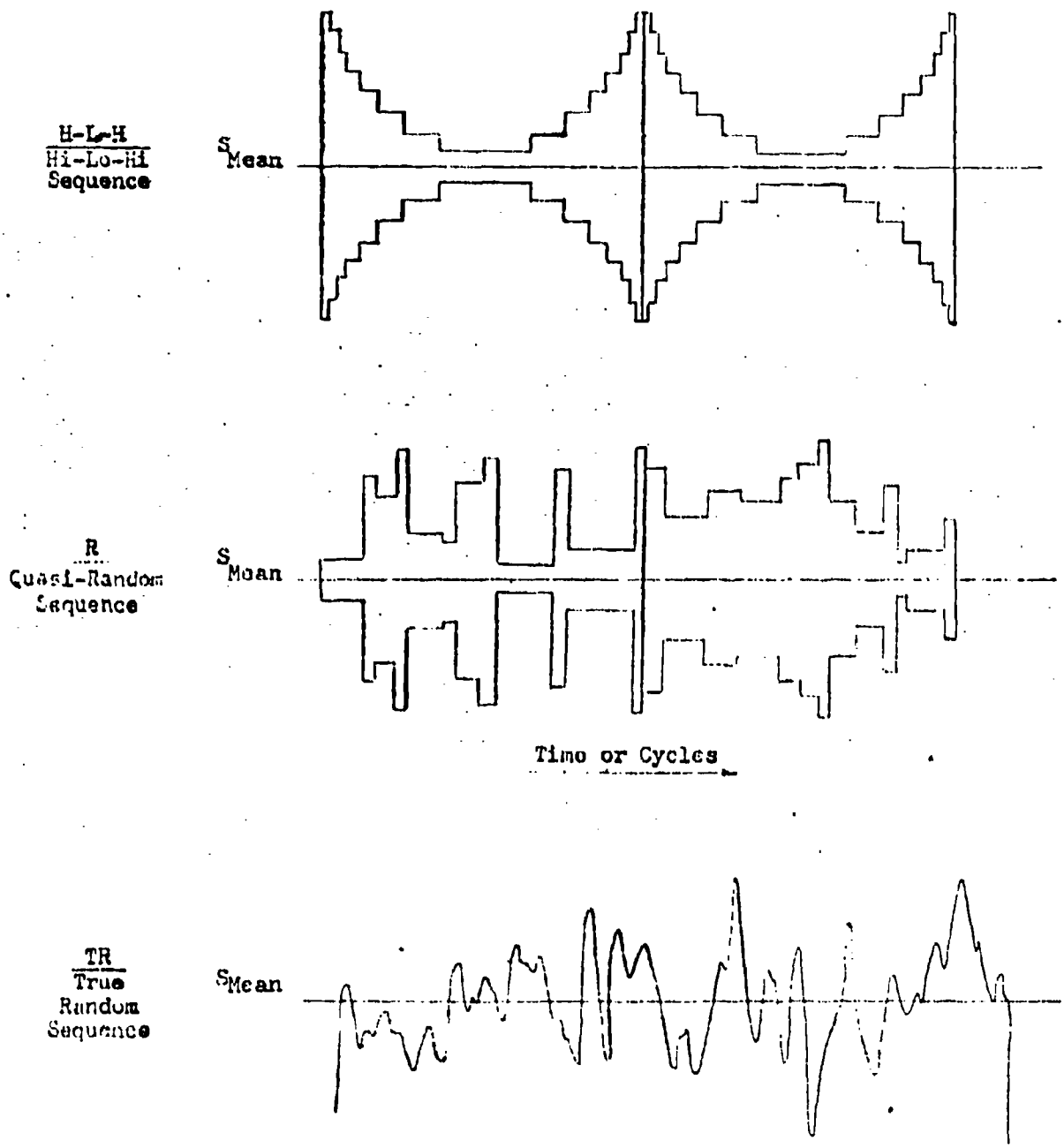
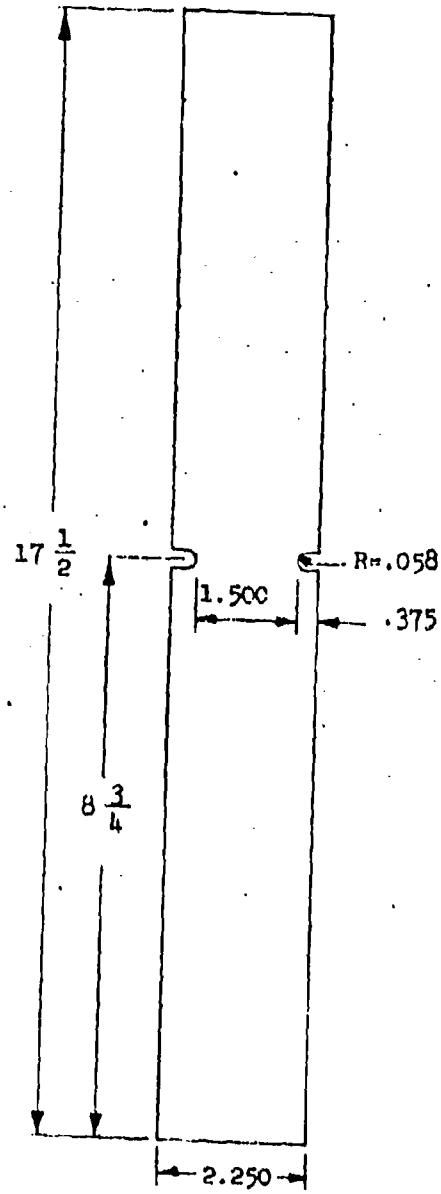
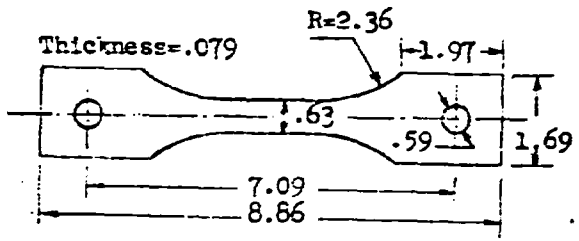



Figure61 (continued) Schematic Diagrams of Gust Loading Sequences

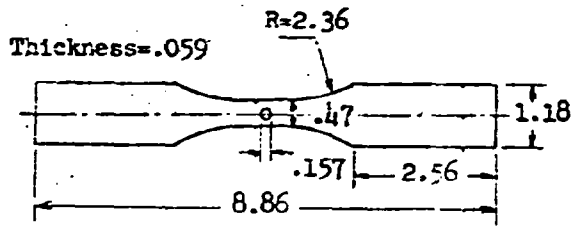



Theoretical Elastic Stress
Concentration Factor $K_T = 4.0$

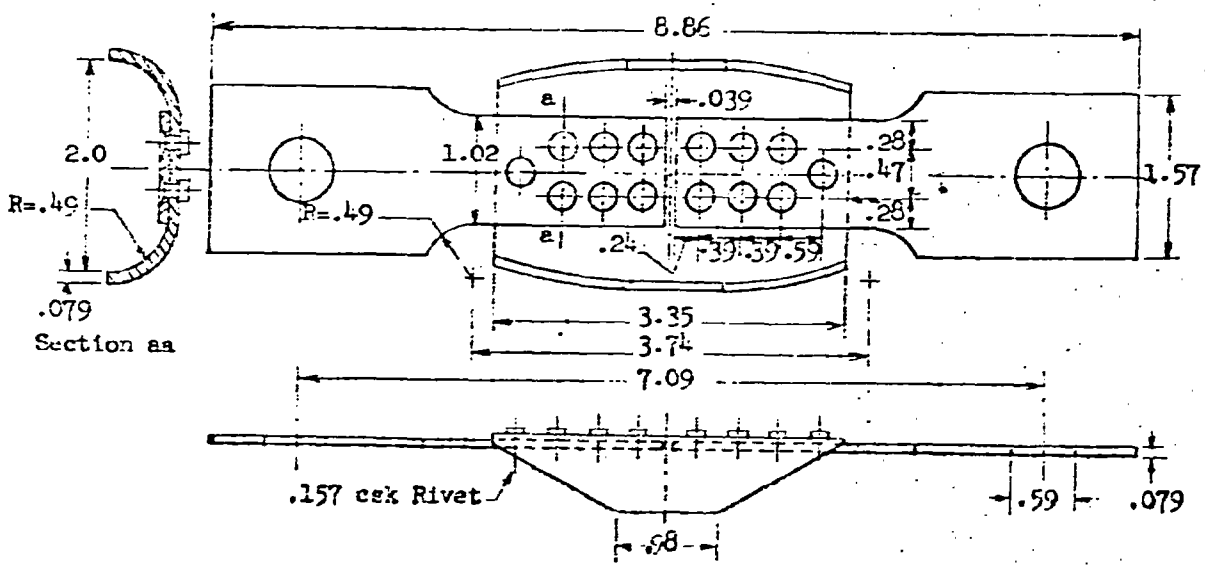
Figure 64 Notched Sheet Specimen for which Fatigue Test Data are Presented in Reference 16



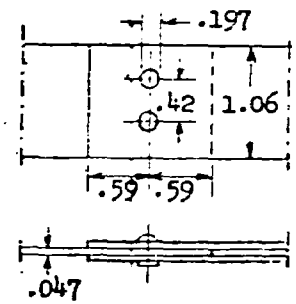

Unnotched Sheet Specimen
7075-T6 Alclad




Polished Strip Specimen Notched
by a Centrally Drilled Hole
Cr-Mo Steel

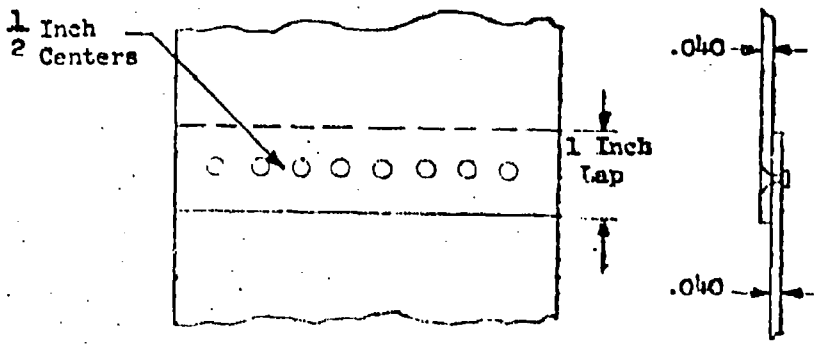



Butt Joint
7075-T6 Alclad

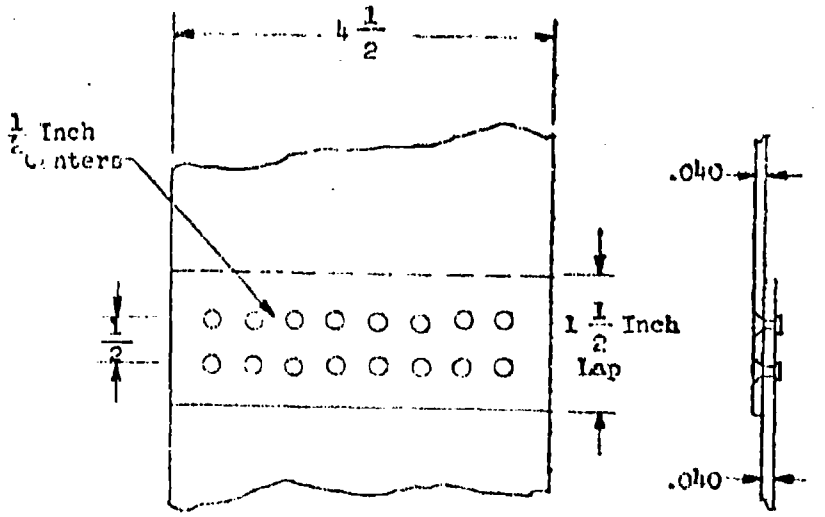



Double Shear
Riveted Joint
2024-T3 Alclad

Figure 65 Specimens for which Fatigue Test Data are Presented in Reference 17




Single - Row Flush-Riveted Lap Joint




Double-Row Flush-Riveted Lap Joint

(Length between Grips is Approximately 12 Inches)

Figure 66 Riveted - Lap Joint Specimens for which Fatigue Test Data are Presented in Reference 18

D.T.D. 363A Aluminum Alloy

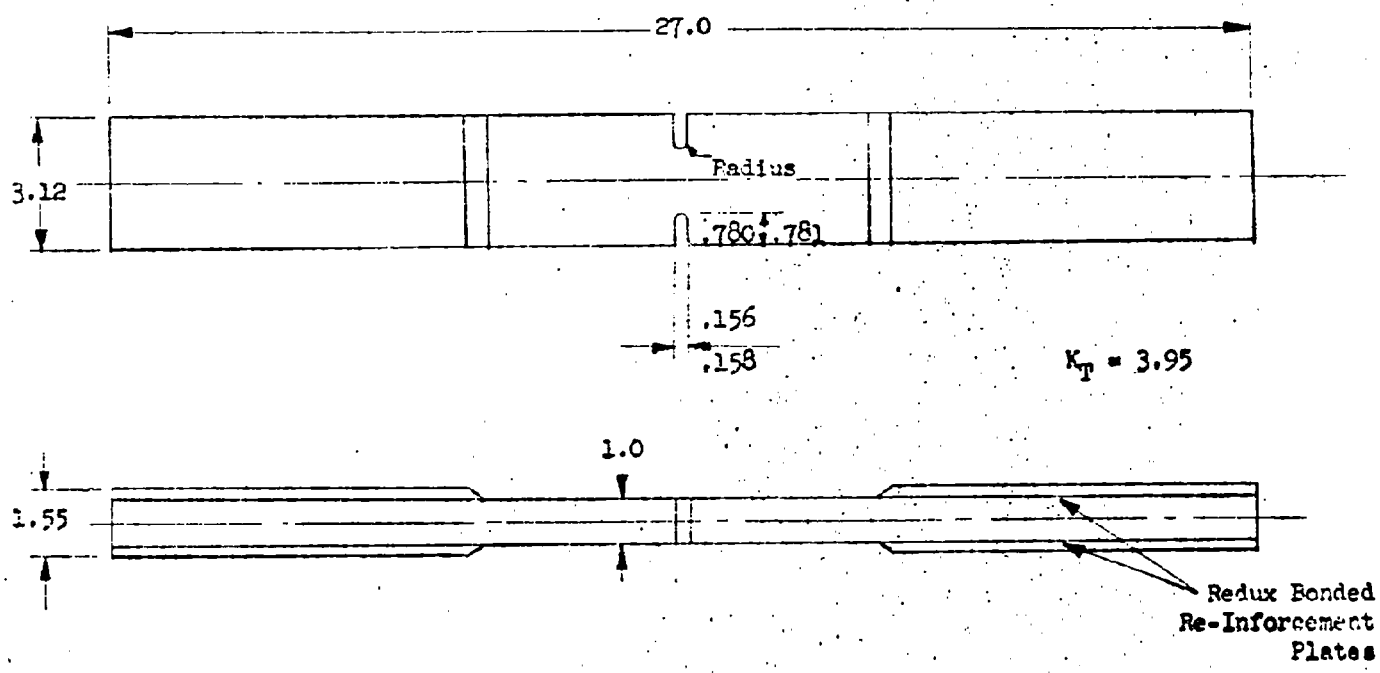
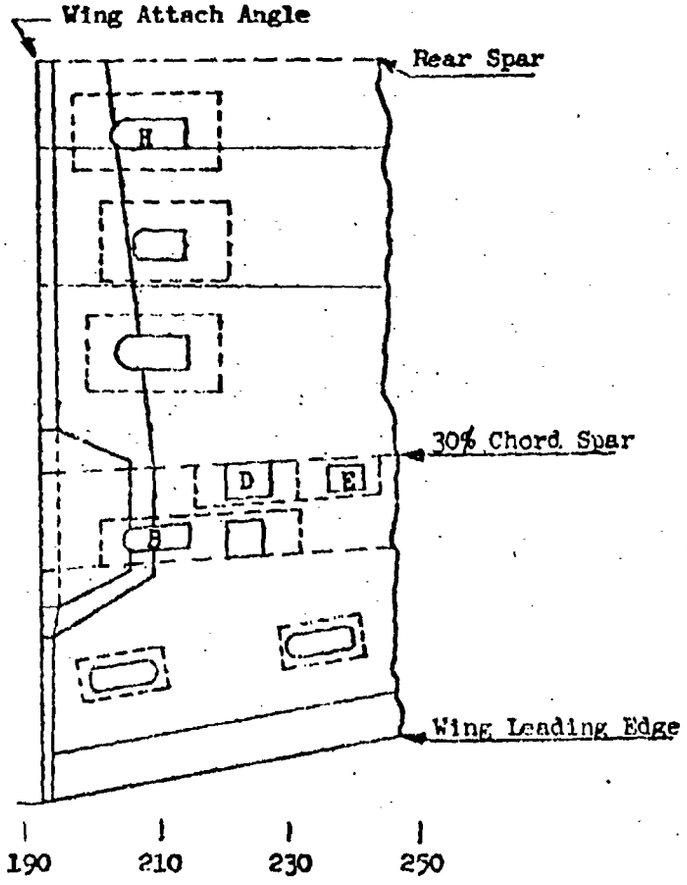



Figure 67 Notched Plate Specimen for which Fatigue Test Data are Presented in Reference 19




D Internal Doubler
E Internal Doubler
H Corner of Cutout

Figure 68 C-46 Wing Specimen for which Fatigue Test Data are Presented in References 20 and 23

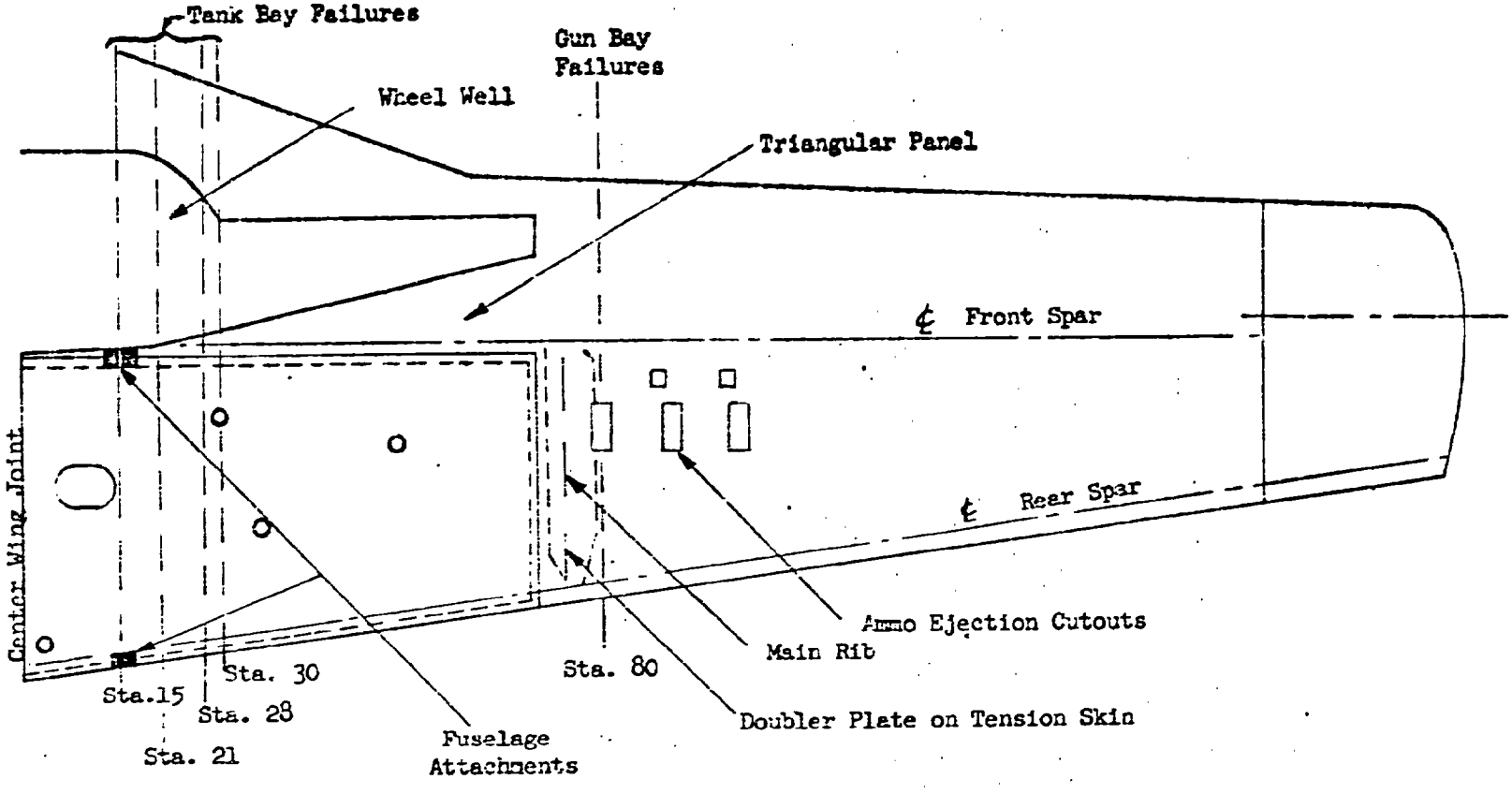



Figure 69 P51 Wing Specimen for Which Fatigue Test Data are Presented in Reference 21

TABLE 31

UNIT GUST LOADING SPECTRA AND S-N DATA FOR NOTCHED SHEET SPECIMENS
2024-T3 ALUMINUM ALLOY
(Reference 16)

$F_{tu}$ = 72.1 KSI (Net Area)

| Loading Step | $f_{max}$ KSI | $S_v$ | n | N | $f_{max}$ KSI | $S_v$ | n | N |
|---|---|---|---|---|---|---|---|---|
| | Gust Spectrum B $f_{mean}$ = 17.4 KSI $S_{mean}$ = .241 | | | | Gust Spectrum A $f_{mean}$ = 17.4 KSI $S_{mean}$ = .241 | | | |
| 1 | 18.1 | .010 | 62000 | - | 18.1 | .010 | 46800 | - |
| 2 | 19.5 | .029 | 24000 | - | 19.5 | .029 | 27200 | - |
| 3 | 20.9 | .049 | 9400 | - | 20.9 | .049 | 14500 | - |
| 4 | 22.3 | .068 | 3400 | 1300000 | 22.3 | .068 | 6800 | 1300000 |
| 5 | 23.7 | .087 | 880 | 270000 | 23.7 | .087 | 2750 | 270000 |
| 6 | 25.1 | .107 | 220 | 96000 | 25.1 | .107 | 1120 | [illegible] |
| 7 | 26.5 | .126 | 60 | 44500 | 26.5 | .126 | 450 | 44500 |
| 8 | 27.9 | .146 | 26 | 26000 | 27.9 | .146 | 200 | 26000 |
| 9 | 29.3 | .165 | 7.8 | 15000 | 29.3 | .165 | 80 | 15000 |
| 10 | 30.7 | .185 | 3.2 | 9200 | 30.7 | .185 | 39 | 9200 |
| 11 | 32.1 | .204 | 1.8 | 6100 | 32.1 | .204 | 18 | 6100 |
| 12 | 33.5 | .223 | .5 | 4200 | 33.5 | .223 | 7.6 | 4200 |
| 13 | 34.9 | .243 | .34 | 2900 | 34.9 | .243 | 3.0 | 2900 |
| 14 | 36.3 | .262 | .16 | 2050 | 36.3 | .262 | 1.3 | 2050 |
| 15 | 37.7 | .282 | .08 | 1540 | 37.7 | .282 | .6 | 1540 |
| 16 | 39.1 | .301 | .054 | 1150 | 39.1 | .301 | .3 | 1150 |
| 17 | 40.5 | .320 | .024 | 860 | 40.5 | .320 | .25 | 860 |
| 18 | 41.9 | .340 | .012 | 700 | 41.9 | .340 | .09 | 700 |
| | (G1 to G5****) | | $\Sigma$100000 * | | | (G6) | $\Sigma$100000 | |
| | Gust Spectrum A $f_{mean}$ = 17.4 KSI $S_{mean}$ = .241 | | | | Gust Spectrum A $f_{mean}$ = 0 KSI $S_{mean}$ = 0 | | | |
| 1 | 19.5 | .029 | 82000 | - | 2.2 | .031 | 41000 | - |
| 2 | 22.5 | .071 | 15000 | 900000 | 8.0 | .111 | 7850 | 4200000 |
| 3 | 25.6 | .114 | 2800 | 73000 | 13.2 | .183 | 980 | 800000 |
| 4 | 28.7 | .157 | 350 | 18500 | 18.5 | .257 | 143 | 100000 |
| 5 | 31.9 | .201 | 46 | 6500 | 23.8 | .330 | 23 | 19000 |
| 6 | 35.1 | .246 | 7.4 | 2760 | 29.2 | .405 | 3 | 4800 |
| 7 | 38.4 | .292 | 1.6 | 1320 | 34.8 | .463 | .73 | 1700 |
| 8 | 41.5 | .334 | .35 | 750 | 40.4 | .561 | .11 | 580 |
| | (G7 to G12) | | $\Sigma$100205 ** | | (G13 & G14) | | $\Sigma$50000 *** | |

* tests also made at 5n (G2, G4, & G5)
** tests also made at $\frac{n}{2}$ (G11)
*** tests also made at 2n (G14)
**** Test Group No.

TABLE 32

UNIT GUST LOADING SPECTRA AND S-N DATA FOR NOTCHED SHEET SPECIMENS
7075-T6 ALUMINUM ALLOY
(Reference 16)

$F_{tu}$ = 82.9 KSI (Net Area)

| Loading Step | $f_{max}$ KSI | $S_v$ | n | N |
|---|---|---|---|---|
| Gust Spectrum A; $f_{mean}$ = 20 KSI; $S_{mean}$ = .241 | | | | |
| 1 | 21.5 | .018 | 42000 | – |
| 2 | 25.3 | .064 | 7500 | 160000 |
| 3 | 28.7 | .105 | 1190 | 16600 |
| 4 | 32.6 | .152 | 175 | 5800 |
| 5 | 36.3 | .197 | 23 | 2900 |
| 6 | 40.1 | .242 | 2.5 | 1490 |
| 7 | 43.9 | .288 | 0.5 | 820 |
| 8 | 47.5 | .332 | 0.1 | 480 |
| | (G15 & G21**) | | > 30000 * | |
| Gust Spectrum A; $f_{mean}$ = 15 KSI; $S_{mean}$ = .121 | | | | |
| 1 | 13.0 | .036 | 24400 | – |
| 2 | 17.1 | .086 | 4700 | 520000 |
| 3 | 21.9 | .144 | 1000 | 20000 |
| 4 | 27.2 | .206 | 92 | 4400 |
| 5 | 31.7 | .262 | 14 | 1650 |
| 6 | 36.8 | .323 | 1.8 | 670 |
| 7 | 42.5 | .392 | 0.3 | 280 |
| 8 | 47.0 | .446 | 0.07 | 160 |
| | (G22 & G23) | | > 30000 | |
| Gust Spectrum A; $f_{mean}$ = 0 KSI; $S_{mean}$ = 0 | | | | |
| 1 | 3.8 | .046 | 24400 | – |
| 2 | 9.1 | .110 | 4800 | 2300000 |
| 3 | 15.0 | .181 | 690 | 27500 |
| 4 | 21.2 | .256 | 98 | 4200 |
| 5 | 27.2 | .328 | 14 | 1050 |
| 6 | 33.7 | .406 | 1.8 | 320 |
| 7 | 39.9 | .481 | 0.33 | 130 |
| 8 | 46.3 | .559 | 0.074 | 58 |
| | (G24 to G27) | | > 30000 | |

* Tests also made at $\frac{n}{5}$ (G15, G18, & G20)

** Test Group No.

TABLE 33

UNIT GUST LOADING SPECTRA AND S-N DATA FOR DOUBLE SHEAR RIVETED JOINTS
2024-T3 ALCLAD
(Reference 17)

$F_{tu}$ = 61.1 KSI (Net Area)

| Loading Step | $S_{max}$ | $S_v$ | n | N | $S_{max}$ | $S_v$ | n | N |
|---|---|---|---|---|---|---|---|---|
| | $S_{mean}$ = .253 | | | | $S_{mean}$ = .152 | | | |
| 1 | .278 | .025 | 281000 | 2300000 | .167 | .015 | 281000 | - |
| 2 | .327 | .074 | 65700 | 120000 | .196 | .044 | 65700 | 650000 |
| 3 | .376 | .123 | 11500 | 54000 | .226 | .074 | 11500 | 260000 |
| 4 | .426 | .173 | 1440 | 29000 | .256 | .104 | 1440 | 160000 |
| 5 | .475 | .222 | 432 | 18000 | .285 | .133 | 432 | 100000 |
| 6 | .524 | .272 | 131 | 11700 | .315 | .163 | 131 | 72000 |
| 7 | .574 | .321 | 50 | 7800 | .345 | .193 | 50 | 53000 |
| 8 | .623 | .370 | 16 | 5400 | .374 | .222 | 16 | 38000 |
| 9 | .672 | .419 | 10 | 3700 | .404 | .252 | 10 | 29000 |
| | | (028*) | $\Sigma$ 360280 | | | (029) | $\Sigma$ 360280 | |
| | $S_{mean}$ = .101 | | | | $S_{mean}$ = .0806 | | | |
| 1 | .111 | .010 | 281000 | - | .089 | .008 | 281000 | - |
| 2 | .131 | .030 | 65700 | - | .105 | .024 | 65700 | - |
| 3 | .150 | .049 | 11500 | 1500000 | .120 | .039 | 11500 | - |
| 4 | .170 | .069 | 1440 | 610000 | .136 | .055 | 1440 | 3500000 |
| 5 | .190 | .089 | 432 | 390000 | .152 | .071 | 432 | 880000 |
| 6 | .209 | .108 | 131 | 270000 | .168 | .087 | 131 | 520000 |
| 7 | .229 | .128 | 50 | 200000 | .184 | .103 | 50 | 380000 |
| 8 | .249 | .148 | 16 | 145000 | .199 | .118 | 16 | 300000 |
| 9 | .268 | .167 | 10 | 120000 | .215 | .134 | 10 | 220000 |
| | | (030) | $\Sigma$ 360280 | | | (031) | $\Sigma$ 360280 | |

*Test Group No.

TABLE 34

UNIT GUST LOADING SPECTRA AND S-N DATA FOR UNNOTCHED SHEET
7075-T6 ALCLAD
(Reference 17)

$F_{tu}$ = 76.8 KSI

| Loading Step | $S_{max}$ | $S_r$ | n | N |
|---|---|---|---|---|
| | | $S_{mean}$ = .201 | | |
| 1 | .221 | .020 | 281000 | - |
| 2 | .260 | .059 | 65700 | - |
| 3 | .299 | .098 | 11500 | 5000000 |
| 4 | .339 | .138 | 1440 | 360000 |
| 5 | .378 | .177 | 432 | 180000 |
| 6 | .417 | .216 | 131 | 105000 |
| 7 | .457 | .256 | 50 | 66000 |
| 8 | .496 | .295 | 16 | 44000 |
| 9 | .535 | .334 | 10 | 31000 |
| | | (G32*) | $\Sigma$ 360280 | |
| | | $S_{mean}$ = .161 | | |
| 1 | .177 | .016 | 281000 | - |
| 2 | .208 | .047 | 65700 | - |
| 3 | .240 | .079 | 11500 | - |
| 4 | .271 | .110 | 1440 | 1500000 |
| 5 | .302 | .141 | 432 | 330000 |
| 6 | .334 | .173 | 131 | 181000 |
| 7 | .365 | .204 | 50 | 120000 |
| 8 | .397 | .236 | 16 | 82000 |
| 9 | .428 | .267 | 10 | 60000 |
| | | (G33) | $\Sigma$ 360280 | |
| | | $S_{mean}$ = .145 | | |
| 1 | .159 | .014 | 281000 | - |
| 2 | .187 | .042 | 65700 | - |
| 3 | .216 | .071 | 11500 | - |
| 4 | .244 | .099 | 1440 | - |
| 5 | .272 | .127 | 432 | 550000 |
| 6 | .301 | .156 | 131 | 260000 |
| 7 | .329 | .184 | 50 | 165000 |
| 8 | .357 | .212 | 16 | 120000 |
| 9 | .385 | .240 | 10 | 85000 |
| | | (G34) | $\Sigma$ 360280 | |

* Test Group No.

TABLE 35

UNIT GUST LOADING SPECTRA AND S-N DATA FOR BUTT JOINTS
7075-T6 ALCLAD
(Reference 17)

$F_{tu}$ = 53.0 KSI (Gross Area)

| Loading Step | $S_{max}$ | $S_v$ | n | N |
|---|---|---|---|---|
| | | $S_{mean}$ = .250 | | |
| 1 | .275 | .025 | 281000 | - |
| 2 | .323 | .073 | 65700 | 380000 |
| 3 | .372 | .122 | 11500 | 95000 |
| 4 | .421 | .171 | 1440 | 31000 |
| 5 | .470 | .220 | 432 | 15000 |
| 6 | .518 | .268 | 131 | 8000 |
| 7 | .567 | .317 | 50 | 4200 |
| 8 | .616 | .366 | 16 | 2400 |
| 9 | .665 | .415 | 10 | 1400 |
| | | (035*) | $\Sigma$ 360280 | |
| | | $S_{mean}$ = .167 | | |
| 1 | .183 | .016 | 281000 | - |
| 2 | .216 | .049 | 65700 | - |
| 3 | .248 | .081 | 11500 | 650000 |
| 4 | .281 | .114 | 1440 | 300000 |
| 5 | .313 | .146 | 432 | 150000 |
| 6 | .346 | .179 | 131 | 75000 |
| 7 | .378 | .211 | 50 | 42000 |
| 8 | .411 | .244 | 16 | 23000 |
| 9 | .443 | .276 | 10 | 14500 |
| | | (036) | $\Sigma$ 360280 | |
| | | $S_{mean}$ = .125 | | |
| 1 | .137 | .012 | 281000 | - |
| 2 | .162 | .037 | 65700 | - |
| 3 | .186 | .061 | 11500 | - |
| 4 | .210 | .085 | 1440 | 1100000 |
| 5 | .235 | .110 | 432 | 460000 |
| 6 | .259 | .134 | 131 | 260000 |
| 7 | .284 | .159 | 50 | 170000 |
| 8 | .308 | .183 | 16 | 110000 |
| 9 | .332 | .207 | 10 | 72000 |
| | | (037) | $\Sigma$ 360280 | |

*Test Group No.

TABLE 36

UNIT GUST LOADING SPECTRA AND S-N DATA FOR STRIPS
WITH CENTRALLY LOCATED HOLE
Cr-Mo STEEL
(Reference 17)

$F_{tu}$ = 150.8 KSI (Net Area)

| Loading Step | $S_{max}$ | $S_v$ | n | N |
|---|---|---|---|---|
| | | $S_{mean}$ = .286 | | |
| 1 | .314 | .028 | 281000 | - |
| 2 | .370 | .084 | 65700 | - |
| 3 | .426 | .140 | 11500 | 260000 |
| 4 | .481 | .195 | 1440 | 92000 |
| 5 | .537 | .251 | 432 | 43000 |
| 6 | .593 | .307 | 131 | 22000 |
| 7 | .649 | .363 | 50 | 11000 |
| 8 | .705 | .419 | 16 | 5400 |
| 9 | .760 | .474 | 10 | 2600 |
| | | (038*) | $\Sigma$ 360280 | |
| | | $S_{mean}$ = .222 | | |
| 1 | .244 | .022 | 281000 | - |
| 2 | .288 | .066 | 65700 | - |
| 3 | .330 | .108 | 11500 | - |
| 4 | .374 | .152 | 1440 | 270000 |
| 5 | .417 | .195 | 432 | 111000 |
| 6 | .460 | .238 | 131 | 56000 |
| 7 | .503 | .281 | 50 | 32000 |
| 8 | .547 | .325 | 16 | 18000 |
| 9 | .590 | .368 | 10 | 11000 |
| | | (039) | $\Sigma$ 360280 | |
| | | $S_{mean}$ = .182 | | |
| 1 | .199 | .017 | 281000 | - |
| 2 | .235 | .053 | 65700 | - |
| 3 | .270 | .088 | 11500 | - |
| 4 | .306 | .124 | 1440 | - |
| 5 | .341 | .159 | 432 | 320000 |
| 6 | .377 | .195 | 131 | 125000 |
| 7 | .412 | .230 | 50 | 64000 |
| 8 | .448 | .266 | 16 | 37000 |
| 9 | .483 | .301 | 10 | 25000 |
| | | (040) | $\Sigma$ 360280 | |

* Test Group No.

TABLE 37

UNIT GUST LOADING SPECTRA AND S-N DATA FOR SINGLE-ROW FLUSH-RIVETED LAP JOINTS
2024-T3 ALCLAD
(Reference 18)

Ultimate Load = 4600 lbs. (Gross Area)

| Loading Step | Maximum Load-lbs. | $S_{max}$ | $S_v$ | n | N | Maximum Load-lbs. | $S_{max}$ | $S_v$ | n | N |
|---|---|---|---|---|---|---|---|---|---|---|
| | Mean Load = 759 lbs. | | | | | $S_{mean}$ = .212 | | | | |
| | Six Loading Steps | | | | | Five Loading Steps | | | | |
| 1 | 1130 | .246 | .034 | 1670000 | - | | | | | |
| 2 | 1450 | .315 | .103 | 207500 | 280000 | 1450 | .315 | .103 | 415000 | 280000 |
| 3 | 1770 | .384 | .172 | 19200 | 91000 | 1770 | .384 | .172 | 38400 | 91000 |
| 4 | 2080 | .452 | .240 | 1920 | 40300 | 2080 | .452 | .240 | 3840 | 40300 |
| 5 | 2400 | .520 | .308 | 192 | 19200 | 2400 | .520 | .308 | 384 | 19200 |
| 6 | 2700 | .588 | .376 | 19 | 10000 | 2700 | .588 | .376 | 38 | 10000 |
| | | (G41,G42 & G43**) | | $\Sigma$ 1895830* | | | | (G44) | $\Sigma$ 457660 | |

* Tests also made at 1.2n and 1.5n. (G42 & G43, respectively)

** Test Group No.

TABLE 38

UNIT GUST LOADING SPECTRUM AND S-N DATA
FOR DOUBLE-ROW FLUSH-RIVETED LAP JOINTS
2024-T3 ALCLAD
(Reference 18)

Ultimate Load = 8690 lbs. (Gross Area)

| Loading Step | Maximum Load-lbs. | $S_{max}$ | $S_r$ | n | N |
|---|---|---|---|---|---|
| Mean Load = 1840 lbs. | | | | $S_{mean}$ = .212 | |
| Five Loading Steps | | | | | |
| 1 | 2734 | .315 | .103 | 143800 | 250000 |
| 2 | 3333 | .384 | .172 | 18500 | 75000 |
| 3 | 3923 | .452 | .240 | 1850 | 31500 |
| 4 | 4514 | .520 | .308 | 185 | 13400 |
| 5 | 5104 | .588 | .376 (.415*) | 19 | 6000 |
| | | | | $\Sigma$ 164350 | |

* Test Group No.

TABLE 39

UNIT GUST LOADING SPECTRA AND S-N DATA FOR SINGLE-ROW FLUSH-RIVETED LAP JOINTS
7075-T6 ALCLAD
(Reference 18)

Ultimate Load = 4975 lbs. (Gross Area)

| Loading Step | Maximum Load-lbs. | $S_{max}$ | $S_v$ | n | N | Maximum Load-lbs. | $S_{max}$ | $S_v$ | n | N |
|---|---|---|---|---|---|---|---|---|---|---|
| | Mean Load = 1055 lbs. | | | | | $S_{mean}$ = .212 | | | | |
| | Six Loading Steps | | | | | Five Loading Steps | | | | |
| 1 | 1222 | .246 | .034 | 1080000 | - | | | | | |
| 2 | 1567 | .315 | .103 | 134000 | 98000 | 1567 | .315 | .103 | 79100 | 98000 |
| 3 | 1910 | .384 | .172 | 12400 | 40500 | 1910 | .384 | .172 | 12400 | 40500 |
| 4 | 2248 | .452 | .240 | 1240 | 22100 | 2248 | .452 | .240 | 1240 | 22100 |
| 5 | 2587 | .520 | .308 | 124 | 12300 | 2587 | .520 | .308 | 124 | 12300 |
| 6 | 2920 | .588 | .376 (G47*) | 12<br>$\Sigma$ 1227780 | 7100 | 2920 | .588 | .376 (G46) | 12<br>$\Sigma$ 92880 | 7100 |

* Test Group No.

TABLE 40

UNIT GUST LOADING SPECTRA AND S-N DATA
FOR NOTCHED PLATE SPECIMENS
D.T.D. 363A ALUMINUM ALLOY
(British Zinc-Aluminum Alloy Similar to 7075-T6)
(Reference 19)

$F_{tu}$ = 85 KSI (Net Area)
$f_{mean}$ = 14 KSI
$S_{mean}$ = .165

| Loading Step | $f_v$ KSI | $S_v$ | n | N |
|---|---|---|---|---|
| | | Nine Loading Steps | | |
| 1 | 2.62 | .030 | 7400 | - |
| 2 | 3.68 | .043 | 3100 | 150000 |
| 3 | 4.73 | .056 | 1500 | 48000 |
| 4 | 5.78 | .068 | 700 | 26000 |
| 5 | 6.84 | .080 | 325 | 17000 |
| 6 | 7.88 | .093 | 150 | 12500 |
| 7 | 8.93 | .105 | 67 | 9200 |
| 8 | 9.98 | .118 | 31 | 6800 |
| 9 | 11.02 | .130 | 15 | 5200 |
| | | (048*) | $\Sigma$ 13290 | |
| | | Nine Loading Steps Different Frequency | | |
| 1 | 2.62 | .030 | 4400 | - |
| 2 | 3.68 | .043 | 600 | 150000 |
| 3 | 4.73 | .056 | 700 | 48000 |
| 4 | 5.78 | .068 | 280 | 26000 |
| 5 | 6.84 | .080 | 180 | 17000 |
| 6 | 7.88 | .093 | 66 | 12500 |
| 7 | 8.93 | .105 | 33 | 9200 |
| 8 | 9.98 | .118 | 21 | 6800 |
| 9 | 11.02 | .130 | 13 | 5200 |
| | | (049) | $\Sigma$ 6290 | |
| | | Ten Loading Steps | | |
| 1 | 2.62 | .030 | 810 | - |
| 2 | 3.68 | .043 | 1800 | 150000 |
| 3 | 4.73 | .056 | 1650 | 48000 |
| 4 | 5.78 | .068 | 747 | 26000 |
| 5 | 6.84 | .080 | 193 | 17000 |
| 6 | 7.88 | .093 | 103 | 12500 |
| 7 | 8.93 | .105 | 60 | 9200 |
| 8 | 9.98 | .118 | 27 | 6800 |
| 9 | 11.02 | .130 | 12 | 5200 |
| 10 | 11.60 | .137 | 8 | 4000 |
| | | (050) | $\Sigma$ 5410 | |

* Test Group No.

TABLE 41

UNIT GUST LOADING SPECTRUM AND S-N DATA
FOR WING STATIONS 180, 214, 228, AND 239 OF C-46 WING
2024-T ALUMINUM ALLOY
(Reference 20 and 23)

Ultimate Load Factor = 5.0 * (Gross Area)
$S_{mean}$ = .2

| Loading Step | $\Delta g$ | $S_v = \frac{\Delta g}{5}$ | n | N | | | |
|---|---|---|---|---|---|---|---|
| | | | | WS 180 | WS 214 | WS 228 | WS 239 |
| | | | | See Note on Figure 92 | | | |
| 1 | .225 | .045 | 39312 | 6600000 | 5000000 | 6000000 | 1750000 |
| | .375 | .075 | 15444 | 1170000 | 1500000 | 1300000 | 520000 |
| | .525 | .105 | 3510 | 320000 | 550000 | 470000 | 240000 |
| 4 | .675 | .135 | 1067 | 132000 | 260000 | 210000 | 130000 |
| 5 | .825 | .165 | 235 | 66000 | 150000 | 110000 | 81000 |
| 6 | .975 | .195 | 73 | 35000 | 92000 | 62000 | 56000 |
| 7 | 1.125 | .225 | 20 | 20500 | 65000 | 39000 | 40000 |
| 8 | 1.275 | .255 | 5.86 | 12500 | 48000 | 27000 | 29000 |
| 9 | 1.425 | .285 | 1.48 | 8600 | 35000 | 18500 | 21500 |
| 10 | 1.575 | .315 | .69 | 6000 | 28000 | 14000 | 16000 |
| 11 | 1.725 | .345 | .19 | 4500 | 23000 | 10200 | 12500 |
| 12 | 1.875 | .375 | .12 | 3300 | 18000 | 8000 | 10000 |
| 13 | 2.025 | .405 | .06 | 2500 | 14500 | 6200 | 8500 |
| 14 | 2.175 | .435 | .02 | 1900 | 12000 | 4800 | 7000 |
| 15 | 2.325 | .465 | .02 | 1520 | 10000 | 4000 | 6000 |
| 16 | 2.475 | .495 | .01 | 1250 | 8800 | 3700 | 5200 |
| | (G51 to G54**) | | $\Sigma$ 59670 | | | | |

* Arbitrary

** Test Group No.

TABLE 42

UNIT GUST LOADING SPECTRUM AND S-N DATA FOR COMPLETE C-46 WING
2024-T ALUMINUM ALLOY
(Reference 20)

Ultimate Load Factor = 5.0 * (Gross Area) $S_{mean} = .2$

| Loading Step | $\Delta g$ | $S_v = \frac{\Delta g}{5}$ | n | N First Crack | N Critical Crack | N Final Failure |
|---|---|---|---|---|---|---|
| 1 | .225 | .045 | 39312 | 3100000 | 4300000 | 6600000 |
| 2 | .375 | .075 | 15444 | 790000 | 1070000 | 1650000 |
| 3 | .525 | .105 | 3510 | 260000 | 400000 | 590000 |
| 4 | .675 | .135 | 1067 | 140000 | 200000 | 280000 |
| 5 | .825 | .165 | 235 | 72000 | 110000 | 152000 |
| 6 | .975 | .195 | 73 | 41000 | 65000 | 95000 |
| 7 | 1.125 | .225 | 20 | 24000 | 40000 | 57000 |
| 8 | 1.275 | .255 | 5.86 | 15000 | 26000 | 37000 |
| 9 | 1.425 | .285 | 1.48 | 9500 | 17000 | 24000 |
| 10 | 1.575 | .315 | .69 | 6200 | 11500 | 16000 |
| 11 | 1.725 | .345 | .19 | 4000 | 7900 | 11000 |
| 12 | 1.875 | .375 | .12 | 2700 | 5400 | 8000 |
| 13 | 2.025 | .405 | .06 | 1800 | 3700 | 5900 |
| 14 | 2.175 | .435 | .02 | 1200 | 2600 | 4500 |
| 15 | 2.325 | .465 | .02 | 850 | 1820 | 3400 |
| 16 | 2.475 | .495 | .01 | 580 | 1270 | 2600 |
| | (G55 to G57**) | | $\Sigma$ 59670 | | | |

* Arbitrary

** Test Group No.

## TABLE 43

UNIT GUST LOADING SPECTRA AND S-N DATA FOR P51 WING
2024-T ALUMINUM ALLOY
(Reference 21 & 24)

Ultimate Load = 89600 lbs. (Gross Area)

$S_{mean}$ = .200

| Loading Step | $S_v$ | n | N Initial Failure Gun Bay | N Initial Failure Tank Bay | N Final Failure Gun Bay | N Final Failure Tank Bay |
|---|---|---|---|---|---|---|
| | | | Eleven Loading Steps | | | |
| 1 | .0324 | 275300 | - | - | - | - |
| 2 | .0540 | 118200 | 1585000 | 3020000 | 2089000 | 5888000 |
| 3 | .0756 | 64310 | 346700 | 616600 | 660700 | 501200 |
| 4 | .0972 | 26080 | 123000 | 211300 | 309000 | 218800 |
| 5 | .1188 | 9452 | 53090 | 93330 | 152200 | 112200 |
| 6 | .1512 | 5110 | 17780 | 38020 | 75860 | 53700 |
| 7 | .1944 | 1139 | 5248 | 15140 | 33110 | 23500* |
| 8 | .2376 | 220.7 | 1950 | 7590 | 15850 | 10960 |
| 9 | .2808 | 51.32 | 813 | 4360 | 7800* | 5623 |
| 10 | .3240 | 10.69 | 355 | 2660 | 4169 | 3020 |
| 11 | .4100 | 4.343 | 83 | 1120 | 1120 | 1072 |
| (G58, G60, G62 & G64***) | | $\Sigma$ 499880 ** | | | | |
| | | | Three Loading Steps | | | |
| 1 | .055 | 26500 | 1513600 | 2691500 | 1905500 | 4365200 |
| 2 | .075 | 5300 | 363080 | 630000* | 676080 | 524810 |
| 3 | .1325 | 1060 | 32359 | 61659 | 114820 | 81283 |
| (G59, G61, G63 & G65) | | $\Sigma$ 32860 | | | | |

* These values have been corrected. The values listed in reference 21 are apparently in error.

** Specified in reference 21 as the number of positive load peaks in $10^6$ load selections.

*** Test Group No.

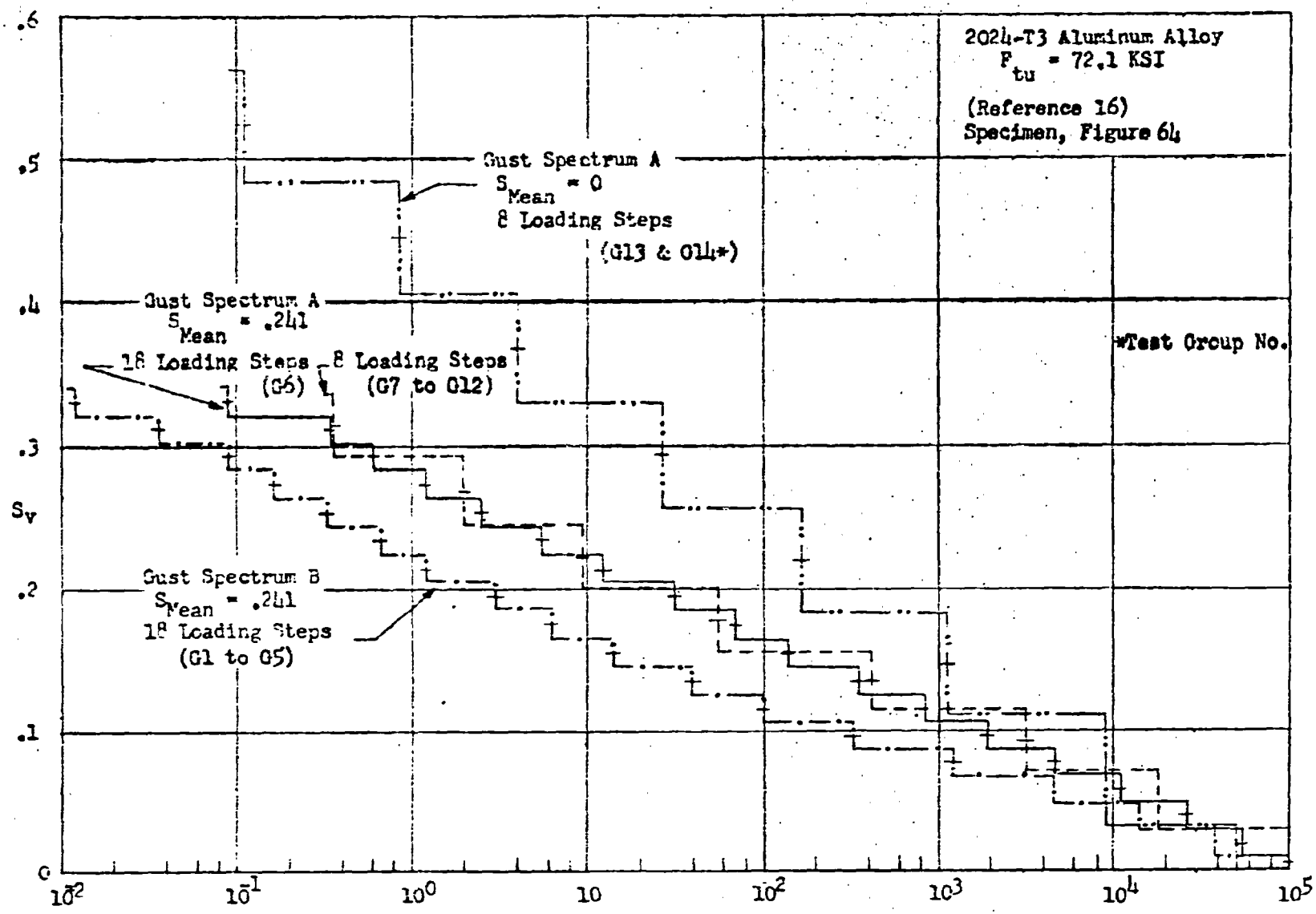



Figure 70 Unit Gust Loading Spectra For Notched Sheet Specimens

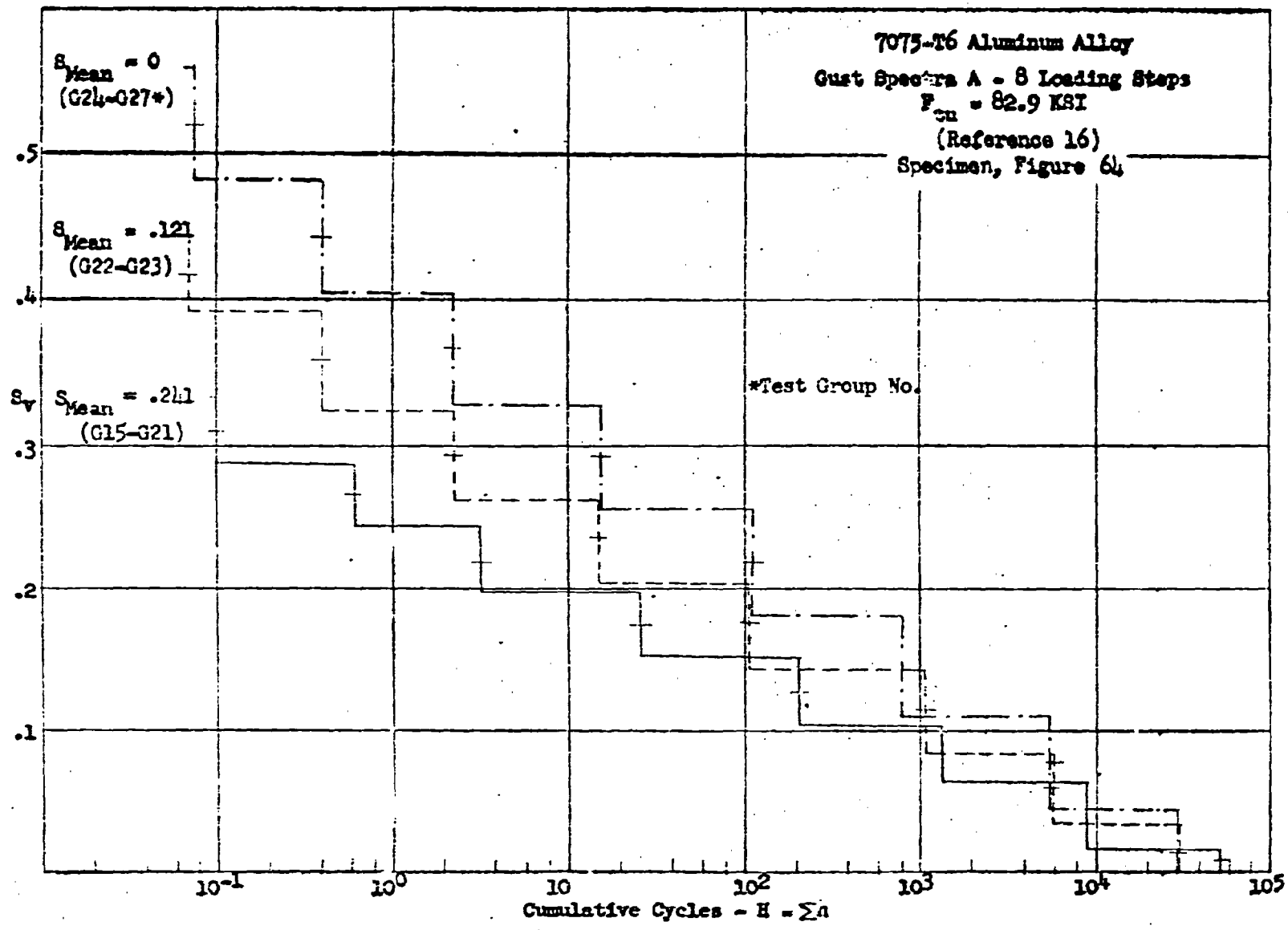



Figure 71 Unit Loading Spectra for Notched Sheet Specimens.

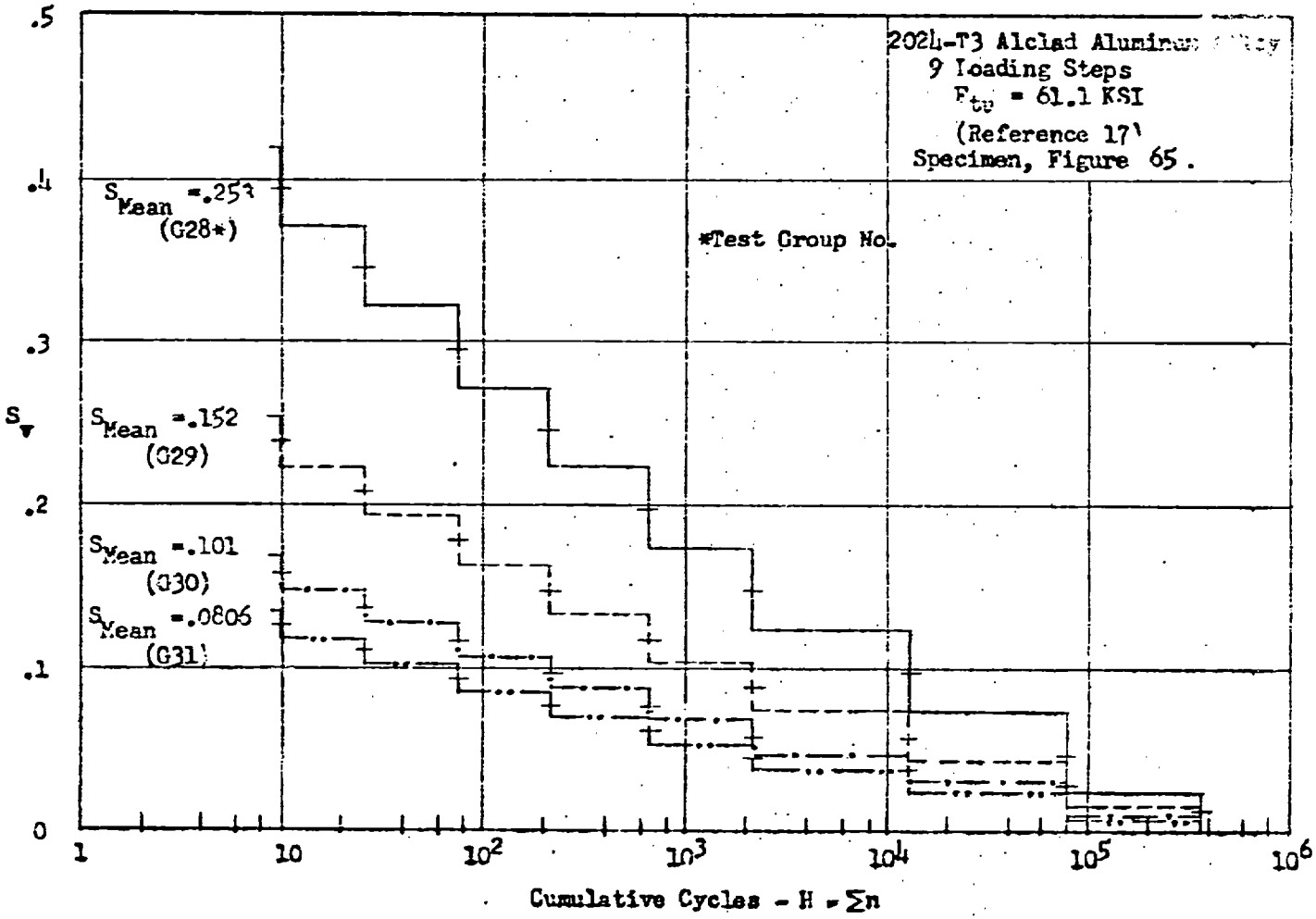



Figure 72 Unit Gust Loading Spectra for Double Shear Riveted Joint Specimens

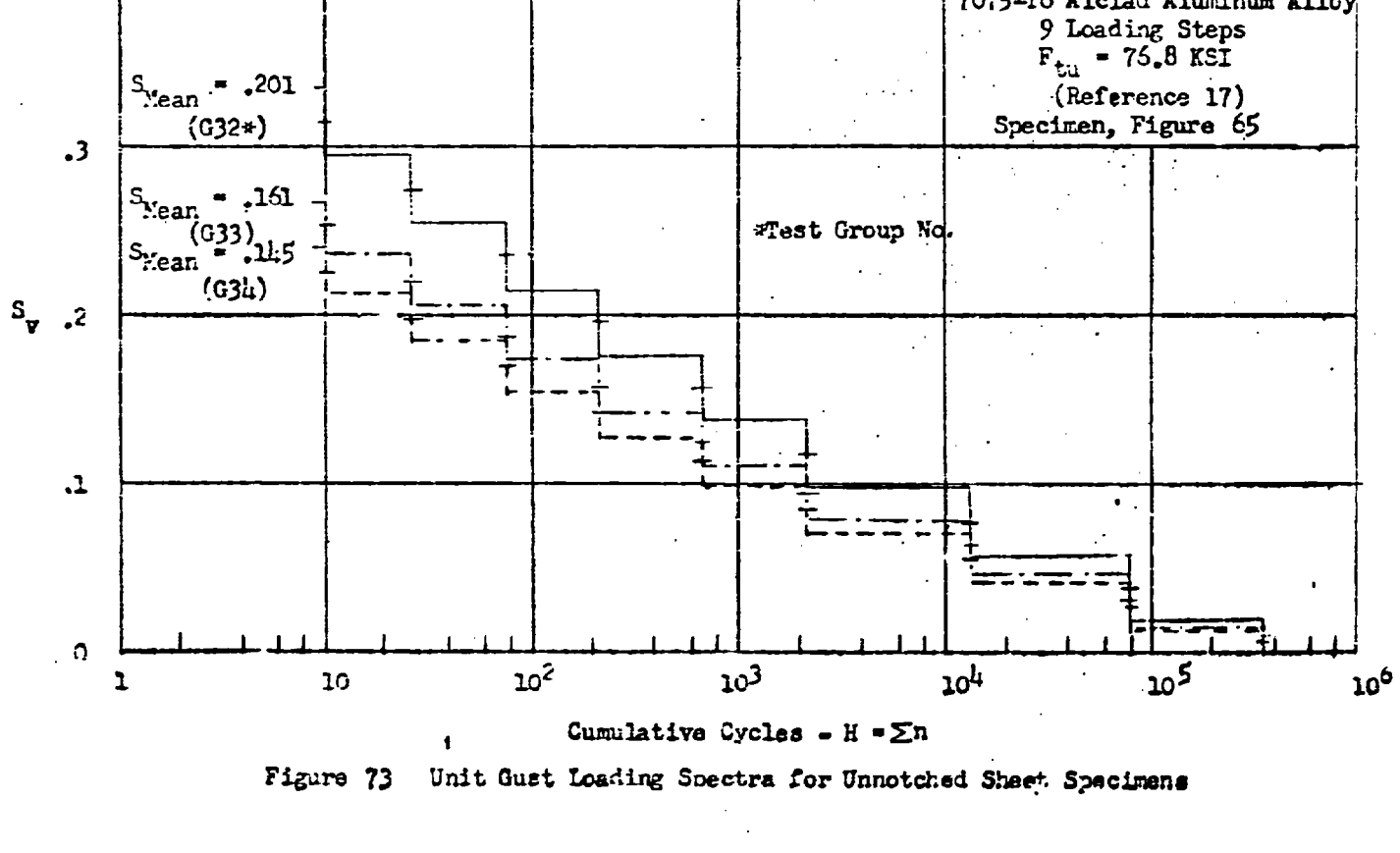



Figure 73 Unit Gust Loading Spectra for Unnotched Sheet Specimens

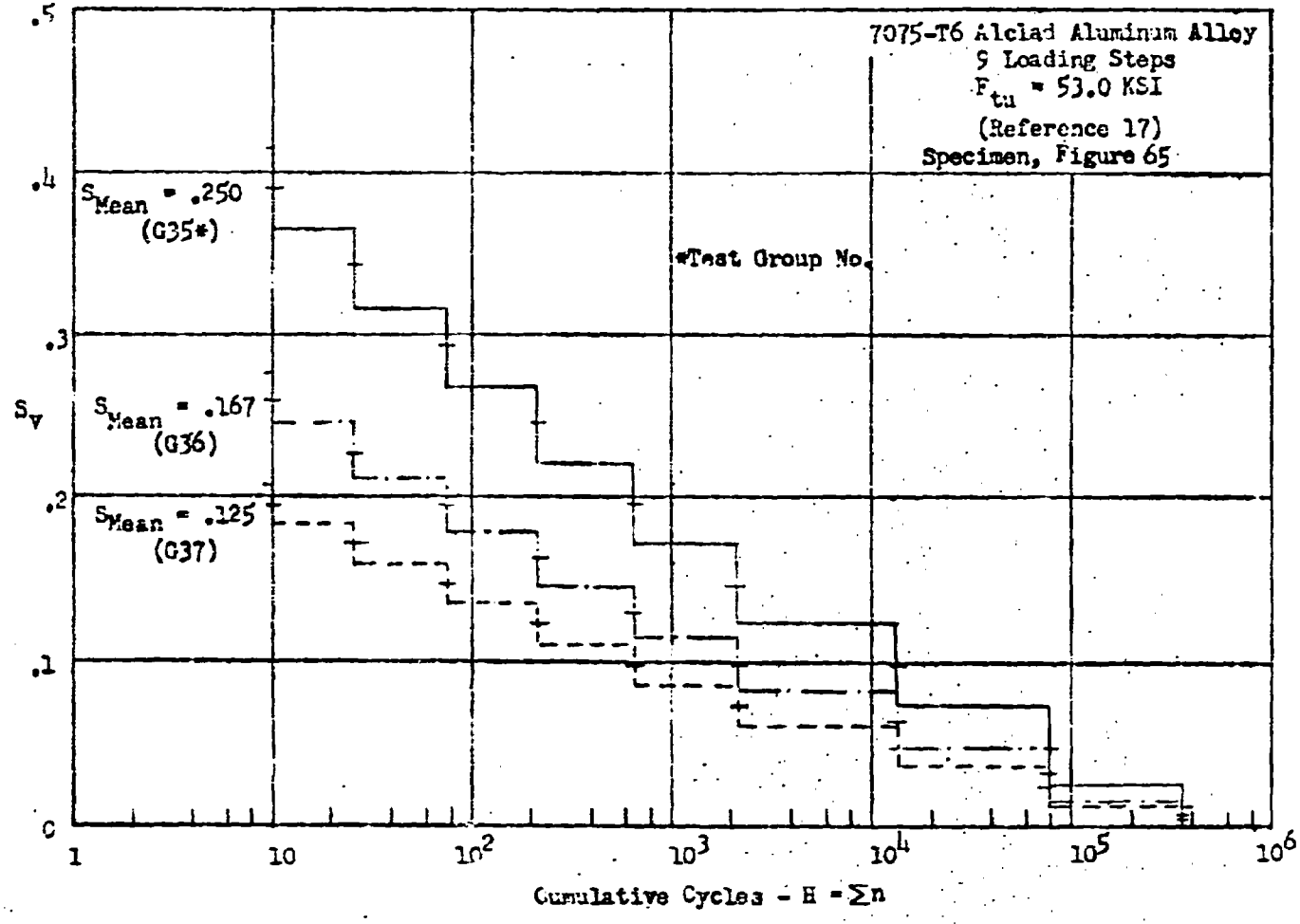



Figure 74 Unit Gust Loading Spectra for Butt Joint Specimens

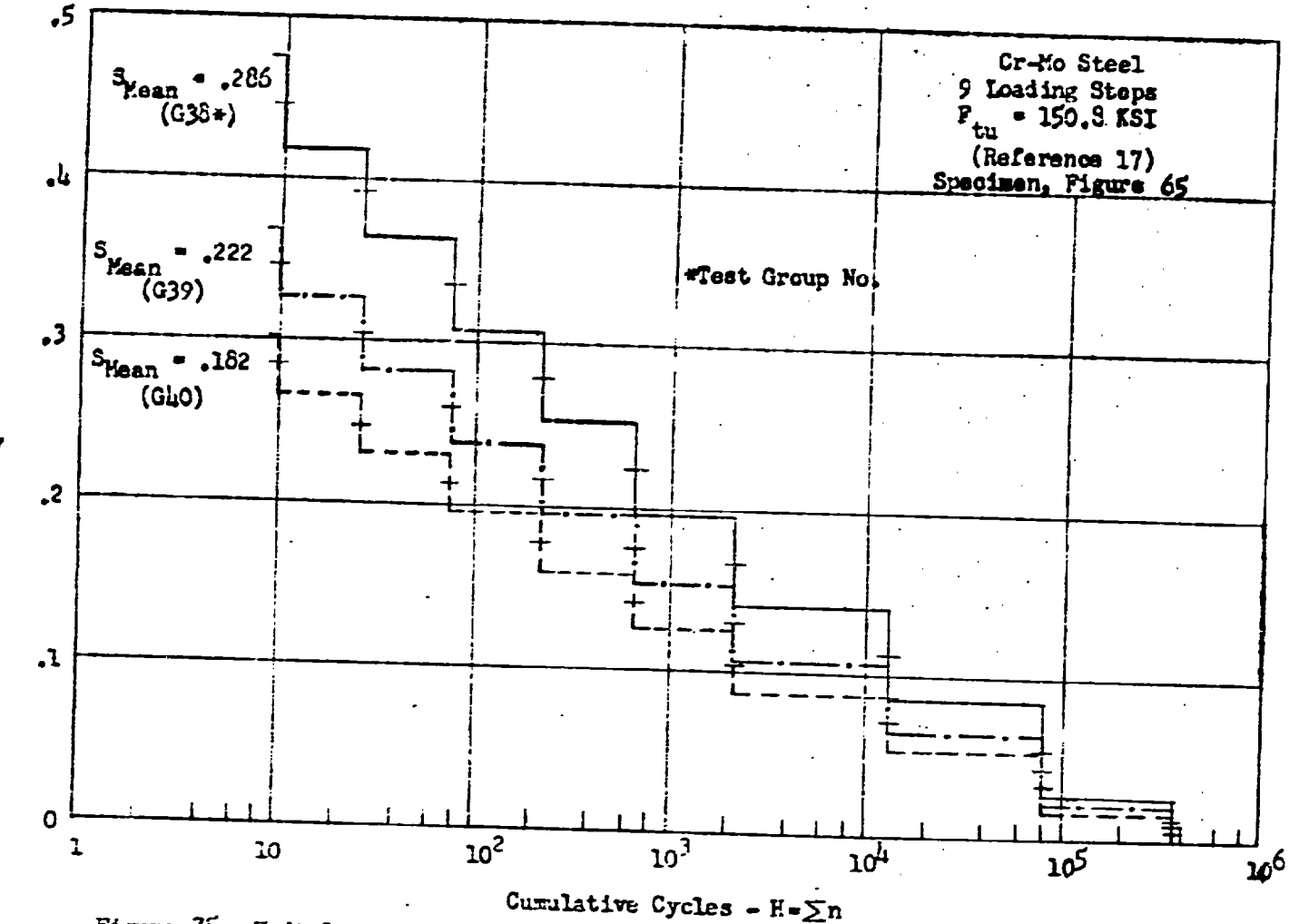



Figure 75 Unit Gust Loading Spectra for Strip Specimens with Centrally Located Hole

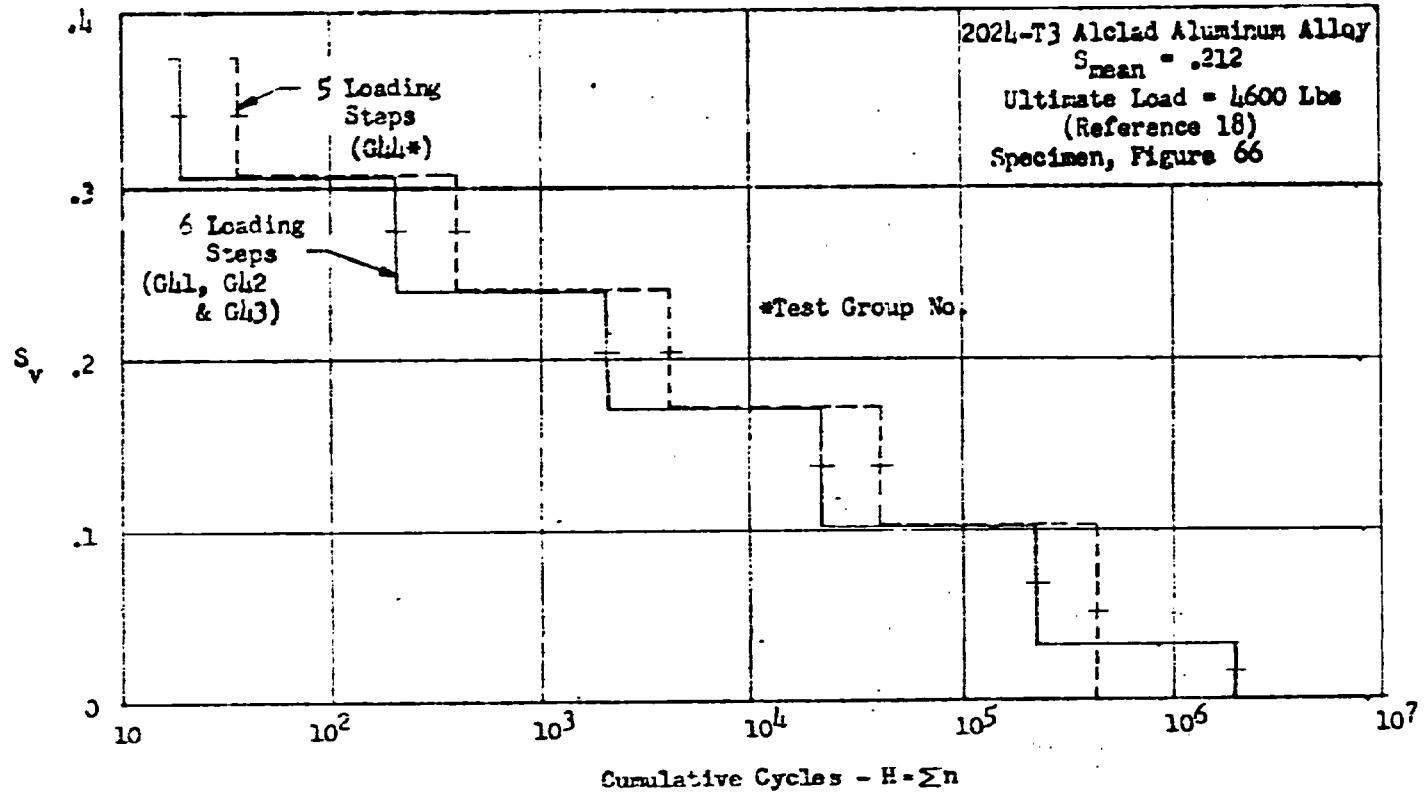



Figure 76 Unit Gust Loading Spectra for Lap Joint Specimens with a Single Row of Flush Rivets

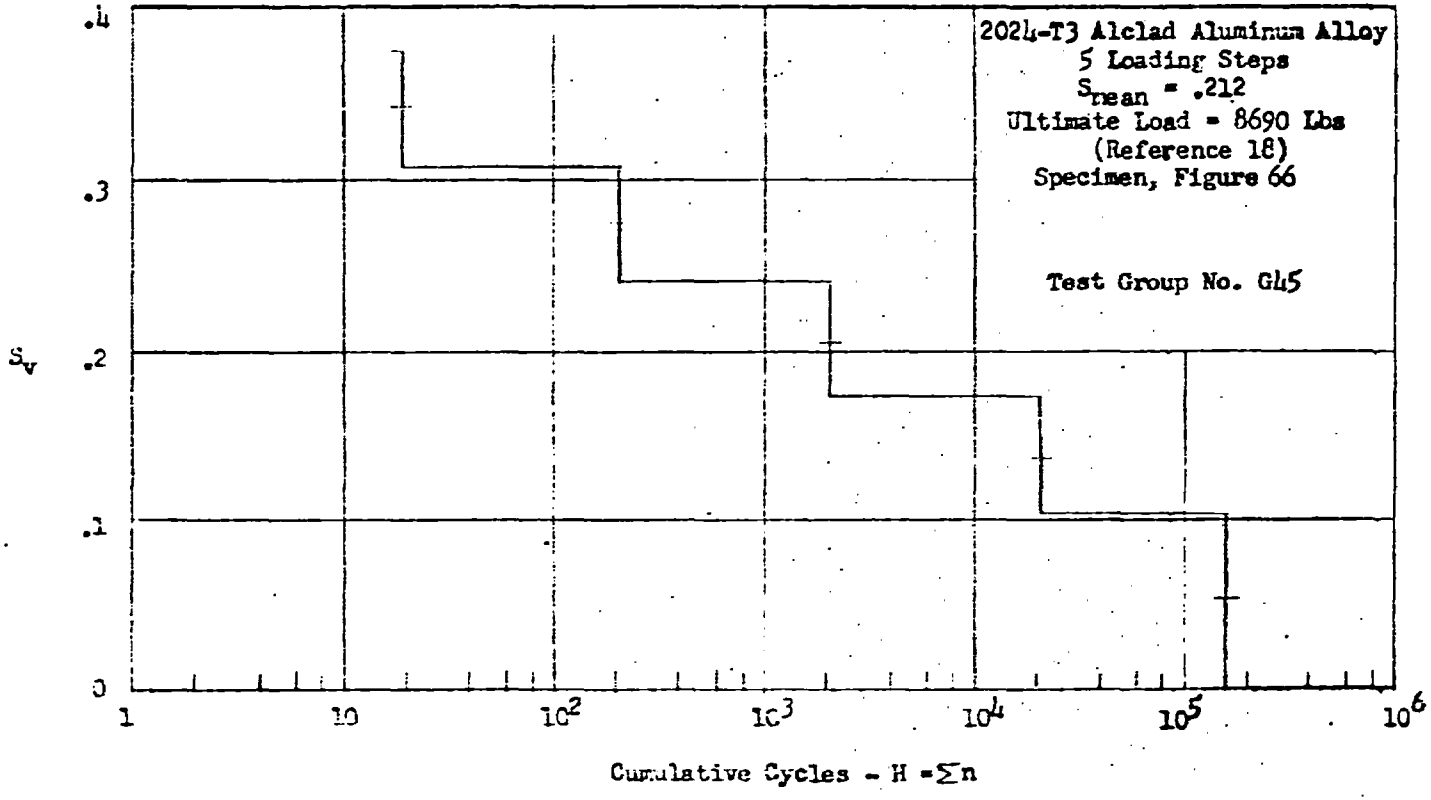



Figure 77 Unit Gust Loading Spectrum for Lap Joint Specimen with a Double Row of Flush Rivets

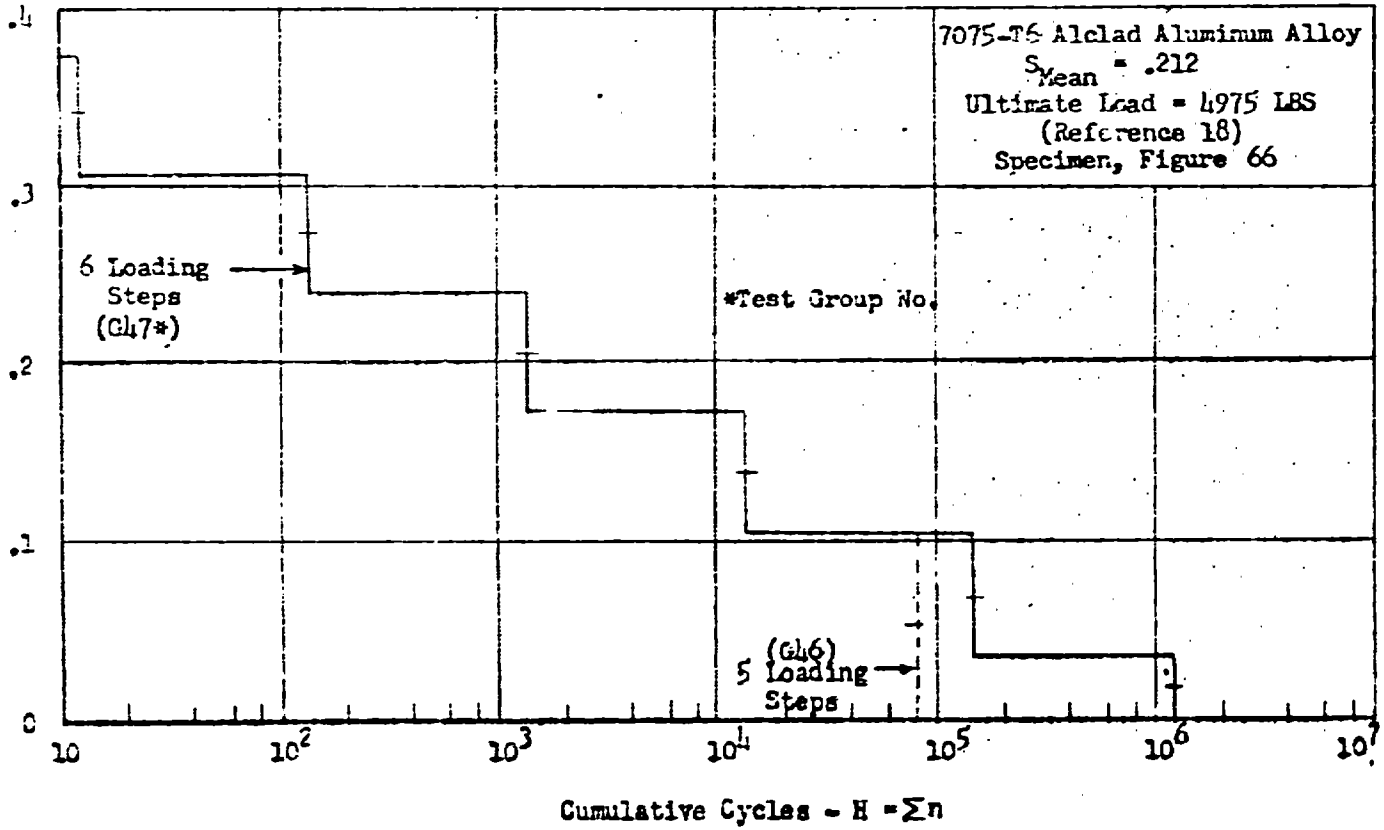



Figure 73 Unit Gust Loading Spectra for Lap Joint Specimens with a Single Row of Flush Rivets

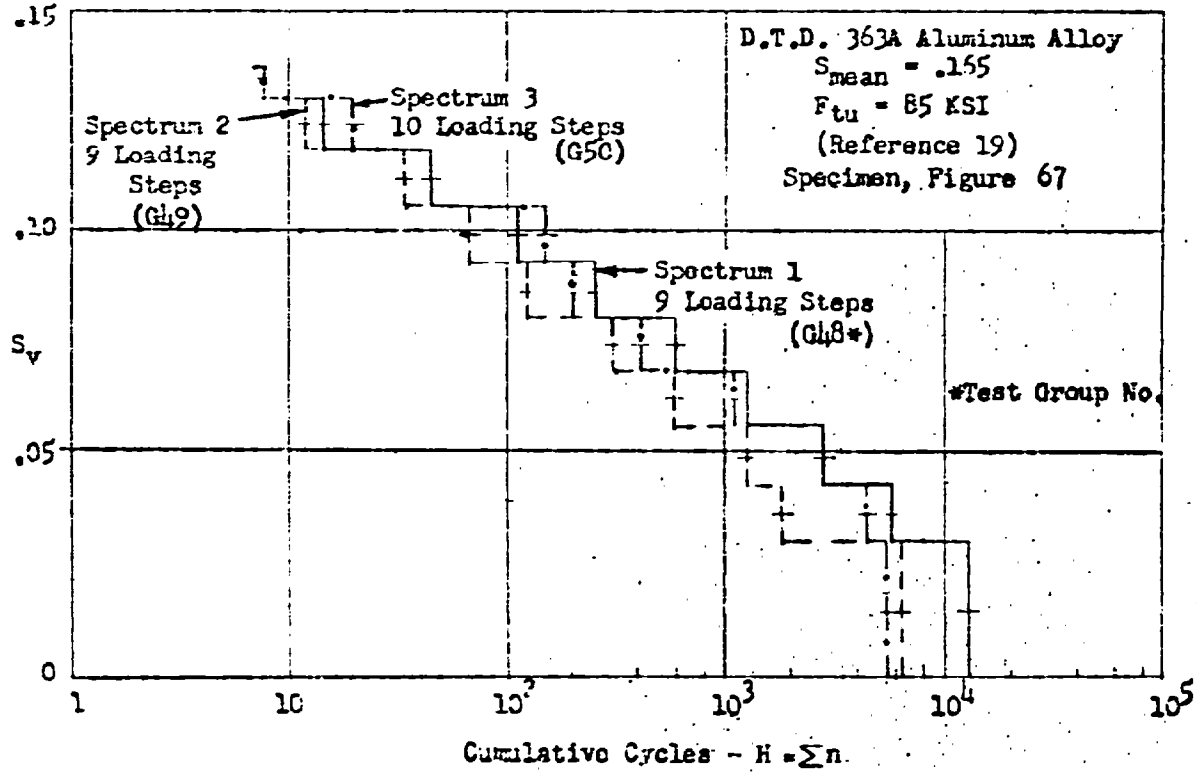



Figure 79 Unit Gust Loading Spectra for Notched Plate Specimens

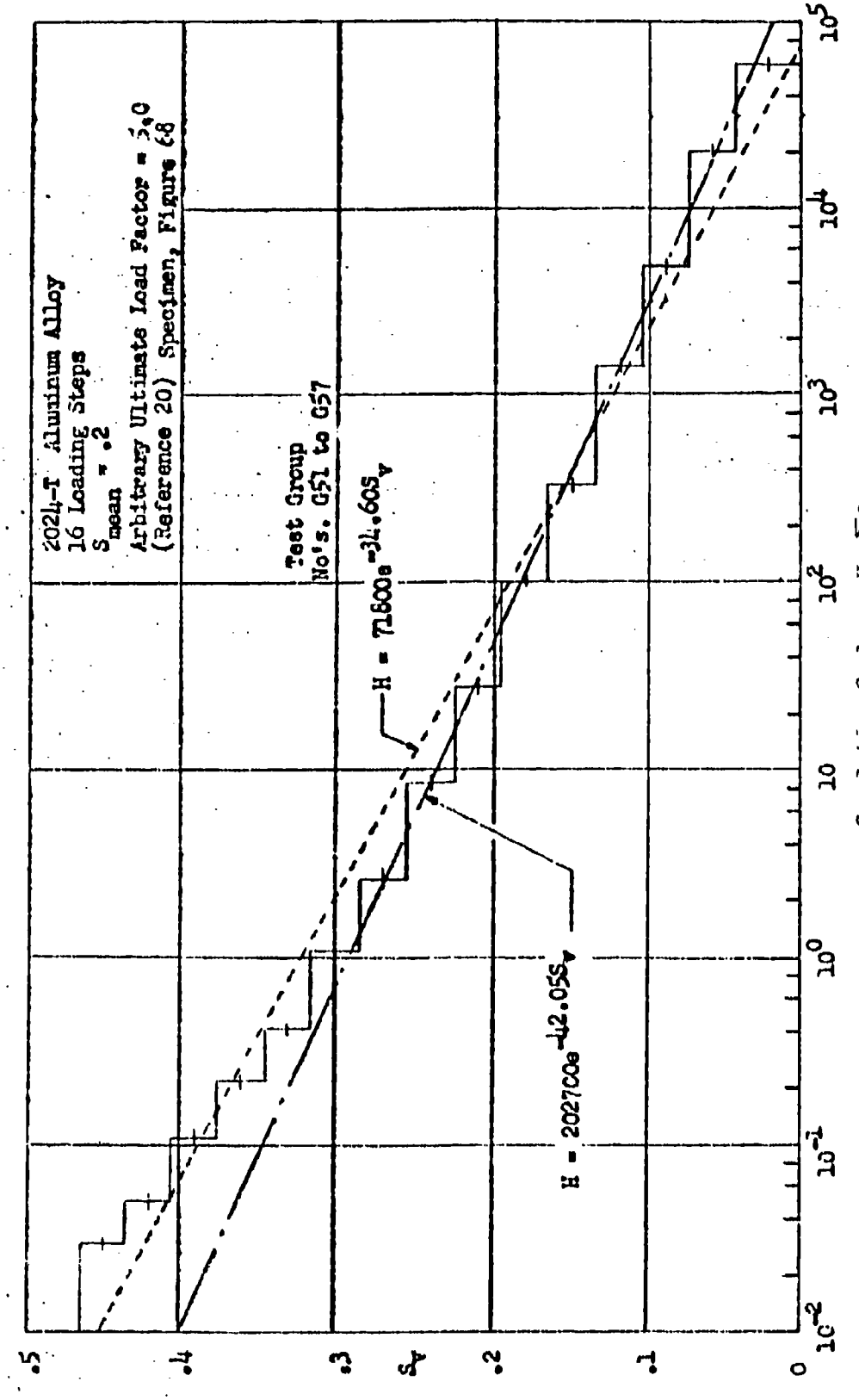



Figure 60. Unit Gust Loading Spectrum for C-46 Wing

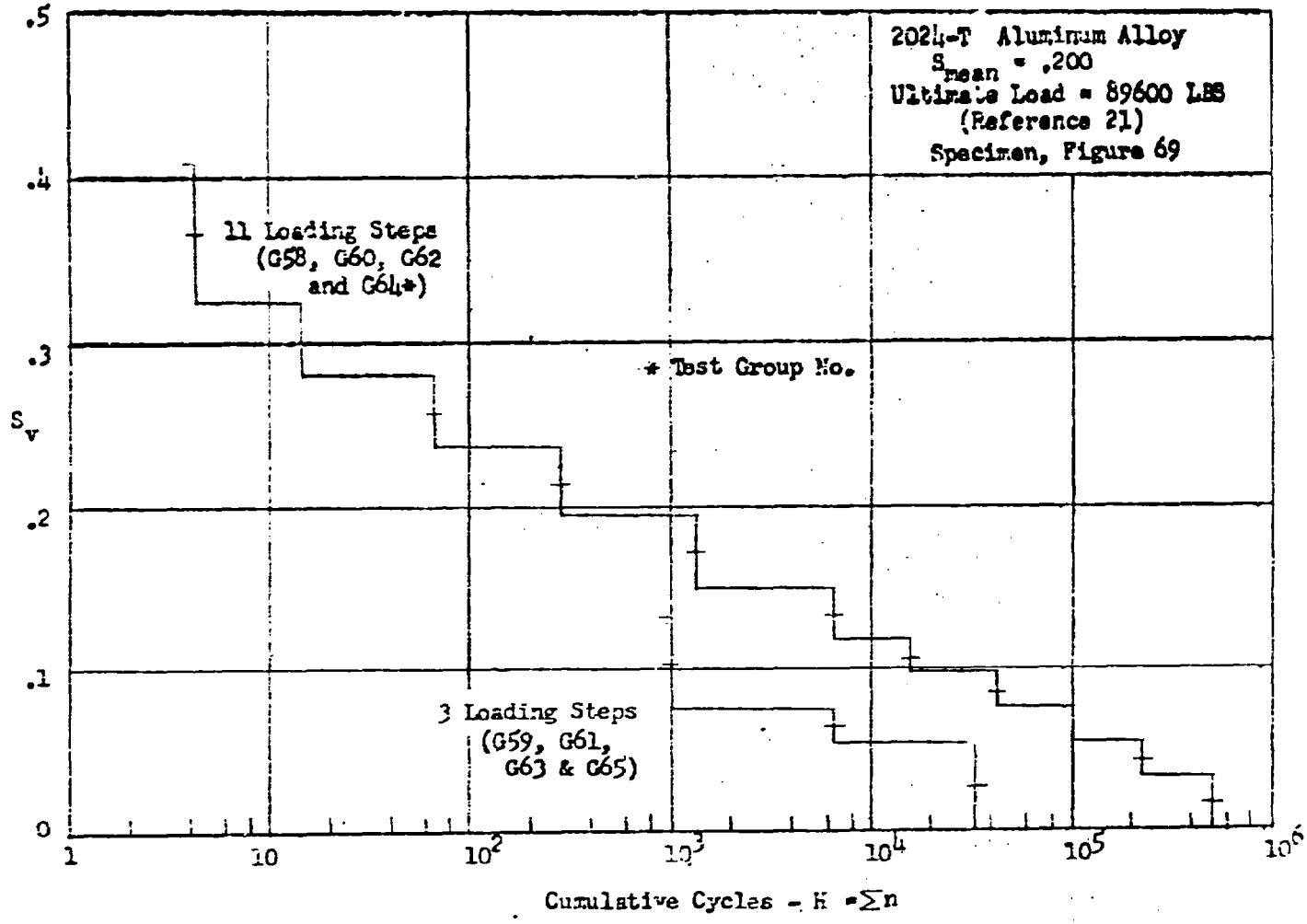



Figure 81 Unit Gust Loading Spectra for P51 Wing

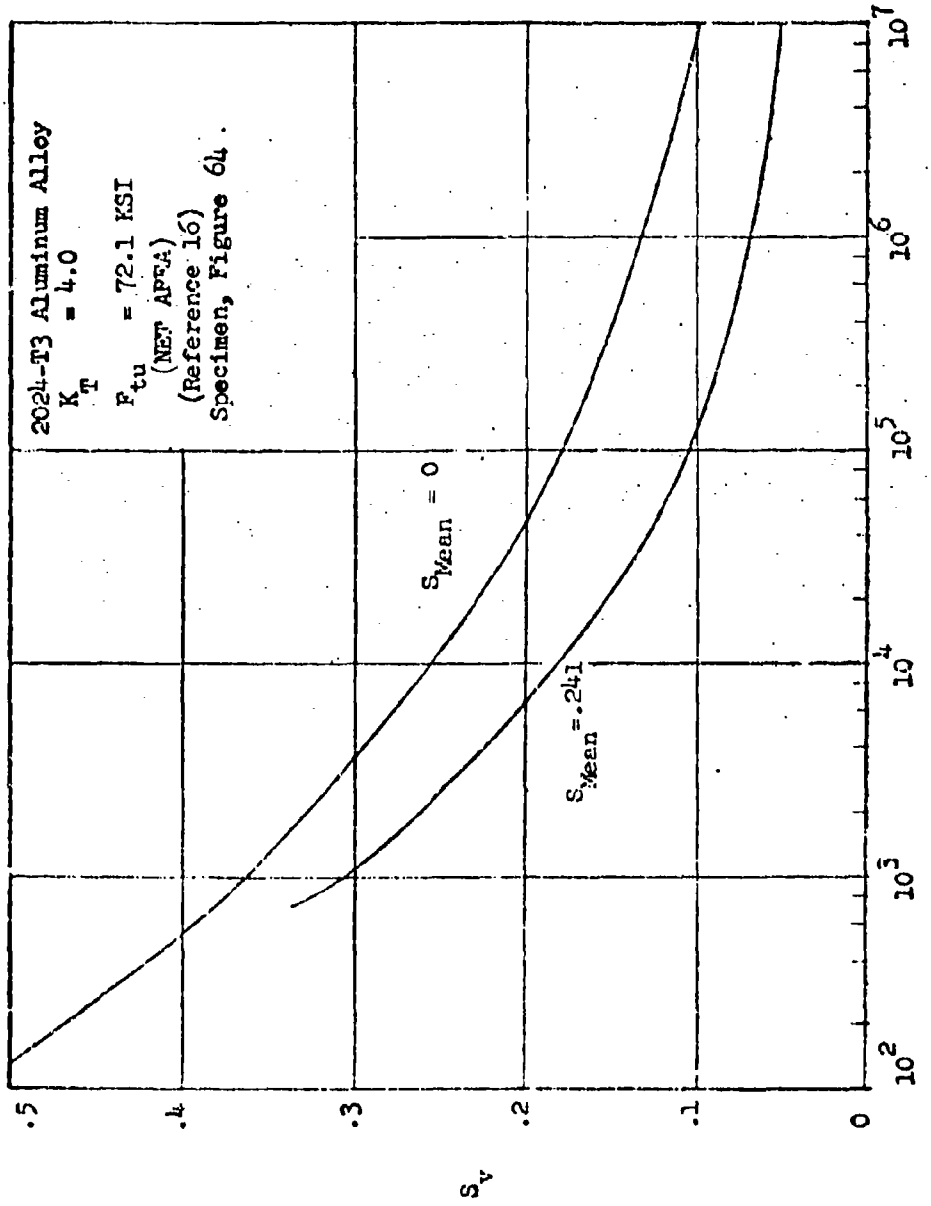



Figure 82 S-N Curves for Notched Sheet Specimens

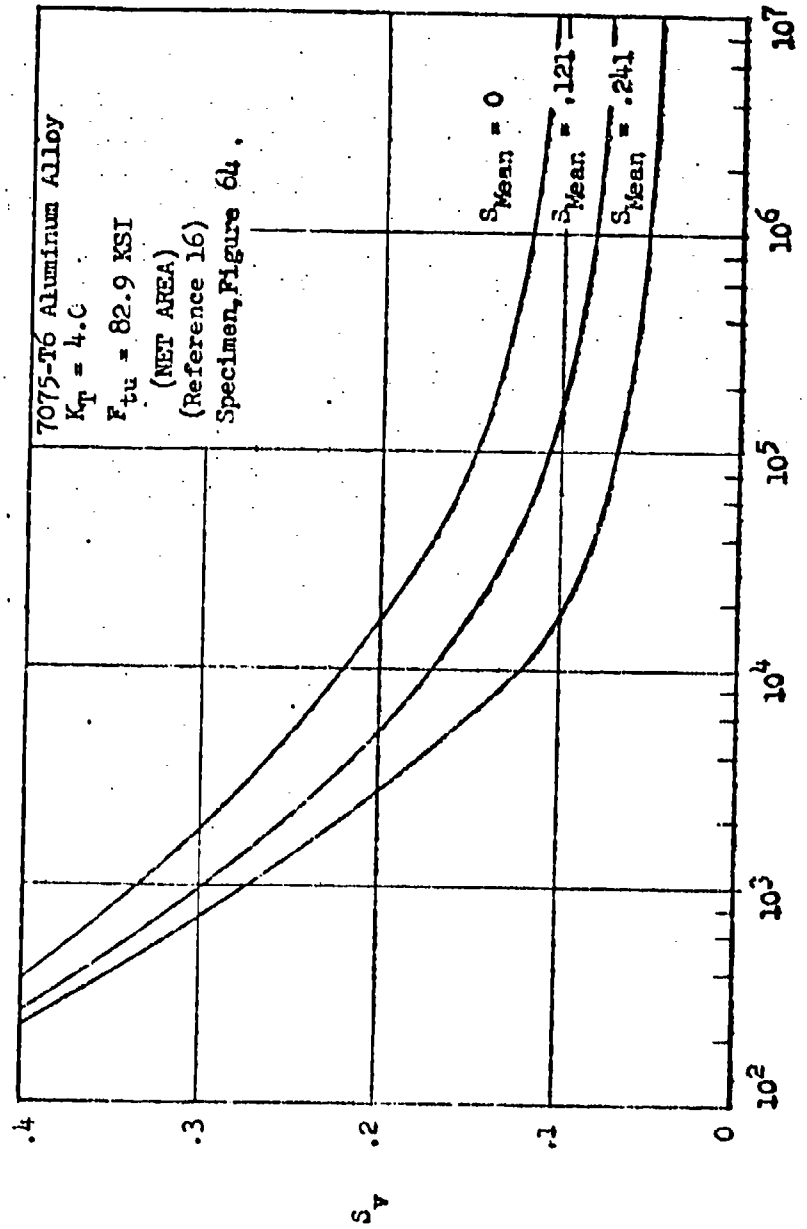



Figure 83 S-N Curves for Notched Sheet Specimens

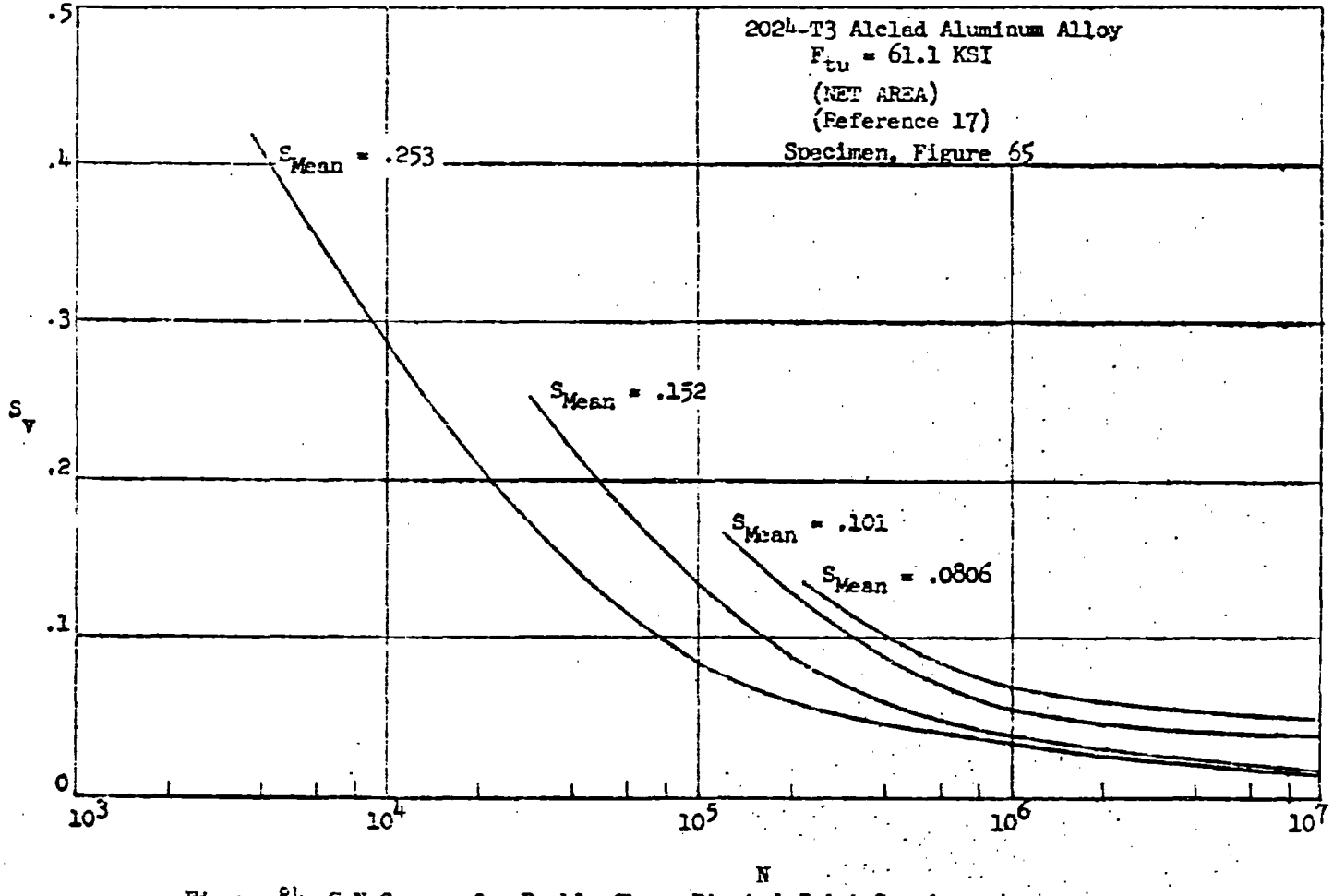



Figure 84 S-N Curves for Double Shear Riveted Joint Specimens

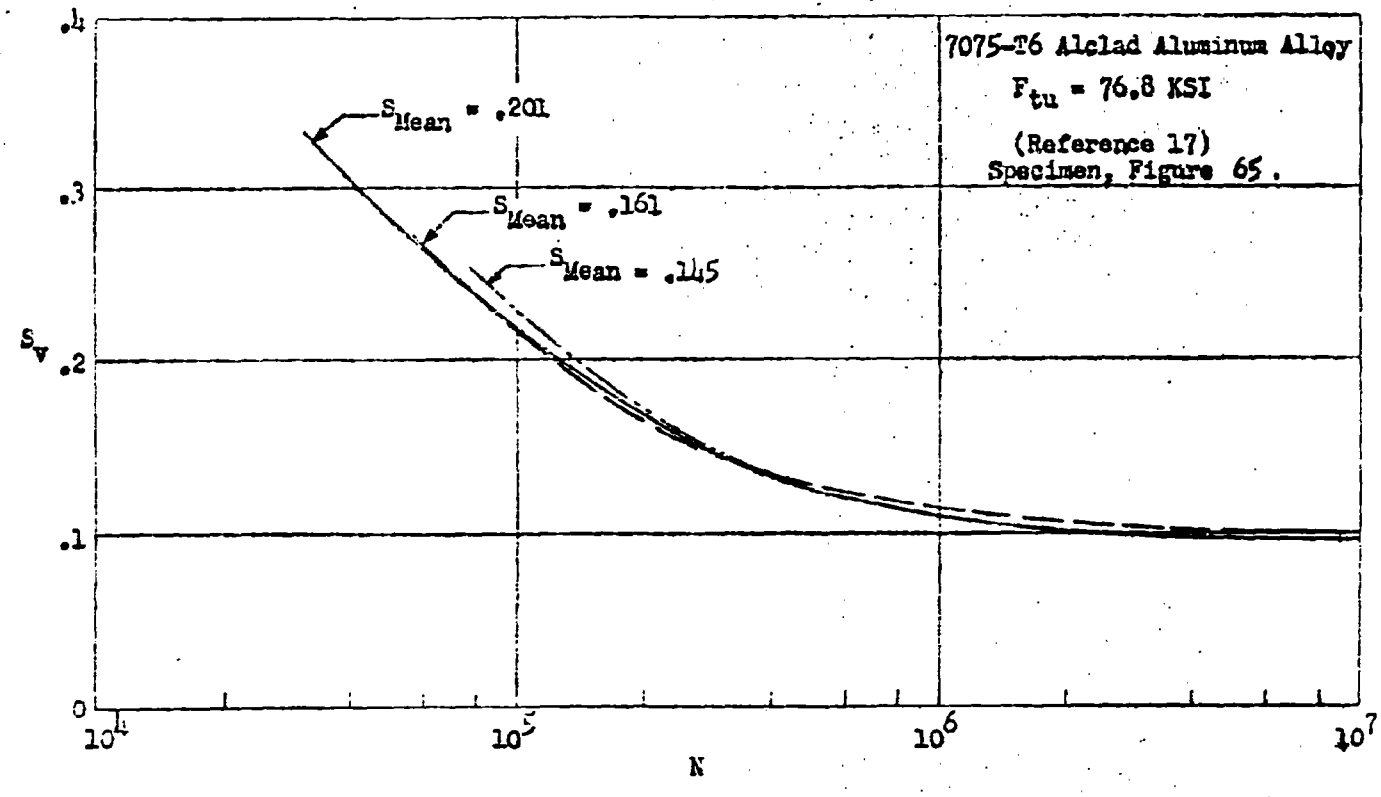



Figure 85 S-N Curves for Unnotched Sheet Specimens

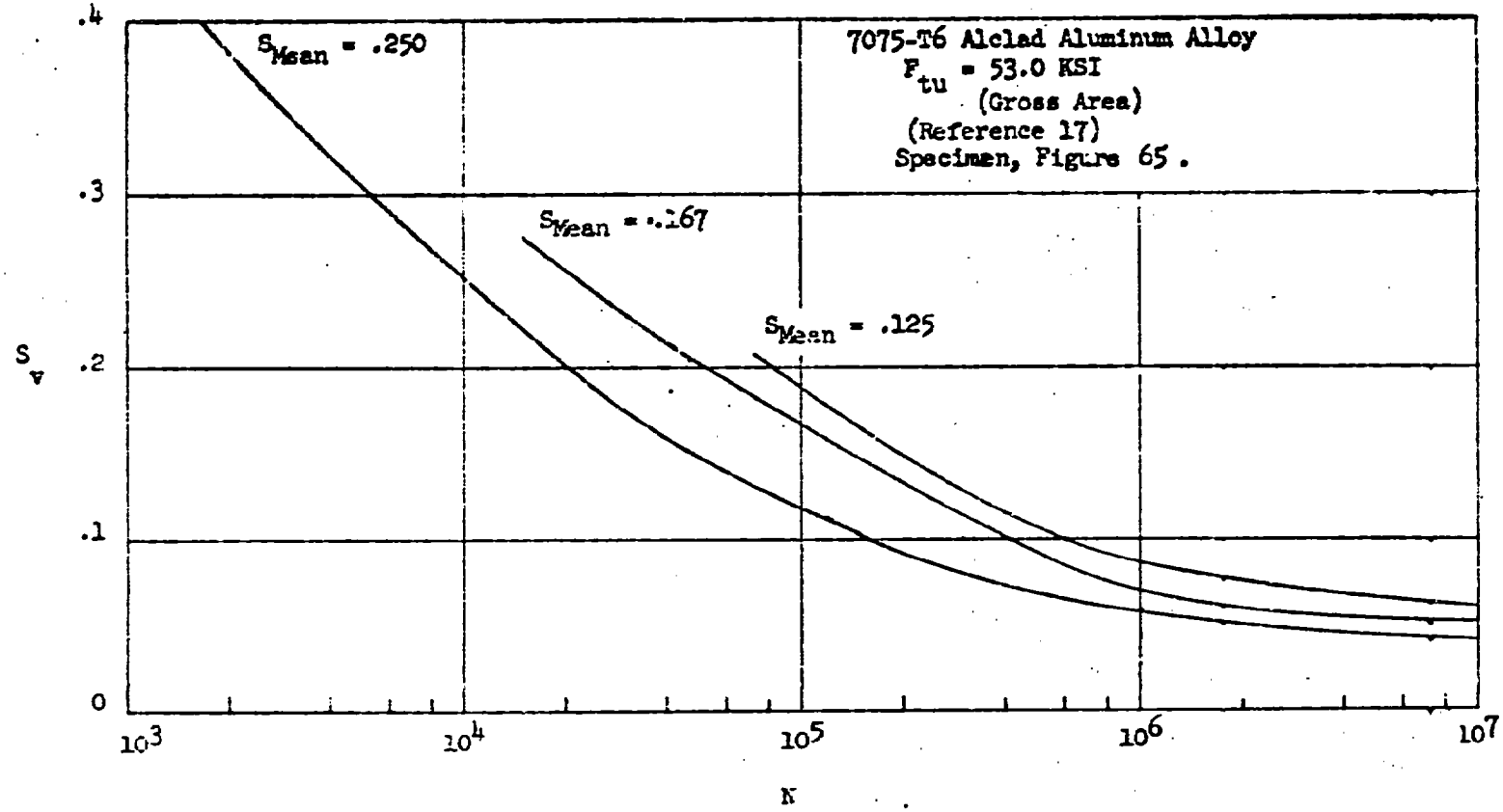



Figure 86 S-N Curves for Butt Joint Specimens

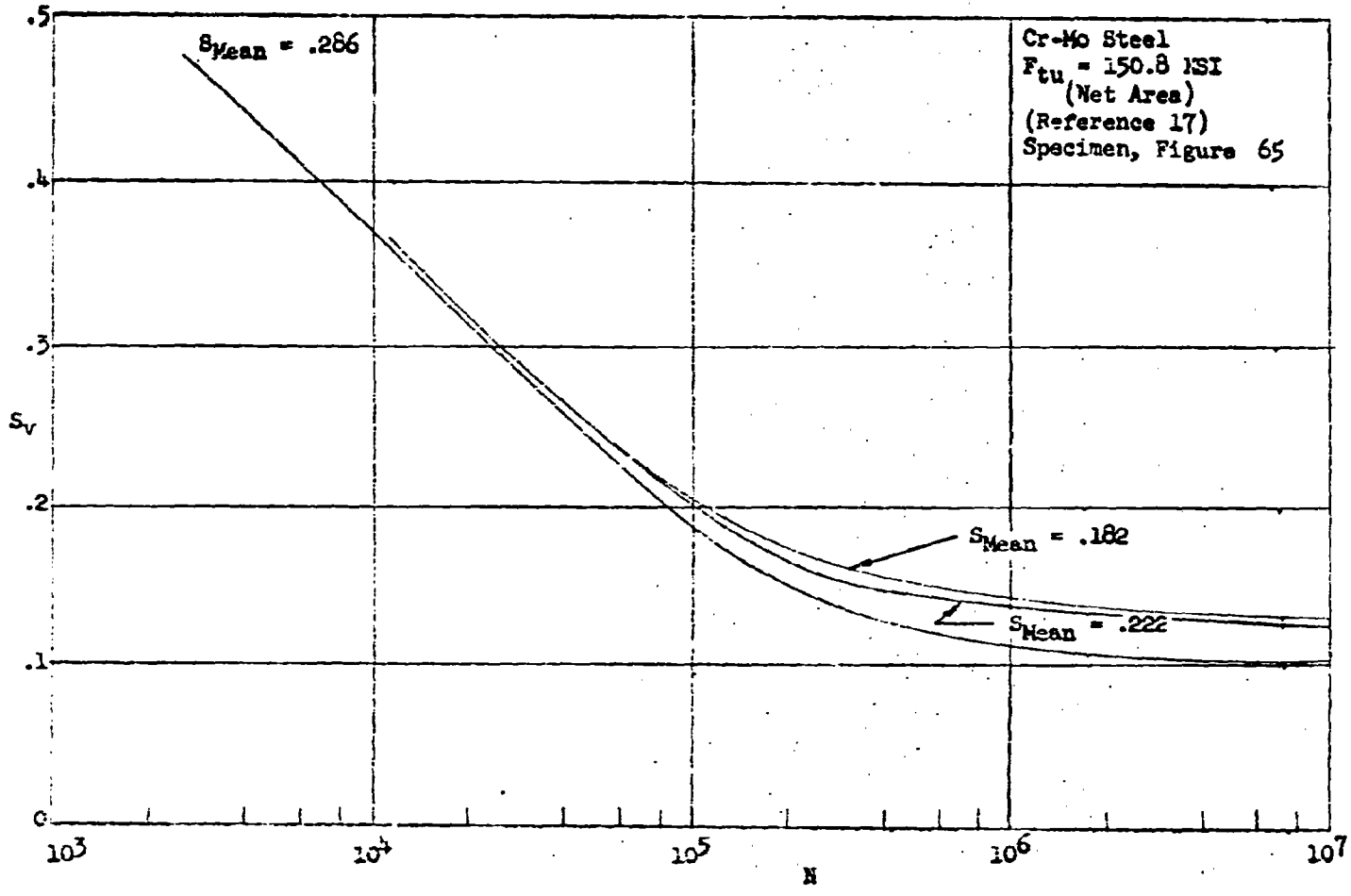



Figure 87 S-N Curves for Strip Specimens with Centrally Located Hole

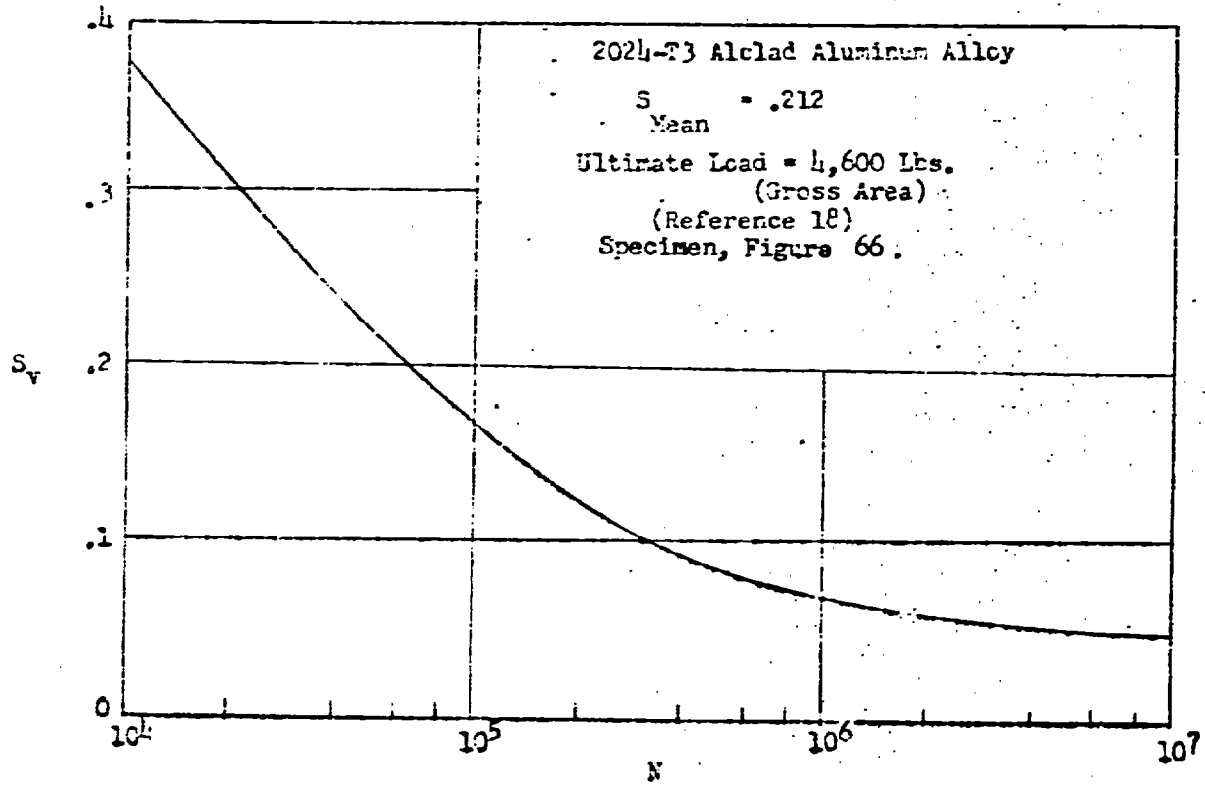



Figure 88 S-N Curve for Lap Joint Specimens with a Single Row of Flush Rivets

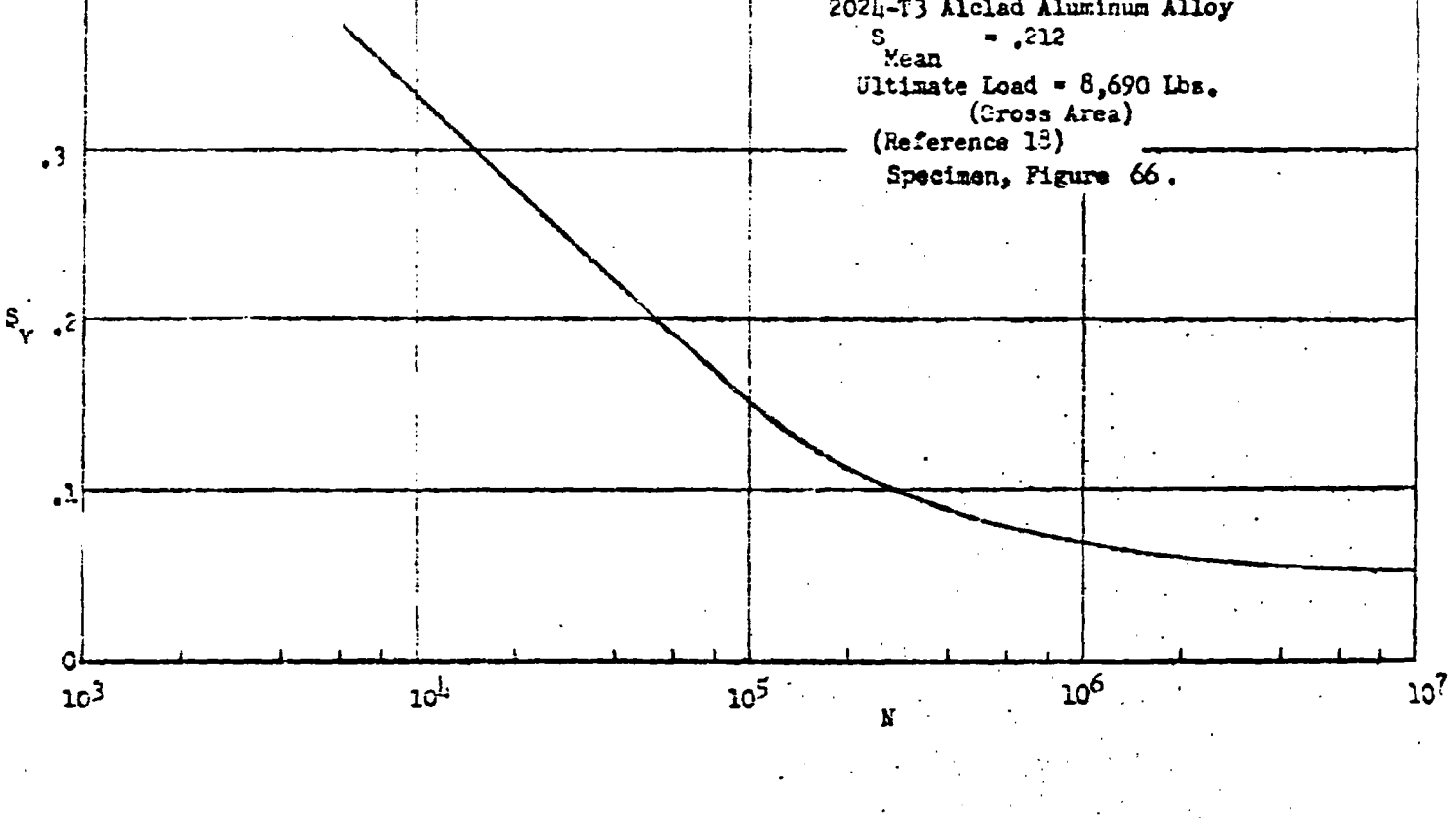



Figure 89 S-N Curve for Lap Joint Specimen with a Double Row of Flush Rivets

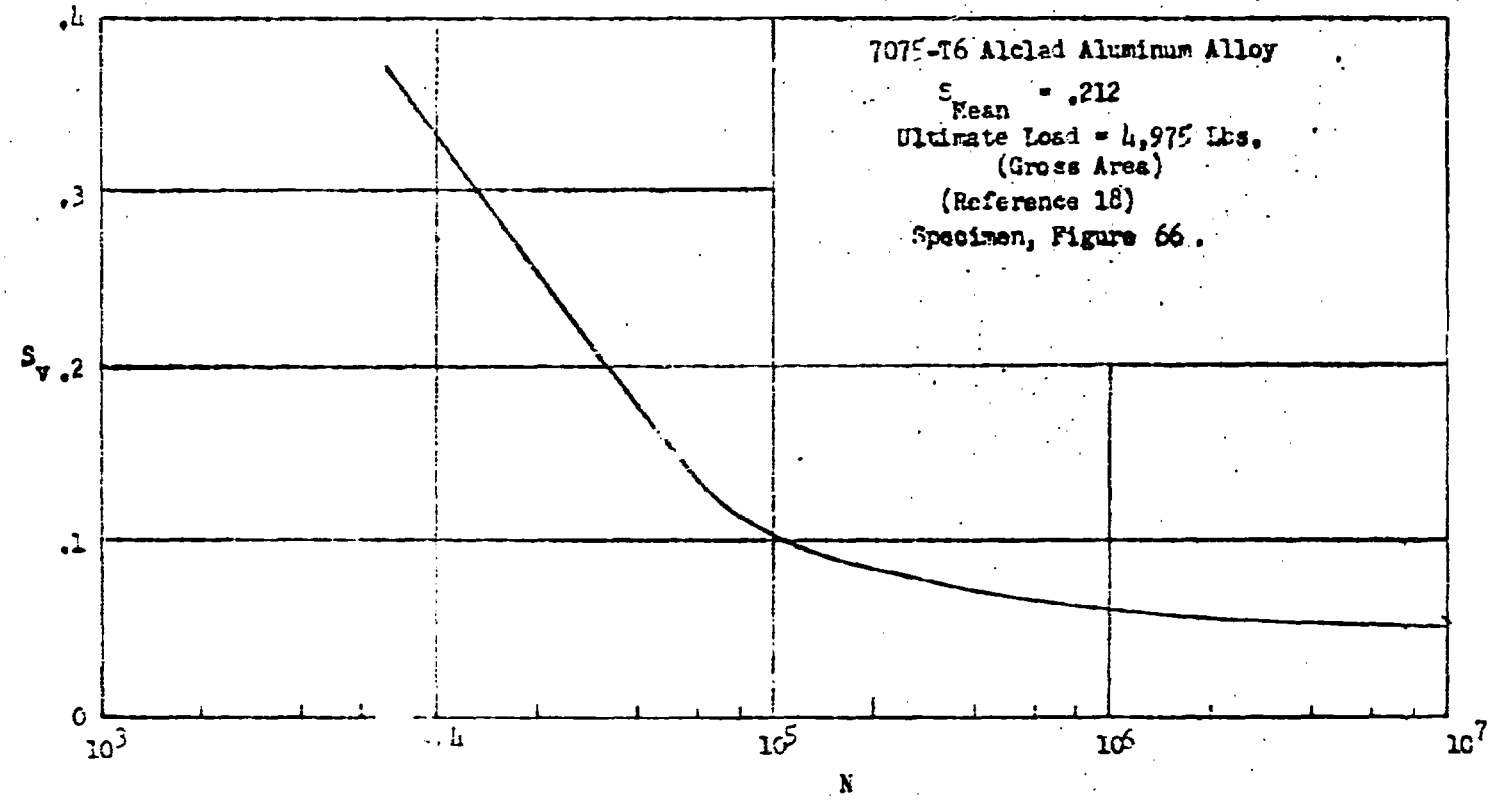



Figure 90 S-N Curve for Lap Joint Specimens with a Single Row of Flush Rivets

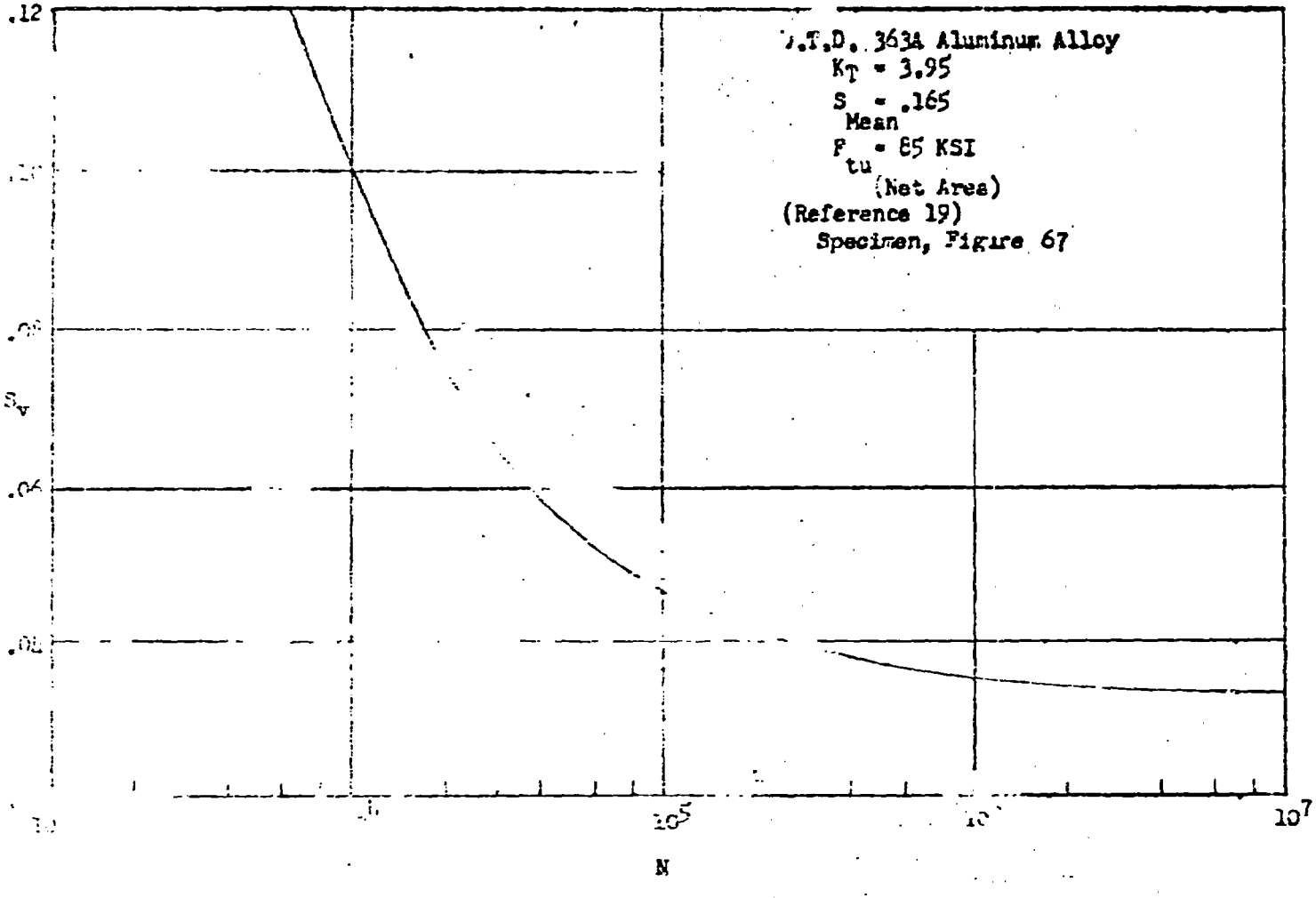
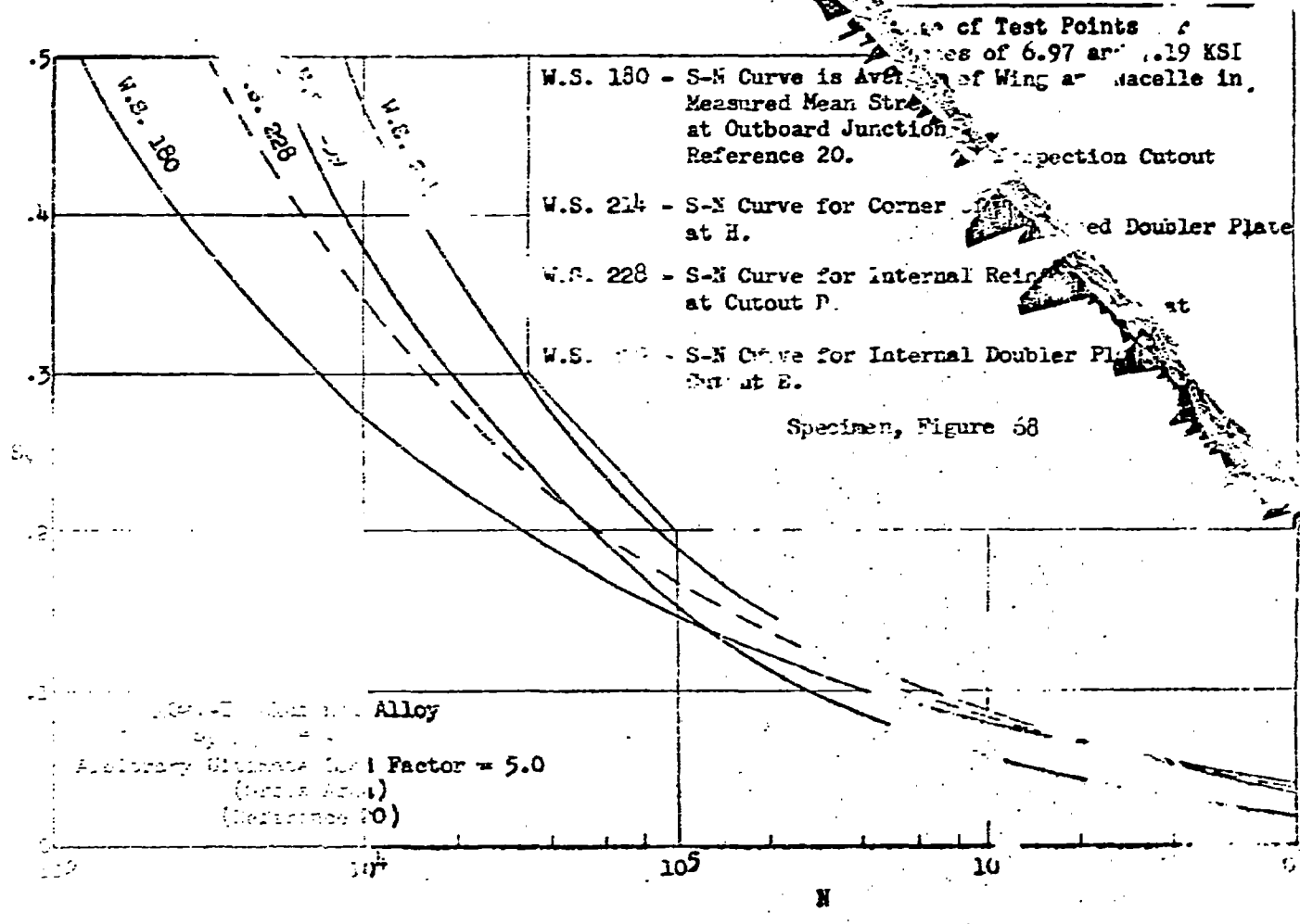



Figure [illegible] S-N Curve for Notched Plate Specimens




...of Test Points ...
...es of 6.97 ar... .19 KSI

W.S. 180 - S-N Curve is Ave... of Wing a... Nacelle in... Measured Mean Stre... at Outboard Junction... Reference 20. ...pection Cutout

W.S. 214 - S-N Curve for Corner ... ...ed Doubler Plate at H.

W.S. 228 - S-N Curve for Internal Rein... at Cutout P. ... at

W.S. ... - S-N Curve for Internal Doubler Pl... Cutout E.

Specimen, Figure 68

Figure ... S-N Curves for Wing Stations 180, 214, 228, and 239 of C...

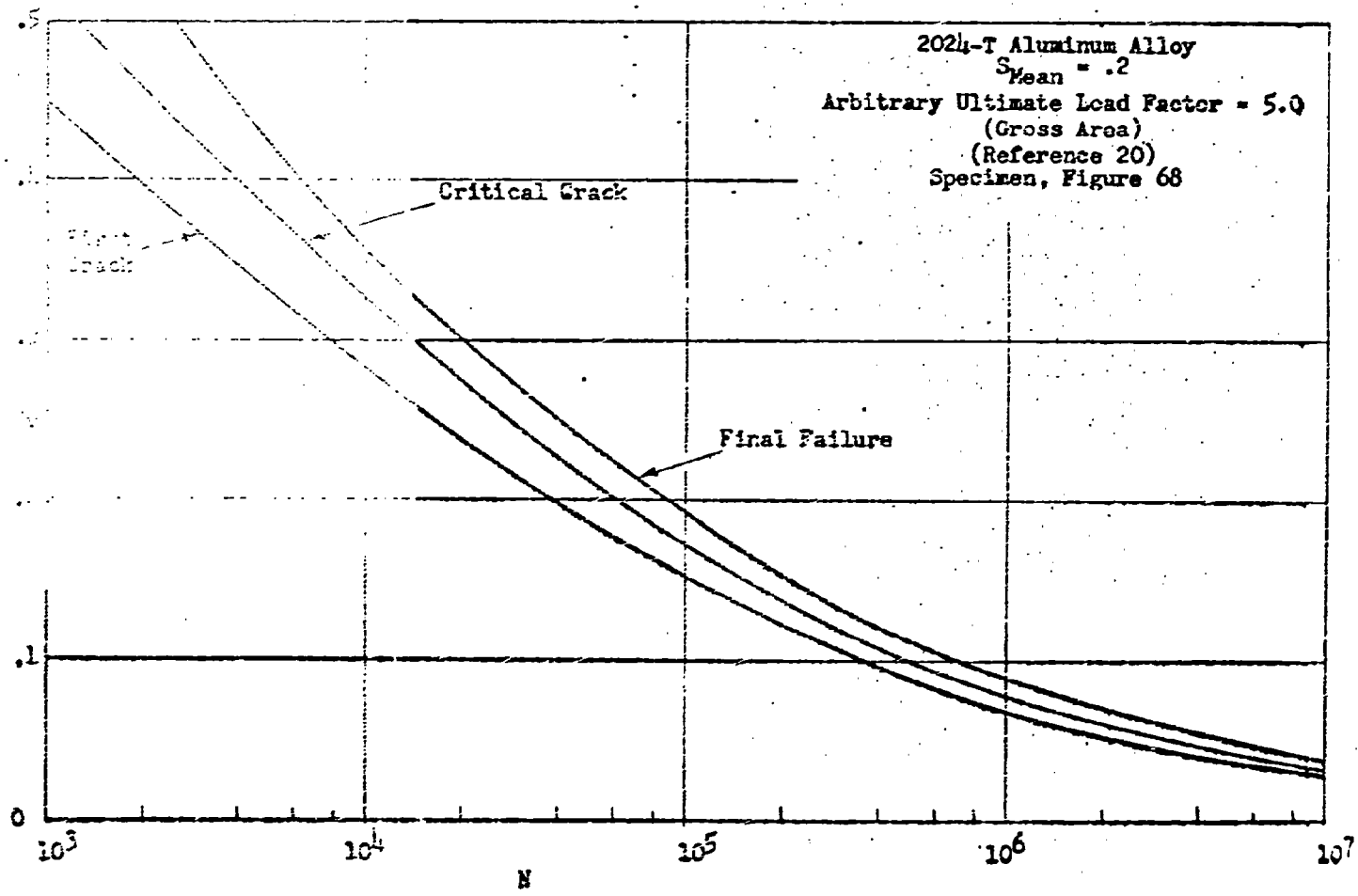



Figure 93 Average S-N Curves for Complete C-46 Wing

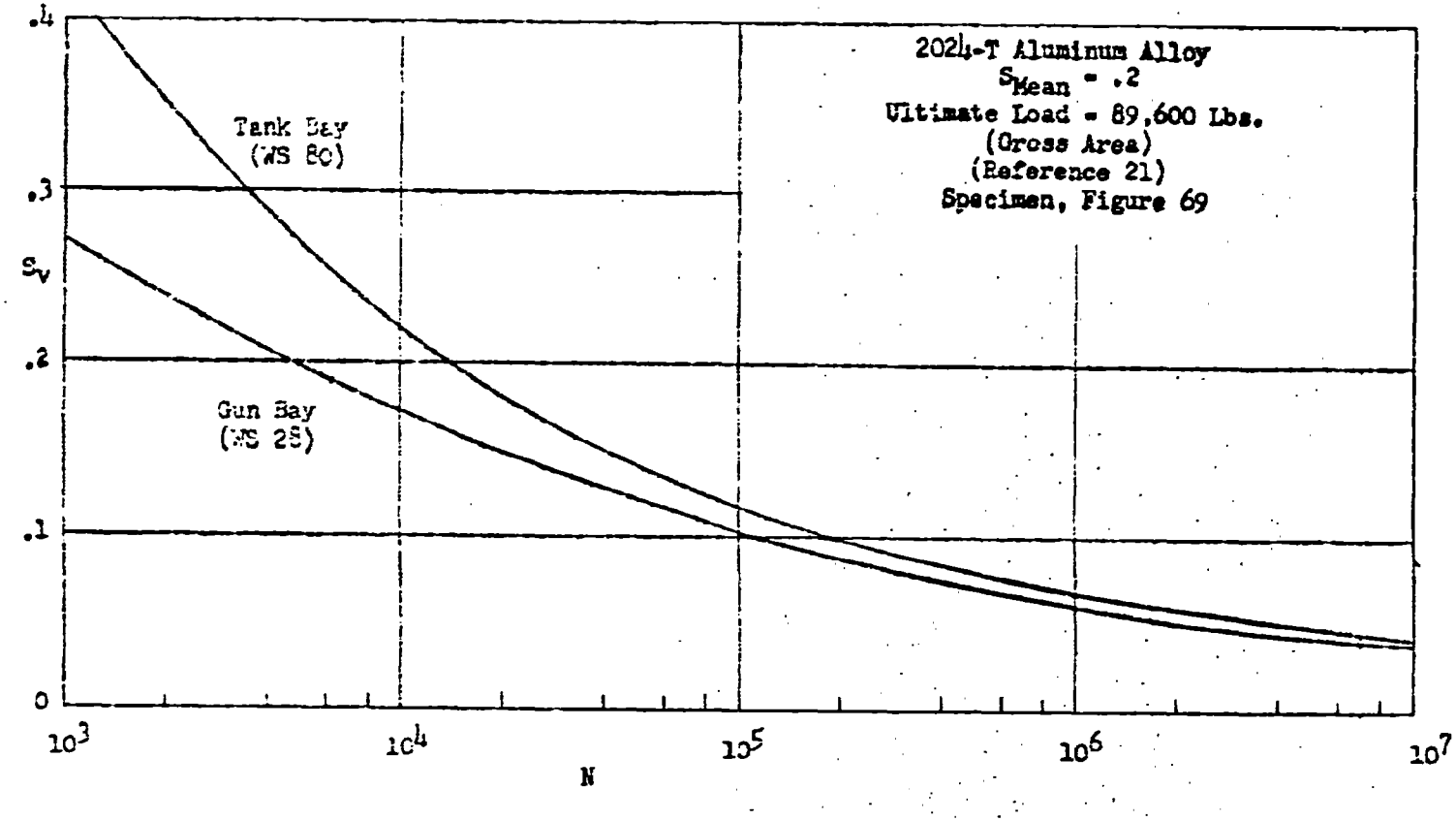



Figure 94 S-N Curves for Initial Failure of P51 Wing

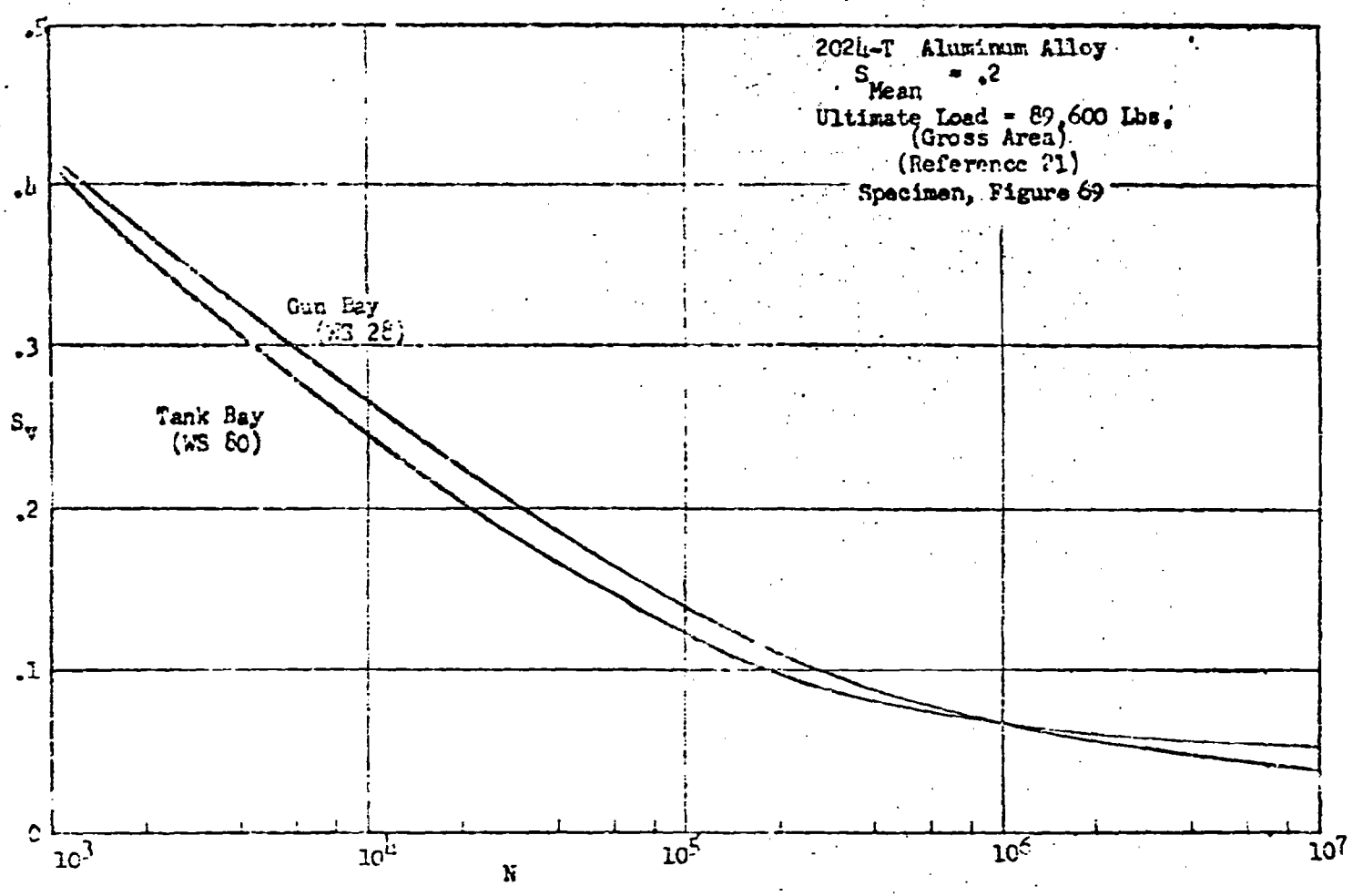



Figure 95 S-N Curves for Final Failure of P51 Wing

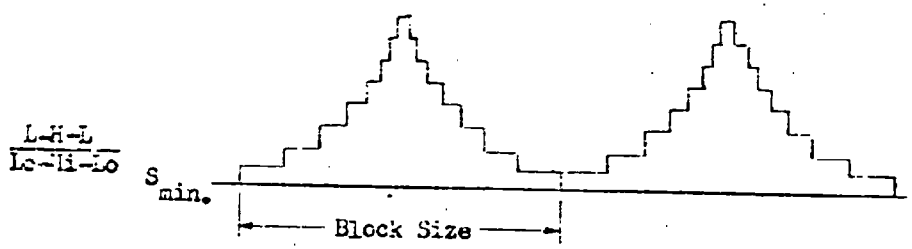



Figure 96 Schematic Diagram of Lo-Hi-Lo Maneuver Loading Sequence

TABLE 44

UNIT MANEUVER LOADING SPECTRA AND S-N DATA
FOR DOUBLE SHEAR RIVETED JOINTS
2024-T3 ALCLAD
(Reference 17)

$F_{tu}$ = 61.1 KSI (Net Area)

| Loading Step | $S_{max}$ | $S_v$ | n | N |
|---|---|---|---|---|
| | | $S_{min}$ = .0833 | | |
| 1 | .117 | .0169 | 3200 | - |
| 2 | .183 | .0499 | 1800 | 540000 |
| 3 | .250 | .0833 | 1100 | 170000 |
| 4 | .317 | .1169 | 620 | 77000 |
| 5 | .383 | .1499 | 350 | 42000 |
| 6 | .450 | .1833 | 200 | 24000 |
| 7 | .517 | .2169 | 120 | 14000 |
| 8 | .583 | .2499 | 68 | 9300 |
| 9 | .650 | .2833 | 39 | 6000 |
| | | (M1*) | $\Sigma$ 7497 | |
| | | $S_{min}$ = .0625 | | |
| 1 | .088 | .0128 | 3200 | - |
| 2 | .138 | .0378 | 1800 | 9000000 |
| 3 | .188 | .0628 | 1100 | 420000 |
| 4 | .238 | .0878 | 620 | 190000 |
| 5 | .288 | .1128 | 350 | 97000 |
| 6 | .338 | .1378 | 200 | 57000 |
| 7 | .388 | .1628 | 120 | 35000 |
| 8 | .438 | .1878 | 68 | 24000 |
| 9 | .488 | .2128 | 39 | 16000 |
| | | (M2) | $\Sigma$ 7497 | |
| | | $S_{min}$ = .050 | | |
| 1 | .070 | .010 | 3200 | - |
| 2 | .110 | .030 | 1800 | - |
| 3 | .150 | .050 | 1100 | 1300000 |
| 4 | .190 | .070 | 620 | 400000 |
| 5 | .230 | .090 | 350 | 200000 |
| 6 | .270 | .110 | 200 | 120000 |
| 7 | .310 | .130 | 120 | 76000 |
| 8 | .350 | .150 | 68 | 50000 |
| 9 | .390 | .170 | 39 | 35000 |
| | | (M3) | $\Sigma$ 7497 | |

* Test Group No.

TABLE 45

UNIT MANEUVER LOADING SPECTRA AND S-N DATA FOR UNNOTCHED SHEET
7075-T6 ALCLAD
(Reference 17)

$F_{tu}$ = 76.8 KSI (Net Area)

| Loading Step | $S_{max}$ | $S_v$ | n | N | $S_{max}$ | $S_v$ | n | N |
|---|---|---|---|---|---|---|---|---|
| | $S_{min}$ = .125 | | | | $S_{min}$ = .100 | | | |
| 1 | .175 | .025 | 3200 | - | .140 | .020 | 3200 | - |
| 2 | .275 | .075 | 1800 | - | .220 | .060 | 1800 | - |
| 3 | .375 | .125 | 1100 | 470000 | .300 | .100 | 1100 | 6000000 |
| 4 | .475 | .175 | 620 | 140000 | .380 | .140 | 620 | 300000 |
| 5 | .575 | .225 | 350 | 71000 | .460 | .180 | 350 | 140000 |
| 6 | .675 | .275 | 200 | 40000 | .540 | .220 | 200 | 80000 |
| 7 | .775 | .325 | 120 | 22000 | .620 | .260 | 120 | 52000 |
| 8 | .875 | .375 | 68 | 9000 | .700 | .300 | 68 | 34000 |
| 9 | .975 | .425 | 39 | 1300 | .780 | .340 | 39 | 20000 |
| | | (M4*) | $\Sigma$ 7497 | | | (M5) | $\Sigma$ 7497 | |
| | $S_{min}$ = .0833 | | | | $S_{min}$ = .0625 | | | |
| 1 | .117 | .0168 | 3200 | - | .088 | .0128 | 3200 | - |
| 2 | .183 | .0498 | 1800 | - | .138 | .0378 | 1800 | - |
| 3 | .250 | .0834 | 1100 | - | .188 | .0628 | 1100 | - |
| 4 | .317 | .1168 | 620 | 680000 | .238 | .0878 | 620 | - |
| 5 | .383 | .1498 | 350 | 230000 | .288 | .1128 | 350 | 850000 |
| 6 | .450 | .1834 | 200 | 135000 | .338 | .1378 | 200 | 340000 |
| 7 | .517 | .2168 | 120 | 86000 | .388 | .1628 | 120 | 200000 |
| 8 | .583 | .2498 | 68 | 58000 | .438 | .1878 | 68 | 130000 |
| 9 | .650 | .2834 | 39 | 41000 | .488 | .2128 | 39 | 92000 |
| | | (M6) | $\Sigma$ 7497 | | | (M7) | $\Sigma$ 7497 | |

*Test Group No.

TABLE 46

UNIT MANEUVER LOADING SPECTRA AND S-N DATA FOR BUTT JOINTS
7075-T6 ALCLAD
(Reference 17)

$F_{tu}$ = 53.0 KSI (Gross Area)

| Loading Step | $S_{max}$ | $S_v$ | n | N |
|---|---|---|---|---|
| | | $S_{min}$ = .100 | | |
| 1 | .14 | .02 | 3200 | - |
| 2 | .22 | .06 | 1800 | 2700000 |
| 3 | .30 | .10 | 1100 | 300000 |
| 4 | .38 | .14 | 620 | 71000 |
| 5 | .46 | .18 | 350 | 20000 |
| 6 | .54 | .22 | 200 | 8600 |
| 7 | .62 | .26 | 120 | 4200 |
| 8 | .70 | .30 | 68 | 2000 |
| 9 | .78 | .34 | 39 | 900 |
| | | (48*) | $\Sigma$ 7497 | |
| | | $S_{min}$ = .0833 | | |
| 1 | .117 | .0168 | 3200 | - |
| 2 | .183 | .0498 | 1800 | - |
| 3 | .250 | .0833 | 1100 | 700000 |
| 4 | .317 | .1168 | 620 | 190000 |
| 5 | .383 | .1498 | 350 | 62000 |
| 6 | .450 | .1833 | 200 | 21000 |
| 7 | .517 | .2168 | 120 | 10000 |
| 8 | .583 | .2498 | 68 | 5500 |
| 9 | .650 | .2833 | 39 | 3100 |
| | | (49) | $\Sigma$ 7497 | |
| | | $S_{min}$ = .0625 | | |
| 1 | .088 | .0127 | 3200 | - |
| 2 | .138 | .0377 | 1800 | - |
| 3 | .188 | .0627 | 1100 | - |
| 4 | .238 | .0877 | 620 | 750000 |
| 5 | .288 | .1127 | 350 | 270000 |
| 6 | .338 | .1377 | 200 | 120000 |
| 7 | .388 | .1627 | 120 | 50000 |
| 8 | .438 | .1877 | 68 | 23000 |
| 9 | .488 | .2127 | 39 | 12500 |
| | | (410) | $\Sigma$ 7497 | |

* Test Group No.

TABLE 47

UNIT MANEUVER LOADING SPECTRA AND S-N DATA
FOR STRIPS WITH CENTRALLY LOCATED HOLE
Cr-Mo STEEL
(Reference 17)

$F_{tu}$ = 150.8 KSI (Net Area)

| Loading Step | $S_{max}$ | $S_v$ | n | N |
|---|---|---|---|---|
| | | $S_{min}$ = .111 | | |
| 1 | .156 | .0225 | 3200 | - |
| 2 | .244 | .0665 | 1800 | - |
| 3 | .333 | .1110 | 1100 | - |
| 4 | .422 | .1555 | 620 | 220000 |
| 5 | .511 | .2000 | 350 | 84000 |
| 6 | .600 | .2445 | 200 | 40000 |
| 7 | .689 | .2890 | 120 | 21000 |
| 8 | .778 | .3335 | 68 | 10000 |
| 9 | .867 | .3780 | 39 | 3800 |
| | | (M11*) | $\Sigma$ 7497 | |
| | | $S_{min}$ = .100 | | |
| 1 | .140 | .020 | 3200 | - |
| 2 | .220 | .060 | 1800 | - |
| 3 | .300 | .100 | 1100 | - |
| 4 | .380 | .140 | 620 | 400000 |
| 5 | .460 | .180 | 350 | 130000 |
| 6 | .540 | .220 | 200 | 59000 |
| 7 | .620 | .260 | 120 | 32000 |
| 8 | .700 | .300 | 68 | 17500 |
| 9 | .780 | .340 | 39 | 9000 |
| | | (M12) | $\Sigma$ 7497 | |
| | | $S_{min}$ = .0833 | | |
| 1 | .117 | .0168 | 3200 | - |
| 2 | .183 | .0498 | 1800 | - |
| 3 | .250 | .0834 | 1100 | - |
| 4 | .317 | .1168 | 620 | - |
| 5 | .383 | .1498 | 350 | 280000 |
| 6 | .450 | .1834 | 200 | 120000 |
| 7 | .517 | .2168 | 120 | 63000 |
| 8 | .583 | .2498 | 68 | 38000 |
| 9 | .650 | .2834 | 39 | 23000 |
| | | (M13) | $\Sigma$ 7497 | |

* Test Group No.

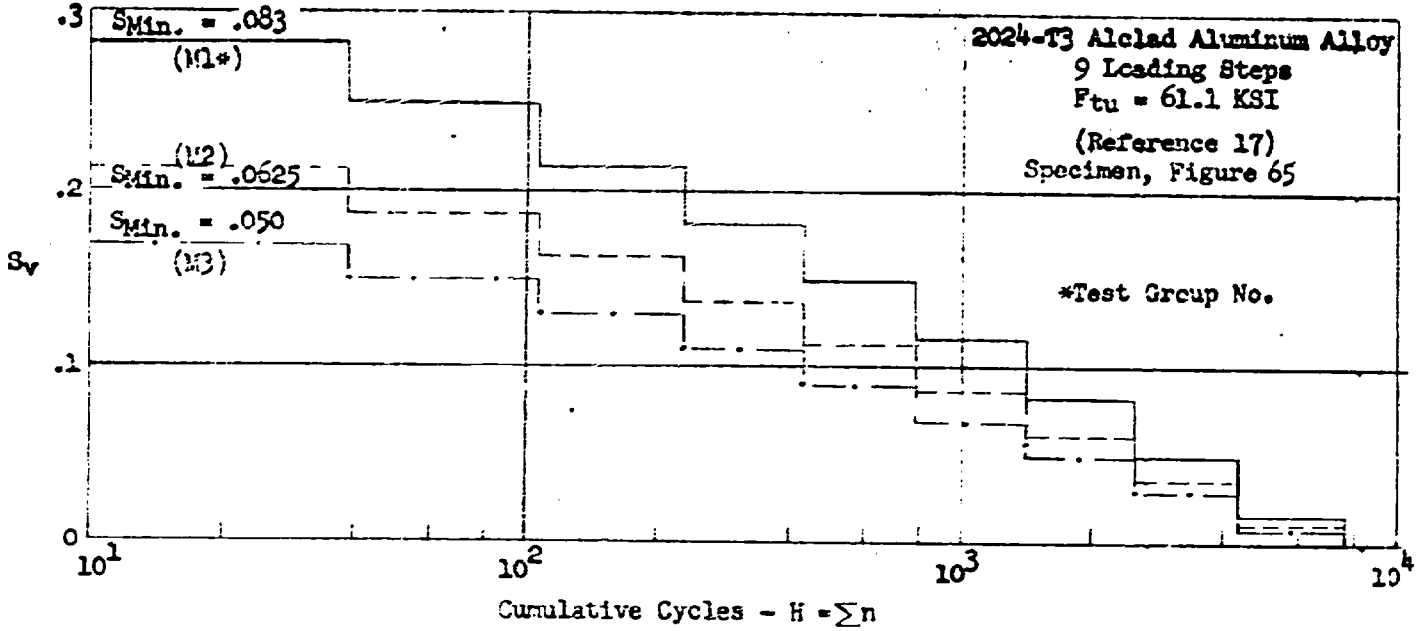



Figure 97 Unit Maneuver Loading Spectra for Double Shear Riveted Joint Specimens.

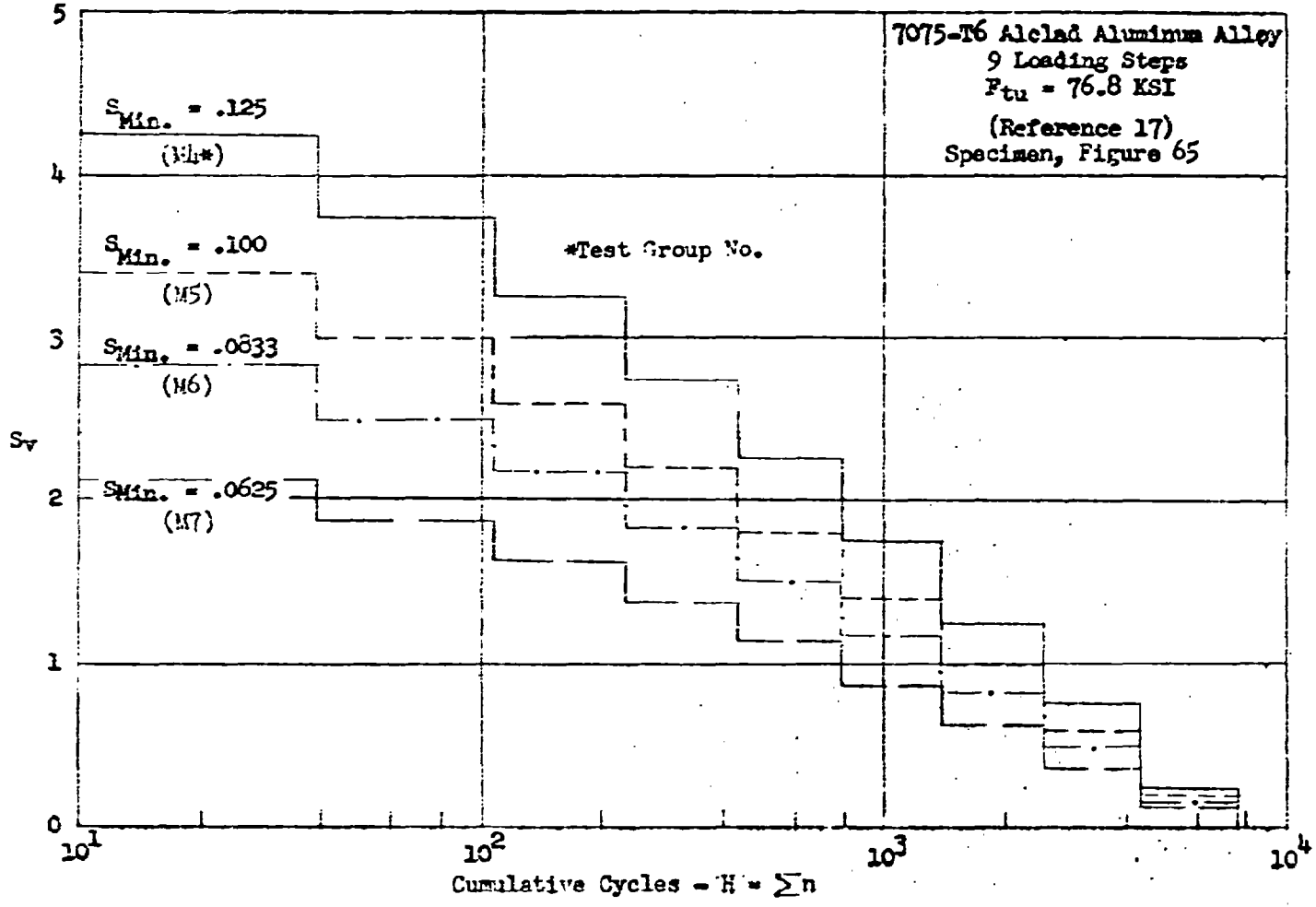



Figure 98 Unit Maneuver Loading Spectra for Unnotched Sheet Specimens.

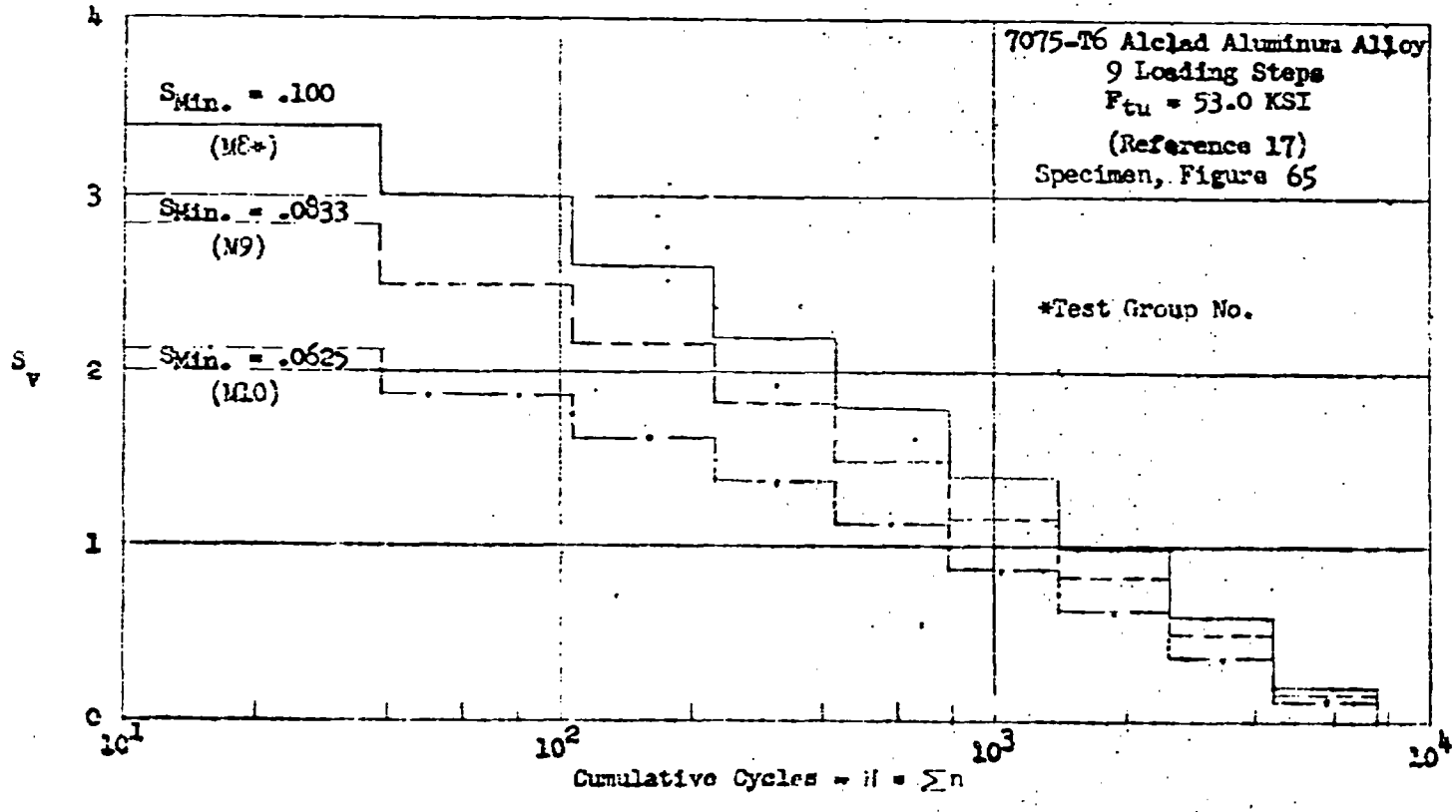



Figure 99 Unit Maneuver Loading Spectra for Butt Joint Specimens.

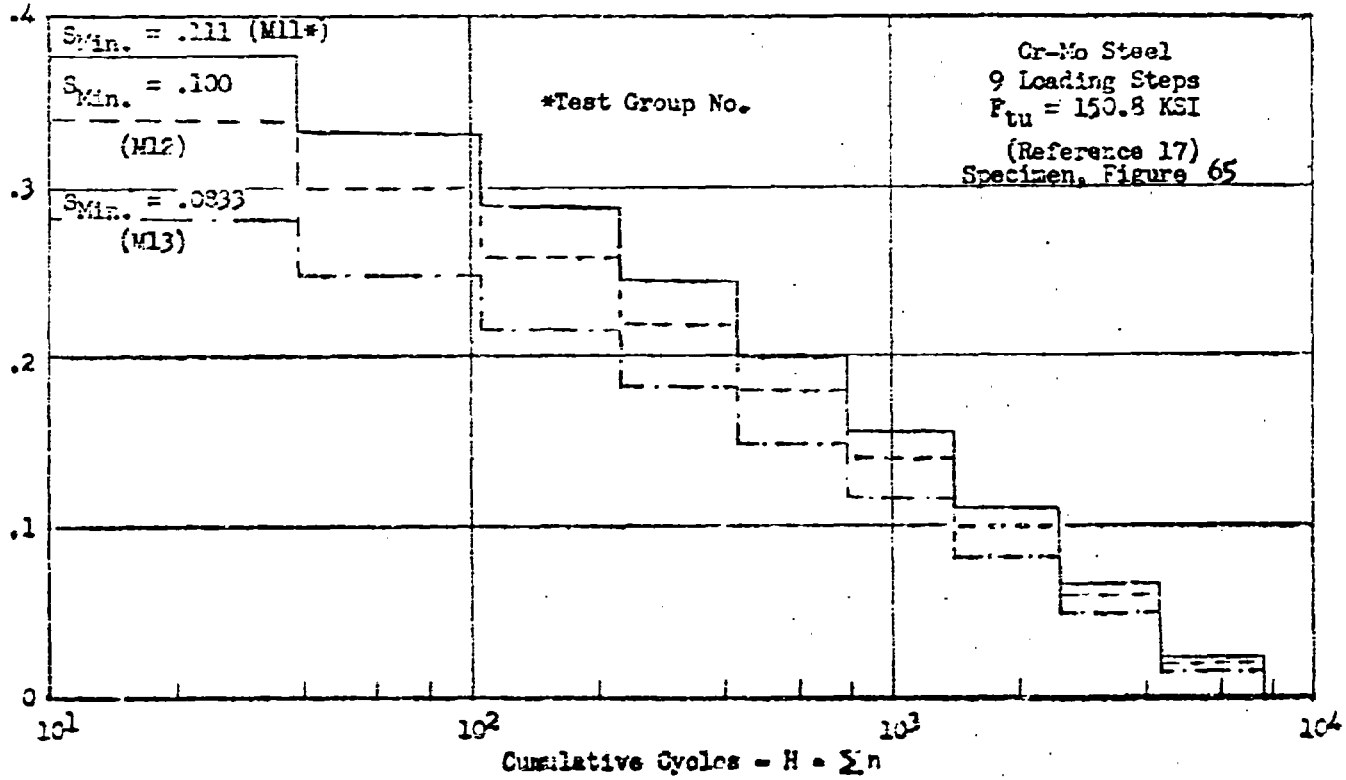



Figure 100 Unit Maneuver Loading Spectra for Strip Specimens with a Centrally Located Hole.

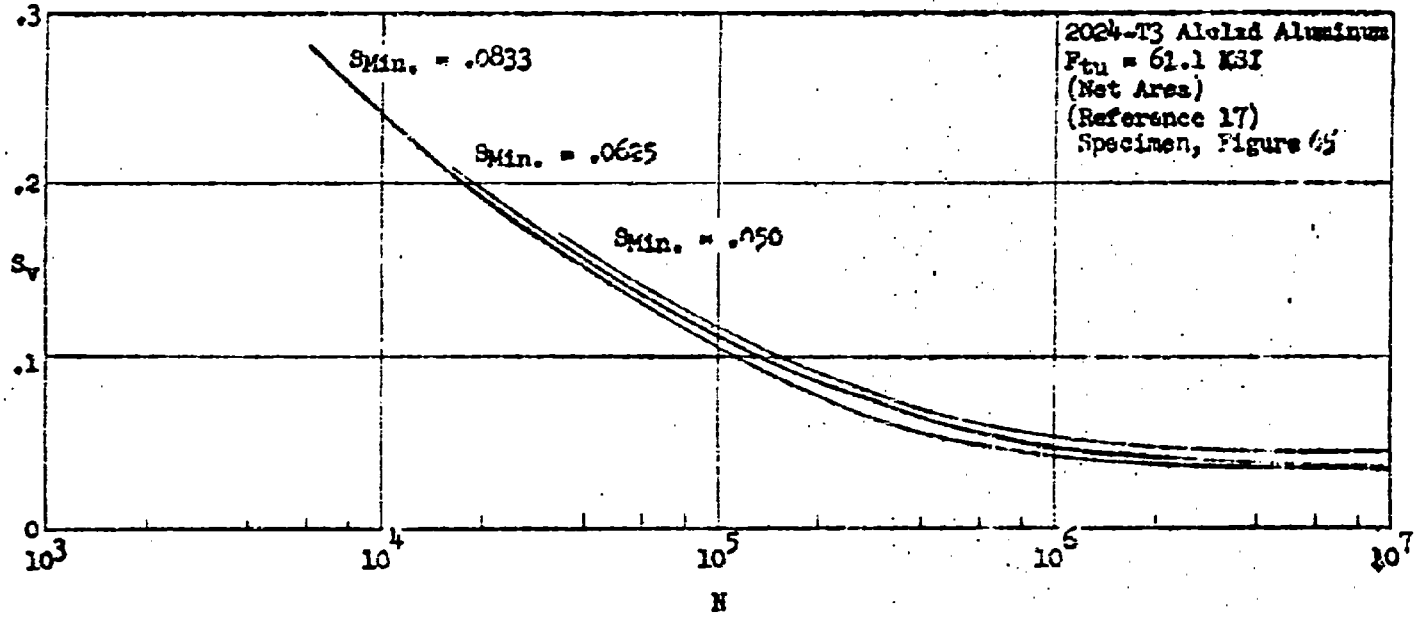



Figure 10L S-N Curves for Double Shear Riveted Joint Specimens. Constant Minimum Stress. (For Maneuver Type Loading)

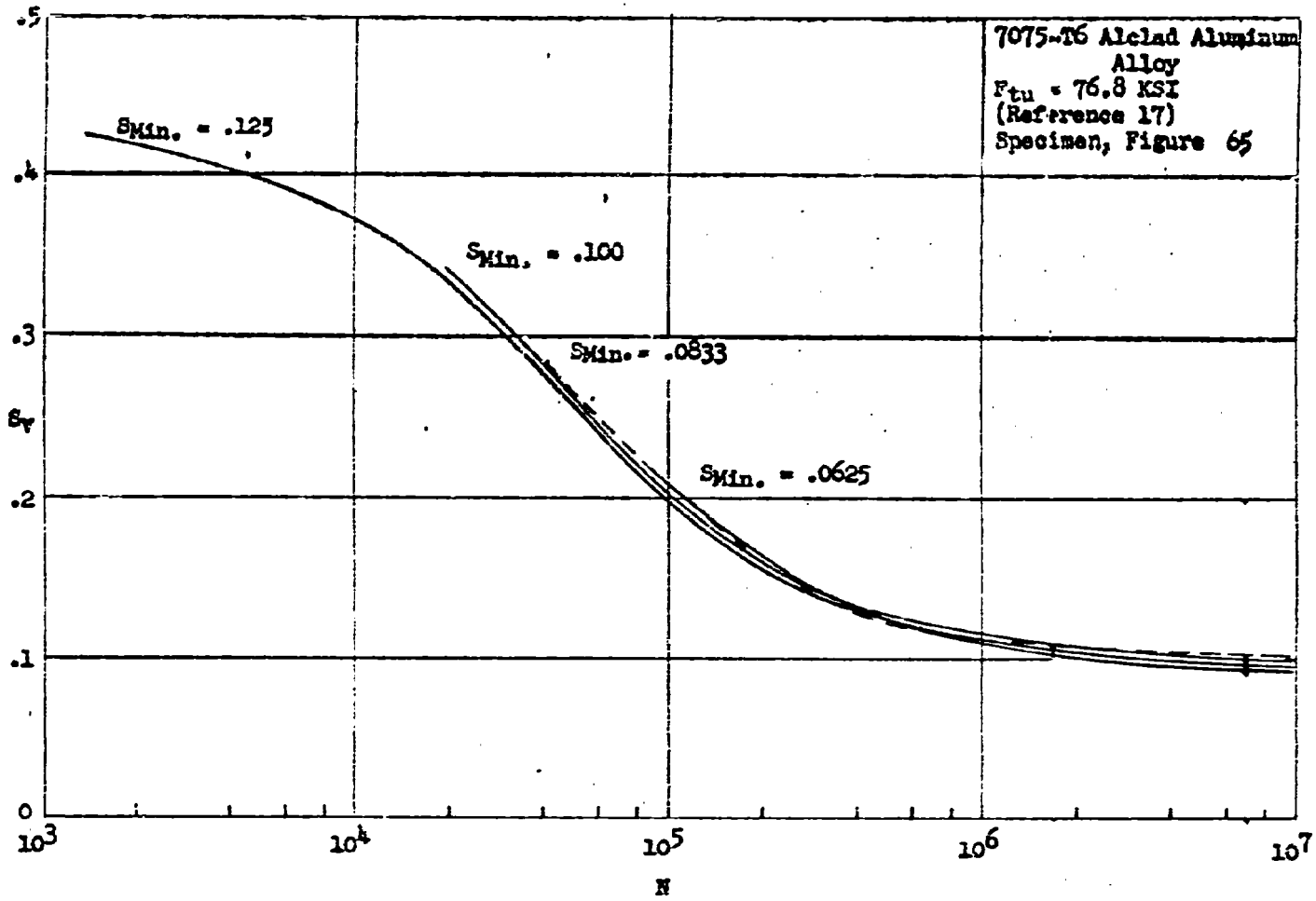



Figure 102 S-N Curves for Unnotched Sheet Specimens.
Constant Minimum Stress. (For Maneuver Type Loading)

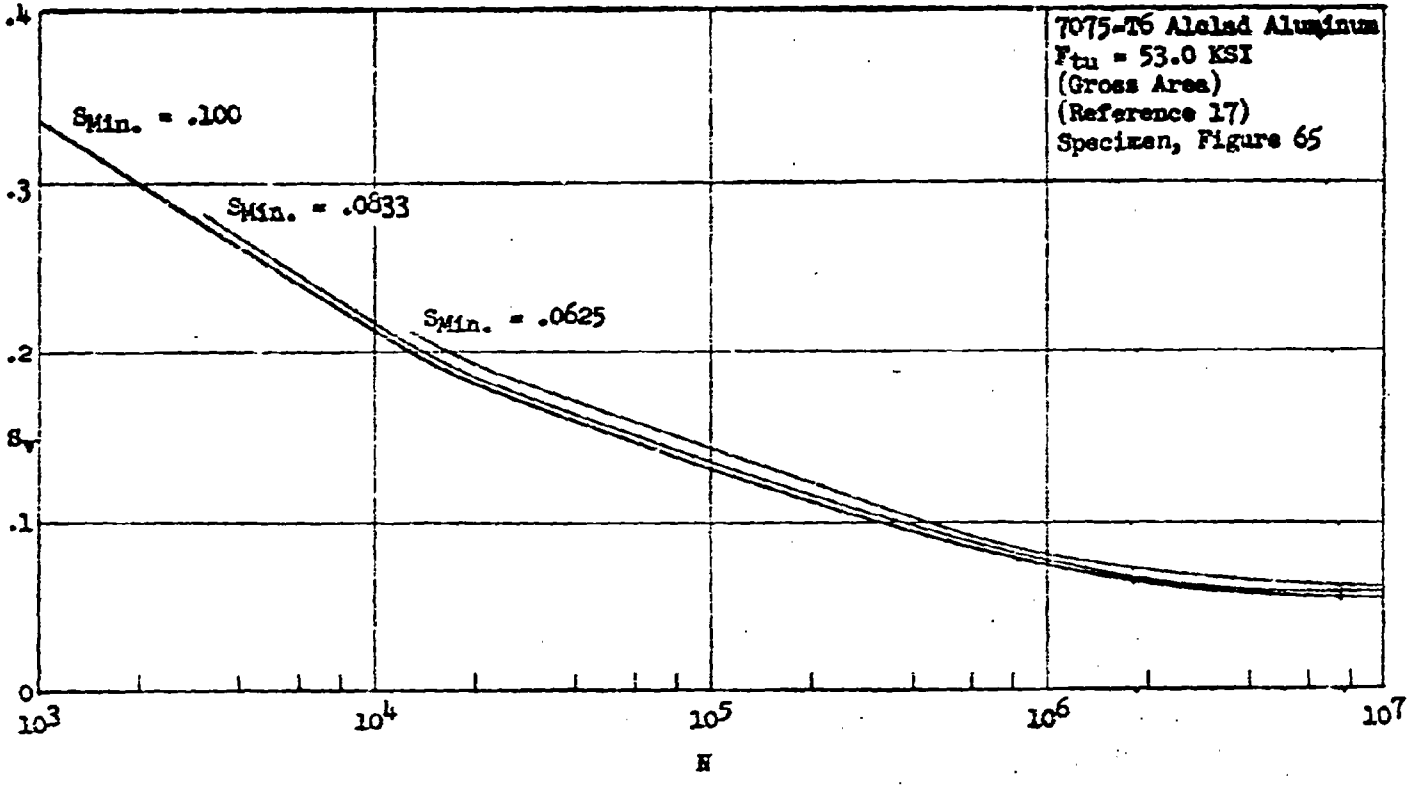



Figure 103 S-N Curves for Butt Joint Specimens.
Constant Minimum Stress. (For Maneuver Type Loading)

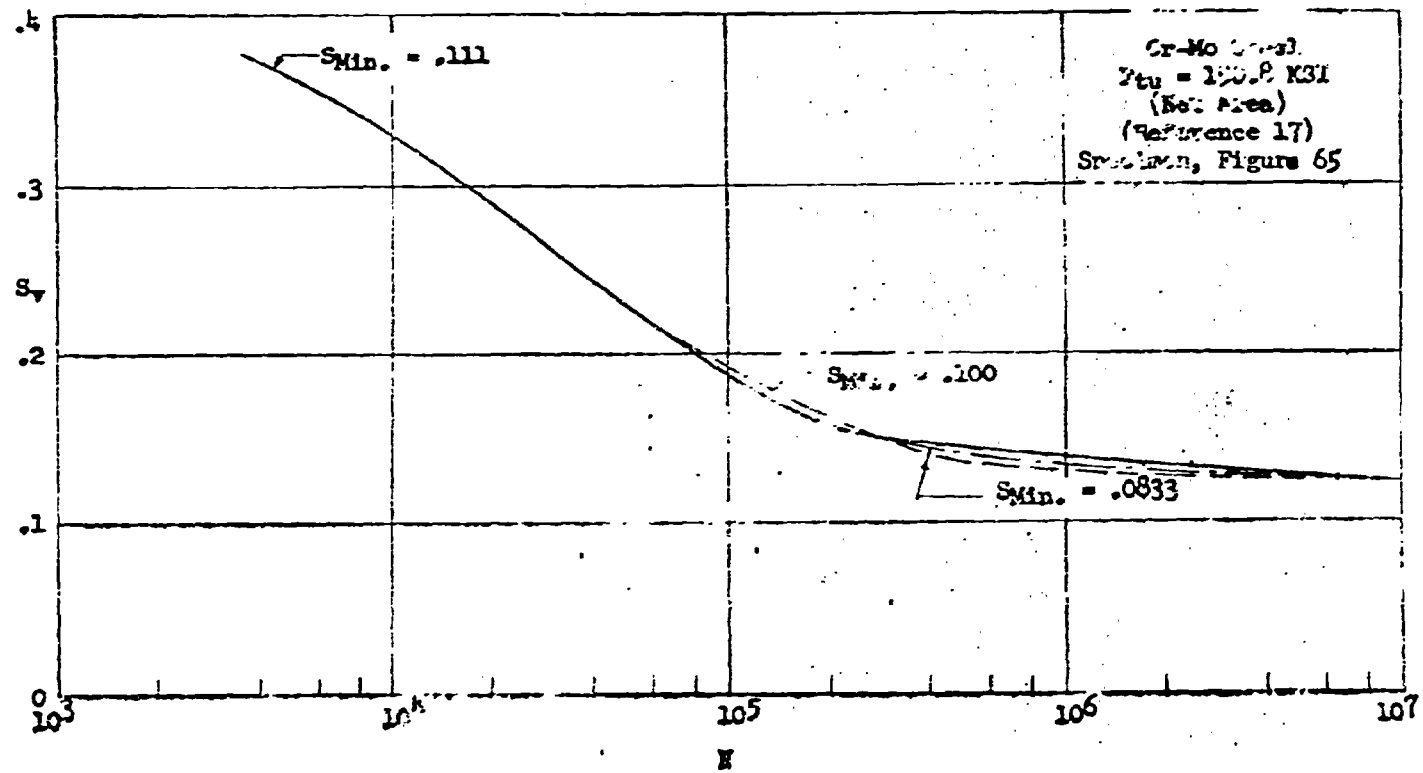



Figure 434 $S_v$ Curves for Strip Specimens with Centrally Located Hole. Constant Minimum Stress. (For Maneuver Type Loading)

TABLE 48

EXPERIMENTAL FATIGUE LIVES FOR GUST LOADING SPECTRA

(Table is Continued on Next Two Pages)

| Test Group No. | Material | Specimen | $S_{Mean}$ | Number of Loading Steps | Type of Spectrum Curve | Sequence | Block Size | Number of Specimens | Test Life ($10^6$ Cycles) Minimum | Maximum | Geometric Mean | Ref. |
|---|---|---|---|---|---|---|---|---|---|---|---|---|
| G1 | 2024-T3 | Notched Sheet | .241 | 18 | Gust B | Lo-Hi | 10200 | 3 | 8.000 | 8.100 | 8.049 | |
| G2 | | | | | | Lo-Hi | 50900 | 9 | 2.500 | 5.000 | 3.872 | |
| G3 | | | | | | Hi-Lo | 10200 | 3 | 7.410 | 17.700 | 11.888 | |
| G4 | | | | | | Hi-Lo | 50900 | 6 | 8.506 | 26.036 | 14.555 | |
| G5 | | | | | | QR | 500000 | 8 | 3.654 | 10.143 | 6.938 | |
| G6 | | | | 18 | Gust A | | 100000 | 4 | 1.403 | 2.501 | 1.824 | |
| G7 | | | | 8 | | Lo-Hi | 100200 | 3 | .501 | .701 | .595 | |
| G8 | | | | | | Hi-Lo | 100200 | 3 | 2.007 | 2.609 | 2.294 | |
| G9 | | | | | | Lo-Hi-Lo | | 3 | 1.454 | 1.854 | 1.612 | |
| G10 | | | | | | Hi-Lo-Hi | 100200 | 3 | 1.376 | 1.756 | 1.519 | |
| G11 | | | | | | QR | 50100 | 3 | 1.704 | 2.353 | 2.020 | |
| G12 | | | .241 | | | | 100200 | 4 | .903 | 1.503 | 1.215 | |
| G13 | | | 0 | | | | 50000 | 6 | .350 | .647 | .479 | |
| G14 | 2024-T3 | | 0 | | | QR | 100000 | 3 | .302 | .476 | .364 | 16 |
| G15 | 7075-T6 | | .241 | | | Lo-Hi | 10200 | 3 | .377 | .571 | .443 | |
| G16 | | | | | | Lo-Hi | 50900 | 4 | .356 | .578 | .452 | |
| G17 | | | | | | Hi-Lo | 50900 | 4 | 1.121 | 1.527 | 1.268 | |
| G18 | | | | | | Lo-Hi-Lo | 10200 | 4 | .509 | 1.013 | .762 | |
| G19 | | | | | | Hi-Lo-Hi | 50900 | 4 | .866 | 1.069 | .976 | |
| G20 | | | | | | QR | 10200 | 3 | .590 | .736 | .661 | |
| G21 | | | .241 | | | QR | 50900 | 4 | .458 | .712 | .600 | |
| G22 | | | .121 | | | Lo-Hi-Lo | 30200 | 3 | .297 | .468 | .385 | |
| G23 | | | .121 | | | QR | 30200 | 6 | .211 | .400 | .282 | |
| G24 | | | 0 | | | Lo-Hi | 30000 | 6 | .180 | .510 | .253 | |
| G25 | | | | | | Hi-Lo | | 5 | .390 | .600 | .496 | |
| G26 | | Notched Sheet | | | | Lo-Hi-Lo | | 3 | .405 | .615 | .498 | |
| G27 | 7075-T6 | | 0 | 8 | Gust A | QR | 50000 | 6 | .210 | .775 | .394 | |

TABLE 48
(Table is completed on next page.)

| Test Group No. | Material | Type of Specimen | $S_{Mean}$ | Number of Loading Steps | Sequence | Block Size | Number of Specimens | Test Life ($10^6$ Cycles) Minimum | Maximum | Geometric Mean | Ref. |
|---|---|---|---|---|---|---|---|---|---|---|---|
| G28 | | Double | .253 | 9 | Lo-Hi-Lo | 360280 | 2 | .324 | .522 | .411 | |
| G29 | 2024-T3 | Shear | .152 | | | | 3 | 3.260 | 5.980 | 4.788 | |
| G30 | Alclad | Riveted | .101 | | | | 3 | 13.690 | 27.400 | 21.732 | |
| G31 | | Joints | .081 | | | | 2 | 62.400 | 270.000 | 129.700 | |
| G32 | | Unnotched | .201 | | | | 2 | 24.100 | 27.400 | 25.710 | |
| G33 | | Sheet | .161 | | | | 2 | 58.700 | 98.000 | 75.875 | |
| G34 | 7075-T6 | | .145 | | | | 2 | 127.000 | 181.000 | 151.966 | 17 |
| | Alclad | | | | | | | | | | |
| G35 | | Butt | .250 | | | | 4 | 2.050 | 4.030 | 2.994 | |
| G36 | | Joints | .167 | | | | 2 | 27.000 | 28.100 | 27.558 | |
| G37 | | | .125 | | | | 2 | 72.700 | 140.000 | 100.986 | |
| G38 | | Strips | .286 | | | | 2 | 3.310 | 4.970 | 4.060 | |
| G39 | Cr-Mo Steel | w/hole | .222 | | | | 2 | 12.100 | 26.600 | 17.902 | |
| G40 | | | .182 | 9 | Lo-Hi-Lo | 360280 | 3 | 45.000 | 63.000 | 50.367 | |
| G41 | | (a) | .212 | 6 | Lo-Hi-(c) | 1599000 | 1 | | | 1.599 | |
| G42 | 2024-T3 | | | 6 | Hi-Lo-(c) | 2279000 | 1 | | | 2.279 | |
| G43 | Alclad | | | 6 | | 2848000 | 1 | | | 2.848 | |
| G44 | | | | 5 | | 457700 | 1 | | | .458 | 16 |
| G45 | | (b) | | 5 | | 164400 | 1 | | | .164 | |
| G46 | 7075-T6 | | | 5 | Hi-Lo (c) | 92900 | 1 | | | .093 | |
| G47 | Alclad | (a) | .212 | 6 | Lo-Hi (c) | 1228000 | 1 | | | 1.228 | |
| G48 | D.T.D. 363A | Notched | .165 | 9 | Lo-Hi-Lo | 13290 | 6 | .093 | .279 | .133 | |
| G49 | Aluminum | Plate | .165 | 9 | Lo-Hi-Lo | 6290 | 6 | .088 | .145 | .127 | 19 |
| G50 | Alloy | | .165 | 10 | Lo-Hi-Lo | 5410 | 5 | .032 | .282 | .074 | |

(a) lap joint with one row of flush rivets
(b) lap joint with two rows of flush rivets
(c) sequence applied only once

TABLE 48

(Concluding Page of Table)

| Test Group No. | Material | | Type of Specimen | $S_{Mean}$ | Number of Loading Steps | Sequence | Block Size | Number of Specimens | Test Life ($10^6$ Cycles) Minimum | Maximum | Geometric Mean | Ref. |
|---|---|---|---|---|---|---|---|---|---|---|---|---|
| G51 | 2024-T | C-46 Wing | WS 180 | .20 | 16 | CR | 59670 | 4 | .970 | 8.314 | 4.179 | |
| G52 | | | WS 214 | | | | | 6 | 3.487 | 8.712 | 4.453 | |
| G53 | | | WS 228 | | | | | 5 | .354 | 7.459 | 2.307 | |
| G54 | | | WS 239 | | | | | 5 | 1.253 | 3.879 | 2.070 | 20 |
| G55 | | | (d) | | | | | 6 | .354 | 2.507 | 1.252 | |
| G56 | | | (e) | | | | | 6 | 1.418 | 6.906 | 3.344 | |
| G57 | | | (f) | | 16 | CR | 59670 | 6 | 7.160 | 13.100 | 9.656 | |
| G58 | | P51 Wing | Gun Bay Initial Failure | | 11 | TR | 500000 | 3 | .276 | .596 | .417 | |
| G59 | | | | | 3 | Lo-Hi-Lo | 32860 | 4 | .240 | 1.120 | .557 | |
| G60 | | | Tank Bay Initial Failure | | 11 | TR | 500000 | 2 | 1.260 | 1.835 | 1.521 | |
| G61 | | | | | 3 | Lo-Hi-Lo | 32860 | 7 | .669 | 1.470 | .953 | 21 |
| G62 | | | Gun Bay Final Failure | | 11 | TR | 500000 | 4 | 2.025 | 3.150 | 2.520 | |
| G63 | | | | | 3 | Lo-Hi-Lo | 32860 | 3 | .990 | 2.300 | 1.495 | |
| G64 | | | Tank Bay Final Failure | | 11 | TR | 500000 | 2 | 1.782 | 2.280 | 2.017 | |
| G65 | 2024-T | | | .20 | 3 | Lo-Hi-Lo | 32860 | 5 | .774 | 1.935 | 1.039 | |

(d) first crack initiated in complete wing
(e) Initiation of critical crack that propagated to failure when loading continued
(f) final failure of complete wing

TABLE 49

EXPERIMENTAL FATIGUE LIVES FOR MANEUVER LOADING SPECTRA

(Reference 17)

| Test Group No. | Material | Type of Specimen | $S_{min}$ | Number of Loading Steps | Sequence | Block Size | Number of Specimens | Test Life ($10^6$ Cycles) Min. | Max. | Geometric Mean |
|---|---|---|---|---|---|---|---|---|---|---|
| M1 | 2024-T3 Alclad | Double Shear Riveted Joint | .0833 | 9 | Lo-Hi-Lo | 7497 | 2 | .282 | .334 | .308 |
| M2 | | | .0625 | | | | 2 | .465 | .532 | .499 |
| M3 | | | .050 | | | | 2 | .825 | .990 | .903 |
| M4 | 7075-T6 Alclad | Unnotched Sheet | .125 | | | | 2 | .206 | .206 | .206 |
| M5 | | | .100 | | | | 2 | .645 | .787 | .716 |
| M6 | | | .0833 | | | | 3 | .630 | 1.120 | .903 |
| M7 | | | .0625 | | | | 2 | 1.454 | 3.369 | 2.219 |
| M8 | | Butt Joint | .100 | | | | 2 | .066 | .071 | .069 |
| M9 | | | .0833 | | | | 2 | .190 | .243 | .214 |
| M10 | | | .0625 | | | | 2 | 1.095 | 1.994 | 1.477 |
| M11 | Cr-Mo Steel | Strip w/hole | .111 | | | | 2 | .188 | .208 | .198 |
| M12 | | | .100 | | | | 2 | .352 | .389 | .370 |
| M13 | | | .0833 | 9 | Lo-Hi-Lo | 7497 | 2 | 1.042 | 1.042 | 1.042 |

## APPENDIX D

## ORIGINAL TEST RESULTS

This appendix presents a description of the test equipment, descriptions of the test specimens, and tabulation and graphical results of the experimental work completed in this program. Also included is the statistical analysis of the constant amplitude coupon S-N data. These data are presented in three part

Part 1. Constant amplitude axial load S-N data from simple coupons.

Statistical analysis of constant amplitude S-N data.

Experimental S-N data.

Construction of S-N Curves by interpolation.

Part 2. Spectral Axial load data from simple coupons.

Description of equipment and procedures for obtaining experimental data on coupon specimens.

Unit Loading Spectra

Experimental Lives

Test Histories . . .

Part 3. Fatigue Test Results of a Complex Specimen

Specimen Description

Test Set-up

Test Results

## APPENDIX D

### PART 1 - CONSTANT AMPLITUDE AXIAL LOAD S-N DATA FROM SIMPLE COUPONS

#### Statistical Analysis of Constant Amplitude S-N Data

The multiple variables and the limited number of individual test specimens per test condition (five coupons each) led to the use of special statistical methods for small samples. The method of linear regression was chosen to analyze the results of the constant amplitude S-N test data. This method has been suggested by Weibull in reference 33, as well as by other investigators. It considers the frequency distribution of log $(S_T - S_E)$ when log N is held constant. While Figure 105 shows that this method can lead to an approximately normal distribution, the small sample size for each combination of stress concentration factor $K_T$ and mean stress $f_{mean}$ in Table 50 does not always make it possible to arrive at statistically significant conclusions with a high degree of confidence.

TABLE 50

TEST CONFIGURATIONS FOR S-N DATA

| $K_T$ | $f_{mean}$, gross area, KSI | | | | |
|---|---|---|---|---|---|
| | -10 | -5 | 0 | 10 | 15 |
| 3 | X | X | | X | X |
| 4 | X | X | X | X | X |
| 7 | X | X | X | X | X |
| 10 | X | X | | X | X |

The eighteen test configurations listed comprise the 450 specimens in Table 52. Twenty-five specimens were tested for each combination of $K_T$ and $f_{mean}$, with five of these specimens being tested at each of five convenient varying stress levels, which did not exceed 25 KSI. Some additional test configurations are given in Table 53 which were not statistically analyzed.

In Weibull's use of the method of linear regression with small sample size, the (n = 5 x 5) or twenty-five specimens are pooled and the following S-N function is assumed (reference 33).

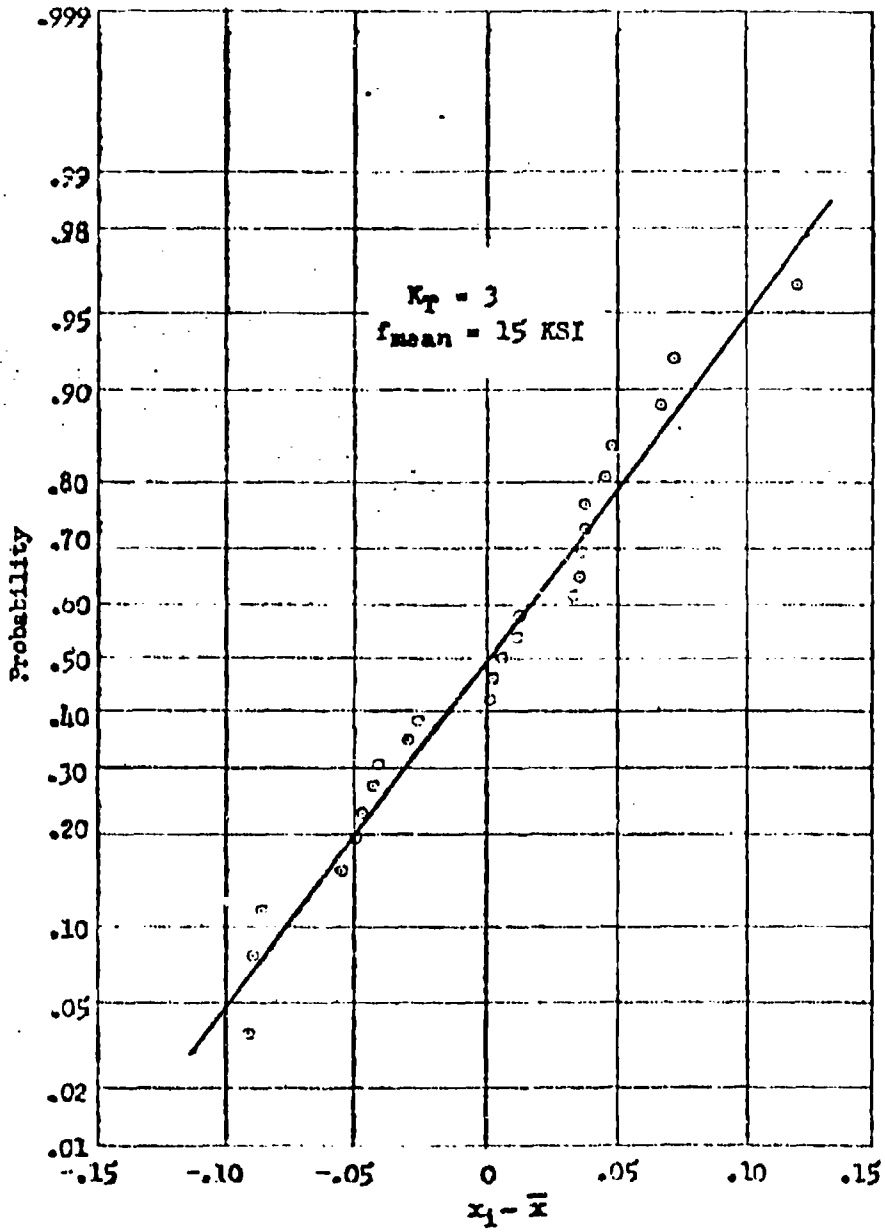



Figure 105 Deviation in $\Delta$ Log $S_v$ from the Least Square Best Fit Straight Line on a Plot of Log $S_v$ versus Log N

$$S_v = S_E + p\,N^u \tag{D1}$$

This form corresponds to Equation (A6) of Appendix A when

$$p = \alpha C^u$$

and

$$u = \frac{1}{\beta}$$

The endurance limit $S_E$ is itself a statistical variate, and Equation (D1) must be solved for known or estimated values of $S_E$. For a given value of $S_E$, Equation (D1) can be written in the form

$$\log (S_v - S_E) = \log p + u \log N \tag{D2}$$

Designating $y = \log (S_v - S_E)$ as the dependent and $x = \log N$ as the independent variable, the method of linear regression may be applied with

$$y = y_o + u\,x \tag{D3}$$

and the coefficients u and $y_o$ of the straight regression line are determined by

$$u = \frac{\sum (x_i - \bar{x})\,(y_i - \bar{y})}{\sum (x_i - \bar{x})^2} \tag{D4}$$

and

$$y_o = \log p = \bar{y} - u\,\bar{x} \tag{D5}$$

where

$$\bar{x} = \frac{\sum x_i}{n} \quad ; \quad \bar{y} = \frac{\sum y_i}{n} \tag{D6}$$

The method is strictly correct only if the population variances of y are homogeneous; that means, the standard deviation in y is independent of x. The deviations from the regression line should be normally distributed. An unbiased estimate of the variance from regression of the population ($n = \infty$) is given by

$$\{\text{var}\} = \frac{\sum [y_i - (y_o + u\,x_i)]^2}{n - 2} \tag{D7}$$

For any given value $x^*$, confidence limits for the computed value $y^* = y_o + u\,x^*$ are easily set according to Cramer (reference 34).

Upper confidence limit

$$y_u = (y_o + u\,x^*) + (t_{\alpha/2;\nu}) \sqrt{\{\text{var}\} \left\{\frac{1}{n} + \frac{(x^* - \bar{x})^2}{\sum (x_i - \bar{x})^2}\right\}} \qquad \text{(D8)}$$

Lower confidence limit

$$y_l = (y_o + u\,x^*) - (t_{\alpha/2;\nu}) \sqrt{\{\text{var}\} \left\{\frac{1}{n} + \frac{(x^* - \bar{x})^2}{\sum (x_i - \bar{x})^2}\right\}} \qquad \text{(D9)}$$

Values of $t_{\alpha/2;\nu}$ corresponding to the required confidence coefficient $(1 - \alpha)$ and the given degree of freedom $\nu = n - 2$ can be found in reference 34; for instance, the values are given in Table 51 for $n = 25$ test specimens.

TABLE 51

Student's t - value for $\nu = 23$ Degree of Freedom

| Confidence ( % ) | 20 | 40 | 60 | 80 | 90 | 95 | 98 | 99 | 99.9 |
|---|---|---|---|---|---|---|---|---|---|
| t - value | .256 | .532 | .858 | 1.319 | 1.714 | 2.069 | 2.500 | 2.807 | 3.767 |

Plausible values must be assumed for the endurance limit before this statistical procedure can be applied to S-N data. The actual value selected for the endurance limit, $S_E$, as pointed out in reference 33, will have only a small effect on the analytical matching of S-N data in the mid-stress range. A more accurate linear interpretation of S-N data over the entire stress range may sometimes be provided by a statistical fit of Equation (D10) to S-N data.

$$N = \frac{\gamma}{S_V^{\delta}} \qquad \text{(D10)}$$

The improvement in matching S-N data in the high and low stress ranges occurs when S-N data follow the linear trend that is indicated in Figure 47. When plotted in the form of log $(S_V - S_E)$ versus log N, the straight

line variation in Figure 47 degenerates into a curve as shown in Figure 57, where two portions of the resulting curve are approximated by straight lines. This curvilinear variation with log $(S_a - S_g)$ led to the use of linear regression based on Equation (D10). Statistical parameters for this equation constitute a special case for Equation (D1), being the same as that secured by setting $S_g$ equal to zero in Equation (D1) and in the subsequent statistical development.

The use of linear regression with Equation (D10) lead to more likely conditions for a straight line fit to the entire stress range of S-N data. It led to the S-N curves in Figures 106 to 123 that were faired within the $\pm$ 90 per cent confidence limits. This fairing was made to reduce as much as possible the merging and intersections in cross plots of the data. The faired S-N curves intersected in only one case at the upper end ($f_y$ = 25 ksi) and were tangent in one place near the endurance limit. Agreement was generally good with the test data although the resulting S-N curves did not flatten out in the vicinity of the assumed endurance limit at $N = 10^7$ cycles.

TABLE 52
S-N DATA FOR NOTCHED SHEET COUPONS
(Table is continued on the next two pages)
All Stresses are Based on Gross Area

| $K_T = 3$ $f_{mean} = -10$ | | $K_T = 3$ $f_{mean} = -5$ | | $K_T = 3$ $f_{mean} = 10$ | | $K_T = 3$ $f_{mean} = 15$ | | $K_T = 4$ $f_{mean} = -10$ | | $K_T = 4$ $f_{mean} = -5$ | |
|---|---|---|---|---|---|---|---|---|---|---|---|
| $f_v$ KSI | N | $f_v$ KSI | N | $f_v$ KSI | N | $f_v$ KSI | N | $f_v$ KSI | N | $f_v$ KSI | N |
| 25 | 601 | 25 | 901 | 25 | 786 | 25 | 660 | 25 | 1215 | 25 | 500 |
| 25 | 640 | 25 | 1081 | 25 | 1509 | 25 | 915 | 25 | 1519 | 25 | 610 |
| 25 | 1425 | 25 | 1384 | 25 | 1866 | 25 | 965 | 25 | 1697 | 25 | 806 |
| 25 | 2044 | 25 | 1642 | 25 | 2476 | 25 | 1072 | 25 | 2424 | 25 | 812 |
| 25 | 5055 | 25 | 2760 | 25 | 2621 | 25 | 1101 | 25 | 2843 | 25 | 873 |
| 20 | 2144 | 20 | 3300 | 20 | 2765 | 20 | 3272 | 20 | 1290 | 20 | 1245 |
| 20 | 6200 | 20 | 3954 | 20 | 3130 | 20 | 3904 | 20 | 2445 | 20 | 1650 |
| 20 | 7500 | 20 | 3960 | 20 | 4611 | 20 | 4269 | 20 | 3379 | 20 | 1686 |
| 20 | 7573 | 20 | 6315 | 20 | 6264 | 20 | 4998 | 20 | 3600 | 20 | 2274 |
| 20 | 11060 | 20 | 6377 | 20 | 8091 | 20 | 5200 | 20 | 5179 | 20 | 2460 |
| 15 | 10600 | 15 | 10800 | 15 | 9000 | 15 | 7995 | 15 | 12600 | 15 | 3600 |
| 15 | 37800 | 15 | 12600 | 15 | 10800 | 15 | 8722 | 15 | 12600 | 15 | 5400 |
| 15 | 39600 | 15 | 23400 | 15 | 10800 | 15 | 10655 | 15 | 11400 | 15 | 6550 |
| 15 | 43200 | 15 | 27000 | 15 | 16200 | 15 | 10707 | 15 | 16200 | 15 | 6800 |
| 15 | 108000 | 15 | 41400 | 15 | 19800 | 15 | 11295 | 15 | 16200 | 15 | 7050 |
| 10 | 100800 | 10 | 7200 | 10 | 27000 | 10 | 23400 | 12.5 | 13860 | 10 | 27600 |
| 10 | 135000 | 10 | 36000 | 10 | 27540 | 10 | 32400 | 12.5 | 15300 | 10 | 63000 |
| 10 | 203400 | 10 | 75600 | 10 | 49680 | 10 | 34200 | 12.5 | 16920 | 10 | 62800 |
| 10 | 302400 | 10 | 270000 | 10 | 52800 | 10 | 43600 | 12.5 | 51600 | 10 | 86400 |
| 10 | 385200 | 10 | 295560 | 10 | 55800 | 10 | 84600 | 12.5 | 79740 | 10 | 93600 |
| 7.5 | 484200 | 5 | 374400 | 5 | 196560 | 5 | 176400 | 10 | 37440 | 5.5 | 163000 |
| 7.5 | 525600 | 5 | 522000 | 5 | 198000 | 5 | 180000 | 10 | 91800 | 5.5 | 189000 |
| 7.5 | 698400 | 5 | 1644500 | 5 | 198540 | 5 | 232200 | 10 | 117000 | 5.5 | 1306800 |
| 7.5 | 1674000 | 5 | * | 5 | 201600 | 5 | 246600 | 10 | 124200 | 5.5 | 1998000 |
| 7.5 | 2719600 | 5 | * | 5 | 239400 | 5 | 460800 | 10 | 3700000 | 5.5 | 3601000 |

* $10^7$ cycles (no failure)

TABLE 52
(Table is completed on next page)
All Stresses are Based on Gross Area

| $K_T = 4$ $f_{mean} = 0$ | | $K_T = 4$ $f_{mean} = 10$ | | $K_T = 4$ $f_{mean} = 15$ | | $K_T = 7$ $f_{mean} = -10$ | | $K_T = 7$ $f_{mean} = -5$ | | $K_T = 7$ $f_{mean} = 0$ | |
|---|---|---|---|---|---|---|---|---|---|---|---|
| $f_v$ KSI | N | $f_v$ KSI | N | $f_v$ KSI | N | $f_v$ KSI | N | $f_v$ KSI | N | $f_v$ KSI | N |
| 25 | 331 | 25 | 150 | 25 | 171 | 20 | 343 | 25 | 36 | 20 | 142 |
| 25 | 342 | 25 | 250 | 25 | 175 | 20 | 450 | 25 | 119 | 20 | 215 |
| 25 | 393 | 25 | 260 | 25 | 180 | 20 | 516 | 25 | 140 | 20 | 224 |
| 25 | 445 | 25 | 324 | 25 | 212 | 20 | 590 | 25 | 172 | 20 | 277 |
| 25 | 537 | 25 | 350 | 25 | 315 | 20 | 664 | 25 | 183 | 20 | 360 |
| 20 | 670 | 20 | 521 | 20 | 491 | 15 | 474 | 20 | 195 | 15 | 386 |
| 20 | 741 | 20 | 531 | 20 | 540 | 15 | 743 | 20 | 226 | 15 | 413 |
| 20 | 914 | 20 | 640 | 20 | 890 | 15 | 1006 | 20 | 247 | 15 | 573 |
| 20 | 975 | 20 | 820 | 20 | 1030 | 15 | 1200 | 20 | 293 | 15 | 636 |
| 20 | 1316 | 20 | 1001 | 20 | 1203 | 15 | 1883 | 20 | 296 | 15 | 884 |
| 15 | 3600 | 15 | 1860 | 15 | 1471 | 10 | 9540 | 15 | 455 | 10 | 1200 |
| 15 | 4283 | 15 | 2500 | 15 | 2325 | 10 | 12600 | 15 | 672 | 10 | 1800 |
| 15 | 4468 | 15 | 2900 | 15 | 2600 | 10 | 14400 | 15 | 748 | 10 | 2310 |
| 15 | 6480 | 15 | 5946 | 15 | 3053 | 10 | 41100 | 15 | 753 | 10 | 3150 |
| 15 | 7200 | 15 | 6150 | 15 | 3170 | 10 | 52200 | 15 | 813 | 10 | 4633 |
| 10 | 26280 | 10 | 9000 | 10 | 6300 | 7.5 | 14580 | 10 | 6150 | 7.5 | 14400 |
| 10 | 28800 | 10 | 9600 | 10 | 6450 | 7.5 | 40140 | 10 | 6300 | 7.5 | 16740 |
| 10 | 29700 | 10 | 10500 | 10 | 7200 | 7.5 | 102780 | 10 | 7672 | 7.5 | 19800 |
| 10 | 36180 | 10 | 12600 | 10 | 7950 | 7.5 | 147600 | 10 | 8100 | 7.5 | 32400 |
| 10 | 37800 | 10 | 27000 | 10 | 15040 | 7.5 | 148500 | 10 | 8620 | 7.5 | 34200 |
| 5 | 2096500 | 4 | 61200 | 3 | 90000 | 5 | 185000 | 4 | 178200 | 5 | 51400 |
| 5 | 3979600 | 4 | 63000 | 3 | 174600 | 5 | 240000 | 4 | 847800 | 5 | 101500 |
| 5 | 5440000 | 4 | 64800 | 3 | 370800 | 5 | 390400 | 4 | 911700 | 5 | 102600 |
| 5 | 6378000 | 4 | 92800 | 3 | 406800 | 5 | 651600 | 4 | 1000000 | 5 | 111900 |
| 5 | 8109720 | 4 | 872000 | 3 | 2196000 | 5 | 691700 | 4 | * | 5 | 941600 |

* $10^7$ cycles (no failure)

TABLE 52
(Concluding Page of Table)
All Stresses are Based on Gross Area

| $K_T = 7$ $f_{mean} = 10$ | | $K_T = 7$ $f_{mean} = 15$ | | $K_T = 10$ $f_{mean} = -10$ | | $K_T = 10$ $f_{mean} = -5$ | | $K_T = 10$ $f_{mean} = 10$ | | $K_T = 10$ $f_{mean} = 15$ | |
|---|---|---|---|---|---|---|---|---|---|---|---|
| $f_v$ KSI | N | $f_v$ KSI | N | $f_v$ KSI | N | $f_v$ KSI | N | $f_v$ KSI | N | $f_v$ KSI | N |
| 20 | 100 | 20 | 90 | 20 | 147 | 15 | 450 | 15 | 155 | 15 | 125 |
| 20 | 130 | 20 | 160 | 20 | 263 | 15 | 450 | 15 | 168 | 15 | 184 |
| 20 | 240 | 20 | 180 | 20 | 336 | 15 | 562 | 15 | 177 | 15 | 199 |
| 20 | 250 | 20 | 190 | 20 | 415 | 15 | 753 | 15 | 179 | 15 | 202 |
| 20 | 350 | 20 | 230 | 20 | 501 | 15 | 1855 | 15 | 200 | 15 | 242 |
| 15 | 383 | 15 | 360 | 15 | 360 | 10 | 780 | 10 | 493 | 10 | 450 |
| 15 | 425 | 15 | 430 | 15 | 478 | 10 | 1031 | 10 | 728 | 10 | 605 |
| 15 | 440 | 15 | 460 | 15 | 575 | 10 | 1231 | 10 | 766 | 10 | 655 |
| 15 | 663 | 15 | 480 | 15 | 685 | 10 | 2331 | 10 | 794 | 10 | 761 |
| 15 | 706 | 15 | 1033 | 15 | 3387 | 10 | 3300 | 10 | 1021 | 10 | 861 |
| 10 | 1500 | 10 | 500 | 10 | 1660 | 7.5 | 916 | 7.5 | 772 | 5 | 4331 |
| 10 | 2450 | 10 | 900 | 10 | 2215 | 7.5 | 3600 | 7.5 | 1391 | 5 | 4500 |
| 10 | 3600 | 10 | 1510 | 10 | 3215 | 7.5 | 4438 | 7.5 | 1462 | 5 | 4924 |
| 10 | 4189 | 10 | 1880 | 10 | 4500 | 7.5 | 7200 | 7.5 | 1501 | 5 | 5100 |
| 10 | 4950 | 10 | 2040 | 10 | 9011 | 7.5 | 22544 | 7.5 | 1766 | 5 | 6300 |
| 5 | 12600 | 5 | 10800 | 7.5 | 28800 | 5.5 | 23800 | 5 | 2880 | 2.5 | 25200 |
| 5 | 12600 | 5 | 12600 | 7.5 | 45000 | 5.5 | 36000 | 5 | 6176 | 2.5 | 28800 |
| 5 | 14400 | 5 | 12960 | 7.5 | 66600 | 5.5 | 36000 | 5 | 6343 | 2.5 | 30600 |
| 5 | 17460 | 5 | 14250 | 7.5 | 72000 | 5.5 | 43200 | 5 | 6999 | 2.5 | 57600 |
| 5 | 25200 | 5 | 17280 | 7.5 | 73800 | 5.5 | 88200 | 5 | 7258 | 2.5 | 64800 |
| 2.5 | 88200 | 2 | 84600 | 5 | 185400 | 4 | 48600 | 2.5 | 25200 | 1.5 | 340200 |
| 2.5 | 83200 | 2 | 84600 | 5 | 352800 | 4 | 55800 | 2.5 | 36000 | 1.5 | 648000 |
| 2.5 | 129600 | 2 | 185400 | 5 | 658800 | 4 | 144000 | 2.5 | 73440 | 1.5 | 1104900 |
| 2.5 | 691000 | 2 | 342000 | 5 | 1420200 | 4 | 824760 | 2.5 | 82620 | 1.5 | 4696200 |
| 2.5 | 1296000 | 2 | * | 5 | 3216600 | 4 | 888480 | 2.5 | 576000 | 1.5 | * |

* $10^7$ cycles (no failure)

## TABLE 53

S-N DATA FOR NOTCHED SHEET COUPONS
All Stresses are Based on Gross Area

| $K_T$=4; $f_{mean}$= 1.125 KSI | | $K_T$=4; $f_{mean}$= 4.5 KSI | | $K_T$=4; $f_{mean}$= 7 KSI | | $K_T$=4; $f_{mean}$= 2.4 KSI | |
|---|---|---|---|---|---|---|---|
| $f_v$ KSI | N | $f_v$ KSI | N | $f_v$ KSI | N | $f_v$ KSI | N |
| 4.225 | $>10^7$ | 7.5 | 25200 | 15 | 3342 | 10.4 | 12015 |
| 4.225 | $>10^7$ | 7.5 | 32400 | 15 | 3465 | 10.4 | 14856 |
| 4.225 | $>1.5\ (10)^7$ | 7.5 | 41400 | 15 | 3537 | | |
| | | 7.5 | 43400 | 15 | 4075 | | |
| | | 7.5 | 43800 | 15 | 4330 | | |
| | | 7.5 | 45000 | | | | |

| $K_T$=7; $f_{mean}$= 1.125 KSI | | $K_T$=7; $f_{mean}$= 4.5 KSI | | $K_T$=7; $f_{mean}$= 7 KSI | | $K_T$=7; $f_{mean}$= 2.6 KSI | |
|---|---|---|---|---|---|---|---|
| $f_v$ KSI | N | $f_v$ KSI | N | $f_v$ KSI | N | $f_v$ KSI | N |
| 4.225 | 364000 | 7.5 | 9900 | 15 | 485 | 10.2 | 1356 |
| 4.225 | 144000 | 7.5 | 10600 | 15 | 502 | 10.2 | 1332 |
| 4.225 | 148000 | 7.5 | 11900 | 15 | 503 | | |
| 4.225 | $>10^7$ | 7.5 | 13700 | 15 | 529 | | |
| 4.225 | $>10^7$ | 7.5 | 14600 | 15 | 540 | | |
| 4.225 | $>10^7$ | 7.5 | 14700 | | | | |

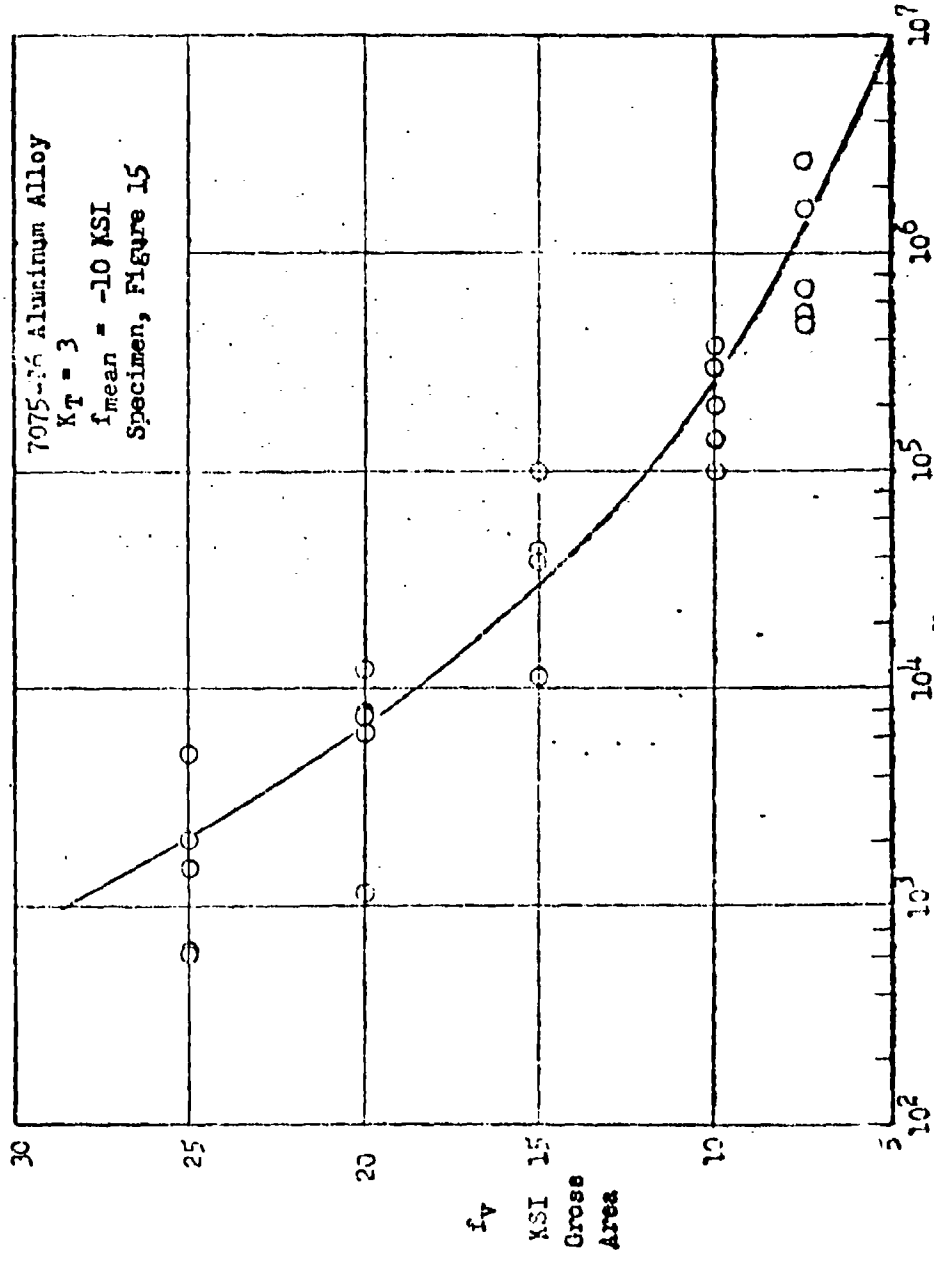



Figure 106 Experimental S-N Curve for Notched Sheet Coupons

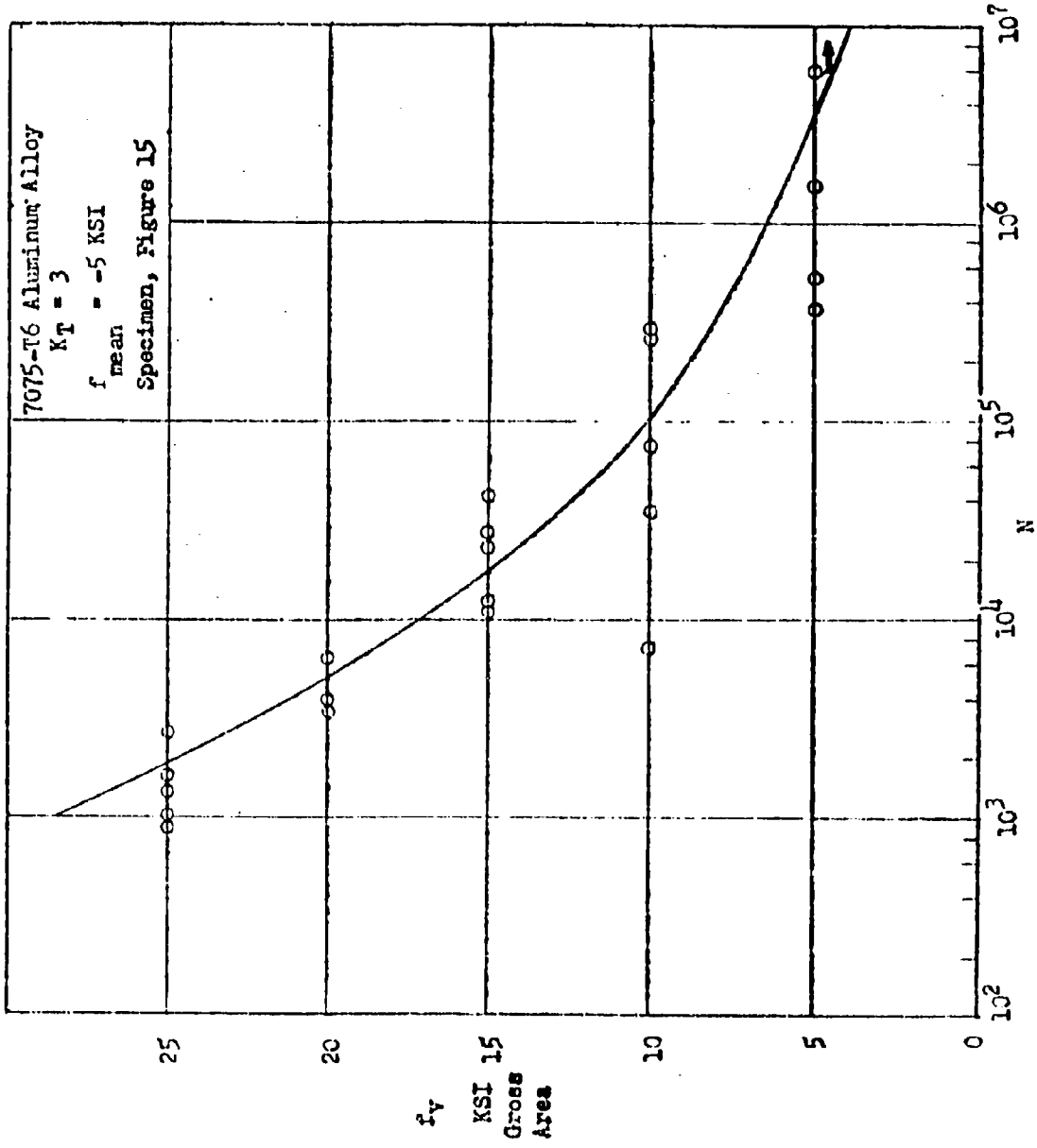



Figure 107 Experimental S-N Curve for Notched Sheet Coupons

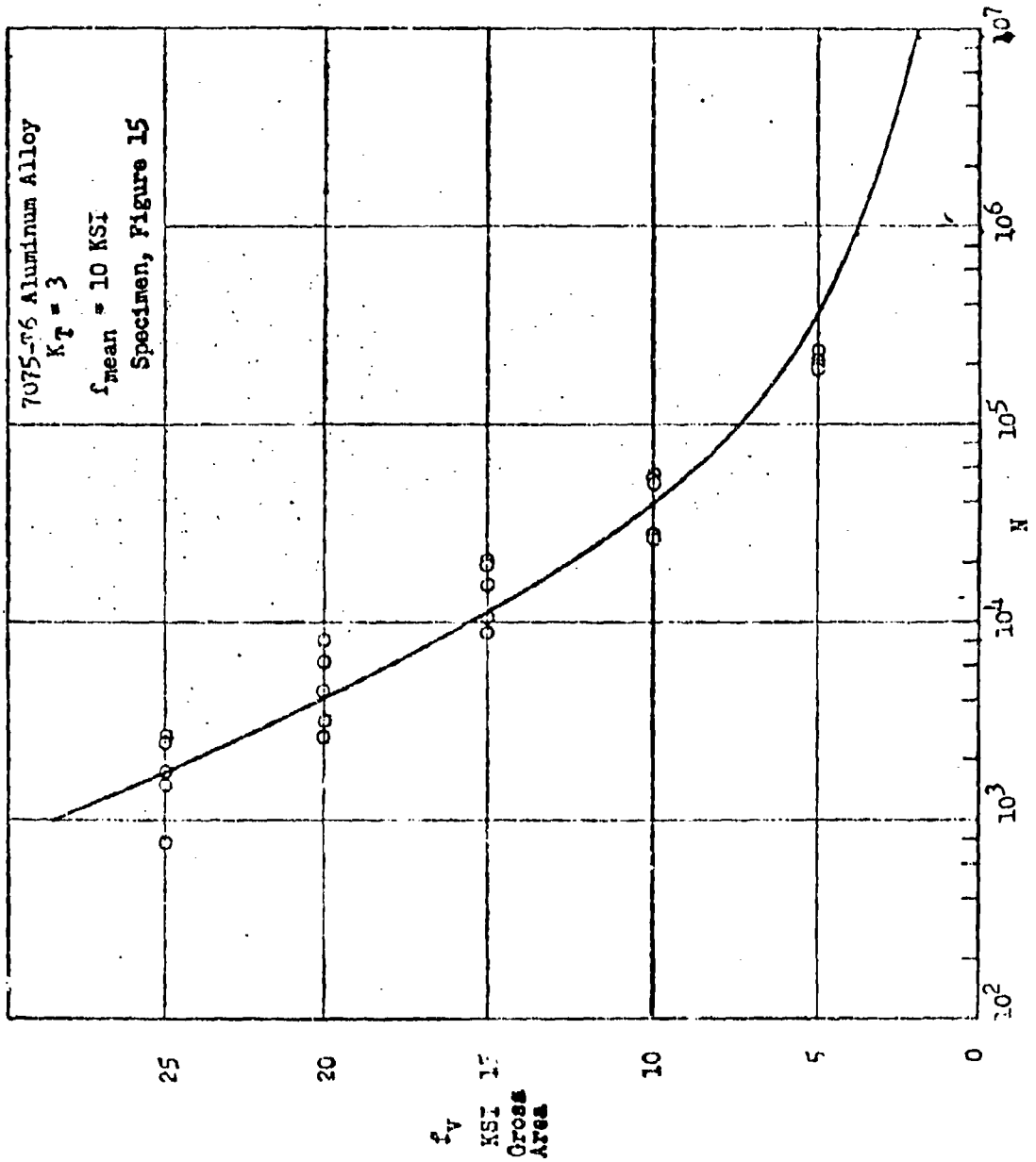



Figure 108 Experimental S-N Curve for Notched Sheet Coupons

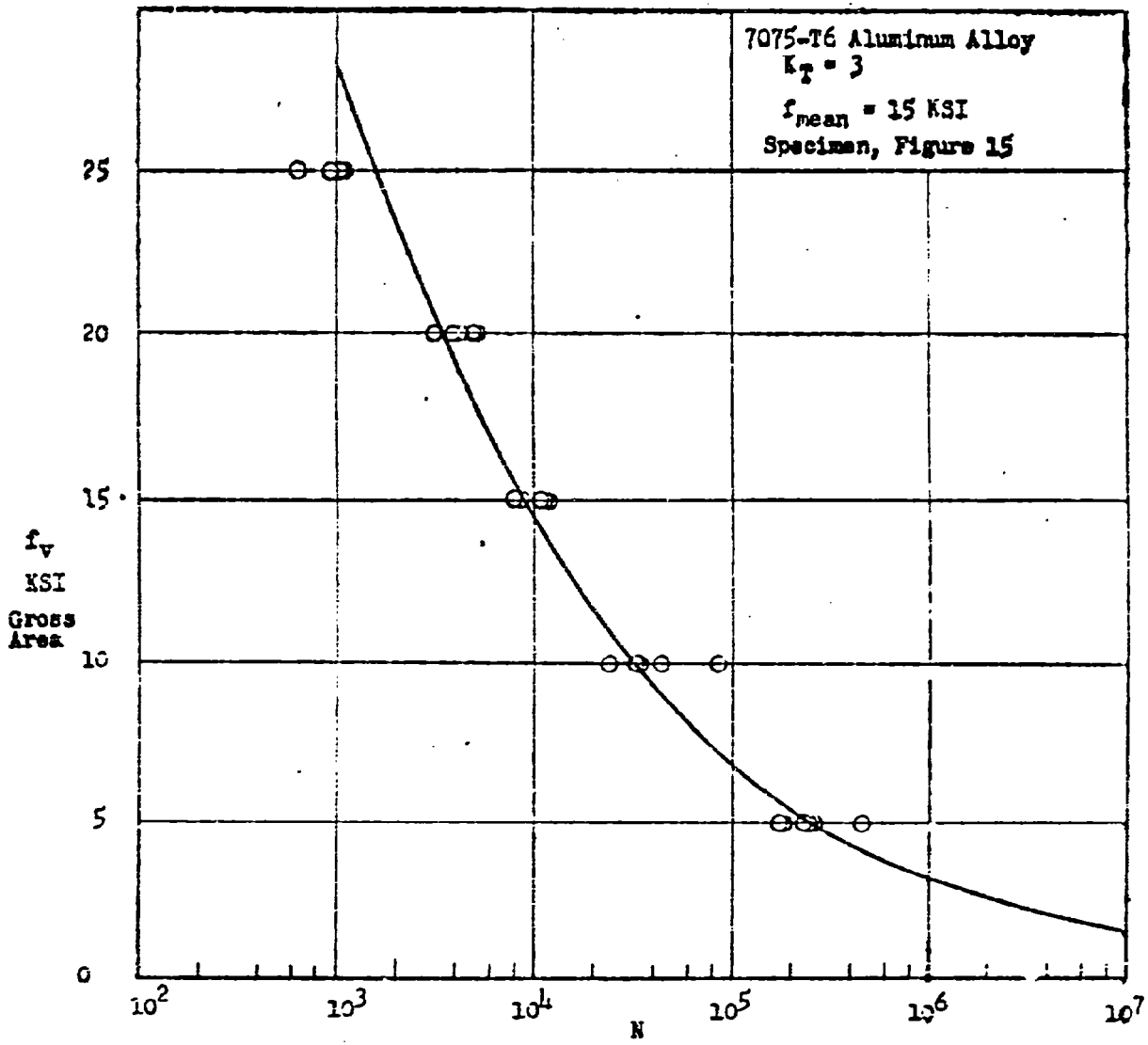



Figure 109 Experimental S-N Curve for Notched Sheet Coupons

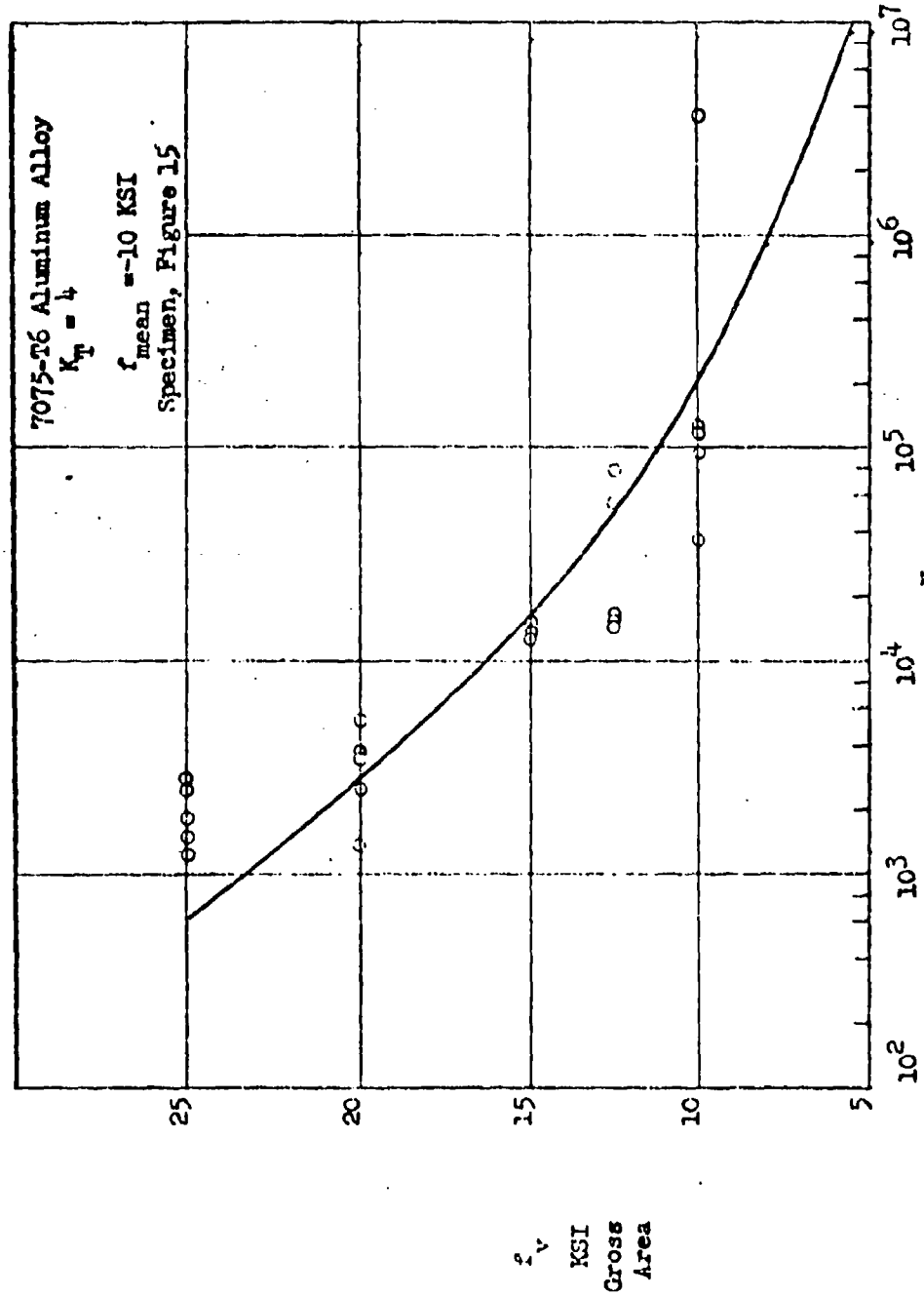



Figure 110 Experimental S-N Curve for Notched Sheet Coupons

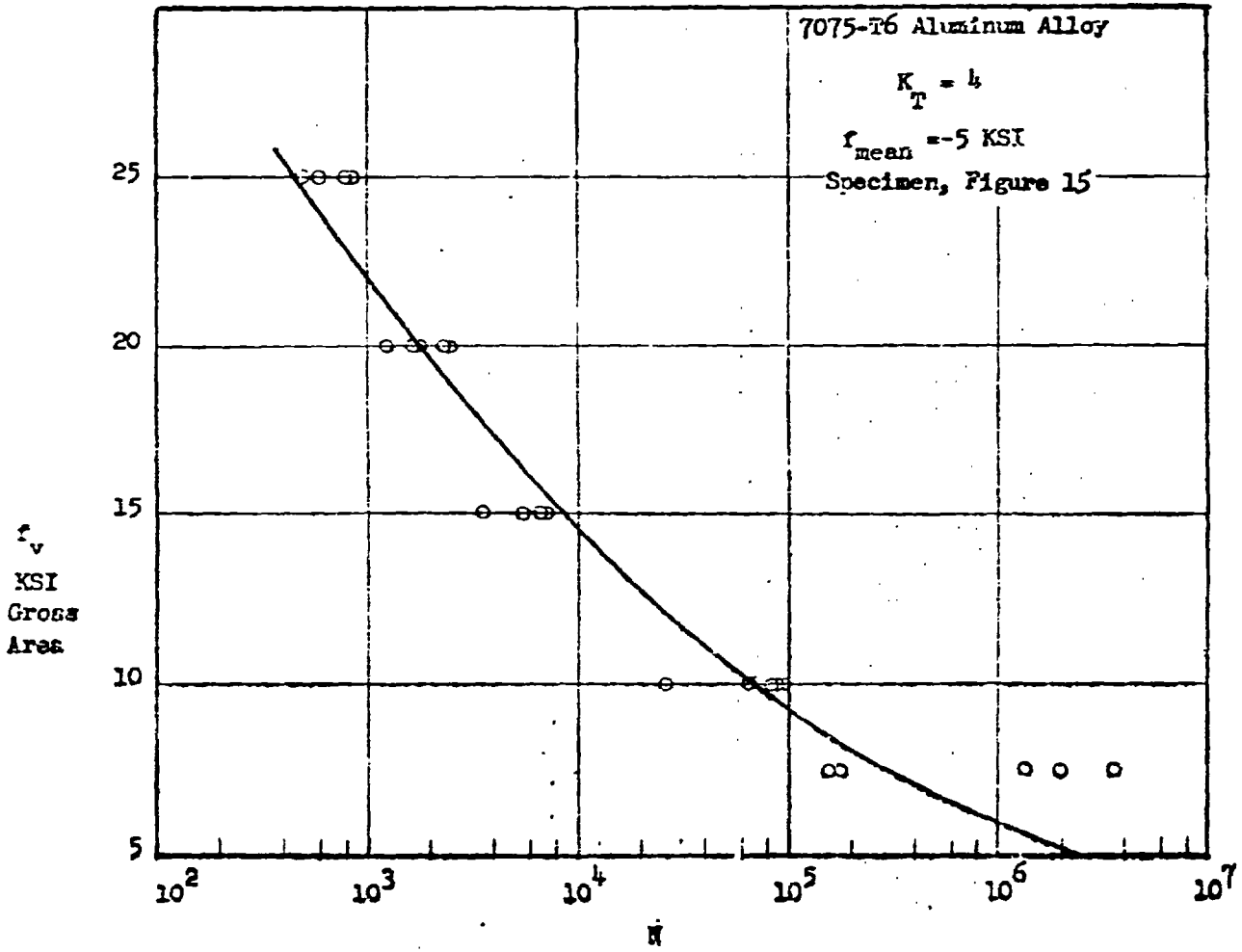
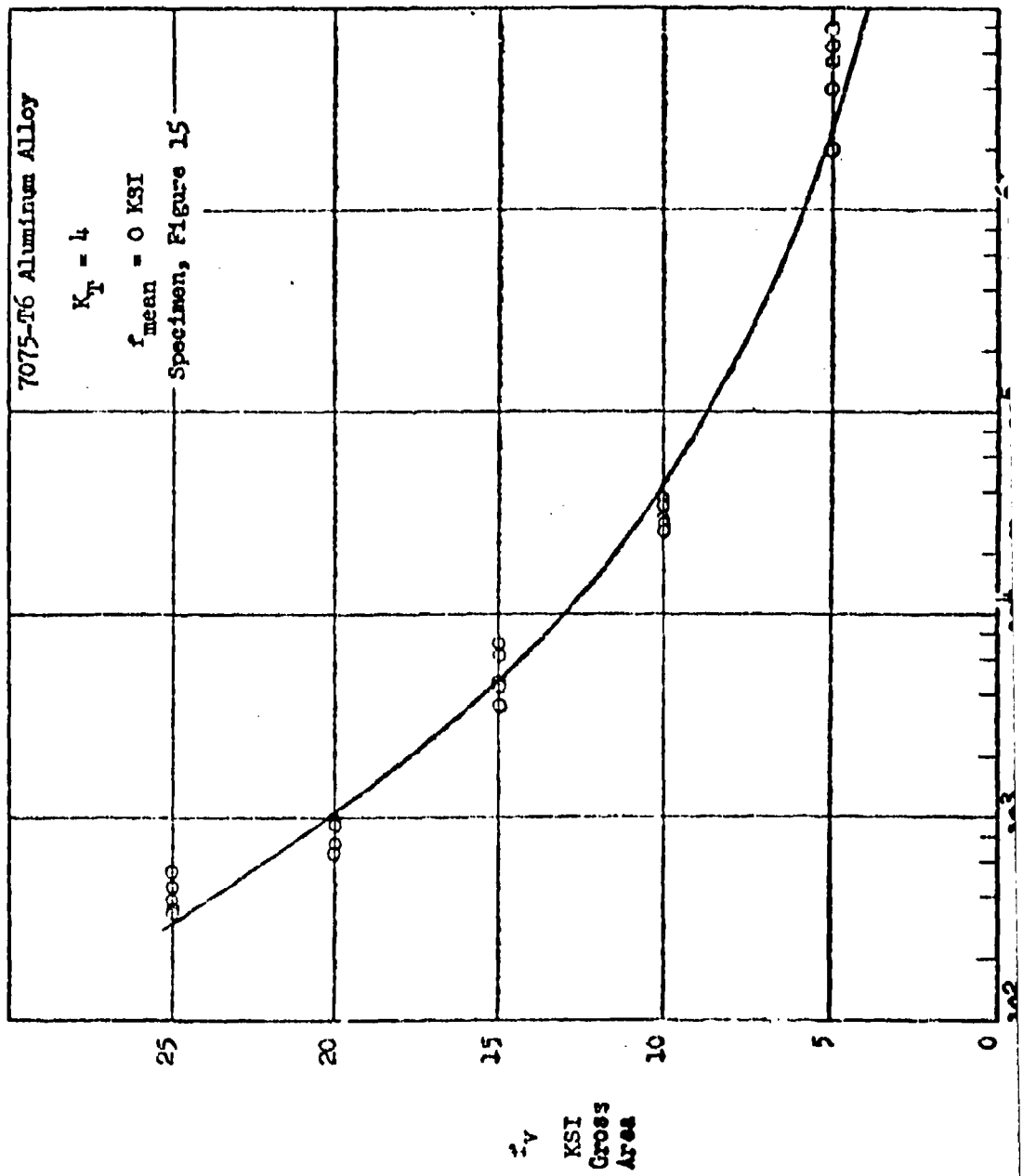



Figure 111 Experimental S-N Curve for Notched Sheet Coupons


7075-T6 Aluminum Alloy
$K_T$ = 4
$f_{mean}$ = 0 KSI
Specimen, Figure 15
25
20
15
10
5
0
KSI
Gross
Area

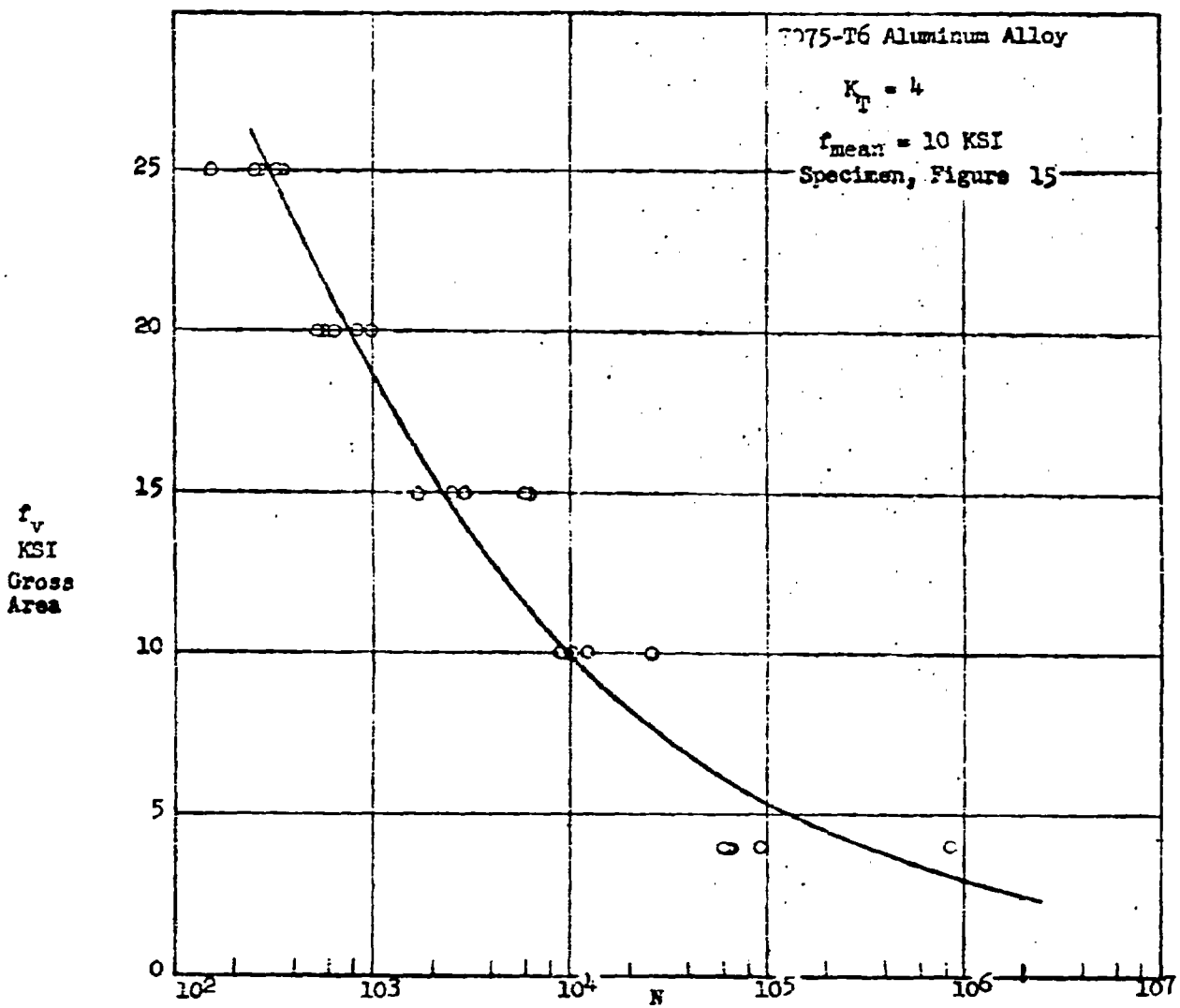



Figure 113 Experimental S-N Curve for Notched Sheet Coupons

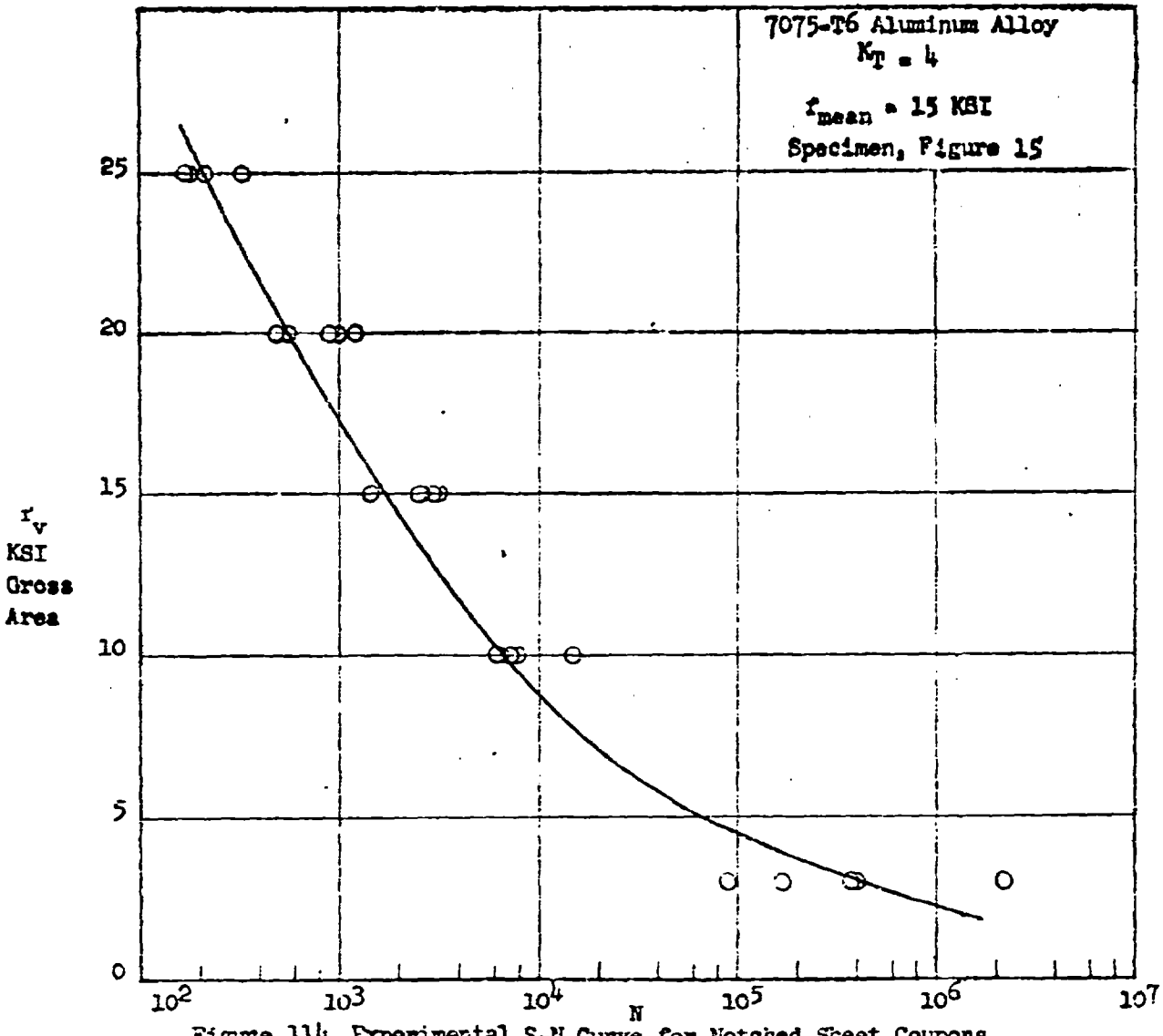



Figure 114 Experimental S-N Curve for Notched Sheet Coupons

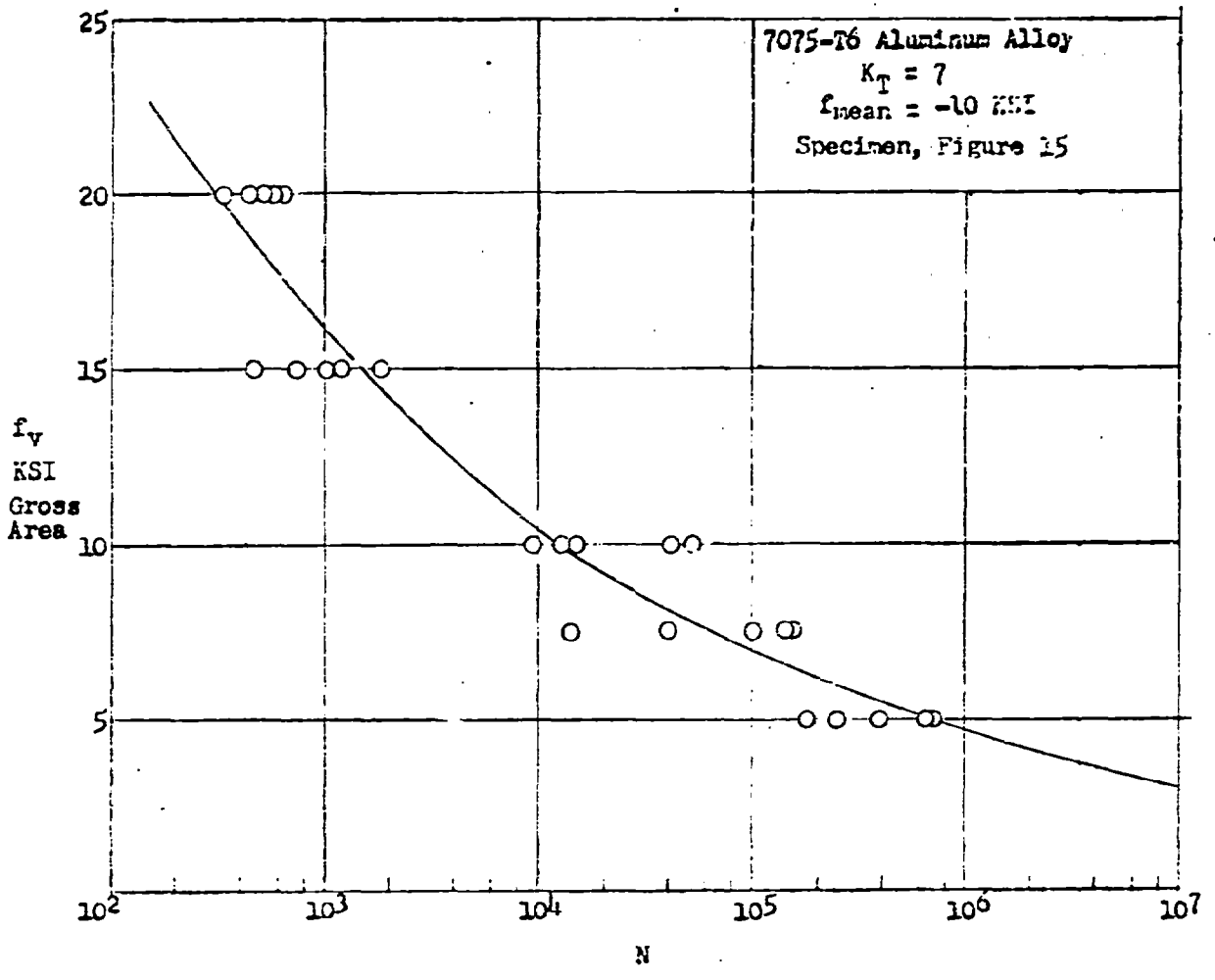



Figure 115 Experimental S-N Curve for Notched Sheet Coupons

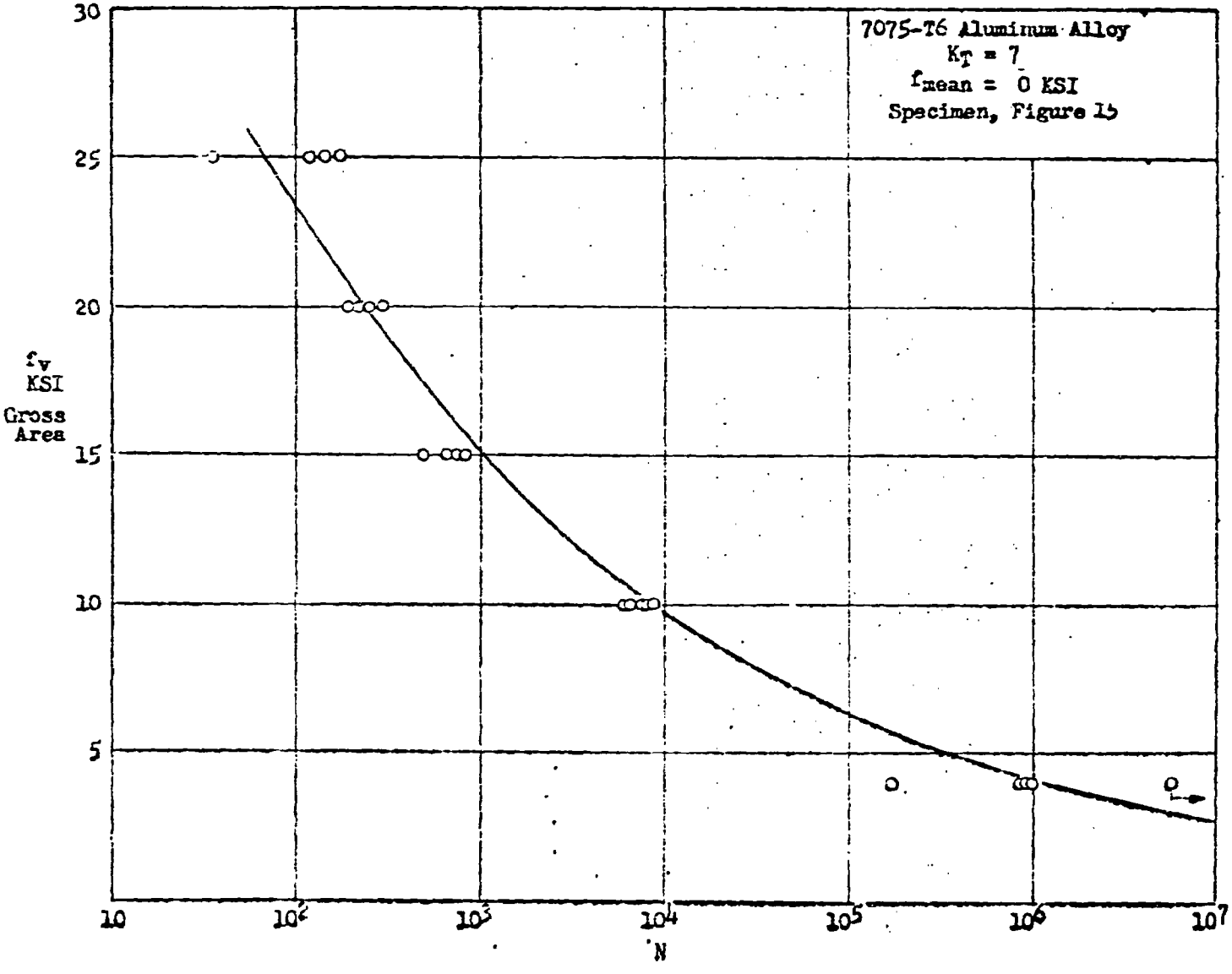



Figure 116 Experimental S-N Curve for Notched Sheet Coupons

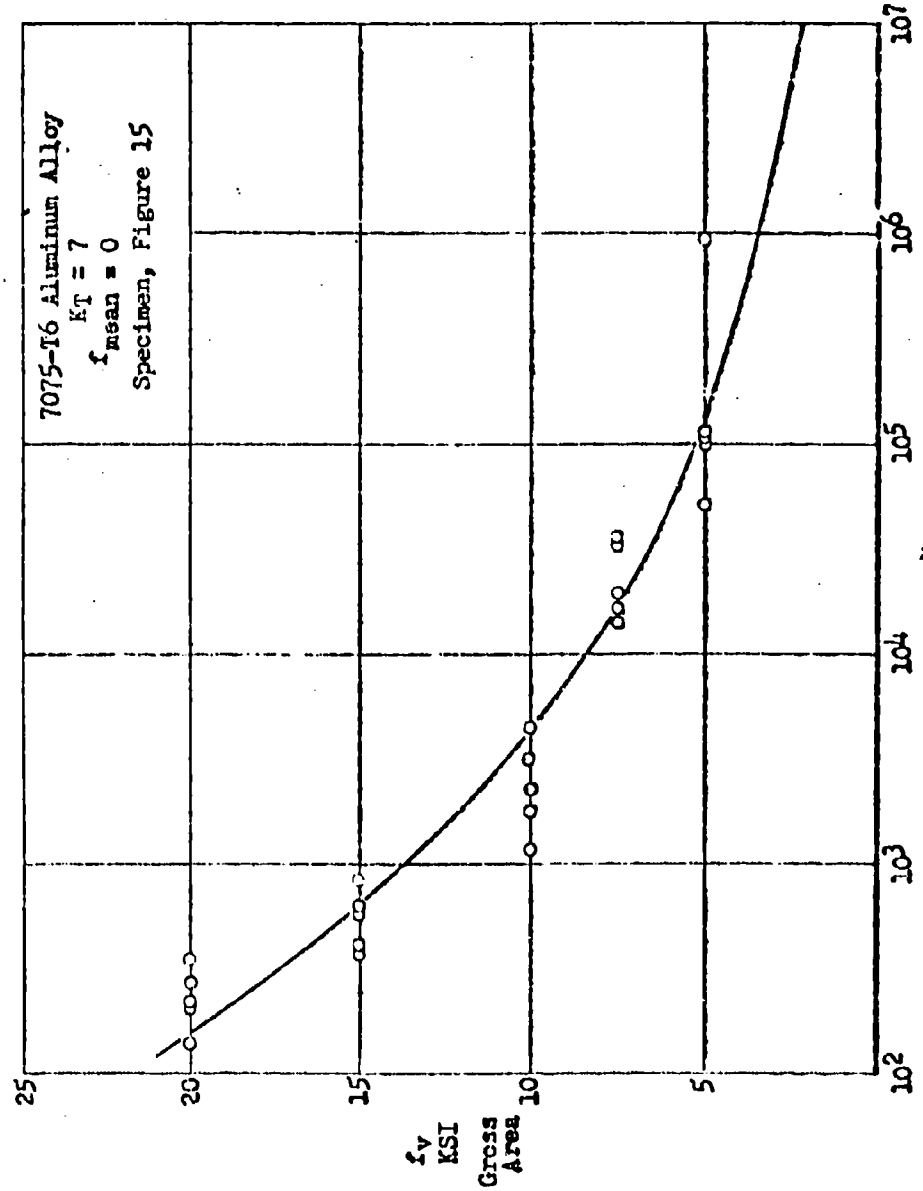



Figure 117 Experimental S-N Curve for Notched Sheet Coupons

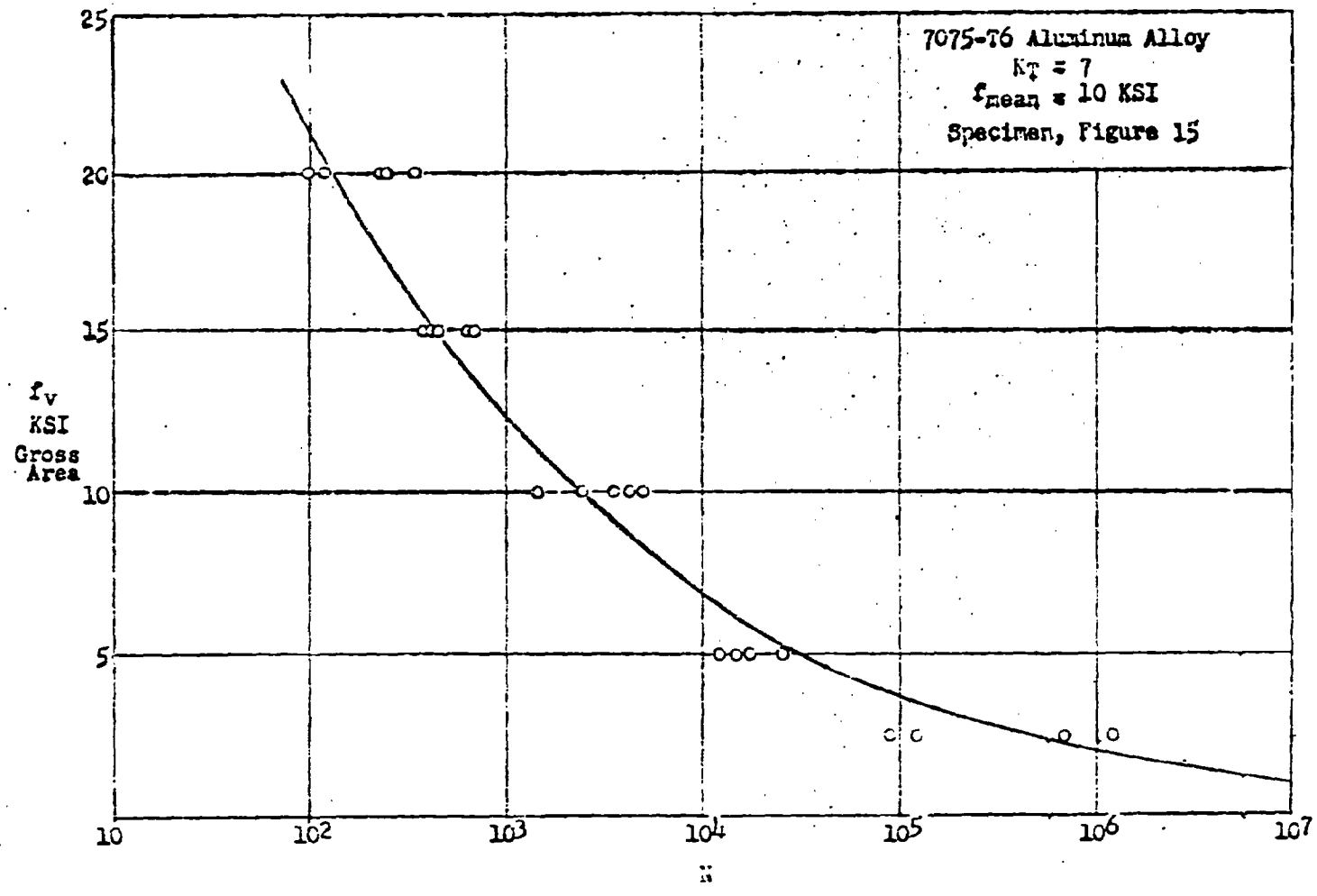



Figure 118 Experimental S-N Curve for Notched Sheet Coupons

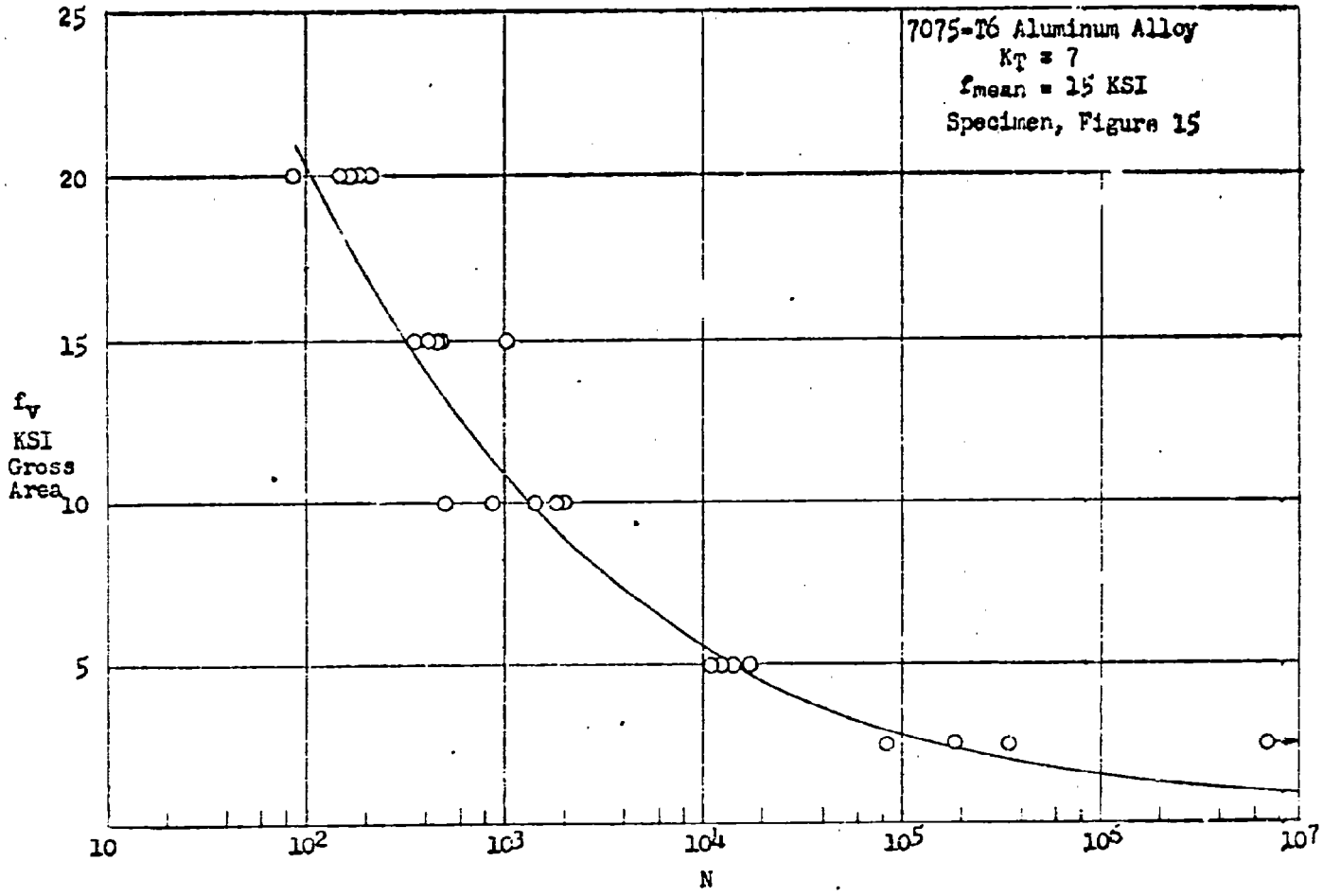



Figure 119 Experimental S-N Curve for Notched Sheet Coupons

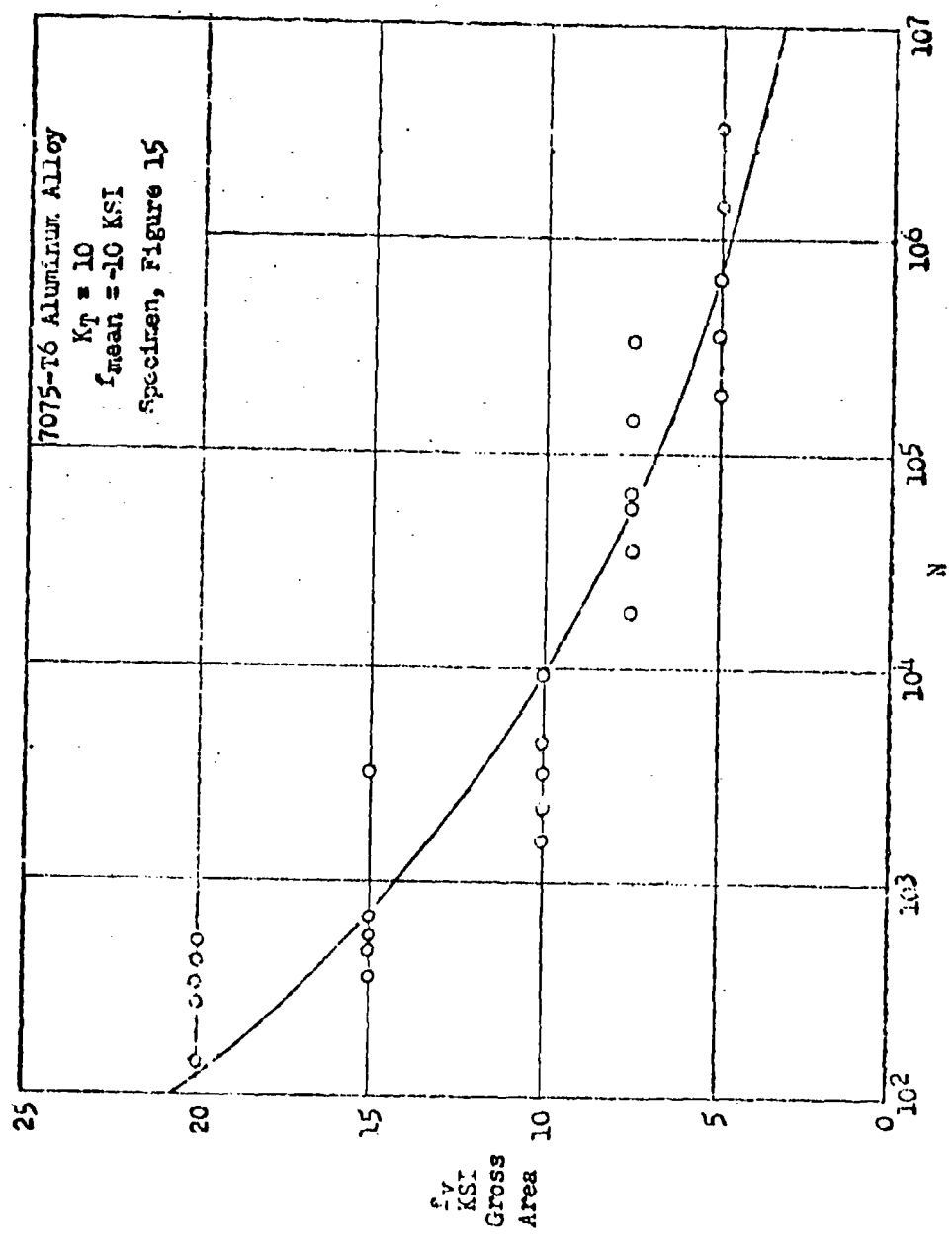



Figure 120 Experimental S-N Curve for Notched Sheet Coupons

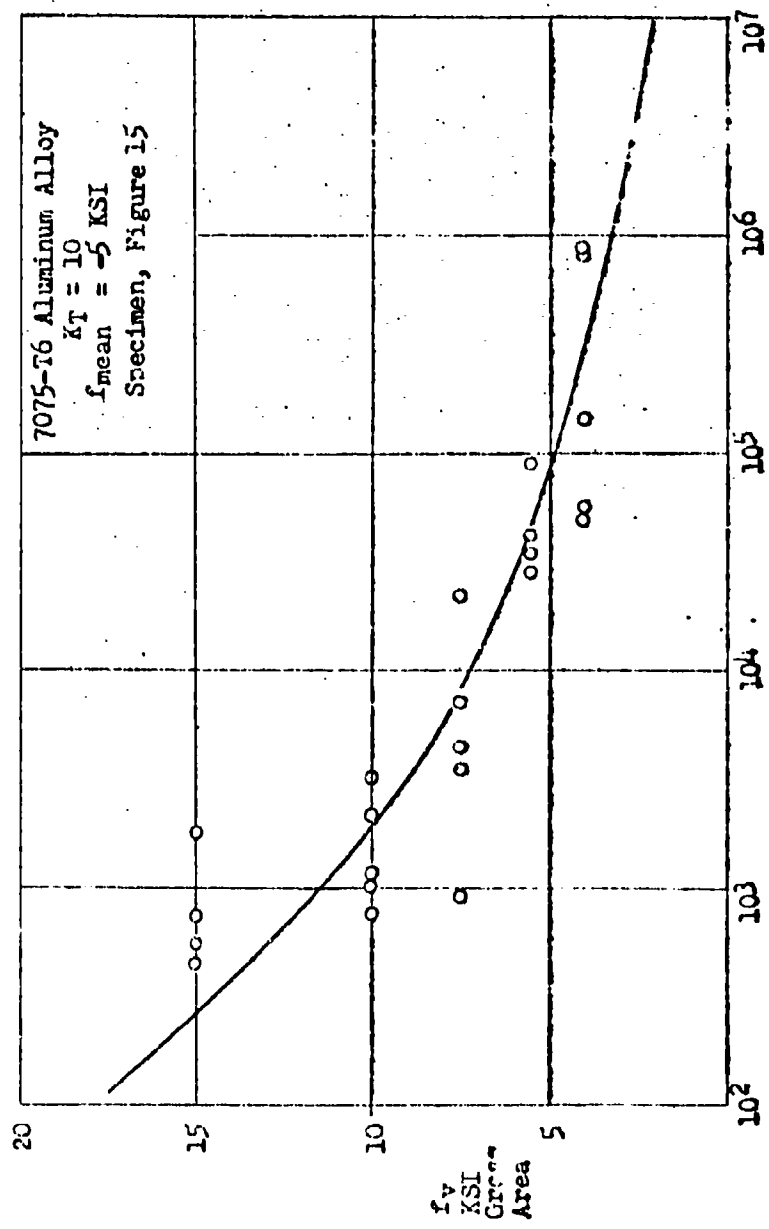



Figure 121 Experimental S-N Curve for Notched Sheet Coupons

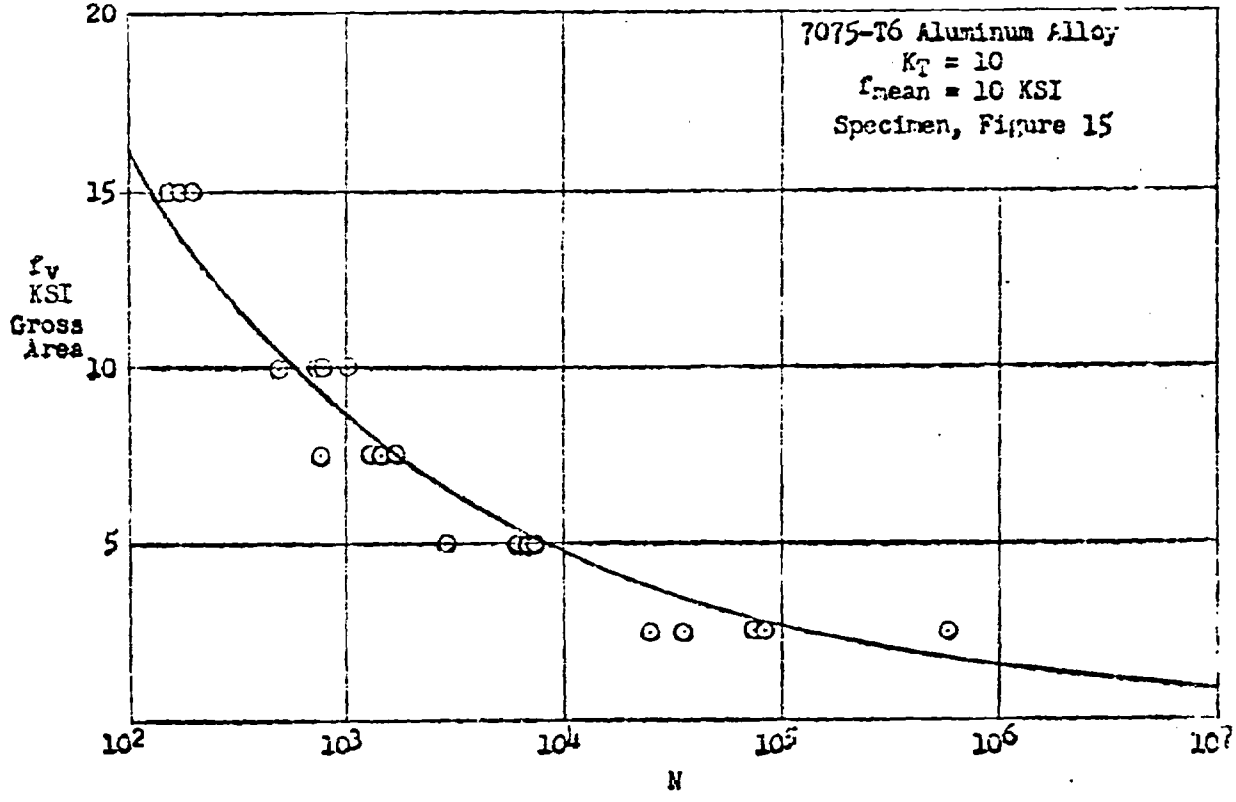



Figure 122 Experimental S-N Curve for Notched Sheet Coupons

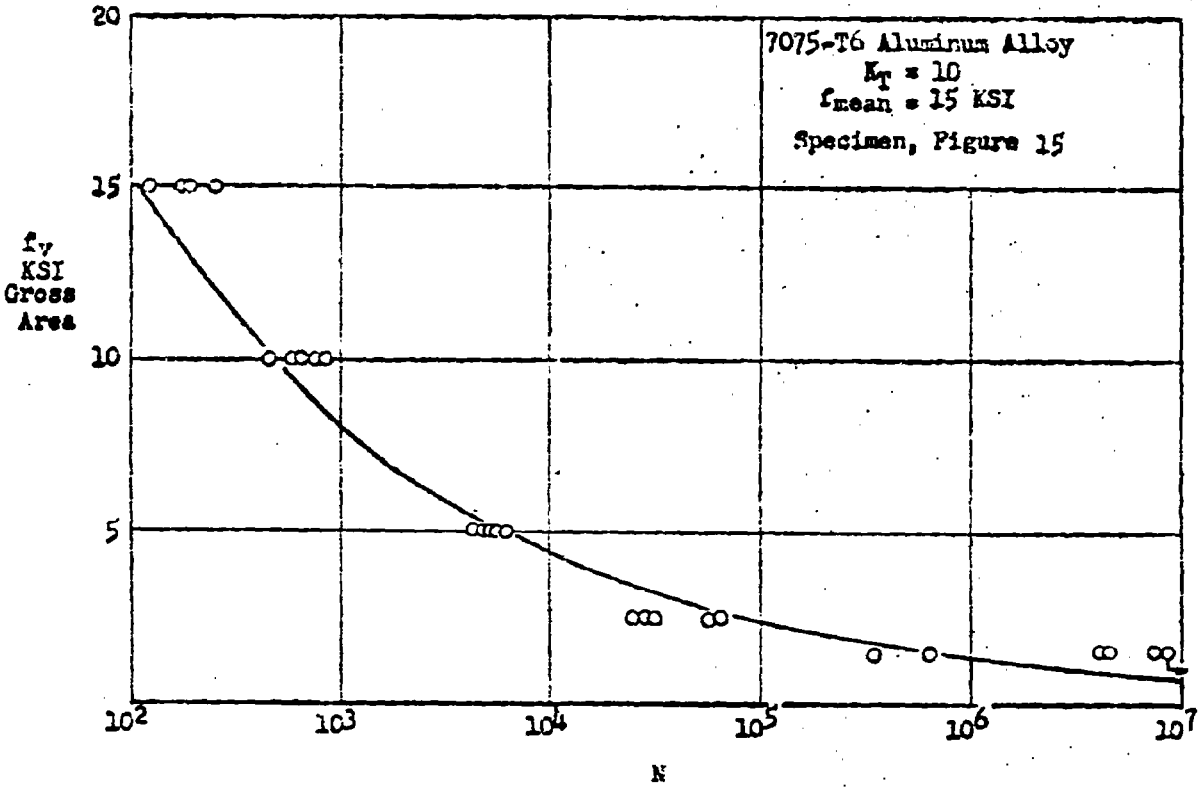



Figure 123 Experimental S-N Curve for Notched Sheet Coupons

## CONSTRUCTION OF S-N CURVES BY INTERPOLATION

The complete fatigue loading history for an airframe structure contains several types of varying load spectra, each acting at different mean load levels. One spectrum in particular, the high-performance fighter-trainer maneuver load history, is characterized by an essentially constant minimum load with the varying load excursions to a maximum magnitude and returning to the original minimum. For fighter-maneuver spectra, the normally defined mean load thus varies with each cycle. Interpolation procedures are required to provide the S-N curves for each of these two basic types of loading.

A. S-N curves of allowable symmetrical varying stresses about a constant mean stress of any specified value are most readily obtained from interpolation of S-N data plotted on a Christensen diagram along lines of the specified constant mean stress. Figure 124 illustrates this operation. The S-N curves in Figure 126 were obtained in this manner from Figure 124, and those in Figure 127 were obtained in a similar manner from Figure 125.

B. S-N curves of allowable unsymmetrical varying stresses above a constant minimum stress of any specified value are readily obtained by interpolation of S-N data plotted on a Christensen diagram along lines of the specified constant minimum stress. Figure 124 illustrates how this procedure results in a 45° line originating at the constant minimum stress in the rectilinear plot that leads to the S-N curve plotted in Figure 128. This latter figure also contains an S-N curve that was derived in the same manner from Figure 125.

C. S-N curves of allowable stresses with any ratio of $R = \frac{F_{min}}{F_{max}}$ may be obtained by interpolation along a radial line of slope $\frac{1}{R}$ on the $F_{min} - F_{max}$ scale.

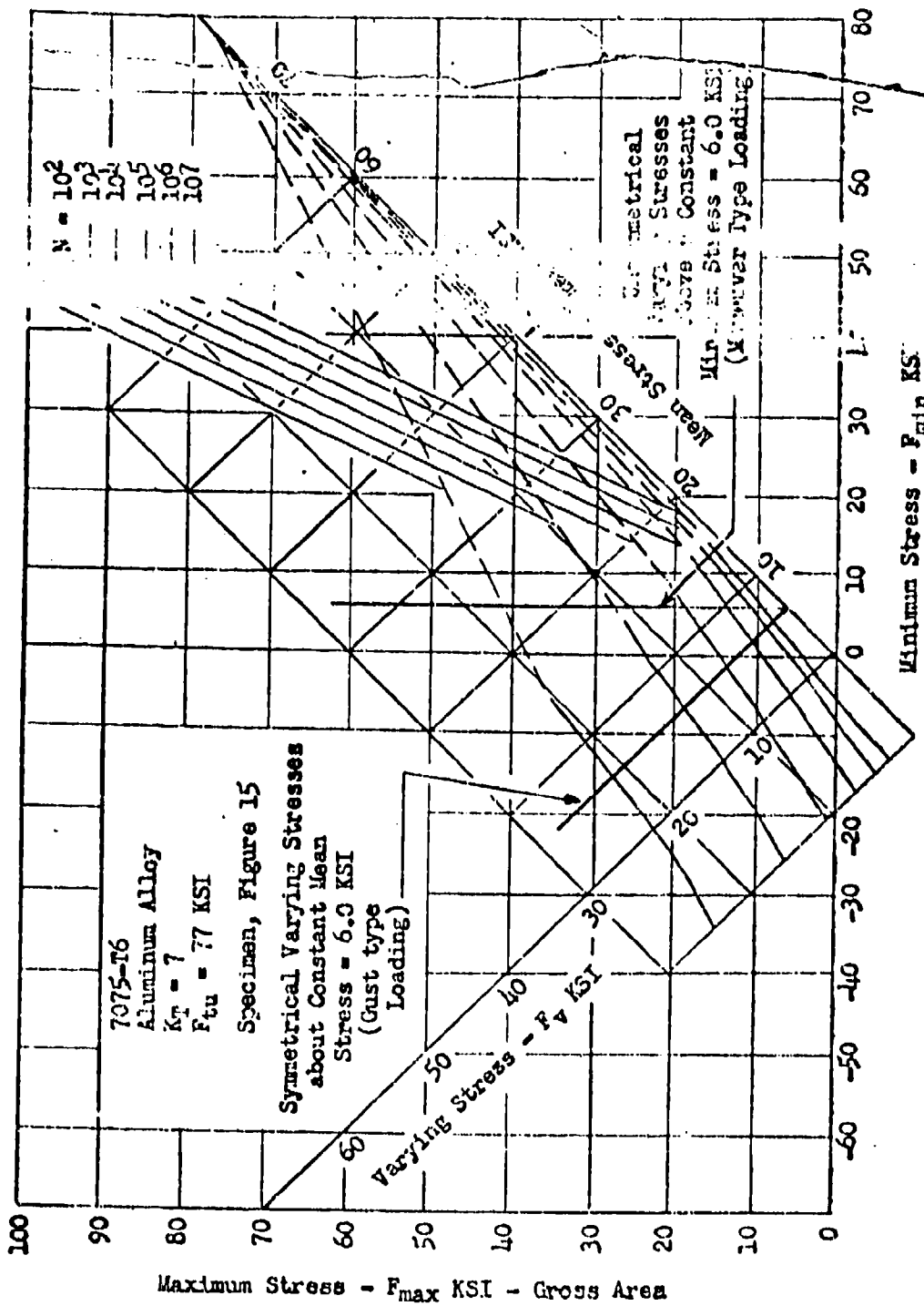



Figure 124 Christensen Diagram-Axial Loading, Coupon Test S-N Data - $K_t$ = 7

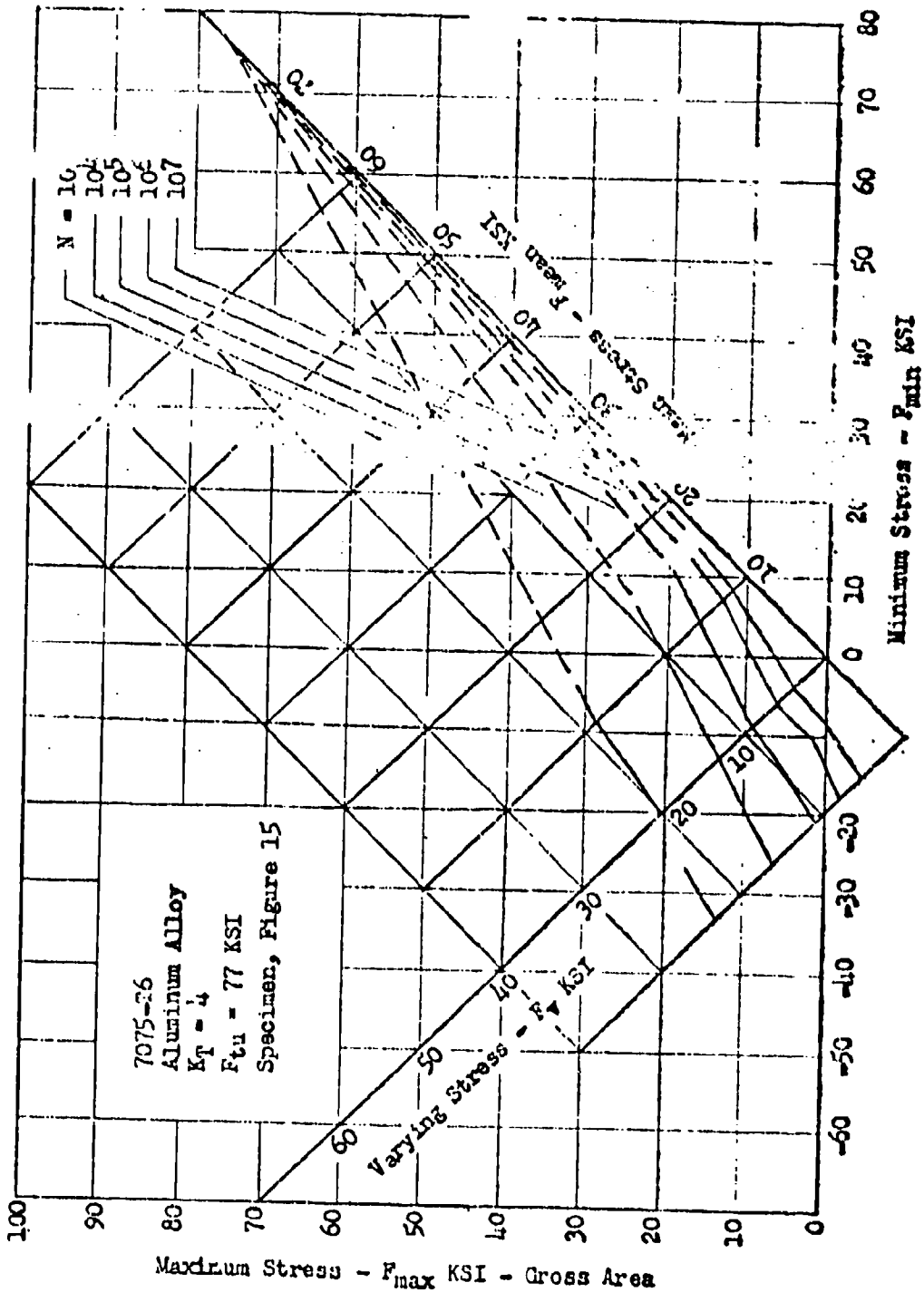



Figure 125 Goodman Diagram-Axial Loading, Coupon Test S-N Data - $K_T$ = 4

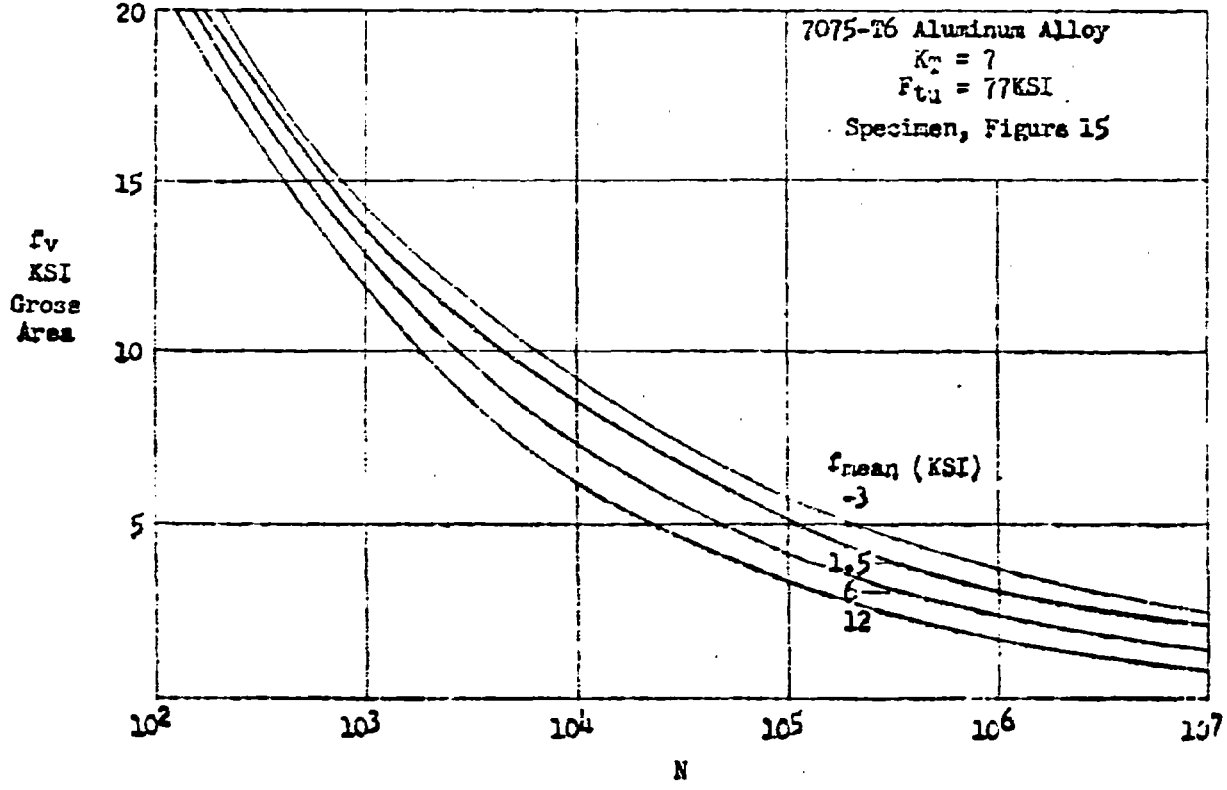



Figure 126 Interpolated S-N Curves for Notched Sheet Coupons - $K_T$ = 7

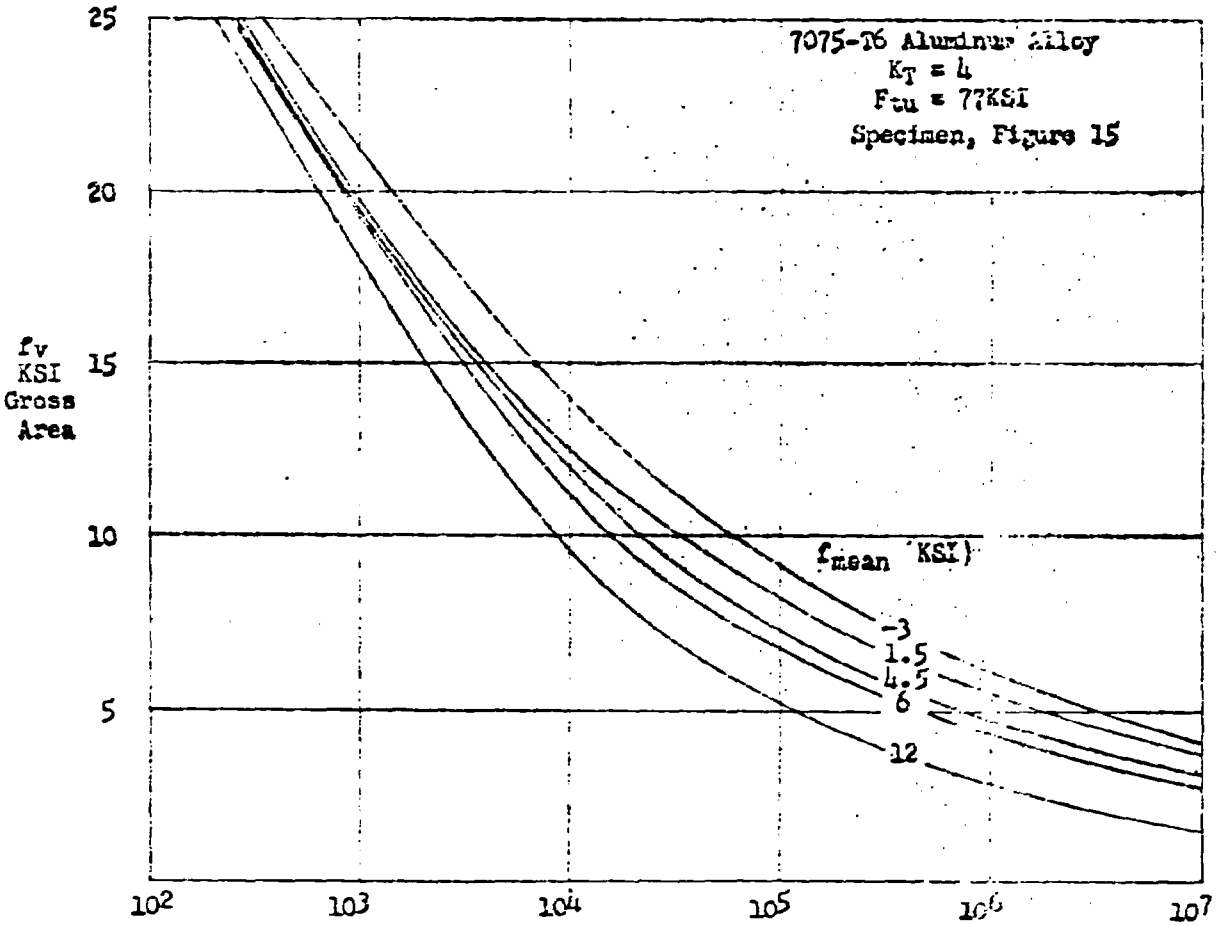



Figure 127 Interpolated S-N Curves for Notched Sheet Coupons - $K_T$ = 4

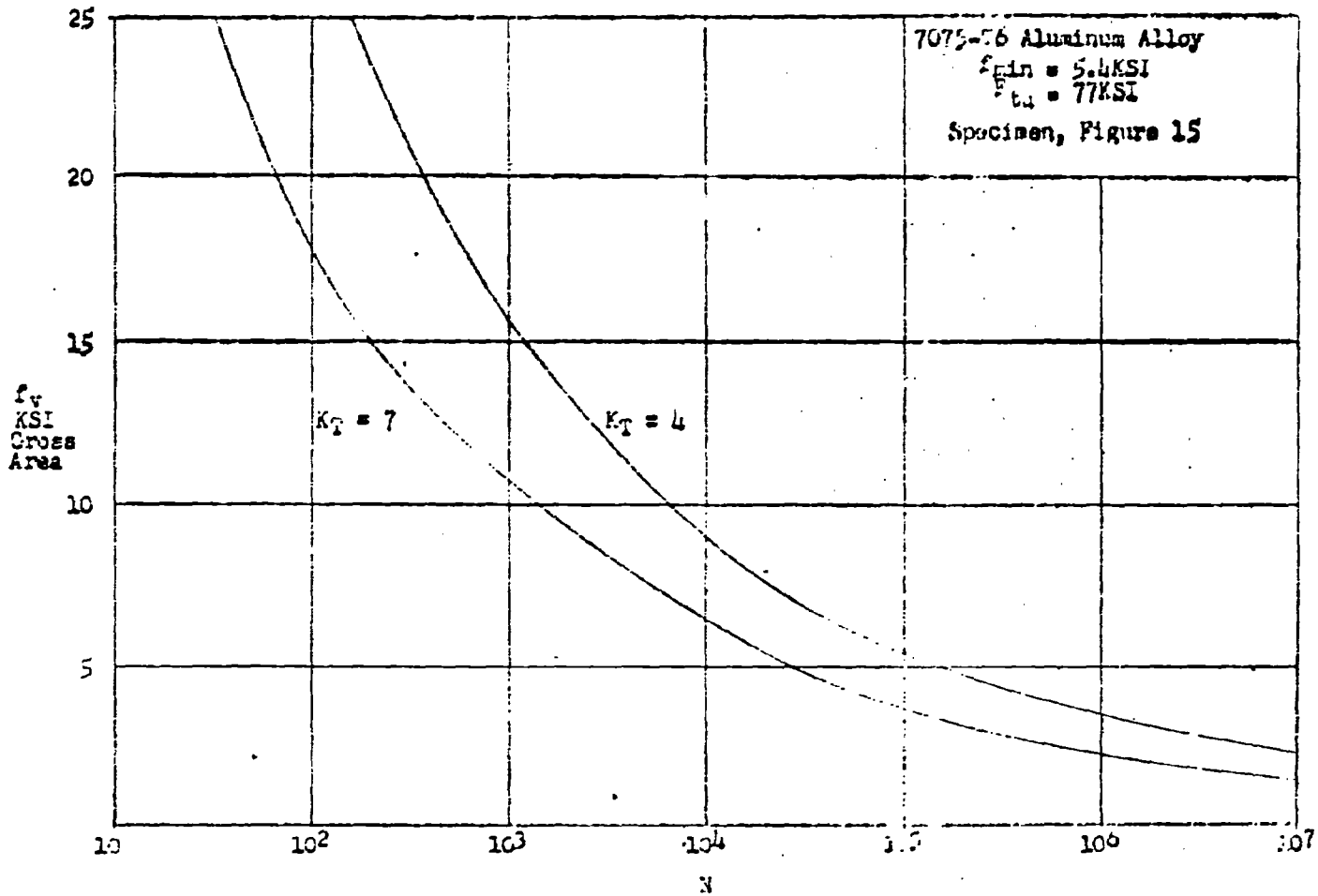



Figure 126 Interpolated S-N Curves for Notched Sheet Coupons Constant Minimum Stress (For Maneuver Type Loading)

## APPENDIX D

## PART 2 - SPECTRAL AXIAL LOAD DATA FROM SIMPLE COUPONS

### DESCRIPTION OF EQUIPMENT AND PROCEDURES FOR OBTAINING EXPERIMENTAL DATA ON COUPON SPECIMENS

This appendix describes the procedures and equipment employed in accomplishing the experimental and data processing phases of this investigation. An analysis is also presented of the degree of accuracy of the specimen loading histories as a reflection of the command signal emanating from the programming tape. In addition, discussion is presented relative to significant problems encountered in development of methods and equipment.

### CONSTRUCTION OF LOADING TAPES

#### Random Gust Loading Tapes

A one-inch multi-channel magnetic tape recording of a complete flight of an instrumented B-47 airplane was obtained from the Boeing Airplane Company. A photograph of the equipment which was used for converting the flight data to test input tapes is shown as Figure 130. A full length oscillograph of this instrumentation tape was visually scanned in order to identify signals of high cyclic activity. The signals representing the bending moments occurring at the wing root during a 96-minute low altitude pass (800 feet at 280 knots) was selected for adaptation to specimen loading signals for this investigation.

The selected flight record was transcribed on dual-channel 1/4-inch magnetic tape, as shown schematically on Figure 131. The flight record was passed through an electronic scanning system which continuously determined and subtracted out variations of mean load from the initial mean value. The mean variations were recorded on Channel No. 2 and the resulting dynamic signal was recorded on Channel No. 1. In order to obtain the shortest testing time possible within the frequency limitations of the testing equipment, the 96-minute flight histories were compressed to about 6 minutes for the wing root trace. Ten copies of the transcribed wing root trace were recorded and spliced together into one-hour continuous programming tape.

In an effort to obtain a random trace with a markedly different spectrum shape, the dynamic signal (Channel No. 1) of the wing root programming tape was re-recorded through a non-linear amplification system. To illustrate the change in shape produced, spectral representations based on zero crossing peak counts of the wing root, modified wing root unit programming tapes are shown on Figure 132.

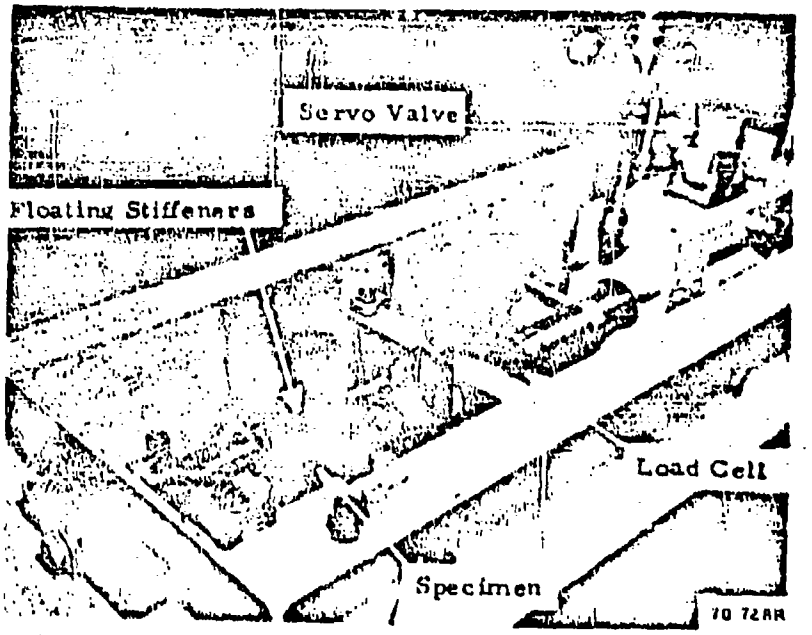



Figure 129 Close-up of Specimen Installation

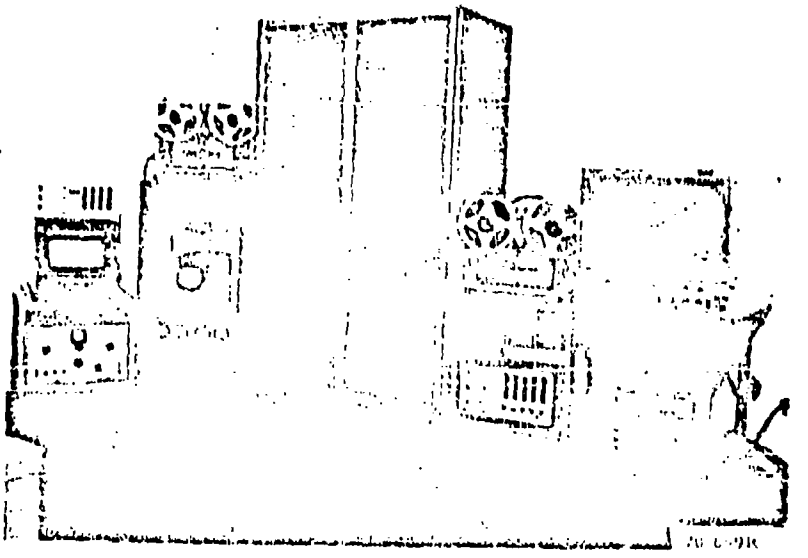


Figure 130 General View of Tape Construction and Data Reduction Equipment

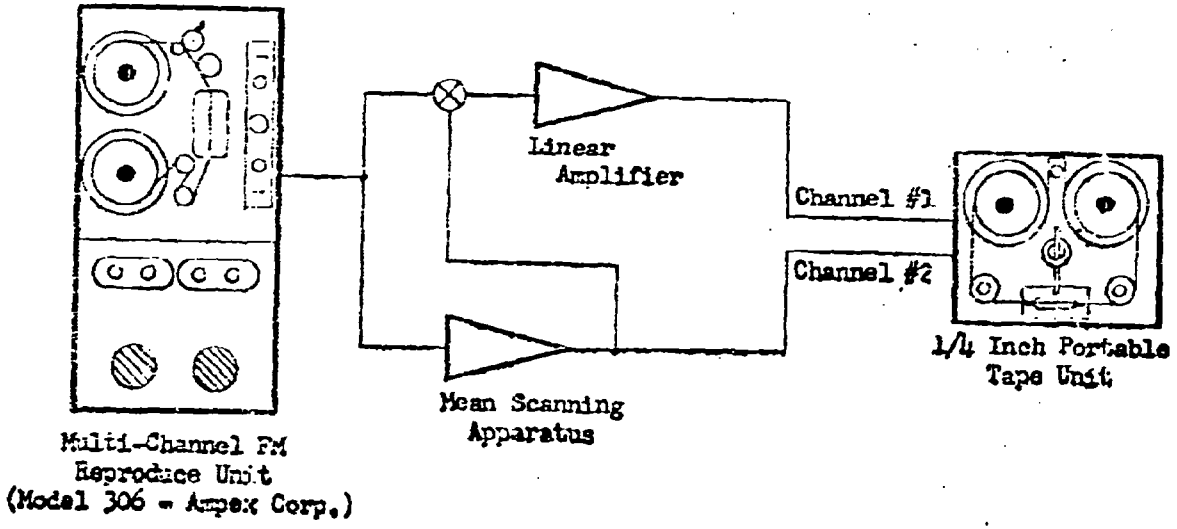



Figure 131 Schematic of Transcription of Flight Record

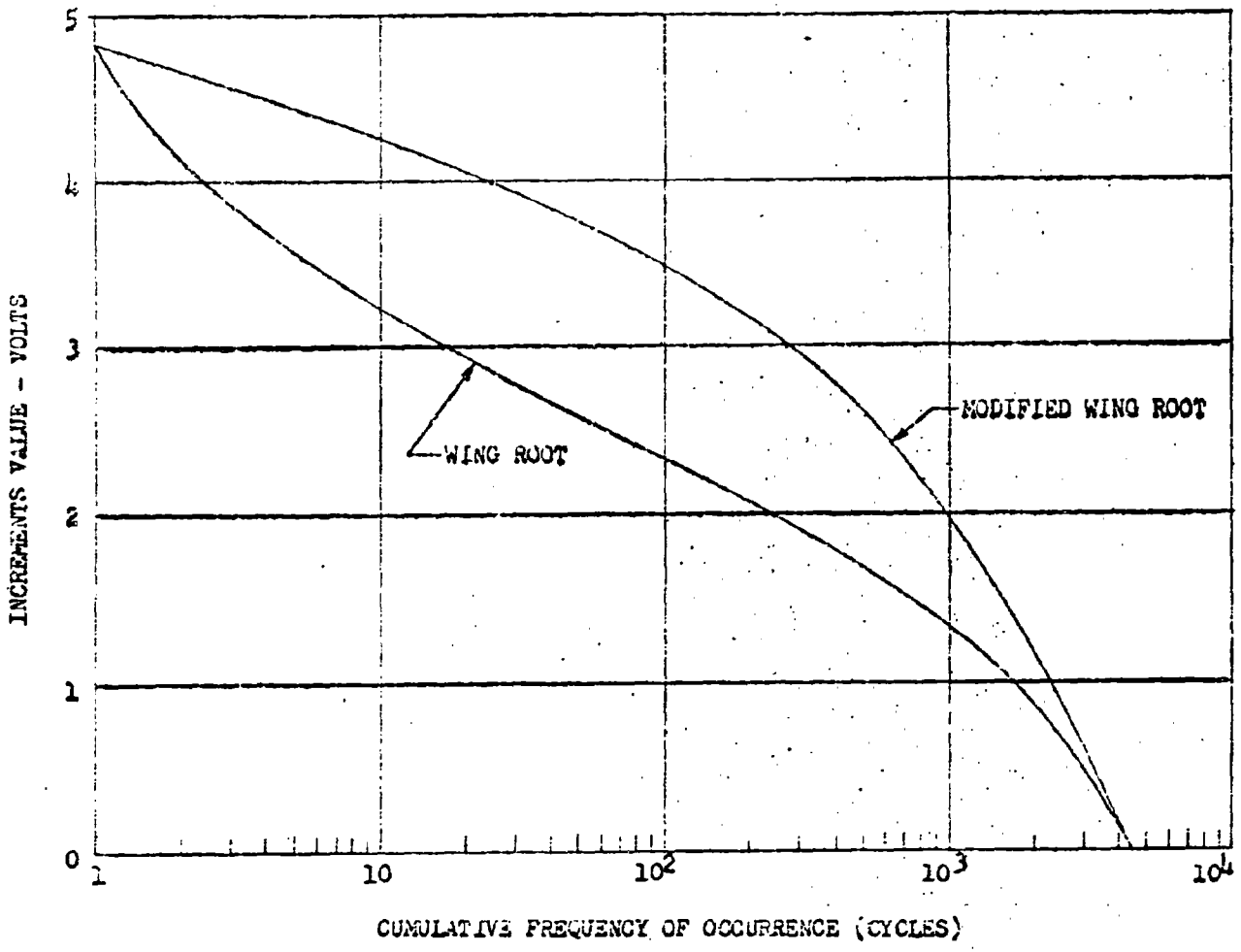



FIGURE 132 MEAN CROSSING PEAK COUNT-WING ROOT AND MODIFIED WING ROOT TRACES

The system used to electrically alter the spectrum shape of a random trace is shown schematically on Figure 133. A desired input-output voltage pattern was drawn on the oscilloscope display screen and the non-linear amplification system was calibrated to match this relationship. Spectrum modification was accomplished by rerecording the tape through this calibrated setup.

## FATIGUE TESTING PROGRAM

The limited flight loading histories recorded by the 96-minute wing trace was insufficient to provide the desired characteristics of a representative extende random service loading history. To obtain the desired loading history, the random wing root programming signal was modified. The maximum positive and nega tive loads were made symmetrical and larger loads were inserted so as to repres a longer service loading spectrum.

Repetitions of 10 basic sections of the random signal (identified as $A_1$, $A_2$, $B_1$ $B_2$ ..... $E_1$, $E_2$) were spliced together to make four programming tapes, each approximately one hour long. The $A_1$ section was obtained by rerecording the the basic wing root signal through a non-linear amplifier such that the maximum negative excursion was limited to match the maximum positive excursion. This operation is similar to that used in making the unit modified wing trace and was shown schematically on Figure 133. The $B_1$ section was obtained by rerecording the $A_1$ section through the non-linear amplifier such that the maximum positive and negative excursions are increased about 15%, the next smaller excursions are amplified only slightly and the smallest excursions experience negligible change. The $C_1$, $D_1$ and $E_1$ sections are obtained in the same manner with the maximum positive and negative excursions increased by approximately 20%, 30%, and 40% respectively, over the maximum $A_1$ excursions. The $A_2$ through $E_2$ sections were obtained by rerecording the $A_1$ through $E_1$ sections through a 75% linear amplification system. These 10 basic sections are summarized below.

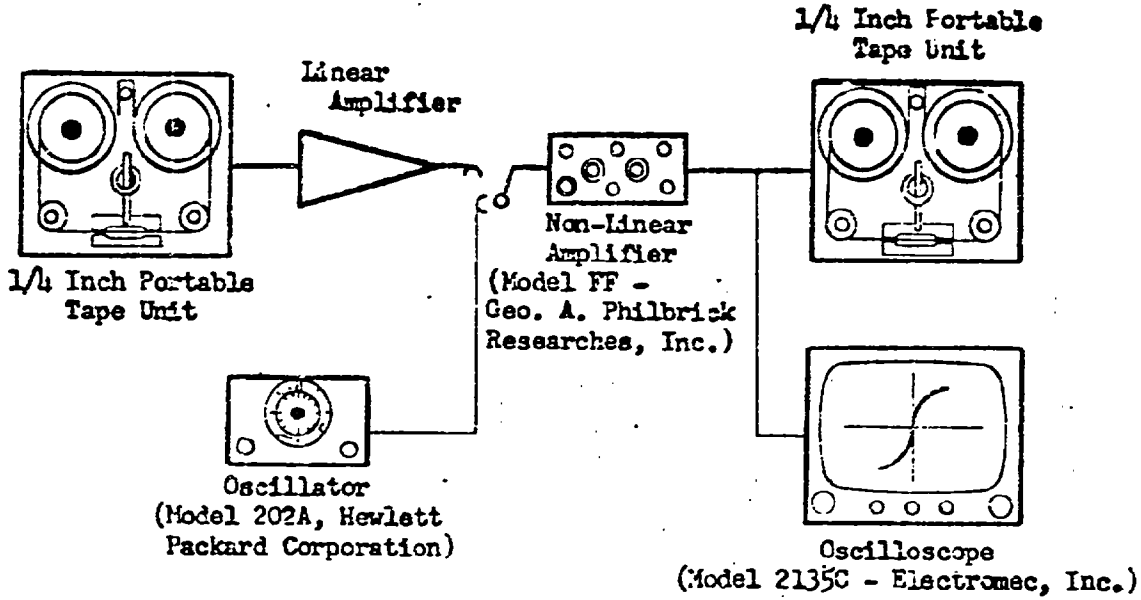



Figure 133 Schematic of System for Altering Spectrum Shapes

| | |
|---|---|
| $A_1$ | Unit wing root signal modified so that maximum positive and negative excursions are approximately equal. |
| $A_2$ | Section $A_1$ x 75% (linear amplifications) |
| $B_1$ | Section $A_1$ modified so that maximum positive and negative excursions amplified approximately 15%. |
| $B_2$ | Section $B_1$ x 75% (linear amplification) |
| $C_1$ | Section $A_1$ modified so that maximum positive and negative excursions amplified approximately 20% |
| $C_2$ | Section $C_1$ x 75% (linear amplification) |
| $D_1$ | Section $A_1$ modified so that maximum positive and negative excursions amplified approximately 30% |
| $D_2$ | Section $D_1$ x 75% (linear amplification) |
| $E_1$ | Section $A_1$ modified so that maximum positive and negative excursions amplified approximately 40% |
| $E_2$ | Section $E_1$ x 75% (linear amplification) |

Four programming tapes (identified as Tape Nos. 49, 50, 51 and 52) were then constructed by splicing the 10 basic sections together in the following sequence.

Tape No. 49

| | | | | | | | | | |
|---|---|---|---|---|---|---|---|---|---|
| $A_1$ | $A_2$ | $A_1$ | $A_2$ | $C_1$ | $A_2$ | $A_1$ | $A_2$ | $A_1$ | $C_2$ |

Tape No. 50

| | | | | | | | | | |
|---|---|---|---|---|---|---|---|---|---|
| $A_1$ | $A_2$ | $A_1$ | $A_2$ | $D_1$ | $A_2$ | $A_1$ | $A_2$ | $A_1$ | $D_2$ |

Tape No. 51

| | | | | | | | | | |
|---|---|---|---|---|---|---|---|---|---|
| $A_1$ | $A_2$ | $A_1$ | $A_2$ | $E_1$ | $A_2$ | $A_1$ | $A_2$ | $A_1$ | $E_2$ |

Tape No. 52

| | | | | | | | | | |
|---|---|---|---|---|---|---|---|---|---|
| $A_1$ | $A_2$ | $A_1$ | $B_2$ | $B_1$ | $A_1$ | $A_2$ | $A_2$ | $B_1$ | $B_2$ |

These four tapes were utilized for testing specimens in the following 11-hour sequence to obtain the desired extended random gust loading spectrum.

| Test Sequence | Loading Tape No. |
|---|---|
| 1 | 52 |
| 2 | 49 |
| 3 | 52 |
| 4 | 52 |
| 5 | 50 |
| 6 | 49 |
| 7 | 49 |
| 8 | 52 |
| 9 | 50 |
| 10 | 52 |
| 11 | 52 |
| 12 | 52 |
| 13 | 49 |
| 4 | 51 |

Random Military Maneuver Tape

Because of the unavailability of an appropriate recording of representative military maneuver loadings, a tape was constructed to be consistent with the loading spectrum for fighter aircraft which is described in specification MIL-A-8866.

The unit wing root programming trace was played through the non-linear amplification system so that the negative excursions were suppressed and the positive excursions were modulated to match the spectrum described above. This operation was similar to that described in making the modified wing root trace which was shown schematically in Figure 132.

Step Ordered Gust Loading Tapes

Cyclic step-ordered loading tapes were constructed to simulate the average test life of a given group of random loading histories. Three combinations of stress interval and block size were used:

(1) 1,000 psi stress interval and 1/10 block size
(2) 1,000 psi stress interval and 1/20 block size
(3) 4,000 psi stress interval and 1/20 block size

The system used to construct the step-ordered loading tapes is shown schematically on Figure 134.

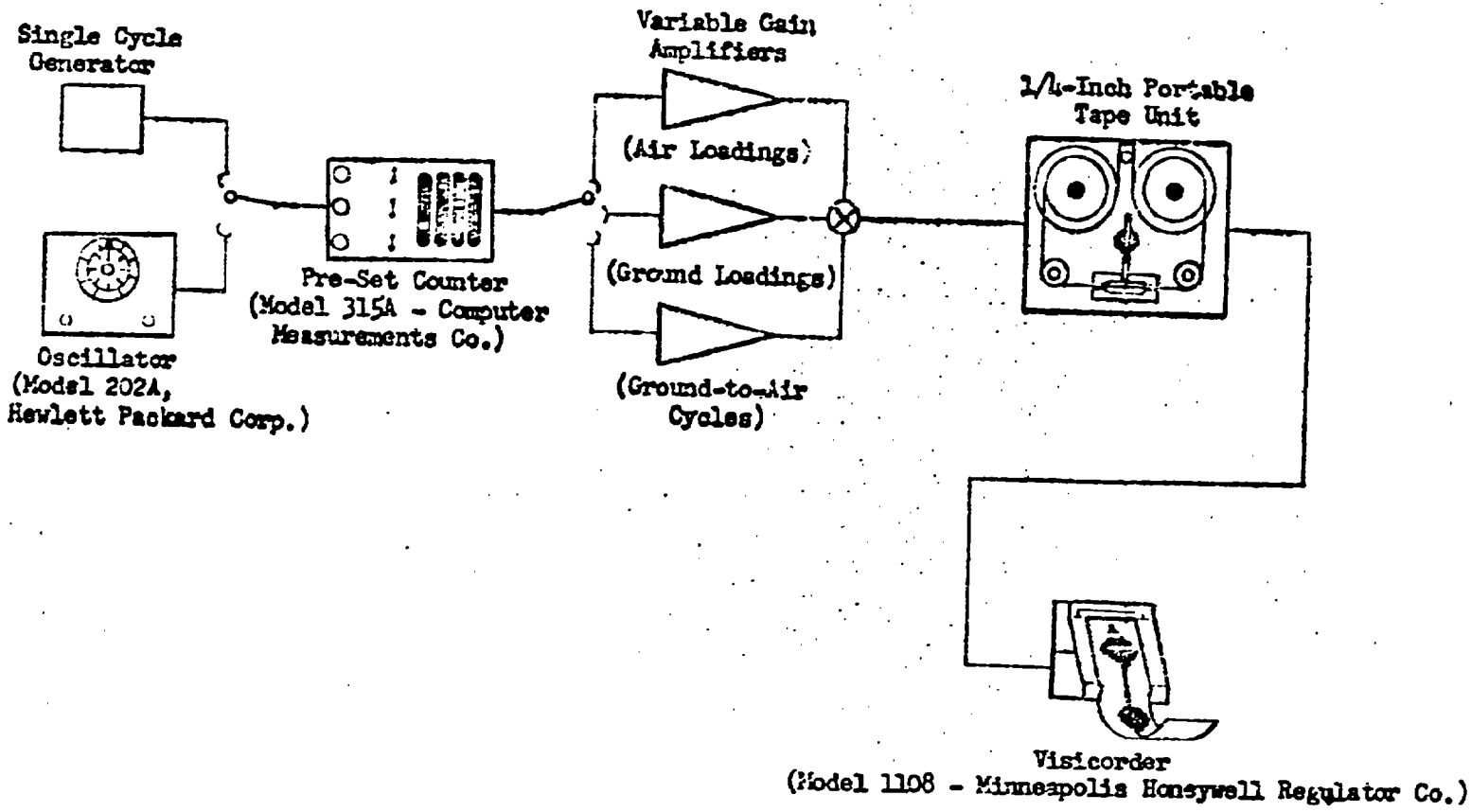
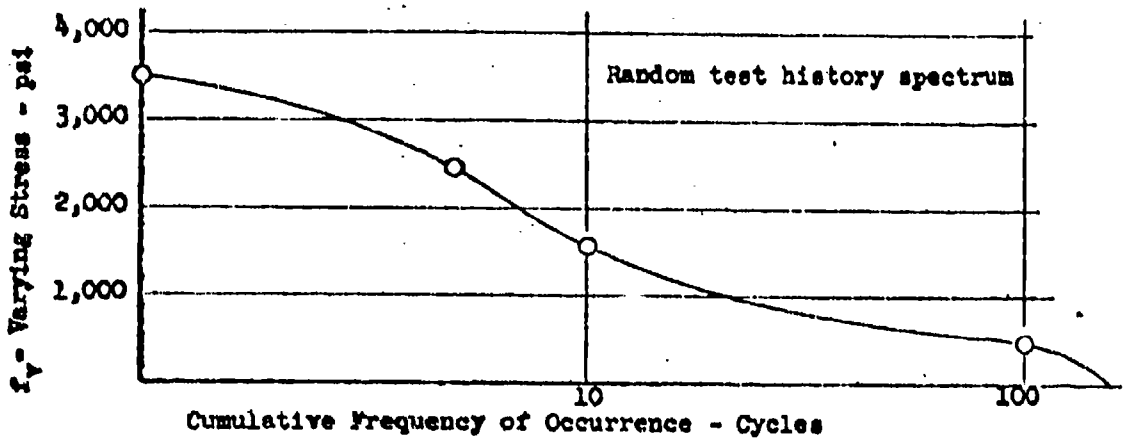



Figure 134 Schematic of Step Ordered Tape Generation

The procedure used in constructing an ordered loading tape is shown in the following example.

For a given average random test history, construct an ordered programming tape of 1,000 psi stress interval size, and 1/10 block size.

(1) Graph the random test history spectrum.
(2) Observe and record in columnar form the cumulative frequency count at the half range intervals (500 psi, 1500 psi, 2500 psi, etc.) on the random spectrum.



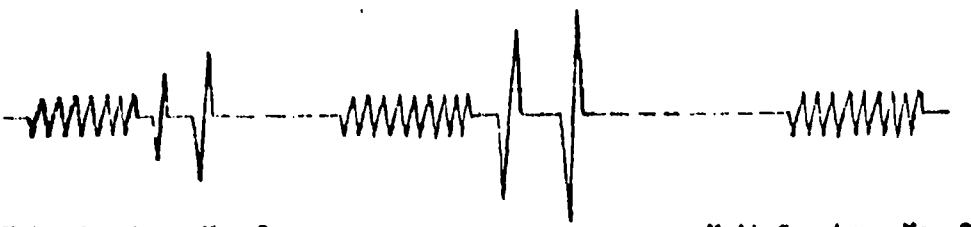

(3) Determine the total number of cycles to be applied at each stress level (1000 psi, 2000 psi, 3000 psi, etc.) by calculating differences between the cumulative counts observed in step (2).

(4) Divide the total number of cycles for each stress level calculated in step (3) by ten. This determines the number of cycles to be applied in each unit spectrum at each stress level. Distribute each fractional cycle to the corresponding half life.

(5) Construct a test programming schedule for the "stress level-cycle" combinations from step (4).

| $f_v$ | $\sum n$ | n | Unit Spectrum Number | | | | | | | | | |
|---|---|---|---|---|---|---|---|---|---|---|---|---|
| | | | (1) | (2) | (3) | (4) | (5) | (6) | (7) | (8) | (9) | (10) |
| 500 | 100 | | | | | | | | | | | |
| 1,000 | | 90 | 9 | 9 | 9 | 9 | 9 | 9 | 9 | 9 | 9 | 9 |
| 1,500 | 10 | | | | | | | | | | | |
| 2,000 | | 5 | 1 | | 1 | | 1 | | 1 | | 1 | |
| 2,500 | 5 | | | | | | | | | | | |
| 3,000 | | 4 | 1 | | | 1 | | 1 | | | 1 | |
| 3,500 | 1 | 1 | | | | | 1 | | | | | |

(6) Employing an "oscillator-preset counter-recorder" combination, (shown schematically in Figure 134) record the ordered loading tape as described in the programming schedule constructed in step (5).



Unit Spectrum No. 1 Unit Spectrum No. 2 Unit Spectrum No. 3

Step Ordered Military Maneuver Loadings

Step ordered loading tapes were constructed representing the average random military maneuver test histories. These ordered loading tapes were constructed utilizing the same procedure used in making the step ordered gust loading tapes except that the negative excursions were suppressed by passing the generated signal through a diode.

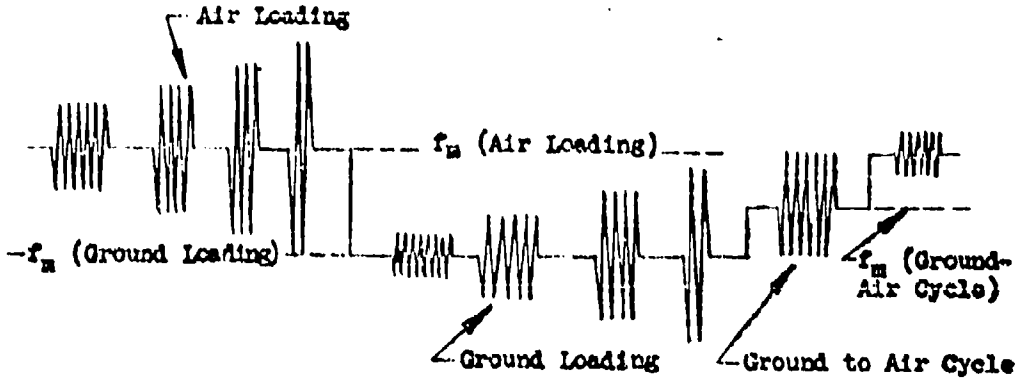
Step Ordered Composite Loading Tapes

Step ordered programming tapes were constructed representing random composite test histories. These ordered tapes were constructed for both gust and military maneuver type air loadings employing the same procedure described in the example above. Air loadings, ground loadings, and ground-to-air transitions were treated as three separate random spectra and separate programming schedules were made for each spectrum. The complete ordered composite tape was made as follows:

(1) The first unit spectrum of air loadings was recorded, as tabulated on its programming schedule, about the mean load for which the corresponding random air loadings were applied.

(2) The first unit spectrum of ground loadings was also recorded, as shown on its programming schedule, at the mean load at which the corresponding random ground loadings were applied.

(3) The first unit spectrum of ground-to-air cycles was recorded such that the peak-to-peak excursion extended from the air loading mean to the ground loading mean.




The procedure described above was used to generate the first unit composite loading spectrum. The succeeding spectrum units were constructed in the same manner.

The standard equipment items used in this tape construction work are indicated on the schematics on Figures 133 and 134. The portable tape unit is a two-channel frequency-modulated 1/4-inch record and playback unit. The tape deck is a series 30 recorder manufactured by American Electronics, Inc., and the electronics were designed and developed by Lockheed. Characteristic of this unit are:

Carrier frequency - 3,400 cps
Tape speed - 7 1/2 inches per second
Minimum signal to noise ratio - 40 db
Maximum record voltage - 9.0 volts
Playback filtering - 60 or 500 cps

## SPECIMEN LOADING

The specimen loading system which was developed for this investigation was basically simple in mechanical detail, utilizing for the most part standard commercial equipment for signal input, hydraulic load control and loading readout. However, to appreciate the demands upon the system it must be realized that in this investigation the primary testing requirement involved application of specimen loadings which faithfully followed command signals of a very complex nature. The controlled application of such loadings dictated the selection and development of servo control circuitry and the development of special test monitoring techniques. A description of the loading system is presented below followed by a brief discussion of several problems encountered during testing.

### DESCRIPTION OF SPECIMEN LOADING EQUIPMENT

Fatigue loading equipment was developed for the rapid application of the loadings defined by signals on the magnetic tapes described in preceding paragraphs. This equipment basically provides an electro-hydraulic servo system consisting of a test specimen in series with a servo valve-jack combination, with the loadings programmed by the signal from magnetic tape. This system is shown schematically on Figure 135.

As shown on this figure, the output signal from the programmer is fed into the servo loop through the summing junction. The amplified input signal programs the action of the servo valve in metering cyclic flow of oil to the fore and aft parts of the servo jack. The output signal of the load transducer strain gage is amplified and fed back into the summing junction closing the loop. The instantaneous summing of these two opposing signals at the input side of the servo valve ideally results in the specimen experiencing the loading history represented by the signal on the loading tape. In utilizing such a system due cognizance was given to inherent mechanical and electrical limitations of the entire system, especially with respect to frequency response and flow characteristics of the servo valve.

The 1/4 inch programming tape unit used for spectral loading input is the same basic unit as the 1/4 inch portable tape unit which was used for preparation of the program tapes except that it does not have recording capabilities. The servo loop command and feed-back electronics were basically Model K2-W operational amplifiers in series with Model K2-P chopper stabilizing amplifiers, manufactured by George A. Philbrick Researches, Inc. A diode clipper was mounted in the electrical circuit between the tape unit and the summing junction which limited the amplitude of the programming signal supplied to the summing junction in case of signal overload. This diode clipper was also basically a Model K2-W operational amplifier.

The servo jack was a Lockheed designed hydraulic actuator with a maximum static force rating of 17,000 pounds. The servo valve employed to program the action of the hydraulic actuator was a Model 26 Flow Control Valve, manufactured by Hydraulic Research and Manufacturing Company. This servo valve has a flow control range from 0.15 to 10 gpm for an operating pressure range of

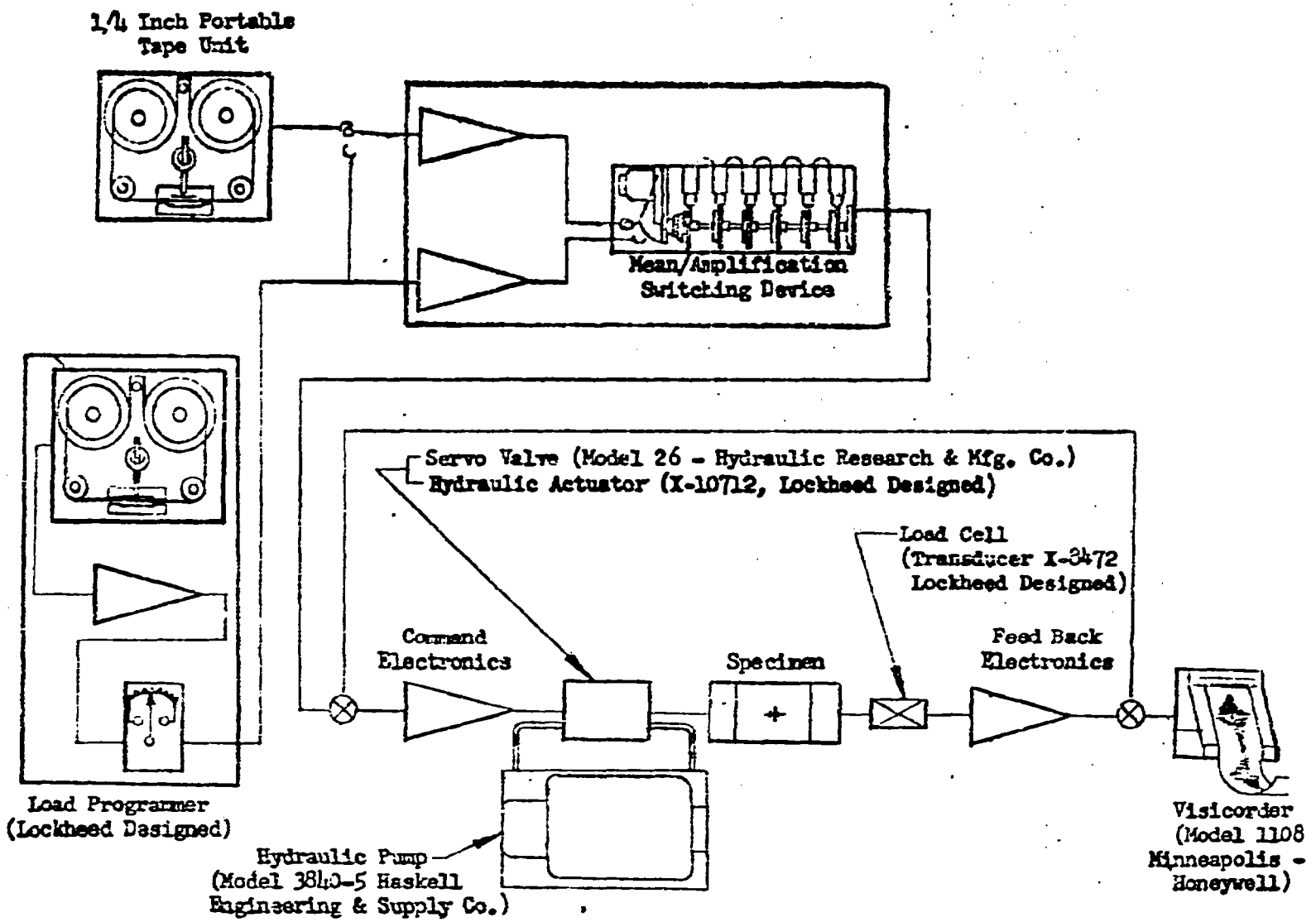



Figure 135 Schematic of Test Loading System

150 to 4,000 psi. The transducer used as the sensing unit in the system was a Lockheed designed strain gaged load cell. This transducer is cylindrical in constructional detail and is equipped with a full bridge gage installation, the electrical output being essentially insensitive to bending strain. Four complete loading systems were developed for this testing program and are shown in operation on Figure 136. The tape playback unit, the electronics and associated components for programming two separate servo loops were mounted in a self-contained unit as shown on Figure 137. A photograph of a valve-jack combination, load transducer and specimen, all rigidly mounted in one of the loading fixtures, is shown on Figure 129. The specimen was mounted in the test fixture by rigid friction grips, and floating stiffeners were used on the unsupported edges of the specimen to prevent buckling as shown in Figure 129. A failure wire was cemented to the specimen in the area of maximum stress concentration and connected to a relay. Upon initiation of a fatigue crack the failure wire circuit was interrupted, instantaneously blocking off hydraulic flow to the actuator.

PROCEDURE FOR SPECTRAL LOADING OF SPECIMENS

Prior to the application of loads to each specimen, the loading system was calibrated and adjusted to produce the applicable loading history represented on programming tape. Although several steps in the calibration and dynamic loading procedure were common to all spectral tests, certain steps were followed only for particular types of loading history. Outlines of the procedures follow.

Loading Histories Having Constant Mean Load Values

(1) From known transducer data, a calibration factor of load versus electrical output was determined which related the maximum signal voltage on the program tape to the highest load to be applied to the specimen. This maximum signal was recorded on an oscillograph for later reference.

(2) A dummy specimen, serving merely as a load link during calibration was installed in the test fixture and the static mean load was applied by dialing in the equivalent voltage to the servo valve circuit.

(3) The required dynamic signal amplification was set, based on the loading tape voltage calibration factor.

(4) The maximum dynamic load was applied to the dummy specimen and the load cell signal output was recorded on an oscillograph for comparison with the static signal previously recorded.

(5) Deviation of the maximum loading cycle from the desired load level was corrected by a compensating adjustment of the signal amplification, and step 4 was repeated.

(6) When the desired loading level for the maximum cycle was obtained the calibrating system was replaced by a test specimen.

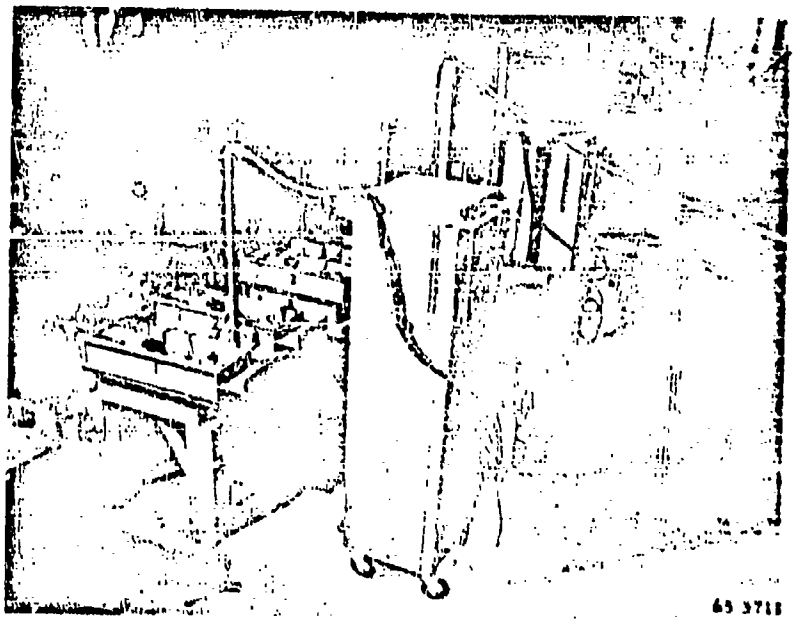


Figure 136 General View of Specimen Loading Apparatus

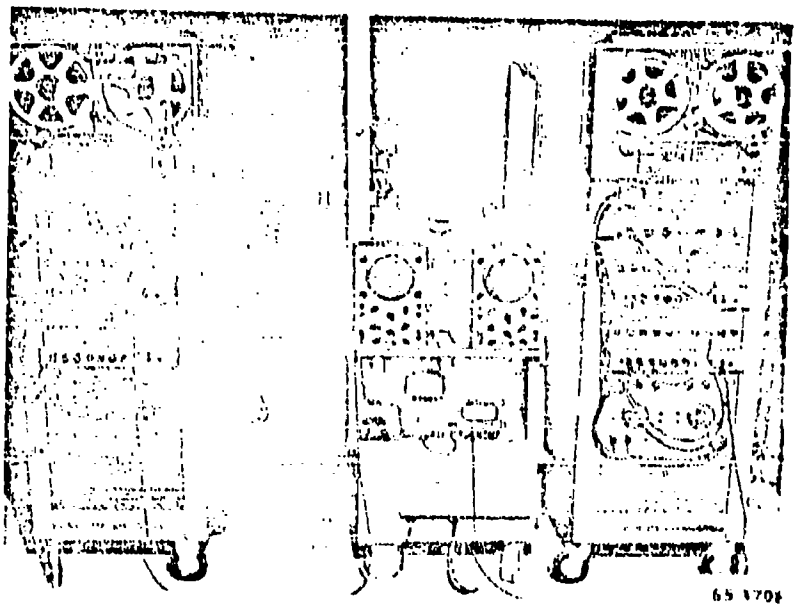


Figure 137 Magnetic Tape Loading Control Units

(7) The loading trace was then applied to the test specimen. The maximum loading cycle was periodically monitored on the oscillograph and required adjustments made to the amplification of the dynamic signal to maintain the desired loading level.

(8) Testing was continued until the initiation of a fatigue crack interrupted the failure wire circuit terminating the loadings. In addition, interruption of the failure wire circuit cut off the power source to the electrical timing device recording the duration of specimen life.

The full range of random loadings applied to the test specimen were periodically monitored to determine the spectrum content of the applied loads, and as an added check on the stability of the frequency response of the loading system. Monitoring of these random loadings was accomplished by recording on magnetic tape the output signal from the load transducer for each unit loading trace applied. These unit monitor tapes were then electrically counted as described later in the data reduction section.

Periodic monitoring checks were also made of the ordered loadings applied to the specimen. Monitoring of the ordered loadings applied in the preliminary investigation was accomplished in the manner described above for the random loadings. Monitoring of the step ordered loadings consisted of periodic recording on an oscillograph of the load transducer output signal for the complete ordered loading trace. The loads for each group of cycles were calculated from the oscillographic record and compared with the schedule from which the loading tape was constructed.

Loading Histories Having Variable Mean Load Values

Random composite loadings with gust type air loadings were produced by using the same loading tape signal for both air loadings and ground loadings. The ground loading trace was similar to the air loadings except that different static mean load and amplification of the dynamic signal were used. The loading tape signal was routed through an electro-mechanical device which periodically shifted both static mean load and amplification of the dynamic trace. The procedure for alternately applying these two loading traces from the same input signal was as follows:

(1) A calibration factor for the load programming system was determined relating specimen load to loading tape voltage and a calibration signal was recorded on an oscillograph. The input voltage relationships required to define the desired loading history were then calculated.

(2) With a dummy specimen installed in the loading fixture, the switching device was locked in one of the spectrum loading positions and the static mean load was applied with a bias voltage.

(3) The required dynamic signal amplification was set based on the loading tape voltage relationships calculated in Step 1 above.

(4) The maximum dynamic signal was applied to the calibrating specimen and recorded on an oscillograph for comparison with the previously recorded loading system calibration factor.

(5) Deviation of the maximum loading cycle from the desired load level was corrected by a compensating adjustment of the signal amplification and the repetition of Step 4.

(6) The switching device was then locked in the second loading condition and Steps 2 through 5 were repeated to obtain its desired dynamic trace amplification.

(7) After the desired loading levels for the maximum loading cycle were obtained, the calibrating specimen was replaced by a test specimen.

(8) The loading trace was then applied to the specimen and the switching device was started at the commencement of the dynamic signal.

(9) The maximum composite loading cycle was periodically monitored on the oscillograph and the required adjustments were made to the amplification of the dynamic signal to maintain the desired loading level.

(10) Testing was continued until a fatigue crack developed. The loading was terminated by failure of the previously described failure wire and the test duration was recorded.

Random composite military maneuver loadings were produced by employing the signals from two separate loading tapes. To apply these loadings the portable tape unit used in the tape construction work was operated in parallel with the programming tape unit as shown schematically on Figure 135. These two signals were fed into the same switching device used in applying the random composite gust loadings. The switching apparatus alternately switched static mean loads and the dynamic signal inputs. The setup, calibration, testing and monitoring were also accomplished in the manner described above for random composite gust loadings.

Ordered composite loading tapes were constructed so that the relationship between the static mean load and the dynamic loading level was recorded on the tape. Thus only one signal amplification was required for the composite tape to apply the desired composite loading spectra. The procedure for setting the loading levels, testing and monitoring, was the same as described for the single spectrum loadings.

Discussion of Loading System Development

In developing this loading system a number of problems were encountered. The resolution of the overall problem of applying the same loading history to the specimen for repeated applications of the same loading trace required considerable effort. Many factors contributing to this overall problem complicated the development of a completely reliable loading system throughout a major portion of the preliminary investigation. Some of the contributing problems are discussed in the following paragraphs.

In order to extend the operating frequency range of the servo valve and system, electrical lead networks were developed. A flat frequency response over the range of 0 to 45 cps with attenuation of 3 db at 60 cps within a

maximum allowable deviation of ±2% was set up as the performance standard. Values for the lead network components were determined from the frequency response of the basic system. In addition individual lead networks were tailored to compensate for the cumulative effect of the characteristics of each servo loop in order to meet these requirements.

In the continued effort to improve the overall loading system performance, the meter originally used in setting the level of the input loading trace was replaced by a direct reading oscillograph (Visicorder). The use of the oscillograph permitted utilization of a dynamic signal for calibrating the loading tapes. This more realistic method of setting the loading level with a dynamic signal in the frequency range of the applied loading cycles greatly improved the control of variations in frequency response.

Due to deterioriation in servo valve performance and aging of electronic components, it was necessary to monitor continuously the frequency response of the servo system. A function generator was used in conjunction with an oscillograph to check the servo system response and by adjustment of the forward and feedback gains of the servo amplifier, the system response could be maintained within the limits of the ±2% deviation.

Variations were noted, during the early testing stage, between loading histories sampled at discrete intervals for the same input trace. This was concluded to be due mainly to large fluctuations of the hydraulic oil temperature occurring over a normal operating period since corresponding fluctuations were also observed in the frequency response of the loading system. Stabilization of the hydraulic oil temperature through the use of an immersion heater or regulation of cooling water through a heat exchanger greatly reduced these response variations.

Proper mechanical operation of the servo valve demands that the hydraulic fluid be filtered of all particles which are greater than approximately 25 microns in diameter. In order to assure reasonable filter life the entire hydraulic system was maintained as free as practicable of contaminants. The formation of varnish or generation of corrosion particles results in costly shutdown periods and is a constant threat to the attainment of reliable test data. Therefore MIL H 5606-A hydraulic fluid was selected because of its stable and non-corrosive characteristics. This particular problem proved to be a costly one during the early stages of the testing phase of this investigation.

Bearing in mind that the specimen loading system was, of necessity, highly responsive to tape signal command, it can readily be seen that it was imperative that loading input tapes remain as free as possible of extraneous signals which might affect testing validity. These false signals may be of such strength to cause serious overloading or destruction of the specimen. In an effort to produce and maintain loading input tapes essentially free of false signals, special tape handling procedures were adopted. Electrical means were also employed to repress false signals of any significant magnitude, during load application.

In passing a magnetic tape across a signal reproduce-head any irregularity of the tape surface causes a momentary loss of playback signal known as a drop-out, resulting in the appearance of a maximum voltage at the output terminals of the tape unit reproduce-electronics. The response characteristics of an electro hydraulic servo loop are such that the loading system instantaneously applies the maximum possible load to the test specimen. The major causes of tape drop-outs are improper tape splices, flaking of the magnetic surface, and minute dust particles collecting on the tape surface. A method of completely eliminating drop-outs was not achieved, but by a continual effort in guarding against conditions conducive to their origin, their occurrence was effectively minimized.

The principal efforts extended in minimizing the occurrence of drop-outs were as follows:

1. Dust protective shields were installed around the area of the loading tape and signal reproduce-equipment. A practice of periodic cleaning was rigorously followed.

2. Multi-pass loading tapes were constructed by splicing together recorded sections of the unit loading trace. These loading tapes were rerecorded onto splice-free tape for use on the load programming units. In the event of accidental damage or flaking of the magnetic coating of the test loading tape, resulting in a permanent drop-out, a duplicate splice-free copy was made of the originally spliced multi-pass tape.

3. Where single drop-outs or other strong extraneous signals existed which were not the result of splicing, electrical means involving the use of diode clippers were utilized to subdue the strength of the signal. To this end the clipper circuit was adjusted to cut off all signal strength which was in excess of that signal representing the highest spectral load.

CONSTANT LOAD AMPLITUDE TESTING EQUIPMENT

As noted in the main body of the report, sets of S-N curves were developed as reference data for the random loading and spectrum loading tests. The S-N tests were conducted in resonant beam fatigue test machines. In this type of fatigue machine, loads are developed by means of a motor-driven rotating eccentric weight fastened at the free end of a pivoted beam. This beam is tuned to a frequency slightly higher than the driving frequency produced by the motor (1800 rpm). The test specimen is mounted normal to the axis of the beam and so is loaded axially by the beam displacements. Static and dynamic loads are measured and monitored using the output of strain gages mounted on a load cell which is loaded in series with the test specimen.

## DATA REDUCTION

### DESCRIPTION OF COUNT METHODS

At the start of this program a large number of count methods were reviewed in terms of their applicability. All of these methods were variations of three basic count methods: "Peak Count," "Range Count" and "Interval Crossing Count." One of these three basic types of count methods was then selected for further use as applied to the gust data records used in this study. This was the mean crossing peak count method. The manner in which the selected count method was applied is described below.

### Mean Crossing Peak Count

Given load-time trace $y = f(t)$

(1) Establish load levels of interest $y_1, y_2, y_3 \ldots y_n$ above and below mean

$$\bar{y} = \frac{1}{T}\int_0^T f(t)dt$$

(2) Establish all points at which $y = \bar{y}$, that is , where load-time trace crosses mean.

(3) Between two successive crossings of the mean establish:

a) The maximum value of load-time trace for portions greater than mean (peak).

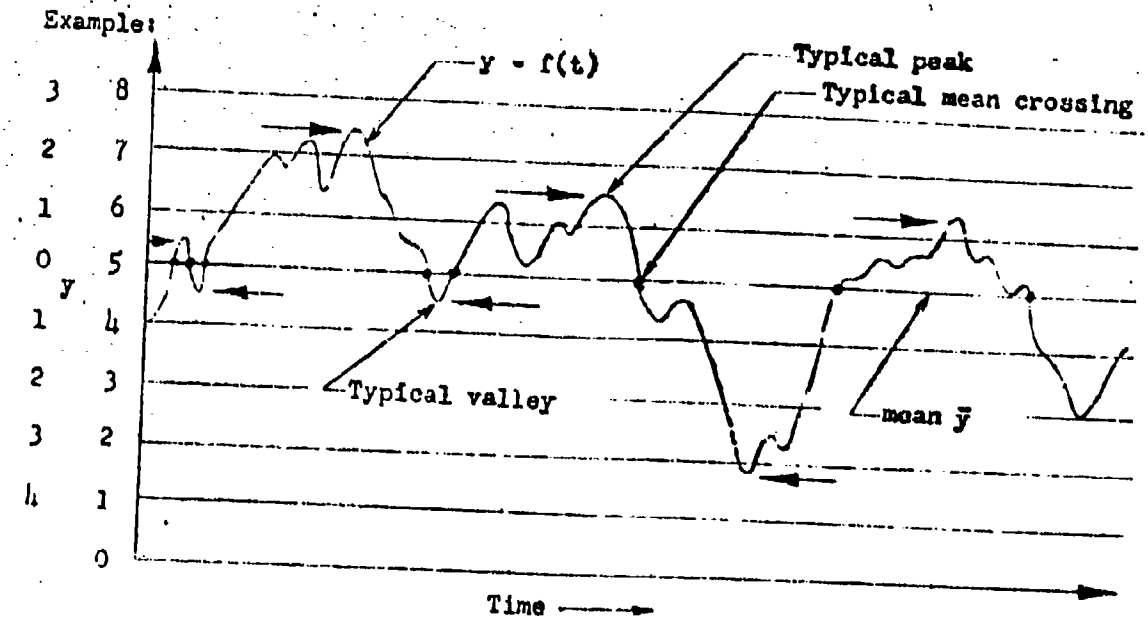
b) The minimum value of load-time trace for portions less than mean (valley).

(4) Count the number of peak maximum values above any paticular level of interest.

(5) Count the number of valley minimum values below any particular level of interest.

(6) Summarize counts.

This Procedure is Illustrated in Figure 138.




| Level of Interest | 0 | 1 | 2 | 3 | 4 |
|---|---|---|---|---|---|
| Peak Count | 4 | 3 | 1 | 0 | 0 |
| Valley Count | 3 | 1 | 1 | 1 | 0 |

Figure 138 Definition of the Mean Crossing Peak Count Method

ELECTRICAL COUNTING SYSTEMS

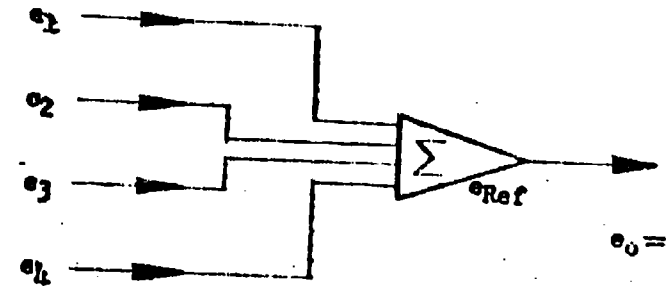
An integrated system was developed for high speed statistical analysis of random and ordered spectra employing analog methods. A counting system was developed for obtaining a mean crossing peak count at counting rates up to 500 cycles per second. This integrated system basically consists of a magnetic tape input unit, an analog computer and an electronic totalizing counter. Figure 130 shows this system programmed for counting.

The magnetic tape input unit was the 1/4 inch portable tape unit used in the construction of the loading tapes. A Model 521C electronic counter manufactured by the Hewlett Packard Corporation was employed to record the statistical data from the counting circuit.

The analog computer consists of eight standard K5-U computing amplifiers and twenty K2-W operational amplifiers manufactured and packaged in a self-contained unit by George Philbrick Researches, Inc. Four separate input signals can be scaled, the polarity inverted, and then summed in the K5-U computing amplifiers. In addition, a reference voltage of either polarity can be subtracted from its final output. The K2-W is a basic operational amplifier in that no input or feedback resistors are associated with it. By adding resistors, capacitors, and diodes externally the K2-W can be made to operate as an inverter, filter, mean integrator, buffer, peak follower, or voltage crossing detector. Schematical representations are shown on Figures 139 and 140 for the operational configurations in which these amplifiers were employed in the counting circuit . In addition, the counting circuit developed for the mean crossing peak count method is shown schematically in Figure 141.

The initial calibration of this circuit was based on use of a five-minute section of the original B-47 wing root loading trace. This trace was recorded on 1/4 inch magnetic tape suitable for electrical counting and an oscillograph was made. The visible trace was scanned and the mean crossing peak count was tabulated. This tabulation was then used as a guide in assessing the performance of the counting circuit.

In the development of this counting system certain problems were encountered which were largely due to the demand for unique applications of analog computer elements. A number of possible circuits were evaluated in the search for counting systems which were accurate and reliable. The selection and use of high quality components was a requisite to the reliable performance of all circuits. Precision carbon resistors and high quality mylar capacitors were used exclusively in all operational amplifier circuitry. Silicon crystal diodes were used in the initial phases of counting circuit development but later proved to possess insufficient reverse impedance to reset the peak follower in all instances. Vacuum tube diodes were substituted, providing reliable operation of the peak follower circuit.



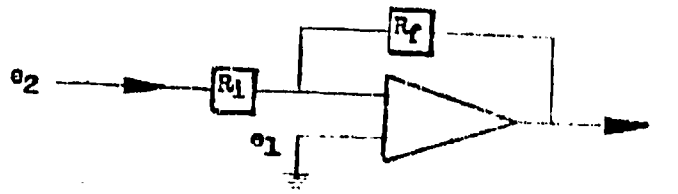

$$e_o = e_{Ref} + \sum (a_1e_1 + a_2e_2 + a_3e_3 + a_4e_4)$$

K5-U Computing Amplifier




$$e_o \approx e_1$$

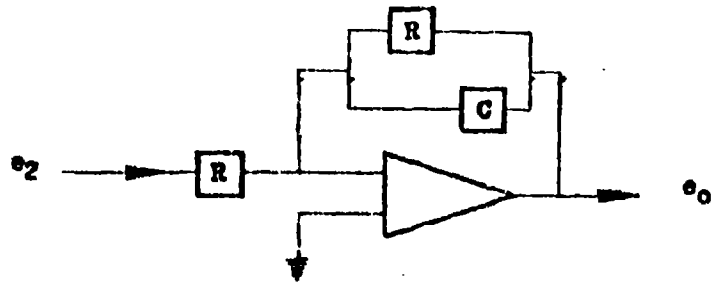
Buffer - K2-W Operational Amplifier




$$e_o \approx - \frac{R_f}{R_1} e_2$$

Inverter - K2-W Operational Amplifier

Figure 139 Applications of Basic Computer Elements

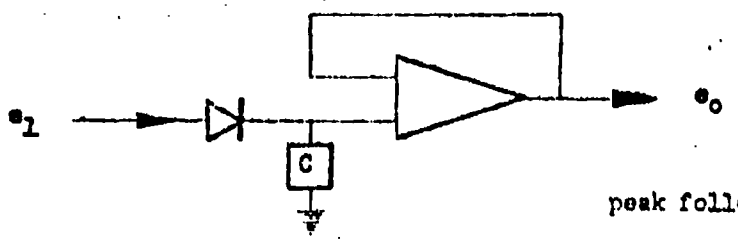



for filter RC $\ll$ 1, $e_o \approx - e_2$

for mean integrator RC $\gg$ 1,

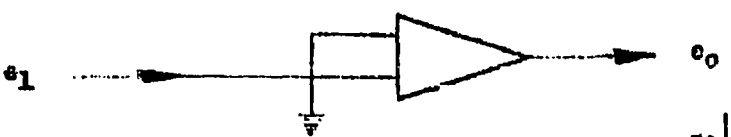
$$e_o = \frac{1}{t} \int_o^t e_2 dt$$

Filter and Mean Integrator
K2-W Operational Amplifier




peak follower $e_o \simeq + \left| + e_{i_{max}} \right|$

Peak Follower - K2-W Operational Amplifier




$e_o = +70 \Big|_{e_1 > 0}$ ; $e_o = -70 \Big|_{e_1 < 0}$

Voltage Crossing Detector
K2-W Operational Amplifier

Figure 140 Applications of Basic Computer Elements

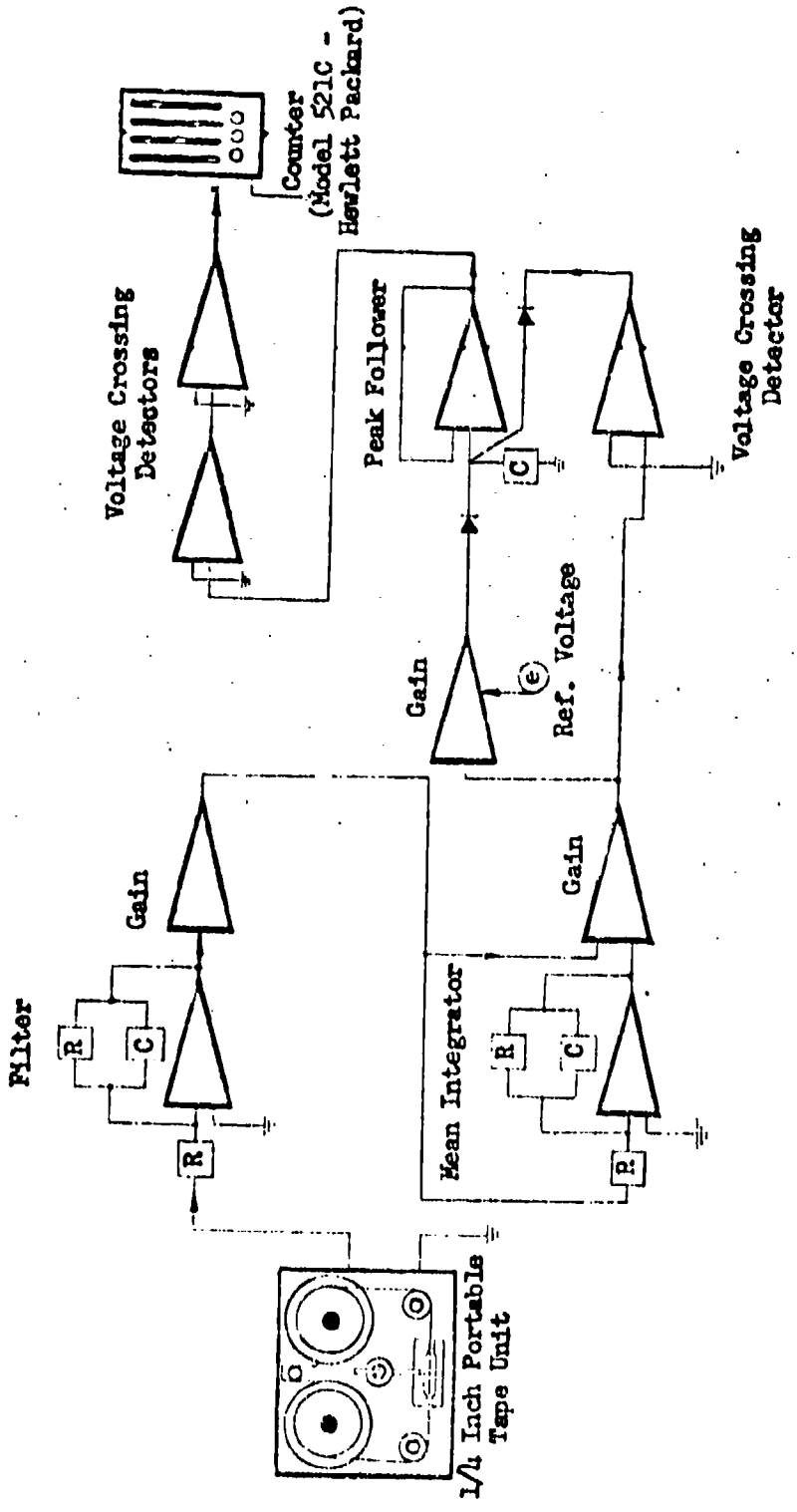



Figure 141 Schematic of Computing Circuit for the Mean Crossing Peak Count

Procedure for Counting Random Spectra

Monitor tapes for the load transducer output signal, representing the specimen loading history, were recorded for a unit section of each random programming tape. These unit loading signals were then programmed through the computing circuit and their count distributions were recorded in columnar form.

The counting of a particular monitor tape was accomplished in the following manner:

(1) The counting circuit was installed on the analog computer and a schedule was made of the load levels at which counts were desired.

(2) The load level was dialed into the computer and the monitor tape signal was programmed to the counting circuit.

(3) Cumulative counts were displayed on the electronic counter as the unit section of monitor signal was transmitted through the computing circuit.

(4) When all of the monitor tape signals had been played through the computing circuit, the total cumulative counts were recorded for permanent record and the sequence was repeated for each load level in the counting schedule.

Procedure for Counting Ordered Spectra

Monitor tapes were also recorded from the load transducer output signal for a unit section of each ordered loading tape constructed in the preliminary investigation. These monitor tapes were counted in the same manner as described above for counting the random spectra.

Counting of the monitor tape output signal for the step ordered loading tapes constructed in the principal part of this investigation was obtained in the following manner.

(1) An oscillographic record was made of the load transducer output signal for the full length of each step ordered programming tape.

(2) The amplitude at each load interval was scaled and the load level determined by comparison with a known calibration.

## ANALYSIS OF ACCURACY

A step by step procedure of the testing, monitoring, and counting operation is summarized below. The values of maximum possible error at each step in this procedure are shown. The nature of such error sources is noted in the procedure outline and also keyed to the schematic diagram shown in Figure 142.

These individual errors were added directly to obtain the maximum error limits shown graphically on Figure 143. However, a more realistic evaluation of the accuracy of the presented data is obtained from the 95% probability error limits presented graphically on Figure 144.

| TEST PROCEDURE USING MULTI-PASS LOADING SPECTRUM PROGRAMMING TAPE | % of Error |
|---|---|
| (1) Apply static calibration of load cell H to Visicorder (J) | |
| a) Load cell calibration | ±1.0 |
| (2) Start tape transport (A) and play output signal thru tape electronics (B) and servo loop (D-E-F-H) and record load cell (H) output on Visicorder J. Compare maximum dynamic range to static calibration on Visicorder (step 1) and adjust gain pot C to apply desired maximum specimen stress | |
| a) Stability of programmer electronics (B) | ±0.5 |
| b) Stability of servo command electronics (D) | ±0.02 |
| c) Frequency response deviation (E) | ±2.0 |
| d) Specimen cross sectional area variation (F) | ±1.5 |
| e) Stability of load cell monitor electronics (I) | ±0.02 |
| f) Visicorder frequency response (J) | ±3.0 |
| g) Reading accuracy - comparison Visicorder calibrations (J) | ±2.0 |
| (3) Continuous loading applied to specimen with calibration techniques (steps 1 and 2) applied periodically | |
| a) Variation of frequency response | ±0.5 |

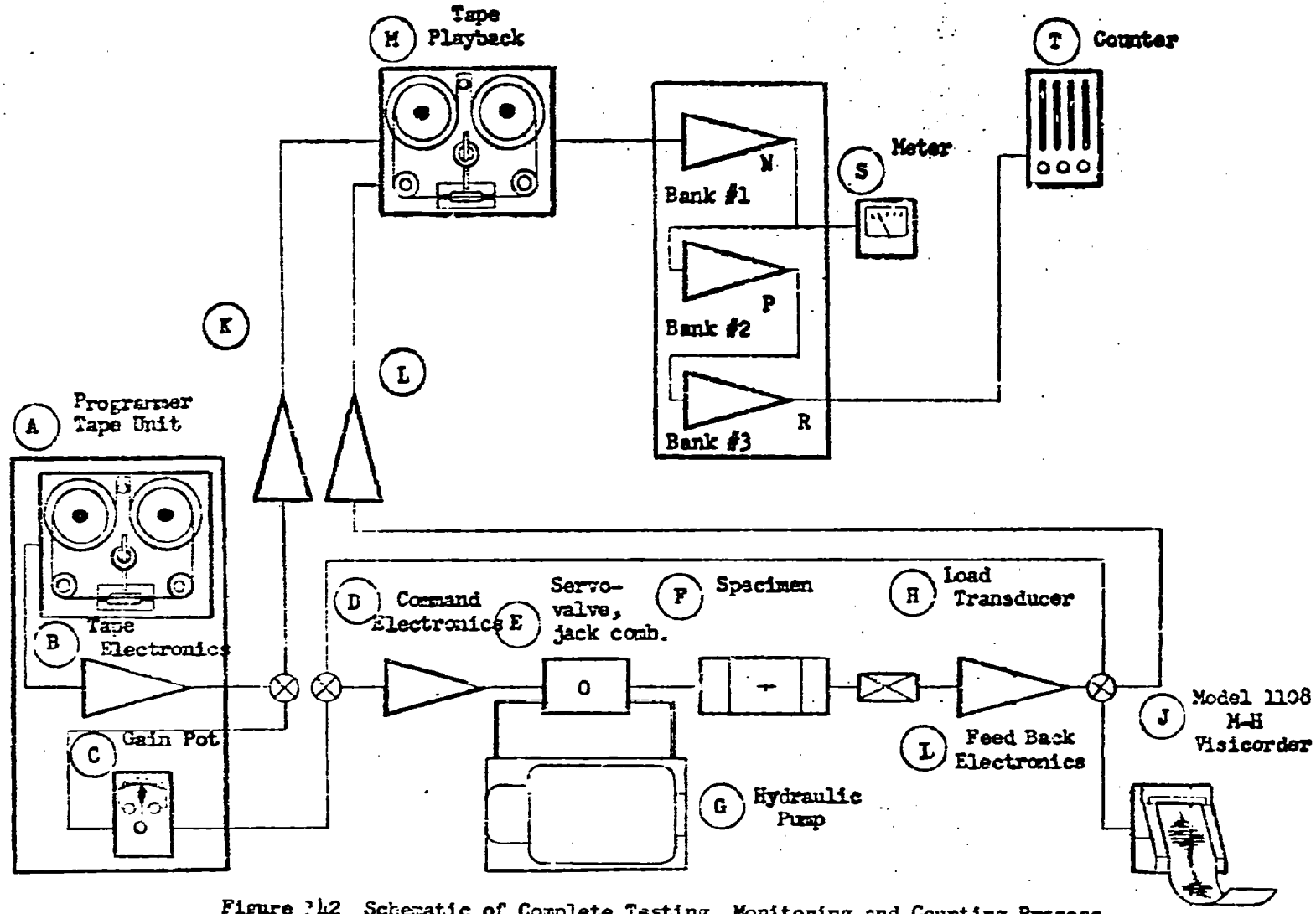



Figure 142 Schematic of Complete Testing, Monitoring and Counting Process

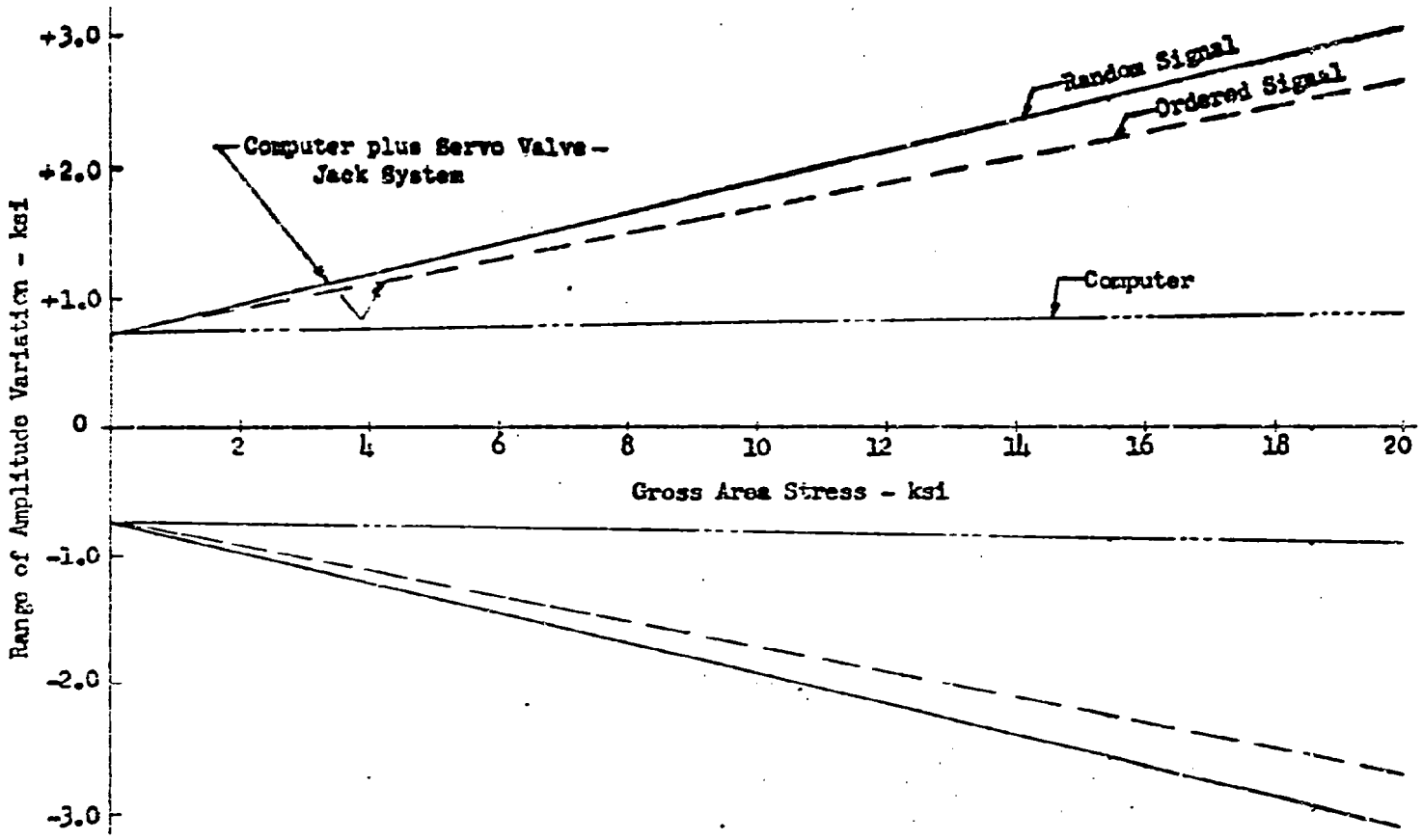



Figure 143 Maximum Error Limits

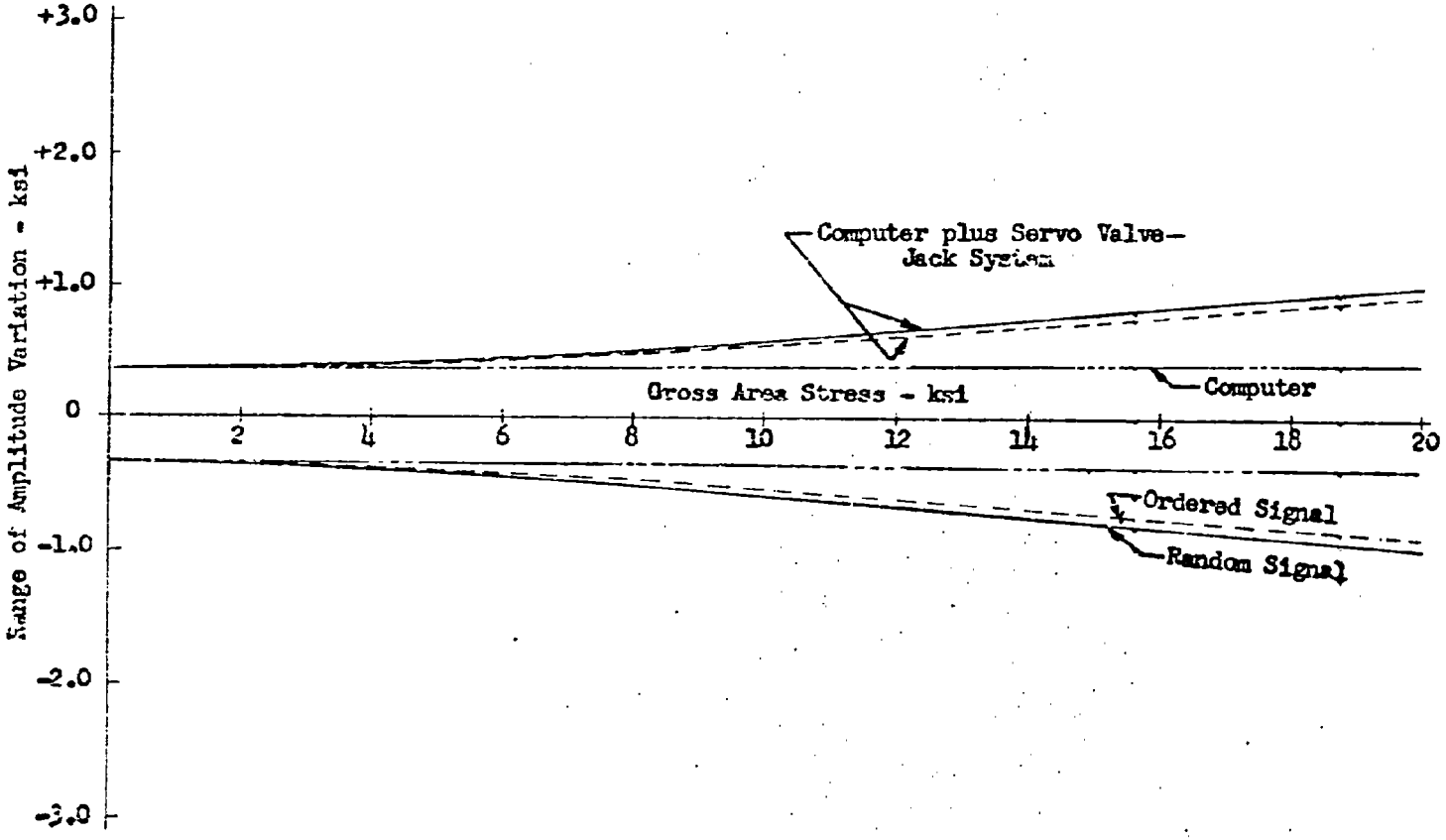



FIGURE 144 95% PROBABILITY ERROR LIMITS

PROCEDURE FOR RECORDING MONITOR TAPE
OF SPECIMEN LOADING HISTORY

| | % of Error |
|---|---|
| (1) Output signal of load cell (H) played through monitor electronics (L) and unit section of basic data recorded on recorder (M). | |
| a) Stability of load cell monitor electronics (I). | --- |
| b) Stability of recorder electronics (L). | ±0.5 |

PROCEDURE FOR COUNTING MONITOR TAPE

| | |
|---|---|
| (1) Program monitor signal into computer (N), (P) & (R) and observe occurrences of data characteristics on counter (R). | |
| a) Balance computer bank No. 2 (P). | ±0.09 * |
| b) Balance computer bank No. 3 (R). | ±0.09 * |
| c) Zero output computer bank No. 1 (N) (read meter (S)) for "tape-zero" input. | ±0.09 * |
| d) Adjust output computer bank No. 1 (N) (read meter (S)) for tape calibration input to desired signal amplification level. | ±0.225 * |
| e) Dial desired signal count level in computer bank No. 3 (R) and observe number of counts on counter (T). | --- |
| f) Stability of computer bank No. 1 (N). | ±0.5 |
| g) Stability of computer bank No. 2 (P). | ±0.2475 * |
| h) Stability of computer bank No. 3 (R). | ±0.2 |

It should be noted that the error analysis described above applies to the complete testing-counting process. It therefore establishes the accuracy of the specimen test history curves presented in the report.

* KSI Constant

## MATERIAL STRENGTH

The results of static tensile tests on the 7075-T6 bare aluminum material used in the investigation are presented in Table 54. The geometry of the rectangular 2 inch gage length conformed to ASTM Standard E8-57T. The longitudinal grained tensile test specimens were taken along the longitudinal axis of each sheet of material.

TABLE 54

STATIC TENSILE PROPERTIES OF
7075-T6 BARE ALUMINUM SHEET, .040 GAGE

| Spec. No. | Sheet No. 1 | | | Sheet No. 2 | | | Sheet No. 3 | | | Sheet No. 4 | | | Sheet No. 5 | | |
|---|---|---|---|---|---|---|---|---|---|---|---|---|---|---|---|
| | $F_{tu}$ (ksi) | $F_{ty}$ (ksi) | % Elong. | $F_{tu}$ (ksi) | $F_{ty}$ (ksi) | % Elong. | $F_{tu}$ (ksi) | $F_{ty}$ (ksi) | % Elong. | $F_{tu}$ (ksi) | $F_{ty}$ (ksi) | % Elong. | $F_{tu}$ (ksi) | $F_{ty}$ (ksi) | % Elong. |
| 1 | 85.4 | 78.2 | 11.0 | 85.4 | 78.5 | 11.5 | 85.8 | 78.6 | 11.0 | 84.9 | 77.2 | 11.0 | 85.7 | 78.6 | 11.0 |
| 2 | 86.1 | 79.0 | 12.0 | 85.2 | 78.3 | 10.5 | 84.8 | 77.7 | 11.0 | 85.4 | 78.3 | 11.0 | 85.5 | 78.4 | 10.5 |
| 3 | 85.4 | 77.8 | 11.0 | 84.5 | 77.1 | 11.0 | 85.1 | 78.3 | 11.0 | 85.4 | 78.5 | 10.5 | 86.0 | 78.1 | 11.0 |
| 4 | 85.7 | 78.7 | 10.5 | 84.3 | 76.2 | 11.0 | 85.9 | 78.8 | 11.0 | 84.8 | 76.5 | 11.0 | 84.5 | 76.7 | 9.0 |
| 5 | 85.0 | 77.4 | 11.0 | 85.1 | 77.9 | 11.5 | 85.9 | 78.7 | 12.0 | 85.6 | 78.3 | 12.0 | 84.5 | 76.4 | 10.0 |
| 6 | 85.2 | 77.2 | 12.0 | 84.7 | 77.9 | 11.0 | 85.4 | 77.0 | 10.5 | 85.8 | 78.7 | 11.0 | 86.1 | 79.2 | 12.0 |
| 7 | 85.2 | 78.3 | 11.0 | 84.7 | 77.4 | 11.5 | 85.5 | 78.5 | 11.5 | 86.1 | 78.8 | 11.0 | 85.9 | 78.7 | 11.0 |
| 8 | 85.6 | 78.1 | 12.0 | 85.3 | 78.3 | 10.0 | 85.1 | 78.2 | 11.5 | 85.4 | 78.5 | 11.0 | 86.0 | 78.8 | 12.5 |
| 9 | 84.8 | 76.8 | 13.0 | 84.0 | 76.3 | 11.0 | 85.1 | 77.5 | 10.5 | 85.6 | 78.7 | 11.5 | 85.9 | 76.6 | 11.0 |
| 10 | 85.3 | 78.1 | 11.0 | 85.6 | 78.5 | 11.0 | 85.8 | 79.1 | 11.0 | 85.4 | 78.5 | 11.0 | 85.3 | 78.0 | 11.0 |
| 11 | 84.8 | 77.2 | 11.5 | 85.2 | 77.9 | 11.5 | 85.1 | 78.1 | 10.5 | 85.0 | 77.9 | 11.0 | 85.7 | 78.2 | 11.0 |
| 12 | 85.7 | 78.3 | 12.0 | 85.3 | 78.1 | 12.0 | 84.1 | 76.5 | 11.5 | 85.4 | 78.5 | 11.0 | 85.6 | 78.5 | 11.0 |
| 13 | 85.1 | 78.1 | 12.0 | 84.9 | 77.2 | 12.0 | 85.0 | 78.0 | 10.5 | | | | | | |
| 14 | 85.9 | 79.1 | 11.0 | 85.5 | 78.3 | 12.0 | 83.6 | 75.3 | 11.5 | | | | | | |
| 15 | 83.7 | 76.3 | 12.0 | 84.5 | 77.8 | 11.0 | 84.4 | 77.6 | 12.0 | | | | | | |
| 16 | 84.8 | 77.5 | 12.0 | 84.6 | 77.2 | 12.0 | 84.6 | 77.6 | 11.5 | | | | | | |

Note: The static test specimens were selected along the longitudinal centerline of each 48 x 144 inch sheet. The longitudinal axis of each specimen was parallel to the direction of sheet rolling.

TABLE 55

UNIT LOW PEAK GUST LOADING SPECTRA AND S-N DATA FOR NOTCHED SHEET COUPONS
7075-T6 ALUMINUM ALLOY

$K_T = 4$

$f_{mean} = 6$ KSI $\quad S_{mean} = .071$

$F_{tu} = 85$ KSI (Gross Area)

| Loading Step | $f_v$ KSI | $S_v$ | n | N |
|---|---|---|---|---|
| | | 18 LOADING STEPS | | |
| 1 | .60 | .0071 | 715900 | -- |
| 2 | 1.78 | .0209 | 511588 | -- |
| 3 | 2.97 | .0349 | 280342 | 6000000 |
| 4 | 4.16 | .0489 | 112479 | 1200000 |
| 5 | 5.35 | .0629 | 32231 | 320000 |
| 6 | 6.54 | .0769 | 7519 | 120000 |
| 7 | 7.42 | .0873 | 1184 | 68000 |
| 8 | 8.02 | .0944 | 561 | 46000 |
| 9 | 8.60 | .1012 | 379 | 32000 |
| 10 | 9.20 | .1082 | 211 | 24000 |
| 11 | 9.75 | .1147 | 119 | 18500 |
| 12 | 10.35 | .1218 | 125 | 14000 |
| 13 | 11.15 | .1312 | 81 | 10200 |
| 14 | 11.75 | .1382 | 18 | 8400 |
| 15 | 11.98 | .1409 | 4 | 7800 |
| 16 | 12.28 | .1445 | 17 | 7200 |
| 17 | 12.80 | .1506 | 15 | 6000 |
| 18 | 13.55 | .1594 | 13 | 4800 |
| | | (066*) | $\Sigma$ 1662800 | |
| | | 4 LOADING STEPS | | |
| 1 | 4.20 | .0494 | 25408 | 1000000 |
| 2 | 8.15 | .0959 | 582 | 43000 |
| 3 | 12.00 | .1412 | 11 | 7800 |
| 4 | 14.00 | .1647 | .10 | 4200 |
| | | | $\Sigma$ 26000 | |

* Test Group No.

TABLE 56

UNIT LOW PEAK GUST LOADING SPECTRA AND S-N DATA FOR NOTCHED SHEET COUPONS
7075-T6 ALUMINUM ALLOY
$K_T = 4$
$f_{mean}$ = 6 KSI  $S_{mean}$ = .071

$P_{tu}$ = 85 KSI (Gross Area)

| Loading Step | $f_v$ KSI | $S_v$ | n | N | $f_v$ KSI | $S_v$ | n | N |
|---|---|---|---|---|---|---|---|---|
| | | | 14 LOADING STEPS | | | | | |
| 1 | 1.10 | .0129 | 25057 | | 1.09 | .0128 | 50098 | ∞ |
| 2 | 2.10 | .0247 | 17005 | | 2.14 | .0236 | 34105 | ∞ |
| 3 | 3.10 | .0365 | 9986 | 4500000 | 3.05 | .0359 | 19970 | 5200000 |
| 4 | 4.15 | .0488 | 5231 | 1100000 | 4.03 | .0474 | 10422 | 1300000 |
| 5 | 5.00 | .0588 | 1832 | 450000 | 5.05 | .0594 | 3636 | 440000 |
| 6 | 6.05 | .0712 | 627 | 180000 | 6.03 | .0709 | 1248 | 180000 |
| 7 | 7.00 | .0824 | 163 | 90000 | 7.03 | .0827 | 324 | 86000 |
| 8 | 8.00 | .0941 | 59 | 47000 | 8.05 | .0947 | 118 | 45000 |
| 9 | 9.05 | .1065 | 23 | 26000 | 9.07 | .1067 | 45 | 25000 |
| 10 | 10.00 | .1176 | 9.9 | 16500 | 10.25 | .1206 | 20 | 15000 |
| 11 | 11.00 | .1294 | 4.5 | 11000 | 10.60 | .1247 | 8.8 | 13000 |
| 12 | 12.00 | .1412 | 1.5 | 7800 | 11.40 | .1341 | 3.9 | 9500 |
| 13 | 12.95 | .1524 | .74 | 5800 | 12.60 | .1482 | .98 | 6400 |
| 14 | 14.00 | .1647 | .25 | 4200 | 14.00 | .1647 | .50 | 4200 |
| | | (068*) | $\Sigma$ 60000 | | | (069) | $\Sigma$ 120000 | |

* Test Group No.

TABLE 57

UNIT LOW PEAK GUST LOADING SPECTRA AND S-N DATA FOR NOTCHED SHEET COUPONS
7075-T6 ALUMINUM ALLOY

$K_T = 7$

$f_{mean} = 6$ KSI $\quad S_{mean} = .071$

$F_{tu} = 85$ KSI (Gross Area)

| Loading Step | $f_v$ KSI | $S_v$ | n | N | $f_v$ KSI | $S_v$ | n | N |
|---|---|---|---|---|---|---|---|---|
| | 17 LOADING STEPS | | | | 13 LOADING STEPS | | | |
| 1 | .60 | .0071 | 100308 | | 1.10 | .0129 | 4497 | $\infty$ |
| 2 | 1.78 | .0209 | 71917 | 3900000 | 1.95 | .0229 | 2124 | 2400000 |
| 3 | 2.97 | .0349 | 39417 | 980000 | 2.79 | .0328 | 1291 | 520000 |
| 4 | 4.16 | .0489 | 15803 | 110000 | 3.72 | .0438 | 703 | 170000 |
| 5 | 5.35 | .0629 | 4551 | 42000 | 4.66 | .0548 | 256 | 70000 |
| 6 | 6.54 | .0769 | 1068 | 17000 | 5.66 | .0666 | 89 | 32000 |
| 7 | 7.42 | .0873 | 166 | 9900 | 6.68 | .0786 | 23 | 15000 |
| 8 | 8.02 | .0944 | 100 | 6900 | 7.70 | .0906 | 10 | 8000 |
| 9 | 8.60 | .1012 | 35 | 5100 | 8.76 | .1031 | 3.5 | 4800 |
| 10 | 9.20 | .1082 | 29 | 3800 | 9.75 | .1147 | 1.5 | 3000 |
| 11 | 9.75 | .1147 | 18 | 3000 | 11.00 | .1294 | .70 | 1800 |
| 12 | 10.35 | .1218 | 18 | 2300 | 11.91 | .1401 | .20 | 1300 |
| 13 | 11.15 | .1312 | 10 | 1700 | 13.10 | .1541 | .10 | 890 |
| 14 | 11.75 | .1382 | 4.0 | 1400 | | | | |
| 15 | 11.98 | .1409 | 1.0 | 1300 | | | | |
| 16 | 12.28 | .1445 | 2.4 | 1150 | | | | |
| 17 | 12.80 | .1506 | 2.0 | 950 | | | | |
| | | (070*) | $\Sigma$ 233400 | | | (071) | $\Sigma$ 9000 | |

* Test Group No.

TABLE 58

UNIT HIGH PEAK GUST LOADING SPECTRA AND S-N DATA FOR NOTCHED SHEET COUPONS
7075-T6 ALUMINUM ALLOY
$K_T = 4$
$f_{mean} = 12$ KSI $S_{mean} = .141$

$F_{tu} = 85$ KSI (Gross Area)

| Loading Step | $f_v$ KSI | $S_v$ | n | N |
|---|---|---|---|---|
| | | 23 LOADING STEPS | | |
| 1 | .5 | .0059 | 107200 | ∞ |
| 2 | 1.5 | .0176 | 83784 | 10000000 |
| 3 | 2.5 | .0294 | 70408 | 1500000 |
| 4 | 3.5 | .0412 | 49593 | 420000 |
| 5 | 4.5 | .0529 | 32123 | 170000 |
| 6 | 5.5 | .0647 | 19296 | 80000 |
| 7 | 6.5 | .0765 | 9663 | 41000 |
| 8 | 7.5 | .0882 | 4035 | 24000 |
| 9 | 8.5 | .1000 | 1658 | 15000 |
| 10 | 9.5 | .1118 | 691 | 10000 |
| 11 | 10.5 | .1235 | 287 | 7400 |
| 12 | 11.5 | .1353 | 151 | 5500 |
| 13 | 12.5 | .1471 | 77 | 4100 |
| 14 | 13.5 | .1588 | 42 | 3100 |
| 15 | 14.5 | .1706 | 29 | 2400 |
| 16 | 15.5 | .1824 | 16 | 1900 |
| 17 | 16.10 | .1894 | 2.0 | 1600 |
| 18 | 16.51 | .1942 | 6.0 | 1500 |
| 19 | 16.92 | .1991 | 1.0 | 1300 |
| 20 | 17.50 | .2059 | 5.0 | 1200 |
| 21 | 18.14 | .2134 | 1.3 | 960 |
| 22 | 18.64 | .2193 | 1.5 | 890 |
| 23 | 19.26 | .2266 | .70 | 760 |
| | | (G72*) | $\Sigma$ 379100 | |
| | | 5 LOADING STEPS | | |
| 1 | 4.13 | .0486 | 8389 | 230000 |
| 2 | 8.25 | .0971 | 828 | 17000 |
| 3 | 12.35 | .1453 | 30 | 4300 |
| 4 | 16.05 | .1888 | 2.9 | 1590 |
| 5 | 18.30 | .2153 | .096 | 940 |
| | | (G73) | $\Sigma$ 9250 | |

* Test Group No.

TABLE 59

UNIT HIGH PEAK GUST LOADING SPECTRA AND S-N DATA FOR NOTCHED SHEET COUPONS
7075-T6 ALUMINUM ALLOY

$K_T = 4$

$f_{mean} = 12$ KSI $\quad S_{mean} = .141$

$F_{tu} = 85$ KSI (Gross Area)

| Loading Step | $f_v$ KSI | $S_v$ | n | N | $f_v$ KSI | $S_v$ | n | N |
|---|---|---|---|---|---|---|---|---|
| | | | | 19 LOADING STEPS | | | | |
| 1 | .96 | .0113 | 5033 | -- | 1.49 | .0175 | 10043 | 10000000 |
| 2 | 1.79 | .0211 | 3511 | 4500000 | 2.46 | .0289 | 6993 | 1600000 |
| 3 | 2.65 | .0312 | 3290 | 1100000 | 3.34 | .0393 | 6594 | 500000 |
| 4 | 3.55 | .0418 | 1842 | 380000 | 4.50 | .0529 | 3697 | 170000 |
| 5 | 4.48 | .0527 | 1139 | 175000 | 5.30 | .0624 | 2298 | 88000 |
| 6 | 5.45 | .0641 | 592 | 81000 | 6.36 | .0748 | 1199 | 45000 |
| 7 | 6.35 | .0747 | 355 | 45000 | 7.35 | .0865 | 708 | 26000 |
| 8 | 7.35 | .0865 | 133 | 26000 | 8.40 | .0988 | 263 | 15000 |
| 9 | 8.38 | .0986 | 59 | 16000 | 9.50 | .1118 | 117 | 10000 |
| 10 | 9.35 | .1100 | 23 | 10000 | 10.50 | .1235 | 45 | 7400 |
| 11 | 10.85 | .1276 | 9.9 | 5500 | 11.60 | .1365 | 20 | 5200 |
| 12 | 11.90 | .1400 | 4.9 | 4900 | 12.50 | .1471 | 9.8 | 4100 |
| 13 | 12.80 | .1506 | 3.0 | 3800 | 13.60 | .1600 | 5.9 | 3000 |
| 14 | 13.80 | .1624 | 2.0 | 2900 | 13.80 | .1624 | 3.8 | 2900 |
| 15 | 14.90 | .1753 | .99 | 2200 | 15.10 | .1776 | 2.0 | 2100 |
| 16 | 15.90 | .1871 | .50 | 1700 | 15.90 | .1871 | .98 | 1700 |
| 17 | 17.20 | .2024 | .30 | 1250 | 17.00 | .2000 | .56 | 1300 |
| 18 | 18.05 | .2124 | .10 | 1000 | 18.00 | .2118 | .21 | 1000 |
| 19 | 18.30 | .2153 | .10 | 960 | 18.30 | .2153 | .21 | 960 |
| | | (074*) | $\Sigma$16000 | | | (075) | $\Sigma$32000 | |

* Test Group No.

TABLE 60

UNIT HIGH PEAK GUST LOADING SPECTRA AND S-N DATA FOR NOTCHED SHEET COUPONS
7075-T6 ALUMINUM ALLOY

$K_T = 7$

$f_{mean} = 12$ KSI $\quad S_{mean} = .141$

$F_{tu} = 85$ KSI (Gross Area)

| Loading Step | $f_v$ KSI | $S_v$ | n | N | $f_v$ KSI | $S_v$ | n | N |
|---|---|---|---|---|---|---|---|---|
| | 14 LOADING STEPS | | | | 17 LOADING STEPS | | | |
| 1 | .84 | .0099 | 25147 | 9000000 | 1.05 | .0124 | 767 | 5400000 |
| 2 | 2.50 | .0294 | 18066 | 280000 | 2.00 | .0235 | 621 | 700000 |
| 3 | 4.16 | .0489 | 9964 | 41000 | 3.00 | .0353 | 444 | 140000 |
| 4 | 5.84 | .0687 | 4005 | 13000 | 3.90 | .0459 | 286 | 54000 |
| 5 | 7.50 | .0882 | 1170 | 5100 | 4.90 | .0576 | 194 | 24000 |
| 6 | 9.16 | .1078 | 278 | 2400 | 5.80 | .0682 | 102 | 13000 |
| 7 | 10.42 | .1226 | 43 | 1500 | 6.80 | .0800 | 48 | 7000 |
| 8 | 11.24 | .1322 | 21 | 1150 | 8.00 | .0941 | 20 | 3900 |
| 9 | 12.08 | .1421 | 15 | 900 | 9.00 | .1059 | 8.9 | 2600 |
| 10 | 12.92 | .1520 | 7 | 710 | 9.80 | .1152 | 3.6 | 1900 |
| 11 | 13.66 | .1607 | 4.6 | 570 | 10.60 | .1247 | 1.4 | 1400 |
| 12 | 14.48 | .1704 | 4.4 | 480 | 11.70 | .1376 | .91 | 980 |
| 13 | 15.58 | .1833 | 3.2 | 350 | 12.70 | .1494 | .40 | 740 |
| 14 | 16.40 | .1929 | .60 | 290 | 14.00 | .1647 | .31 | 530 |
| 15 | | | | | 14.90 | .1753 | .15 | 420 |
| 16 | | | | | 16.00 | .1882 | .10 | 320 |
| 17 | | | | | 16.20 | .1906 | .044 | 300 |
| | | (G76*) | $\Sigma$ 58700 | | | (G77) | $\Sigma$ 2500 | |

* Test Group No.

TABLE 61

UNIT CONCAVE UPWARD AND CONCAVE DOWNWARD GUST LOADING SPECTRA AND S-N DATA FOR NOTCHED SHEET COUPONS
7075-T6 ALUMINUM ALLOY
$K_T = 4$
$f_{mean} = 12$ KSI $S_{mean} = .141$

$F_{tu} = 85$KSI (Gross Area)

7 Loading Steps

| Loading Step | $f_v$ KSI | $S_v$ | n | N | $f_v$ KSI | $S_v$ | n | N |
|---|---|---|---|---|---|---|---|---|
| | | | | Concave Upward | | | | |
| 1 | 1 | .0118 | 157310 | 20000000 | 1 | .0118 | 456200 | 20000000 |
| 2 | 3 | .0353 | 62150 | 750000 | 3 | .0353 | 269000 | 750000 |
| 3 | 5 | .0588 | 44890 | 110000 | 5 | .0588 | 83450 | 110000 |
| 4 | 7 | .0824 | 6900 | 31000 | 7 | .0824 | 15070 | 31000 |
| 5 | 9 | .1059 | 1140 | 12000 | 9 | .1059 | 1450 | 12000 |
| 6 | 11 | .1294 | 190 | 6300 | 11 | .1294 | 350 | 6300 |
| 7 | 12.75 | .1500 | 50 | 3800 | 12.75 | .1500 | 80 | 3800 |
| | | (G78*) | $\Sigma$272600 | | | (G79) | $\Sigma$825600 | |
| | | | | Concave Downward | | | | |
| 1 | 1 | .0118 | 65590 | 20000000 | 1 | .0118 | 38340 | 20000000 |
| 2 | 3 | .0353 | 61210 | 750000 | 3 | .0353 | 42920 | 750000 |
| 3 | 5 | .0588 | 32800 | 110000 | 5 | .0588 | 27000 | 110000 |
| 4 | 7 | .0824 | 24920 | 31000 | 7 | .0824 | 19970 | 31000 |
| 5 | 9 | .1059 | 9960 | 12000 | 9 | .1059 | 12020 | 12000 |
| 6 | 11 | .1294 | 2030 | 6300 | 11 | .1294 | 4490 | 6300 |
| 7 | 12.75 | .1500 | 210 | 3800 | 12.75 | .1500 | 400 | 3800 |
| | | (G80) | $\Sigma$196700 | | | (G81) | $\Sigma$145100 | |

* Test Group No.

TABLE 62

UNIT FIGHTER MANEUVER LOADING SPECTRA AND S-N DATA FOR NOTCHED SHEET COUPONS
7075-T6 ALUMINUM ALLOY

$K_T = 4$

$f_{min} = 5.4$ KSI $\quad S_{min} = .064$

$F_{tu} = 85$ KSI (Gross Area)

| Loading Step | $f_v$ KSI | $S_v$ | n | N | $f_v$ KSI | $S_v$ | n | N |
|---|---|---|---|---|---|---|---|---|
| | | | | 11 LOADING STEPS | | | | |
| 1 | .71 | .0084 | 5971 | ∞ | 1.68 | .0198 | 350 | ∞ |
| 2 | 2.13 | .0251 | 4795 | ∞ | 3.50 | .0412 | 235 | 1000000 |
| 3 | 4.27 | .0502 | 7085 | 350000 | 5.75 | .0676 | 175 | 78000 |
| 4 | 7.10 | .0835 | 5029 | 26000 | 7.80 | .0918 | 125 | 18000 |
| 5 | 9.92 | .1167 | 2860 | 7000 | 10.00 | .1176 | 85 | 6600 |
| 6 | 12.78 | .1504 | 1351 | 2400 | 12.10 | .1424 | 56 | 3100 |
| 7 | 14.90 | .1753 | 264 | 1200 | 14.20 | .1671 | 29 | 1500 |
| 8 | 16.30 | .1918 | 104 | 820 | 16.50 | .1941 | 12 | 780 |
| 9 | 18.45 | .2171 | 113 | 500 | 18.30 | .2153 | 5.4 | 520 |
| 10 | 20.25 | .2382 | 12 | 360 | 20.15 | .2371 | 1.6 | 360 |
| 11 | 20.81 | .2448 | 6.3 | 320 | 21.00 | .2471 | .28 | 310 |
| | | (M14*) | $\Sigma$ 27700 | | | (M15) | $\Sigma$ 1100 | |

* Test Group No.

TABLE 63

UNIT FIGHTER MANEUVER LOADING SPECTRA AND S-N DATA FOR NOTCHED SHEET COUPONS
7075-T6 ALUMINUM ALLOY

$K_T = 4$

$f_{min} = 5.4$ KSI $\quad S_{min} = .064$

$F_{tu} = 85$ KSI (Gross Area)

| Loading Step | $f_v$ KSI | $S_v$ | n | N | Loading Step | $f_v$ KSI | $S_v$ | n | N |
|---|---|---|---|---|---|---|---|---|---|
| | | | | 40 LOADING STEPS | | | | | |
| 1 | .470 | .0055 | 100 | -- | 21 | 10.450 | .1229 | 15 | 5700 |
| 2 | .845 | .0099 | 75 | -- | 22 | 11.050 | .1300 | 15 | 4400 |
| 3 | 1.175 | .0138 | 75 | -- | 23 | 11.750 | .1382 | 12 | 3500 |
| 4 | 1.555 | .0183 | 75 | -- | 24 | 12.250 | .1441 | 11 | 2900 |
| 5 | 1.930 | .0227 | 75 | -- | 25 | 12.850 | .1512 | 7.8 | 2300 |
| 6 | 2.400 | .0282 | 60 | 7200000 | 26 | 13.550 | .1594 | 5.9 | 1800 |
| 7 | 2.920 | .0344 | 55 | 2600000 | 27 | 14.150 | .1665 | 5.9 | 1600 |
| 8 | 3.500 | .0412 | 45 | 1000000 | 28 | 14.650 | .1724 | 5.8 | 1300 |
| 9 | 3.955 | .0465 | 45 | 510000 | 29 | 15.150 | .1782 | 3.9 | 1100 |
| 10 | 4.475 | .0526 | 45 | 300000 | 30 | 15.700 | .1847 | 2.9 | 940 |
| 11 | 5.000 | .0588 | 40 | 155000 | 31 | 16.300 | .1918 | 2.0 | 820 |
| 12 | 5.555 | .0654 | 35 | 88000 | 32 | 16.850 | .1982 | 2.0 | 710 |
| 13 | 6.050 | .0712 | 35 | 58000 | 33 | 17.350 | .2041 | 1.5 | 640 |
| 14 | 6.650 | .0782 | 32 | 37000 | 34 | 17.850 | .2100 | .98 | 570 |
| 15 | 7.150 | .0841 | 30 | 26000 | 35 | 18.300 | .2153 | .96 | 520 |
| 16 | 7.750 | .0912 | 25 | 18000 | 36 | 18.850 | .2218 | .70 | 470 |
| 17 | 8.300 | .0976 | 23 | 14000 | 37 | 19.400 | .2282 | .58 | 420 |
| 18 | 8.550 | .1006 | 20 | 12000 | 38 | 20.000 | .2353 | .50 | 370 |
| 19 | 9.400 | .1106 | 20 | 8600 | 39 | 20.300 | .2388 | .40 | 350 |
| 20 | 10.000 | .1176 | 19 | 6700 | 40 | 21.000 | .2471 | .30 | 310 |
| | | | | | | | (M16*) | $\Sigma$ 1000 | |

* Test Group No.

TABLE 64

UNIT GROUND LOADING SPECTRA AND S-N DATA FOR NOTCHED SHEET COUPONS

7075-T6 ALUMINUM ALLOY

$K_T = 7$

$f_{mean} = -3$ KSI $\qquad S_{mean} = -.035$

$F_{tu} = 85$ KSI (Gross Area)

| Loading Step | $f_v$ KSI | $S_v$ | n | N | $f_v$ KSI | $S_v$ | n | N |
|---|---|---|---|---|---|---|---|---|
| | 18 Loading Steps | | | | 11 Loading Steps | | | |
| 1 | .48 | .0056 | 236392 | - | 1.10 | .0129 | 10553 | - |
| 2 | 1.44 | .0169 | 174558 | - | 2.07 | .0244 | 7010 | - |
| 3 | 2.38 | .0280 | 96152 | - | 3.10 | .0365 | 2831 | 2900000 |
| 4 | 3.32 | .0391 | 38265 | 1800000 | 4.07 | .0479 | 980 | 580000 |
| 5 | 4.28 | .0504 | 10869 | 470000 | 5.15 | .0606 | 98 | 180000 |
| 6 | 5.23 | .0615 | 2542 | 160000 | 6.25 | .0735 | 38 | 70000 |
| 7 | 5.94 | .0699 | 409 | 90000 | 7.32 | .0861 | 15 | 33000 |
| 8 | 6.42 | .0755 | 184 | 62000 | 8.50 | .1000 | 4.3 | 15000 |
| 9 | 6.89 | .0811 | 124 | 43000 | 9.05 | .1065 | 1.5 | 10500 |
| 10 | 7.36 | .0866 | 71 | 31000 | 9.90 | .1165 | .41 | 6800 |
| 11 | 7.80 | .0918 | 44 | 23000 | 10.50 | .1235 | .19 | 5000 |
| 12 | 8.28 | .0974 | 42 | 18000 | | | | |
| 13 | 8.90 | .1047 | 25 | 12000 | | | | |
| 14 | 9.38 | .1104 | 8 | 9000 | | | | |
| 15 | 9.56 | .1125 | 2 | 7800 | | | | |
| 16 | 9.80 | .1153 | 4.3 | 7000 | | | | |
| 17 | 10.22 | .1202 | 4.3 | 5400 | | | | |
| 18 | 10.80 | .1271 | 3.8 | 4200 | | | | |
| | | (T1*) | $\Sigma$ 559700 | | | (T2) | $\Sigma$ 21500 | |

* Test Group No.

## TABLE 65

UNIT COMPOSITE LOW PEAK GUST, GROUND AND GROUND-AIR-GROUND LOADING SPECTRUM, AND S-N DATA FOR NOTCHED SHEET COUPONS

7075-T6 ALUMINUM ALLOY
$K_T = 4$
$F_{tu}$ = 85 KSI (GROSS AREA)

| LOADING STEP | $f_v$ KSI | $S_v$ | n | N |
|---|---|---|---|---|
| | 26 LOADING STEPS | | | |
| | LOW PEAK GUST LOADING | | | |
| | $f_{mean}$ = 6 KSI; $S_{mean}$ = .071 | | | |
| 1 | 1.15 | .0135 | 5549 | ∞ |
| 2 | 2.20 | .0259 | 4036 | ∞ |
| 3 | 3.25 | .0382 | 2018 | 8400000 |
| 4 | 4.35 | .0512 | 940 | 900000 |
| 5 | 5.35 | .0629 | 386 | 330000 |
| 6 | 6.40 | .0753 | 114 | 135000 |
| 7 | 7.45 | .0876 | 27 | 65000 |
| 8 | 8.25 | .0971 | 9.9 | 40000 |
| 9 | 9.15 | .1076 | 4.0 | 24000 |
| 10 | 10.15 | .1194 | 2.4 | 15000 |
| 11 | 11.20 | .1318 | .99 | 10000 |
| 12 | 12.05 | .1418 | .41 | 8600 |
| 13 | 13.00 | .1529 | .19 | 5700 |
| | | | Σ13100 | |
| | GROUND LOADING | | | |
| | $f_{mean}$ = -3 KSI; $S_{mean}$ = -.035 | | | |
| 14 | 1.20 | .0141 | 2969 | ∞ |
| 15 | 2.20 | .0259 | 2078 | ∞ |
| 16 | 3.30 | .0388 | 1088 | ∞ |
| 17 | 4.50 | .0529 | 495 | 5200000 |
| 18 | 5.65 | .0665 | 208 | 1500000 |
| 19 | 6.75 | .0794 | 64 | 550000 |
| 20 | 7.60 | .0894 | 15 | 270000 |
| 21 | 8.65 | .1018 | 5.9 | 136000 |
| 22 | 9.40 | .1106 | 2.0 | 90000 |
| 23 | 10.30 | .1212 | .99 | 52000 |
| 24 | 11.45 | .1347 | .60 | 29000 |
| 25 | 12.00 | .1412 | .41 | 22600 |
| | | | Σ6930 | |
| | GROUND-AIR-GROUND LOADING | | | |
| | $f_{mean}$ = 1.5 KSI; $S_{mean}$ = .018 | | | |
| 26 | 4.90 | .0576 | 1170 | 2100000 |
| Total | | (CG1*) | Σ21200 | |

* Test Group No.

TABLE 66

UNIT COMPOSITE LOW PEAK GUST, GROUND AND GROUND-AIR-GROUND LOADING SPECTRUM, AND S-N DATA FOR NOTCHED SHEET COUPONS

7075-T6 ALUMINUM ALLOY
$K_T = 7$
$F_{tu} = 85$ KSI (GROSS AREA)

| LOADING STEP | $f_v$ KSI | $S_v$ | n | N |
|---|---|---|---|---|
| | 21 LOADING STEPS | | | |
| | LOW PEAK GUST LOADING $f_{mean} = 6$ KSI; $S_{mean} = .071$ | | | |
| 1 | 1.30 | .0153 | 511 | ∞ |
| 2 | 2.30 | .0271 | 325 | 2900000 |
| 3 | 3.20 | .0376 | 220 | 320000 |
| 4 | 4.20 | .0494 | 90 | 110000 |
| 5 | 5.10 | .0600 | 34 | 49000 |
| 6 | 6.00 | .0706 | 12 | 25000 |
| 7 | 7.20 | .0847 | 2.5 | 11000 |
| 8 | 8.70 | .1024 | .81 | 4900 |
| 9 | 9.10 | .1071 | .35 | 4000 |
| 10 | 10.00 | .1176 | .21 | 2700 |
| 11 | 11.00 | .1294 | .052 | 1800 |
| | | | Σ1200 | |
| | GROUND LOADING $f_{mean} = -3$ KSI; $S_{mean} = -.035$ | | | |
| 12 | 1.30 | .0153 | 290 | ∞ |
| 13 | 2.30 | .0271 | 190 | ∞ |
| 14 | 3.30 | .0388 | 84 | 1800000 |
| 15 | 4.30 | .0506 | 29 | 450000 |
| 16 | 5.20 | .0612 | 5.2 | 165000 |
| 17 | 6.25 | .0735 | 1.1 | 69000 |
| 18 | 7.25 | .0853 | .35 | 34000 |
| 19 | 8.35 | .0982 | .16 | 17000 |
| 20 | 8.85 | .1041 | .052 | 12000 |
| | | | Σ600 | |
| | GROUND-AIR-GROUND LOADING $f_{mean} = 1.5$ KSI; $S_{mean} = .018$ | | | |
| 21 | 4.65 | .0547 | 102 | 140000 |
| Total | | | (CG2*) Σ1900 | |

* Test Group No.

TABLE 67

UNIT COMPOSITE HIGH PEAK GUST, GROUND AND GROUND-AIR-GROUND LOADING SPECTRA, AND S-N DATA FOR NOTCHED SHEET COUPONS
7075-T6 ALUMINUM ALLOY
$K_T = 4$
$F_{tu} = 85$ KSI (GROSS AREA)

| LOADING STEP | $f_v$ KSI | $S_v$ | n | N | $f_v$ KSI | $S_v$ | n | N |
|---|---|---|---|---|---|---|---|---|
| | 28 LOADING STEPS | | | | | | | |
| | High Peak Gust Loading; $f_{mean} = 12$ KSI; $S_{mean} = .141$ | | | | | | | |
| 1 | 1.15 | .0135 | 606 | ∞ | 1.10 | .0129 | 2560 | ∞ |
| 2 | 2.40 | .0282 | 505 | 1800000 | 2.30 | .0271 | 2560 | 2000000 |
| 3 | 3.40 | .0400 | 429 | 470000 | 3.00 | .0353 | 1598 | 770000 |
| 4 | 4.30 | .0506 | 257 | 190000 | 3.90 | .0459 | 1064 | 280000 |
| 5 | 5.40 | .0635 | 158 | 86000 | 4.80 | .0565 | 580 | 132000 |
| 6 | 6.35 | .0747 | 84 | 46000 | 5.85 | .0688 | 387 | 63000 |
| 7 | 7.65 | .0900 | 40 | 22000 | 7.00 | .0824 | 169 | 31000 |
| 8 | 8.55 | .1006 | 17 | 14300 | 8.00 | .0941 | 73 | 18500 |
| 9 | 9.55 | .1124 | 5.9 | 9800 | 9.00 | .1059 | 24 | 12000 |
| 10 | 10.60 | .1247 | 3.0 | 7100 | 10.20 | .1200 | 13 | 8100 |
| 11 | 11.50 | .1353 | 1.4 | 5500 | 11.05 | .1300 | 4.8 | 5500 |
| 12 | 12.60 | .1462 | .69 | 4000 | 12.10 | .1424 | 3.4 | 4600 |
| 13 | 13.60 | .1600 | .39 | 3000 | 13.05 | .1535 | 1.5 | 3500 |
| 14 | 14.80 | .1741 | .21 | 2259 | 14.00 | .1647 | .97 | 2760 |
| 15 | 15.40 | .1812 | .16 | 1960 | 14.90 | .1753 | .51 | 2200 |
| 16 | 15.80 | .1859 | .092 | 1760 | 16.0 | .1882 | .34 | 1670 |
| 17 | 16.30 | .1918 | .046 | 1560 | 16.85 | .1982 | .11 | 1360 |
| 18 | — | — | — | — | 18.30 | .2153 | .11 | 960 |
| | | | Σ2110 | | | | Σ9040 | |
| | Ground Loading; $f_{mean} = -3$ KSI; $S_{mean} = -.035$ | | | | | | | |
| 19 | 1.25 | .0147 | 553 | ∞ | 1.10 | .0129 | 455 | ∞ |
| 20 | 2.10 | .0247 | 286 | ∞ | 2.05 | .0241 | 342 | ∞ |
| 21 | 3.10 | .0365 | 133 | ∞ | 3.05 | .0359 | 126 | ∞ |
| 22 | 4.20 | .0494 | 44 | 7800000 | 4.00 | .0471 | 46 | 10000000 |
| 23 | 5.00 | .0588 | 6.9 | 3000000 | 5.00 | .0588 | 9.2 | 3000000 |
| 24 | 6.00 | .0706 | 2.0 | 1070000 | 6.05 | .0712 | 2.4 | 980000 |
| 25 | 6.90 | .0812 | .64 | 480000 | 7.00 | .0824 | .63 | 450000 |
| 26 | 7.95 | .0935 | .25 | 220000 | 8.05 | .0947 | .40 | 192000 |
| 27 | 8.65 | .1018 | .046 | 134000 | 9.30 | .1094 | .11 | 93000 |
| 28 | 8.95 | .1053 | .046 | 116000 | — | — | — | — |
| | | | Σ1030 | | | | Σ970 | |
| | Ground-Air-Ground Loading; $f_{mean} = 4.5$ KSI; $S_{mean} = .053$ | | | | | | | |
| 29 | 7.95 | .0935 | 182 | 65000 | 7.85 | .0924 | 89 | 67000 |
| Total | (CG3 *) Σ3320 | | | | (CG4) Σ10100 | | | |

* Test Group No.

## TABLE 68

UNIT COMPOSITE FIGHTER MANEUVER, GROUND AND GROUND-AIR-GROUND LOADING SPECTRUM, AND S-N DATA FOR NOTCHED SHEET COUPONS 7075-T6 Aluminum Alloy

$K_T = 4$

$F_{tu} = 85$ KSI (Gross Area)

| Loading Steps | $f_v$ KSI | $S_v$ | n | N |
|---|---|---|---|---|
| | | 29 Loading Steps | | |
| | | FIGHTER MANEUVER LOADING | | |
| | | $f_{min} = 5.45$ KSI; $S_{min} = .064$ | | |
| 1 | .71 | .0084 | 1870 | ∞ |
| 2 | 2.13 | .0251 | 1496 | 13000000 |
| 3 | 4.27 | .0502 | 2224 | 340000 |
| 4 | 7.10 | .0835 | 1574 | 27000 |
| 5 | 9.92 | .1167 | 896 | 6500 |
| 6 | 12.78 | .1504 | 423 | 2400 |
| 7 | 14.90 | .1753 | 83 | 1200 |
| 8 | 16.30 | .1918 | 51 | 820 |
| 9 | 18.42 | .2167 | 35 | 510 |
| 10 | 20.25 | .2382 | 3.9 | 340 |
| 11 | 20.80 | .2447 | 2.0 | 310 |
| | | | ∑8660 | |
| | | GROUND LOADING | | |
| | | $f_{mean} = -3$ KSI; $S_{mean} = -.035$ | | |
| 12 | .42 | .0049 | 849 | ∞ |
| 13 | 1.44 | .0169 | 628 | ∞ |
| 14 | 2.38 | .0280 | 345 | ∞ |
| 15 | 3.32 | .0391 | 138 | ∞ |
| 16 | 4.28 | .0504 | 39 | 7000000 |
| 17 | 5.22 | .0614 | 9.1 | 2200000 |
| 18 | 5.94 | .0699 | 1.5 | 1100000 |
| 19 | 6.42 | .0755 | .63 | 740000 |
| 20 | 6.89 | .0811 | .44 | 500000 |
| 21 | 7.36 | .0866 | .25 | 330000 |
| 22 | 7.80 | .0918 | .15 | 240000 |
| 23 | 8.28 | .0974 | .21 | 170000 |
| 24 | 8.90 | .1047 | .037 | 120000 |
| 25 | 9.38 | .1104 | .055 | 90000 |
| 26 | 9.56 | .1125 | .002 | 80000 |
| 27 | 9.80 | .1153 | .016 | 70000 |
| 28 | 10.22 | .1202 | .003 | 54000 |
| | | | ∑2010 | |
| | | GROUND-AIR-GROUND LOADING | | |
| | | $f_{mean} = 1.22$ KSI; $S_{mean} = .014$ | | |
| 29 | 4.22 | .0496 | 287 | 5000000 |
| Total | | | (CML*) ∑11000 | |

* Test Group No.

## TABLE 69

### EXPERIMENTAL FATIGUE LIVES FOR GUST LOADING SPECTRA 7075-T6 ALUMINUM ALLOY

(Table is completed on next three pages)

| Test Group No. | Specimen No. | Type of Specimen | $K_T$ | $S_{mean}$ | No. of Loading Steps | Type of Spectrum Curve | Sequence | Block Size | Test Life ($10^6$ Cycles) |
|---|---|---|---|---|---|---|---|---|---|
| G56 | 318 | Notched Sheet Coupon | 4 | .071 | 18 | Low Peak | True Random | 1662800 (Avg.) | 1.936 |
| | 362 | | | | | | | | 1.470 |
| | 393 | | | | | | | | 1.792 |
| | 305 | | | | | | | | 1.453 |
| | | | | | | | | | 1.650* |
| G67 | 364 | | | | 4 | | Lo-Hi | 26000 | 1.394 |
| | 365 | | | | | | | | .458 |
| | 368 | | | | | | | | 2.103 |
| | 370 | | | | | | | | 2.046 |
| | 377 | | | | | | | | 1.030 |
| | | | | | | | | | 1.230 * |
| G68 | 372 | | | | 14 | | Lo-Hi | 60000 | 4.918 |
| | 376 | | | | | | | | 3.178 |
| | 381 | | | | | | | | 4.189 |
| | 385 | | | | | | | | 3.777 |
| | 394 | | | | | | | | 5.070 |
| | | | | | | | | | 4.165 * |
| G69 | 378 | | 4 | | 14 | | Lo-Hi | 120000 | 4.553 |
| | 387 | | | | | | | | 5.386 |
| | 388 | | | | | | | | 5.390 |
| | 392 | | | | | | | | 5.874 |
| | 391 | | | | | | | | 10.056 |
| | | | | | | | | | 6.005 * |
| G70 | 299 | Notched Sheet Coupon | 7 | .071 | 17 | Low Peak | True Random | 233400 (Avg.) | .252 |
| | 300 | | | | 15 | | | | .170 |
| | 301 | | | | 17 | | | | .239 |
| | 302 | | | | 17 | | | | .200 |
| | 303 | | | | 17 | | | | .326 |
| | 304 | | | | 17 | | | | .213 |
| | | | | | | | | | .228 * |

* Geometric mean of test life

TABLE 69

EXPERIMENTAL FATIGUE LIVES FOR GUST LOADING SPECTRA
7075-T6 ALUMINUM ALLOY

(Table is continued on next page)

| Test Group No. | Specimen No. | Type of Specimen | $K_T$ | $S_{mean}$ | No. of Steps | Type of Loading Spectrum Curve | Sequence | Block Size | Test Life ($10^6$ Cycles) |
|---|---|---|---|---|---|---|---|---|---|
| G71 | 348 | Notched Sheet Coupon | 7 | .071 | 13 | Low Peak | Low-Hi | 9000 | .211 |
| | 350 | | | | | | | | .289 |
| | 351 | | | | | | | | .305 |
| | 355 | | | | | | | | .254 |
| | 356 | | 7 | .071 | | Low Peak | | | .228 |
| | | | | | | | | | .255* |
| G72 | 279 | | 4 | .111 | 23 | High Peak | True Random | 379100 (Avg.) | .652 |
| | 285 | | | | 21 | | | | .396 |
| | 287 | | | | 21 | | | | .457 |
| | 288 | | | | 21 | | | | .335 |
| | 290 | | | | 21 | | | | .239 |
| | 291 | | | | 21 | | | | .326 |
| | 292 | | | | 21 | | | | .248 |
| | | | | | | | | | .359* |
| G73 | 326 | | | | 5 | | Lo-Hi | 9250 | .304 |
| | 331 | | | | | | | | .145 |
| | 332 | | | | | | | | .153 |
| | 334 | | | | | | | | .188 |
| | 336 | | | | | | | | .306 |
| | 337 | | | | | | | | .207 |
| | 339 | | | | | | | | .498 |
| | 340 | | | | | | | | .353 |
| | | | | | | | | | .248* |
| G74 | 313 | Notched Sheet Coupon | 4 | .111 | 13 | High Peak | Lo-Hi | 16000 | .415 |
| | 320 | | | | | | | | .470 |
| | 328 | | | | | | | | .814 |
| | 335 | | | | | | | | .441 |
| | 341 | | | | | | | | .928 |
| | | | | | | | | | .579* |

* Geometric mean of test life

TABLE 69

EXPERIMENTAL FATIGUE LIVES FOR GUST LOADING SPECTRA
7075-T6 ALUMINUM ALLOY

(Table is concluded on next page)

| Test Group No. | Specimen No. | Type of Specimen | $K_T$ | $S_{mean}$ | No. of Loading Steps | Type of Spectrum Curve | Sequence | Block Size | Test Life ($10^6$ Cycles) |
|---|---|---|---|---|---|---|---|---|---|
| G75 | 307 | Notched Sheet Coupon | 4 | .141 | 19 | High Peak | Lo-Hi | 32000 | .319 |
| | 308 | | | | | | | | .289 |
| | 309 | | | | | | | | .288 |
| | 310 | | | | | | | | .224 |
| | 312 | | 4 | | | | | | .257 |
| | | | | | | | | | .274 * |
| G76 | 274 | | 7 | | 13 | | True Random | 58700 (Avg.) | .0566 |
| | 280 | | | | 14 | | | | .0957 |
| | 281 | | | | 13 | | | | .0566 |
| | 282 | | | | 13 | | | | .0392 |
| | 283 | | | | 13 | | | | .0522 |
| | 284 | | | | 13 | | | | .0522 |
| | | | | | | | | | .0567* |
| G77 | 293 | Notched Sheet Coupon | 7 | .141 | 17 | High Peak | Lo-Hi | 2500 | .0630 |
| | 294 | | | | | | | | .0582 |
| | 295 | | | | | | | | .0630 |
| | 296 | | | | | | | | .0589 |
| | 297 | | | | | | | | .0413 |
| | 298 | | | | | | | | .0555 |
| | | | | | | | | | .0517* |

* Geometric mean of test life

TABLE 69

EXPERIMENTAL FATIGUE LIVES FOR GUST LOADING SPECTRA
7075-T6 ALUMINUM ALLOY
(Concluding page of table)

| Test Group No. | Specimen No. | Type of Specimen | $K_T$ | $S_{mean}$ | No. of Loading Steps | Type of Spectrum Curve | Sequence | Block Size | Test Life ($10^6$ Cycles) |
|---|---|---|---|---|---|---|---|---|---|
| G78 | 70 | Notched Sheet Coupon | 4 | .141 | 7 | Concave Upward | True Random | 272600 (Avg.) | .300 |
| | 72 | | | | | | | | .309 |
| | 85 | | | | | | | | .260 |
| | 88 | | | | | | | | .254 |
| | 92 | | | | | | | | .277 |
| | 93 | | | | | | | | .240 |
| | 114 | | | | | | | | .262 |
| | 115 | | | | | | | | .228 |
| | 126 | | | | | | | | .359 |
| | 128 | | | | | | | | .239 |
| | | | | | | | | | .270* |
| G79 | 251 | | | | 7 | Concave Upward | Lo-Hi | 825600 (Avg.) | 1.020 |
| | 252 | | | | | | | | .780 |
| | 255 | | | | | | | | .536 |
| | 256 | | | | | | | | .808 |
| | 258 | | | | | | | | .985 |
| | | | | | | | | | .804* |
| G80 | 173 | | | | 7 | Concave Downward | True Random | 196700 (Avg.) | .168 |
| | 175 | | | | | | | | .259 |
| | 176 | | | | | | | | .157 |
| | 177 | | | | | | | | .203 |
| | | | | | | | | | .193* |
| G81 | 246 | Notched Sheet Coupon | 4 | .141 | 7 | Concave Downward | Lo-Hi | 145100 (Avg.) | .134 |
| | 247 | | | | | | | | .118 |
| | 248 | | | | | | | | .147 |
| | 249 | | | | | | | | .141 |
| | 250 | | | | | | | | .187 |
| | | | | | | | | | .144* |

* Geometric Mean of Test Life

TABLE 70

EXPERIMENTAL FATIGUE LIVES FOR GROUND LOADING SPECTRA

7075-T6 ALUMINUM ALLOY

| Test Group No. | Specimen No. | Type of Specimen | $K_T$ | $S_{mean}$ | No. of Loading Steps | Sequence | Block Size | Test Life ($10^6$ cycles) |
|---|---|---|---|---|---|---|---|---|
| T1 | 416 | Notched Sheet Coupon | 7 | -.035 | 18 | True Random | 559700 (Avg.) | .783 |
| | 417 | | | | | | | .500 |
| | 418 | | | | | | | .552 |
| | 419 | | | | | | | .579 |
| | 422 | | | | | | | .496 |
| | 423 | | | | | | | .448 |
| | | | | | | | | .550 * |
| T2 | 461 | Notched Sheet Coupon | 7 | -.035 | 11 | Lo-Hi | 21500 | .775 |
| | 462 | | | | | | | .748 |
| | 465 | | | | | | | 1.010 |
| | 466 | | | | | | | 1.268 |
| | 469 | | | | | | | .900 |
| | 471 | | | | | | | 1.309 |
| | | | | | | | | .978 * |

* Geometric mean of test life

TABLE 71

EXPERIMENTAL FATIGUE LIVES FOR FIGHTER MANEUVER LOADING SPECTRA
7075-T6 ALUMINUM ALLOY

| Test Group No. | Specimen No. | Type of Specimen | $K_T$ | $S_{min}$ | No. of Loading Steps | Sequence | Block Size | Test Life ($10^6$ Cycles |
|---|---|---|---|---|---|---|---|---|
| M14 | 342 | Notched Sheet Coupon | 4 | .064 | 11 | True Random | 27700 (Avg.) | .0264 |
| | 343 | | | | | | | .0220 |
| | 344 | | | | | | | .0176 |
| | 345 | | | | | | | .0308 |
| | 346 | | | | | | | .0440 |
| | 347 | | | | | | | .0264 |
| | 349 | | | | | | | .0264 |
| | | | | | | | | .0267* |
| M15 | 399 | | | .064 | 11 | Lo-Hi | 1100 | .0129 |
| | 400 | | | | | | | .0129 |
| | 401 | | | | | | | .0097 |
| | 404 | | | | | | | .0193 |
| | 406 | | | | | | | .0150 |
| | | | | | | | | .0136 * |
| M16 | 410 | Notched Sheet Coupon | 4 | .064 | 40 | Lo-Hi | 1000 | .0082 |
| | 411 | | | | | | | .0174 |
| | 413 | | | | | | | .0123 |
| | 414 | | | | | | | .0123 |
| | 415 | | | | | | | .0133 |
| | | | | | | | | .0123 * |

* Geometric mean of test life

TABLE 72

EXPERIMENTAL FATIGUE LIVES FOR COMPOSITE MANEUVER LOADING SPECTRUM
7075-T6 ALUMINUM ALLOY

True Random Loading Sequence

| Test Group No. | Specimen No. | Type of Specimen | $K_T$ | $S_{min}$ | $S_{mean}$ | No. of Loading Steps | Block Size | Test Life ($10^6$ Cycles) |
|---|---|---|---|---|---|---|---|---|
| CM1 | 488 | Notched Sheet Coupon | 4 | Fighter Maneuver .064 | Ground -.035 G-A-G .014 | 29 | 11000 (Avg.) | .0091 |
| | 489 | | | | | | | .0103 |
| | 490 | | | | | | | .0121 |
| | 499 | | | | | | | .0098 |
| | 500 | | | | | | | .0135 |
| | | | | | | | | .0108* |

* Geometric Mean of Test Life

TABLE 73

EXPERIMENTAL FATIGUE LIVES FOR COMPOSITE GUST LOADING SPECTRA

7075-T6 ALUMINUM ALLOY

Lo-Hi Loading Sequence

| Test Group No. | Specimen No. | Type of Specimen | $K_T$ | $S_{mean}$ | No. of Loading Stops | Block Size | Test Life ($10^6$ cycles) |
|---|---|---|---|---|---|---|---|
| CG1 | 475 | Notched Sheet Coupon | 4 | Gust .071 Ground -.035 G-A-G .018 | 26 | 21200 | 1.092 |
| | 480 | | | | | | .571 |
| | 481 | | | | | | 1.242 |
| | 485 | | | | | | .754 |
| | 487 | | | | | | 1.694 |
| | | | | | | | .998 * |
| CG2 | 478 | | 7 | Gust .071 Ground -.035 G-A-G .018 | 21 | 1900 | .134 |
| | 479 | | | | | | .138 |
| | 482 | | | | | | .083 |
| | 484 | | | | | | .110 |
| | 486 | | | | | | .084 |
| | | | | | | | .107 * |
| CG3 | 467 | | 4 | Gust .141 Ground -.035 G-A-G .053 | 28 | 3300 | .145 |
| | 470 | | | | | | .191 |
| | 472 | | | | | | .117 |
| | 473 | | | | | | .118 |
| | 474 | | | | | | .151 |
| | | | | | | | .142 * |
| CG4 | 509 | Notched Sheet Coupon | 4 | Gust .141 Ground -.035 G-A-G .053 | 28 | 10100 | .200 |
| | 510 | | | | | | .259 |
| | 511 | | | | | | .338 |
| | 512 | | | | | | .221 |
| | 513 | | | | | | .276 |
| | 514 | | | | | | .269 |
| | 517 | | | | | | .177 |
| | 518 | | | | | | .301 |
| | | | | | | | .250 * |

* Geometric mean of test data

TABLE 74

LOW PEAK RANDOM GUST LOADING HISTORIES
(MEAN CROSSING PEAK COUNTS)
$f_{mean}$ = 6,000 psi
$K_T$ = 4.0

Test Group No. G66

| Varying Stress (psi) | Cumulative Frequency of Load Cycle Occurrences | | | |
|---|---|---|---|---|
| | Specimen No.305 | Specimen No.318 | Specimen No.362 | Specimen No.393 |
| 0 | 1,452,900 | 1,935,750 | 1,470,300 | 1,792,200 |
| 1,190 | 827,300 | 1,102,600 | 837,050 | 1,020,600 |
| 2,380 | 380,300 | 507,050 | 384,750 | 469,100 |
| 3,560 | 135,380 | 180,500 | 136,990 | 166,960 |
| 4,750 | 37,113 | 49,490 | 37,539 | 45,774 |
| 5,950 | 8,952 | 11,939 | 9,057 | 11,043 |
| 7,120 | 2,382.7 | 3,181.5 | 2,411.3 | 2,938.6 |
| 7,720 | 1,326.0 | 1,811.2 | 1,371.7 | 1,672.6 |
| 8,310 | 859.5 | 1,148.4 | 869.1 | 1,060.0 |
| 8,900 | 527.7 | 705.3 | 534.3 | 650.8 |
| 9,500 | 344.1 | 460.3 | 348.7 | 424.3 |
| 10,000 | 239.9 | 321.5 | 243.3 | 295.6 |
| 10,700 | 91.1 | 122.4 | 93.1 | 112.3 |
| 11,600 | 60.2 | 80.7 | 61.7 | 74.0 |
| 11,900 | 22.6 | 30.5 | 23.7 | 27.6 |
| 12,050 | 21.0 | 28.6 | 22.0 | 25.6 |
| 12,500 | 10.2 | 13.2 | 10.2 | 11.5 |
| 13,100 | 7.7 | 10.0 | 7.7 | 8.7 |
| 14,000 | 2.0 | 3.0 | 2.0 | 2.0 |

TABLE 75

LOW PEAK ORDERED GUST LOADING HISTORIES

Stress Interval = 4,000 psi
Unit Spectrum = 1/20 avg. random test history
$f_{mean}$ = 6,000 psi
$K_T$ = 4.0

Test Group No. 067

| Varying Stress (psi) | Cumulative Frequency of Load Cycle Occurrences | | | | |
|---|---|---|---|---|---|
| | Specimen No. 364 | Specimen No. 365 | Specimen No. 368 | Specimen No. 370 | Specimen No. 377 |
| 2,100 | 1,393,865 | 457,862 | 2,103,148 | 2,045,683 | 1,029,604 |
| 6,180 | 31,805 | 10,202 | 48,008 | 46,808 | 23,404 |
| 10,080 | 588 | 189 | 888 | 866 | 433 |
| 14,000 | 5 | 2 | 8 | 8 | 4 |
| No. of Blocks | 53.61 | 17.61 | 80.89 | 78.68 | 39.60 |

TABLE 76

LOW PEAK ORDERED GUST LOADING HISTORIES

Stress Interval = 1,000 psi
Unit Spectrum = 1/20 avg. random test life
$f_{mean}$ = 6,000 psi
$K_T$ = 4.0

Test Group No. G68

| Varying Stress (psi) | Cumulative Frequency of Load Cycle Occurrences | | | | |
|---|---|---|---|---|---|
| | Specimen No. 372 | Specimen No. 376 | Specimen No.381 | Specimen No.385 | Specimen No.394 |
| 550 | 4,918,201 | 3,177,840 | 4,189,201 | 3,777,001 | 5,070,000 |
| 1,600 | 2,868,201 | 1,852,840 | 2,439,201 | 2,202,001 | 2,945,000 |
| 2,600 | 1,474,201 | 951,840 | 1,249,201 | 1,131,001 | 1,512,000 |
| 3,620 | 654,201 | 421,840 | 552,001 | 501,001 | 672,000 |
| 4,580 | 223,701 | 143,590 | 189,751 | 170,501 | 231,000 |
| 5,520 | 72,901 | 46,800 | 62,101 | 55,801 | 75,600 |
| 6,520 | 21,466 | 13,780 | 18,285 | 16,431 | 22,260 |
| 7,500 | 8,101 | 5,200 | 6,901 | 6,201 | 8,400 |
| 8,520 | 3,241 | 2,080 | 2,761 | 2,481 | 3,360 |
| 9,520 | 1,378 | 884 | 1,174 | 1,055 | 1,428 |
| 10,500 | 568 | 364 | 484 | 435 | 588 |
| 11,500 | 203 | 130 | 173 | 156 | 210 |
| 12,480 | 81 | 52 | 69 | 63 | 84 |
| 14,000 | 20 | 13 | 17 | 16 | 21 |
| No. of Blocks | 81.97 | 52.96 | 69.82 | 62.95 | 84.50 |

TABLE 77

LOW PEAK ORDERED GUST LOADING HISTORIES

Stress Interval = 1,000 psi
Unit Spectrum = 1/10 avg. random test history
$f_{mean}$ = 6,000 psi
$K_T$ = 4.0

Test Group No. G69

| Varying Stress (psi) | Cumulative Frequency of Load Cycle Occurrences | | | | |
|---|---|---|---|---|---|
| | Specimen No.378 | Specimen NO.387 | Specimen No.388 | Specimen No.391 | Specimen No.392 |
| 540 | 4,552,819 | 5,385,622 | 5,390,422 | 10,056,042 | 5,874,024 |
| 1,620 | 2,652,819 | 3,135,622 | 3,140,422 | 5,856,042 | 3,424,024 |
| 2,590 | 1,360,819 | 1,605,622 | 1,610,422 | 3,000,042 | 1,758,024 |
| 3,540 | 600,819 | 705,622 | 710,422 | 1,328,042 | 778,024 |
| 4,540 | 203,519 | 242,022 | 242,022 | 456,542 | 264,024 |
| 5,540 | 66,619 | 79,222 | 79,222 | 149,442 | 86,424 |
| 6,530 | 19,629 | 23,342 | 23,342 | 44,032 | 25,464 |
| 7,540 | 7,419 | 8,822 | 8,822 | 16,642 | 9,624 |
| 8,600 | 2,979 | 3,542 | 3,542 | 6,682 | 3,864 |
| 9,660 | 1,277 | 1,518 | 1,518 | 2,864 | 1,656 |
| 10,420 | 537 | 638 | 638 | 1,204 | 696 |
| 11,000 | 204 | 242 | 242 | 457 | 264 |
| 12,000 | 56 | 66 | 66 | 125 | 72 |
| 14,000 | 19 | 22 | 22 | 42 | 24 |
| No. of Blocks | 37.94 | 44.88 | 44.92 | 83.80 | 48.95 |

TABLE 78

LOW PEAK RANDOM GUST LOADING HISTORIES
(MEAN CROSSING PEAK COUNTS)
$f_{mean}$ = 6,000 psi
$K_T$ = 7.0

Test Group No. 070

| Varying Stress (psi) | Cumulative Frequency of Load Cycle Occurrences | | | | | |
|---|---|---|---|---|---|---|
| | Specimen No.299 | Specimen No.300 | Specimen No.301 | Specimen No.302 | Specimen No.303 | Specimen No.304 |
| 0 | 252,300 | 169,650 | 239,250 | 200,100 | 326,250 | 213,150 |
| 1,190 | 143,700 | 97,050 | 136,500 | 114,100 | 185,900 | 121,600 |
| 2,380 | 65,900 | 44,800 | 62,700 | 52,450 | 85,500 | 56,000 |
| 3,560 | 23,480 | 15,980 | 22,360 | 18,630 | 30,460 | 19.940 |
| 4,750 | 6,437 | 4,440 | 6,157 | 5,142 | 8,349 | 5,507 |
| 5,950 | 1,552 | 1,079.5 | 1,488 | 1,246 | 2,018.5 | 1,338 |
| 7,120 | 411.8 | 286.0 | 397.3 | 328.3 | 538.6 | 354.3 |
| 7,720 | 234.4 | 163.6 | 227.2 | 187.6 | 306.2 | 202.0 |
| 8,310 | 148.5 | 103.5 | 144.1 | 118.9 | 193.7 | 127.7 |
| 8,900 | 90.9 | 62.7 | 88.3 | 72.3 | 119.2 | 77.6 |
| 9,500 | 60.0 | 40.8 | 58.4 | 47.5 | 77.4 | 50.6 |
| 10,000 | 41.8 | 28.4 | 40.8 | 33.3 | 53.7 | 35.3 |
| 10,700 | 16.1 | 11.3 | 16.1 | 13.6 | 19.7 | 13.6 |
| 11,600 | 10.6 | 7.3 | 10.6 | 9.0 | 12.9 | 9.0 |
| 11,900 | 3.9 | 1.1 | 3.9 | 2.6 | 5.0 | 2.6 |
| 12,050 | 3.6 | 1.0 | 3.6 | 2.5 | 4.6 | 2.5 |
| 12,500 | 1.4 | | 1.4 | 1.3 | 1.4 | 1.3 |
| 13,100 | 1.0 | | 1.0 | 1.0 | 1.0 | 1.0 |

TABLE 79

LOW PEAK ORDERED GUST LOADING HISTORIES

Stress Interval = 1,000 psi
Unit Spectrum = 1/20 avg. random test history
$f_{mean}$ = 6,000 psi
$K_T$ = 7.0

Test Group No. G71

| Varying Stress (psi) | Cumulative Frequency of Load Cycle Occurrences | | | | |
|---|---|---|---|---|---|
| | Specimen No.348 | Specimen No.350 | Specimen No.351 | Specimen No.355 | Specimen No.356 |
| 550 | 211,141 | 289,080 | 305,371 | 253,531 | 228,242 |
| 1,520 | 104,421 | 145,280 | 153,731 | 127,121 | 113,502 |
| 2,370 | 55,201 | 76,800 | 80,971 | 67,201 | 60,002 |
| 3,260 | 25,301 | 35,200 | 36,771 | 30,801 | 27,502 |
| 4,190 | 8,971 | 12,480 | 12,871 | 10,921 | 9,752 |
| 5,160 | 2,991 | 4,160 | 4,291 | 3,641 | 3,252 |
| 6,170 | 921 | 1,280 | 1,321 | 1,121 | 1,002 |
| 7,190 | 300 | 416 | 430 | 365 | 327 |
| 8,230 | 139 | 192 | 199 | 169 | 152 |
| 9,260 | 58 | 80 | 83 | 71 | 64 |
| 10,380 | 23 | 32 | 33 | 29 | 26 |
| 11,460 | 7 | 9 | 10 | 9 | 8 |
| 13,100 | 2 | 3 | 3 | 3 | 3 |
| No. of Blocks | 23.46 | 32.12 | 33.93 | 28.17 | 25.36 |

TABLE 80

HIGH PEAK RANDOM GUST LOADING HISTORIES
(MEAN CROSSING PEAK COUNTS)

$f_{mean}$ = 12,000 psi
$K_T$ = 4.0

Test Group No. G72

| Varying Stress (psi) | Cumulative Frequency of Load Cycle Occurrences | | | | | | |
|---|---|---|---|---|---|---|---|
| | Specimen No.279 | Specimen No.285 | Specimen No.287 | Specimen No.288 | Specimen No.290 | Specimen No.291 | Specimen No.292 |
| 0 | 652,500 | 395,850 | 456,750 | 334,950 | 239,250 | 326,250 | 247,950 |
| 1,000 | 467,600 | 283,800 | 327,500 | 240,300 | 171,700 | 234,100 | 177,900 |
| 2,000 | 323,760 | 196,350 | 226,600 | 166,250 | 118,700 | 161,950 | 123,000 |
| 3,000 | 202,550 | 122,850 | 141,750 | 104,050 | 74,250 | 101,350 | 76,950 |
| 4,000 | 117,200 | 71,020 | 82,020 | 60,220 | 42,960 | 58,670 | 44,510 |
| 5,000 | 61,880 | 37,520 | 43,300 | 31,800 | 22,720 | 30,970 | 23,550 |
| 6,000 | 28,650 | 17,345 | 20,075 | 14,710 | 10,585 | 14,335 | 10,960 |
| 7,000 | 12,030 | 7,225 | 8,445 | 6,180 | 4,455 | 6,025 | 4,610 |
| 8,000 | 5,100 | 3,082 | 3,582 | 2,615 | 1,893 | 2,550 | 1,958 |
| 9,000 | 2,250 | 1,364 | 1,583 | 1,157.5 | 833.5 | 1,129 | 862 |
| 10,000 | 1,145 | 697 | 805 | 590.0 | 424.0 | 575 | 439 |
| 11,000 | 567.3 | 346.2 | 400 | 292.6 | 210.2 | 285.6 | 217.2 |
| 12,000 | 311.4 | 190.2 | 219.6 | 160.2 | 115.7 | 156.6 | 119.3 |
| 13,000 | 179.7 | 109.5 | 126.4 | 91.9 | 67.1 | 90.0 | 69.0 |
| 14,000 | 108.4 | 65.7 | 76.0 | 54.8 | 40.6 | 53.8 | 41.6 |

(Continued on next page)

TABLE 80 (Continued)

| Varying Stress (psi) | Cumulative Frequency of Load Cycle Occurrences | | | | | | |
|---|---|---|---|---|---|---|---|
| | Specimen No.279 | Specimen No.285 | Specimen No.287 | Specimen No.288 | Specimen No.290 | Specimen No.291 | Specimen No.292 |
| 15,000 | 39.7 | 22.9 | 27.3 | 18.7 | 15.1 | 18.7 | 15.1 |
| 16,000 | 28.8 | 16.6 | 19.8 | 13.6 | 11.0 | 13.6 | 11.0 |
| 16,190 | 27.3 | 15.7 | 18.7 | 12.8 | 10.4 | 12.8 | 10.4 |
| 16,830 | 9.2 | 6.2 | 6.2 | 4.6 | 3.6 | 4.6 | 3.6 |
| 17,000 | 4.9 | 3.0 | 3.0 | 1.5 | 1.5 | 1.5 | 1.5 |
| 18,000 | 3.7 | 2.2 | 2.2 | 1.1 | 1.1 | 1.1 | 1.1 |
| 18,290 | 3.4 | 2.0 | 2.0 | 1.0 | 1.0 | 1.0 | 1.0 |
| 19,000 | 1.2 | | | | | | |
| 19,520 | 1.0 | | | | | | |

(End of Table 80 )

TABLE 81

HIGH PEAK ORDERED GUST LOADING HISTORIES

Stress Interval = 4,000 psi
Unit Spectrum = 1/20 avg. random test history
$f_{mean}$ = 12,000 psi
$K_T$ = 4.0

Test Group No. G73

| Varying Stress (psi) | Cumulative Frequency of Load Cycle Occurrences | | | |
|---|---|---|---|---|
| | Specimen No.326 | Specimen No.331 | Specimen No.332 | Specimen No.334 |
| 2,070 | 304,232 | 144,578 | 152,718 | 188,145 |
| 6,190 | 28,000 | 13,126 | 14,001 | 17,500 |
| 10,350 | 1,056 | 496 | 529 | 660 |
| 14,200 | 96 | 46 | 49 | 60 |
| 18,300 | 3 | 2 | 2 | 2 |
| Spectrum Units | 32.89 | 15.63 | 16.51 | 20.34 |
| Varying Stress (psi) | Cumulative Frequency of Load Cycle Occurrences | | | |
| | Specimen No.336 | Specimen No.337 | Specimen No.339 | Specimen No.340 |
| 2,070 | 305,713 | 207,478 | 497,650 | 353,350 |
| 6,190 | 28,875 | 19,250 | 46,375 | 33,250 |
| 10,350 | 1,089 | 726 | 1,749 | 1,254 |
| 14,200 | 99 | 66 | 159 | 114 |
| 18,300 | 3 | 2 | 5 | 4 |
| No. of Blocks | 33.05 | 22.43 | 53.80 | 38.20 |

TABLE 82

HIGH PEAK ORDERED GUST LOADING HISTORIES

Stress Interval = 1,000
Unit Spectrum = 1/20 avg. random test history
$f_{mean}$ = 12,000 psi
$K_T$ = 4.0

Test Group No. G74

| Varying Stress (psi) | Cumulative Frequency of Load Cycle Occurrences | | | | |
|---|---|---|---|---|---|
| | Specimen No.313 | Specimen No.320 | Specimen No.328 | Specimen No.335 | Specimen No.341 |
| 480 | 414,882 | 470,401 | 813,600 | 441,281 | 928,161 |
| 1,320 | 284,882 | 320,401 | 558,600 | 301,281 | 638,001 |
| 2,220 | 193,882 | 217,501 | 380,100 | 203,281 | 435,001 |
| 3,100 | 108,082 | 121,801 | 211,800 | 113,401 | 243,601 |
| 4,020 | 59,982 | 68,151 | 117,500 | 63,451 | 136,301 |
| 4,960 | 30,082 | 34,801 | 60,000 | 32,400 | 69,601 |
| 5,900 | 15,002 | 17,401 | 30,000 | 16,201 | 34,801 |
| 6,850 | 6,002 | 6,961 | 12,000 | 6,481 | 13,921 |
| 7,860 | 2,627 | 3,046 | 5,250 | 2,836 | 6,091 |
| 8,860 | 1,127 | 1,306 | 2,250 | 1,216 | 2,611 |
| 10,100 | 552 | 639 | 1,100 | 595 | 1,277 |
| 11,380 | 302 | 349 | 600 | 325 | 697 |
| 12,350 | 177 | 204 | 350 | 190 | 407 |
| 13,300 | 102 | 117 | 200 | 109 | 233 |
| 14,350 | 52 | 59 | 100 | 55 | 117 |
| 15,400 | 27 | 30 | 50 | 28 | 59 |
| 16,550 | 14 | 15 | 25 | 14 | 30 |
| 17,620 | 6 | 6 | 10 | 6 | 12 |
| 18,300 | 3 | 3 | 5 | 3 | 6 |
| No. of Blocks | 25.93 | 29.40 | 50.85 | 27.58 | 58.01 |

TABLE 83

HIGH PEAK ORDERED GUST LOADING HISTORIES

Stress Interval = 1,000
Unit Spectrum = 1/10 avg. random test history
$f_{mean}$ = 12,000
$K_T$ = 4.0

Test Group No. G75

| Varying Stress (psi) | Cumulative Frequency of Load Cycle Occurrences | | | | |
|---|---|---|---|---|---|
| | Specimen No.307 | Specimen No.308 | Specimen No.309 | Specimen No.310 | Specimen No.312 |
| 750 | 319,040 | 288,960 | 288,000 | 224,319 | 256,961 |
| 1,980 | 219,040 | 198,000 | 198,000 | 153,999 | 176,001 |
| 2,900 | 149,040 | 135,000 | 135,000 | 104,999 | 120,001 |
| 3,920 | 83,040 | 75,600 | 75,600 | 58,799 | 67,201 |
| 4,900 | 46,040 | 42,300 | 42,300 | 32,899 | 37,601 |
| 5,830 | 23,040 | 21,600 | 21,600 | 16,799 | 19,201 |
| 6,850 | 11,040 | 10,800 | 10,800 | 8,399 | 9,601 |
| 7,880 | 4,320 | 4,320 | 4,320 | 3,359 | 3,841 |
| 8,950 | 1,890 | 1,890 | 1,890 | 1,469 | 1,681 |
| 10,000 | 810 | 810 | 810 | 629 | 721 |
| 11,050 | 396 | 396 | 396 | 307 | 353 |
| 12,050 | 216 | 216 | 216 | 167 | 193 |
| 13,050 | 126 | 126 | 126 | 97 | 113 |
| 13,700 | 72 | 72 | 72 | 55 | 65 |
| 14,450 | 36 | 36 | 36 | 27 | 33 |
| 15,500 | 18 | 18 | 18 | 13 | 17 |
| 16,450 | 9 | 9 | 9 | 6 | 9 |
| 17,500 | 4 | 4 | 4 | 2 | 4 |
| 18,300 | 2 | 2 | 2 | 1 | 2 |
| No. of Blocks | 9.97 | 9.03 | 9.00 | 7.01 | 8.03 |

TABLE 84

HIGH PEAK RANDOM GUST LOADING HISTORIES
(MEAN CROSSING PEAK COUNTS)
$f_{mean}$ = 12,000 psi
$K_T$ = 7.0

Test Group No. G76

| Varying Stress (psi) | Cumulative Frequency of Load Cycle Occurrences | | | | | |
|---|---|---|---|---|---|---|
| | Specimen No.274 | Specimen No.280 | Specimen No.281 | Specimen No.282 | Specimen No.283 | Specimen No.284 |
| 0 | 56,550 | 95,700 | 56,550 | 39,150 | 52,200 | 52,200 |
| 1,670 | 32,400 | 54,500 | 32,400 | 22,600 | 29,800 | 29,800 |
| 3,330 | 15,000 | 25,100 | 15,000 | 10,600 | 13,700 | 13,700 |
| 5,000 | 5,360 | 9,000 | 5,360 | 3,880 | 4,860 | 4,860 |
| 6,670 | 1,504 | 2,479 | 1,504 | 1,092 | 1,354 | 1,354 |
| 8,330 | 369 | 606 | 369 | 267.5 | 329 | 329 |
| 10,000 | 99.1 | 159.1 | 99.1 | 70.8 | 86.6 | 86.6 |
| 10,830 | 56.8 | 88.9 | 56.8 | 40.5 | 49.6 | 49.6 |
| 11,660 | 35.6 | 55.5 | 35.6 | 25.8 | 31.2 | 31.2 |
| 12,500 | 21.1 | 33.5 | 21.1 | 15.8 | 18.4 | 18.4 |
| 13,330 | 13.5 | 21.5 | 13.5 | 10.3 | 11.9 | 11.9 |
| 14,000 | 9.2 | 14.7 | 9.2 | 7.2 | 8.2 | 8.2 |
| 14,960 | 3.1 | 5.0 | 3.1 | 3.1 | 3.1 | 3.1 |
| 16,190 | 2.0 | 3.3 | 2.0 | 2.0 | 2.0 | 2.0 |
| 16,620 | | 1.0 | | | | |

## TABLE 85

### HIGH PEAK ORDERED GUST LOADING HISTORIES

Stress Interval = 1,000 psi
Unit Spectrum = 1/20 avg. random test history
$f_{mean}$ = 12,000 psi
$K_T$ = 7.0

Test Group No. 077

| Varying Stress (psi) | Cumulative Frequency of Load Cycle Occurrences | | | | | |
|---|---|---|---|---|---|---|
| | Specimen No.293 | Specimen No.294 | Specimen No.295 | Specimen No.296 | Specimen No.297 | Specimen No.298 |
| 530 | 63,002 | 58,249 | 63,002 | 68,001 | 41,253 | 55,501 |
| 1,550 | 43,752 | 40,249 | 43,752 | 47,251 | 28,503 | 38,501 |
| 2,500 | 28,127 | 25,874 | 28,127 | 30,376 | 18,003 | 24,751 |
| 3,450 | 16,877 | 15,524 | 16,877 | 18,226 | 10,803 | 14,851 |
| 4,400 | 9,627 | 8,854 | 9,627 | 10,396 | 6,163 | 8,471 |
| 5,350 | 4,702 | 4,323 | 4,702 | 5,077 | 3,011 | 4,137 |
| 6,300 | 2,127 | 1,954 | 2,127 | 2,296 | 1,363 | 1,871 |
| 7,400 | 902 | 827 | 902 | 973 | 579 | 793 |
| 8,500 | 402 | 367 | 402 | 433 | 259 | 353 |
| 9,400 | 177 | 160 | 177 | 190 | 115 | 155 |
| 10,200 | 84 | 75 | 84 | 90 | 56 | 73 |
| 11,150 | 49 | 43 | 49 | 52 | 33 | 42 |
| 12,200 | 26 | 22 | 26 | 27 | 18 | 22 |
| 13,300 | 16 | 13 | 16 | 16 | 11 | 13 |
| 14,450 | 8 | 6 | 8 | 8 | 6 | 6 |
| 15,500 | 4 | 3 | 4 | 4 | 3 | 3 |
| 16,200 | 3 | 2 | 3 | 3 | 2 | 2 |
| No. of Blocks | 25.19 | 23.29 | 25.19 | 27.24 | 16.52 | 22.23 |

TABLE 86

TEST LOADING SPECTRA

| Specimen No. | 70 | 72 | 85 | 88 | 92 |
|---|---|---|---|---|---|
| Trace | Wing Root | Wing Root | Wing Root | Wing Root | Wing Root |
| $K_T$ | 4 | 4 | 4 | 4 | 4 |
| Record No. | 17M-P4-4 | 17M-P4-4 | 17M-P4-4 | 17M-P4-4 | 17M-P3-3 |
| Mean Stress (psi) | 12,000 | 12,000 | 12,000 | 12,000 | 12,000 |
| Trace Repetitions | 69.7 | 71.8 | 60.5 | 59.1 | 79.2 |
| Varying Stress (Gross Area) KSI | Random | Random | Random | Random | Random |
| | Cumulative Frequency of Occurrences (Cycles) | | | | |
| | Test Group No. G78 | | | | |
| 0 | 299,710 | 308,740 | 260,150 | 254,130 | 277,200 |
| 1.5 | | | | | |
| 2 | 153,340 | 157,960 | 133,100 | 130,020 | 67,320 |
| 4 | 66,215 | 68,210 | 57,475 | 56,145 | 39,600 |
| 6 | 9,061 | 9,334 | 7,865 | 7,683 | 8,712 |
| 8 | 1,533 | 1,580 | 1,331 | 1,300 | 1,584 |
| 10 | 293 | 302 | 254 | 248 | 396 |
| 11 | | | | | |
| 12 | 118 | 122 | 103 | 100 | 135 |
| 13.5 | 70 | 72 | 61 | 59 | 79 |

TABLE 66

TEST LOADING SPECTRA
(Continued)

| Specimen No. | 93 | 114 | 115 | 126 | 128 |
|---|---|---|---|---|---|
| Trace | Wing Root | Wing Root | Wing Root | Wing Root | Wing Root |
| $K_T$ | 4 | 4 | 4 | 4 | 4 |
| Record No. | 17M-P4-4 | 17M-P3-3 | 17M-P4-4 | 17M-P3-3 | 17M-P4-4 |
| Mean Stress (psi) | 12,000 | 12,000 | 12,000 | 12,000 | 12,000 |
| Trace Repetitions | 55.7 | 74.8 | 53.0 | 102.5 | 55.6 |
| Varying Stress (Gross Area) KSI | Random | Random | Random | Random | Random |
| | Cumulative Frequency of Occurrences (Cycles) | | | | |
| | Test Group No. G78 | | | | |
| 0 | 239,510 | 261,600 | 227,900 | 358,750 | 239,080 |
| 1.5 | | | | | |
| 2 | 122,540 | 63,580 | 116,600 | 87,125 | 122,320 |
| 4 | 52,915 | 37,400 | 50,350 | 51,250 | 52,820 |
| 6 | 7,241 | 8,228 | 6,890 | 11,275 | 7,228 |
| 8 | 1,225 | 1,496 | 1,166 | 2,050 | 1,223 |
| 10 | 234 | 374 | 223 | 512 | 234 |
| 12 | 95 | 127 | 90 | 174 | 94 |
| 12.25 | | | | | |
| 13.5 | 56 | 75 | 53 | 102 | 56 |

TABLE 86

TEST LOADING SPECTRA
(Continued)

| Specimen No. | 251 | 252 | 255 | 256 | 258 |
|---|---|---|---|---|---|
| Trace | Wing Root | Wing Root | Wing Root | Wing Root | Wing Root |
| $K_T$ | 4 | 4 | 4 | 4 | 4 |
| Record No. | 46M-P4-4 | 46M-P2-1 | 46M-P4-4 | 46M-P4-4 | 46M-P2-1 |
| Mean Stress (psi) | 12,000 | 12,000 | 12,000 | 12,000 | 12,000 |
| Trace Repetitions | 217.0 | 156.0 | 114.0 | 172.0 | 197.0 |
| Varying Stress (Gross Area) KSI | Ordered | Ordered | Ordered | Ordered | Ordered |
| | Cumulative Frequency of Occurrences (Cycles) | | | | |
| | Test Group No. G79 | | | | |
| 0 | 1,019,900 | 780,000 | 535,800 | 808,400 | 985,000 |
| 2 | 477,400 | 327,600 | 250,800 | 378,400 | 413,700 |
| 4 | 130,200 | 88,920 | 68,400 | 103,200 | 112,290 |
| 6 | 21,700 | 15,600 | 11,400 | 17,200 | 19,700 |
| 8 | 2,604 | 1,872 | 1,368 | 2,064 | 2,364 |
| 10 | 673 | 640 | 353 | 533 | 808 |
| 12 | 282 | 265 | 148 | 224 | 335 |
| 13.5 | 217 | 156 | 114 | 172 | 197 |

TABLE 66

TEST LOADING SPECTRA
(Continued)

| | Cumulative Frequency of Occurrences (Cycles) | | | |
|---|---|---|---|---|
| Specimen No. | 173 | 175 | 176 | 177 |
| Trace | Mod. Wing Root | Mod. Wing Root | Mod. Wing Root | Mod. Wing Root |
| $K_T$ | 4 | 4 | 4 | 4 |
| Record No. | 30M-P4-4 | 30M-P4-4 | 30M-P4-4 | 30M-P4-4 |
| Mean Stress (psi) | 12,000 | 12,000 | 12,000 | 12,000 |
| Trace Repetitions | 37.3 | 57.6 | 34.9 | 45.1 |
| Varying Stress (Gross Area) KSI | Random | Random | Random | Random |
| | Test Group No. G60 | | | |
| 0 | 167,850 | 259,200 | 157,050 | 202,950 |
| 2 | 111,900 | 172,800 | 104,700 | 135,300 |
| 4 | 59,680 | 92,160 | 55,840 | 72,160 |
| 6 | 31,705 | 48,960 | 29,665 | 38,335 |
| 8 | 10,444 | 16,128 | 9,772 | 12,628 |
| 8.6 | | | | |
| 9.6 | | | | |
| 10 | 1,940 | 2,995 | 1,815 | 2,345 |
| 10.35 | | | | |
| 11.55 | | | | |
| 12 | 213 | 328 | 199 | 257 |
| 13.5 | 37 | 58 | 35 | 45 |

TABLE 86

TEST LOADING SPECTRA
(Concluded)

| | Cumulative Frequency of Occurrences (Cycles) | | | | |
|---|---|---|---|---|---|
| Specimen No. | 246 | 247 | 248 | 249 | 250 |
| Trace | Mod. Wing Root | Mod. Wing Root | Mod. Wing Root | Mod. Wing Root | Mod. Wing Root |
| $K_T$ | 4 | 4 | 4 | 4 | 4 |
| Record No. | 44M-P2-1 | 44M-P4-4 | 44M-P2-1 | 44M-P4-4 | 44M-P2-1 |
| Mean Stress (psi) | 12,000 | 12,000 | 12,000 | 12,000 | 12,000 |
| Trace Repetitions | 31.1 | 27.4 | 34.1 | 32.7 | 43.5 |
| Varying Stress (Gross Area) KSI | Ordered | Ordered | Ordered | Ordered | Ordered |
| | Test Group No. 681 | | | | |
| 0 | 133,730 | 117,820 | 146,630 | 140,610 | 187,050 |
| 2 | 99,520 | 84,940 | 109,120 | 101,370 | 139,200 |
| 4 | 62,200 | 46,580 | 68,200 | 55,590 | 87,000 |
| 6 | 37,320 | 24,660 | 40,920 | 29,430 | 52,200 |
| 8 | 18,038 | 9,264 | 19,778 | 11,772 | 25,230 |
| 10 | 4,976 | 3,288 | 5,456 | 3,924 | 6,960 |
| 12 | 404 | 329 | 443 | 392 | 566 |
| 13.5 | 31 | 27 | 34 | 33 | 44 |

## TABLE 87

RANDOM MILITARY MANEUVER LOADING HISTORIES
(PEAK COUNTS)
Minimum Stress = 5,450 psi
$K_t$ = 4.0

Test Group No. M14

| Incremental Stress (psi) | Cumulative Frequency of Load Cycle Occurrences | | | | | |
|---|---|---|---|---|---|---|
| | Specimen No.342 | Specimen No.343 | Specimen No.344 | Specimen No.345 | Specimen No.346 | Specimen No. 347 & No. 349 |
| 0 | 26,400 | 22,000 | 17,600 | 30,800 | 44,000 | 26,400 |
| 2,840 | 20,700 | 17,250 | 13,800 | 24,150 | 34,500 | 20,700 |
| 5,680 | 16,100 | 13,450 | 10,760 | 18,830 | 26,900 | 16,100 |
| 11,400 | 9,360 | 7,800 | 6,240 | 10,920 | 15,600 | 9,360 |
| 17,000 | 4,560 | 3,800 | 3,040 | 5,320 | 7,600 | 4,560 |
| 22,700 | 1,830 | 1,525 | 1,220 | 2,135 | 3,050 | 1,830 |
| 28,400 | 540 | 450 | 360 | 630 | 900 | 540 |
| 31,200 | 288 | 240 | 192 | 336 | 480 | 288 |
| 34,000 | 132 | 110 | 88 | 154 | 220 | 132 |
| 39,800 | 24 | 20 | 16 | 28 | 40 | 24 |
| 41,200 | 12 | 10 | 8 | 14 | 20 | 12 |
| 42,050 | 6 | 5 | 4 | 7 | 10 | 6 |

## TABLE 88

ORDERED MILITARY MANEUVER LOADING HISTORIES

Stress Interval = 4,000 psi
Unit Spectrum = 1/20 avg. random test history
Minimum Stress = 5,450 psi
$K_T$ = 4.0

Test Group No. M15

| Incremental Stress (psi) | Cumulative Frequency of Load Cycle Occurrences | | | | |
|---|---|---|---|---|---|
| | Specimen No.399 | Specimen No.400 | Specimen No.401 | Specimen No.404 | Specimen No.406 |
| 1,680 | 12,900 | 12,898 | 9,676 | 19,345 | 15,001 |
| 5,180 | 8,700 | 8,698 | 6,526 | 13,045 | 10,101 |
| 9,250 | 5,880 | 5,878 | 4,411 | 8,815 | 6,811 |
| 13,550 | 3,780 | 3,778 | 2,836 | 5,665 | 4,361 |
| 17,800 | 2,280 | 2,278 | 1,711 | 3,415 | 2,611 |
| 22,100 | 1,260 | 1,258 | 946 | 1,885 | 1,421 |
| 26,300 | 588 | 586 | 442 | 877 | 637 |
| 30,700 | 240 | 238 | 181 | 355 | 260 |
| 34,800 | 84 | 82 | 64 | 121 | 91 |
| 38,450 | 24 | 22 | 19 | 34 | 26 |
| 42,000 | 3 | 3 | 3 | 5 | 4 |
| No. of Blocks | 12.00 | 11.99 | 9.00 | 17.99 | 13.95 |

TABLE 89

ORDERED MILITARY MANEUVER LOADING HISTORIES

Stress Interval = 1,000 psi
Unit Spectrum = 1/20 avg. random test history
Minimum Stress = 5,450 psi
$K_T$ = 4.0

Test Group No. M16

| Incremental Stress (psi) | Cumulative Frequency of Load Cycle Occurrences | | | |
|---|---|---|---|---|
| | Specimen No.410 | Specimen No.411 | Specimen Nos.413&414 | Specimen No.415 |
| 470 | 8,201 | 17,425 | 12,298 | 13,271 |
| 1,320 | 7,401 | 15,725 | 11,098 | 11,971 |
| 2,020 | 6,801 | 14,450 | 10 198 | 10,996 |
| 2,730 | 6,201 | 13,175 | 9.298 | 10,021 |
| 3,480 | 5,601 | 11,900 | 8,398 | 9,046 |
| 4,330 | 5,001 | 10,625 | 7,498 | 8,071 |
| 5,320 | 4,521 | 9,605 | 6,778 | 7.291 |
| 6,420 | 4,081 | 8,670 | 6,118 | 6,576 |
| 7,460 | 3,721 | 7,905 | 5,578 | 5,991 |
| 8,430 | 3,361 | 7,140 | 5,038 | 5,406 |
| 9,480 | 3,001 | 6,375 | 4,498 | 4,821 |
| 10,560 | 2,721 | 5,780 | 4,078 | 4.366 |
| 11,600 | 2,401 | 5,100 | 3.598 | 3,846 |
| 12,700 | 2,121 | 4,505 | 3,178 | 3,391 |
| 13,800 | 1,881 | 3,995 | 2,818 | 3,001 |
| 14,900 | 1,681 | 3,570 | 2,518 | 2.676 |
| 16,050 | 1,425 | 3,026 | 2,134 | 2,260 |
| 16,850 | 1,241 | 2,635 | 1,858 | 1,961 |
| 17,950 | 1,081 | 2.295 | 1,618 | 1,701 |
| 19,400 | 921 | 1,955 | 1,378 | 1,441 |
| 20,450 | 769 | 1,632 | 1,150 | 1,194 |
| 21,500 | 649 | 1,377 | 970 | 999 |
| 22,800 | 529 | 1,122 | 790 | 804 |
| 24,000 | 441 | 935 | 658 | 661 |
| 25,100 | 345 | 731 | 514 | 517 |
| 26,400 | 281 | 595 | 418 | 421 |
| 27,700 | 233 | 493 | 346 | 349 |
| 28,800 | 185 | 391 | 274 | 277 |
| 29,800 | 137 | 289 | 202 | 205 |
| 30,850 | 105 | 221 | 154 | 157 |
| 32,000 | 81 | 170 | 118 | 121 |
| 33,150 | 65 | 136 | 94 | 97 |
| 34,200 | 49 | 102 | 70 | 73 |
| 35,200 | 37 | 77 | 52 | 55 |
| 36,150 | 29 | 60 | 40 | 43 |
| 37,150 | 21 | 43 | 29 | 31 |
| 38,250 | 15 | 31 | 21 | 22 |
| 39,400 | 10 | 21 | 14 | 15 |
| 40,300 | 7 | 16 | 11 | 11 |
| 42,000 | 4 | 9 | 6 | 6 |
| No. of Blocks | 8.00 | 17.00 | 11.99 | 12.95 |

TABLE 90

RANDOM GROUND LOADING HISTORIES
(MEAN CROSSING PEAK COUNTS)
$f_{mean}$ = -3,000 psi
$K_T$ = 7.0

Test Group No. T1

| Varying Stress (psi) | Cumulative Frequency of Load Cycle Occurrences | | | | | |
|---|---|---|---|---|---|---|
| | Specimen No.416 | Specimen No.417 | Specimen No.418 | Specimen No.419 | Specimen No.422 | Specimen No.423 |
| 0 | 783,000 | 500,250 | 552,450 | 578,550 | 495,900 | 448,050 |
| 950 | 452,400 | 289,000 | 319,300 | 334,200 | 286,250 | 258,700 |
| 1,920 | 208,250 | 133,000 | 146,850 | 153,800 | 131,550 | 119,050 |
| 2,850 | 73,600 | 47,040 | 51,950 | 54,400 | 46,450 | 42,150 |
| 3,800 | 20,050 | 12,846 | 14,168 | 14,818 | 12,656 | 11,460 |
| 4,750 | 4,843 | 3,107.5 | 3,424 | 3,583 | 3,057.5 | 2,770 |
| 5,700 | 1,287 | 827.9 | 911.2 | 953.7 | 813.9 | 738.5 |
| 6,180 | 715.9 | 461.0 | 507.3 | 530.4 | 453.4 | 410.9 |
| 6,650 | 458.9 | 295.6 | 325.1 | 339.4 | 290.1 | 262.9 |
| 7,130 | 286.2 | 184.3 | 202.6 | 211.6 | 180.3 | 164.3 |
| 7,600 | 187.4 | 120.4 | 133.2 | 138.0 | 117.6 | 107.2 |
| 8,000 | 129.4 | 83.0 | 91.8 | 94.8 | 80.9 | 73.7 |
| 8,550 | 48.8 | 31.1 | 34.6 | 34.6 | 29.8 | 26.6 |
| 9,250 | 32.8 | 20.8 | 23.1 | 23.1 | 19.8 | 17.8 |
| 9,500 | 11.0 | 6.7 | 7.8 | 7.8 | 6.7 | 6.7 |
| 9,620 | 10.2 | 6.2 | 7.2 | 7.2 | 6.2 | 6.2 |
| 9,980 | 4.4 | 2.7 | 2.7 | 2.7 | 2.7 | 2.7 |
| 10,450 | 3.4 | 2.0 | 2.0 | 2.0 | 2.0 | 2.0 |
| 11,150 | 1.0 | | | | | |

## TABLE 91

ORDERED CROUNT LOADING HISTORIES

Stress Interval = 1,000 psi
Unit Spectrum = 1/20 avg. random test history
$f_{mean}$ = -3,000 psi
$\dot{n}_T$ = 7.0

Test Group No. 72

| Varying Stress (psi) | Cumulative Frequency of Load Cycle Occurrences | | | | | |
|---|---|---|---|---|---|---|
| | Specimen No.461 | Specimen No.462 | Specimen No.465 | Specimen No.466 | Specimen No.469 | Specimen No.471 |
| 550 | 775,438 | 747,757 | 1,010,085 | 1,268,351 | 900,009 | 1,309,422 |
| 1,580 | 396,008 | 380,257 | 516,585 | 648,851 | 459,009 | 668,922 |
| 2,580 | 144,008 | 136,007 | 187,585 | 235,851 | 165,009 | 241,192 |
| 3,580 | 41,408 | 39,107 | 53,635 | 67,701 | 47,159 | 69,012 |
| 4,610 | 5,768 | 5,447 | 7,370 | 9,291 | 6,569 | 9,612 |
| 5,700 | 2,168 | 2,047 | 2,770 | 3,491 | 2,469 | 3,612 |
| 6,780 | 692 | 653 | 884 | 1,113 | 788 | 1,152 |
| 7,910 | 296 | 279 | 378 | 475 | 337 | 492 |
| 8,780 | 87 | 82 | 111 | 139 | 99 | 144 |
| 9,480 | 22 | 20 | 28 | 34 | 25 | 36 |
| 10,500 | 7 | 6 | 9 | 11 | 8 | 12 |
| No. of Blocks | 36.07 | 34.78 | 46.98 | 58.99 | 41.86 | 60.90 |

TABLE 92

ORDERED COMPOSITE LOADING HISTORIES

(Spectra Based on Tests Having Approx. 11 Random Gust Loadings per Flight)

LOW PEAK GUST LOADINGS IN FLIGHT

Stress Interval = 1,000 psi
Unit Spectrum = 1/20 average random test history
$K_T$ = 4.0

Test Group No. CQ1

| Varying Stress (psi) | Cumulative Frequency of Load Cycles Occurrences | | | | |
|---|---|---|---|---|---|
| | Specimen No. 475 | Specimen No. 480 | Specimen No. 481 | Specimen No. 485 | Specimen No. 487 |
| | Gust Loadings $f_{mean}$ = 6,000 psi | | | | |
| 580 | 674,501 | 351,000 | 766,987 | 467,505 | 1,040,000 |
| 1,680 | 388,501 | 202,500 | 442,487 | 269,505 | 600,000 |
| 2,720 | 180,501 | 94,500 | 206,487 | 125,505 | 280,000 |
| 3,800 | 76,501 | 40,500 | 88,487 | 53,505 | 120,000 |
| 4,850 | 28,051 | 14,850 | 32,437 | 19,305 | 44,000 |
| 5,880 | 8,161 | 4,320 | 9,427 | 5,600 | 12,800 |
| 6,920 | 2,296 | 1,215 | 2,647 | 1,575 | 3,600 |
| 7,950 | 919 | 486 | 1,054 | 630 | 1,440 |
| 8,700 | 408 | 216 | 464 | 280 | 640 |
| 9,650 | 205 | 108 | 232 | 140 | 320 |
| 10,680 | 82 | 43 | 93 | 56 | 128 |
| 11,620 | 31 | 16 | 35 | 21 | 48 |
| 13,000 | 10 | 5 | 12 | 7 | 16 |
| | Ground Loadings $f_{mean}$ = -3,000 psi | | | | |
| 600 | 357,001 | 189,000 | 406,232 | 245,000 | 560,000 |
| 1,700 | 204,001 | 108,000 | 232,232 | 140,000 | 320,000 |
| 2,750 | 96,901 | 51,300 | 110,432 | 66,500 | 152,000 |
| 3,900 | 40,801 | 21,600 | 46,632 | 28,000 | 64,000 |
| 5,080 | 15,301 | 8,100 | 17,632 | 10,500 | 24,000 |
| 6,200 | 4,591 | 2,430 | 5,452 | 3,150 | 7,200 |
| 7,180 | 1,276 | 675 | 1,682 | 875 | 2,000 |
| 8,120 | 511 | 270 | 812 | 350 | 800 |
| 9,020 | 205 | 108 | 464 | 140 | 320 |
| 9,850 | 103 | 54 | 116 | 70 | 160 |
| 10,880 | 52 | 27 | 58 | 35 | 80 |
| 12,000 | 21 | 11 | 23 | 14 | 32 |
| | Ground to Air Cycles $f_{mean}$ = 1,500 psi | | | | |
| 4,000 | 60,486 | 31,249 | 68,788 | 41,510 | 94,287 |
| No. of Blocks | 51.54 | 26.96 | 58.62 | 35.59 | 79.97 |

TABLE 93

ORDERED COMPOSITE LOADING HISTORIES
(Spectra Based on Tests having approx. 12 Random Gust Loadings per Flight)

LOW PEAK GUST LOADINGS IN FLIGHT

Stress Interval = 1,000 psi
Unit Spectrum = 1/20 avg. random test history
$K_f$ = 7.0

Test Group No. CG2

| Varying Stress (psi) | Cumulative Frequency of Load Cycle Occurrences | | | | |
|---|---|---|---|---|---|
| | Specimen No. 478 | Specimen No. 479 | Specimen No. 482 | Specimen No. 484 | Specimen No. 486 |
| | | Gust Loadings $f_{mean}$ = 6,000 psi | | | |
| 650 | 84,652 | 87,180 | 52,445 | 69,305 | 52,575 |
| 1,800 | 48,442 | 49,950 | 30,005 | 39,725 | 30,135 |
| 2,750 | 25,367 | 26,225 | 15,705 | 20,875 | 15,835 |
| 3,700 | 9,747 | 10,165 | 6,025 | 8,115 | 6,155 |
| 4,650 | 3,447 | 3,595 | 2,155 | 2,895 | 2,195 |
| 5,550 | 1,067 | 1,113 | 693 | 923 | 699 |
| 6,600 | 227 | 237 | 177 | 227 | 177 |
| 7,950 | 105 | 107 | 61 | 82 | 61 |
| 8,900 | 43 | 43 | 26 | 35 | 27 |
| 9,550 | 18 | 18 | 11 | 15 | 11 |
| 11,000 | 4 | 4 | 2 | 3 | 2 |
| | | Ground Loadings $f_{mean}$ = -3,000 psi | | | |
| 650 | 42,002 | 43,201 | 25,811 | 34,765 | 26,395 |
| 1,800 | 21,702 | 22,321 | 13,341 | 17,945 | 13,635 |
| 2,800 | 8,402 | 8,641 | 5,171 | 6,925 | 5,275 |
| 3,800 | 2,522 | 2,593 | 1,559 | 2,053 | 1,585 |
| 4,750 | 492 | 505 | 312 | 400 | 309 |
| 5,720 | 121 | 123 | 74 | 98 | 76 |
| 6,750 | 40 | 40 | 24 | 32 | 25 |
| 7,800 | 15 | 15 | 9 | 12 | 9 |
| 8,850 | 4 | 4 | 2 | 3 | 2 |
| | | Ground to Air Cycles $f_{mean}$ = 1,500 psi | | | |
| 4,650 | 7,280 | 7,488 | 4,472 | 5,928 | 4,545 |
| No. of Blocks | 70.54 | 72.61 | 43.57 | 57.93 | 43.98 |

## TABLE 94

ORDERED COMPOSITE LOADING HISTORIES
(Spectra Based on Tests having approx. 13 Random Gust Loadings per Flight)

HIGH PEAK GUST LOADINGS IN FLIGHT

Test Group No. C03
Stress Interval = 1,000 psi
Unit Spectrum = 1/20 avg. random test history
$K_T$ = 4.0

| Varying Stress (psi) | Cumulative Frequency of Load Cycles Occurrences | | | | |
|---|---|---|---|---|---|
| | Specimen No. 467 | Specimen No. 470 | Specimen No. 472 | Specimen No. 473 | Specimen No. 474 |
| | | Gust Loadings $f_{mean}$ = 12,000 psi | | | |
| 580 | 91,835 | 120,914 | 74,142 | 75,449 | 95,632 |
| 1,780 | 65,435 | 86,114 | 52,542 | 53,849 | 68,032 |
| 2,900 | 43,435 | 57,114 | 35,002 | 35,849 | 45,032 |
| 3,850 | 24,735 | 32,776 | 20,127 | 20,549 | 25,875 |
| 4,850 | 13,545 | 17,956 | 11,027 | 11,187 | 14,176 |
| 5,880 | 6,665 | 8,836 | 5,427 | 5,427 | 6,976 |
| 7,000 | 3,010 | 3,991 | 2,452 | 2,452 | 3,151 |
| 8,100 | 1,247 | 1,654 | 1,017 | 1,017 | 1,306 |
| 9,050 | 516 | 685 | 422 | 422 | 541 |
| 10,080 | 258 | 343 | 212 | 212 | 271 |
| 11,050 | 129 | 172 | 107 | 107 | 136 |
| 12,050 | 69 | 92 | 58 | 58 | 73 |
| 13,100 | 39 | 52 | 33 | 33 | 41 |
| 14,200 | 22 | 29 | 18 | 18 | 23 |
| 15,100 | 13 | 18 | 11 | 11 | 14 |
| 15,600 | 6 | 9 | 6 | 6 | 7 |
| 16,300 | 2 | 3 | 2 | 2 | 2 |
| | | Ground Loadings $f_{mean}$ = -3,000 psi | | | |
| 620 | 44,720 | 59,281 | 36,401 | 36,401 | 46,800 |
| 1,680 | 20,640 | 27,361 | 16,801 | 16,801 | 21,600 |
| 2,600 | 8,170 | 10,831 | 6,651 | 6,651 | 8,550 |
| 3,650 | 2,365 | 3,136 | 1,926 | 1,926 | 2,475 |
| 4,600 | 430 | 571 | 351 | 351 | 450 |
| 5,500 | 129 | 172 | 106 | 106 | 135 |
| 6,450 | 43 | 58 | 36 | 36 | 45 |
| 7,420 | 15 | 20 | 13 | 13 | 15 |
| 8,300 | 4 | 6 | 4 | 4 | 4 |
| 8,950 | 2 | 3 | 2 | 2 | 2 |
| | | Ground to Air Cycles $f_{mean}$ = 4,500 psi | | | |
| 7,950 | 7,955 | 10,545 | 6,475 | 6,475 | 8,325 |
| No. of Blocks | 43.56 | 57.04 | 35.28 | 35.67 | 45.44 |

## TABLE 95

CRUISE COMPOSITE LOADING HISTORIES
(Spectra Based on Tests having approximately 110 Random Gust Loadings per Flight)

HIGH PEAK GUST LOADINGS IN FLIGHT

Test Group No. CG4
Stress Interval = 1,000 psi
Unit Spectrum = 1/20 avg. random test history
$K_T$ = 4.0

| Varying Stress (psi) | Cumulative Frequency of Load Cycle Occurrences | | | | | | | |
|---|---|---|---|---|---|---|---|---|
| | Specimen No. 509 | Specimen No. 510 | Specimen No. 511 | Specimen No. 512 | Specimen No. 513 | Specimen No. 514 | Specimen No. 517 | Specimen No. 518 |
| | Gust Loadings f(mean) = 12,000 psi | | | | | | | |
| 550 | 179,556 | 231,785 | 302,418 | 197,951 | 246,129 | 240,364 | 158,896 | 269,287 |
| 1,600 | 129,556 | 166,785 | 217,418 | 142,951 | 176,129 | 172,864 | 113,896 | 194,287 |
| 2,650 | 79,556 | 101,785 | 132,418 | 87,951 | 108,002 | 107,864 | 68,896 | 119,287 |
| 3,700 | 47,556 | 60,185 | 79,201 | 52,751 | 64,302 | 64,664 | 40,803 | 71,287 |
| 4,750 | 25,556 | 32,403 | 42,901 | 28,551 | 35,102 | 34,964 | 22,103 | 38,287 |
| 5,820 | 13,556 | 17,503 | 23,101 | 15,351 | 18,902 | 18,764 | 11,903 | 20,302 |
| 6,420 | 5,702 | 7,503 | 9,901 | 6,551 | 8,102 | 7,964 | 5,103 | 8,702 |
| 7,500 | 2,377 | 3,129 | 4,126 | 2,701 | 3,377 | 3,251 | 2,128 | 3,627 |
| 8,500 | 952 | 1,253 | 1,651 | 1,051 | 1,352 | 1,301 | 853 | 1,452 |
| 9,600 | 477 | 623 | 826 | 526 | 667 | 651 | 428 | 727 |
| 10,620 | 230 | 303 | 397 | 253 | 326 | 313 | 207 | 350 |
| 11,580 | 135 | 178 | 232 | 148 | 191 | 183 | 122 | 205 |
| 12,580 | 68 | 90 | 116 | 74 | 96 | 92 | 62 | 103 |
| 13,520 | 39 | 52 | 66 | 42 | 55 | 53 | 36 | 59 |
| 14,450 | 20 | 27 | 33 | 21 | 28 | 27 | 19 | 30 |
| 15,450 | 10 | 14 | 16 | 10 | 14 | 14 | 10 | 15 |
| 16,420 | 4 | 6 | 6 | 4 | 6 | 6 | 4 | 6 |
| 18,300 | 2 | 3 | 3 | 2 | 3 | 3 | 2 | 3 |

(continued on next page)

TABLE 95 (Continued)

| Varying Stress (psi) | Cumulative Frequency of Load Cycle Occurrences | | | | | | | |
|---|---|---|---|---|---|---|---|---|
| | Specimen No. 509 | Specimen No. 510 | Specimen No. 511 | Specimen No. 512 | Specimen No. 513 | Specimen No. 514 | Specimen No. 517 | Specimen No. 518 |
| | Ground Loadings $f_{mean}$ = -3,000 psi | | | | | | | |
| .550 | 19,002 | 25,013 | 33,004 | 21,004 | 27,004 | 26,004 | 17,004 | 29,005 |
| 1,520 | 10,452 | 13,763 | 18,154 | 11,554 | 14,854 | 14,304 | 9,354 | 15,955 |
| 2,550 | 3,612 | 4,763 | 6,274 | 3,994 | 5,134 | 4,944 | 3,234 | 5,515 |
| 3,520 | 1,142 | 1,513 | 1,994 | 1,264 | 1,624 | 1,564 | 1,024 | 1,745 |
| 4,500 | 230 | 313 | 400 | 256 | 328 | 316 | 208 | 353 |
| 5,520 | 66 | 88 | 119 | 77 | 98 | 95 | 63 | 106 |
| 6,520 | 22 | 28 | 36 | 24 | 30 | 30 | 20 | 33 |
| 7,520 | 10 | 13 | 16 | 11 | 14 | 14 | 9 | 15 |
| 9,300 | 2 | 3 | 3 | 2 | 3 | 3 | 2 | 3 |
| | Ground to Air Cycles $f_{mean}$ = 4,500 psi | | | | | | | |
| 7,850 | 1,748 | 2,300 | 3,036 | 1,932 | 2,484 | 2,392 | 1,564 | 2,668 |
| No. of Blocks | 19.85 | 25.67 | 33.54 | 21.89 | 27.31 | 26.63 | 17.58 | 29.82 |

(End of Table)

TABLE 96

RANDOM COMPOSITE LOADING HISTORIES

MILITARY MANEUVER LOADINGS IN FLIGHT
$K_T = 4.0$
Test Group No. CM1

| Dynamic Stress (psi) | Cumulative Frequency of Load Cycle Occurrences Specimen No.488 | Specimen No. 489 | Specimen No. 490 | Specimen No.499 | Specimen No.500 |
|---|---|---|---|---|---|
| (Incremental) | Military Maneuver Loadings Minimum Stress = 5,450 psi | | | | |
| 0 | 7,236 | 8,126 | 9,549 | 7,711 | 10,676 |
| 2,840 | 5,674 | 6,371 | 7,488 | 6,046 | 8,371 |
| 5,680 | 4,424 | 4,968 | 5,838 | 4,714 | 6,527 |
| 11,400 | 2,566 | 2,881 | 3,386 | 2,734 | 3,785 |
| 17,000 | 1,250 | 1,404 | 1,649 | 1,332 | 1,844 |
| 22,700 | 502 | 563 | 662 | 534 | 740 |
| 28,400 | 148 | 166 | 195 | 158 | 218 |
| 31,200 | 78 | 88 | 104 | 84.1 | 116 |
| 34,000 | 36.2 | 40.6 | 47.7 | 38.6 | 53.4 |
| 39,700 | 6.58 | 7.39 | 8.68 | 7.01 | 9.71 |
| 41,200 | 3.29 | 3.69 | 4.34 | 3.50 | 4.85 |
| 42,000 | 1.64 | 1.85 | 2.17 | 1.75 | 2.43 |
| (Varying) | Ground Loadings $f_{mean} = -3,000$ psi | | | | |
| 0 | 1,682 | 1,888 | 2,216 | 1,793 | 2,478 |
| 950 | 971 | 1,090 | 1,280 | 1,036 | 1,431 |
| 1,920 | 446 | 501 | 588 | 476 | 658 |
| 2,850 | 158 | 177 | 208 | 168 | 233 |
| 3,800 | 43.0 | 48.2 | 56.6 | 45.8 | 63.3 |
| 4,750 | 10.4 | 11.6 | 13.7 | 11.1 | 15.3 |
| 5,700 | 2.75 | 3.09 | 3.63 | 2.94 | 4.06 |
| 6,180 | 1.53 | 1.72 | 2.02 | 1.63 | 2.26 |
| 6,650 | 0.982 | 1.10 | 1.29 | 1.05 | 1.45 |
| 7,130 | 0.61 | 0.69 | 0.81 | 0.65 | 0.90 |
| 7,600 | 0.41 | 0.45 | 0.53 | 0.43 | 0.59 |
| 8,000 | 0.28 | 0.31 | 0.36 | 0.29 | 0.41 |
| 8,550 | 0.10 | 0.12 | 0.14 | 0.11 | 0.15 |
| 9,250 | 0.070 | 0.078 | 0.092 | 0.074 | 0.10 |
| 9,500 | 0.024 | 0.026 | 0.031 | 0.025 | 0.035 |
| 9,620 | 0.022 | 0.024 | 0.029 | 0.023 | 0.032 |
| 9,980 | 0.008 | 0.009 | 0.011 | 0.009 | 0.012 |
| 10,450 | 0.006 | 0.007 | 0.008 | 0.006 | 0.009 |
| | Ground-Air-Ground Loading $f_{mean} = 1,225$ psi | | | | |
| 4,225 | 240 | 270 | 317 | 256 | 354 |

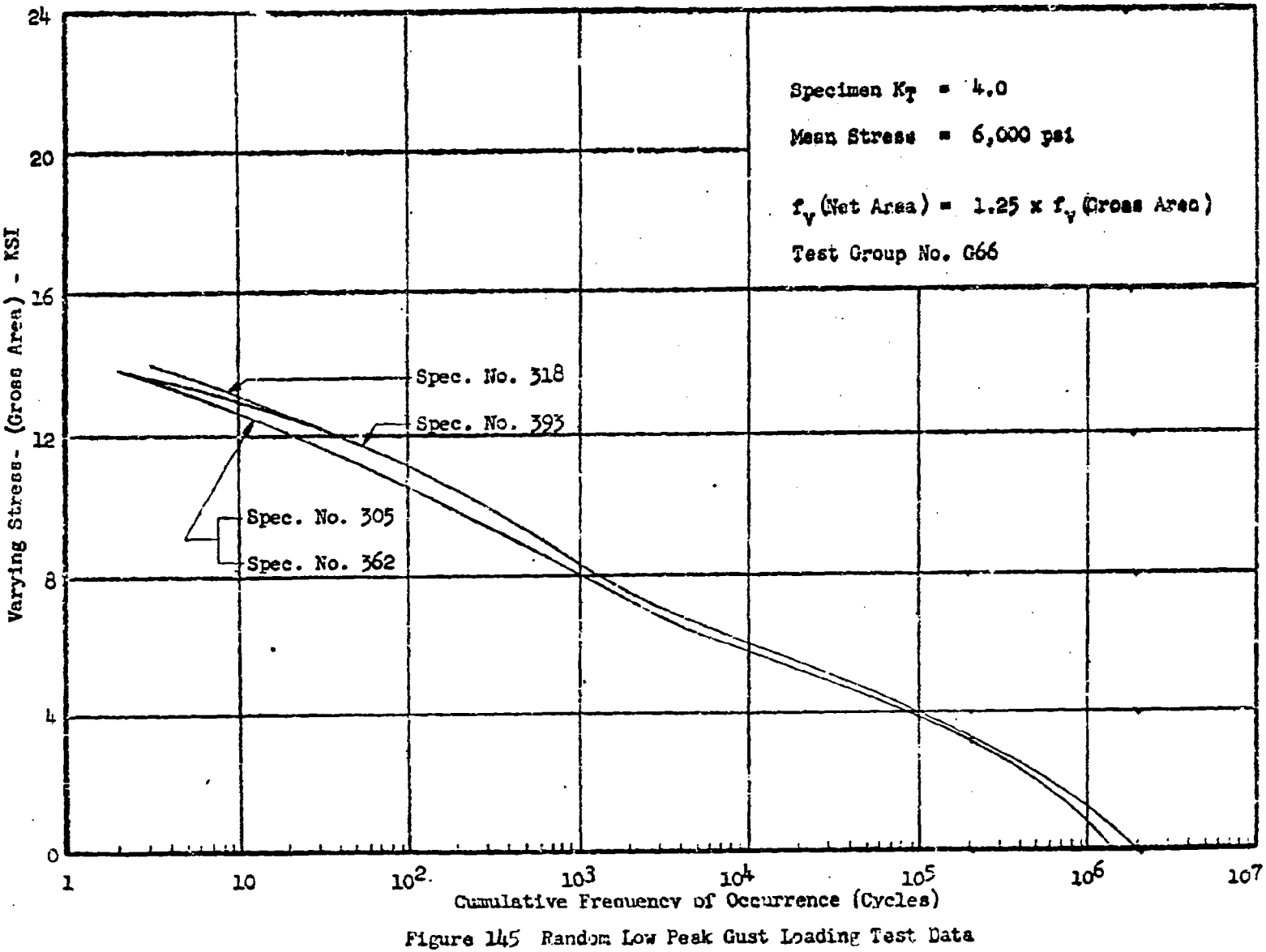



Figure 145 Random Low Peak Gust Loading Test Data

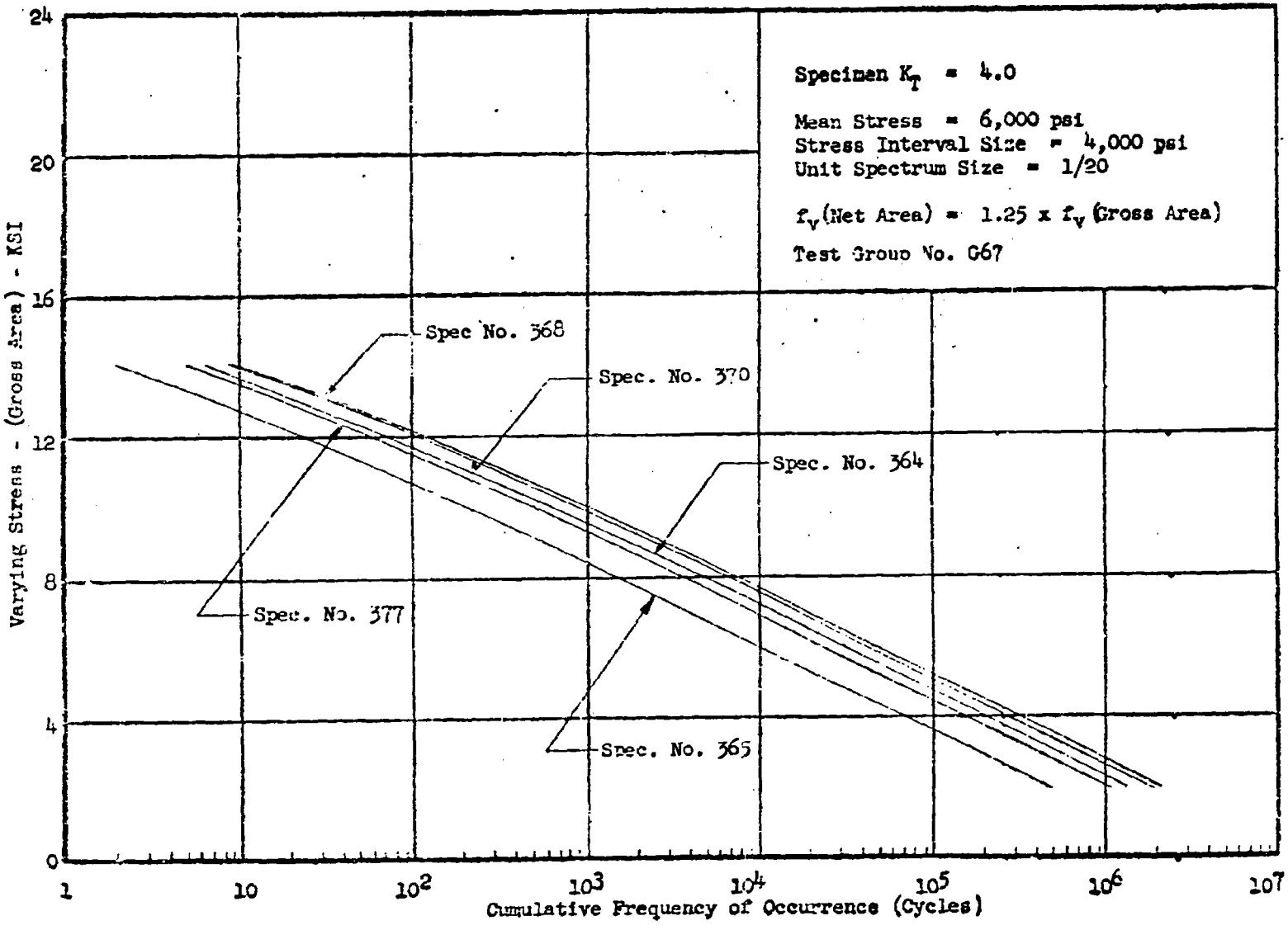



Figure 146 Ordered Low Peak Gust Loading Test Data

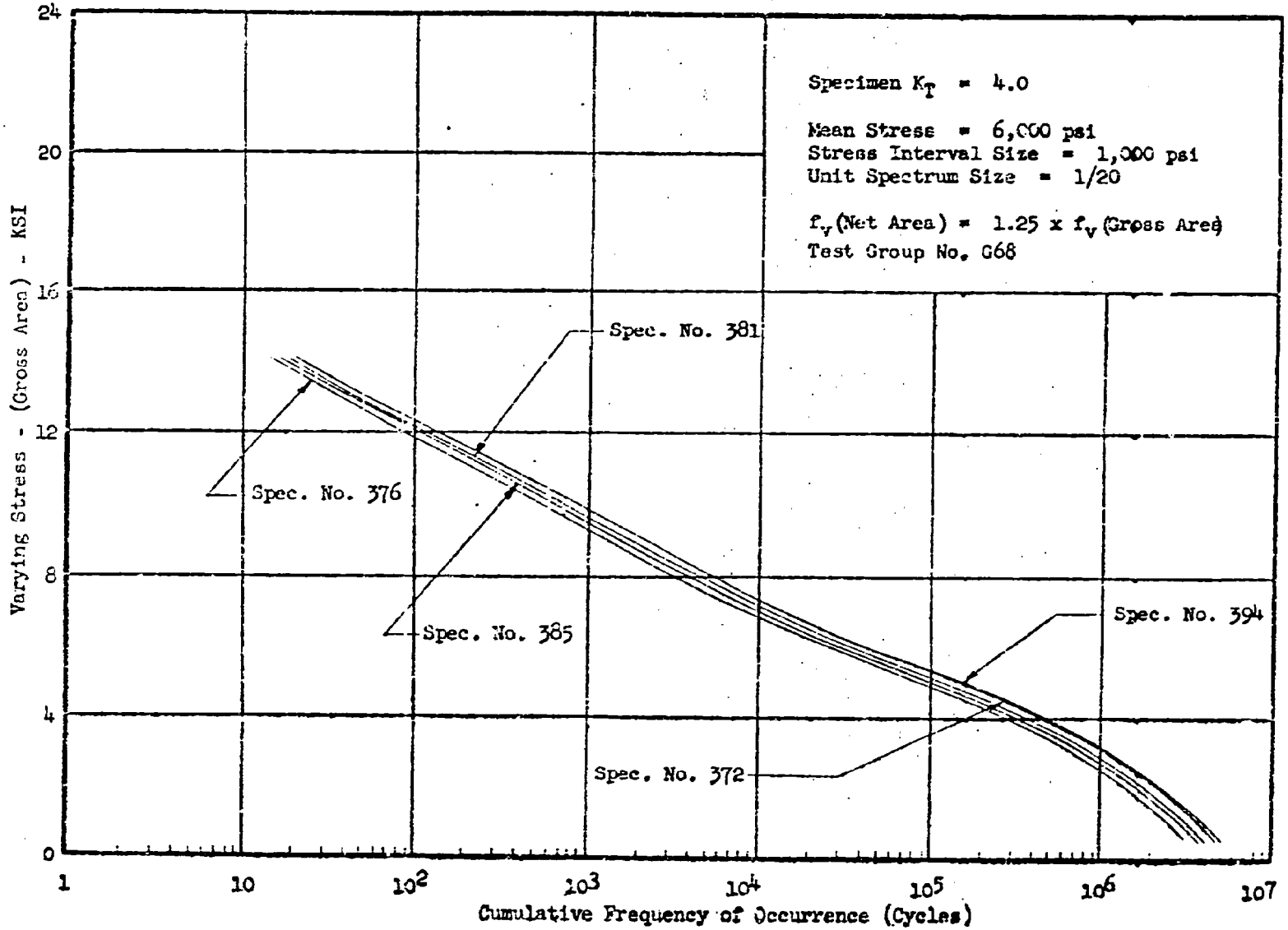



Figure 147 Ordered Low Peak Gust Loading Test Data

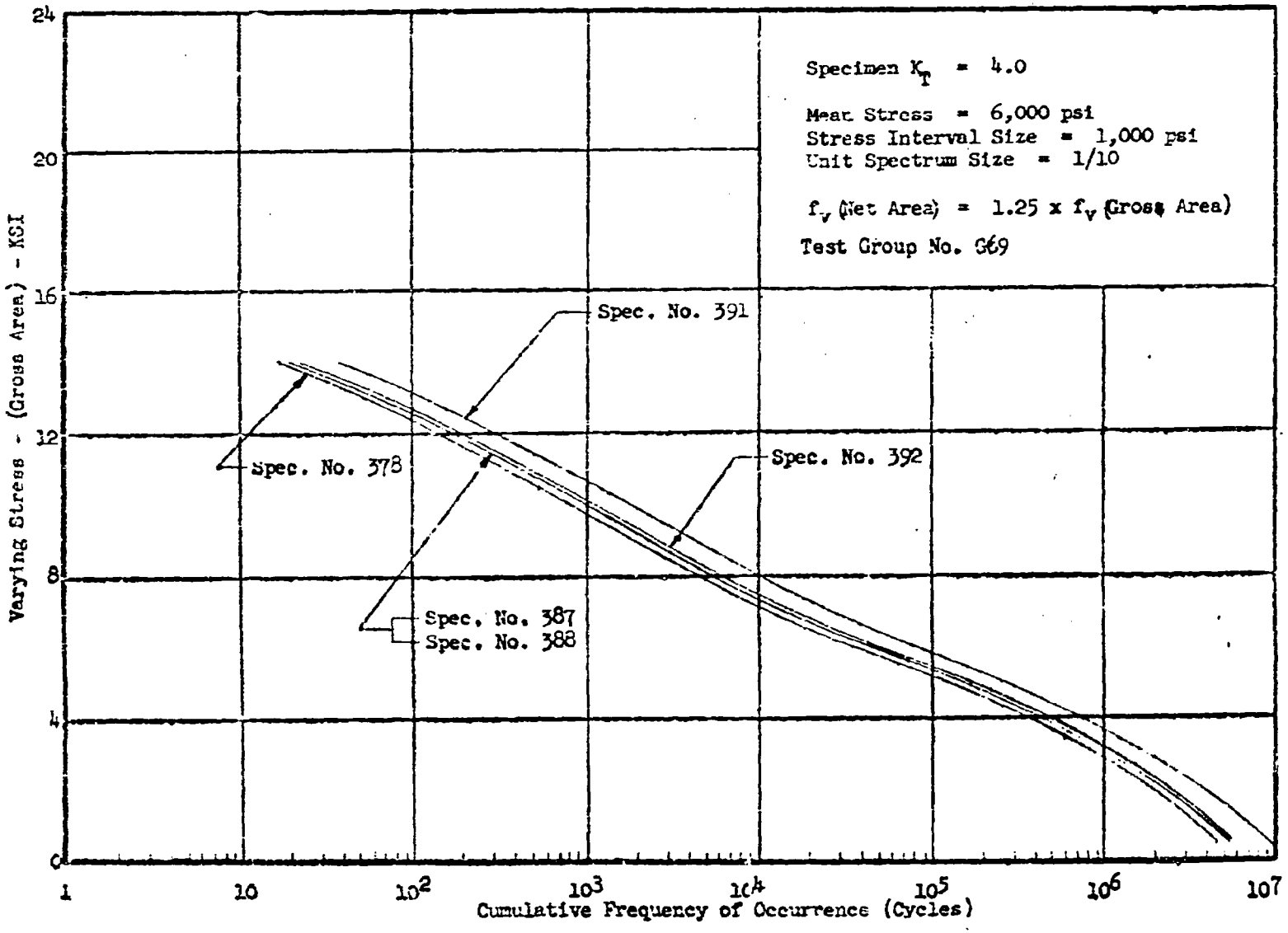



Figure 148 Ordered Low Peak Gust Loading Test Data

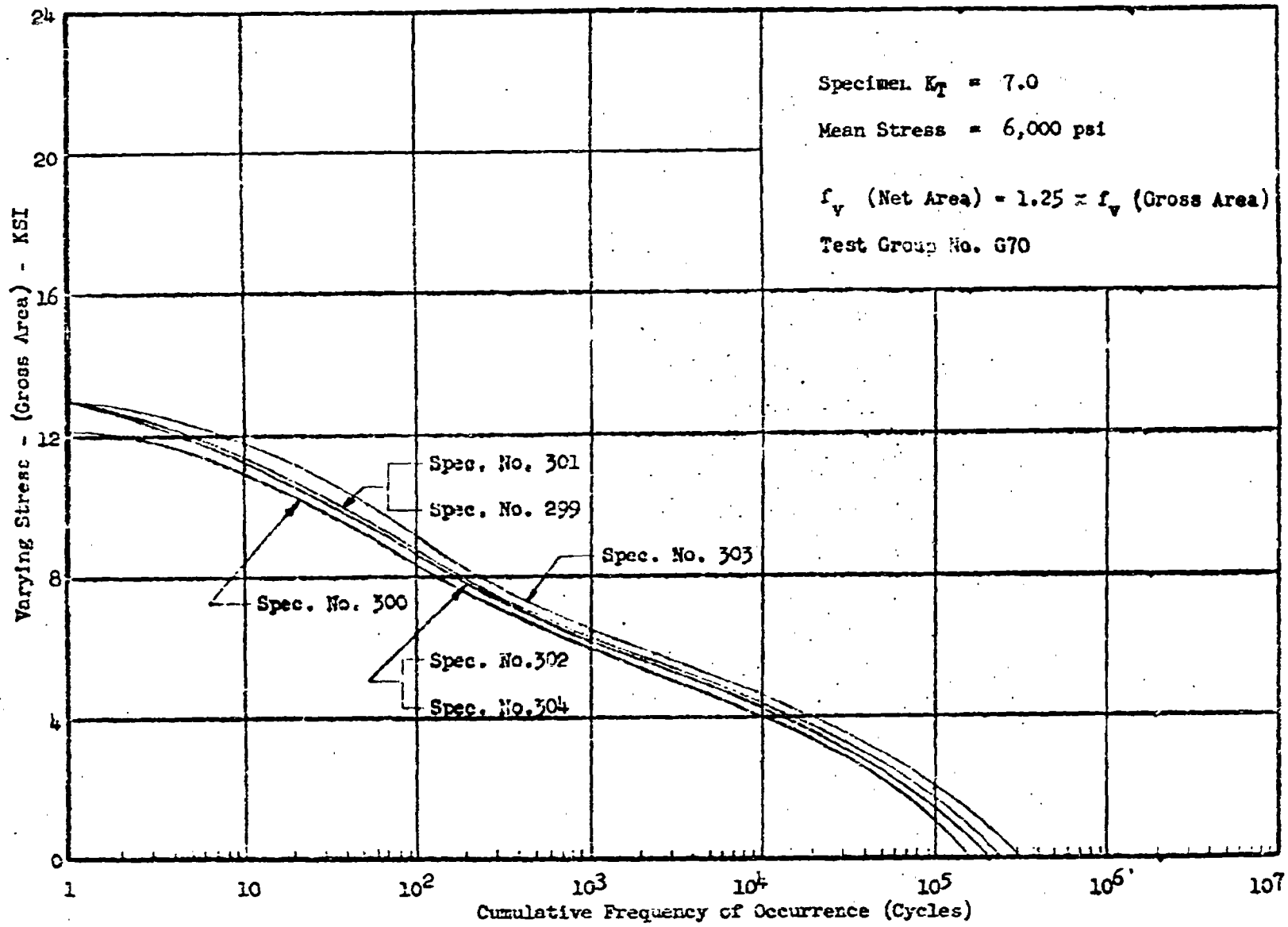



Figure 149 Random Low Peak Gust Loading Test Data

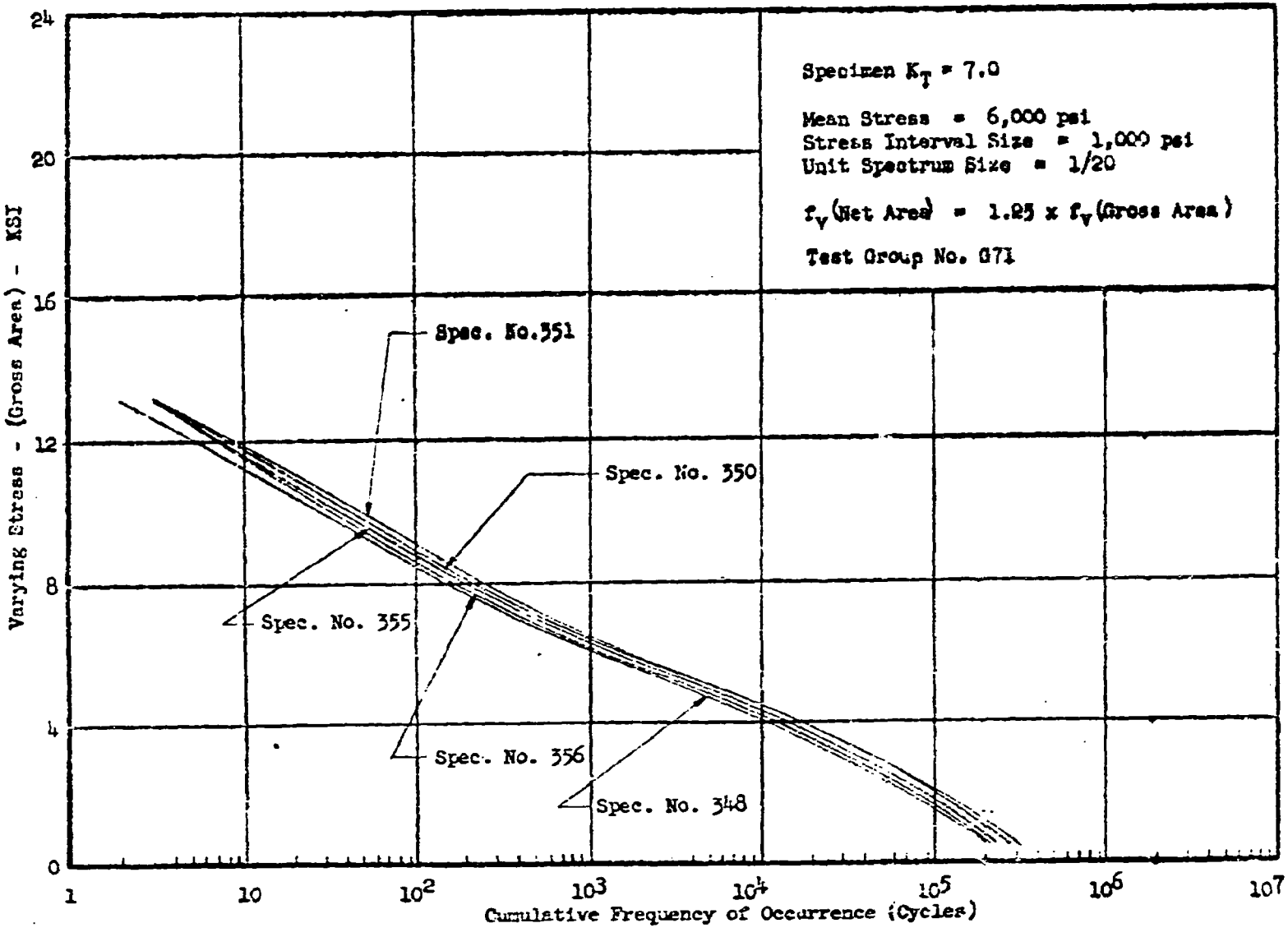



Figure 150 Ordered Low Peak Gust Loading Test Data

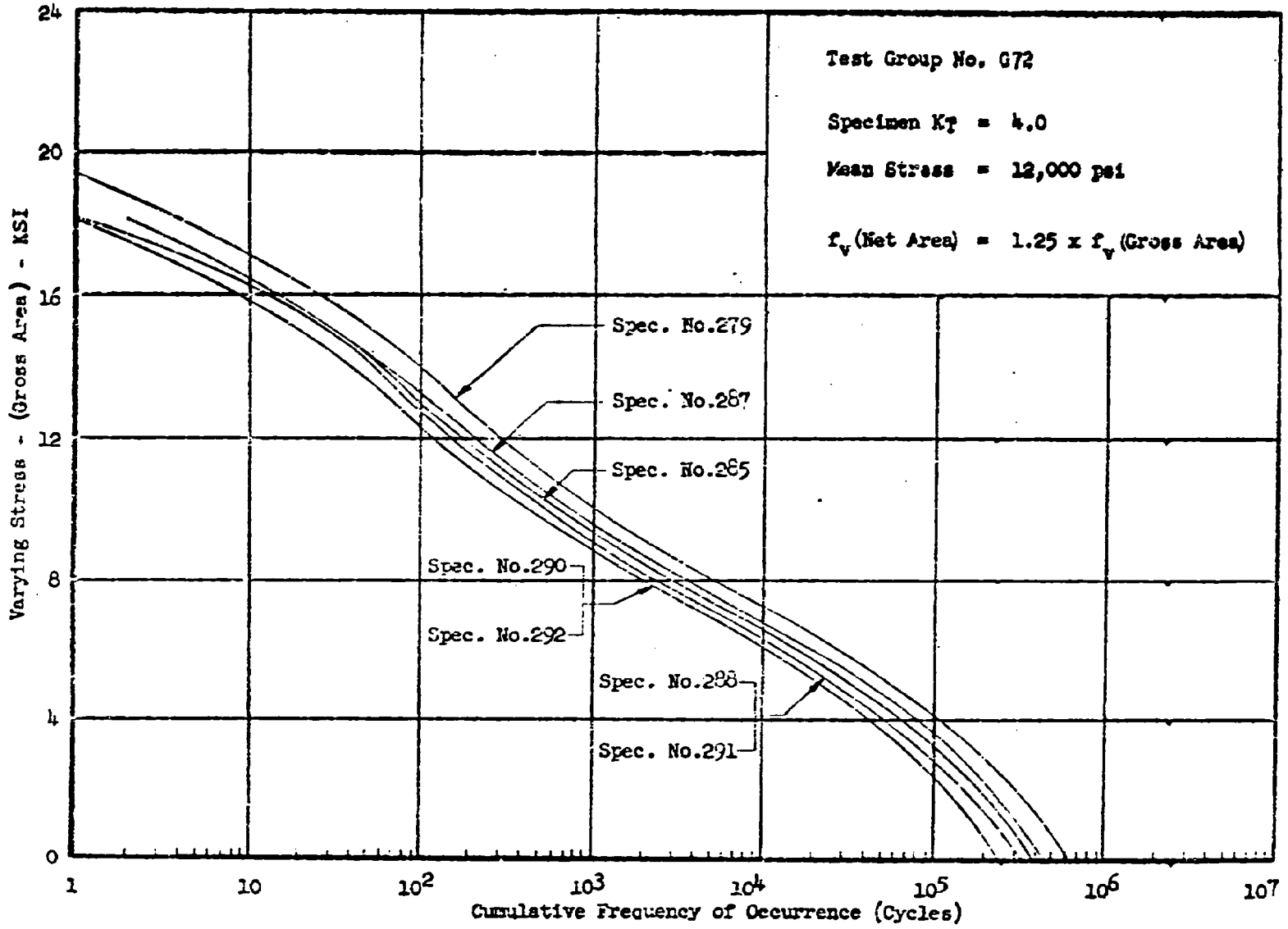



Figure 151 Random Peak Gust Loading Test Data

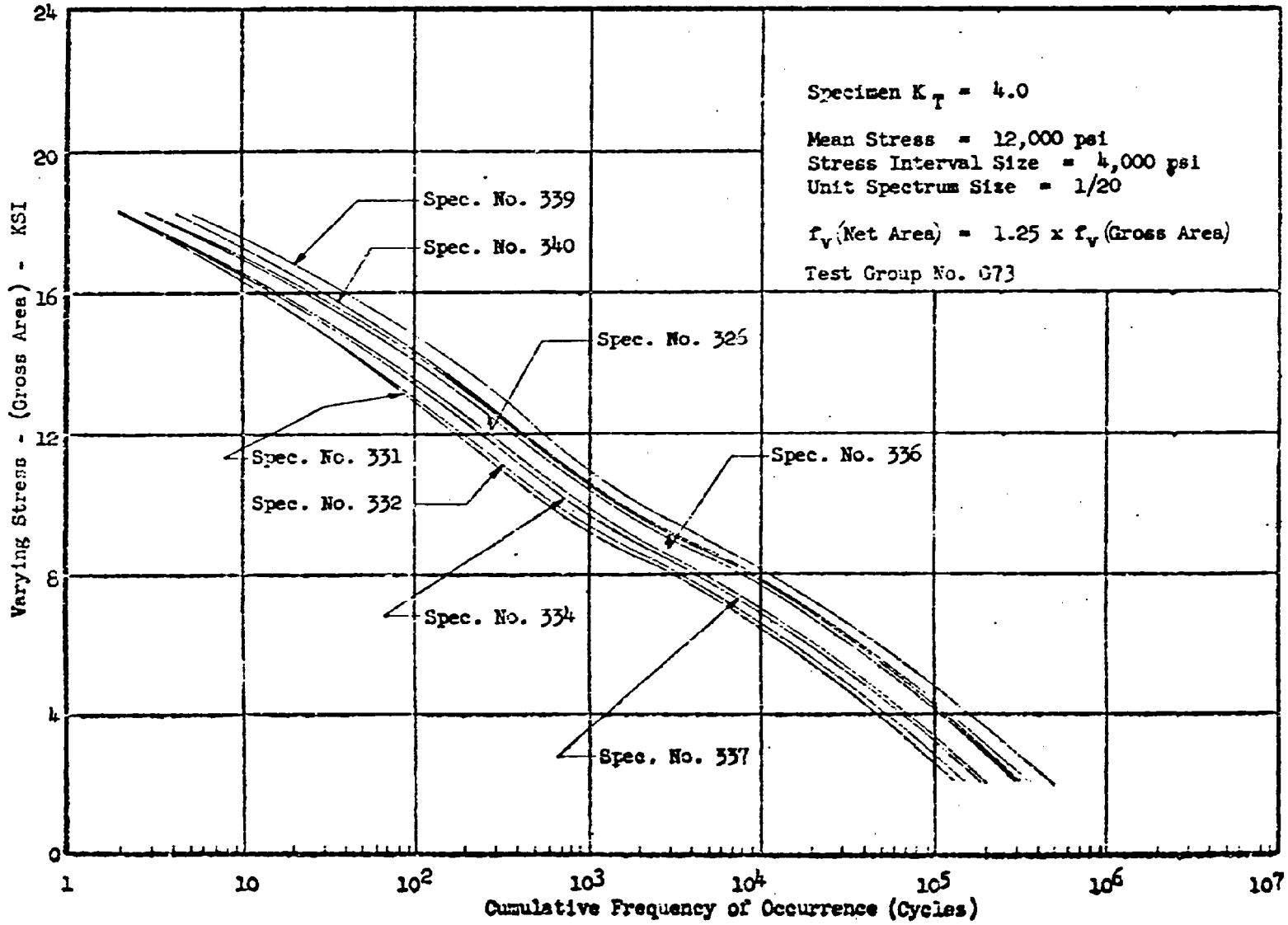



Figure 152 Ordered High Peak Gust Loading Test Data

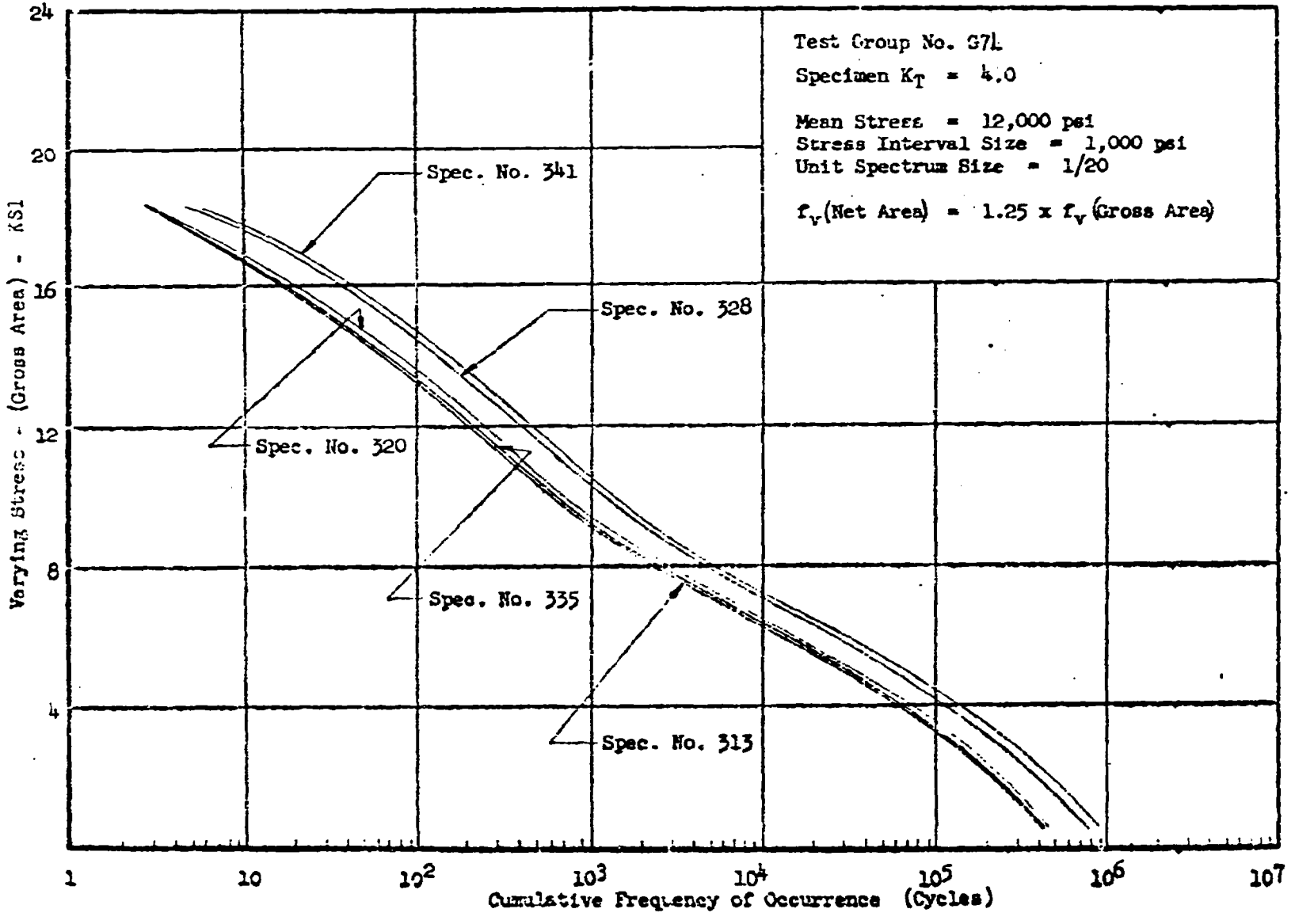



Figure 153 Ordered High Peak Gust Loading Test Data

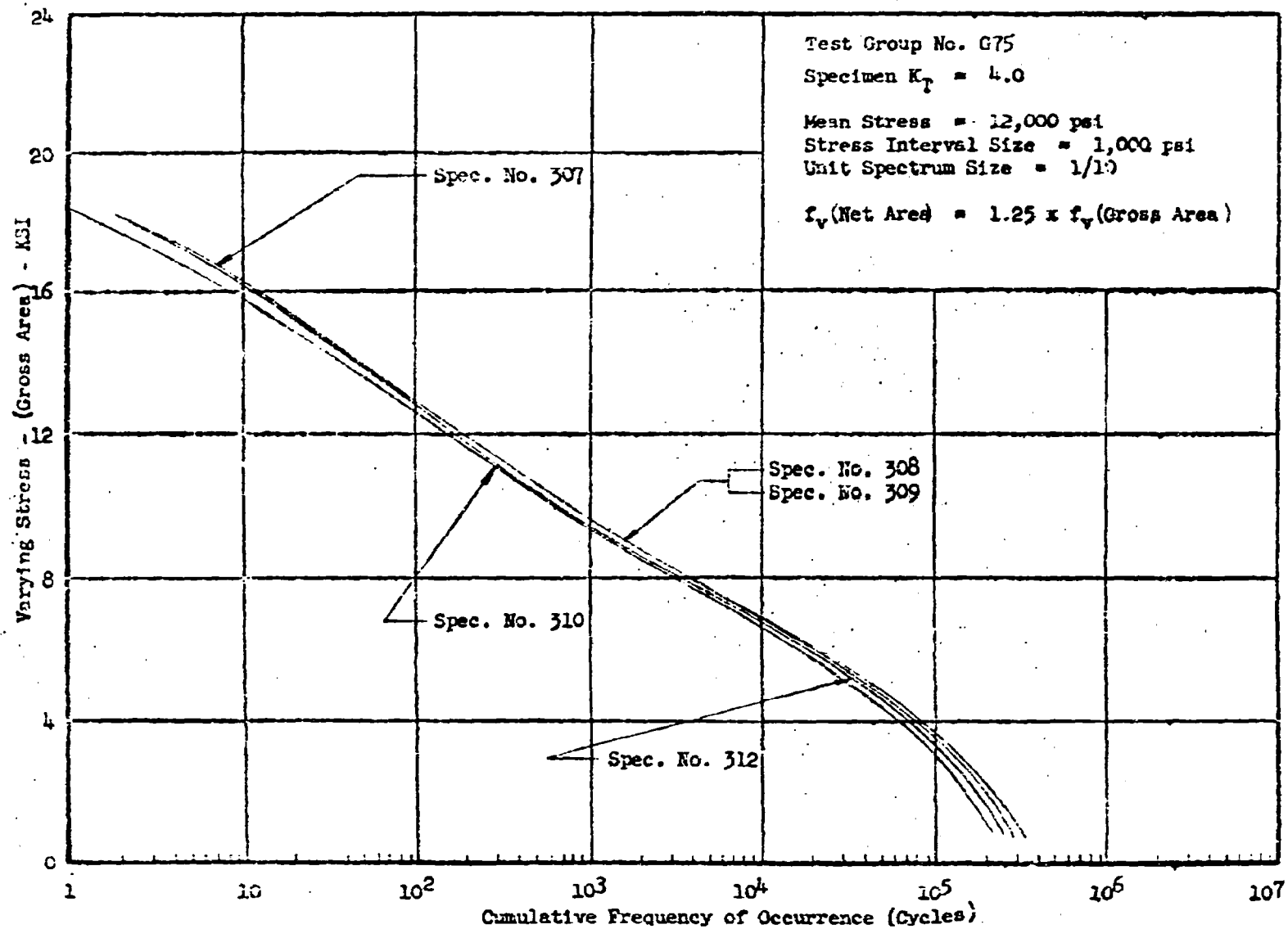



Figure 154 Ordered High Peak Gust Loading Test Data

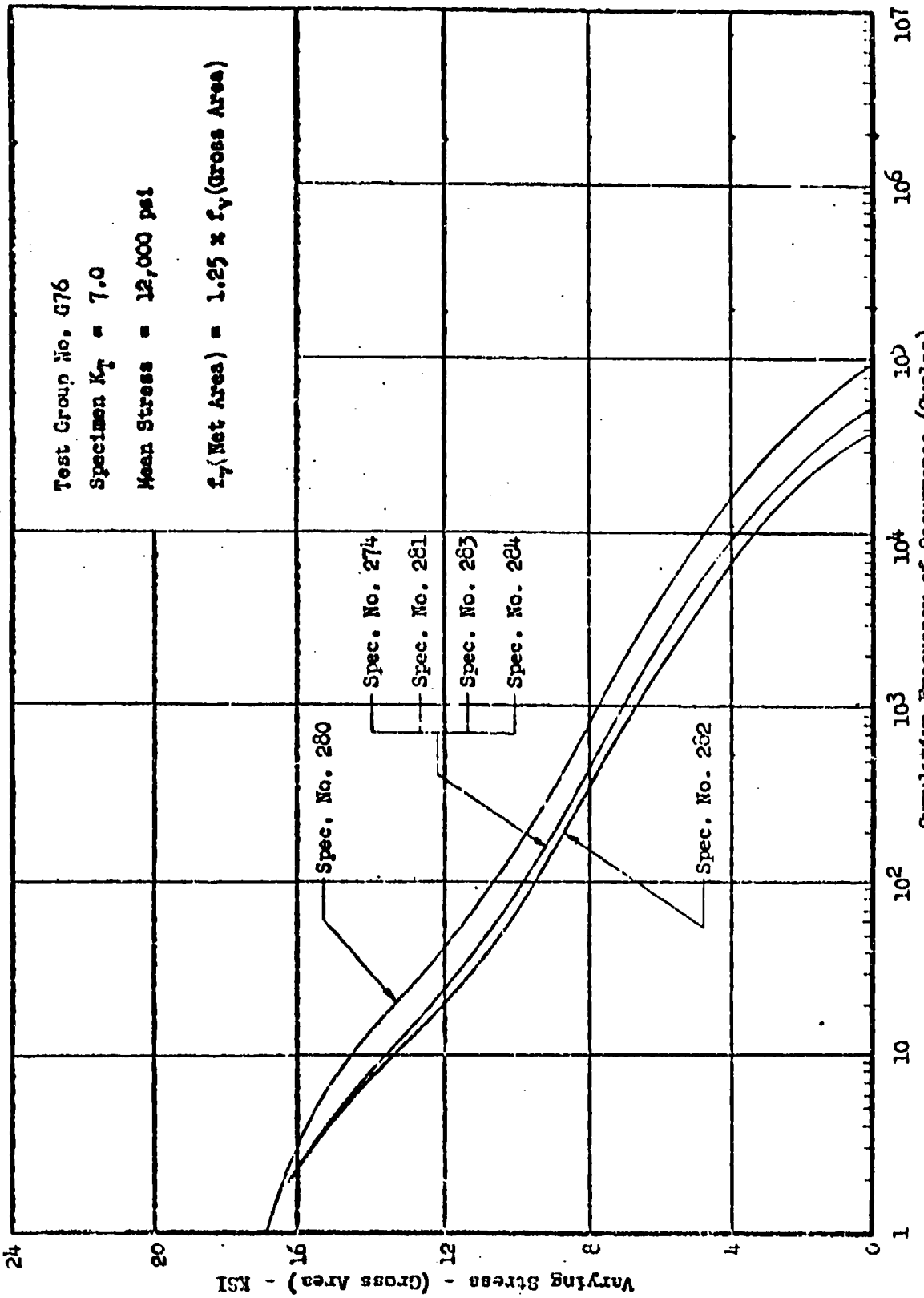



Figure 155 Random High Peak Gust Loading Test Data

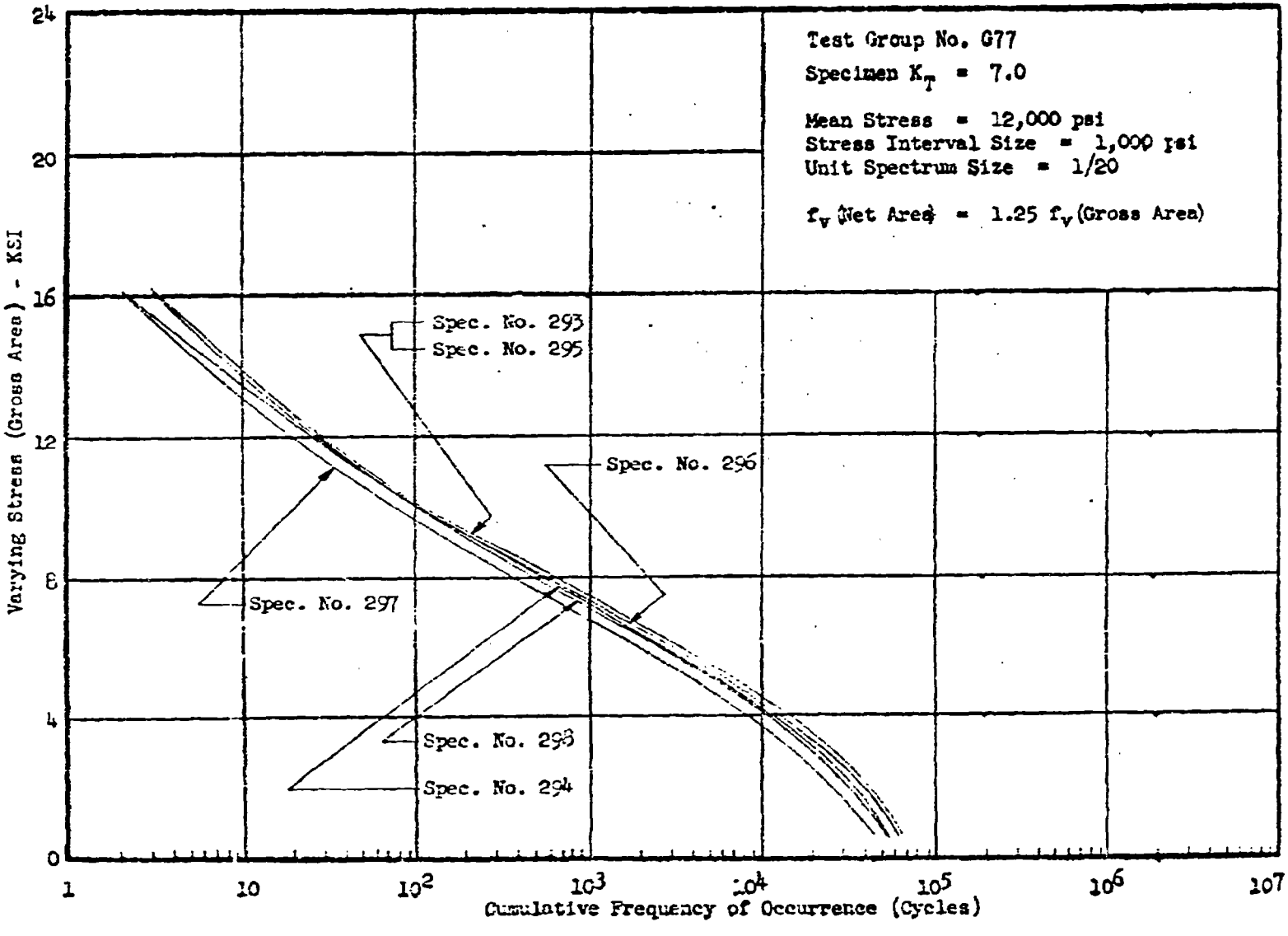



Figure 156 Ordered High Peak Gust Loading Test Data

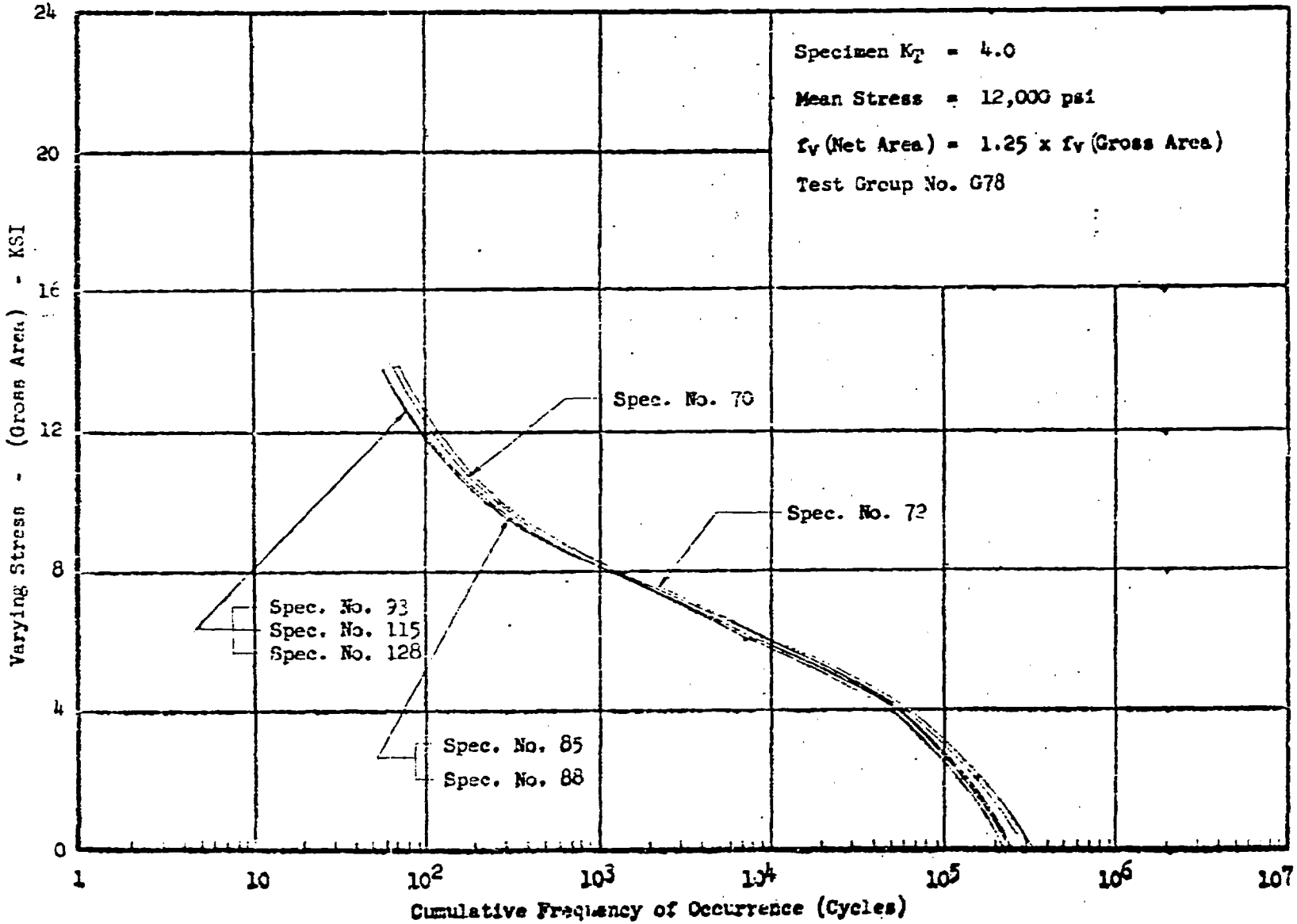



Figure 157 Wing Root Random Loading Test Data (Mean Crossing Peak Count)

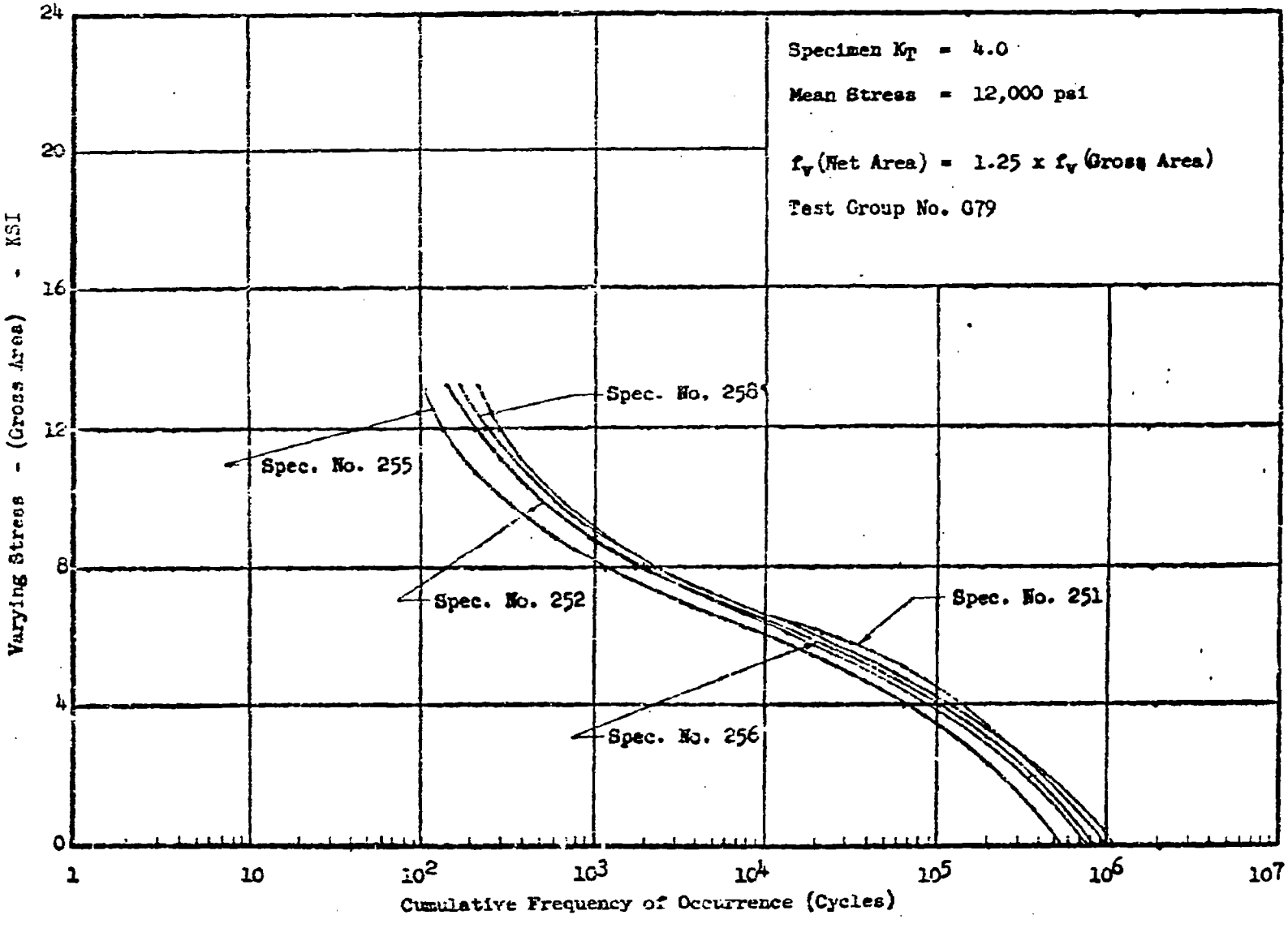



Figure 158 Wing Root Ordered Loading Test Data (Mean Crossing Peak Count)

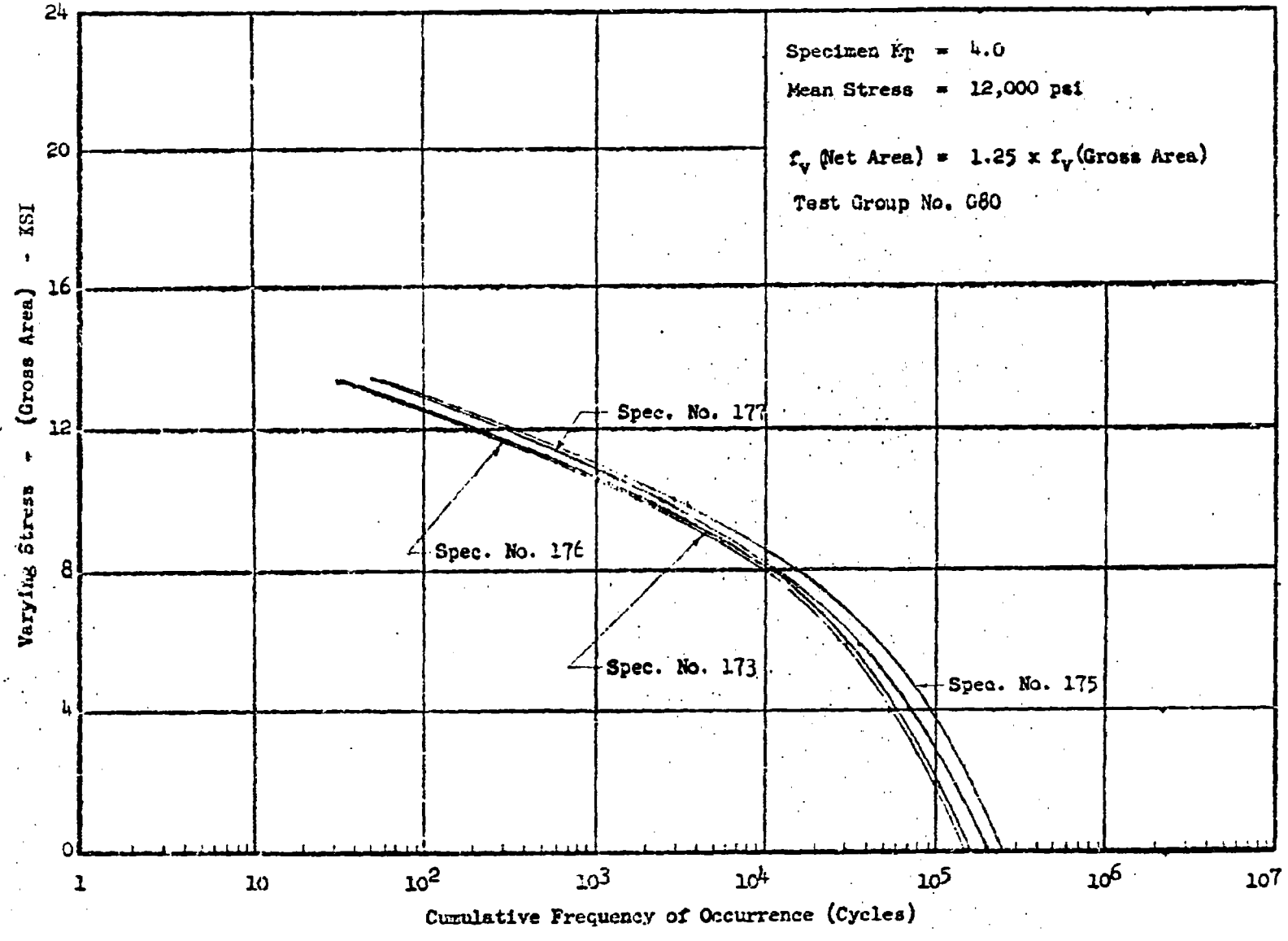



Figure 159 Modified Wing Root Random Loading Test Data (Mean Crossing Peak Count)

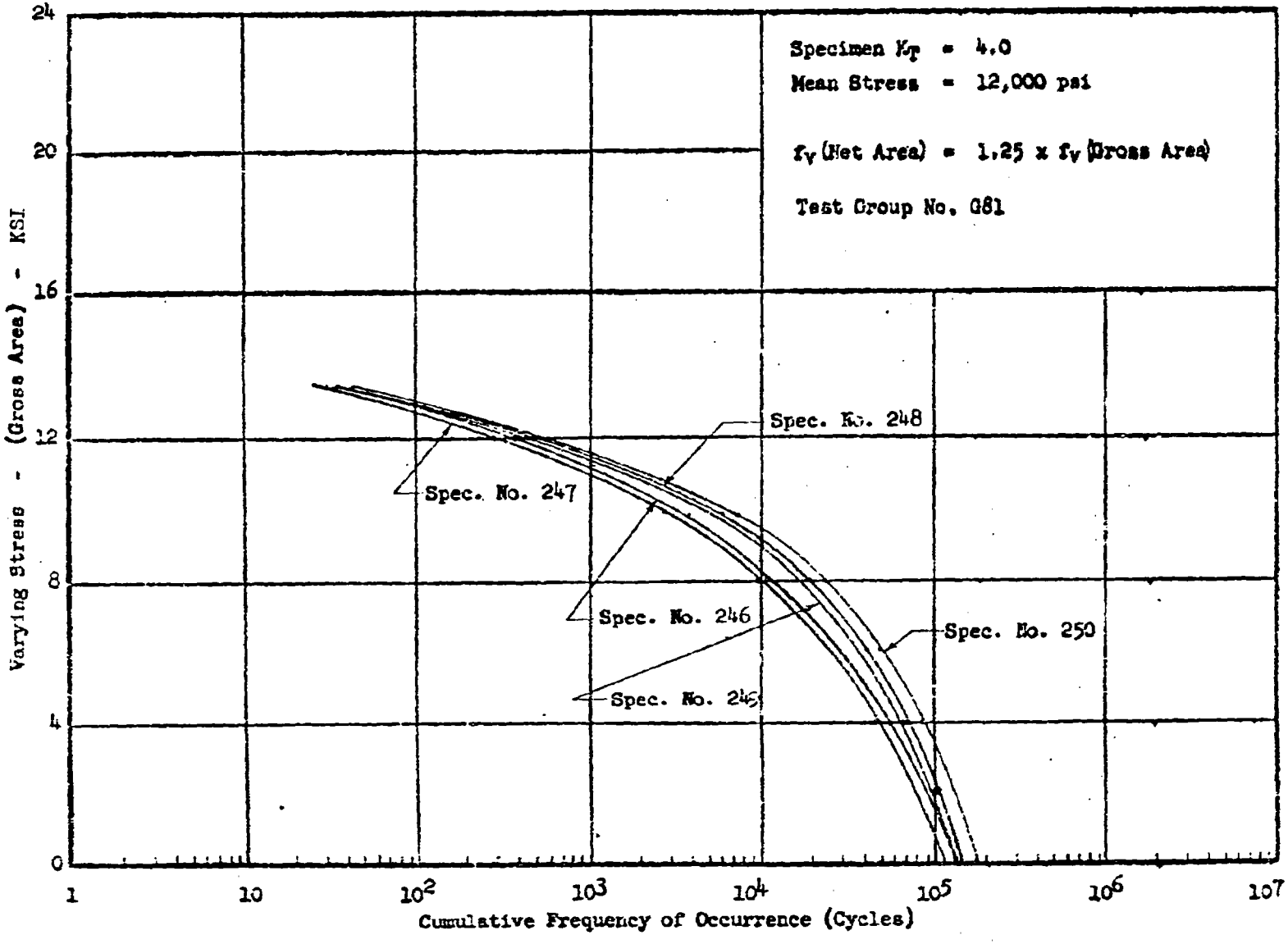



Figure 160 Modified Wing Root Ordered Loading Test Data (M

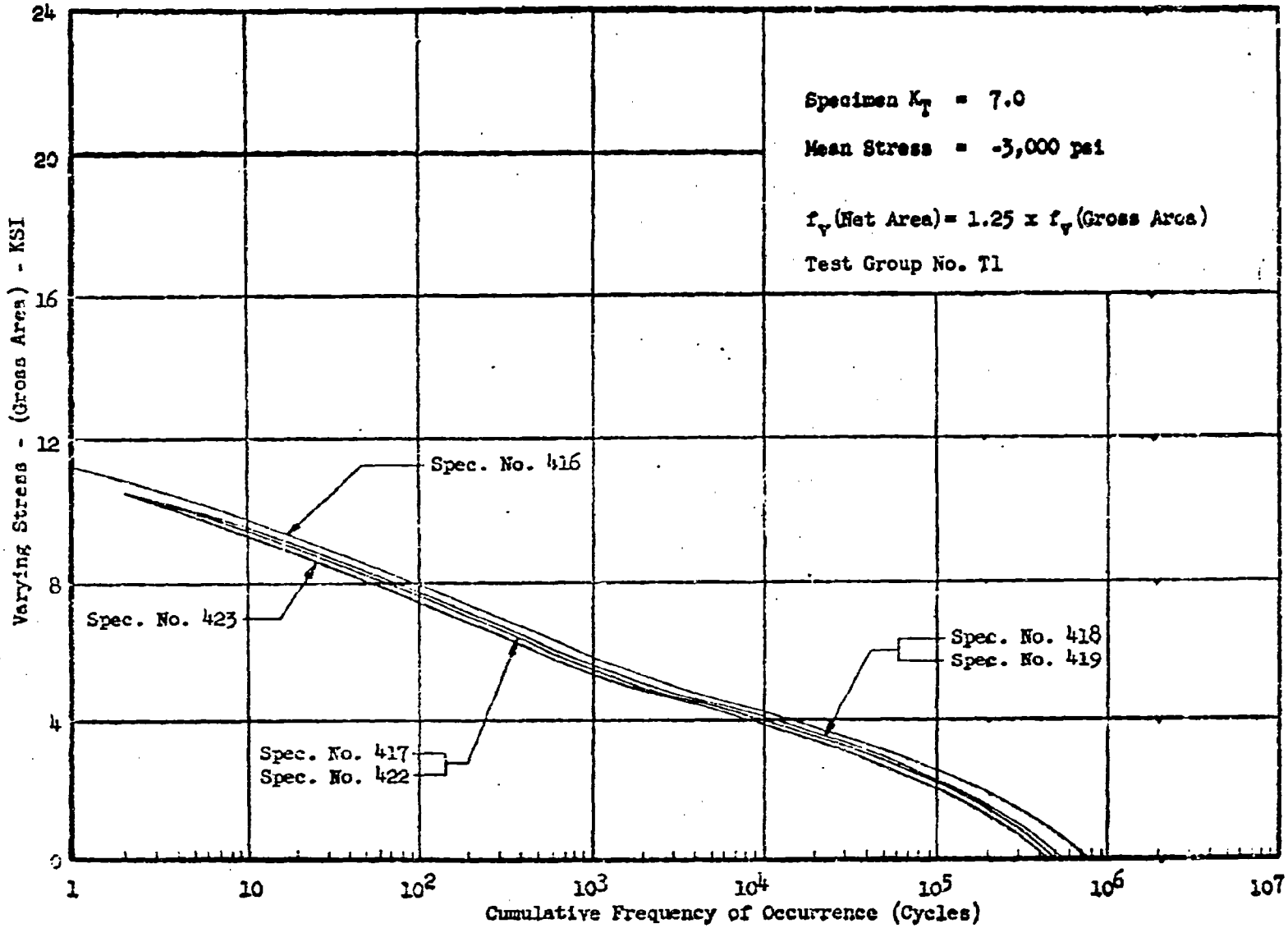
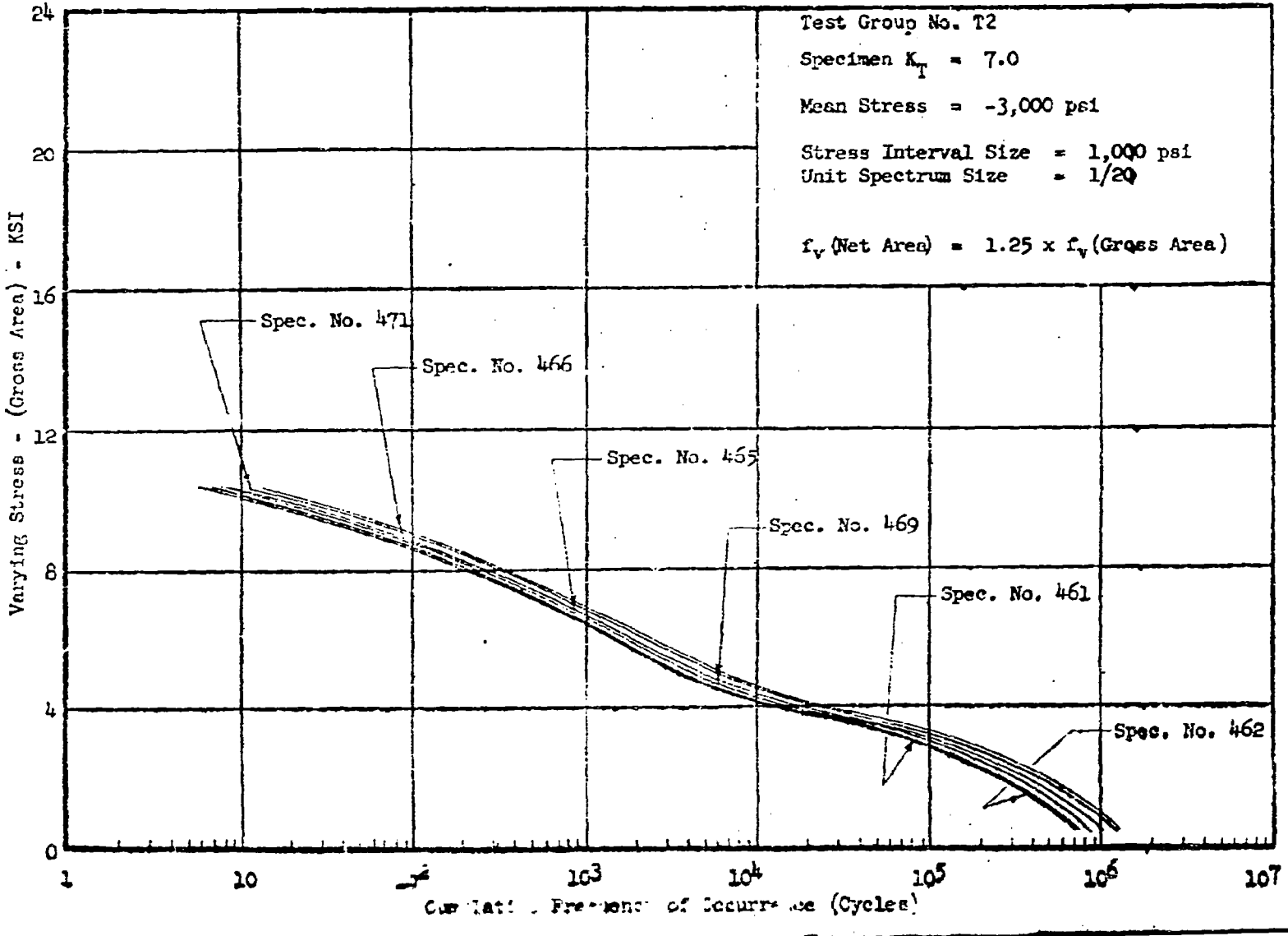



Figure 161 Random Ground Loading Test Data


Test Group No. T2
Specimen $K_T$ = 7.0
Mean Stress = -3,000 psi
Stress Interval Size = 1,000 psi
Unit Spectrum Size = 1/20
$f_v$ (Net Area) = 1.25 x $f_v$ (Gross Area)
Spec. No. 471
Spec. No. 466
Spec. No. 465
Spec. No. 469
Spec. No. 461
Spec. No. 462
Varying Stress - (Gross Area) - KSI
0
4
8
12
16
20
24
1
10
$10^3$
$10^4$
$10^5$
$10^6$
$10^7$
Cumulative Frequency of Occurrence (Cycles)

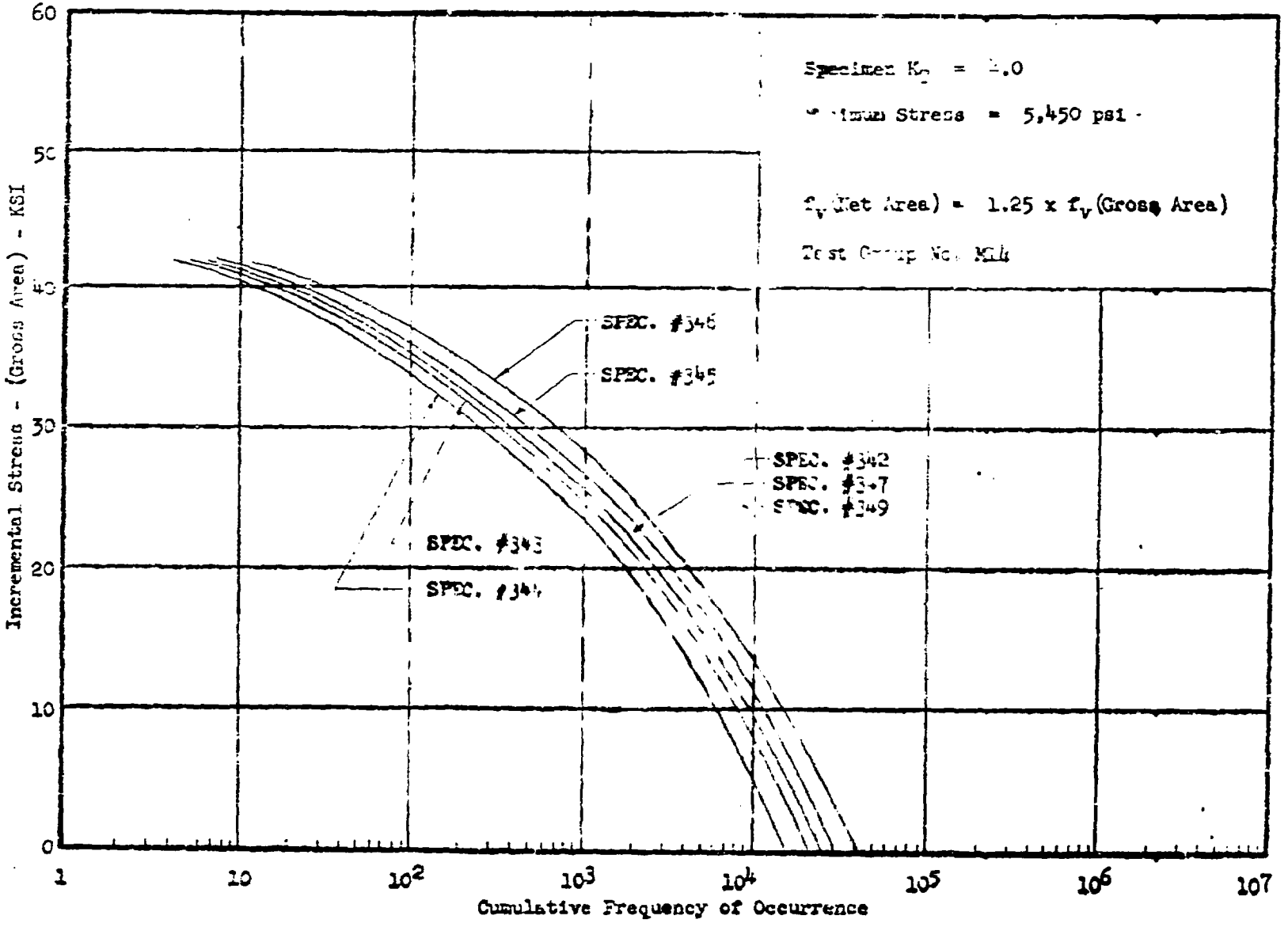



Figure 163 Random Military Maneuver Flight Loading

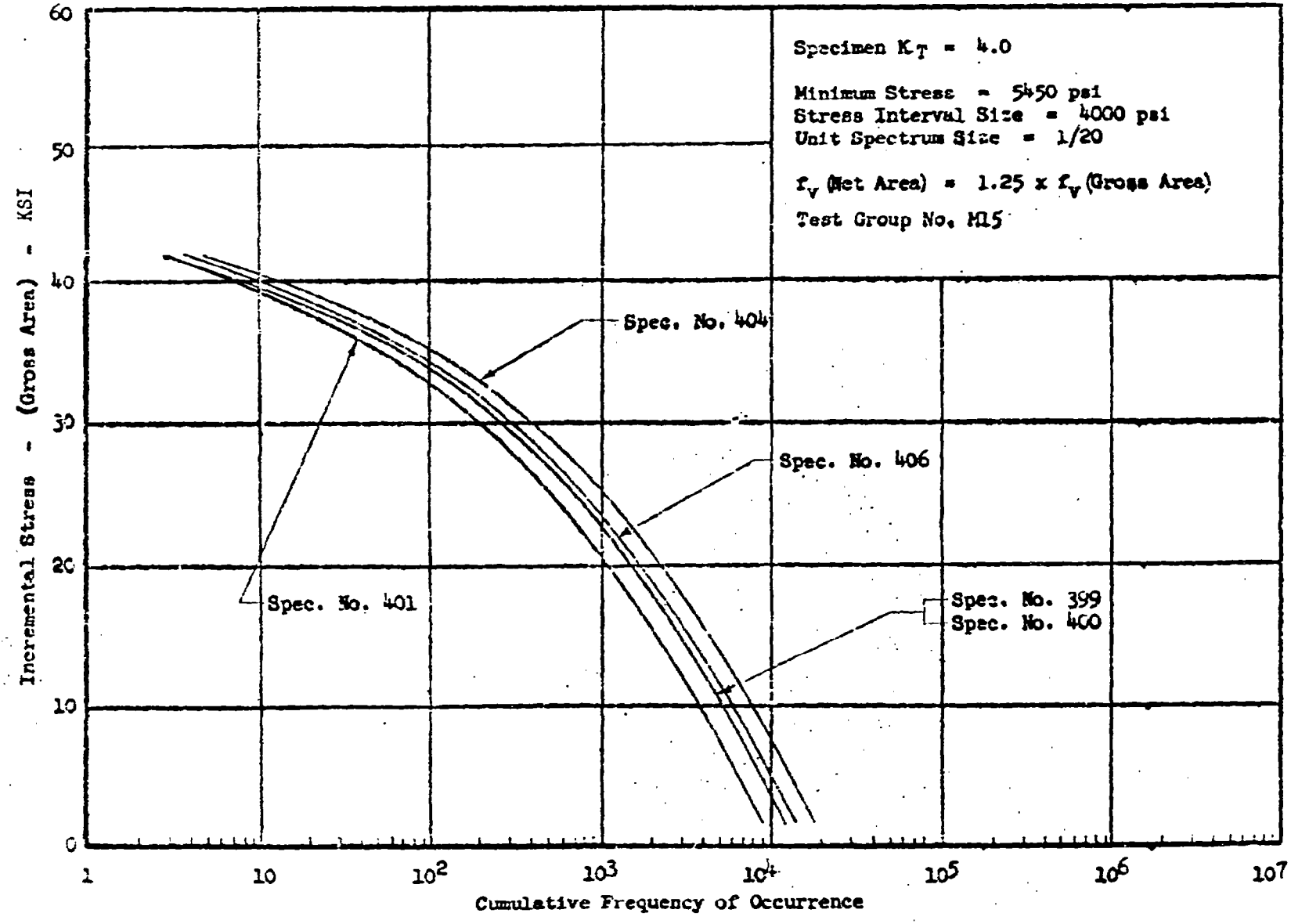



Figure 164 Ordered Military Maneuver Flight Loading Test Data

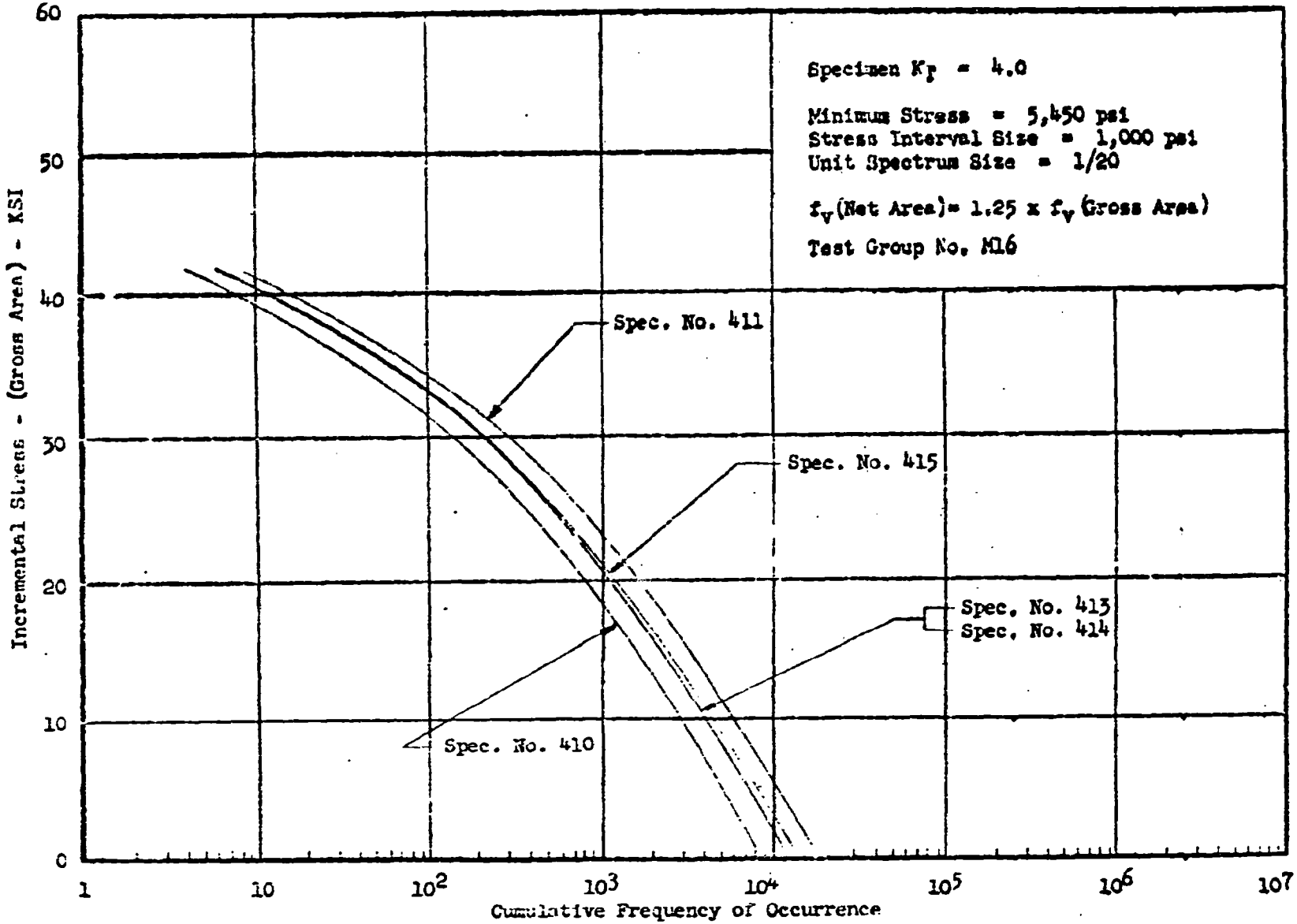



Figure 165 Ordered Military Maneuver Flight Loading Test Data

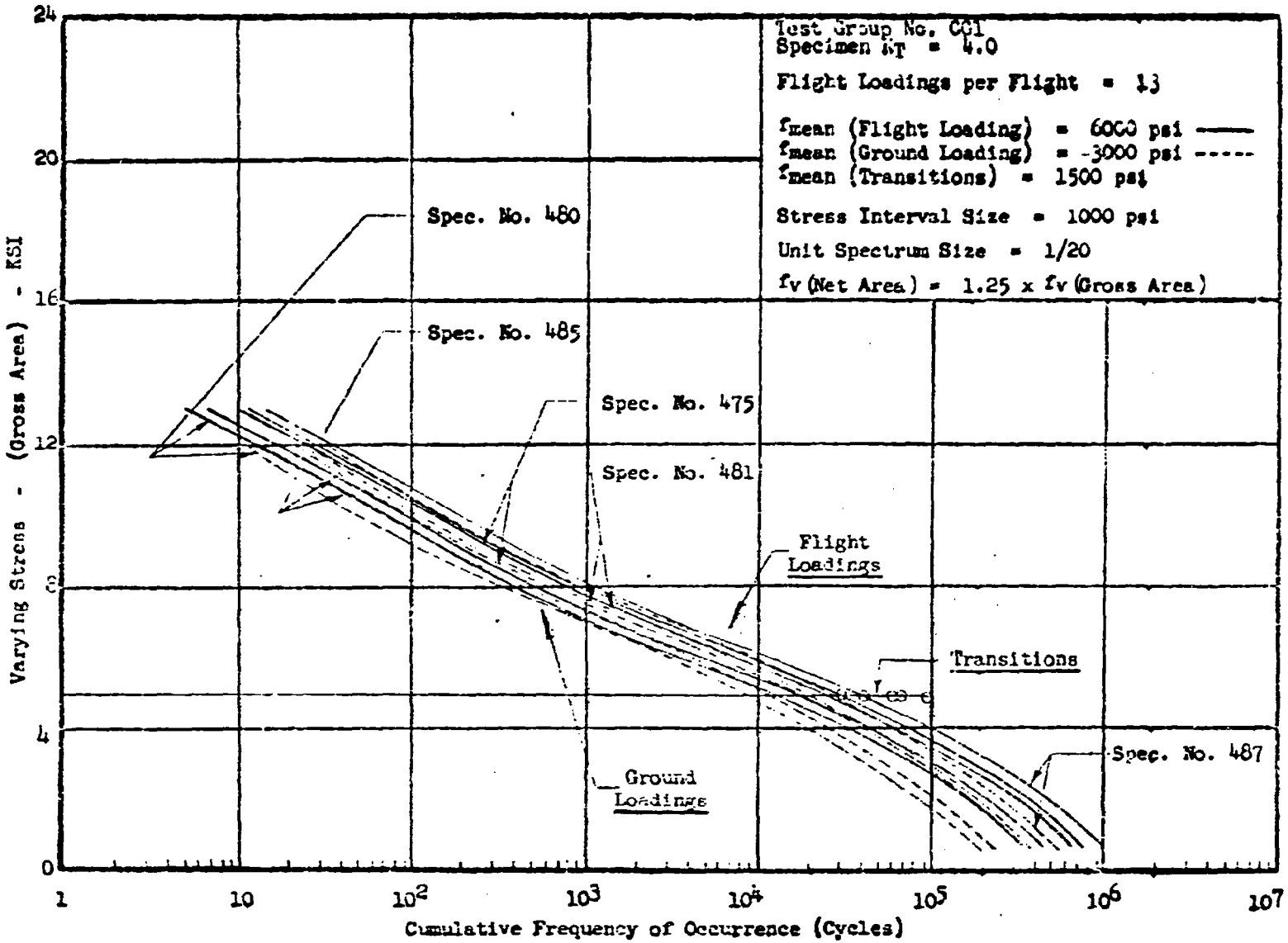



Figure 166 Ordered Composite Loading Test Data (Low Peak Gust Loadings in Flight)

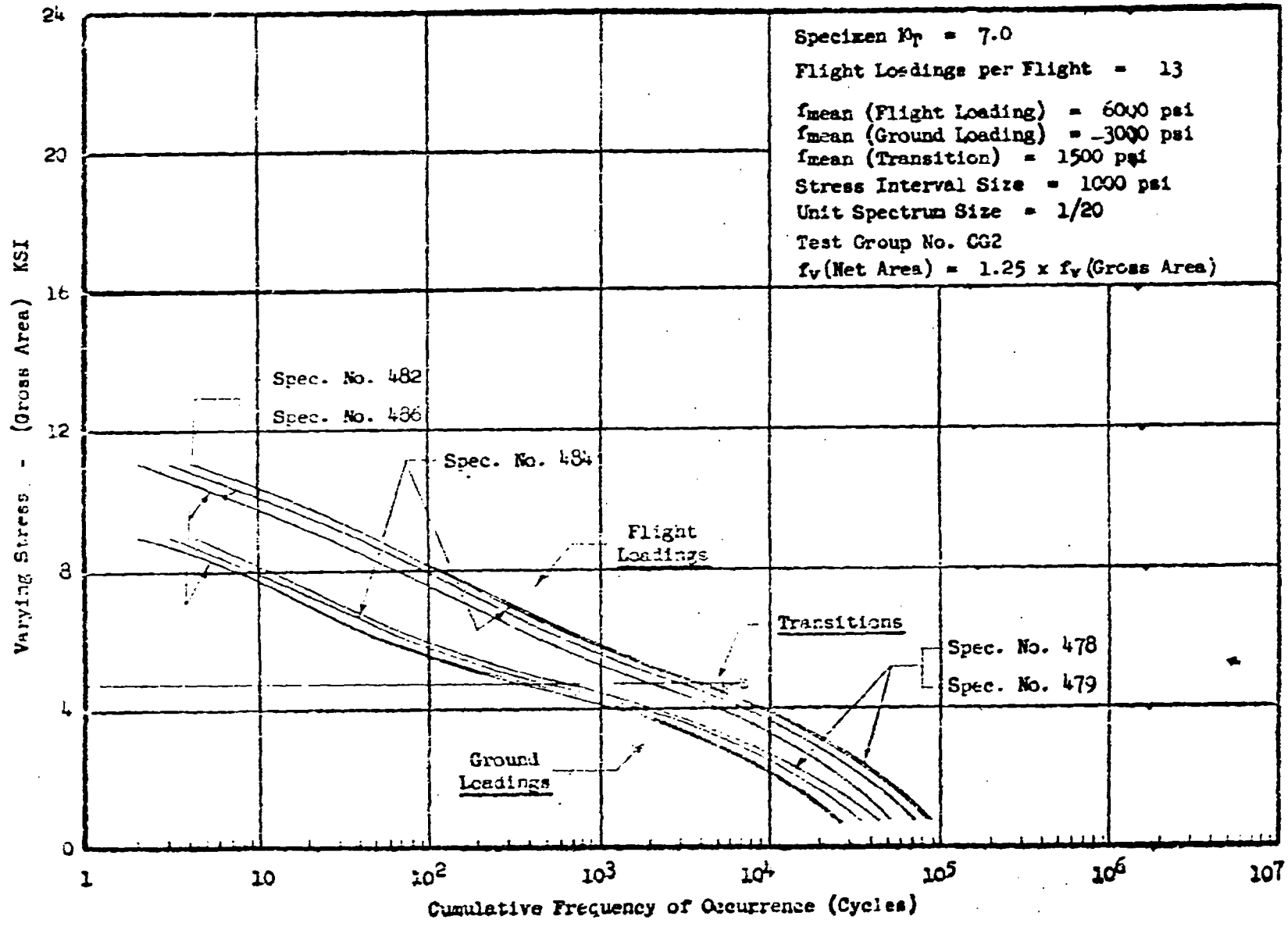



Figure 167 Ordered Composite Loading Test Data (Low Peak Gust Loadings in Flight)

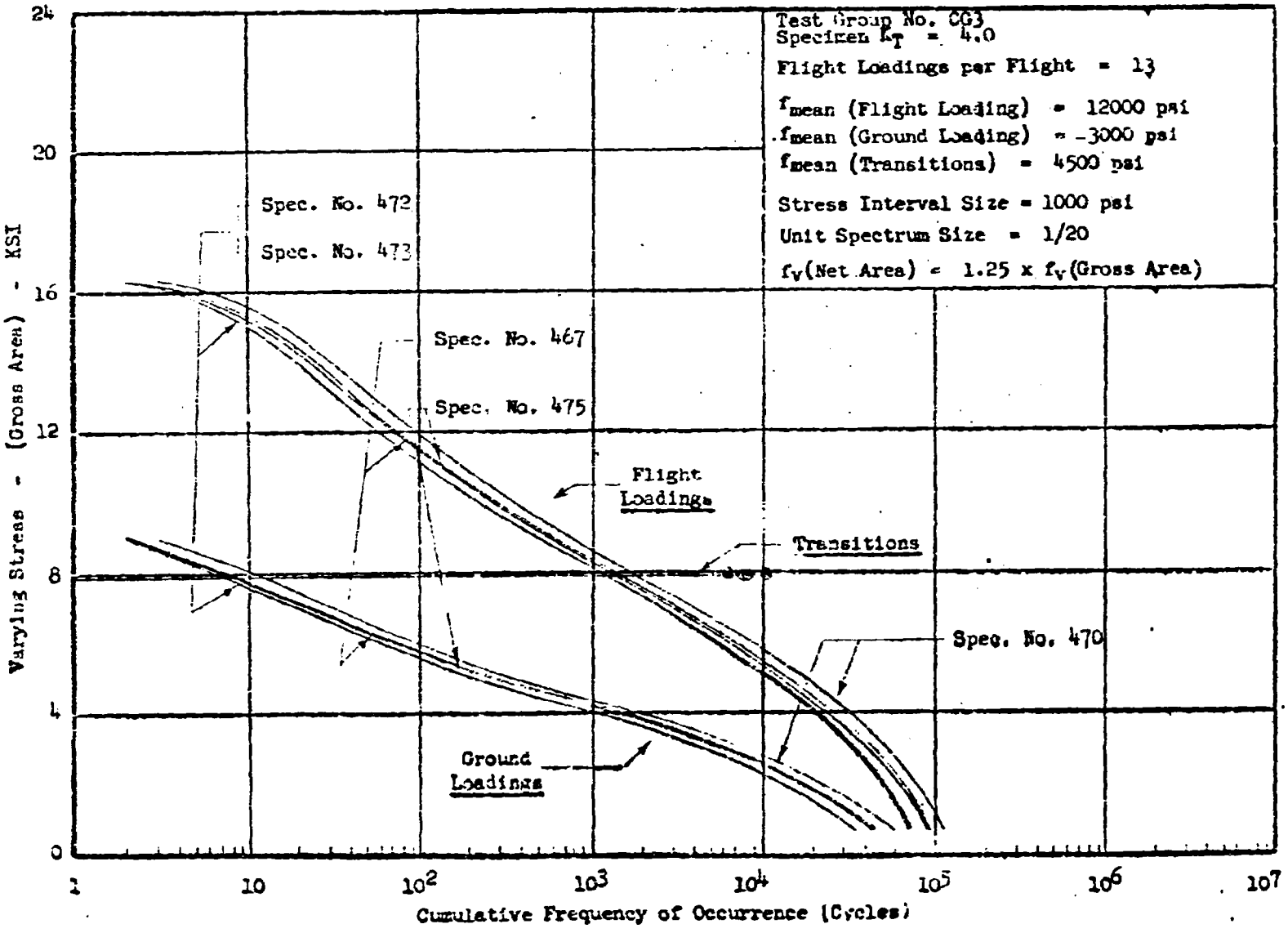



Figure 168 Ordered Composite Loading Data (High Peak Gust Loadings in Flight)

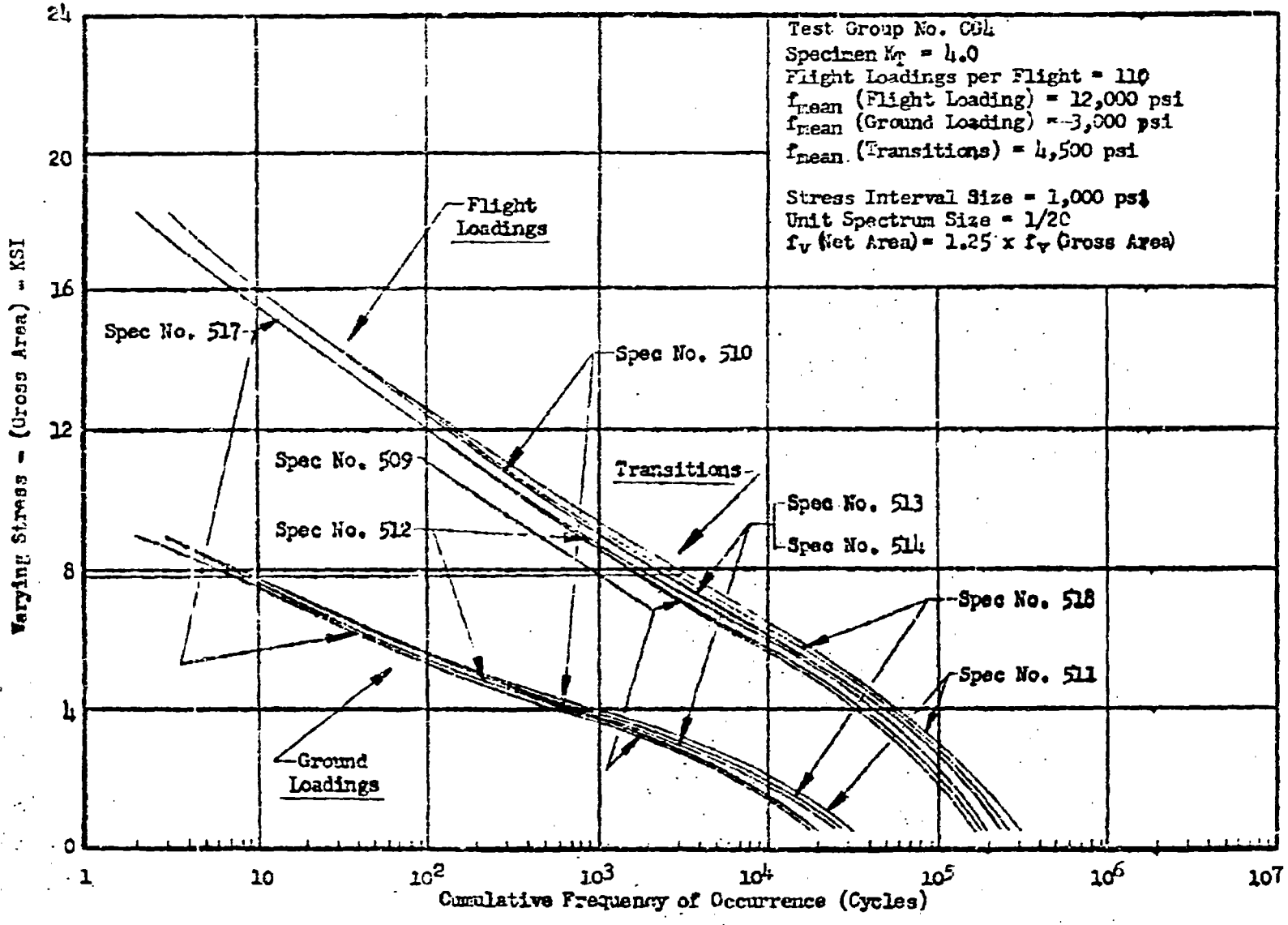



Figure 169 Ordered Composite Loading Test Data (High Peak Gust Loadings in Flight)

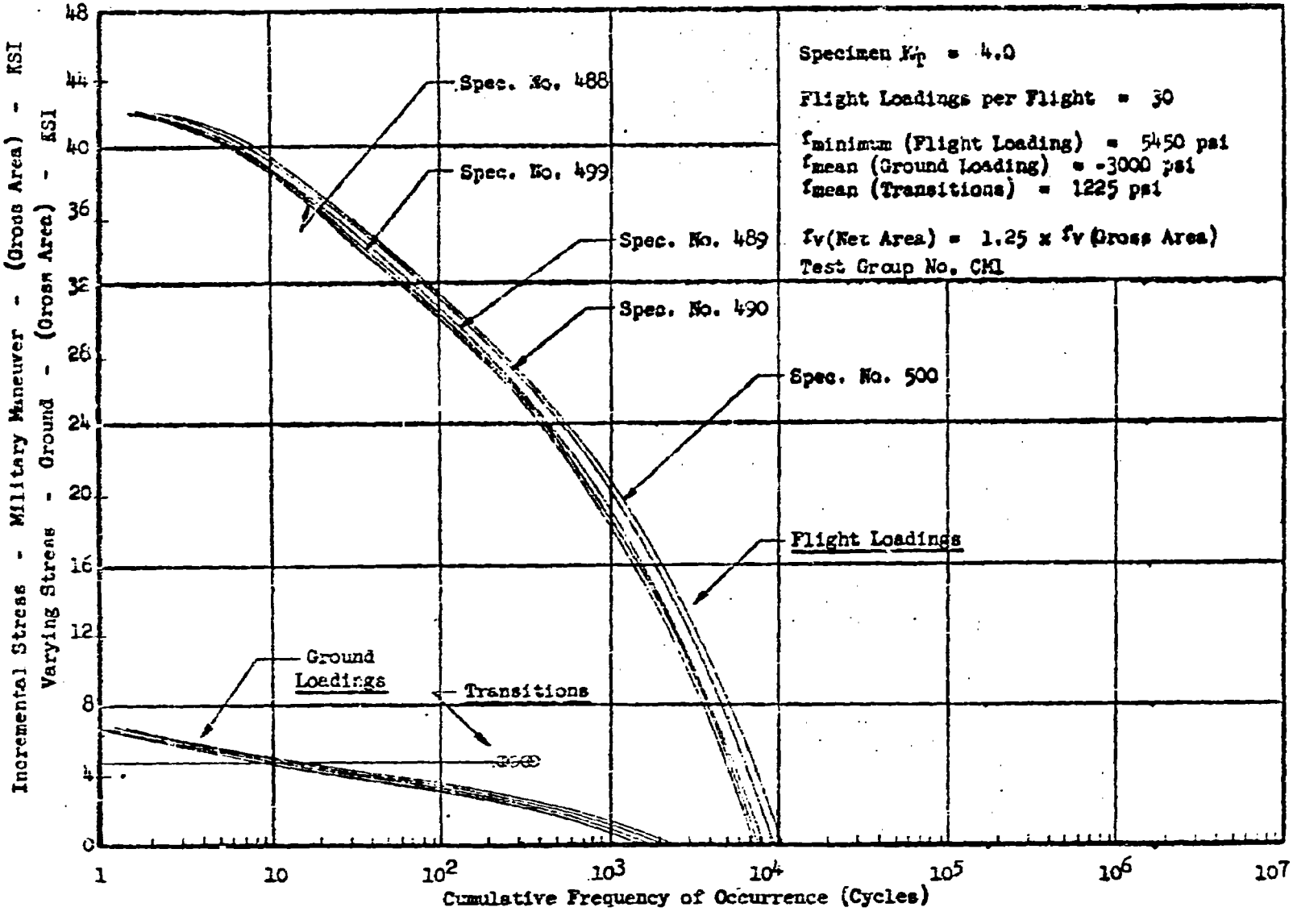



Figure 170 Random Composite Loading (Military Maneuver Flight Loadings)

## APPENDIX D

## PART 3 - FATIGUE TEST RESULTS OF A COMPLEX SPECIMEN

### Introduction

In order to compare the fatigue life results derived from simple coupon data described in other sections of this report, it was planned to fatigue test fifteen typical complex joint specimens representative of contemporary aircraft construction. The joint selected is illustrated in Figure 41. The test spectra to be applied were representative of two types of loading, gust and maneuver, and a composite set in which ground taxi loads and ground-air-ground loading cycles defined by a static mean ground to a static mean flight range were combined with gust loads in flight on one group of specimens, and with maneuver loads in flight in another group of specimens. The test equipment and specimen description, along with the experimental results in tabular, graphical, and photographic form, are presented in this appendix.

### The Specimen

The specimen is constructed of two basically identical panel sections of integrally stiffened skin typical of current wing tension surface design. The two panels are joined by a double shear butt splice arrangement, with one splice plate recessed for flush outer contour, and the other splice plate containing an integral flange for a rib support connection. The material is aluminum alloy extrusion 7075-T6 of Specification QQ-A-277. Mechanical properties determined from tensile coupons of the specimen material are listed in Table 9, which indicates satisfactory agreement with the specification requirements. The panels are assembled with 12 Hi-Lok fasteners of one quarter inch diameter as indicated in Figure 41.

### Test Set-up

Each of the panel assemblies was installed in a Lockheed-designed 500,000-pound fatigue testing machine as shown in Figure 43. To facilitate the fatigue testing, and since it was desired to have these panels tested in groups of three's, the tandem arrangement was adopted. In practice, the first of two such panels to fail was replaced by a third test panel; however, the second panel to fail was replaced simply by a dummy panel in order that the testing might be continued without disturbing the adjustment of the test machine.

Figure 44 presents a schematic diagram of the test machine which is partially shown in Figure 43. This machine, which was designed and built particularly for the ordered spectrum testing of wing surface structure, is a fairly conventional inertia-drive resonance machine utilizing inertia reaction and incorporating a spring-coupled hydraulic static loading system. It is normally operated subresonance with amplification factors of less than 50. Dynamic load control when running is provided by test frequency adjustment, and the driving eccentric weight is manually adjustable over a range of more than 20 to 1 to provide additional set-up control.

For the subject test program an auxiliary, more sensitive, load-measuring transducer was bolted to the face of the permanently installed 500,000-pound transducer in series with the two test panels (Figure 43). This load transducer consisted mainly of an I-section upon which were mounted 16 electrical strain gages arranged to measure axial loads up to plus or minus 100,000 pounds independent of moments in either transverse plane and independent of shear eccentricity.

Test Procedure

In the spectrum testing of the panels, relatively high-amplitude, low-cycle loadings were applied by means of a hydraulic jack, part of the hydraulic static loading system previously mentioned, at frequencies ranging from 1 to 200 cycles per minute. Control of these hydraulic loadings was maintained through a Weston 4-way solenoid valve which in turn was actuated by a special cyclic control device incorporating a Schmitt Trigger. This load control device consisted principally of a two-level voltage sensor, each level of which could be adjusted independently of the other level to "trigger" the solenoid valve whenever a paticular voltage, generated by the previously calibrated load measuring transducer, was amplified and fed into it. And, since the principle function of any electrical strain gage type of transducer is to generate a voltage proportional to the load which is being applied to it, it was simply a case of manually selecting the upper and lower load levels and then allowing the hydraulic jack to cycle back and forth between these points.

Lower amplitude, hi-cycle loadings (dynamic) were applied at approximately 1,200 cycles per minute by means of the rotating eccentric weight shown in Figure 44. These loads were manually selected by means of a hand-operated vari-drive coupled to the eccentric shaft. Loads were visually controlled through a calibrated dynamic strain indicator which, as in the case of the cyclic load control device previously described, was used to determine indirectly the actual load being felt by the load transducer. Calibration of this strain indicator was made at the beginning of each work day using a calibration box which has previously been calibrated against known loads applied directly to the transducer in a Baldwin-Southwark universal test machine at the Lockheed Physical Test Laboratory.

For both types of loadings, hydraulic and dynamic, loads were selected that would give the required stress levels shown in Figures 179 through 184 at the minimum cross section of the panel assemblies. This minimum cross section was always near the center section of one of the two panel sections comprising the panel assembly.

As an additional check on the accuracy of the applied loadings, stresses at minimum cross section of the panels were measured independently (both statically and dynamically) through pairs of strain gages installed on the stringers and on the skin at these areas. These strain surveys showed the stresses at the minimum areas to be within plus or minus 2% of the required axial stresses as determined by measured loads at the transducer.

Test Results

Panel No. 1 was loaded statically in the aforementioned fatigue machine and after 350 applications of the basic air loading spectrum had failed to

produce any evidence of fatigue cracking (Table 98). Careful inspection of this panel, prior to the static test, was made after the panel had been disassembled. The panel was then reassembled, using new Hi-Lok fasteners after it was determined that the only visible fatigue "damage" consisted of minor fretting at the faying surfaces within the joint area (Figure 171).

The static tension load was applied at a steady rate of 500 pounds per second until failure. Failure occurred at 66,000 pounds (giving an ultimate tensile stress of 80,950 psi across the minimum cross section of the smaller of the two panel sections) and consisted of the fracture of both the tee and of one of the panel sections at the joint (Figure 171).

The remaining 14 panels were spectrum tested to failure - Panels 2 through 6 to a spectrum of air loads representing amplifications of the basic spectrum used in the spectrum test of Panel No. 1 (Figure 179 through 181); Panels 7 through 9 to a single maneuver loading spectrum (Figure 182); Panels 10 and 13 to a composite spectrum representing gust, ground-to-air, and ground loadings (Figure 183) and Panels 14 and 15 to a composite spectrum of ground, ground-to-air, and maneuver loadings (Figure 184).

With the exception of Panels 7 through 9, all spectrum loadings were applied one block at a time, with the smallest loads being applied first.

In the case of Panel No. 7, the first 230 blocks were applied one at a time; however, the last seventy were applied ten blocks at a time.

For Panels 8 and 9, the blocks were applied ten at a time from the beginning of the testing, and, in addition, the lowest load level was omitted from the spectrum.

For Panel No. 9, the next two lowest load levels were dropped at the end of 500 blocks.

Panels 11 and 12 are not reported since both panels failed in compression because of a failure in the hydraulic loading system of the fatigue testing machine.

The mechanical properties of the joint material are given in Table 97. Spectral test results for minimum gross area stresses are presented in Tables 99 to 104 and Figures 179 to 184. The stress conversion factors in Table 105 were used to convert the panel stresses for minimum gross area into stresses for gross area at point of fracture in Tables 106 to 108.

The results of these spectral fatigue tests are analysed on the basis of stresses for both minimum gross area and gross area at point of fracture, and compared in Section V of the main body of this report.

## TABLE 97

### MECHANICAL PROPERTIES OF JOINT MATERIAL

| Coupon | Ultimate (KSI) | Yield (KSI) | % Elong.* | Red. Area % |
|---|---|---|---|---|
| A. Integrally Stiffened Panel Coupons Longitudinal Grain | | | | |
| E-1 | 87.6 | 79.4 | 9 | 16 |
| E-2 | 92.3 | 84.2 | 9 | 16 |
| E-3 | 93.0 | 84.9 | 9 | 14 |
| E-4 | 90.1 | 81.4 | 10 | 15 |
| E-5 | 88.6 | 80.2 | 10 | 15 |
| E-6 | 90.5 | 82.6 | 9 | 16 |
| Aver. | 90.4 | 82.1 | 9.3 | |
| Spec. QQ-A-277 | 80 | 72 | 7 | |
| B. Splice Plate Coupons Transverse Grain | | | | |
| S-1 | 74.7 | 63.1 | 12 | |
| S-2 | 71.5 | 59.6 | 12 | |
| S-3 | 73.2 | 61.6 | 12 | |
| S-4 | 74.5 | 62.9 | 10 | |
| S-5 | 72.4 | 61.0 | 11 | |
| S-6 | 73.8 | 62.0 | 12 | |
| S-7 | 72.2 | 60.7 | 12 | |
| S-8 | 75.6 | 64.3 | 11 | |
| Aver. | 73.5 | 61.9 | 11.5 | |
| Spec. QQ-A-287 | 73 | 63 | | |
| C. Splice Tee-Section Coupons Transverse Grain | | | ** | |
| T-1 | 74.1 | 73.3 | F.O.G.L. | |
| T-2 | 74.6 | 73.8 | F.O.G.L. | |
| T-3 | 83.2 | 73.4 | 14 | |
| T-4 | 76.3 | 72.9 | F.O.G.L. | |
| T-5 | 84.0 | 73.8 | 12 | |
| T-6 | 83.7 | 75.6 | 14 | |
| T-7 | 83.1 | 72.7 | 14 | |
| T-8 | 83.7 | 73.7 | F.O.G.L. | |
| Aver. | 80.3 | 73.7 | 13.5 | |
| Spec. QQ-A-277 | 75 | 65 | | |

* 1" Gage Length
** 0.5" Gage Length
F.O.G.L. - Failed Outside Gage Length

TABLE 98

SUMMARY OF PANEL TEST RESULTS
(Continued on next page)

| Panel No. | Min. Area ($in^2$) | Loading Geometry (1) | | No. of Applied Loading Blocks | Description of Panel Failures | | Test Results |
|---|---|---|---|---|---|---|---|
| | | Spectrum Description | Spectrum Step Size | | Mode & Location | Ref. Photos (2) | |
| 1 | .8153 | Air Loading $f_{mean}$ = 12,000 psi | $f_{vary}$ = 1,000 psi | 350 | No fatigue failure. Panel pulled statically. Failure occurred both in the tee & in one of the panel sections at the joint. | Fig. 171 | Fig. 179 |
| 2 | .8137 | Air Loading $f_{mean}$ = 23,400 psi | $f_{vary}$ = 1,965 psi | 52 | No failure. | Figs. 173 & 174 | Fig. 180 |
| | | Air Loading $f_{mean}$ = 30,600 psi | $f_{vary}$ = 2,560 psi | 3<br>Total: 55 | Multiple fatigue failures in the tee between fillet radius and line of hi-lok holes at edge of collars. | | |
| 3 | .8151 | Air Loading $f_{mean}$ = 23,400 psi | $f_{vary}$ = 1,960 psi | 52 | No failure. | Figs. 175 & 176 | Fig. 180 |
| | | Air Loading $f_{mean}$ = 30,600 psi | $f_{vary}$ = 2,560 psi | 9 | 1/4 inch fatigue crack at edge of single hi-lok hole in the tee. | | |
| | | | | 2<br>Total: 63 | Catastrophic failure at intersection of stringer run-out and fillet. | | |

(1) All stresses are those experienced at the minimum cross section of the panel assembly (Fig.41, Sec. B-B).

(2) Photographs, shown in Figs.171 thru 176, were selected as representative of the various types of fatigue failures incurred.

TABLE 98

SUMMARY OF PANEL TEST RESULTS
(Continued on next page)

| Panel No. | Min. Area ($in^2$) | Loading Geometry (1) | | No. of Applied Loading Blocks | Description of Panel Failures | | Test Results |
|---|---|---|---|---|---|---|---|
| | | Spectrum Description | Spectrum Step Size | | Mode & Location | Ref. Photos (2) | |
| 4 | .8162 | Air Loading $f_{mean}$ = 27,000 psi | $f_{vary}$ = 2,240 psi | 56-1/2 | Single failure at intersection of stringer run-out and fillet radius, catastrophic. | Figs. 175 & 176 | Fig.181 |
| 5 | .8204 | Air Loading $f_{mean}$ = 27,000 psi | $f_{vary}$ = 2,240 psi | 48-1/2 | Single fatigue failure (1/2 inch crack) in tee between fillet & line of hi-lok holes at edge of a collar. | Figs. 173 & 174 | Fig.181 |
| 6 | .8332 | Air Loading $f_{mean}$ = 27,000 psi | $f_{vary}$ = 2,240 psi | 58 | Same as Panel No. 9 | Fig. 172 | Fig.181 |
| 7 | .8197 | Maneuver Loading $f_{min}$ = 7,600 psi | $\Delta f_{max}$ = 5,650 psi | 300 | Same as Panel No. 9 | Fig. 172 | Fig.182 |
| 8 | .8462 | Maneuver Loading $f_{min}$ = 7,600 psi | $\Delta f_{max}$ = 5,650 psi | 460 | Multiple fatigue failures in tee at edge of hi-lok holes. | Figs. 177 & 178 | Fig.182 |
| 9 | .8373 | Maneuver Loading $f_{min}$ = 7,600 psi | $\Delta f_{max}$ = 5,650 psi | 600 | Multiple hidden fatigue failures in a panel section at the hi-lok holes, panel failed catastrophically. | Fig. 172 | Fig.182 |

(1) All stresses are those experienced at the minimum cross section of the panel assembly (Fig. 11, Sec. B-B).

(2) Photographs, shown in Figs. 171 thru 178, were selected as representative of the various types of fatigue failures incurred.

TABLE 96

SUMMARY OF PANEL TEST RESULTS

| Panel No. (3) | Min. Area ($in^2$) | Loading Geometry (1) | | No. of Applied Loading Blocks | Description of Panel Failures | | Test Results |
|---|---|---|---|---|---|---|---|
| | | Spectrum Description | Spectrum Step Size | | Mode & Location | Ref. Photos (2) | |
| 10 | .8369 | Air Loading<br>$f_{mean}$ = 27,000 psi<br>G.T.A. Loading<br>$f_{mean}$ = 10,000 psi<br>Ground Loading<br>$f_{mean}$ = -6,700 psi | $f_{vary}$ = 2,240 psi<br>$f_{vary}$ = 16,560 psi<br>$f_{vary}$ = 2,220 psi | 9-1/2 | Same as Panel No. 9 | Fig.172 | Fig. 183 |
| 13 | .8326 | Air Loading<br>$f_{mean}$ = 27,000 psi<br>G.T.A. Loading<br>$f_{mean}$ = 10,000 psi<br>Ground Loading<br>$f_{mean}$ = -6,700 psi | $f_{vary}$ = 2,240 psi<br>$f_{vary}$ = 16,560 psi<br>$f_{vary}$ = 2,220 psi | 10 | Same as Panel No. 4 | Figs.175 & 176 | Fig. 183 |
| 14 | .8340 | Ground Loading<br>$f_{mean}$ = -6,700 psi<br>G.T.A. Loading<br>$f_{mean}$ = 450 psi<br>Maneuver Loading<br>$f_{min}$ = 7,600 psi | $f_{vary}$ = 2,220 psi<br>$f_{vary}$ = 7,160 psi<br>$\Delta f_{max}$ = 5,650 psi | 5 | Catastrophic failure starting at an outside hi-lok hole in the tee. | Figs.177 & 178 | Fig. 184 |
| 15 | .8178 | Ground Loading<br>$f_{mean}$ = -6,700 psi<br>G.T.A. Loading<br>$f_{mean}$ = 450 psi<br>Maneuver Loading<br>$f_{min}$ = 7,600 psi | $f_{vary}$ = 2,220 psi<br>$f_{vary}$ = 7,160 psi<br>$\Delta f_{max}$ = 5,650 psi | 9 | Same as Panel No. 9 except that both panel sections failed. | Fig. 172 | Fig. 184 |

(1) All stresses are those experienced at the minimum cross section of the panel (Figure 41, Section B-B)
(2) Photographs selected are representative of the various types of fatigue failures incurred.
(3) Panels 11 & 12 were accidentally overloaded and were failed in compression.

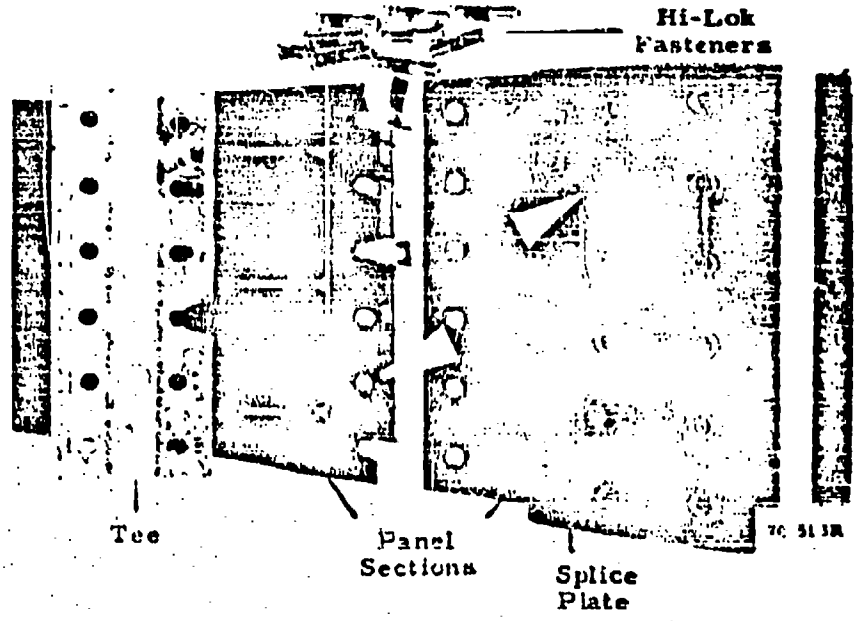



Figure 171 Panel Assembly No. 1, Pulled Statically. Fretting at the faying surfaces (arrows) was caused by previous, low-amplitude cycling.

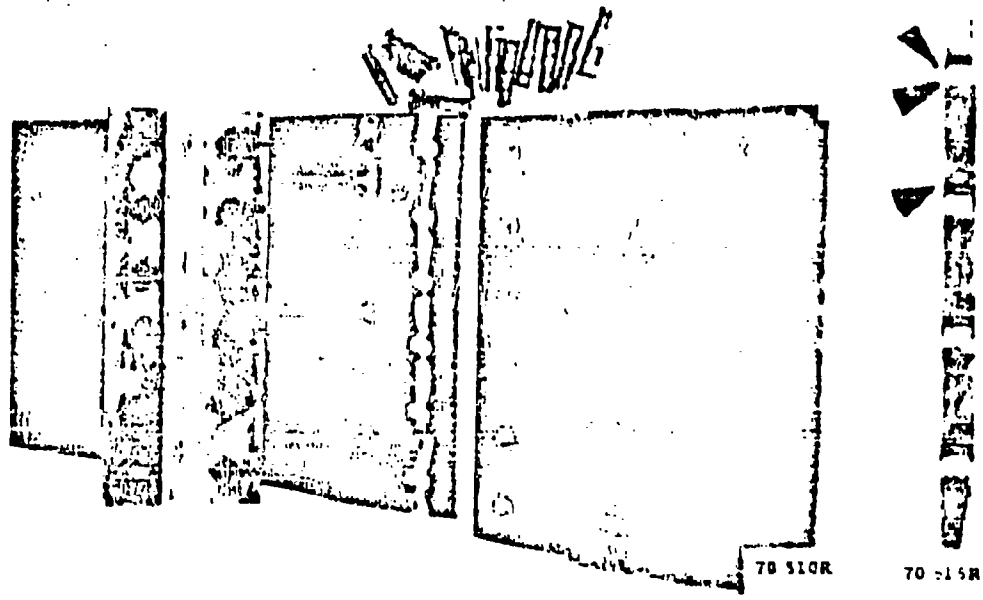
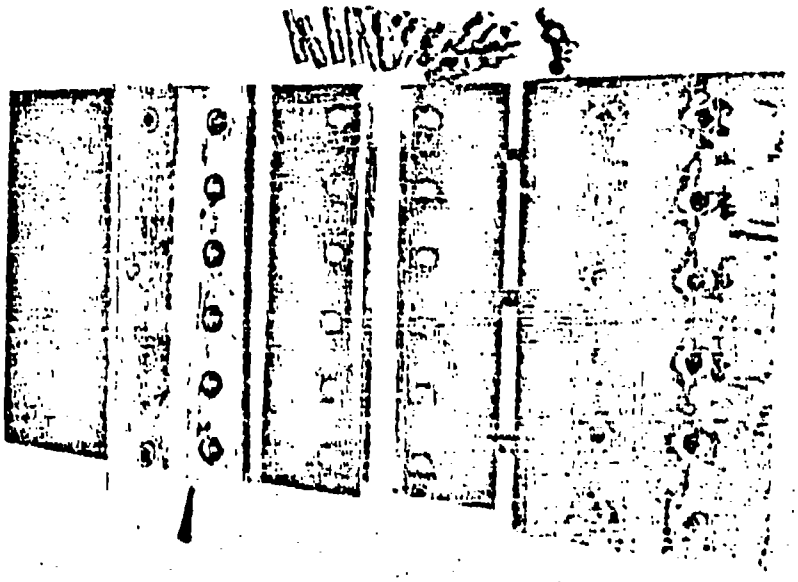
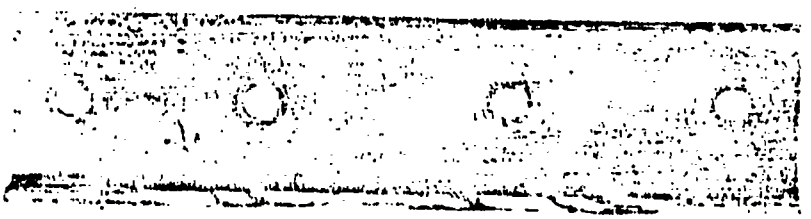


Figure 172 Panel Assembly No. 9. Fatigue failure of a panel section. Edges of all six holes showed evidence of fatigue cracking. Note beach marks (arrows) in the enlarged cross section.



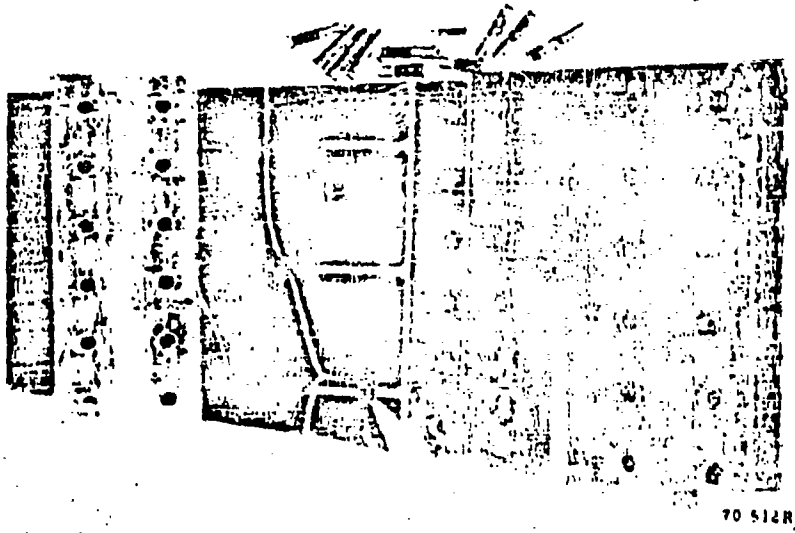
70 514

Figure 173 Panel Assembly No. 2. Fatigue failure of the tee (arrow) between lockbolt holes and the fillet radius.



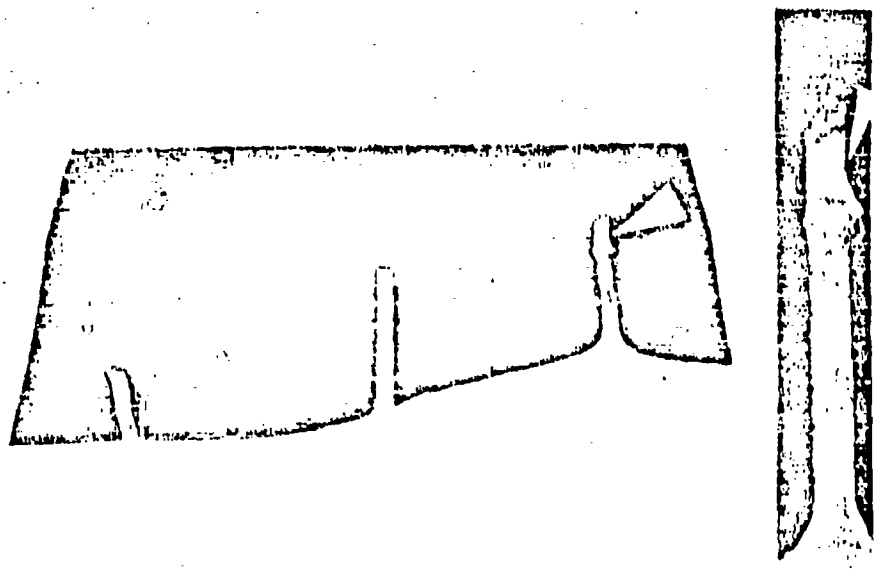
70 519R

Figure 174 Cross section of the tee shown above. Multiple fatigue failures (bright semi-circular areas) coincide with scratches on the upper surface of the tee.



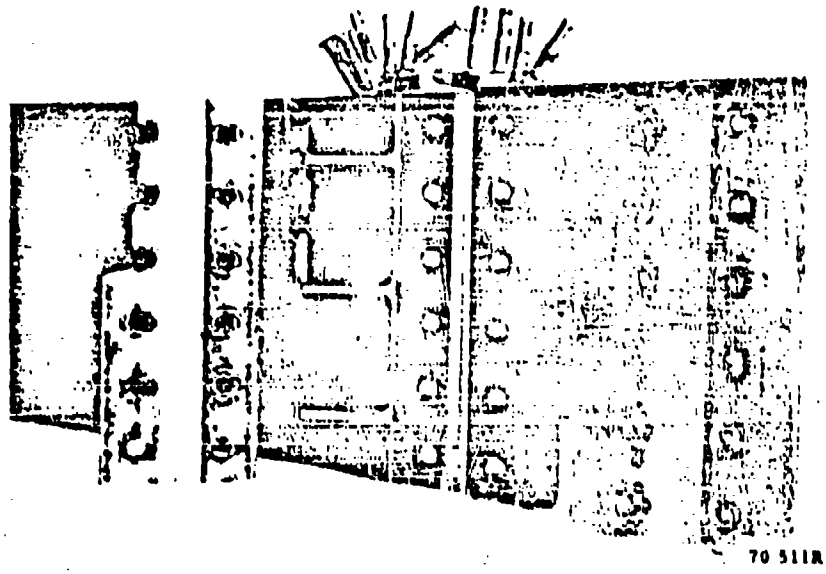
70 512R

Figure 175 Panel Assembly No. 4. Fatigue failure in a panel section near the intersection of a stringer run-out and a fillet radius.



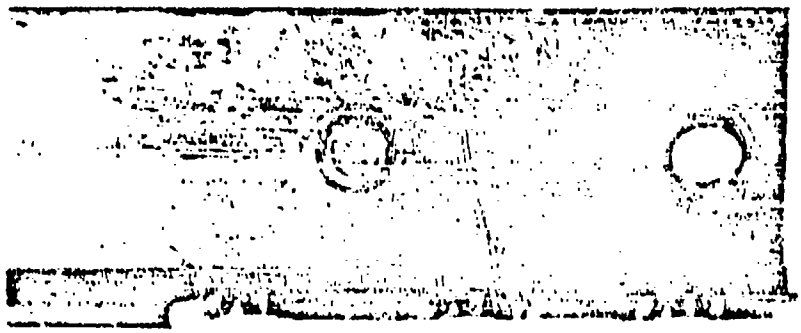
70 516R 70 516R

Figure 176 Two cross section views of the fatigue crack shown in the above photograph.



70 511R

Figure 177 Panel Assembly No. 8. Fatigue failures in the tee section. Cracks originated at the edges of the two outside lockbolt holes.



70 517R

Figure 178 Cross section of the failed tee shown in the above photograph. Note beach marks (arrows).

TABLE 99

GUST LOADING HISTORY
LO-HI LOADING SEQUENCE
PANEL NO. 1
$f_{mean}$ = 12,000 psi

| Varying Stress (psi) * | Simple Frequency (cycles) |
|---|---|
| 1 | 1,750,000 |
| 2 | 1,225,000 |
| 3 | 1,155,000 |
| 4 | 647,500 |
| 5 | 402,500 |
| 6 | 210,000 |
| 7 | 126,000 |
| 8 | 47,250 |
| 9 | 21,000 |
| 10 | 8,050 |
| 11 | 3,500 |
| 12 | 1,750 |
| 13 | 1,050 |
| 14 | 700 |
| 15 | 350 |
| 16 | 175 |
| 17 | 115 |
| 18 | 35 |
| 18.3 | 35 |

*Minimum cross sectional area.

TABLE 100

GUST LOADING HISTORY - LO-HI LOADING SEQUENCE

Test Group No. G82

| PANEL NO. 2 | | PANEL NO. 3 | |
|---|---|---|---|
| Varying Stress (psi) * | Simple Frequency Cycles | Varying Stress (psi) * | Simple Frequency Cycles |
| $f_{mean}$ = 23,448 psi | | $f_{mean}$ = 23,402 psi | |
| 1,954 | 260,000 | 1,951 | 260,000 |
| 3,908 | 182,000 | 3,901 | 182,000 |
| 5,862 | 171,600 | 5,852 | 171,600 |
| 7,816 | 96,200 | 7,803 | 96,200 |
| 9,770 | 59,800 | 9,753 | 59,800 |
| 11,724 | 31,200 | 11,704 | 31,200 |
| 13,678 | 18,720 | 13,654 | 18,720 |
| 15,632 | 7,020 | 15,605 | 7,020 |
| 17,586 | 3,120 | 17,556 | 3,120 |
| 19,540 | 1,196 | 19,506 | 1,196 |
| 21,494 | 520 | 21,458 | 520 |
| 23,448 | 260 | 23,409 | 260 |
| 25,402 | 156 | 25,358 | 156 |
| 27,357 | 104 | 27,309 | 104 |
| 29,311 | 52 | 29,260 | 52 |
| 31,265 | 27 | 31,211 | 27 |
| 33,219 | 17 | 33,162 | 17 |
| 35,173 | 6 | 35,112 | 6 |
| 35,759 | 6 | 35,697 | 6 |
| No Failure - Loads Increased | | No Failure - Loads Increased | |
| $f_{mean}$ = 30,660 psi | | $f_{mean}$ = 30,610 psi | |
| 2,555 | 15,000 | 2,550 | 45,000 |
| 5,110 | 10,500 | 5,101 | 31,500 |
| 7,666 | 9,900 | 7,653 | 29,700 |
| 10,221 | 5,550 | 10,204 | 16,650 |
| 12,776 | 3,450 | 12,755 | 10,350 |
| 15,331 | 1,800 | 15,305 | 5,400 |
| 17,887 | 1,080 | 17,857 | 3,240 |
| 20,442 | 405 | 20,407 | 1,215 |
| 22,997 | 147 | 22,957 | 540 |
| 25,552 | 46 | 25,508 | 207 |
| 28,109 | 20 | 28,061 | 90 |
| 30,662 | 10 | 30,609 | 45 |
| 33,219 | 6 | 33,162 | 27 |
| 35,774 | 4 | 35,713 | 18 |
| 38,329 | 2 | 38,264 | 9 |
| 40,885 | 2 | 40,814 | 5 |
| 43,440 | 1 | 43,365 | 3 |
| 45,995 | 0 | 45,915 | 1 |
| 46,762 | 0 | 46,681 | 1 |

*Minimum cross sectional area.

TABLE 101

GUST LOADING HISTORY
LO-HI LOADING SEQUENCE

Test Group No. G83

| PANEL NO. 4 | | PANEL NO. 5 | | PANEL NO. 6 | |
|---|---|---|---|---|---|
| Varying Stress (psi) * | Simple Frequency (Cycles) | Varying Stress (psi) * | Simple Frequency (Cycles) | Varying Stress (psi) * | Simple Frequency (Cycles) |
| $f_{mean}$ = 27,152 psi | | $f_{mean}$ = 27,033 psi | | $f_{mean}$ = 26,618 psi | |
| 2,262 | 285,000 | 2,252 | 245,000 | 2,218 | 290,000 |
| 4,525 | 199,500 | 4,505 | 171,500 | 4,436 | 203,000 |
| 6,788 | 188,100 | 6,758 | 161,700 | 6,655 | 191,400 |
| 9,051 | 105,450 | 9,011 | 90,650 | 8,873 | 107,300 |
| 11,313 | 65,550 | 11,263 | 56,350 | 11,091 | 66,700 |
| 13,576 | 34,200 | 13,516 | 29,400 | 13,310 | 34,800 |
| 15,839 | 20,520 | 15,770 | 17,280 | 15,582 | 20,880 |
| 18,102 | 7,695 | 18,022 | 6,480 | 17,746 | 7,830 |
| 20,365 | 3,420 | 20,275 | 2,880 | 19,964 | 3,480 |
| 22,627 | 1,311 | 22,527 | 1,104 | 22,182 | 1,334 |
| 24,890 | 570 | 24,780 | 480 | 24,400 | 580 |
| 27,152 | 282 | 27,032 | 240 | 26,618 | 290 |
| 29,415 | 168 | 29,285 | 144 | 28,836 | 174 |
| 31,677 | 112 | 31,537 | 96 | 31,054 | 116 |
| 33,941 | 56 | 33,791 | 48 | 33,273 | 58 |
| 36,203 | 29 | 36,044 | 24 | 35,491 | 29 |
| 38,466 | 18 | 38,296 | 15 | 37,710 | 18 |
| 40,728 | 6 | 40,549 | 5 | 39,927 | 6 |
| 41,408 | 6 | 41,225 | 5 | 40,593 | 6 |

*Minimum cross sectional area.

TABLE 102

FIGHTER MANEUVER LOADING HISTORIES
LO-HI LOADING SEQUENCE
Test Group No. M17

| PANEL NO. 7 | | PANEL NO. 8 | | PANEL NO. 9 | |
|---|---|---|---|---|---|
| Maximum Stress (psi) * | Simple Frequency (Cycles) | Maximum Stress (psi) * | Simple Frequency (Cycles) | Maximum Stress (psi) * | Simple Frequency (Cycles) |
| Minimum Stress = 7,865 psi | | Minimum Stress = 7,601 psi | | Minimum Stress = 7,680 psi | |
| 13,606 | 80,500 | 13,181 | 80,500 | 13,320 | 80,500 |
| 19,363 | 70,500 | 18,759 | 110,450 | 18,957 | 117,500 |
| 25,123 | 52,500 | 24,338 | 82,250 | 24,595 | 87,500 |
| 30,882 | 37,500 | 29,917 | 58,750 | 30,234 | 75,000 |
| 36,641 | 25,500 | 35,497 | 39,950 | 35,872 | 51,000 |
| 42,399 | 16,800 | 41,075 | 26,320 | 41,509 | 33,600 |
| 46,158 | 8,700 | 46,654 | 13,630 | 47,147 | 17,400 |
| 53,917 | 3,900 | 52,233 | 6,110 | 52,786 | 7,800 |
| 59,675 | 1,450 | 57,811 | 2,350 | 58,423 | 2,972 |
| 65,434 | 508 | 63,391 | 810 | 64,061 | 1,033 |
| 68,314 | 90 | 66,181 | 144 | 66,851 | 164 |

*Minimum cross sectional area.

TABLE 103

COMPOSITE LOADING HISTORIES
GUST LOADINGS IN FLIGHT - LO-HI LOADING SEQUENCE

Test Group No. C05

| PANEL NO. 10 | | PANEL NO. 13 | |
|---|---|---|---|
| Varying Stress (psi) * | Simple Frequency (Cycles) | Varying Stress (psi) * | Simple Frequency (Cycles) |
| **Gust Loadings** | | | |
| $f_{mean}$ = 26,500 psi | | $f_{mean}$ = 26,800 psi | |
| 2,208 | 123,750 | 2,220 | 165,000 |
| 4,416 | 86,535 | 4,439 | 115,380 |
| 6,626 | 80,190 | 6,660 | 106,920 |
| 8,834 | 44,955 | 8,880 | 59,940 |
| 11,042 | 28,905 | 11,099 | 37,260 |
| 13,250 | 16,200 | 13,319 | 19,440 |
| 15,459 | 9,700 | 15,540 | 11,664 |
| 17,667 | 3,650 | 17,759 | 5,103 |
| 19,876 | 1,620 | 19,979 | 1,620 |
| 22,084 | 621 | 22,199 | 621 |
| 24,292 | 270 | 24,418 | 270 |
| 26,500 | 135 | 26,638 | 135 |
| 28,708 | 81 | 28,858 | 81 |
| 30,916 | 54 | 31,077 | 54 |
| 33,126 | 29 | 33,298 | 27 |
| 35,334 | 14 | 35,518 | 14 |
| 37,542 | 8 | 37,737 | 8 |
| 39,750 | 3 | 39,957 | 3 |
| 40,413 | 3 | 40,624 | 2 |
| **Ground Loadings** | | | |
| $f_{mean}$ = -6,630 psi | | $f_{mean}$ = -6,660 psi | |
| 2,208 | 110,250 | 2,220 | 110,250 |
| 4,416 | 61,200 | 4,439 | 61,200 |
| 6,626 | 25,200 | 6,660 | 25,200 |
| 8,834 | 10,080 | 8,880 | 10,080 |
| 11,042 | 2,150 | 11,099 | 2,150 |
| 13,250 | 450 | 13,319 | 450 |
| 15,459 | 120 | 15,540 | 120 |
| 17,667 | 54 | 17,759 | 54 |
| 19,876 | 29 | 19,979 | 28 |
| 22,084 | 6 | 22,199 | 6 |
| 24,292 | 1 | 24,418 | 1 |
| 24,591 | 1 | 24,748 | 1 |
| **Ground to Air Cycles** | | | |
| $f_{mean}$ = 9,980 psi | | $f_{mean}$ = 10,000 psi | |
| 16,561 | 32,500 | 16,617 | 32,500 |

*Minimum cross sectional area.

TABLE 104

COMPOSITE LOADING HISTORIES
FIGHTER MANEUVER LOADINGS IN FLIGHT
LO-HI LOADING SEQUENCE
Test Group No. CM2

| PANEL NO. 14 | | PANEL NO. 15 | |
|---|---|---|---|
| Dynamic Stress (psi) * | Simple Frequency (Cycles) | Dynamic Stress (psi) * | Simple Frequency (Cycles) |
| Maximum Stress | | | |
| Maneuver Loadings | | | |
| Minimum Stress = 7,725 psi | | Minimum Stress = 7,875 psi | |
| 13,372 | 24,500 | 13,629 | 44,100 |
| 19,032 | 20,750 | 19,397 | 37,350 |
| 24,692 | 18,500 | 25,166 | 33,300 |
| 30,353 | 15,250 | 30,935 | 27,450 |
| 36,013 | 9,250 | 36,704 | 16,650 |
| 41,672 | 5,750 | 42,471 | 10,350 |
| 47,333 | 2,500 | 48,241 | 4,500 |
| 52,993 | 2,000 | 54,010 | 3,600 |
| 58,653 | 661 | 59,778 | 1,485 |
| 64,313 | 112 | 65,547 | 228 |
| 67,144 | 28 | 68,432 | 56 |
| Varying Stress | | | |
| Ground Loadings | | | |
| $f_{mean}$ = -6,650 psi | | $f_{mean}$ = -6,780 psi | |
| 2,216 | 61,250 | 2,258 | 110,250 |
| 4,432 | 34,000 | 4,517 | 61,200 |
| 6,648 | 14,000 | 6,776 | 25,200 |
| 8,864 | 5,600 | 9,034 | 10,080 |
| 11,080 | 1,075 | 11,293 | 1,935 |
| 13,296 | 225 | 13,551 | 405 |
| 15,513 | 60 | 15,810 | 108 |
| 17,728 | 27 | 18,068 | 49 |
| 19,944 | 14 | 20,327 | 26 |
| 22,160 | 3 | 22,585 | 5 |
| 24,376 | 1 | 24,843 | 1 |
| 24,750 | 0 | 25,179 | 1 |
| Ground to Air Cycles | | | |
| $f_{mean}$ = 442 psi | | $f_{mean}$ = 450 psi | |
| 7,280 | 3,325 | 7,360 | 5,980 |

*Minimum cross sectional area.

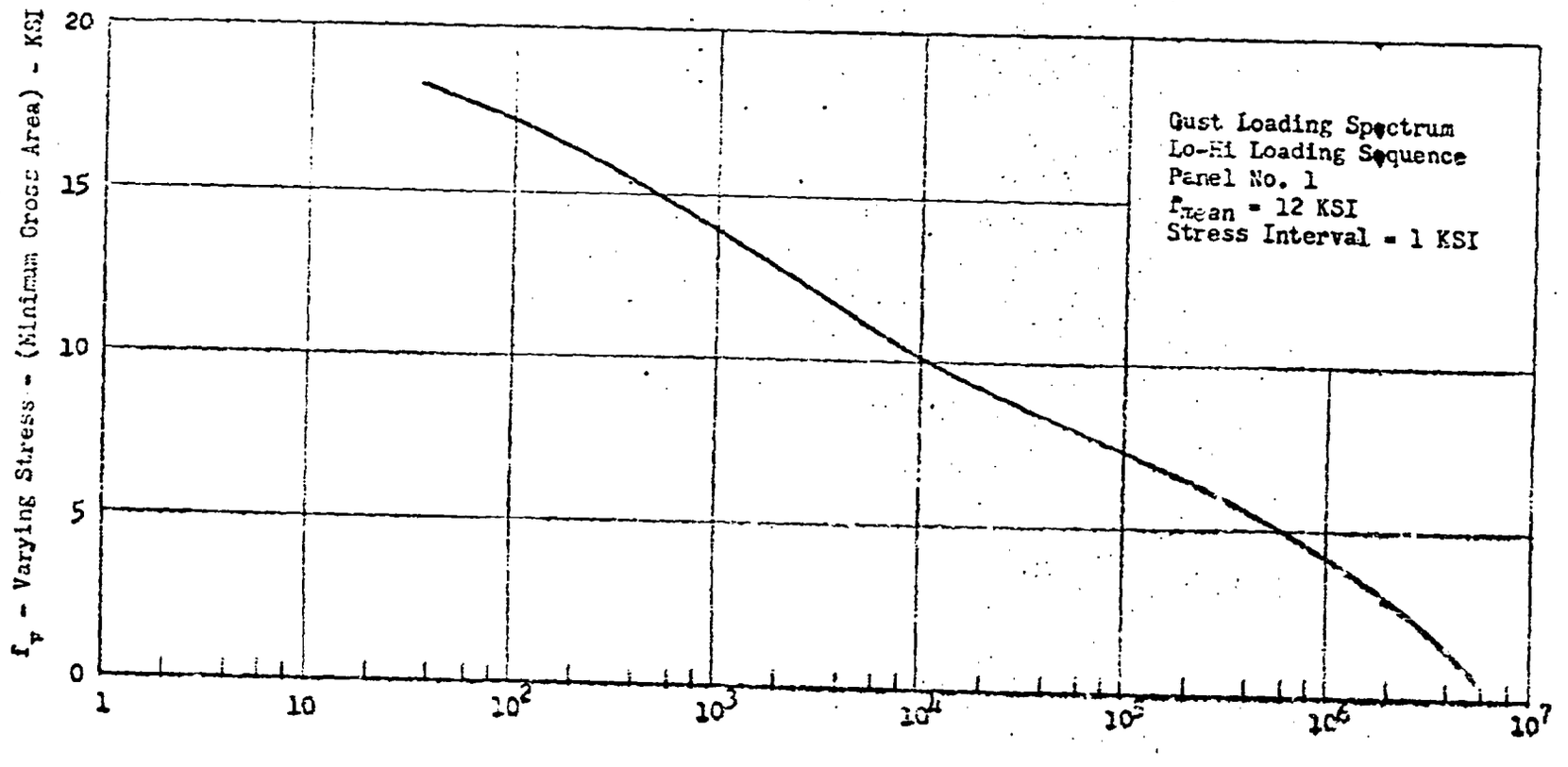



Figure 179. Ordered Test Load History

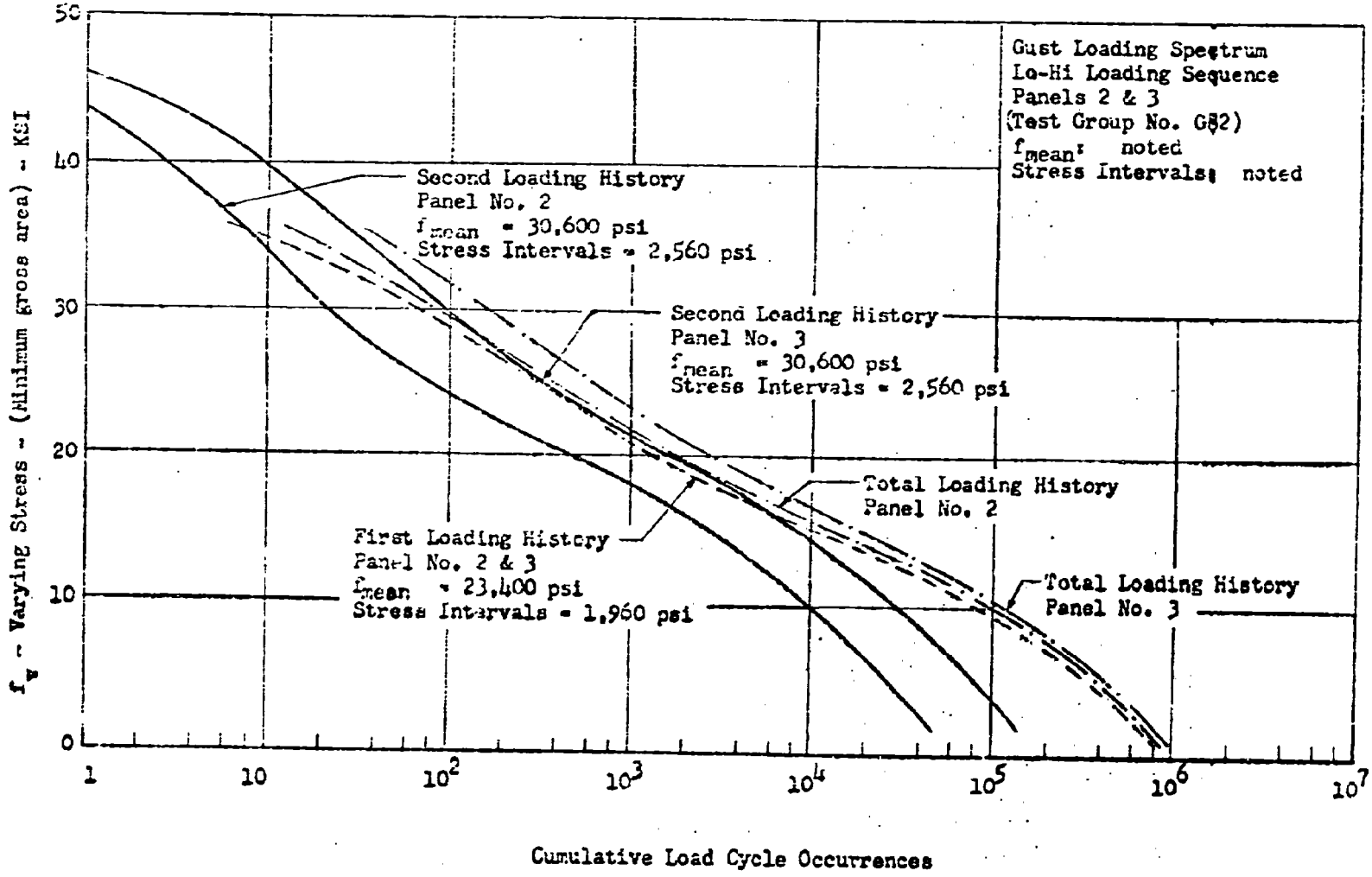



Figure 180. Ordered Test Loading History

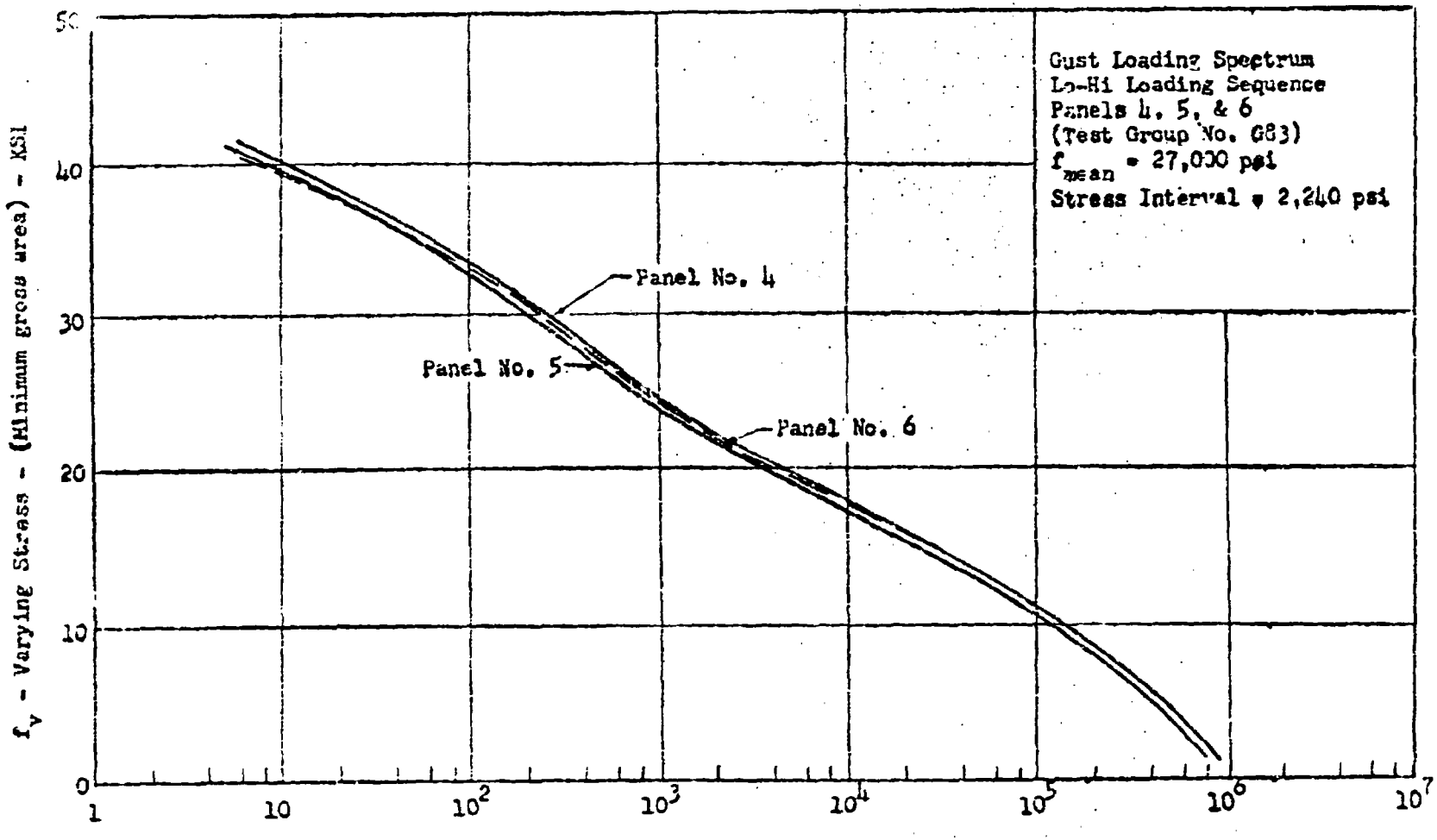





Figure 181. Ordered Test Loading History

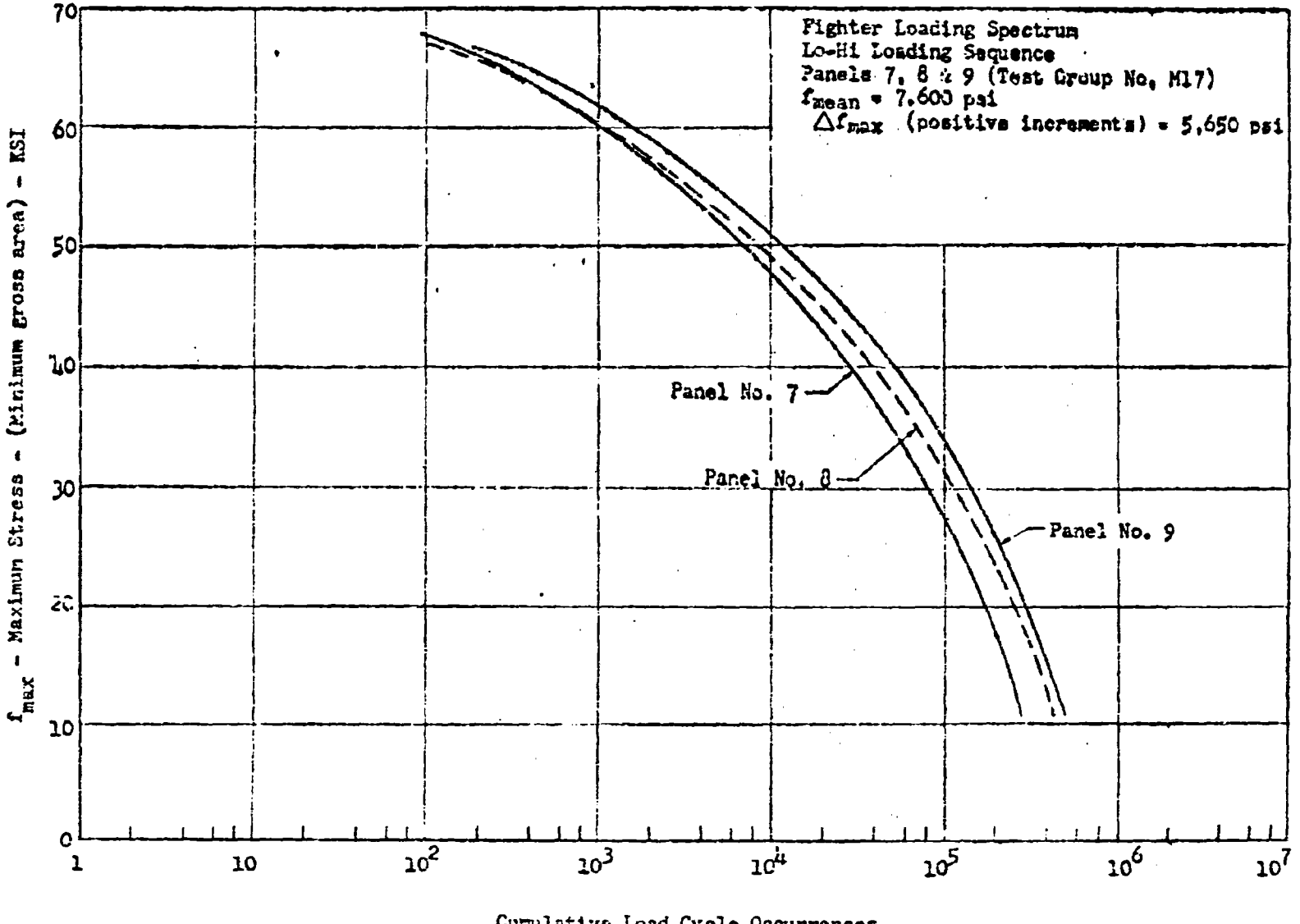



Figure 122. Ordered Test Loading History

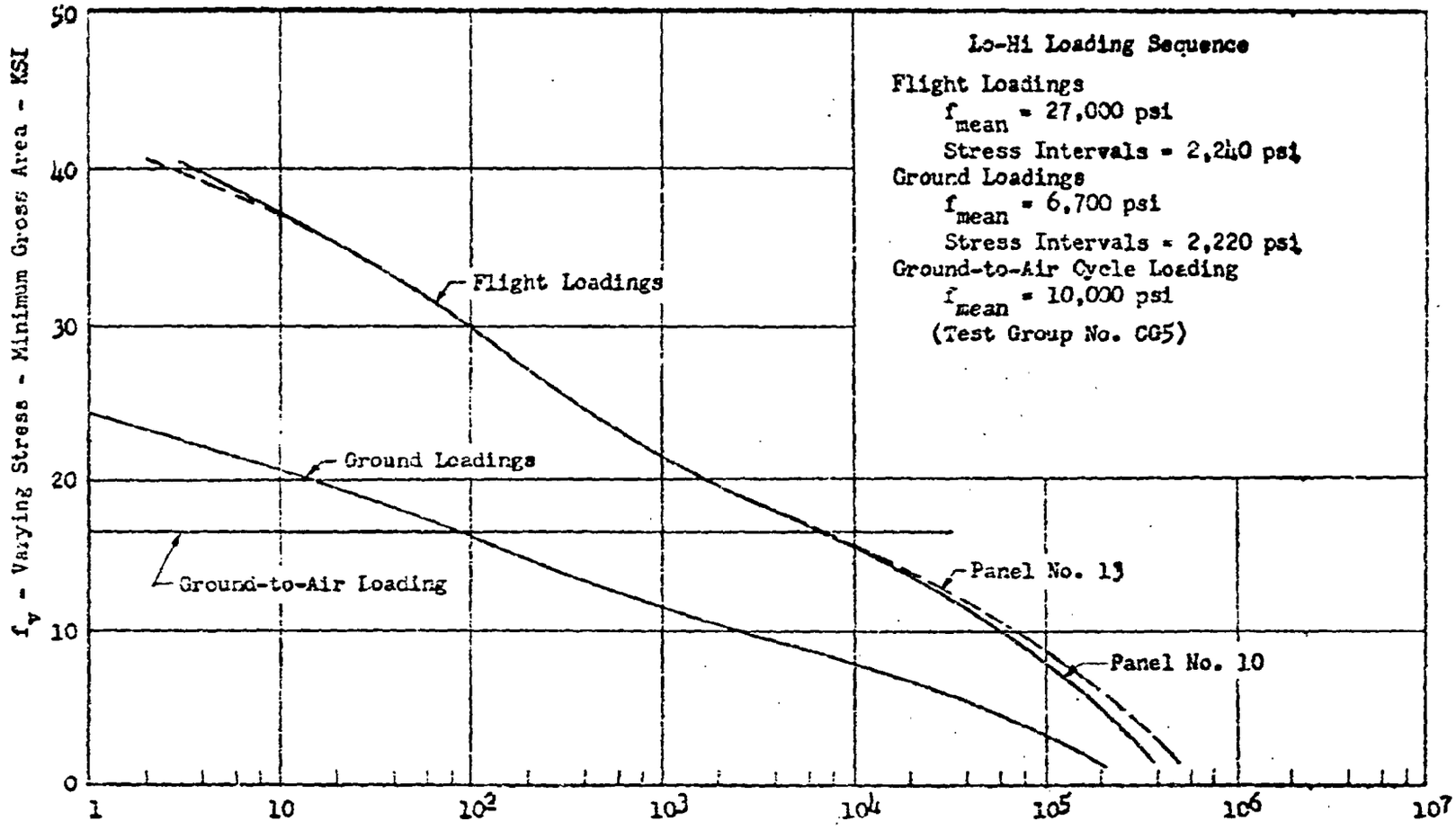



Figure 183. Ordered Composite Gust Loading Test Histories

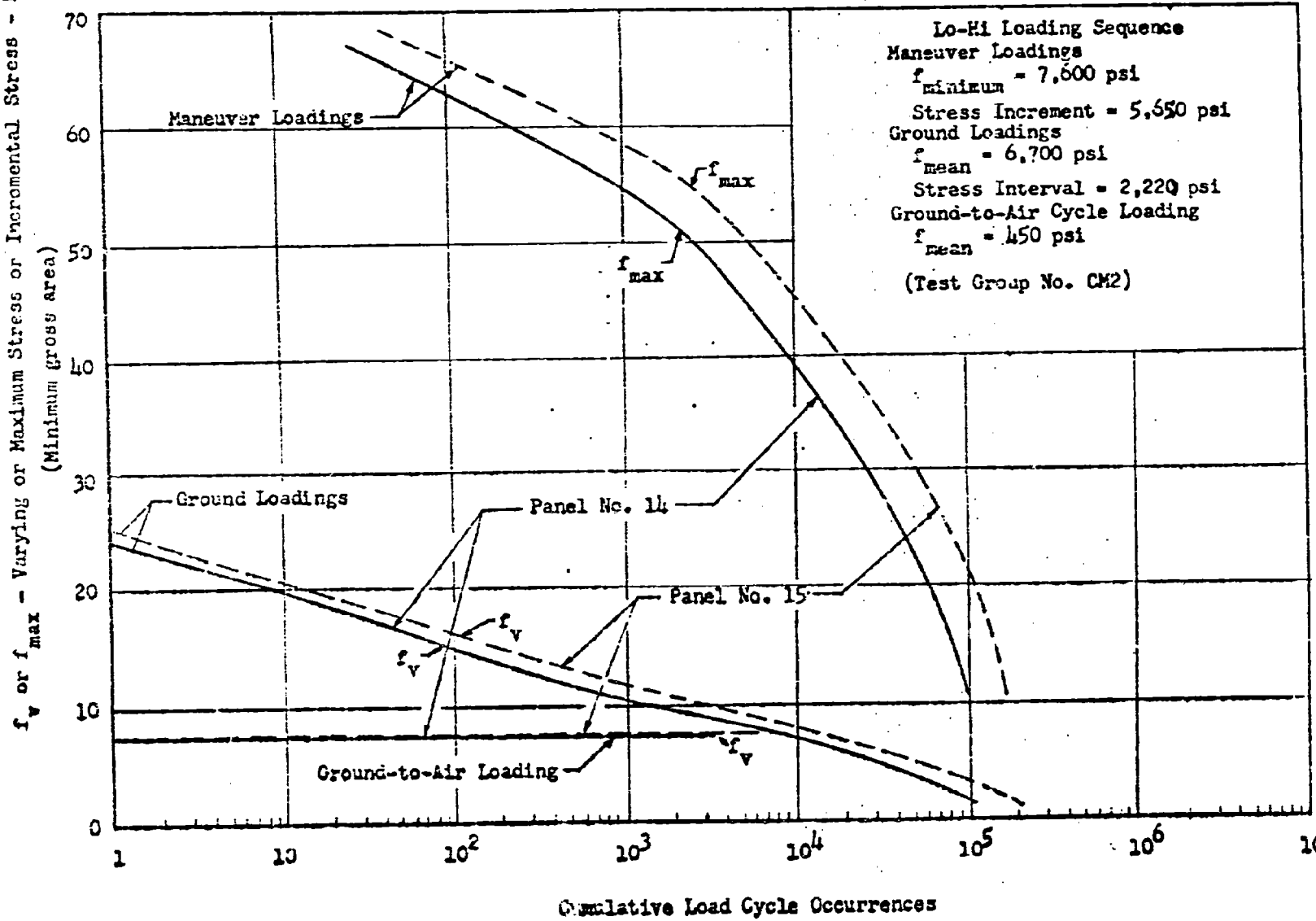



Figure 184. Ordered Composite Maneuver Loading Test Histories

TABLE 105

FACTORS USED TO CONVERT PANEL STRESSES FOR MINIMUM GROSS AREA INTO STRESSES FOR GROSS AREA AT POINT OF FRACTURE

| Panel No. | Minimum Gross Area ($in.^2$) | Point of Fracture | Area of Tee ($in.^2$) | Area of Splice Plate ($in.^2$) | Fractured Gross Area ($in.^2$) | Stress Conversion Factors (1) |
|---|---|---|---|---|---|---|
| 2 | .8137 | Tee | .7892 | 1.232 | .2021(2) | .403 |
| 3 | .8151 | Tee | .7864 | 1.236 | 2.022(2) | .403 |
| | | Stringer Run-out | | | 1.742(3) | .468 |
| 4 | .8168 | Stringer Run-out | | | 1.543(3) | .529 |
| 5 | .8204 | Tee | .7869 | 1.226 | 2.013(2) | .406 |
| 6 | .8332 | Panel at Joint | | | 1.649 | .505 |
| 7 | .8197 | Panel at Joint | | | 1.615 | .508 |
| 8 | .8462 | Tee | .7892 | 1.228 | 2.017(2) | .420 |
| 9 | .8373 | Panel at Joint | | | 1.580 | .530 |
| 10 | .8369 | Panel at Joint | | | 1.648 | .508 |
| 13 | .8326 | Stringer Run-out | | | 1.794(3) | .448 |
| 14 | .8340 | Tee | .7866 | 1.235 | 2.022(2) | .412 |
| 15 | .8178 | Panel at Joint | | | 1.640 | .499 |

1. Stress conversion factor is the ratio of minimum gross area to fractured gross area.
2. Total area for tee and splice plate.
3. Effective area of panel and stringer in vicinity of stringer run-out at joint.

TABLE 106

GROSS AREA STRESS SPECTRA IN VICINITY OF FRACTURE IN PANEL 2 AT TEE AND IN PANEL 3* AT STRINGER RUN-OUT

Test Group No. G82

| Loading Step | Panel 2 $f_v$ KSI | Panel 2 n | Panel 3* $f_v$ KSI | Panel 3* n |
|---|---|---|---|---|
| | $f_{mean}$ = 9.45 KSI | | $f_{mean}$ = 11.00 KSI | |
| 1 | .79 | 260000 | .91 | 260000 |
| 2 | 1.57 | 182000 | 1.83 | 182000 |
| 3 | 2.36 | 171600 | 2.74 | 171600 |
| 4 | 3.15 | 96200 | 3.65 | 96200 |
| 5 | 3.94 | 59800 | 4.56 | 59800 |
| 6 | 4.72 | 31200 | 5.48 | 31200 |
| 7 | 5.51 | 18720 | 6.39 | 18720 |
| 8 | 6.30 | 7020 | 7.30 | 7020 |
| 9 | 7.09 | 3120 | 8.22 | 3120 |
| 10 | 7.87 | 1196 | 9.13 | 1196 |
| 11 | 8.66 | 520 | 10.00 | 520 |
| 12 | 9.45 | 260 | 11.00 | 260 |
| 13 | 10.20 | 156 | 11.90 | 156 |
| 14 | 11.00 | 104 | 12.80 | 104 |
| 15 | 11.80 | 52 | 13.70 | 52 |
| 16 | 12.60 | 27 | 14.60 | 27 |
| 17 | 13.40 | 17 | 15.50 | 17 |
| 18 | 14.20 | 6 | 16.40 | 6 |
| 19 | 14.40 | 6 | 16.70 | 6 |
| | | $\Sigma$ 832004 | | $\Sigma$ 832004 |
| | No Failure - Loads Increased | | | |
| | $f_{mean}$ = 12.4 KSI | | $f_{mean}$ = 14.3 KSI | |
| 20 | 1.01 | 15000 | 1.19 | 15000 |
| 21 | 2.06 | 10500 | 2.39 | 31500 |
| 22 | 3.09 | 9900 | 3.58 | 29700 |
| 23 | 4.12 | 5550 | 4.78 | 16650 |
| 24 | 5.15 | 3450 | 5.97 | 10350 |
| 25 | 6.18 | 1800 | 7.16 | 5400 |
| 26 | 7.21 | 1080 | 8.36 | 3240 |
| 27 | 8.24 | 405 | 9.55 | 1215 |
| 28 | 9.27 | 147 | 10.70 | 540 |
| 29 | 10.30 | 46 | 11.90 | 207 |
| 30 | 11.30 | 20 | 13.10 | 90 |
| 31 | 12.40 | 10 | 14.30 | 45 |
| 32 | 13.40 | 6 | 15.50 | 27 |
| 33 | 14.40 | 4 | 16.70 | 18 |
| 34 | 15.40 | 2 | 17.90 | 9 |
| 35 | 16.50 | 2 | 19.10 | 5 |
| 36 | 17.50 | 1 | 20.30 | 3 |
| 37 | - | - | 21.50 | 1 |
| 38 | - | - | 21.80 | 1 |
| | | $\Sigma$ 47931 | | $\Sigma$ 144001 |
| TOTAL | | $\Sigma$ 879935 | | $\Sigma$ 976005 |

* Stresses at point of fracture in Panel 3 are based on stress conversion factor (Table 105) for catastrophic failure at stringer run-out rather than stress conversion factor for initial failure at tee.

TABLE 107

GROSS AREA STRESS SPECTRA IN VICINITY OF FRACTURE IN PANEL 4 AT STRINGER RUN-OUT, IN PANEL 5 AT TEE AND IN PANEL 6 AT JOINT

Test Group No. G83

| Loading Step | Panel 4 $f_v$ KSI | Panel 4 n | Panel 5 $f_v$ KSI | Panel 5 n | Panel 6 $f_v$ KSI | Panel 6 n |
|---|---|---|---|---|---|---|
| 1 | 1.20 | 255000 | .92 | 245000 | 1.12 | 290000 |
| 2 | 2.39 | 199500 | 1.84 | 171500 | 2.24 | 203000 |
| 3 | 3.59 | 186100 | 2.76 | 161700 | 3.36 | 151400 |
| 4 | 4.79 | 105450 | 3.68 | 90650 | 4.48 | 107300 |
| 5 | 5.98 | 65550 | 4.60 | 56350 | 5.60 | 66700 |
| 6 | 7.18 | 34200 | 5.51 | 29400 | 6.72 | 34800 |
| 7 | 8.38 | 20520 | 6.43 | 17280 | 7.87 | 20880 |
| 8 | 9.58 | 7695 | 7.35 | 6480 | 8.96 | 7830 |
| 9 | 10.80 | 3420 | 8.27 | 2880 | 10.10 | 3480 |
| 10 | 12.00 | 1311 | 9.19 | 1104 | 11.20 | 1334 |
| 11 | 13.20 | 570 | 10.10 | 480 | 12.30 | 580 |
| 12 | 14.40 | 282 | 11.00 | 240 | 13.40 | 290 |
| 13 | 15.60 | 168 | 11.90 | 144 | 14.60 | 174 |
| 14 | 16.80 | 112 | 12.90 | 96 | 15.70 | 116 |
| 15 | 18.00 | 56 | 13.80 | 48 | 16.80 | 58 |
| 16 | 19.20 | 29 | 14.70 | 24 | 17.90 | 29 |
| 17 | 20.30 | 18 | 15.60 | 15 | 19.00 | 18 |
| 18 | 21.50 | 6 | 16.50 | 5 | 20.20 | 6 |
| 19 | 21.90 | 6 | 16.80 | 5 | 20.50 | 6 |
| | | $\Sigma$ 911993 | | $\Sigma$ 783401 | | $\Sigma$ 928001 |

TABLE 108

GROSS AREA STRESS SPECTRA IN VICINITY OF FRACTURE IN PANELS 7 AND 9 AT JOINT AND IN PANEL 8 AT TEE

Test Group No. M17

| Loading Step | Panel 7 | | Panel 8 | | Panel 9 | |
|---|---|---|---|---|---|---|
| | $f_v$ KSI | n | $f_v$ KSI | n | $f_v$ KSI | n |
| | $f_{min}$ = 4.00 KSI | | $f_{min}$ = 3.19 KSI | | $f_{min}$ = 4.07 KSI | |
| 1 | 1.46 | 80500 | 1.37 | 80500 | 1.49 | 80500 |
| 2 | 2.92 | 70500 | 2.74 | 110450 | 2.99 | 117500 |
| 3 | 4.38 | 52500 | 3.51 | 82250 | 4.48 | 87500 |
| 4 | 5.85 | 37500 | 4.69 | 58750 | 5.98 | 75000 |
| 5 | 7.31 | 25500 | 5.86 | 39950 | 7.47 | 51000 |
| 6 | 8.77 | 16800 | 7.03 | 26320 | 8.96 | 33600 |
| 7 | 10.20 | 8700 | 8.20 | 13630 | 10.60 | 17400 |
| 8 | 11.70 | 3900 | 9.37 | 6110 | 12.00 | 7800 |
| 9 | 13.20 | 1450 | 10.50 | 2350 | 13.40 | 2972 |
| 10 | 14.60 | 508 | 11.70 | 810 | 14.90 | 1033 |
| 11 | 15.40 | 90 | 12.80 | 144 | 15.70 | 184 |
| | | $\Sigma$ 297915 | | $\Sigma$ 421254 | | $\Sigma$ 473989 |

TABLE 109

GROSS AREA STRESS SPECTRA IN VICINITY OF FRACTURE IN PANEL 10 AT JOINT AND PANEL 13 AT STRINGER RUN-OUT

Test Group No. CG5

| Loading Step | Panel 10 | | Panel 13 | |
|---|---|---|---|---|
| | $f_v$ KSI | n | $f_v$ KSI | n |
| | Gust Loading | | | |
| | $f_{mean}$ = 13.50 KSI | | $f_{mean}$ = 12.40 KSI | |
| 1 | 1.12 | 123750 | 1.03 | 165000 |
| 2 | 2.24 | 86535 | 2.06 | 115380 |
| 3 | 3.37 | 80190 | 3.09 | 106920 |
| 4 | 4.49 | 44955 | 4.12 | 59940 |
| 5 | 5.61 | 28905 | 5.15 | 37260 |
| 6 | 6.73 | 16200 | 6.18 | 19440 |
| 7 | 7.85 | 9700 | 7.12 | 11664 |
| 8 | 8.97 | 3650 | 8.24 | 5103 |
| 9 | 10.10 | 1620 | 9.27 | 1620 |
| 10 | 11.20 | 612 | 10.30 | 612 |
| 11 | 12.30 | 270 | 11.30 | 270 |
| 12 | 13.50 | 135 | 12.40 | 135 |
| 13 | 14.60 | 81 | 13.40 | 81 |
| 14 | 15.70 | 54 | 14.40 | 54 |
| 15 | 16.80 | 29 | 15.50 | 27 |
| 16 | 17.90 | 14 | 16.50 | 14 |
| 17 | 19.10 | 8 | 17.50 | 8 |
| 18 | 20.20 | 3 | 18.50 | 3 |
| 19 | 20.50 | 3 | 18.80 | 2 |
| | | $\Sigma$ 396723 | | $\Sigma$ 515542 |
| | Ground Loading | | | |
| | $f_{mean}$ = 3.37 KSI | | $f_{mean}$ = 3.09 KSI | |
| 20 | 1.12 | 110250 | 1.03 | 110250 |
| 21 | 2.24 | 61200 | 2.06 | 61200 |
| 22 | 3.37 | 25200 | 3.09 | 25200 |
| 23 | 4.49 | 10080 | 4.12 | 10080 |
| 24 | 5.16 | 2150 | 5.15 | 2150 |
| 25 | 6.73 | 450 | 6.18 | 450 |
| 26 | 7.85 | 120 | 7.21 | 120 |
| 27 | 8.97 | 54 | 8.24 | 54 |
| 28 | 10.10 | 29 | 9.27 | 28 |
| 29 | 11.20 | 6 | 10.30 | 6 |
| 30 | 12.30 | 1 | 11.30 | 1 |
| 31 | 13.50 | 1 | 11.50 | 1 |
| | | $\Sigma$ 209541 | | $\Sigma$ 209540 |
| | Ground-Air-Ground Loading | | | |
| | $f_{mean}$ = 5.05 KSI | | $f_{mean}$ = 4.64 KSI | |
| 32 | 8.41 | 32500 | 7.72 | 32500 |
| TOTAL | | $\Sigma$ 638764 | | $\Sigma$ 757582 |

TABLE 110

GROSS AREA STRESS SPECTRA IN VICINITY OF FRACTURE IN PANEL 14 AT TEE AND IN PANEL 15 AT JOINT

Test Group No. CM2

| Loading Step | Panel 14 | | Panel 15 | |
|---|---|---|---|---|
| | $f_v$ KSI | n | $f_v$ KSI | n |
| | Fighter Maneuver Loading | | | |
| | $f_{min}$ = 3.18 KSI | | $f_{min}$ = 3.93 KSI | |
| 1 | 1.16 | 24500 | 1.44 | 44100 |
| 2 | 2.33 | 20750 | 2.87 | 37350 |
| 3 | 3.50 | 18500 | 4.31 | 33300 |
| 4 | 4.66 | 15250 | 5.75 | 27450 |
| 5 | 5.83 | 9250 | 7.19 | 16650 |
| 6 | 6.99 | 5750 | 8.63 | 10350 |
| 7 | 8.16 | 2500 | 10.10 | 4500 |
| 8 | 9.33 | 2000 | 11.50 | 3600 |
| 9 | 10.50 | 661 | 12.90 | 1485 |
| 10 | 11.70 | 112 | 14.40 | 228 |
| 11 | 12.20 | 28 | 15.10 | 56 |
| | | $\Sigma$ 99301 | | $\Sigma$ 179069 |
| | Ground Loading | | | |
| | $f_{mean}$ = -2.74 KSI | | $f_{mean}$ = -3.38 KSI | |
| 12 | .91 | 61250 | 1.13 | 110250 |
| 13 | 1.83 | 34000 | 2.25 | 61200 |
| 14 | 2.74 | 14000 | 3.38 | 25200 |
| 15 | 3.65 | 5600 | 4.51 | 10080 |
| 16 | 4.56 | 1075 | 5.64 | 1935 |
| 17 | 5.48 | 225 | 6.76 | 405 |
| 18 | 6.39 | 60 | 7.89 | 108 |
| 19 | 7.30 | 27 | 9.02 | 49 |
| 20 | 8.22 | 14 | 10.10 | 25 |
| 21 | 9.13 | 3 | 11.30 | 5 |
| 22 | 10.00 | 1 | 12.40 | 1 |
| 23 | - | - | 12.60 | 1 |
| | | $\Sigma$ 116255 | | $\Sigma$ [illegible] |
| | Ground-Air-Ground Loading | | | |
| | $f_{mean}$ = .18 KSI | | $f_{mean}$ = .22 KSI | |
| 24 | 3.00 | 3326 | 3.67 | 5980 |
| TOTAL | | [illegible]081 | | $\Sigma$ 394309 |

Aeronautical Systems Division, W-PAFB, Ohio. Rpt No. ASD-TR-61-434, AN ENGINEERING EVALUATION OF METHODS FOR THE PREDICTION OF FATIGUE LIFE IN AIRFRAME STRUCTURES. Mar 62, [illegible] p. incl illus., tables, 15 refs

Unclassified Report

Results of study are presented for comparison and verification of fatigue-life prediction methods suitable for handling complex problems encountered in design and operation of modern aircraft. Problems of airframe fatigue are analyzed from overall viewpoint of a system of design, development testing, and interpretation of flight service history. From study of 25 proposed fatigue-life prediction methods, 10 were evaluated numerically with 78 complex spectral test results representing about 200 specimens.

( over )

1. Airframes
2. Fatigue

I. AFSC Project 1:67, Task 1:6710
II. Contract AF33(616)-6674
III. Lockheed-California Co., A Div. of Lockheed Aircraft Corp., Burbank, California
IV. W. J. Crichlow, A. J. McCulloch, L. Young, et al
V. In ASTIA collection

Aeronautical Systems Division, W-PAFB, Ohio. Rpt No. ASD-TR-61-434, AN ENGINEERING EVALUATION OF METHODS FOR THE PREDICTION OF FATIGUE LIFE IN AIRFRAME STRUCTURES. Mar 62, [illegible] p. incl illus., tables, 15 refs.

Unclassified Report

Results of study are presented for comparison and verification of fatigue-life prediction methods suitable for handling complex problems encountered in design and operation of modern aircraft. Problems of airframe fatigue are analyzed from overall viewpoint of a system of design, development testing, and interpretation of flight service history. From study of 25 proposed fatigue-life prediction methods, 10 were evaluated numerically with 78 complex spectral test results representing about 200 specimens.

( over )

1. Airframes
2. Fatigue

I. AFSC Project 1:67, Task 1:6710
II. Contract AF33(616)-6674
III. Lockheed-California Co., A Div. of Lockheed Aircraft Corp., Burbank, California
IV. W. J. Crichlow, A. J. McCulloch, L. Young, et al
V. In ASTIA collection

Experimental program generated constant-amplitude, axial-load, S-N type data on simple notched coupons of 7075-T6 aluminum alloy sheet. New magnetic tape-controlled fatigue test machines were used to apply simple spectra of gust, maneuver, ground, composite spectra of flight gust, ground taxi, and ground-air-ground transitions and composite spectra of flight maneuver, ground taxi, and ground-air-ground transition. Specimens of complex joint were also fatigue-tested to same simple one-for-one gust and maneuver spectra, to the composite spectra of flight gust, ground taxi, and ground-air-ground transition cycles, and to composite flight maneuver, ground taxi, and ground air ground transition cycles. Data were analyzed to confirm or provide means of improving selected fatigue-life prediction methods.

Experimental program generated constant-amplitude, axial-load, S-N type data on simple notched coupons of 7075-T6 aluminum alloy sheet. New magnetic tape-controlled fatigue test machines were used to apply simple spectra of gust, maneuver, ground [illegible] composite spectra of flight gust, ground taxi, and ground-air-ground transitions and composite spectra of flight maneuver, ground taxi, and ground-air-ground transition. Specimens of complex joint were also fatigue-tested to same simple one-for-one gust and maneuver spectra, to the composite spectra of flight gust, ground taxi, and ground-air-ground transition cycles, and to composite flight maneuver, ground taxi, and ground-air-ground transition cycles. Data were analyzed to confirm or provide means of improving selected fatigue-life prediction methods.

REPORT HAS BEEN DELIMITED

AND CLEARED FOR PUBLIC RELEASE

UNDER DOD DIRECTIVE 5200.20 AND

NO RESTRICTIONS ARE IMPOSED UPON

ITS USE AND DISCLOSURE.

DISTRIBUTION STATEMENT A

APPROVED FOR PUBLIC RELEASE;

DISTRIBUTION UNLIMITED.